HYDROGEOLOGICAL AND GEOPHYSICAL INVESTIGATION OF THE GROUNDWATER SYSTEM IN THE KAITUNA VALLEY, BANKS PENINSULA

A thesis

submitted in partial fulfilment

of the requirements for the degree

of

Master of Science in Engineering Geology

in the

University of Canterbury

by

Parviz Namjou

University of Canterbury

1988

FRONTISPIECE: Groundwater utilisation in Kaituna Valley

TO MY MOTHER,
TO WHOM I OWE EVERYTHING

ABSTRACT

In the Kaituna Valley an intensive change in land use has produced an increased demand for water, particularly groundwater. The present study was undertaken in order to provide an adequate data base to develop appropriate water management strategies for the Kaituna Valley and other similar catchments in the area.

Shrinkage fractures within lava flows control the vertical movement of water whilst horizontal water flow occurs mainly within brecciated lava. Chemical and environmental water analysis indicate that local precipitation through volcanic fractures is the main mechanism for groundwater recharge in the area. The impermeable layers (tuff and ash) between lava flows and subvertical dikes divide the subsurface volcanic rocks into a number of groundwater compartments each with its own water level and outlets. Outlets will be into adjacent lower compartments or springs. As a result the groundwater passes through a number of steps down the hillside into the zone adjacent to the valley floor sediments. The outlet through the gravelly layer in this zone is the main mechanism of groundwater replenishment within the valley floor deposits.

Geophysical investigations have identified two aquifers below the valley floor. The lower aquifer with an average transmissivity value of 4.45×10^{-3} m^2/s has a variable thickness ranging between 2 m to 60 m. The average transmissivity for the upper aquifer is 14.5×10^{-3} m^2/s with an average thickness of 24 m.

Using the hydrological water Balance for the monitored water year (June 1986 - May 1987), the total rate of recharge to the groundwater system was 86 mm out of 1900 mm total rainfall.

If groundwater is to be used for drinking, it must be treated for excessive iron content in well M36/1344, and excessive manganese content in wells M36/843 and M36/1344 bot.. of which draw from the lower aquifer.

TABLE OF CONTENTS

CHAPTER THREE GEOPHYSICAL INVESTIGATION

CHAPTER FOUR SURFACE HYDROLOGY

CHAPTER FIVE GROUND WATER HYDROLOGY

CHAPTER SIX HYDROCHEMISTRY AND ENVIRONMENTAL ISOTOPE STUDIES

CHAPTER SEVEN SUMMARY AND CONCLUSIONS

LIST OF FIGURES

Figures (Continued) Page

Figures (Continued) Page

Figures (Continued) Page

LIST OF TABLES

LIST OF PLATES

ACKNOWLEDGEMENTS

The following people and organizations have my sincere thanks for their assistance during the preparation of this thesis.

My supervisors, Mr D.H. Bell and Dr J.R Pettinga for their guidance and encouragement during the course of this project. I am especially grateful to Mr Bell for his reviewing of the draft of this thesis.

The North Canterbury Catchment board and Ministry of Works for provide funding assistance throughout the project with special thank to John Talbot.

Dr Mike Broadbent, for his guidence and encouragements during the geophysical investigation.

Geophysics division of Department of Scientific and Industrial Research for seismic data processings with special thanks to Dr D. Woodward, R. O'Connor, S. Hicks.

The technical staff of the Geology Department of the University of Canterbury for their assistance throughout the project and for the use of technical resources, equipment and facilities of the department, and also Tracey Robinson for her kind assistance in the final printing.

G. Horrell, P. White, P. Callender, for assistance in data processing and Mike simpson, P. Perkins for their help and company in the field.

My classmates, the Mikes, J.K, Ron, Dale, Grant, Vivs, who proofread much of the manuscript and their humour.

CHAPTER ONE

INTRODUCTION

1.1 Project Background

The Kaituna Valley covers an area of about 50 km^2, and is located on the south-west side of Bank Peninsula north-east of the Kaitorete Spit. (Fig. 1.1). It extends more than 11 km from Lake Ellesmere in the south to the Mt Herbert in the north, and relief rises from 1 m at Lake Ellesmere to an altitude of 920 m.

A main problem for successful farming and land use development in the area is the water supply. In the lower part of the valley low rainfall and high evapotranspiration rates make irrigation essential, especially in the south east of the valley where hill slopes face the north-west winds and dry out in summer. Highly saline soils adjacent to the lake regularly require large volumes of water to effect desalting. In addition during recent years there has been a steady change in land use from traditional pastoral farming to more intensive forms of land use, including horticulture, market gardening and dairying. These changes have produced an increased demand for water, particularly groundwater, in the lower-central part of the valley where the main body of the investigation is concentrated.

1.2 Project Objectives

The primary aim of the Kaituna groundwater study has been to assess and delineate the groundwater system, in order to provide an adequate data base to develop appropriate water management strategies for the Kaituna Catchment, and for other similar tributary catchments in the Banks Peninsula.

Within the scope of the this overall direction, specific study objectives have been:

1) Engineering Geological and Hydrogeological mapping of the area in order to determine site development history and geological controls of groundwater movement.

2) Engineering Geophysical investigation including, electrical resistivity surveys, geophysical downhole logging and seismic profiles to

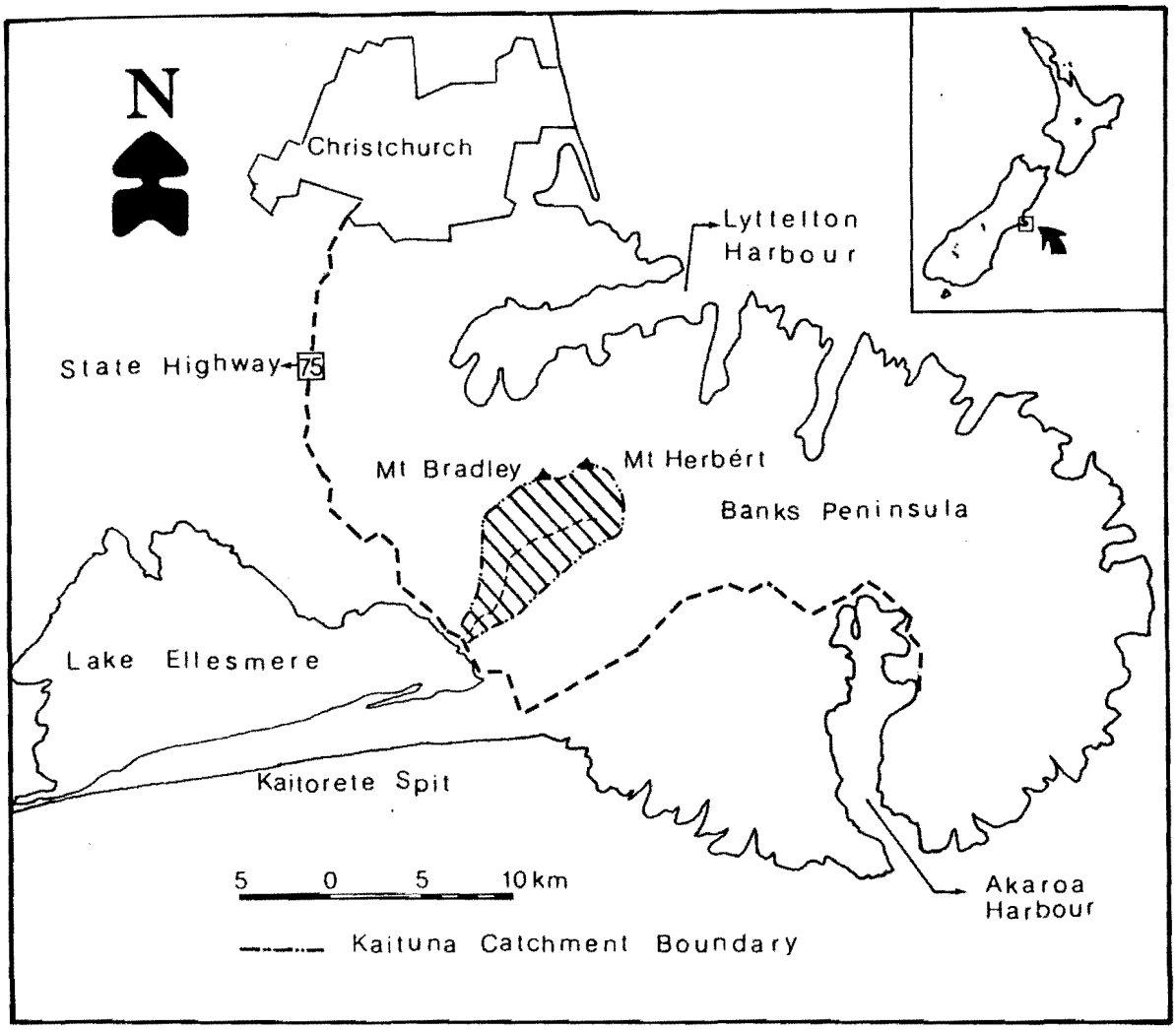

Figure 1.1 Location Map

complement geological observations in defining aquifer distribution.

3) Stream discharge monitoring and catchment meteorological studies (evaporation and rainfall monitoring) to detect any possible interaction between groundwater and stream flow, and to assess the inputs and outputs of the groundwater system for understanding the gross water balance.

4) Aquifer testing (eg. pumping test, free flow test, slug test) to determine hydraulic parameters of the groundwater system.

5) Monitoring of the piezometric surface and study of its fluctuation with time to describe the responses of the aquifers to seasonal hydrological inputs.

6) Spring discharge monitoring in order to identify groundwater discharge mechanisms.

7) Water quality assessment for both spring discharges and valley floor aquifers, including environmental isotope studies. This was undertaken in order to identify groundwater recharge sources and to determine the suitability of groundwater for public water supply, and/or irrigation application.

In pursuing the above objectives, it became apparent that groundwater and surface hydrology of the catchment are closely related. As a result, the original objectives were expanded to include an assessment of the surface hydrology.

1.3 Geological Setting

1.3.1 Banks Peninsula

Banks Peninsula, with an elevated area of 1200 km^2, consists mainly of eroded remains of two large stratovolcanoes-Lyttelton and Akaroa both of Miocene age (Sewell, 1985). These formed between 11 and 5.8 million years ago. For the past 15 million years (from early Pleistocene) Banks Peninsula was an island on the western end of the Chatham Rise. Rapidly downcutting radial drainage pattern were well established on these by Pleistocene. The craters of both the Lyttelton and Akaroa volcanoes eroded completely due to lengthening and widening of the drainage system which have subsequently been drowned by sea, forming the Lyttelton and Akaroa harbors. During the mid-late Pleistocene (20 000 years ago), the volcanic island (Banks Peninsula) gradually became connected to the mainland by outwash fans from the Canterbury Plains.

The pre-Lyttelton rocks (Torlesse Terrane sediments and the Charteris Bay Sandstone) occur up to an elevation of 330 m above sea level near Gebbies Pass.

A general stratigraphic column and simplified geological map of Banks Peninsula is show in Fig. 1.2.

1) Lyttelton Volcanics

Lyttelton Volcanics overlie a basement of Triassic to mid-Miocene volcanic and sedimentary rocks (Sewell, 1985). The volcanics are estimated to have formed a symmetrical cone as high as 1500 m above sea level, between 11 to 10 million years ago. It is largely composed of basic lavas (aa) with intercalated pyroclastic beds. The pyroclastic depositsvary from ash and tuffs to scoria cones. The Lyttelton volcano contain a number of trachyte lava flows and a radial dyke swarm. A trachytic radial dyke swarm was emplaced in fractures in the updomed volcanic cone towards the end of Lyttelton volcanism (9.7 Ma).

2) Mt Herbert Volcanics

The Mt Herbert Volcanics comprise a volcanic complex of mildly alkaline, basalt plugs and lava flow and pyroclastic deposits. It occurred as a series of eruptions within and on the southern flanks of the Lyttelton volcano. The Mt Herbert Volcanics range in age from 9.7 to 8.0 Ma and are subdivided into five formations according to their field, composition and age relationships. These volcanics represent a south-easterly migration of volcanic activity from Lyttelton towards the Akaroa volcanics.

3) Akaroa Volcanics

The Akaroa volcano was active from about 9.0 million years ago (Sewell 1985) to one million years ago. During this period a large volcanic cone (20 km south-east of the Lyttelton volcanics center) consisting of trachyte-basalt lava and pyroclastic beds was constructed. A number of dikes and domes, mainly of trachyte composition, are also identified in the volcanic succession.

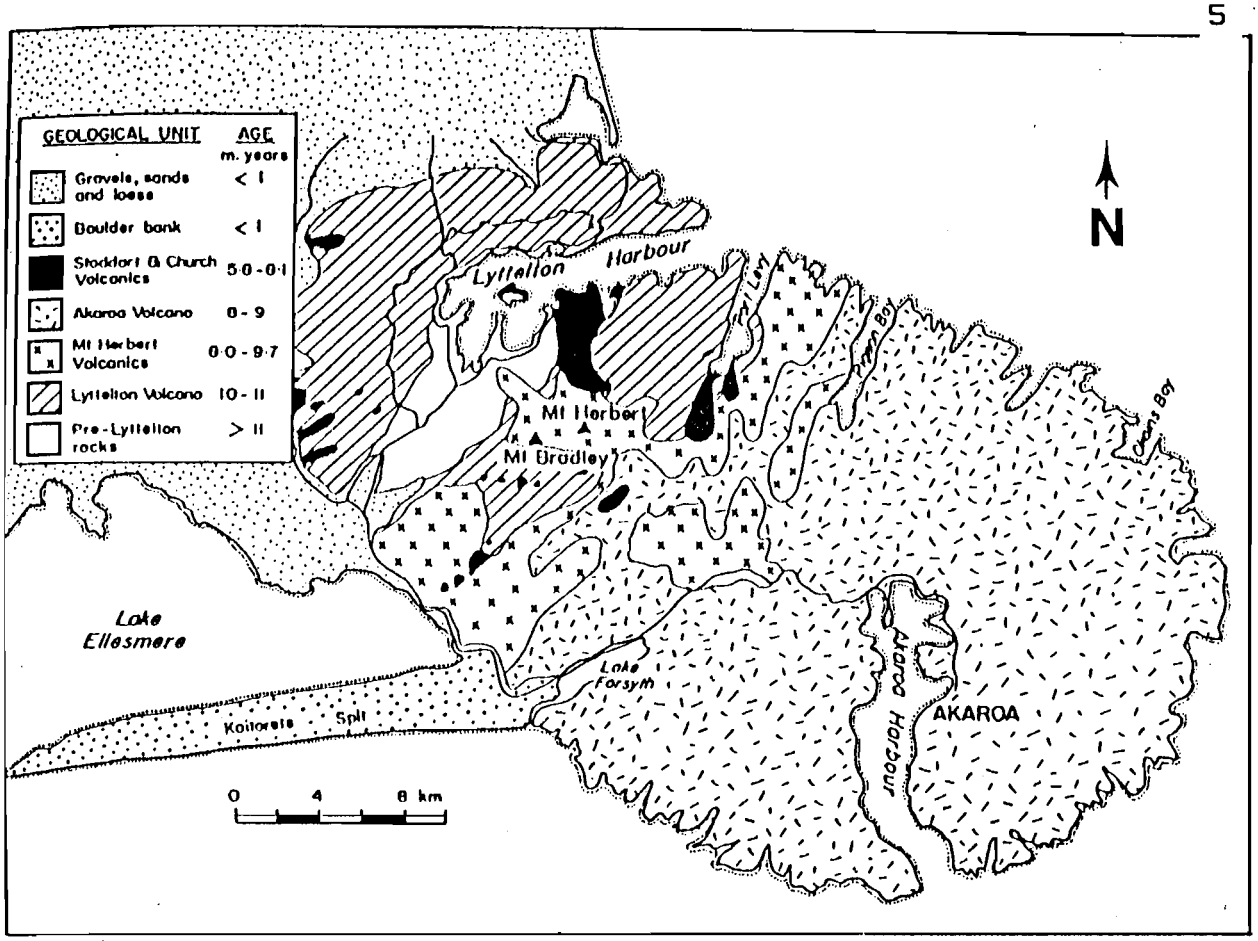

AGE millions of years before present	BANKS PENINSULA GEOLOGY	
	GEOLOGICAL UNIT	LITHOLOGY
QUATERNARY 0 - 1	Recent deposits	loess, gravels and alluvium
	break in succession	no rocks of Pliocene age known
MIOCENE 6 - 8	Diamond Harbour Volcanics	basalt lavas
8 - 10	Akaroa Volcano	basalt - trachyte lavas, dikes, gabbro - syenite
	Mt Herbert Volcanics	basalt lavas, pyroclastics and lake sediments
10 - 12	Lyttelton Volcano	basalt - trachyte lavas and dikes
12 - 14	Governors Bay Volcanics	andesite flows and rhyolite domes
	break in succession	no rocks of Eocene - Oligocene age known
PALEOCENE 50 - 60	Charteris Bay Sandstone	marine, buff - coloured quartz + sandstone
	break in succession	no rocks known
CRETACEOUS 90 - 100	McQueens Volcanics	andesite flows and rhyolite domes
	break in succession folding of Torlesse rocks	no rocks of Jurassic age known
TRIASSIC 210 - 230	Torlesse Terrain	marine, grey sandstones and mudstones, and red cherts

Figure 1.2;
Simplified Geological Map and General Stratigraphic Column of Banks Peninsula (after Weaver et al, 1985).

4) Church Volcanics

The Church Volcanics consist of a newly defined volanic group of basanitoids, alkali olivine-basalts and intercalated volcanogenic sediments (Sewell 1985). Most of these rocks were previously considered as the Church Formation of the Diamond Harbour Group. The volcanics range in age from 8.1 to 7.3 Ma.

5) Stoddart Volcanics

The Stoddart Volcanics comprise the youngest phase of volcanism on Banks Peninsula, occurring between 7.0 and 5.8 Ma. The volcanics consist mainly of olivine-basalt to olivine-hawaiite lavas. The Stoddart volcanic have been found entirely within the area covered by the Lyttelton Volcanics as valley fillings or flat sheets from a number of sources. The major exposures of these rocks are identified in the Diamond Harbour and Port Levy areas (Fig. 1.2).

1.3.2 Geological Succession in the Kaituna Valley

The Kaituna Valley is a good example of an ancient (~10 Ma, following the formation of Lyttelton volcanics) valley system which has been infilled by successive phase of volcanism and then re-excavated (Sewell, 1985). This is evidenced by Stoddart Point olivine-basalt lavas (Fig. 1.3) which are found as remnant valley-fill sequences along the north-side of the valley. The volcanic successions in Kaituna Valley are illustrated in Fig. 1.3 and a summary of the lithology for each volcanic group is presented in Table 1.1.

Lyttelton Volcanics are exposed mainly in the middle and north side of the valley (Fig. 1.3). A large area of volcanic breccia is located near the head of Kaituna valley (GR 885 222). Two Trachytic domes also have also been identified within these volcanics. One is located north of trig D whilst the other occursnorth of the valley between Mt Bradly and Mt Herbert (Fig. 1.3).

The lava flow related to Mt Herbert unconformably overlies the Lyttelton Volcanics on the north side of Kaituna Valley (Fig. 1.3). Three subdivision of these volcanics are identified in the Valley; 1) Port Levy Volcanic suite, 2) Orton-Bradley Volcanic Suite and, 3) Kaituna Olivine Hawaiites. The location of Mt Herbert Volcanics and its subdivisions are

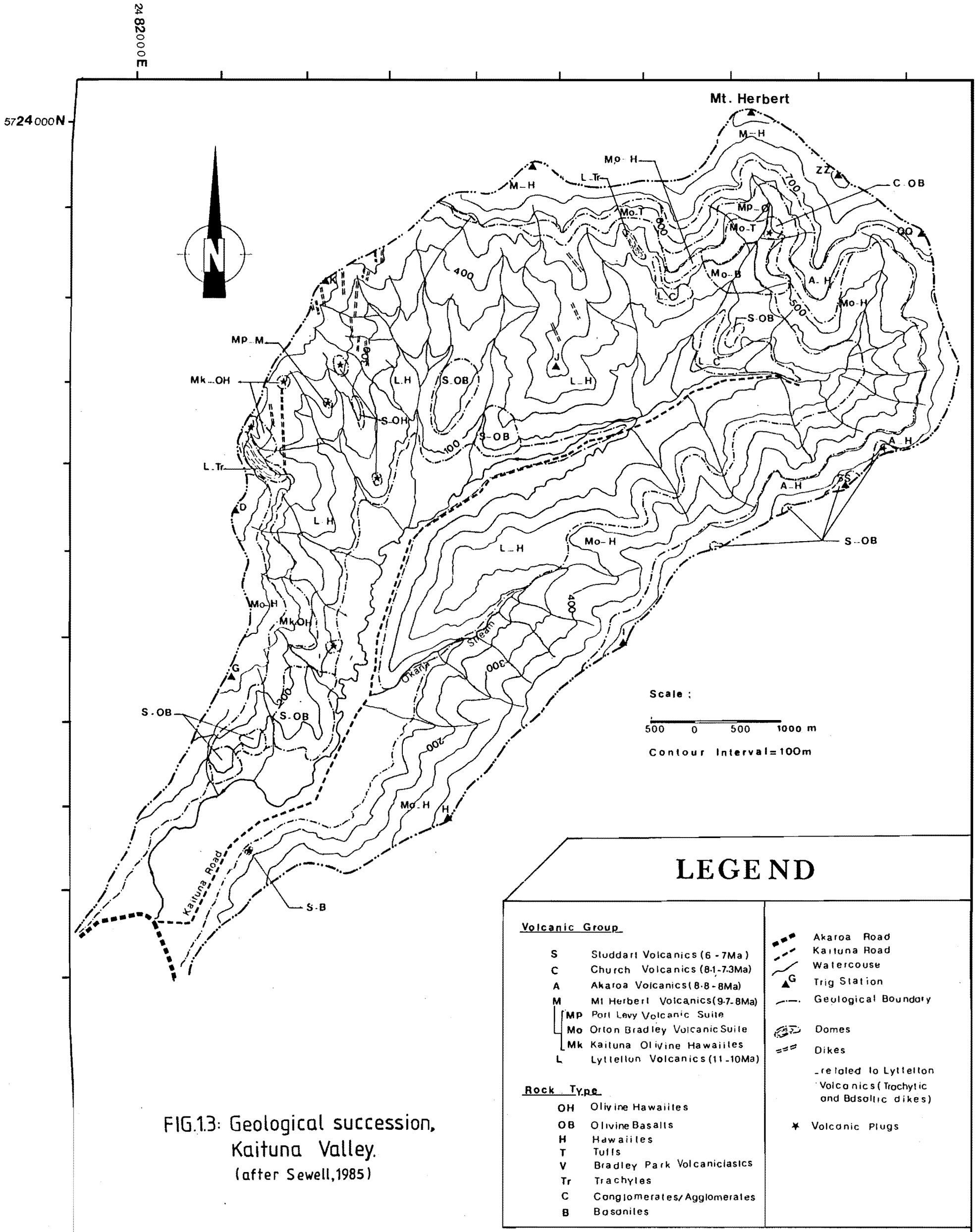

FIG.1.3: Geological succession, Kaituna Valley.
(after Sewell, 1985)

SUMMARY OF STRATIGRAPHY OF CENTRAL BANKS PENINSULA

GROUP	FORMATION	K/Ar AGE RANGE (Ma)	LITHOLOGY	DISTINCTIVE CHEMICAL & MINERALOGICAL FEATURES	MAIN LOCALITIES
STODDART VOLCANICS	STODDART POINT OLIVINE-BASALTS	7·0 - 5·8	Fresh, columnar-jointed, olivine ± clinopyroxene phyric basanites, olivine-basalts and olivine-hawaiites – rare olivine-basalt dikes	No plagioclase phenocrysts. Mg-number 38-66. Low TiO_2 contents. Ne and Hy-normative. Ce_n/Yb_n (c.6·0) $^{87}Sr/^{86}Sr$ (0·70320-0·70370)	Taitapu - Ahuriri, Kaituna Valley Port Levy, Diamond Harbour, Quail Island
	KAIORURU OLIVINE HAWAIITES	6·9 - 6·8	Commonly weathered, vesicular, pale pink, olivine ± clinopyroxene-phyric and aphyric olivine-hawaiites	No plagioclase phenocrysts. Mg-number 36-60. Lower levels of incompatible trace element abundance relative to Stoddart Point lavas. Ce_n/Yb_n (c.6·0). $^{87}Sr/^{86}Sr$ (0·70350)	Diamond Harbour, Quail Island
CHURCH VOLCANICS	CHURCH BAY OLIVINE-BASALTS	7·8 - 7·3	Fresh, columnar-jointed, olivine ± clinopyroxene ± plagioclase-phyric olivine-basalts	Mg-numbers 40-60. Moderate Cr (250 ppm) and Ni (150 ppm). Ce_n/Yb_n (c 9·0) $^{87}Sr/^{86}Sr$ (0·70300)	Diamond Harbour, Quail Island, Taitapu - Ahuriri
	DARRA BASANITOIDS	8·1 - 7·7	Fresh, columnar-jointed olivine ± clinopyroxene-phyric basanitoids – rare basanitoid dikes	Mg-numbers 60-68. High Cr (450ppm) and Ni (200 ppm) content $^{87}Sr/^{86}Sr$ (0·70296)	Diamond Harbour, Quail Island, Ahuriri-Taitapu
AKAROA VOLCANICS		9·0 - 8·0	Fresh, medium to fine-grained, olivine-clinopyroxene-plagioclase-phyric and grey, aphyric hawaiites - rare trachyte domes and dikes	Fractionated series. Trace element abundances generally higher than Lyttelton volcanics. Ce_n/Yb_n (c.7·0) $^{87}Sr/^{86}Sr$ (0·70294-0·70388)	South side of Kaituna Valley - Port Levy
MT HERBERT VOLCANICS	MT HERBERT HAWAIITES	8·5 - 8·0	Grey, columnar-jointed, aphyric and rarely olivine-phyric olivine-hawaiites	Chemical features similar to Akaroa. Ce_n/Yb_n (c.9·0) $^{87}Sr/^{86}Sr$ (0·70306)	Mt Herbert - Mt Bradley
	CASTLE ROCK HAWAIITES	8·5 - 8·0	Grey, columnar to knobbly-jointed aphyric hawaiites	Red/brown apatite microphenocrysts. Sr (>1000ppm), high P_2O_5 (1·4 + %) — Fractionated series	Charteris Bay - Bradley Park
	PORT LEVY VOLCANIC SUITE	8·9 - 8·5	Grey-black, columnar-jointed, aphyric hawaiites-rare porphyritic basalts and mugearites	Mod. P_2O_5 and Nb contents Enriched overall in REE — Ce_n/Yb_n (c.7·0)	Port Levy - Western Valley
	ORTON-BRADLEY VOLCANIC SUITE	9·5 - 8·9	Black, fresh aphyric, olivine-hawaiites & olivine ± clinopyroxene ± plagioclase-phyric olivine-basalts	High TiO_2 and low K_2O contents relative to Port Levy & Castle R. — $^{87}Sr/^{86}Sr$ (0·70298)	Mt Herbert - Mt Bradley
	KAITUNA OLIVINE-HAWAIITES	9·7 - 9·5	Columnar-jointed, dark grey-black, fresh, olivine ± clinopyroxene-phyric olivine-hawaiites	Amphibole/apatite-rich lavas and xenoliths High Ce_n/Yb_n (c.15·0) $^{87}Sr/^{86}Sr$ (0·70332)	Kaituna - McQueens Valleys
LYTTELTON VOLCANICS		11 - 10	Moderately weathered, plagioclase ± olivine ± clinopyroxene-phyric hawaiites - trachyte lava flows and domes - numerous trachytic and basaltic dikes	Fractionated series Commonly plagioclase-phyric. High average Zr/Sr and Zr/Nb ratios compared to other volcanic groups Ce_n/Yb_n (c.8·0) $^{87}Sr/^{86}Sr$ (0·70300-0·70515)	North side of Kaituna Valley - Mt Herbert

Table 1.1 A Summary of Lithology for each Volcanic Group (after Sewell 1985).

shown in Fig. 1.3.

Akaroa Volcanics are identified chiefly above the 500 m contour line on the east side of the valley (Fig. 1.3). They unconformably overlie the oldest volcanic rocks and interfinger with the Mt Herbert Volcanics (Sewell, 1985).

The Stoddart Volcanics (olivine-basalt) in the area are erupted from five vent plugs (Fig. 1.3). The largest vent plug is located in the upper reaches of the valley (GR. 907520). Lava flows related to these volcanics unconformably outcrop against volcanic rocks of the Lyttelton volcanics and Mt Herbert volcanics. The most complete stratigraphic succession is identified in the lower part of the valley (GR. 840 017) where lavas form a thick (130 m) sequence of 48 flows (Sewell, 1985).

1.4 Geomorphology

The Kaituna valley forms a major valley system draining to the south west. The valley, as part of the Banks Peninsula, was largely unaffected by the Kaikura orogeny (probably due to its distance from the main axis of the Southern Alp deformation). Its origin therefore is considered to be due to erosion in the head waters of a major radial drainage system developed following cessation of Lyttelton and Akaroa volcanism. A thick pyroclastic deposit near the head of the Kaituna valley (Fig. 1.3) is likely to have eroded rapidly, and has been responsible for the initial development of the valley drainage system. The topography in the area is controlled by gently southward dipping (average 7 degree) lava flows. The eruption of Stoddart Volcanics from the five sources (Fig. 1.3) as valley filling or flat sheets between 6.9 to 5.8 million years ago has been responsible for the present pattern of the Kaituna valley drainage system.

Although there is no evidence that glaciers ever formed on Banks Peninsula, the morphology of the area has been affected by the glacial period of the last two million years. Fine sand and silt, formed by the milling action of ice on rock, was accumulated as loess (up to 20 m) on the irregular surface of the volcanic rocks.

1.5 Climate

1.5.1 Rain Bearing Winds and Rainfall

The Kaituna valley as a part of Banks Peninsula projects out from,

and its climate is quite different from, the surrounding Canterbury Plains. This is especially apparent with rainfall, with south-westerly and westerly winds flowing over the western part of the Peninsula and shedding their moisture as they cool. While Lyttelton Harbour receives most of its rainfall from a south-westerly direction, the bays to the east are more affected by rainfall from the north-east. The Southern Alps provide no shelter from rain bearing winds from the south and south west, and therefore the higher elevated areas (where snow is expected in winter) are more exposed to southerly rain than the adjacent Canterbury Plains. This is clearly illustrated in the isohyetal map (Fig. 1.4). The contours of equal rainfall depths are based on 35 years (from 1950 to 1985) of rainfall (mean values) for Banks Peninsula.

Winter conditions can linger on into spring due to the persistence of rain from the south and south west. Higher altitude regions of Bank Peninsula are more likely to be affected than the lower altitude regions due to topographic forcing of these unstable air masses. In Kaituna Valley this is documented by observation of 247.4 mm in November 1986 for stn.1 (App. 8.1). The summer period is dominated by anticyclonic conditions, resulting in the lowest rainfall totals at this time of the year. The dry warm north-west wind in early summer have an erosive effect on the hill slopes facing north. During this time relatively frequent rains are quickly dissipated by high evaporation rates.

1.5.2 Temperature

On Banks Peninsula the seasonal temperature range is smaller than that experienced in Christchurch due to the greater maritime influence (being less prone to katabatic drainage of cold air from the plains). This range is of the order of 20° - 30° (Dept. of Lands & Survey 1982). As a result frost are fewer and summer temperatures are low for Canterbury. In general relative humidity is less than 70% between October and February and temperatures often exceed 30° C during these months. In winter, May to September, sub-zero temperatures are common. Ground frosts are recorded on more than 100 days per annum at Lincoln (Depth. of Lands & Survey, 1984), the nearest meteorological station, about 18 km inland. Climatic parameters, obtained from the Lincoln station (between June 1986 and May 1987) are presented in App. 1.

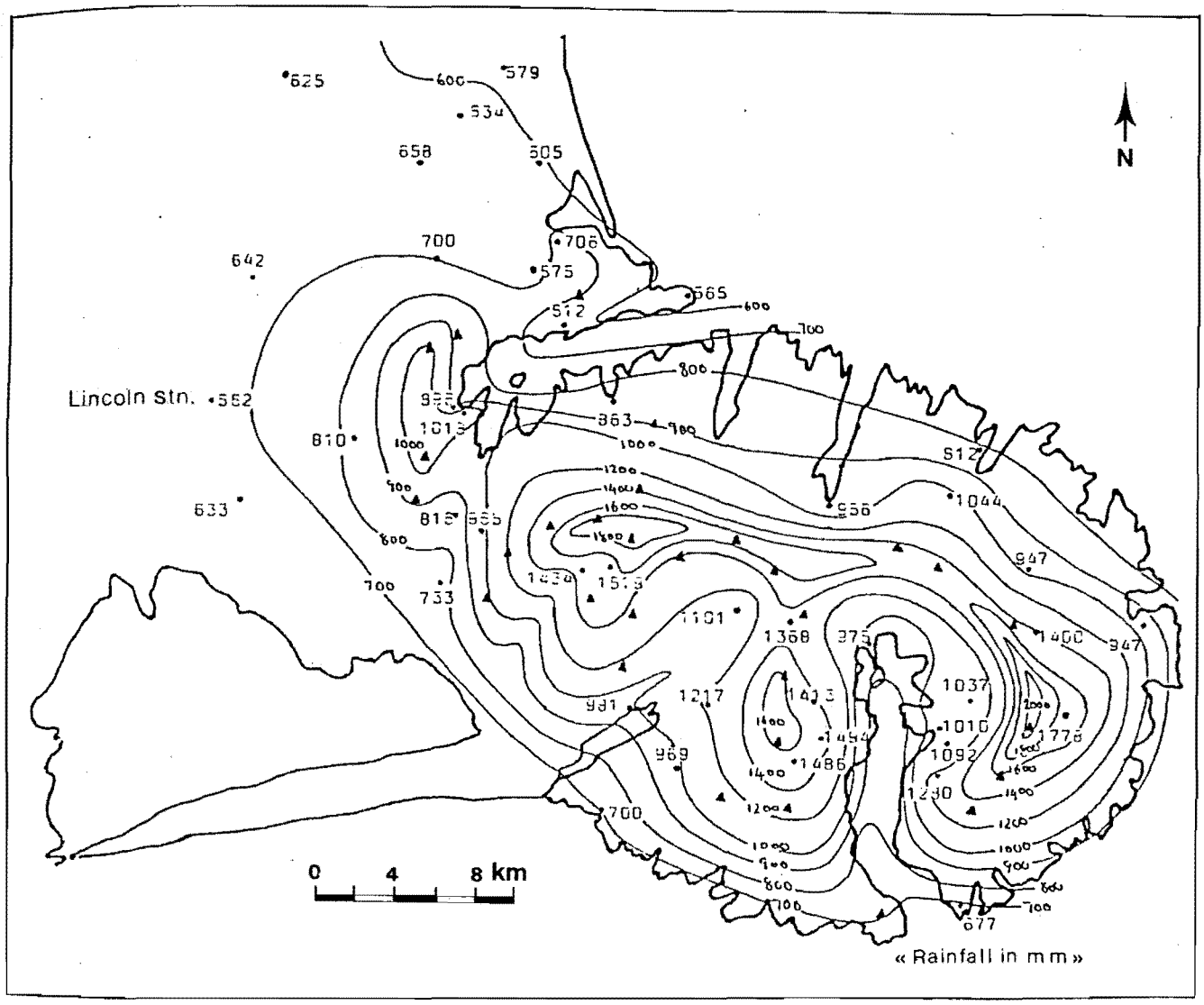

Figure 1.4 Mean Annual RainFall in the Banks Peninsula (based on rainfall data from a period of 1950 to 1985)(after Jayet, 1986).

1.6 Vegetation

Development of the present vegetation in the Kaituna Valley has been greatly influenced by man and is therefore more related to management than to soil and climate. Pre-European vegetation consisted of Podocarp/Hardwood forest, which is now restricted to damper gullies due to burning in both pre-European and European times. Tall forests occupied the rich, flat alluvial ground of the valley floors. Only tiny remnants of forest remain as reserves, because the valley floors were prime candidates for conversion to farmland (Wilson, 1987). There is isolated native bush preserved on the hill sides as well, the largest being located to the south of Mt Herbert in the inaccessible stream headwater (GR M36 895 230).

The main species of the Podocarpaceae family on the valley floor are Kahikatea, Matai and Totara. Hall's (or mountain) Totara is more common at higher elevations. Wilson (1987) notes that the most common type of vegetation which can be used as the indicators of the presence of springs are the Juncus species (rushes) and Carex species (Sedges). Today mixture of pasture land grass and tussock cover most of the valley. On the lower slopes more intensive development has occurred, with improved pastures sown down, while on some steeper slopes there has been colonization by gorse, broom and bracken fern.

Towards Lake Ellesmere there is a distinct zonation of the vegetation parallel to the lake margin; 1) Grassland 2) Juncus dominant 3) Scripus swamp 4) Salt meadow. Factors influencing this zoning are flooding, salinity and soil texture. Flooding has been more effective factor among these categories (Palmer 1982).

1.7 Land Use

The emphasis in the study area is on extensive sheep and cattle grazing, including breeding and some intensive fattening. Soils of the plains and valley floor are, in general, of high value for food production and at present are used for dairying, horticulture, and general cropping. Soils of the rolling land and hills are of low value for food production and can be classified according to their suitability for urban uses. Loess is susceptible to tunnel and gully erosion, making it unsuitable for cropping (especially where the vegetation cover is depleted by overgrazing or removed). However presently some of this land is maintained in pasture.

Fertility is improved by top dressing and soil structure is encouraged to developed so that there is less erosion. The land near the lake has to be leached of salt, protected from flooding and drained before it is suitable for pasture.

The land Use Inventory Code and land use Capability Classification of the valley is shown in the Fig. 1.5 and Tables, 1.2 and 1.3. In this classification the suitability of rural land for productive use can be evaluated after taking account of all physical limitations

In Kaituna Valley three of the land use capability classes (Table 1.3) can be identified;

Class III land has moderately deep to moderately shallow soils on flat to gently undulating slopes (0° - 7°). Land use limitation include a risk of wind erosion, high watertables in winter, or saline soils. These limitations are moderate for intensive grazing, cropping and production forestry.

Class VI Includes land with very shallow stony soils on flat to undulating slopes(16° - 35°) and stable hill slopes. It is considered suitable land for grazing and, with the exception of the shallow stony soils, for production forestry.

Class VII these type of land consists of steep exposed hill slopes (26 - 35) and rolling coastal dunes with a severe wind erosion hazard under pasture. It is not desirable for grazing or production forestry.

1.8 Investigation Techniques

1.8.1 Hydrogeological mapping

Hydrogeological mapping of the Catchment was undertaken from May 1986 until January 1987 using topographic base plans: M36 and N36. The whole catchment and its lower half were mapped at 1/10000 (Fig. 1.6). and 1/20000 (Fig. 1.7) scales respectively.

1.8.2 Laboratory Testing

Laboratory permeability tests (falling head) were carried out (September 1986) on 8 samples obtained from a 6 m hand auger hole. Samples obtained from the auger hole were also analyzed for particle size distribution (by dry sieve and hydrometer), and water content. For a more accu-

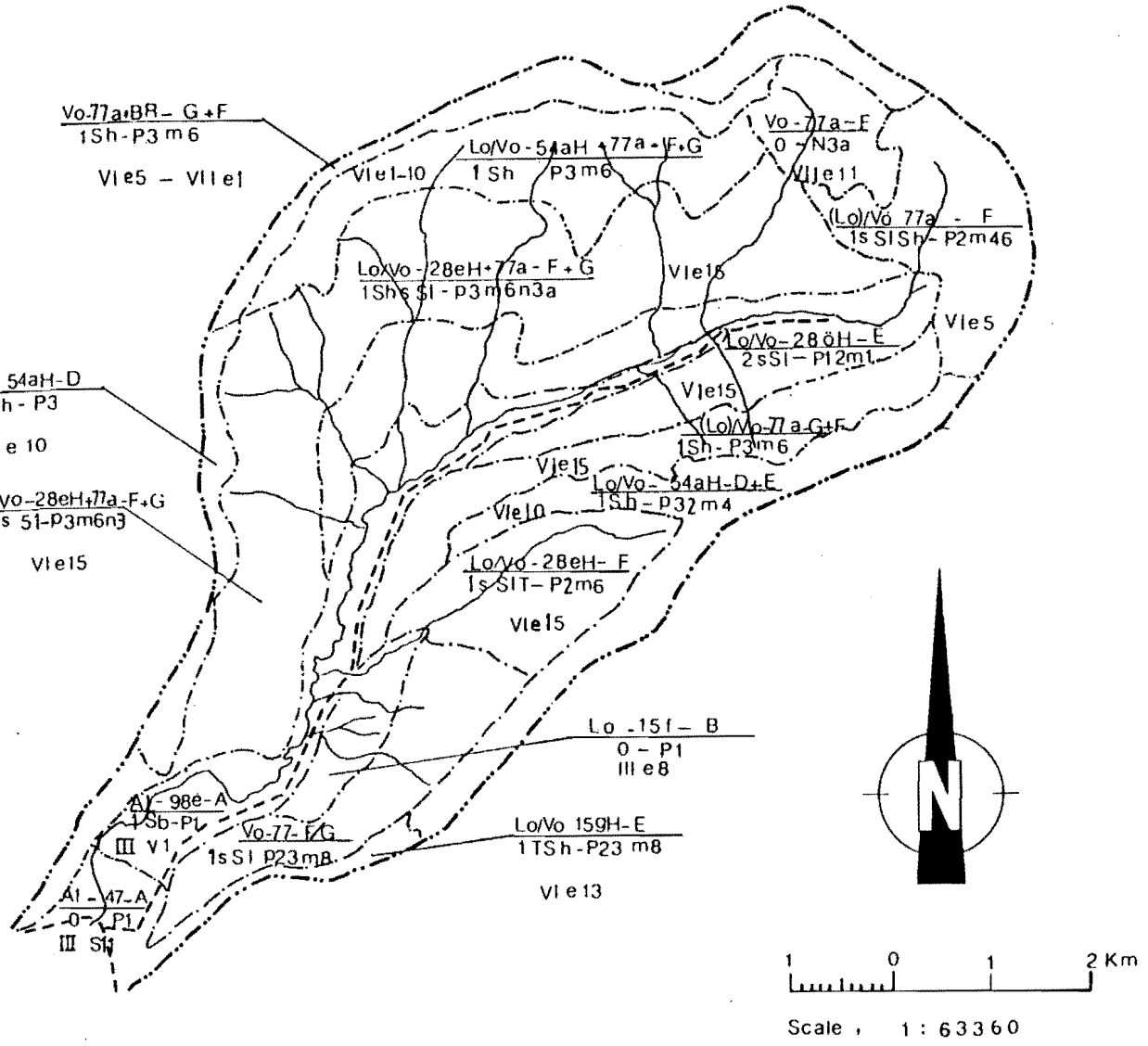

LEGEND

A LAND USE INVENTORY CODE:

Rock type - Soil unit - Slope
Erosion degree . type - Vegetation (Classification in table)

B LAND USE CAPABILITY:

E.G : VIe 15

Class

I	II	Iii	IV	V	VI	VI	VIII
degree of limitation							

Subclass

erosion (e)	wetness (w)	soil (s)	climate (c)
dominant kind of limitation			

Unit

1	2	3	etc
similar management and conservation requirements			

Fig 1.5 LAND USE IN KAITUNA VALLEY
(Based on N.Z Land Resources Inventory Worksheet S84/S94) (NWASCO 1975)

ROCK TYPE

Al	Undifferentiated flood plain alluvium
Vo	Volcanic rock
Lo	loess

SOIL UNIT

15f	TAKAHE (yellow-grey earth)
15gII	TAKAHE - KIWI (same as 15f)
28aII	OKUKU (yellow-grey to yellow-brown earths integra)
28eII	PAWSON (same as 28aII)
47a	KENEPURU (lowland yellow-brown earths)
54aII	BOSSU (Upland and High country yellow-brown earth)
77	EVANS KIWI (brown granular loam and clays)
77a	STEWART SUMMIT (same as 77)
98e	BARRY (recent soils on flood plains)

SLOPE

A	0 - 3
B	4 - 7
C	8 - 15
D	16 - 20
E	21 - 25
F	26 - 35
G	> 35

F + G Compound slopes (first slope dominates)

EROSION

Type	Degree
Sh sheet	0 negligible
sSl soil slip	1 slight
T tunnel gully	
Sb streambank	

Degree of erosion

VEGETATION

Grassland
- P1 High producing pasture
- P2 Low producing or native grassland

Scrubland
- M1 Manuka kanuka
- M4 Fern
- M6 Mixed native scrub assns
- M8 Gorse

Forest
- N3 Podocarp - hardwood
  - (a) Lowland

N.B. Capital letter indicates type of vegetation comprises > 40% of unit area, small letter < 40%.

Table 1.2 Land use inventory code classification (Water and Soil Division, M.W.D. 1979)

Increasing limitation to use ↓

Class	Cropping Suitability	* General Pastoral & Production Forestry Suitability	* General Suitability
I			
II	High		Multiple use of land
III	Medium	High	
IV	Low		
V			
VI		Medium	Pastoral Forestry land
VII	Unsuitable	Low	
VIII		Unsuitable	Catchment protected land

↓ decreasing versatility

* Land use capability classes IV - VII which have wetness as the major limitation and those units in very low rainfall areas or those occurring on shallow soils are normally not suited to production forestry.

Table 1.3 Land use capability classification (Water and Soil Division, M.W.D. 1979)

rate soil description, Atterberg limit tests was also conducted on these samples.

1.8.3 Geophysical investigations

Geophysical downhole logging, electrical resistivity, seismic refraction and seismic reflection were employed for this study.

Downhole logging was carried out using caliper, natural gamma and neutron logging techniques in six boreholes.

A Resistivity survey was undertaken between January 1986 until March 1987, using ABEM DC Terrameter and Terrameter SAS 300 with its Booster. The survey consisted of 42 Schlumberger and 3 Wenner electrical soundings.

Seismic reflection and seismic refraction profiles were conducted using Geophysical Division's SN 338-HR 48 channel recording system mounted in a truck during March and April 1987. Explosive charges, and a minisosie road tamper were used as energy source for the survey(by author, and staff of N.C.C.B and D.S.I.R).

1.8.4 Surface Hydrology

Rainfall monitoring was undertaken using four rainfall gages (circular standard cylinder 20.3 cm in diameter). Rain data for each site was collected on a daily basis (9 am) for a 12 months period (June 1986 -May 1987). Evaporation data was obtained for 12 months using a class A pan evaporimeter.

Stream gauging data was collected using an automatic stage recorder (3m range Foxboro pressure bulb). Measurement of discharge was conducted using a current flow meter (Pygmy current meter).

1.8.5 Groundwater Hydrology

The hydraulic parameter of aquifers were investigated using a pumping test, (step drawdown), slug and free flow tests on seven bore holes Piezometers in eight bores were monitored from June 1986 to May 1987. Water level in bores were monitored using a standard W/A cable electronic probe. Discharge magnitude was monitored on a monthly basis at 27 springs for 12 months (June 1986 - May 1987)(see App.13.1).

1.8.6 Hydrochemistry and Environmental Isotope Studies

Water samples for chemical analysis were collected from a total of five boreholes, three springs and one surface water. Water samples from three boreholes and three springs were forwarded to the Institute of Nuclear Science for analysis of the stable isotope Oxygen-18, and the radio-active isotope Tritium.

1.9 Thesis Organization

The thesis consists of seven chapters. Chapter two present a geological frame work for the valley and its hydrogeological characteristics. In the following chapter application of different geophysical techniques (downhole geophysical logging, resistivity, and seismic refraction and reflection methods) for locating the water bearing potential of valley floor deposits are discussed. Surface and groundwater hydrology components and their interaction are discussed in chapter four and five to develop a water balance and hydrogeological model for the catchment. In chapter six hydrochemistry and isotopic investigation and their application in water quality assessments and groundwater origin are interpreted. The final chapter presents the summary and conclusions of the study.

CHAPTER TWO

HYDROGEOLOGICAL CHARACTERISATION

2.1 Introduction and Objectives

The occurrence and properties of groundwater, its origin, movement, and chemical constituents, are dependent on the geologic framework. The main objective for the following study was therefore to distinguish the most important geological properties (lithology composition, distribution, structure and morphology) which control the water bearing potential of the rocks and sediments within the study area.

The geologic framework in the study area consists of volcanic lava flows, pyroclastic materials, intrusive rocks, regolith deposits and alluvial-coastal sediments.

2.1.1 Lava Flows

Lava flows in the area are related to different volcanics Their composition varies between olivine basalt, olivine hawaiites and hawaiites (Fig 1.3).

Properties of relevance to groundwater storage / migration are discussed below.

1) Flow Thickness and Orientation

Lava flow thickness is irregular, and dependent on distance from the centre of extrusion. Variations in lava thickness are interpreted to be due to the relative proximity of the flows to the eruptive centre. Lava thickness is also controlled by the pre-existing topography on the volcano's flanks. Field data has indicated a maximum thickness of 30 m. and a minimum thickness of 2-3 m for lava flows. The average thickness determined is between 2 and 3 m.

The dip of lava flows was measured at various locations where the top part of the lava was exposed. The value ranges from 6° to 20° toward the south. The average dip for a group of lava flows with similar orientations is shown in Figs 1.6, 1.7.

The gentle dip of lava toward the south is illustrated in Plate 2.1.

2) Flow Morphology

The "aa" type lava flow consists of a basal breccia, a rubbly top, and massive lava in between (Fig. 2.1). A 2-3 m. thick mantle of irregular rubble tops or scoriaceous fragments develop autoclastically by breakup of the solidified crust of the flow during movement. Slabs formed on the steep toe of the active flow fall to the ground, where they form a carpet of rubble over which the flow subsequently advances. These basal breccias are generally thin and less continuous (Plate 2.2) than the brecciated tops, whilst the brecciated lava grades into more massive lava in the center.

3) Jointing

Joint structure is controlled by the flow thickness and the distance from chilled flow margins. The joint density increases toward the margins and spacing, persistence, and aperture of the joints changes rapidly within the same flow. Additionally, from field observations, the different types of volcanics in the valley appear to cause an irregular jointing pattern within the valley. However, in general terms, two sets of joints are dominant in each lava flow, one set approximately normal to the lava flow direction (columnar jointing, Plates 2.3, 2.4,2.5) and the other roughly parallel to it (Plate 2.6). During formation of a lava flow, the movement of the base of the flow is decreased by friction against the underlying ground, and the moving liquid higher up tends to separate into a series of joints parallel to the top and bottom of the flow (parallel joints). In the study area these joints vary in orientation for different lava flows.

As the lava cools it shrinks, and this results in tensional stress, which in turn cause the rock to fissure. Some of the joints thus formed are approximately at right angles to the cooling surface (vertical or columnar jointing). This set of joints are more pronounced in the study area. In the study area, joint spacing for the vertical set averages about 40 cm, but varies between 0.01 m. and 4 m. Joint width is approximately 3 cm, but is reduced in some cases due to weathering and infilling by secondary minerals such as calcite.

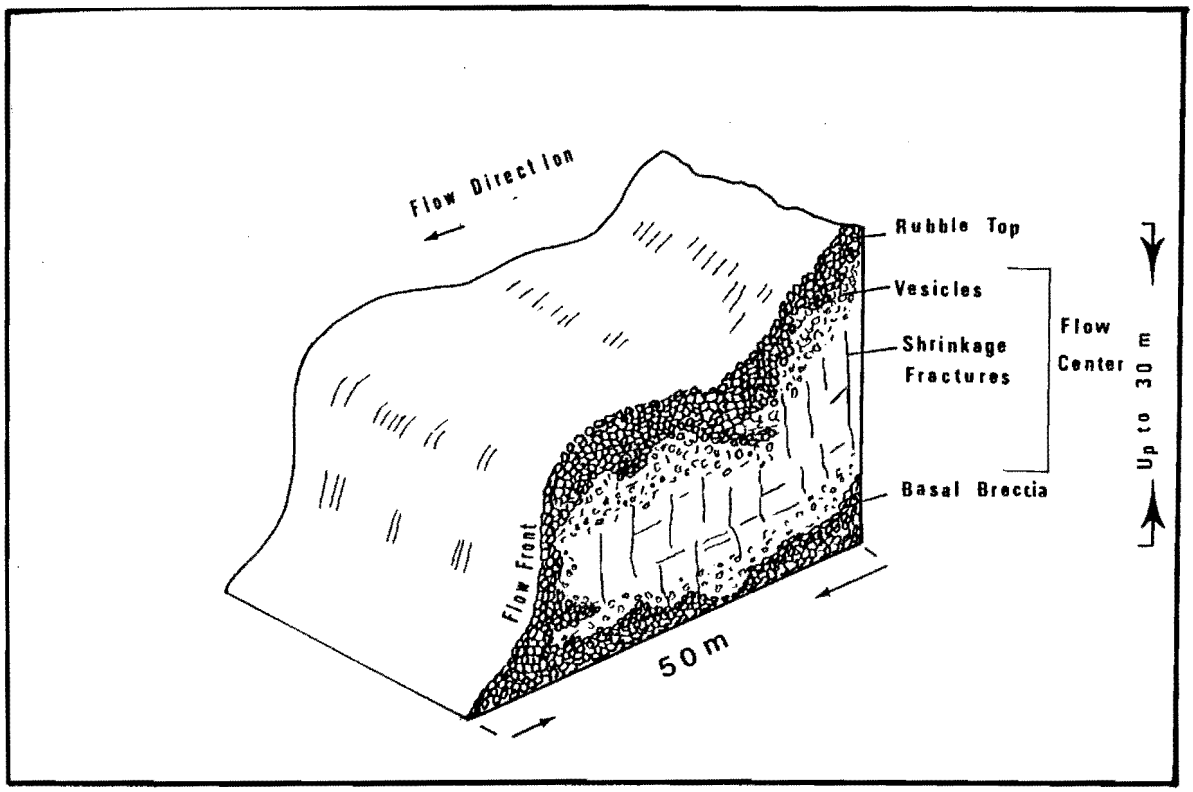

Figure 2.1 aa Lava Flow Morphology

Plate 2.1 The gentle dip of the lava flows towards the south. (G.R. 842 171).

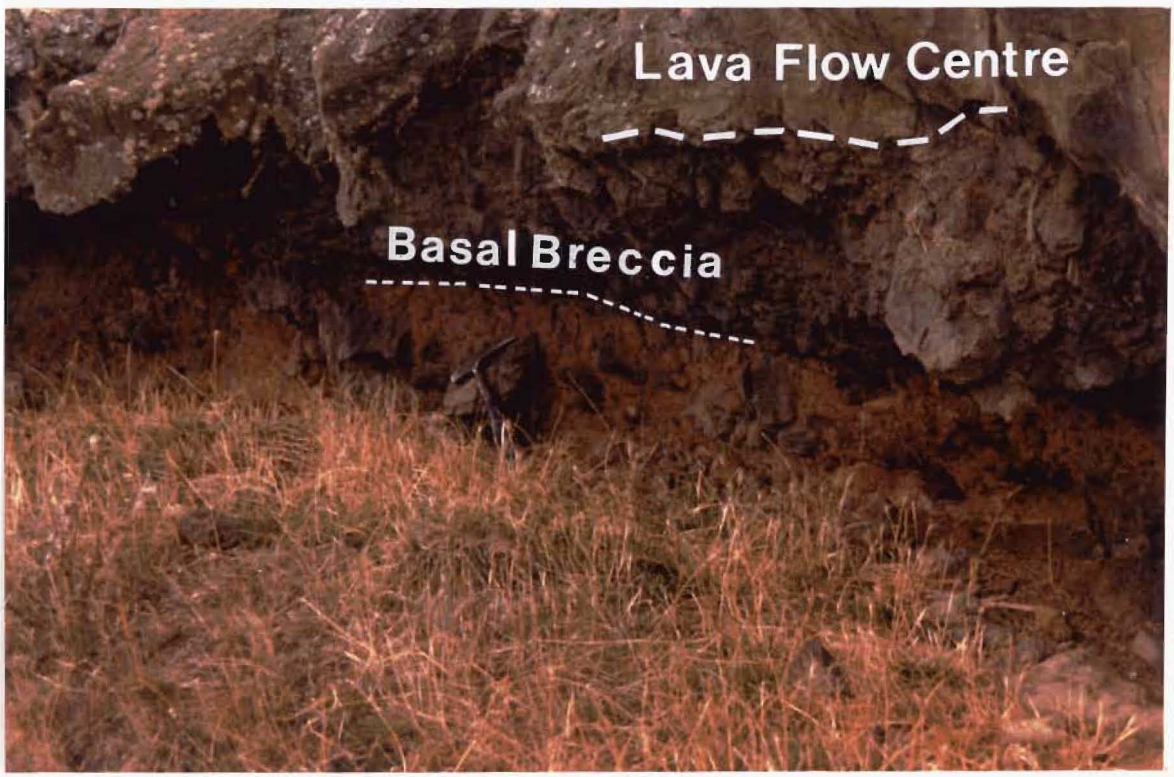

Plate 2.2 Contact between lava flow, basal breccia and ash layer. (G.R. 828 146).

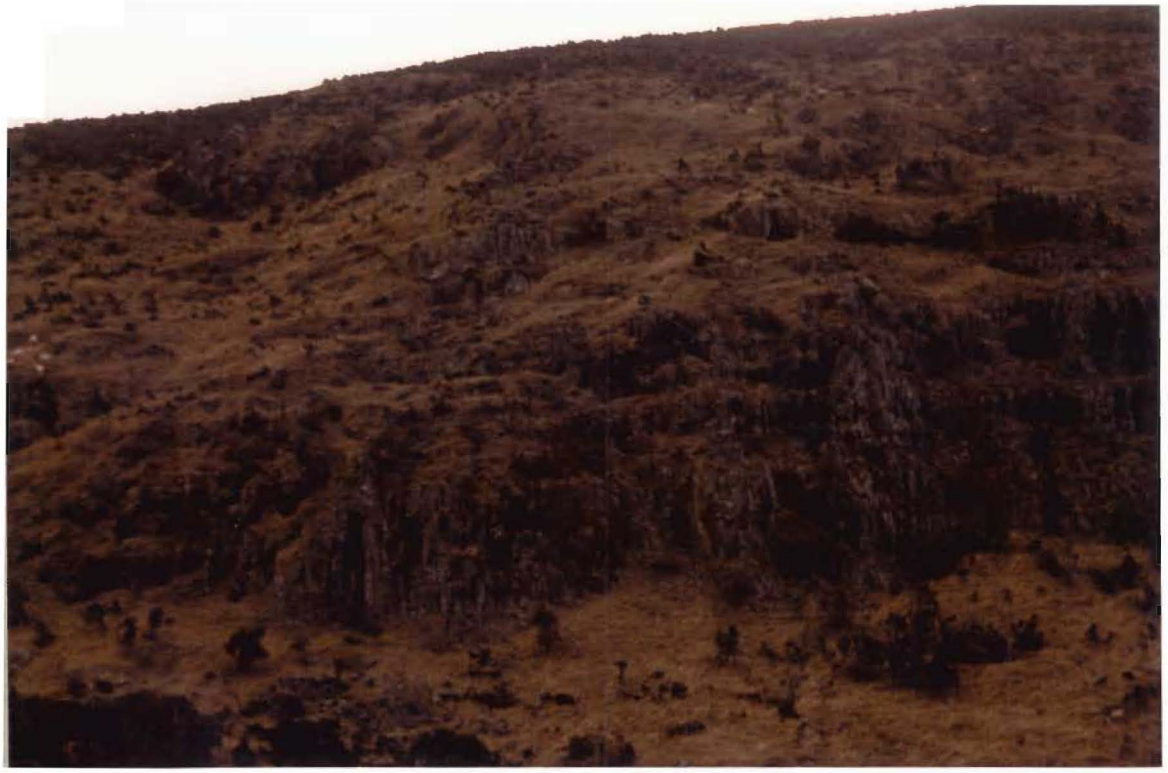

Plate 2.3 Lava Flows with Columnar Joints. (G.R. 843 168)

Plate 2.4 Columnar Joints. (G.R. 842 166)

Plate 2.5 Joints parallel to the lava flow (Parallel joints) (G.R 884 221).

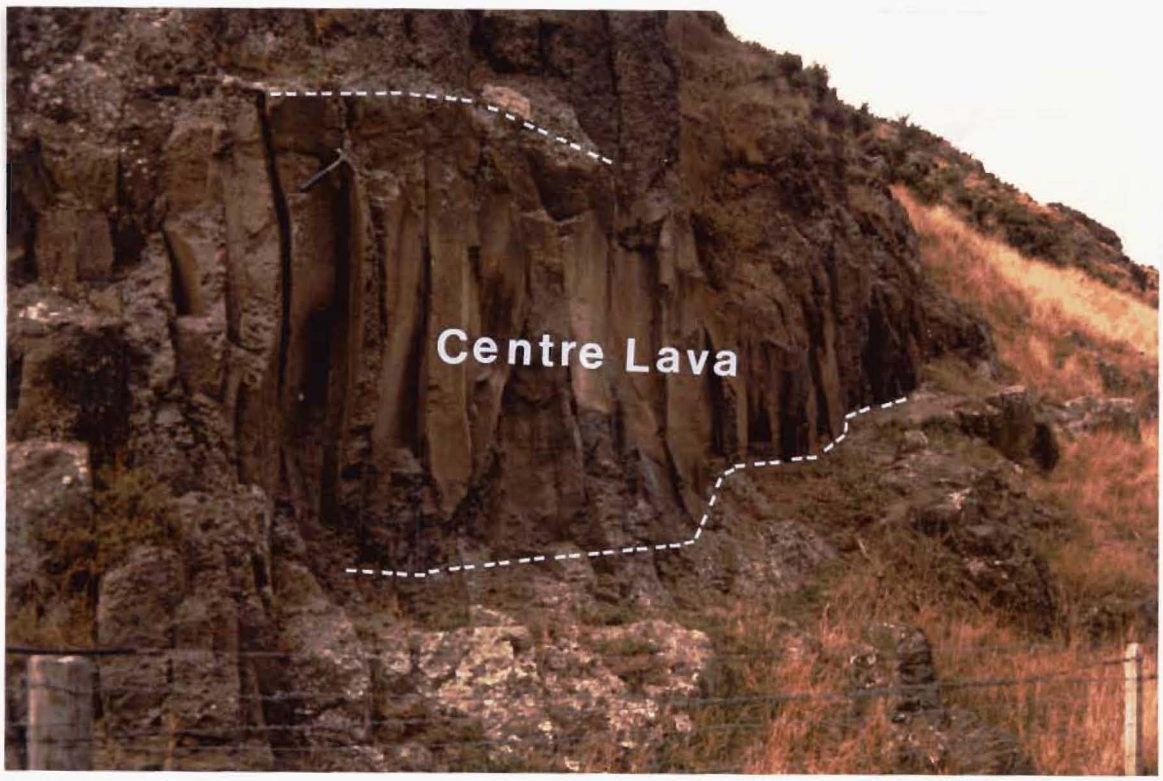

Plate 2.6 Columnar joints and contact between centre lava and brecciated lava. (G.R 841 166).

4) Vesicularity

Vesicles produced by bubbles of gas trapped during the solidification of the lava are occasionally infilled with secondary minerals. If solidification is very slow, all the gas bubbles may escape, leaving the solidified rock dense, but if cooling is rapid, the liquid freezes with the gas bubbles still in it and the rock will be highly vesicular. In the area thin (2 - 3 m) lava flows, and the top and bottom of flows are generally vesicular The vesicles generally have a diameter of less than 1 cm.

2.1.2 Pyroclastic Materials and Intrusive rocks

Accumulations of rock fragments thrown out by volcanic explosions occur throughout the study area. Unconsolidated ash deposits are known as ash layers, ash beds, or ash blankets, while consolidated ash deposits are called tuff. These materials are typically reddish in colour (Plate 2.7) with an average clast size between 1/256 and 2 mm (Sewell, 1985). Some graded bedding is observed within crystal tuff deposits. Tuffs are generally present as thin discontinuous beds of irregular thickness (1 - 3 m.), which pinch out locally). Volcanic agglomerates (average clast size 64 mm), have also been found in the study area. These are present in thicknesses of up to 150 m. (GR M36 885 222, Plate 2.8) Clasts are supported by a matrix of tuffaceous medium sand.

Intrusive rocks in the valley are mainly trachytic and mugearitic. There are also two trachytic domes in the valley. Both domes are weathered with a poorly developed columnar - jointing.

2.2 Water - Bearing Properties of Rock Mass

2.2.1 Rock Mass Model

Hydrogeological properties of rock mass including lava flows, pyroclastics, and intrusive rocks, together with their rock engineering geological descriptions (App. 2) are presented in Table 2.1.

The proposed model is illustrated in Table 2.1. The most suitable medium for water movement within the rocks in the Kaituna valley is considered to be a lava flow with a joint spacing of up to 200 mm. The main perching layer within the rock mass is ash and tuff (average clast size

Plate 2.7 Ash Layer below Brecciated Lava. (Clast Size between 1/256 to 2 mm) (G.R. 856 174)

Plate 2.8 Volcanic Agglomerates (Average Clast Size 64 mm) (G.R. 885 222).

DIAGRAM SHOWING VOLCANIC & INTRUSIVE ROCKS	ENGINEERING GEOLOGICAL DESCRIPTION	HYDROGEOLOGICAL PROPERTIES
LAVA FLOW 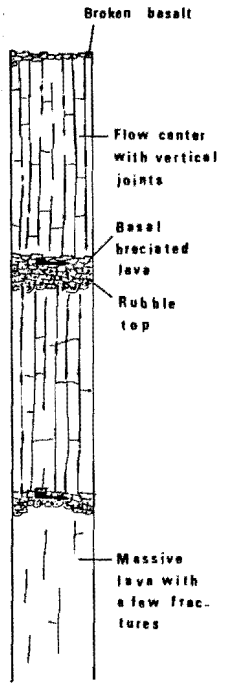	Flow centre slightly to highly weathered, moderately strong to very strong, light to dark grey. medium to finely crystalline Basalt to trachytic rock, often vesicular. - jointing is irregular, however 2 joint sets are dominant. Spacing : <15 to 200cm Aperture: tight to <200cm Average unit block size; medium to large (10 to 100 cm). Rubbly top: slightly to highly weathered basaltic clasts (boulder size), in matrix of slightly to highly weathered, soft to hard light to dark mixture of silt to gravel fragments of basaltic composition. Basal Dreciated Lava: unweathered to slightly weathered, strong, dark grey, clasts of Basalt Trachyte (up to boulder size), with insignificant matrix.	- highly fractured lava is the main medium for vertical water flow. - massive lava with a few shrinkage fracture is a barrier to vertical water movement. - highly weathered lava flow acts as a perching layer, due to a reduction in void ratio. - highly weathered rubbly lava (at top) acts as a perching layer. - slightly weathered rubble lava allows horizontal water flow. - the most suitable zone for horizontal water movement.
PYROCLASTICS 	Ash and Tuff: slightly to highly weathered, moderately weak to moderately strong, light to dark red, massive to finely layerd basaltic tuff and ash. Volcanic Brecia: slightly to highly weathered, moderately weak to moderately strong, grey clasts of Basalt and Trachyte (1-50cm), in a slightly to highly weathered, weak to moderately strong, grey to greyish red, medium massive sandy tuffaceous matrix	- impermeable, and the main barrier for vertical water flow. - barrier for vertical water flow due to its massive and unjointed nature.
INTRUSIVES 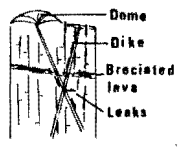	Dikes and Domes: slightly to moderately weathered, strong to very strong, greyish massive Trachytic to basanitic domes and dikes	- barrier for vertical and horizontal water flow due to its massive and unjointed nature.

Table 2.1 Engineering Geological Description and Hydrogeological Properties of Rock Mass

between 1/256 mm and 2 mm.

2.2.2 Water Movement in Lava Flows

Two components of water flow through lava flows have been identified and are discussed in the following sections.

1) Horizontal (Lateral)

The horizontal water flow is a downward movement due to the gentle southward dip of the lava flow (6°- 20°). The basal breccias, rubbly tops, horizontal joints of the lava flows are identified as the main zones of horizontal groundwater flow (Plate 2.9).

Since the horizontal flow path occurs through a layer which was formed contemporaneously with the lava flow, horizontal water flow is considered to be a function of the primary permeability of the rock mass.

The basal breccias have a better potential for groundwater flow than the rubbly top layers since they have been less affected by erosional processes. Erosional processes will tend to reduce the permeability of the rubbly top in the time gap which is present between the formation of succeeding lava flows. Horizontal water flow will depend on any difference in horizontal conductivity between the brecciated lava and underlying layers. Maximum horizontal flow will occur where a perching layer such as tuff underlies the brecciated lava. In the absence of a coherent perching layer, water will percolate to deeper layers through vertical shrinkage joints.

2) Vertical

Vertical shrinkage cracks are the main path for vertical flow of water. Since the joints developed after the formation of the rock mass, this type of flow is due to secondary permeability within the rock mass.

Freeze and Cherry (1979) give a permeability value of up to 10^2 m/s for a jointed lava flow. It was observed in the field that columnar jointed lavas in summit region (Plate 2.10) can absorb all rainfall water with no surplus run off. In contrast, massive and unjointed flows have no potential as a medium for vertical water flow.

Plate 2.9 Horizontal Jointed Lava Flow (Media for Horizontal Water Movement). (G.R. 836 187)

Plate 2.10 Columnar Jointed Lava at Summit (Media for Vertical Water Flow). (G.R. 835 198)

2.2.3 Water Movement in Pyroclastic Materials and Intrusive Rocks

Loose and coarser pyroclastic materials are highly permeable, however permeability is reduced with compaction and weathering (deposition of secondary minerals). Compacted and impermeable tuffs between lava flows (Plate 2.7) divide the volcanic terrain into a number of groundwater compartments.

Intrusive rocks (domes and dikes) act mainly as a barrier to lateral water flow. Joints and shrinkage cracks are generally tighter in these rocks, and the vertical flow path is greatly reduced.

2.3 Regolith Materials.

2.3.1 Types

The regolith materials on Bank peninsula can be divided into the following categories (Bell and Trangmar, 1987):

1) in situ primary airfall loess;
2) loess colluvium;
3) mixed deposits of loess and volcanic colluvium;
4) volcanic colluvium; and
5) residual regolith.

The main element used in this classification is the presence or absence of a loessial component.

A general relationship between landform and regolith type is shown in Fig. 2.2. This model is generally appropriate for Kaituna Valley. The engineering geological description of the regolith deposits in the study area is shown in Table. 2.2.

2.3.2 In Situ Primary Airfall Loess and Loess Colluvium

1) Composition and Occurrence

The in situ loess of the Kaituna Valley is mainly related to the Barry Bay Loess and its eroded phase. The Barry Bay loess is mainly

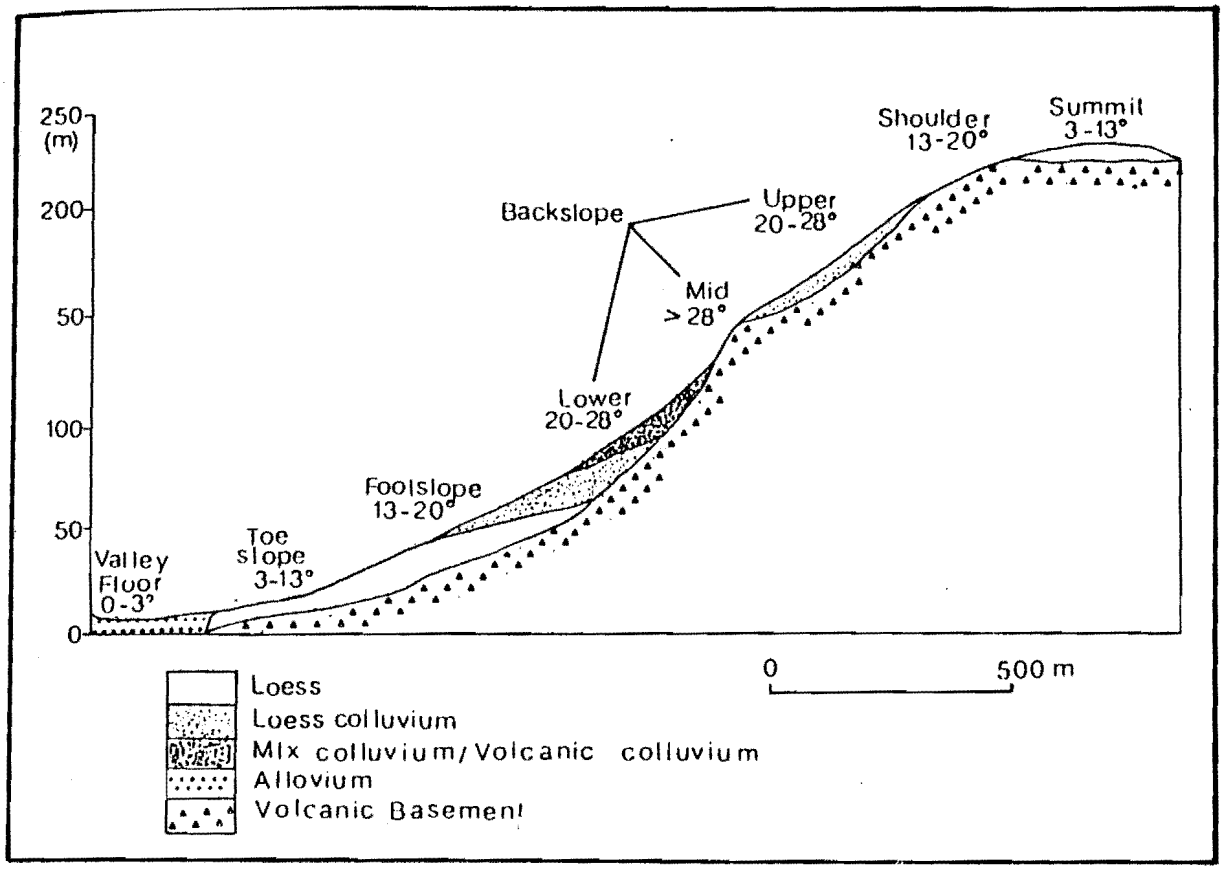

Figure 2.2: A general relationship between landform and regolith (modified for Kaituna Valley), after Bell and Trangmar, 1987.

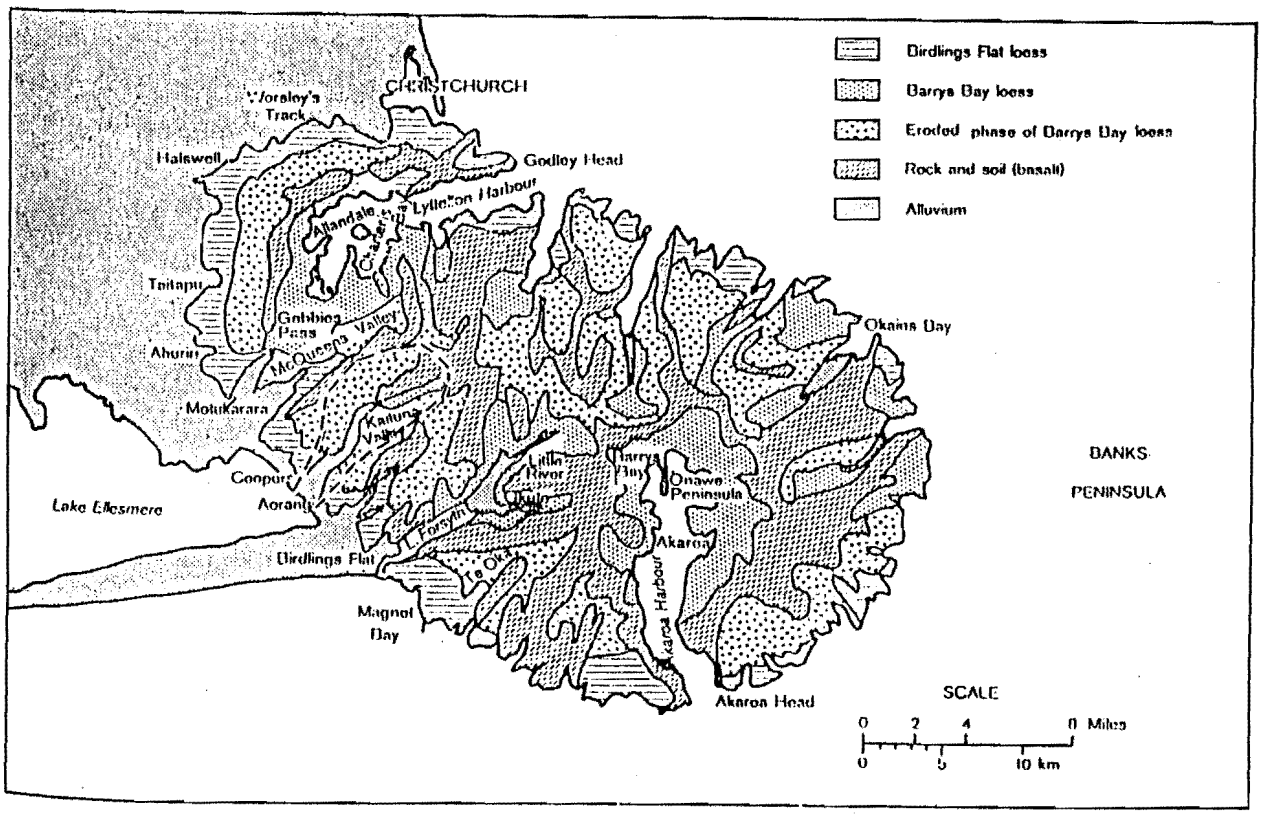

Figure 2.3: Distribution of loess on Banks Peninsula (after Griffiths, 1973).

DIAGRAM SHOWING REGOLITH MATERIALS & WATER FLOW	ENGINEERING GEOLOGICAL FIELD DESCRIPTION	HYDROGEOLOGICAL PROPERTIES
IN SITU LOESS L 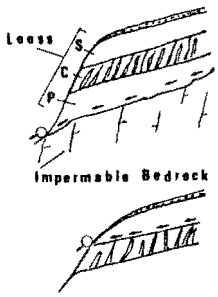	unweathered to slightly weathered, dry to moist, fine to stiff light olive brown (Birdlings Flat & light yellowish brown (Barrys Bay). Lighter concretions and orange mottling due to burrowing massive clayey silt with some sand (at lower elevations). ML.	- low infiltration potential. - common media for water flow are; S layer, where it overlies C layer fragepan and P layer, overling impermeable bedrock
LOESS COLLUVIUM L.C 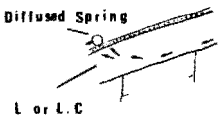	slightly to moderately, weathered, dry to moist, firm, light yellowish brown, or dark brown, massive, silt with some clay, sand, and gravel, ML.	-slightly higher infiltration potential than in situ loess (up to 10% volcanic fragments.
Mixed Colluvium M.C 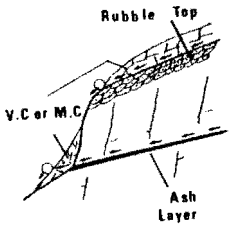	Moderately weathered, dry to moist, firm, dark brown to yellowish brown, massive gravelly clay and silt with some fine coarse gravel, and sand, M.L.	- Higher potential as an infiltration media than loess and loess colluvium (10 to 90% volcanic fragments.)
Volcanic Colluvium V.C	Moderately to highly weathered, dry to saturated, soft to hard, dark reddish brown, silty gravel (fine to coarse) and clay with some sand, GP.	- the best medium for infiltration among the regolith deposits (more than 90% volcanic fragments).

Table 2.2 Engineering Geological Field Description and Hydrogeological Properties of Regolith Materials.

classified as silty loam, with some fine sandy loam at lower altitudes (Bell and Trangmar, 1987). In the lower part of the Valley (Fig 2.3) the loess is part of the Birdling Flat Loess; a calcareous, fine sandy loam. Calcareous concretion are scattered throughout the deposits. The lime has been deposited by seepage around a central core, for example a root, a fragment of rock or soil, or a even a moa bone (Griffiths, 1973). The lime cements the fine silts into sand-sized particles, resulting in an overall increase in porosity (Birrel & Packard, 1953). Salts found in the Birdling Flat Loess include calcium sulphate, calcium chloride, calcium carbonate and sodium sulphate and chloride. Layering in loess colluvium and in situ Loess is illustrated in Fig. 2.4. In the study area the layering is variable and generally discontinuous. The discontinuous nature of the layering is thought to be due to erosion during deposition, and post-Pleistocene slope processes (Griffiths, 1973).

Loess colluvium is mainly composed of quartzo-feldspatic silts and fine sands. It may contain up to 10% volcanic fragments (Plate 2.12) which range in size from pebbles to boulders (Bell & Trangmar 1987). The percentage of volcanic components increases toward the bedrock, where it grades into mixed colluvium and then into volcanic colluvium.

The Birdling Flat loess - colluvium is highly dispersive. It shows distinct and discontinuous layering, related to a series of depositional events and post-glacial soil formation. Birdling Flat Loess covers the bottom part of the valley (Fig. 2.3). Thickness is up to 16 m but decreases with increasing altitude (Plate 2.11).

Barry Bay Loess covers the valley heads and summits of the valley in more humid climatic areas.

In general, in situ loess is thicker at the summit and becomes thinner at the slope shoulders and the footslopes while loess colluvium is more apparent at the shoulders, backslope, footslope and topslopes (Fig. 2.2). Loess colluvium is thickest on accumulative footslopes, where it is layered and covers the in situ loess.

2) Origin and Distribution

Silt-size materials were formed by glacial grinding action during the Pleistocene. They initially accumulated on the fluvio-glacial outwash fan surfaces, and were then transported by north westerly winds and deposited as a blanket on the eroded flanks of Banks Peninsula and the

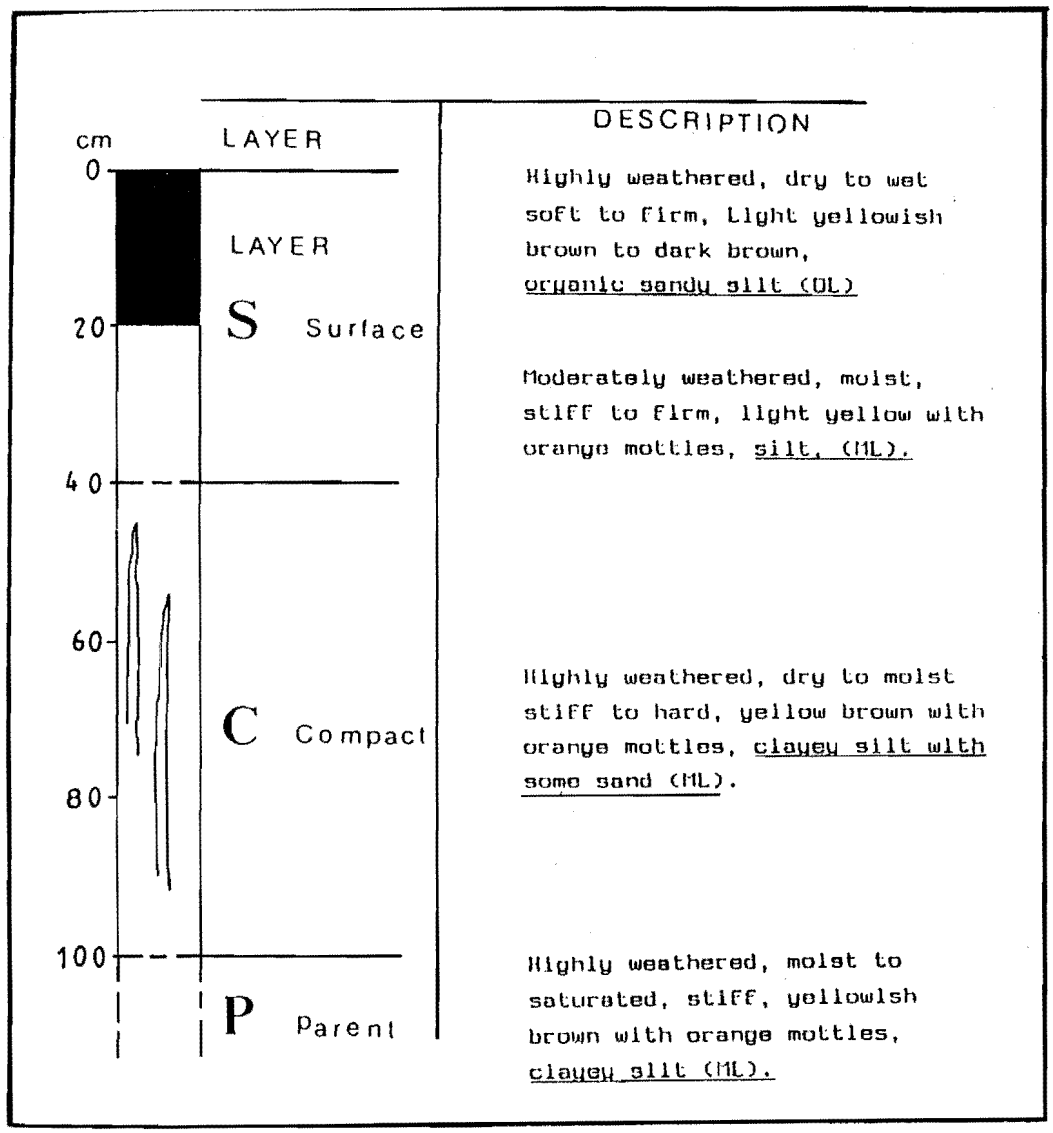

Note: Description guideline is presented in App. 2.2

Fig. 2.4 Layering in In Situ Loess and their general descriptions.

Plate 2.11 Birdlings Flat loess cover at the bottom part of the valley (G.R. 830 149).

Plate 2.12 Loess colluvium contains up to 10% volcanic fragments (which range in size from pebble to boulder) (G.R. 857 176).

Canterbury Plains (Griffiths, 1973).

Loess colluvium is a result of down slope transportation of in situ loess by freeze-thaw induced mass movement during cold-climatic episodes in the Pleistocene.

2.3.3 Mixed colluvium

Mixed colluvium consists of loess intermixed with weathering products derived from the volcanic rocks that outcrop upslope (Bell and Trangmar,1987). The ratio of loess (or loess colluvium) to volcanic fragments ranges from 10% to 90%, therefore the morphology of mixed colluvium is highly variable. Colour ranges from dark brown to yellowish brown, depending on the volcanic fragment/loess ratio. The size of the volcanic fragments range from sand to boulder, decreasing with increasing distance from the outcrop.

Mixed colluvium is traced on backslopes and upper footslopes below outcrops of volcanic rocks (Fig. 2.2). It may overlie in situ loess, older colluvium or bedrock. The thickness of mixed colluvium in Kaituna Valley varies between 0.4 - 2.8 m.

2.3.4 Volcanic Colluvium and Residual Regoliths

1) Volcanic Colluvium

Volcanic colluvium consists of weakly to moderately weathered volcanic rock fragments held in a matrix of highly weathered fines derived from volcanic bedrock, and mixed with a small amount (<10%) of loess materials (Bell & Trangmar, 1987). The size of the fragments varies from fine grit to boulder, with larger fragments found near the outcrops (Plate 2.13) Colour ranges from reddish brown to light brown, depending on the volcanic rock/loess ratio.

Volcanic colluvium is found mainly on the moderately steep mid backslopes immediately below the outcrop. The thickness is extremely variable, reaching a maximum of 1.2 m. and thinning away from the outcrops.

2) Residual Regoliths

Residual regoliths are formed from the in situ weathering of vol-

canic bedrock (Plate 2.14) They contain 5-20% slightly to highly weathered, subangular volcanic fragments in a matrix of reddish brown silty clay loam or clay loam.

Residual Regoliths are found on low angle slopes (3° - 20°) at high altitudes where a lava flow ends, or where lava flows of different resistance to weathering are exposed. The thickness of residual regoliths is usually less than 0.9m. These materials are mapped together with volcanic colluvium, since their infiltration properties are similar.

2.3.5 Water-Bearing Properties of the Regolith materials

Hydraulic conductivity in regolith materials increases with increasing volcanic fragments and decreasing loess component. This is due to a change in composition. An increase in volcanic fragments from 0% in loess (silt size material) to 90% in volcanic colluvium will result in increased permeability, and therefore infiltration potential. This has been documented previously by Bell & Trangmar (1987), and Sanders (1986).

1) In situ loess and Loess-Colluvium

Water flow in in situ loess may occur: 1) at the loess-bedrock interface within the P layer, by percolating through dessication cracks of the C layer fragipan or infiltrating through the loess-bedrock interface, 2) above the C layer fragipan,- where this is developed (Table 2.2).

Loess colluvium has a lower bulk density and a greater permeability than in situ loess (Bell - Trangmar, 1987). Layering within the loess colluvium displays differences in permeability, moisture retention, density, texture dispersion, and strength. Contacts between these layers therefore provide suitable subsurface water flow paths, and water flow within more dispersive layers has resulted in the formation of tunnel gullies (Fig. 1.6 and 1.7).

2) Mixed Colluvium

Mixed colluvium may directly overlie in situ loess, older colluvium or bedrock. Where the underlying layer is firm and massive (eg. in situ loess), water which has percolated through the mixed colluvium flows

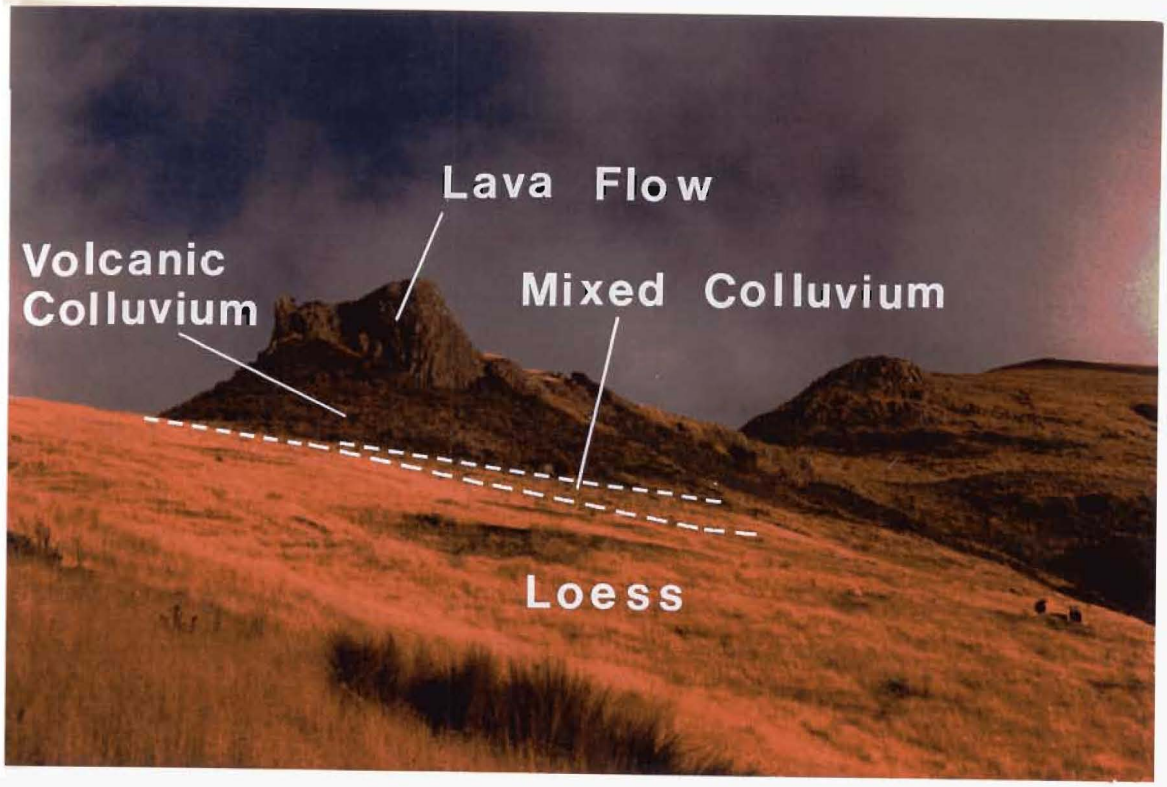

Plate 2.13 Volcanic colluvium forming apron below lava flow outcrop. Also note contact between loess and mixed colluvium at the base of the apron (G.R. 885 205).

Plate 2.14 Residual regolith formed as a result of insitu weathering of volcanic bedrock (G.R. 885 205).

along the interface. In general with an increasing ratio of volcanic fragments/loess, the permeability of the mixed colluvium increases.

3) Volcanic Colluvium and Residual Regoliths

The composition of the volcanic colluvium (poorly sorted volcanic fragment with less than 10% loess), makes it the most suitable medium for water flow among regoliths. Its distribution in Kaituna valley is shown in Figs 1.6 and 1.7. The water flow path is often close to the bedrock interface (Table 2.2). This became evident by observing the disappearance of springs over volcanic colluvium and their reappearance at lower elevations).

Rock flows (free-falling rocks under gravity downward and usually outwards from the source) have been associated with the seepage zone in these units.

2.4 Alluvial and Coastal Sediments

2.4.1 Description

The following discussion is based on information obtained from logged drillholes (Fig. 2.5). Valley floor deposits, and their hydrogeological characteristics will be discussed in detail in Chapters 3 and 5.

Alluvial-coastal sediments in the Kaituna valley floor consist of a wedge of sediments resting on a lakeward inclined surface of the volcanic basement (Fig. 1.7).

Valley floor sediments are composed of clastic materials varying greatly in size and degree of sorting. Both marine and terrestrial materials have been deposited in the valley, and these consist of poorly sorted volcanic rubble, beach gravels, fine grained lagoonal muds and clays (Talbot and Callander, 1986), and terrestrial gravel, silt, clay, and sandy silt (rewashed loess and loess colluvium).

After formation of the volcanic terrain and development of the drainage system within the valley, the steep and unvegetated valley sides were extensively eroded. This resulted in the formation of a poorly sorted volcanic rubble of irregular thickness found on top of the volcanic bedrock (Fig. 2.5).

During periods of high sea level, weathered volcanic fragments were covered by beach gravel and lagoonal muds and clays (with some wood

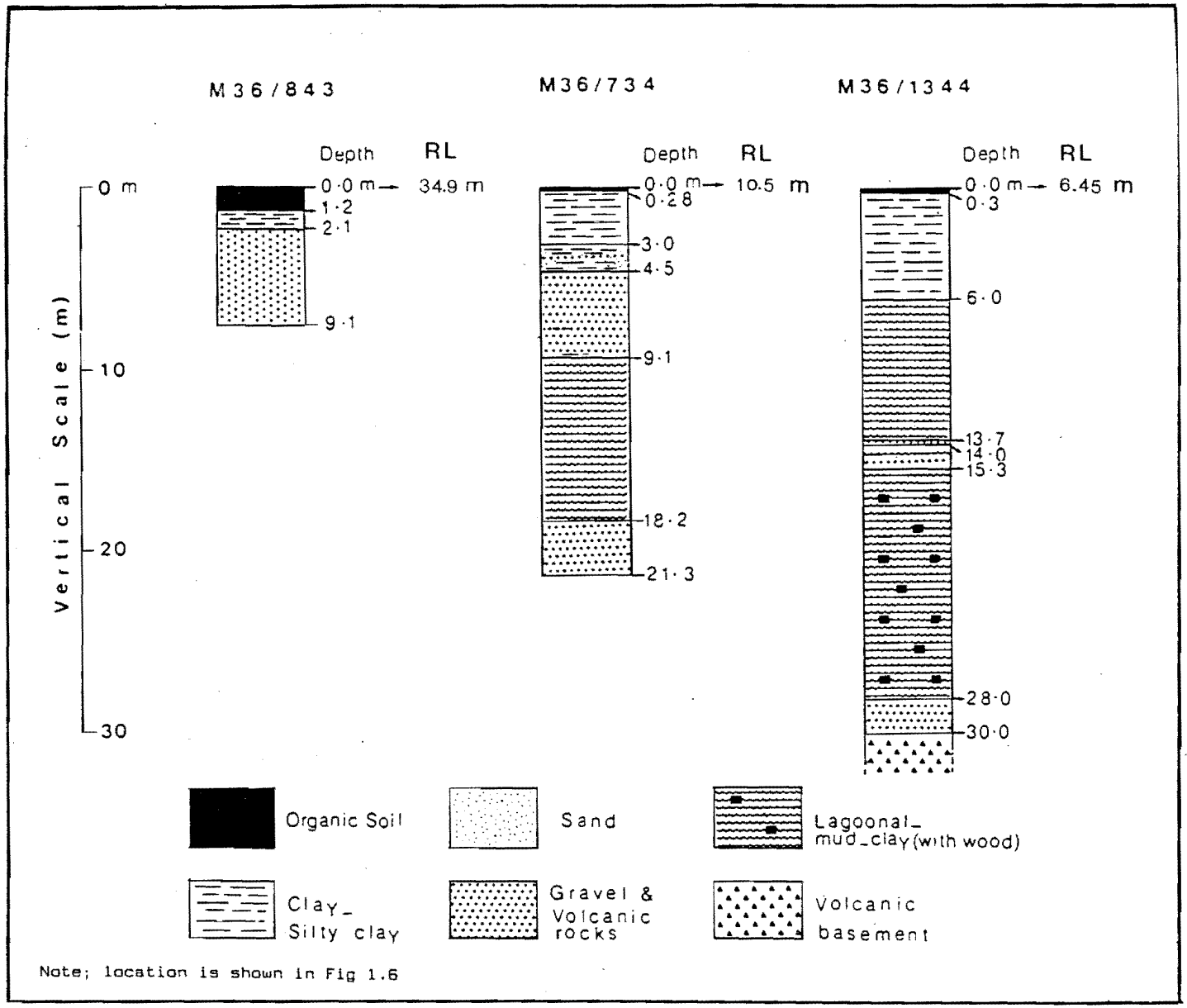

Figure 2.5 Summary Lithological Logs for Three Wells

remnants). The marine sediments were later overlain by terrestrial clay and gravel lenses when sea level was close to its present day position. The top part of the alluvium (especially the modern flood plain) is covered by silt and sandy silt which are sourced from rewashed loess and loess colluvium.

The alternating sequence of marine and terrestrial sediments within the area is related to transgressions and regressions during the Pleistocene. During the full glacial conditions in the Southern Alps (15,000 years ago), sea level was approximately 130 m lower than at present. Then in the early post - glacial (10,000 years ago), sea level was about 20 m lower than now, but rising (during this time a shallow strait existing between the alluvial fan belonging to the Rakaia and Waimakariri rivers, and Banks Peninsula). In the mid post-glacial period (6000 to 4000 years ago), there was a continuing rise in sea level to 3 m above present level. At the beginning of this period the Kaituna Valley was a bay open to the sea. Finally from the late post-glacial (2000 years ago), sea level started falling to the present mean sea level (Palmer, 1982).

2.4.2 Water-Bearing Properties of the Alluvium (at Shallow Depths)

The top six metres of the alluvium were investigated by laboratory permeability, grain size, and water content analysis of the different layers found within a six metre deep auger hole (AH1, in Fig. 1.6). This data, and an engineering geological field description, is presented in Table 2.3.

Permeability tests revealed that the silty layers which cover the top part of the alluvial plain have a very low (App.3.2) hydraulic conductivity (Table 2.3). All samples were well sorted (App. 4), except a silty sand layer between 2.65 and 2.85 m. This sample is composed of 54.07% sand, 40.63% silt and 4.3% clay. The water table was measured at a depth of 5 m. in the augerhole, and laboratory measurements of water content increase toward this depth. Depth to water table varies between 0 (Spring A1, Fig. 1.6) and 5 m (augerhole AH1). Using auger holes at different locations, the average depth to the water table was found to be between 1 and 3 m, decreasing toward the main stream (Kaituna).

The terrestrial sediments formed within or close to river channels are found to be more coarse-grained (sand and gravel) than those deposited on the flood plain (using auger holes).

Sampl No.	Water Content	Permeability m/sec	Textural Terms (Folf 1968)	Depth (cm)	Eng.Geological Field description
				0	
					highly weathered, soft, moist, dark brown, highly organic soil (PT).
				20	
		-7			slightly weathered, soft, moist, dark
A	27%	3.8 . 10	SILT		greyish brown with
			silt=85.7%		orange mottles, silt
			clay=7.25%		with some sand and
			sand=5%		clay (OL).
				70	
					moderately weathered,
		-8			soft, dry, light
B	0%	6.4 . 10	SANDY SILT		greyish brown with
			silt=71%		orange mottles,
			sand=18%		sandy silt with some
			clay=9%		clay (ML).
				150	
					moderately weathered,
		-8			soft, dry, light
C	11%	1.15 . 10	SANDY SILT		yellowish brown with
			silt=68%		orange mottles,
			sand=23%		sandy silt with some
			clay=7%		clay (ML).
				190	
					moderately weathered,
		-7			soft, dry, light
D	11%	6.23 . 10	SANDY SILT		whitish yellow with
			silt=80.48%		orange mottles,
			sand=14%		sandy silt with some
			clay=3.52%		clay (ML).
				265	
		-6			moderately weathered,
E	17%	1.13 . 10	SILTY SAND		soft, wet, dark
			sand=54.07%		greyish brown, silty
			silt=40.63%		sand with some clay
			clay=4.3%		(SM).
				287	
					slightly weathered,
		-8			soft, wet, dark
F	30%	2.26 . 10	SILT		yellowish brown with
			silt=90.5%		a few orang mottles,
			clay=7.5%		silt with some sand
			sand=2%		and clay (CL).
				300	
		-7			slightly weathered,
G	37%	2.4 . 10	SILT		soft, wet, dark
			silt=80.3%		bluish grey, silt
			sand=10%		with some sand and
			clay=7.70%		clay (CL).
				510	
					moderately weathered,
					soft, saturated,
		-7			dark yellowish grey
H	34%	1.55 . 10	SANDY SILT		with orange mottles,
			silt=69%		sandy silt with some
			sand=18%		clay (CL).
			clay=11%	600	

Table2.3 Engineering Geological Field description and Laboratory Permeability, Grain size, Water content tests on samples from Auger Hole AH1

App.4.3

The boundary of alluvial sediments are defined in Fig. 1.6 and 1.8. Between GR M36 894 211 and GR M36 900 210, the stream flow occurs on volcanic bedrock (Plate 2.19) and volcanic colluvium where leakage from the stream is highly probable.

The alluvial sediment overlies a sequence of marine muds, clays, and gravelly layers (Fig. 2.5). Their boundary and hydrogeological characteristics are discussed in the Chapters 3 and 5.

2.5 Springs

2.5.1 Springs Model

The following model is based on geological study and field observation. Impermeable and compacted layers such as tuff, occurring between lava flows and impermeable subvertical dikes divide the volcanic terrain into a number of "groundwater compartments", each with its own water level and its own outlet. This outlet flows either into an adjacent lower compartment, or into a spring which may be from bedrock or through the surficial deposits (Fig. 2.6).

2.5.2 Spring Outlet Morphology

Springs with confined flow (obvious outlet) are observed where the outlet is from a highly permeable layer such as an extensively fractured lava, brecciate lava, or volcanic colluvium (Plate 2.15).

Diffused springs are those which have their outlet through loess, loess colluvium, mixed colluvium, or alluvium, both of which have low permeability. As a result, discharge occurs over a large area (eg. 10 m^2 for spring A1 in alluvium), and the original spring outlet is difficult to detect. These can be located by the presence of special vegetation (eg. Rushes or Carex Species), which occur more commonly in wet grounds a diffuse spring from loess is shown in Plate 2.16.

2.5.3 Spring Distribution

Springs in the area generally occur in clusters, either from the same or several lava flows close together, where they overlie impermeable layers (eg. tuffs). Groundwater outlets can occur where regolith is thin over the scarp edge of the lava flow (Table 2.2).

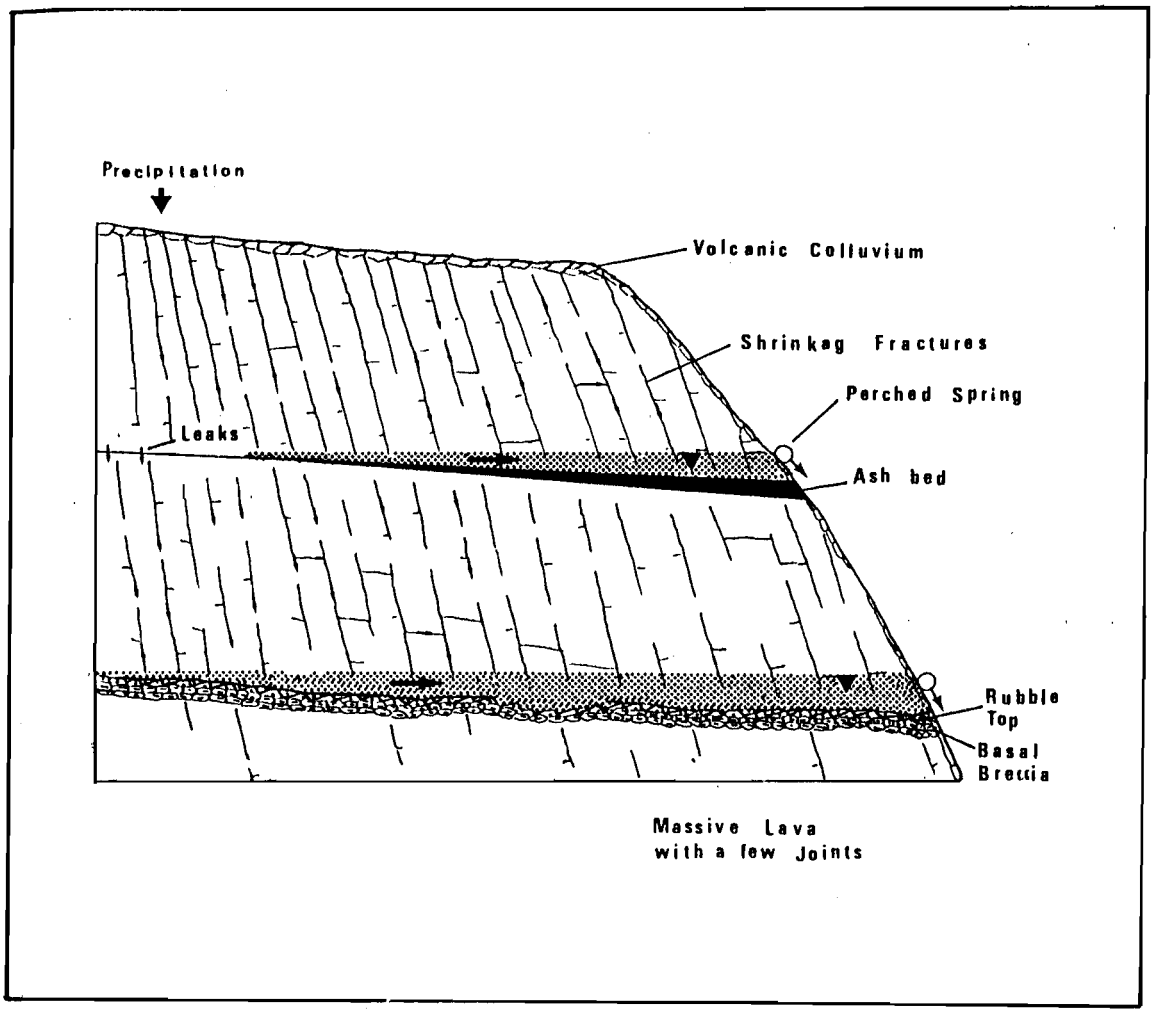

Figure 2.6 Springs in Volcanic Bedrock

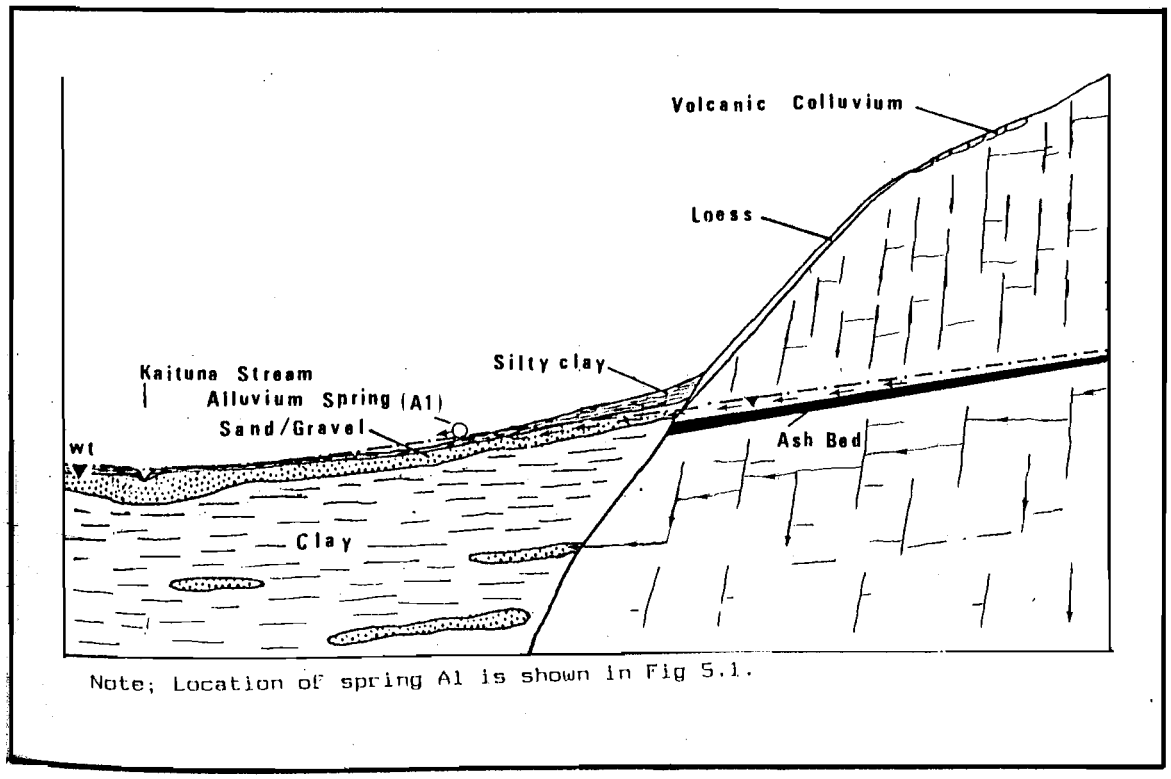

Figure 2.7 Springs in alluvial deposits

Plate 2.15 Confined spring from volcanic colluvium (G.R 836 185).

Plate 2.16 Diffuse spring from loess (G.R. 877 208).

The bedrock control of the spring configuration decreases at lower altitudes, where the main geological control is the permeability contrast within the regolith type materials (eg. existence of the C layer fragipan within the loess layer).

2.5.4 Hydrogeological Classification of Springs

Springs are classified according to the material from which they are observed to flow, regardless of their original infiltration medium. Springs, their flow magnitudes, and their location are presented in Fig. 1.6 and 1.7.

1) Springs in Volcanic Bedrock

Water storage within the volcanic bedrock is the source of the majority of springs in the catchment area (Plates, 2.17 and 2.18).

Only a small proportion (Figs. 1.6, 1.7) flow from the rock itself, as much of the volcanic rock is covered by colluvium and other regolith deposits.

2) Springs in Volcanic and Mixed Colluvium

The largest number of springs in the valley flow from volcanic colluvium (Plate 2.15) which is highly permeable. Springs flowing from mixed colluvium are rare, since these deposits are generally located below the highly permeable layers of volcanic colluvium.

3) Springs in Loess and Loess - Colluvium

Loessial deposits are generally found on low angle slopes below volcanic and mixed colluvium, and are therefore remote from the main recharge area. As a result, springs are rare and diffuse (Plate 2.16). Confined springs are found, however, where tunnel gullying has developed (tunnel gullies are a result of subsurface development of "pipe-like" tunnels, due to subsurface erosion in loessial soils).

Water movement in loess is along the low permeability C layer fragipan (if this is developed), or along the loess-volcanic bedrock interface. Springs occur where this interface is exposed or where the loess layer is locally eroded (Table 2.2).

Plate 2.17 Spring from volcanic rock (G.R. 863 193).

Plate 2.18 Seepage from volcanic rock (G.R. 860 168).

4) Springs in Alluvial Deposits

A few diffuse springs seep from the alluvial materials, marked by swampy ground. The proposed model for the occurrence of one of these springs (A1 on Fig, 1.6) is illustrated in Fig. 2.7. Underground water flows above an impermeable layer (eg. ash or tuff), through basal breccia. The water flow exits from volcanic rock through a sandy layer. The spring occur where the water table intersects the ground surface.

2.6 Synthesis

The geologic framework of the study area consists of volcanic lava flows and intrusive rocks, pyroclastic materials, regolith deposits and alluvial and coastal sediments.

Two types of groundwater flow were distinguished within the volcanic lava flows. Horizontal water flow is a downward movement due to a gentle southward dip of the lava flow (6 -20°). The basal breccias and rubbly tops of the lava flows are the main zones of approximate horizontal flow of groundwater.

Vertical shrinkage cracks are the main cause of vertical flow of water.

The main perching layer within the rock mass is ash and tuff (average clast size between 1/256 mm and 2 mm).

Intrusive rocks (domes and dikes) act mainly as barriers to lateral water flow. Pyroclastic materials (eg. tuff) are generally massive and consolidated.

The composition of volcanic colluvium (poorly sorted volcanic fragments with <10% loess), makes it the most suitable medium for water flow among regoliths.

Alluvial and coastal terrains in the Kaituna valley floor consist of a wedge of sediments resting on the lakeward inclined surface of volcanic basement. Alternations of the marine and terrestrial sediments within the area are related to transgressions and regressions during the Pleistocene.

Permeability tests of different layers within a 6 m Auger hole revealed that the silty layers which cover the top part of the alluvial plain have a very low hydraulic conductivity.

Plate 2.19 Flow of the main stream on volcanic rocks (G.R. 900 210).

CHAPTER THREE

GEOPHYSICAL INVESTIGATION

3.1 Introduction

Geophysical downhole logging, electrical resistivity, and seismic reflection and refraction were used to detect the water bearing potential of the valley floor and to delineate the most promising groundwater areas. The work comprised geophysical logging of 6 bores, 45 electrical soundings (8 geoelectric sections), 2 seismic reflection and 4 seismic refraction lines (Fig. 3.1).

The aim of the Geophysical Downhole Logging was to record physical parameters of valley floor deposits which can be interpreted in terms of the hydrogeological characteristics, the boundary of different the hydrogeological characteristics, and the boundary of different lithological units.

A resistivity survey was undertaken in the Kaituna Valley between January 1986 - February 1987 with a view to assessing the applicability of the method for obtaining subsurface hydrogeological and lithological information.

The seismic reflection and refraction surveys were undertaken (March - April 1987) in the lower part of the valley (Fig. 3.1) with a three major objectives:

1) To investigate the depth to volcanic basement in the survey area.
2) To locate any water bearing zones within the marine and terrestrial sedimentary section of the valley.
3) To assess the applicability of seismic reflection and seismic refraction methods in these types of the sediments.

3.2 Geophysical Logging

The Caliper, Natural Gamma, Gamma Gamma and Neutron logging techniques were used in the survey (App. 5). Geophysical loggings were made in 6 wells, M36/843, M36/734, M36/1344, M36/1437, M36/1421, and M36/727 (The first three wells with drillers geological logs). The location of

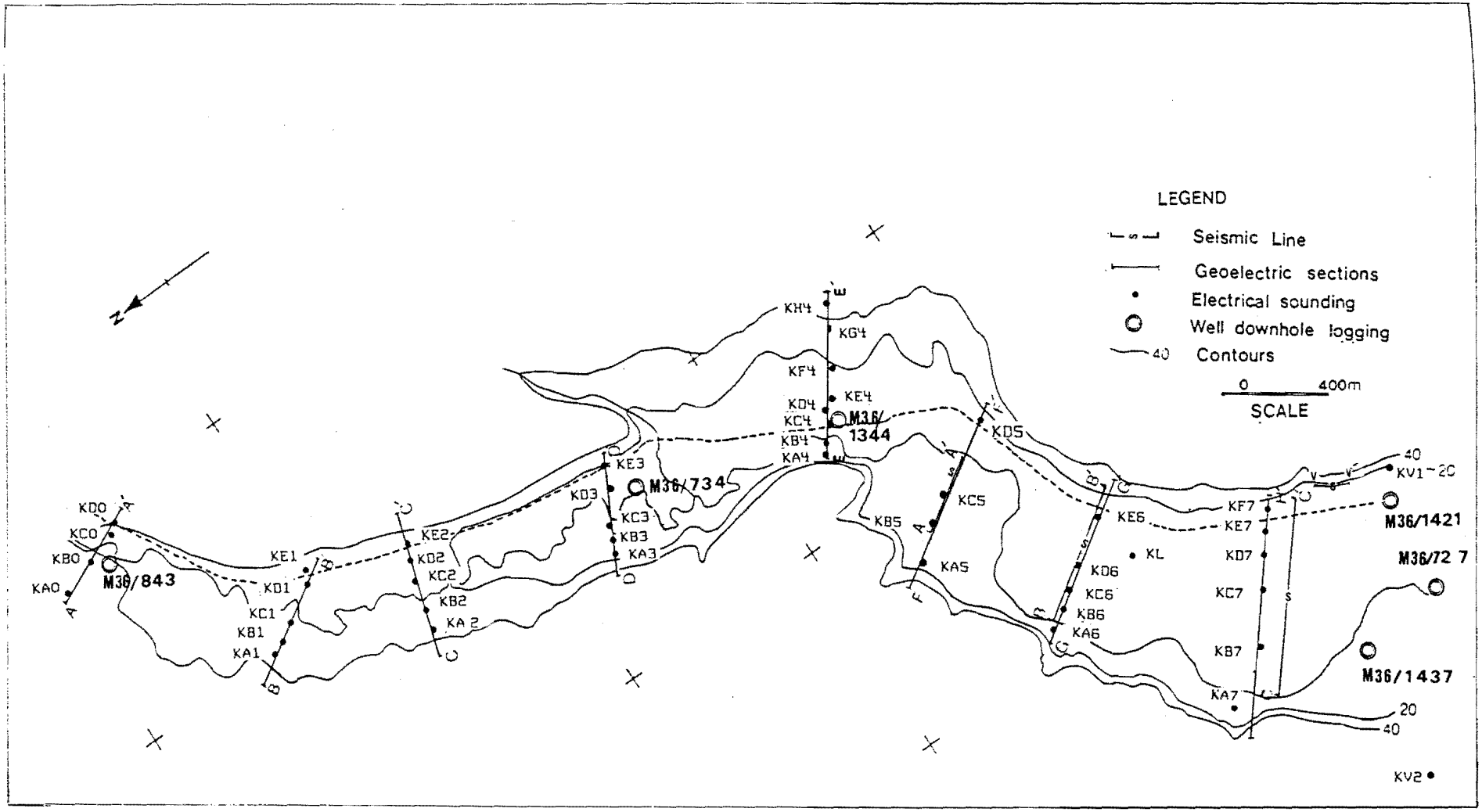

3.1 Location of Geophysical Investigation Sites

the boreholes are shown in Fig. 3.1.

In summary;

1) Caliper logs provide a continuous record of hole diameter and casing, and are useful for interpretation of other geophysical logs.

2) Natural Gamma logs were used to obtain information of lithology because the Gamma ray response decreases as the clay content decreases. Gravel generally had the lowest level of natural gamma radiation.

3) Gamma Gamma logs (Density logs) are mainly used for the identification of the Bulk Density and locating cavities around the well casing, the Count/Second recorded on a Gamma Gamma log increasing with decreasing Bulk density.

4) Neutron Logs provided an indicator as to the amount of fluid and hence material porosity of a deposit, high neutron response being related to sediments with low apparent porosity (apparent porosity or total porosity includes all the pore spaces in a material, regardless whether they are interconnected or not).

Any observed correlation between the low natural gamma signals and the low density or high apparent porosity could be caused by changes in hole diameter around the casings. In general the natural gamma emission is not related to hole size if a correlation exists between low natural gamma and high density, or low apparent porosity. Therefore Natural gamma has been the principal radiation log used for the interpretation.

The logging equipment consisted of three main units, (1) a radiation detector and/or source, (2) signal conditioners, and (3) recorders (Plate 3.1).

3.2.1 Data Processing and Interpretation.

1) Methods Used

Data from the field chart records were transferred into the scale presented in Figs. 3.2 to 3.7 as a common procedure for data presentation. The scale change (depth and/or radiation scale) was made using the Ministry of Work and Development digital computer. Digitizing the coordinates of points was made using a four-button cursor connected to the digitizer. Data was subsequently calibrated to establish the log response values in terms of the count per second (cps) for nuclear logging, and millimetres for Caliper logging.

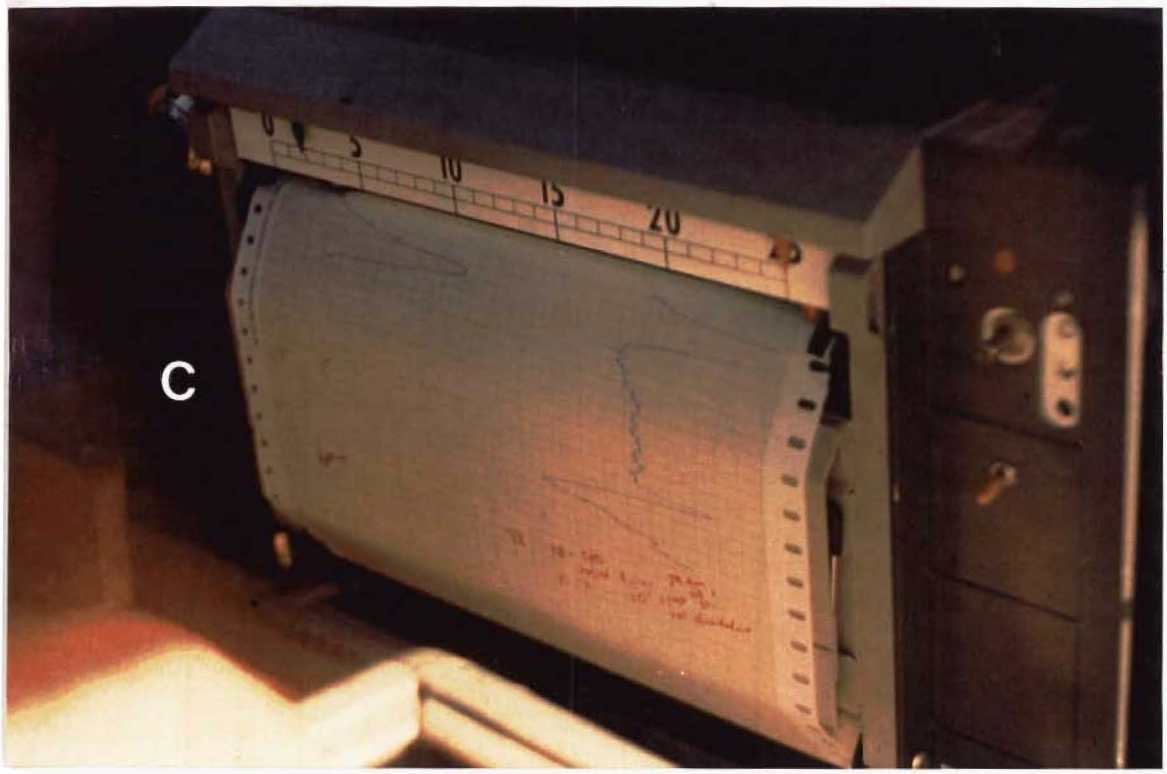

Plate 3.1 Recording System for Geophysical Logging

A - Recorder

B - Mechanical Winching Drum.

C - Gamma Gamma Chart Recorder.

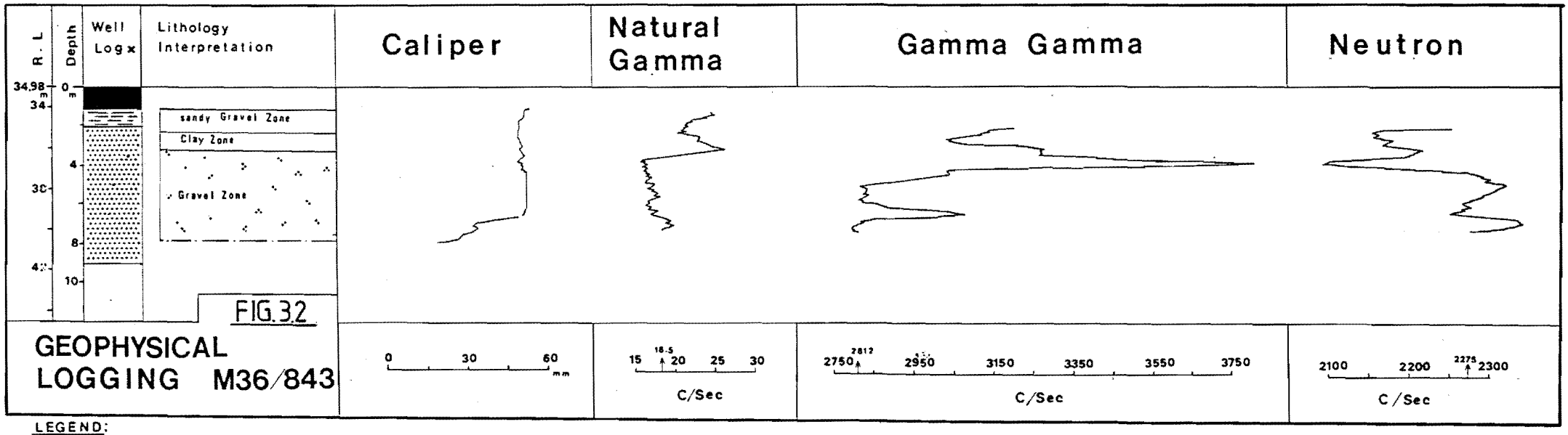

LEGEND:

Organic soil

Clay-Silty clay

Gravel-Volcanic rocks

× See p 59 3.2.1 «1»

Figure 3.2 Interpretation of Geophysical Log M36/843

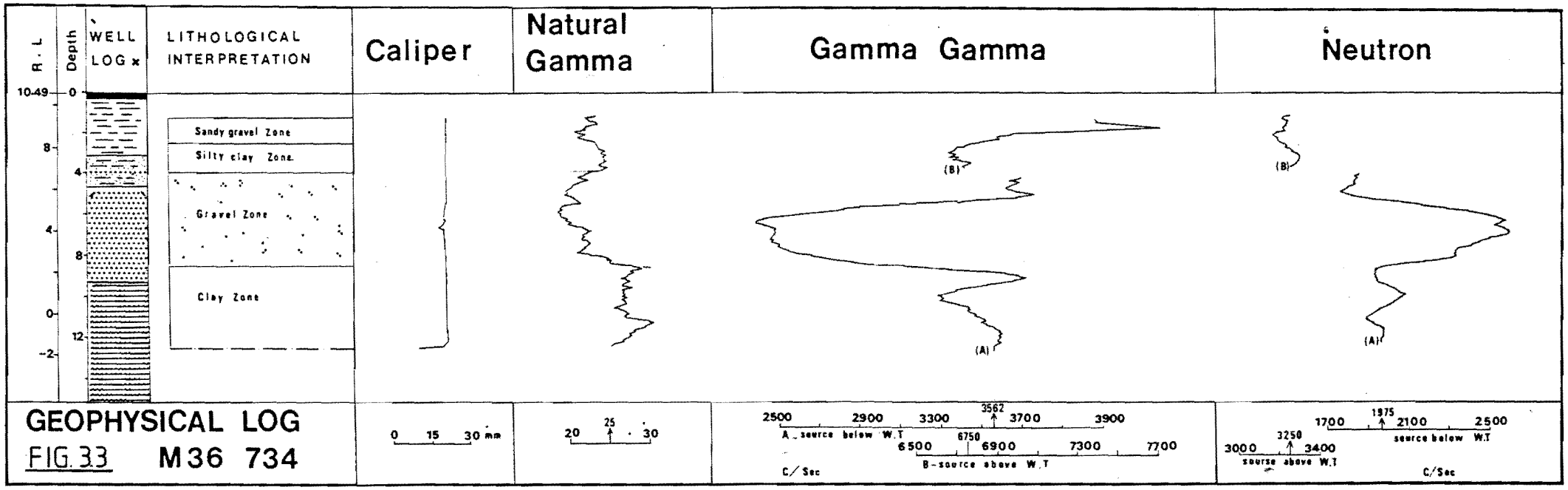

LEGEND:

× See p 59 3.2.1 «1»

Figure 3.3 Interpretation of Geophysical Log M36/743

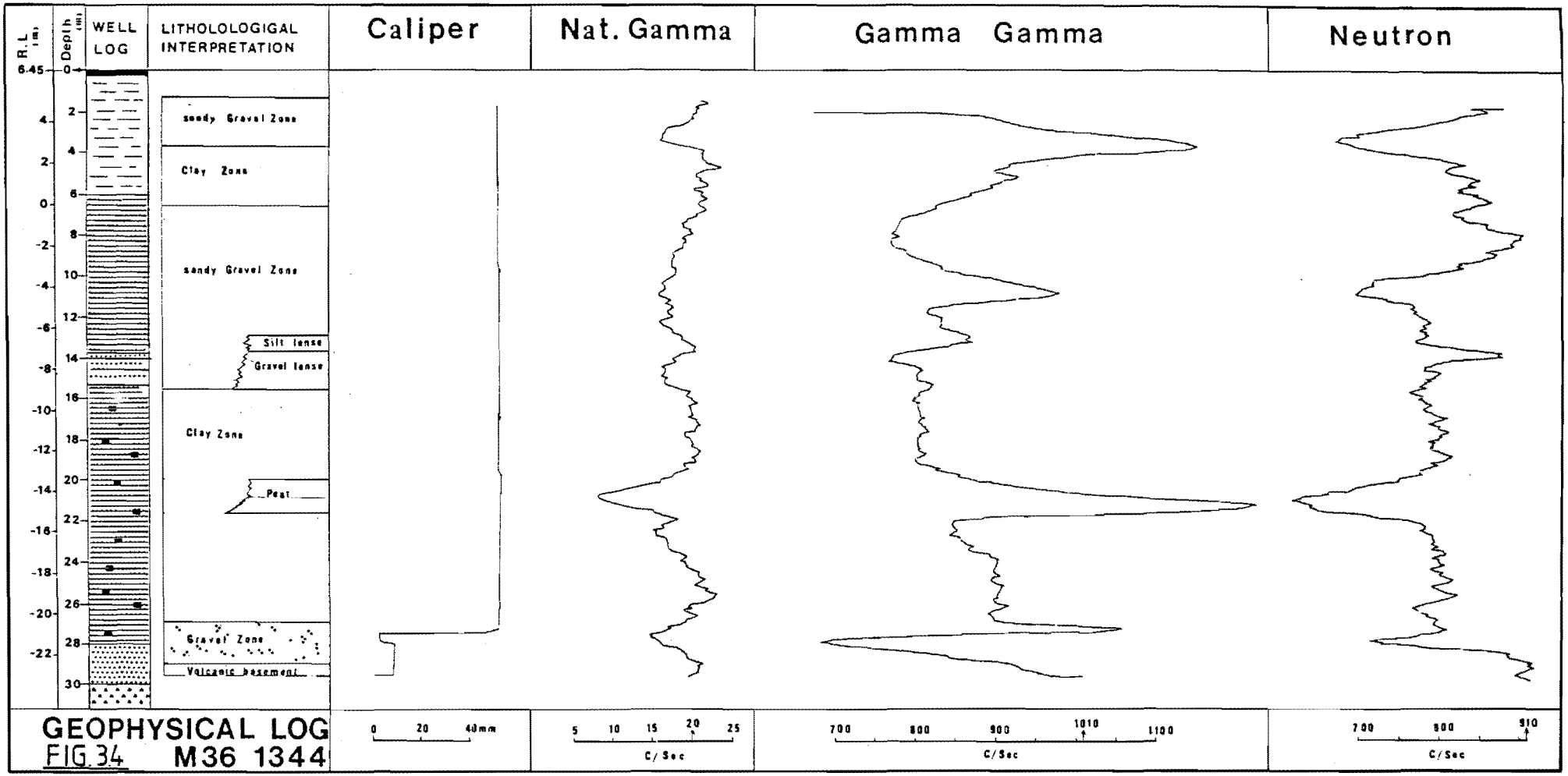

See p 59 3.2.1 «1»

Figure 3.4 Interpretation of Geophysical Log M36/1344

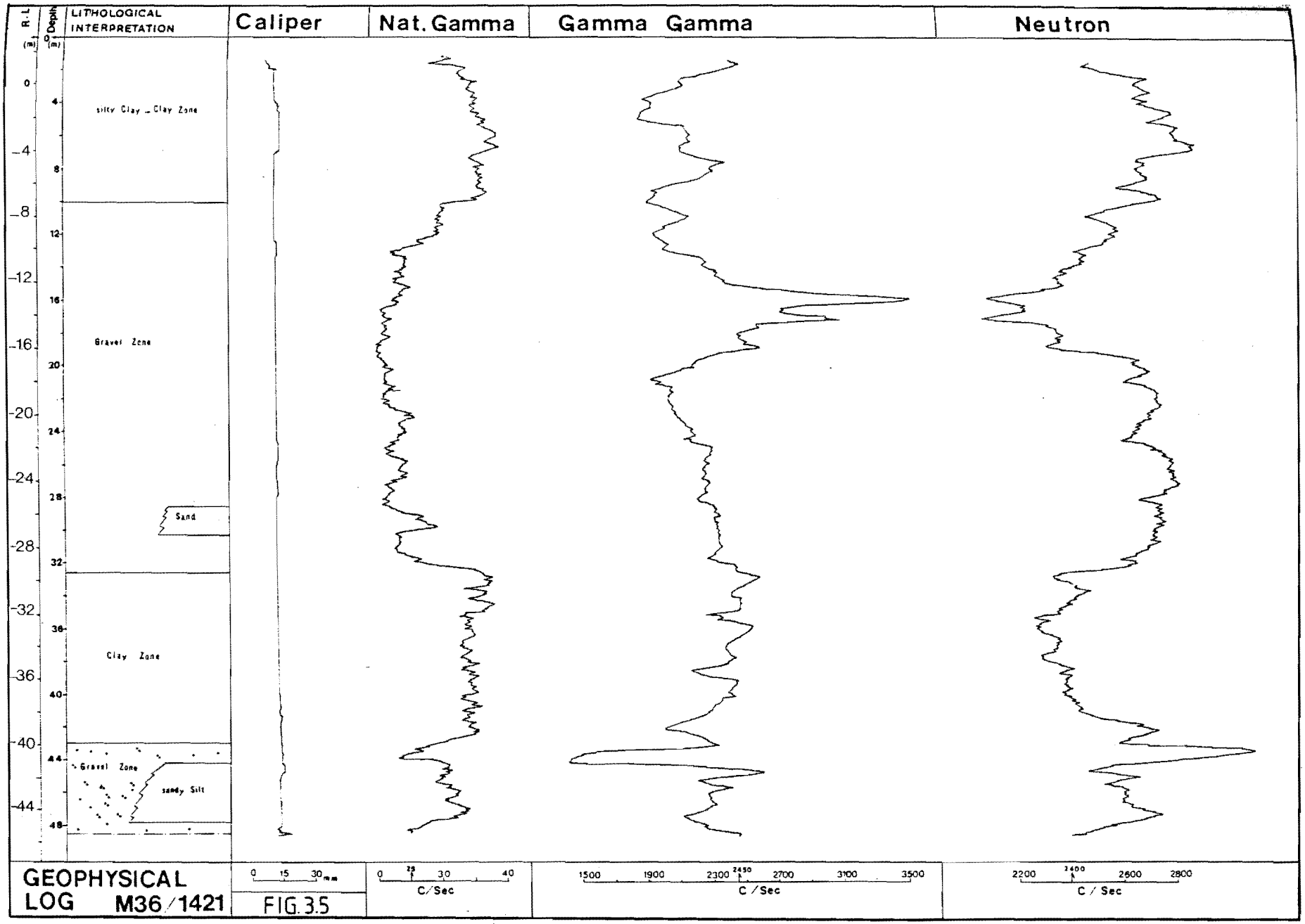

Figure 3.5 Interpretation of Geophysical Log M36/1421

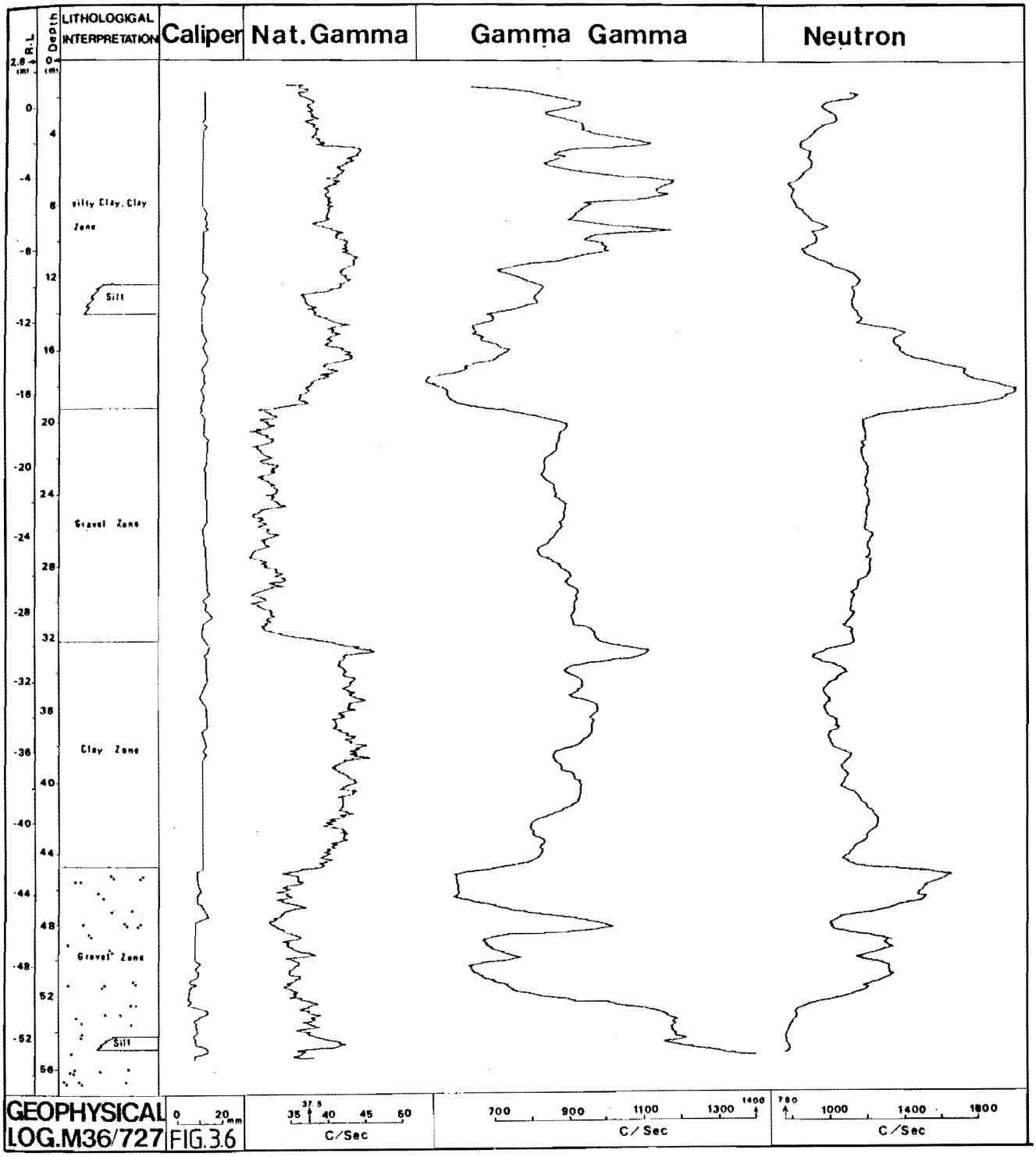

Figure 3.6 Interpretation of Geophysical Log M36/727

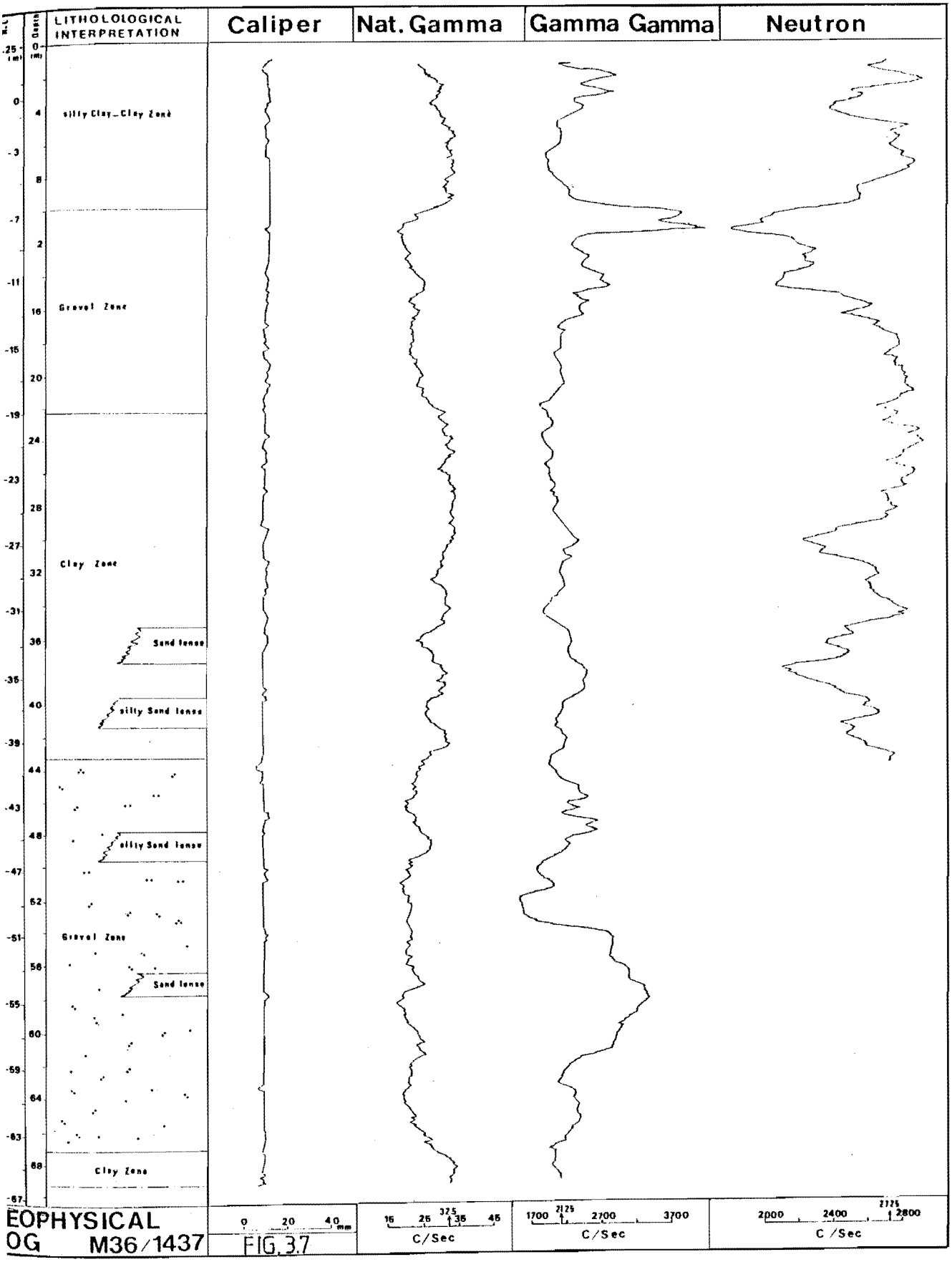

Figure 3.7 Interpretation of Geophysical Log M36/1437

Drillers logs were available for three wells M36/843, M36/734, M36/1344. Although these logs were not obtained by standard procedures or by geologists, they were used during lithological interpretation to define typical geophysical signatures for the sediments throughout the study area. Using variation of radiation intensity of each log, and drillers logs (where applicable), combined with knowledge of the local geology, lithological data was obtained. For each log lithology is divided into a number of zones, each representing a different sedimentation environment, named according to the dominant grain size. In addition major lenses of different materials within each zone were also defined.

2) Geophysical Log, M36/ 843

Three zones have been identified in this site (Fig. 3.2): 1) a low natural gamma activity between 1.2 - 2.4 m indicating a gravelly zone, 2) a zone from 2.4 - 3.2 m with high natural gamma radiation and a lower bulk density indicating clay, identified as a confining layer, and; 3) a second gravelly zone below 3.2 m which according to the well drillers log is the source of water. The sharp decrease in natural Gamma radiation at 3.2 m indicates the contact between the confining layer and the underlying aquifer, whilst the low bulk density (and high apparent porosity) within the first 1.2 m of the gravel layer (3.2 - 4.4 m) indicates the occurrence of caving around the well casing.

3) Geophysical Log, M36/ 734

The downhole logging tool did not reach the bottom of the well (21.3 m) due to the reduction in hole diameter below 12.5 m. However, the three zones recognized at the previous site (M36/843) were still identified in the top part of the log (Fig. 3.3). The top thin gravelly zone (1.1 - 2.3 m) overlies a zone with high natural gamma response (2.3 - 3.7 m), The latter layer being interpreted as a silt and silty clay layer. The third zone (3.7 - 8.2 m) shows a sharp increase in apparent bulk density and a sharp decrease in apparent porosity, which indicates a gravelly layer. This second gravelly layer is underlain (with a sharp contact) by a layer which has the maximum natural gamma radiation in the log. This being identified as a clayey layer below 8.2 m which is the main confining unit for the aquifer at bottom of the well (well drillers log, Fig. 2.5).

4) Geophysical Log, M36/ 1344

The lithological interpretation of this well is identical to the wells described previously. The increase in apparent porosity response in the thin sandy gravel layer at the top (1.5 - 3.8 m) may be due to an increase in hole diameter around the casing. The natural gamma radiation shows a sharp increase in the next zone (3.8 - 6.6 m), indicating the occurrence of clayey deposits. The natural gamma response gradually decreases below a depth of 6.6 m, indicating a transitional zone between the clay and the underlying gravelly zone. A more uniform gravel with higher apparent bulk density and lower apparent porosity is located at the bottom of this zone (13.6 - 15.7 m). Below 15.7 m the natural gamma radiation gradually increases, whilst the apparent bulk density gradually decreases, indicating the existence of a zone (to 27 m) with a high percentage of clay particles, this being identified as the main confining layer at the site. Within this clayey zone a unit occurs between 20.2 - 21.8 m with a very low natural gamma radiation, low neutron count rate (high apparent porosity), and a very low apparent density which together suggest a peat lens. The confining layer covers deposits with low natural gamma radiation, high density and low porosity from 27.2 to 29.8 m (Fig. 3.4), which is the source of water in this well and an aquifer zone (drillers log, Fig. 2.5). The high neutron cps values with high apparent bulk density below 29.8 m is a typical radiation response for basalt. The high neutron-log value in these rocks are due to their high content of chemically-bound water (Rider, 1986).

5) Geophysical Log, M36/ 1421

Downhole logging indicates the occurrence of 4 distinct zones of fine and coarse sediments at the site (Fig. 3.5). The top thin gravelly layer which was identified in all of the previous logs was not detected in this well or in the other wells in this part of the valley. High natural gamma response indicates the existence of the two clayey zones at depths of 1.2 - 10 m and 32.4 - 43 m respectively. There is a very sharp contact between the second clayey zone (identified as the main confining layer) and its top and bottom gravelly layers (at depth of 32.4 and 43 m respectively). The top clayey zone (1.2 - 10 m) becomes more silty toward the surface (as natural gamma response decreases). A transitional contact occurs between this clayey layer and underlying gravelly zone (Fig. 3.5).

Low apparent bulk density (gamma gamma) and high apparent porosity (neutron response) may be due to the occurrence of caving around the casing between 10 and 20 m in the top part of this gravelly zone (10 - 32.4 m). In the top part of the second gravelly zone below 43 m, a thin layer of gravel with a higher apparent bulk density and a lower apparent porosity was identified between 43 and 44.2 m. This becomes more sandy between the depth of 44.2 and 48 m, and the coarse materials below 43 m are interpreted as the water source.

6) Geophysical Log, M36/ 727

The 4 main zones of the previous site (M36/1421) were clearly identified at this locality (Fig. 3.6). The natural gamma activity in the top clayey zone (1.4 - 19.4 m) indicates a few lenses of silt and sand (Fig 3.6). The gamma gamma count rate decreases towards the bottom part of this zone, while the neutron count rate increases, which could be due to higher compaction of the sediment, with a corresponding decrease in apparent porosity. The first gravel layer (19.4 - 32.4 m) shows a sharp contact (sharp increase in natural gamma radiation) with the basal confining clayey layer (32.4 - 45 m). The bottom gravelly zone below 45 m is identified by its high natural gamma response, whilst a drop in the apparent bulk density toward the base of the log is considered to be due to cavities filled with water (decrease in the neutron response).

7) Geophysical Log, M36/ 1437

The previous zones of coarse and fine sediments are again detected in this well (Fig. 3.7) The neutron probe was not able to penetrate below a depth of 43.2 m in this well due to casing oxidation. The first clayey layer (1.3 - 10 m) overlies a zone of coarse deposits from 10 - 22.4 m. The second fine deposit zone (22.4 - 43.2 m), which is considered to be the main confining layer, overlies a second gravelly zone between 43.2 and 67 m. Two main lenses of sand (35.4 - 37.4) and silty sand (39.5 - 41.2 m) are identified within the confined layer by comparing the natural gamma radiations. A decrease in apparent bulk density at two sections (10 - 12 m and 53.5 - 61.7 m within the gravelly zones is considered to be due to an increase in hole diameter around the casing. The gravelly zone contains a major lens of sand from (56.5 to 57.7 m). The gravel between 43.2 and 67 m was identified as the main aquifer within the depth of the bore.

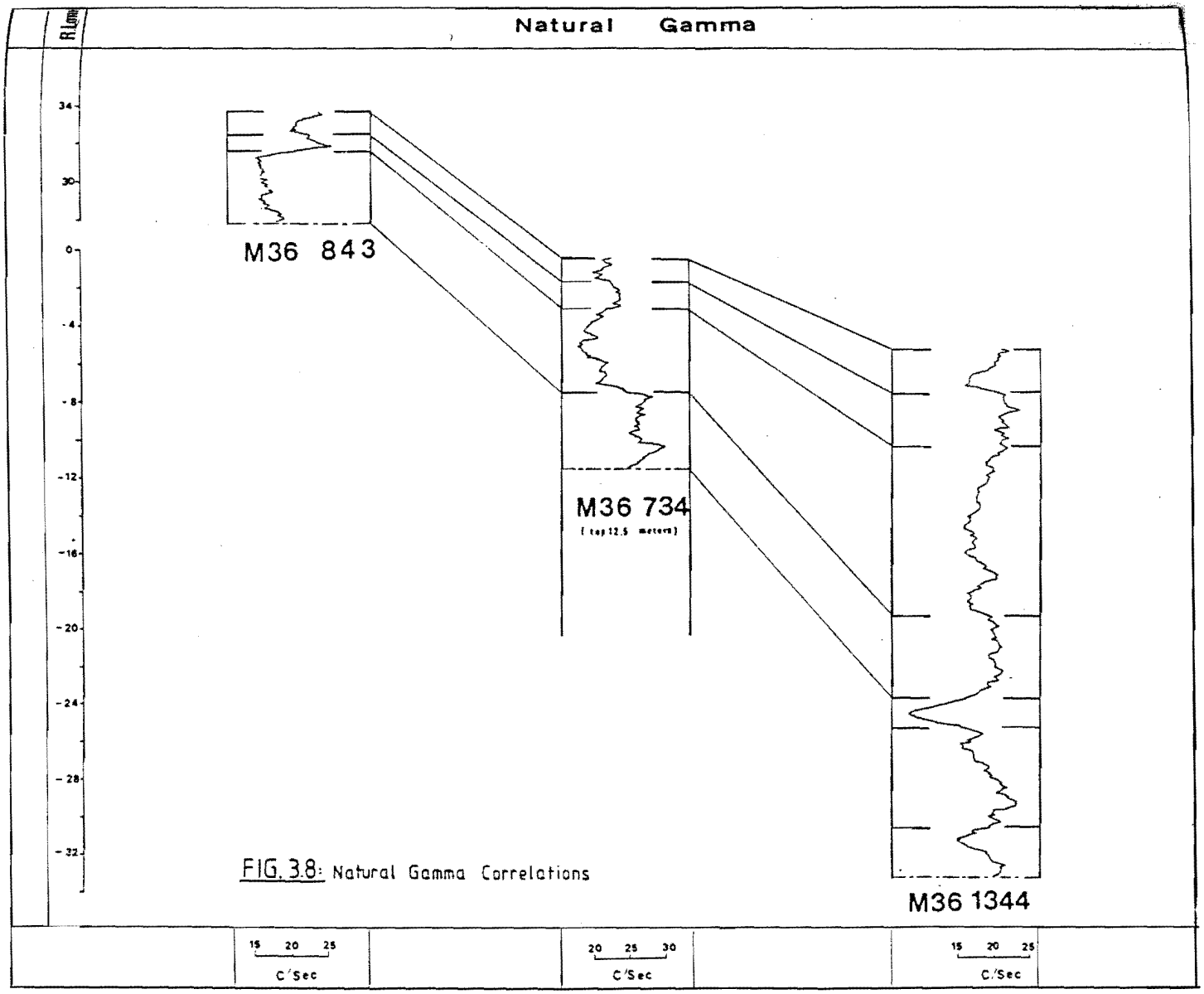

FIG. 3.8: Natural Gamma Correlations

Figure 3.8 Natural Gamma Correlations for Wells M36/843, M36/734, M36/1344

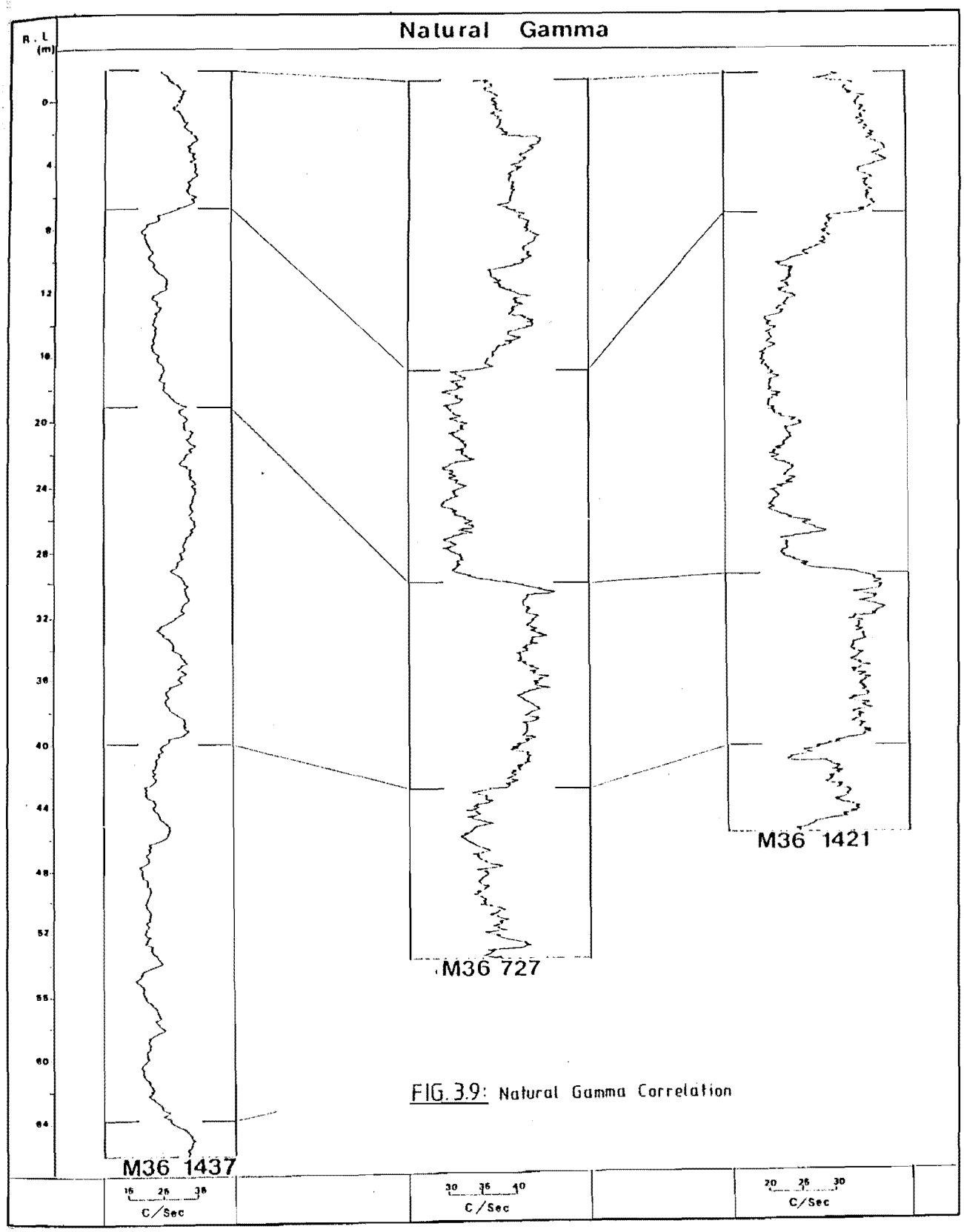

FIG. 3.9: Natural Gamma Correlation

Figure 3.9 Natural Gamma Correlations for Wells M36/1437, M36/727, M36/1421

The natural gamma radiation gradually increases after 64 m, suggesting the occurrence of a clayey zone below 67 m.

3.2.2 Natural Gamma Log Correlation.

Correlation of geophysical logs between different holes is useful for recognizing lithological continuity and variation, especially in holes without reliable geological logs. Only natural gamma log correlations were made as this log is less affected by changes in hole diameter and casing structure, and is more efficient as a lithologic indicator (White, 1985). Plots of all natural gamma logs are produced relative to mean sea level, and the natural gamma correlation is shown in Fig. 3.8 (M36/843, M36/734, M36/1344) and Fig. 3.9 (M36/727, M36/1421, M36/1437).

The lithologic interpretation and correlation of the all 6 geophysical logs is shown in Fig. 3.10.

The three logs from wells 843, 734 and 1344 show a thin gravel zone with a low natural gamma count rate (17 to 20.5 c/sec) close to the surface. This zone is underlain by a fine layer with a radiation intensity of 22 to 26 count/sec in each of the wells.

The natural gamma count rate in the third (gravelly) zone ranges between 16.5 and 20 c/sec, and appears to be more uniform in well M36/843. This zone is underlain by a clayey zone with a higher natural gamma count rate (21 to 28 c/sec) in wells M36/743 and M36/1344. This clayey layer was not detected in well M36/843, and the basal gravel (water source) in this well (M36/843) is confined by the top clay layer (2.4 - 3.2 m).

The thin, top gravelly layer does not appear in the three adjacent wells at the bottom of the valley (M36/1421, M36/727, M36/1437). The four common zones are identical in all three logs. The increased natural gamma count rate in these logs, compared to logs from the previous group, which were located at higher elevations, is considered to be due to an increase in the clay component. The first clayey zone, with a higher count rate (35 to 41 c/sec), is thicker and less uniform in well 727 in the centre of the valley. In the three logs, this layer overlies a gravelly zone (22 to 28 count/sec.). This gravelly zone does not appear to be an aquifer as the wells were drilled specifically to find water (and it is unlikely that all drilling would have passed the base of this gravel zone if it was an aquifer). The main confining layer for these three wells has a natural gamma response between 33.3 and 42.5 count/sec. It overlies a gravelly zone with a natural gamma intensity of 21 to 34 count/ sec which appears

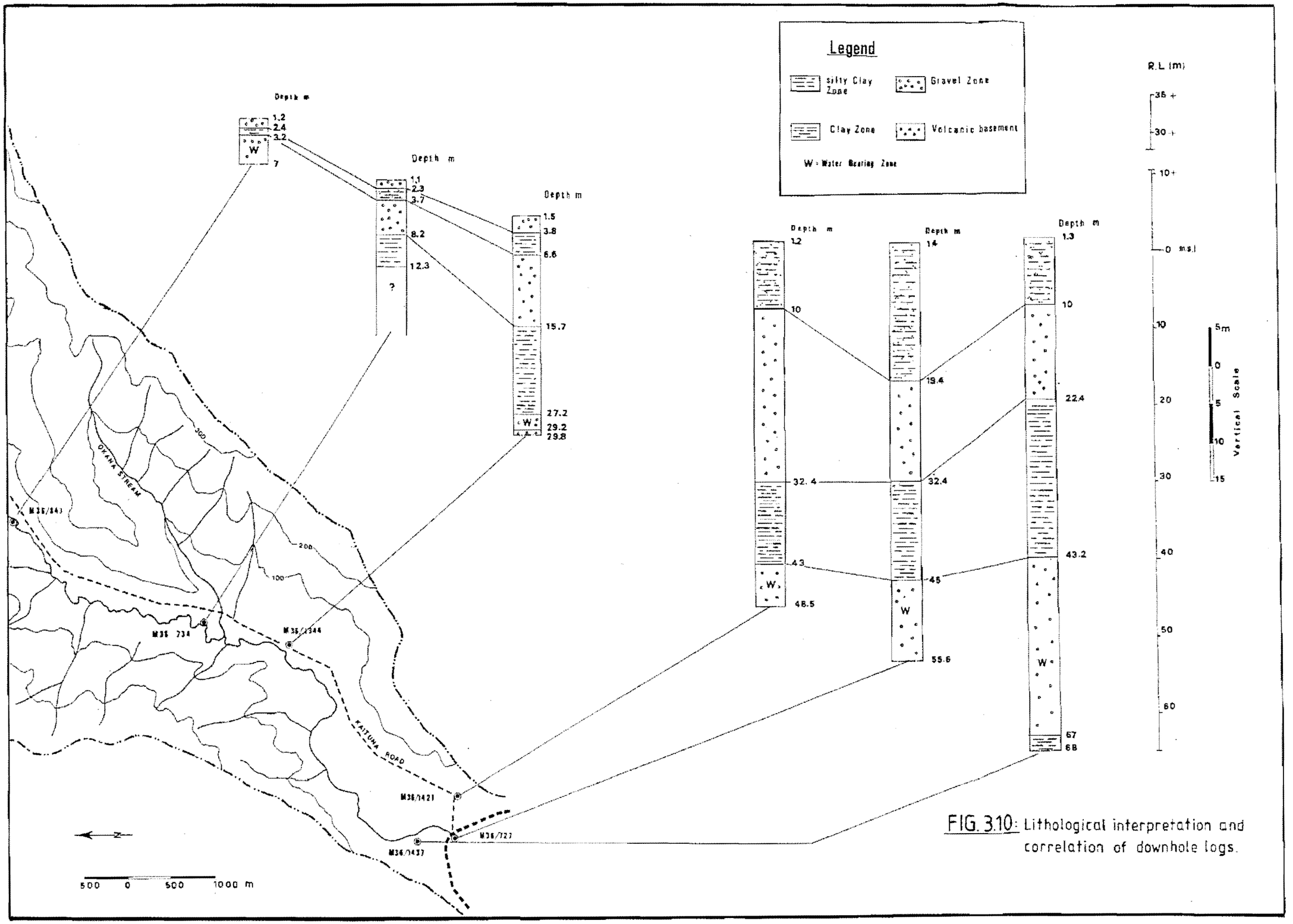

FIG. 3.10: Lithological interpretation and correlation of downhole logs.

to be the main source of water in these wells (Fig. 3.10).

3.3 Electrical Resistivity Survey

3.3.1 Field Techniques and Equipment

The survey consisted of 42 Schlumberger and 3 Wenner electrical soundings at locations indicated in Fig. 3.1. A very brief simplified description of these method is given in App 6.2 and in most textbooks on geophysical prospecting (eg. Telford et al 1970, Dobrin 1981).

The equipment used in the survey consists of an ABEM DC Terrameter, and terrameter SAS 300 with its Booster (Terrameter SAS 2000), Premeasured single conductor sounding cables and Multicore cable (BGS - 256). Specifications of the Terrameters are presented in App. 6.1.

3.3.2 Sounding Sites and Data Processing

Sounding sites were chosen so as to:

a) give measurement at as even intervals along the profile lines as practicable, while keeping the sounding centre away from fences and rough or clearly variable surface conditions; and b) keep all electrodes at about the same elevation throughout a sounding.

The soundings were made parallel to the valley sides in an attempt to ensure homogeneity of material between the electrodes.

The apparent resistivities for each sounding were plotted on Standard 62.5 mm log-log graphs. Each of these sounding curves was then interpreted as horizontal layers, assuming each layer is electrically uniform with horizontal plane boundaries. The graph of the field soundings (App. 6.3) was matched against a theoretical graph which had been computed for particular layer resistivities. If a match is obtained between the various segments of the observed curves and the segments of the published curves, then the subsurface structure can be assumed to be identical with the theoretical structure. A set of theoretical curves is shown in App. 6.4 for a "two layer" structure, and a summary of steps for this stage of interpretation is described in App. 6.5.

The layer resistivities and their boundary depths (App. 6.3) were used as data for a computer programme which modified the models so that apparent resistivities would be more consistent with those observed. The input models and with the modified models, are shown in App. 6.7. The

programme used is based on one published by Merrick (1977), modified by H M Bibby (D.S.I.R) and R Atkins and P White (M.W.D). Some details of the program are given in an unpublished report by White (1985).

3.3.3 Resistivity Interpretation.

The theory upon which the computation of the resistivity depths is based assumes uniform, parallel boundary planes between zones. This condition is rarely observed in reality, therefore the depth determined is an average depth over an area of the boundary between zones of different resistivity. Further differences between the geoelectric profiles and the geologic section are due to electric boundaries which separate layers of different resistivities not necessarily coinciding with boundaries separating layers of different lithologic composition. For example, when the salinity of ground water in a given type of sediment varies with depth, several geoelectric layers may be distinguished within the same lithologic unit. In contrast, units from different lithologies may have the same resistivity and therefore form a single geoelectric layer. In general the resistivity decreases with increasing porosity and with increasing water salinity. Clay saturated with water will be surrounded by a film of partially mobile ions which will migrate under a potential gradient. This migration adds to the normal migration of ions in the fluid, causing a reduction in resistivity of the clay deposits (Davis & Dewiest 1967). The resistivity is higher in the coarser sediments (sands and gravels) which contain water with a low salinity. Within these coarse sediments resistivity increases with increasing permeability, and hence decreases with increasing clay content.

Geological logs (well drillers logs) were used (where possible) for better lithological controls during resistivity interpretation.

1) Formation Factor

Formation Factors are ratios of the resistivity of a sediment containing water (R) to the resistivity of the interstitial water by itself (R_2). The resistivity of the interstitial water is controlled by its ion content and temperature. The higher the ion content and temperature of the interstitial water, the lower the resistivity (Dawson & Thompson 1981).

The formation Factor was measured for a more accurate interpretation of the resistivity data.

Saturated silt samples (at site KC7 and KD4, Fig. 3.1) and water from the wells with known lithological information (M36/843 M36/734 M36/843) were analysed to define the formation factors.

The resistivity of the interstital water was obtained using water conductivity values measured in the laboratory by the Ministry of Works and Development and North Canterbury Catchment Board;

Resistivity (ohm.m at 25°) = 1000 x 1/conductivity (mS/m at 25°)

Average water tempretaure in the field was 15°C. The following equation was therefore used to convert the resistivity value to its equivalent in the field;

$$\frac{R_2}{R_1} = \frac{22.0 + t_1}{22.0 + t_2}$$

where
R_2 = Resistivity at 15°
R_1 = Resistivity at 25°
t_2 = Field temperature (15°)
t_1 = Laboratory temperature (25°)

The formation factors and the resistivity results are summarized in Table 3.1.

site	Sample Depth (m)	R_2 (at 15°) (ohm.m)	R ohm.m	Formation factor
KC7	4	5	11.4	2.3 (C)
KD4	2	22.7	48.5	2.1 (C)
M36/843	8.8	41.40	204	4.9 (G)
M36/734	21.3	23.4	73.8	3.15 (G)
M36/1344	30	17.7	77	4.35 (G)

Table 3.1 Resistivities of water and Formation Factor (C, for silty clay and G, for volcanic colluvium and gravel) at different locations

The gravel layer above the basement in well M36/734 and M36/1344 (drillers log and downhole logging) was not distinguished by the resistivity survey. This is assumed to be due to the lack of sufficient resistivity contrast between the two, and also the small relative thickness of the gravel. Therefore the gravel resistivity (R) is assumed to be the same as the resistivity identified for volcanic rock at these two sites. Results indicate that although the resistivity of the material varies in each locality the formation factor for each lithological unit remains similar. The Formation Factor for gravels is higher (3.15 - 4.9) than silty clay (2.1 - 2.3).

3.3.4 Hydrogeological Interpretation of the Deduced Resistivities

By using the computer model of the Resistivity layers and their related boundary depth from 42 electrical soundings, seven geoelectric sections across the valley have been interpreted (Figs. 3.11 and 3.12).

In the present study the resistivity of the thin (<1 m thick) top soil is excluded from the geoelectric sections and the discussion.

The resistivity of volcanic rock can vary considerable depending upon the extent of the weathering and fracturing. Using the experimental soundings from KV1, and KV2, the resistivity of dry and solid volcanic lava flow was found to be within the range 150 - 250 ohm.m (App. 6.3). The saturated and more weathered lava below a depth of 30 metres (Well 1344 with the lithological log) was found to have a lower resistivity, 70 ohm.m (soundings KC4).

Geoelectric section AA' indicates the occurrence of a gravel layer with an average resistivity of 309 ohm.m. The boundary of this layer is in close agreement with the lithological data obtained from the geological log of well 843 (Fig. 3.2) This layer is overlain by a silty clays with lower average resistivity of 65 ohm.m, whilst the volcanic basement underlying the gravel has a resistivity lying between 42 and 92 ohm.m. At this location the volcanic boundary is deepest at sounding site KB0 (Fig. 3.1) with a gravel layer (18 m) overlying the volcanics (Fig. 3.11). The thickness of this gravel decreases downstream while the thickness of silty clay overlying the gravels shows an increase in thickness (Geoelectric sections BB' CC'). The gravel-volcanic boundary depth at sounding KC1 (section BB') and KB2 (section CC') suggests the existence of an old river channel (Fig. 3.11). The gravel layer in section DD' (sounding KC3) with resistivity of 184 ohm.m occurs immediately below the silt and silty clay layer, and the well drillers log and downhole logging (well 734) also indicates the occurrence of this thin gravel at this site.

The marine clay with a very low resistivity (25.8 - 9.7 ohm.m) was distinguished on geoelectric sections DD', EE',FF' (Figs 3.11 and 3.12) where the resistivity contrast was sufficient. The first evidence of marine clays with a low resistivity (14 ohm.m) is in section DD'. This interpretation was made by comparing the geoelectric section DD' and the lithological log of the well 734, 100 m south of sounding KD3. The presence of marine clay is better established at the section EE' using litho-

logical data from the well 1344. A thin gravel layer within the marine sediment (Lithological log 1344, close to the sounding KC4) is not identified in geoelectric section EE. This is considered to be due to its small relative thickness.

As a result of an increase in conductivity of the water in the top silty clay and (Table 3.1) toward the Lake Ellesmere, the top silty clay in sections FF', GG', HH', shows a very low resistivity (between 9.3 and 23.8 ohm m depending on the degree of saturation. However, the calculated formation factor indicates the similarity of this layer (from a lithological point of view) with the top silt and silty clay in the upstream geoelectric sections (Table 3.1).

Below the silty clay according to the downhole logging there are a several zones of clay and gravel (Fig. 3.10). These are identified as a single layer with resistivity of 22.4 - 46.4 ohm.m in sections FF', GG', HH'. This is considered to be due to;

1) the occurrence of "dirty" gravel (gravel mixed with clay), and 2) an increase in water conductivity.

A "dirty" gravel will show lower resistivity due to the higher free ion content caused by the intermixed clays, hence the intercalating layer of clay and gravel could not be determined because of their lack of resistivity contrast. In addition interstitial water in these sections in the top silty layer shows a very low resistivity (5 ohm.m at site KD7) compared with the resistivity of water in the same layer upper part of the valley (22.7 ohm.m at site Kd7). This also results in masking of the gravelly layers.

Resistivity variation at the bottom of geoelectric sections FF',GG' , HH'is high (with a maximum of 608 ohm.m at site KD5 and a minimum of 32.4, site KA7), The erratic nature of resistivity horizon indicates an occurrence of a gravelly layer rather than volcanic basement. It is interpretated that the volcanic basement is masked by this gravelly layer and therefore was not detected.

3.4 Seismic Refraction and Reflection Surveys

3.4.1 Seismic Techniques and Equipment

Both reflection and refraction techniques were used. A brief and simplified description of these two techniques and the survey configuration used is given in App. 7.1 and 7.2.

The seismic data was collected using Geophysics Division's Sercel SN338 - HR 48 channel recording system mounted in a truck. Two minisosie road tampers (Plate 3.2) and explosive charges (Plate 3.3) were used as energy sources for the reflection and refraction surveys respectively. The technical specification of the main recording system is given in App. 7.4. The location of all seismic reflection and refraction lines is shown in Fig. 3.1 and 1.6.

1) Seismic Reduction Method

For seismic reflection the data were initially recorded on magnetic tape and later reduced in the Geophysics Division seismic processing centre. Software and a Vax 11/750 computer were used in the centre to produce the seismic sections shown in Figs. 3.13 and 3.14. The main objectives of the processing were;

1) to eliminate or at least suppress all noise (all signals not associated with primary reflections).

2) to obtain the greatest possible resolution for the reflection.

In seismic refraction survey the refraction signals stored on digital tape were interpreted using the "plus-minus method" (Hagedoorn, 1959), the "delay time method" (Barry, 1967) (by D.S.I.R and author).

3.4.2 Seismic Reflection Surveys

1) Data Interpretation

In seismic reflection surveys each reflection package shows a combination of physical characteristics that distinguish it from adjacent seismic facies. The seismic facies unit is interpreted to express certain lithology, stratification, and depositional features of the deposits that generate the reflections in the unit (Brown, 1984). The Seismic facies were distinguished by; (1) reflection configuration, (2) reflection continuity, (3) reflection amplitude, (4) reflection termination or lateral change, and (5) Interval velocity.

1) Reflection configuration is controlled by bedding patterns which are related to depositional processes, original depositional topography, and erosion.

2) Reflection continuity depends on the continuity of the density-velocity contrast along the unit surface(s).

Plate 3.2 Minisosie used for Seismic Reflection Survey. Pneumatic hammer vibrates a plate coupled with the ground in a non-controlled random sequence. The signature of the random source energy is recorded by a sensor and transmitted to the recording station.

Kaituna Line BB′

PROJECT NAME : KAITUNA

EAST

RECORDING PARAMETERS

Source type/weight :Minie-Sosie	Spread : Split Spread
Shot spacing : 8m	Receiver pattern : 6 in-line, 1.8m int
Number of channels : 48	Geophone response :28 Hz OYO
Near offset : 32	Receiver spacing: 8 m
Far offset : 252	Sampling rate : 1000 ms
Equipment : Sercel	Record length : 1 sec
Date shot : 6/4/87	Filters: 25 Hz lowcut

PROCESSING SEQUENCE

DEMUX	Demultiplex shot gathers
DEBIAS	
FILTER	Bandpass filter 30-200 Hz
RESAMPLE	2 ms sampling rate
TRMUTE	Bad trace edit
FKTIME	To remove groundroll
AGC	Automatic gain 400 ms window
DECONW	Deconvolution 70 msec operator 14 msec gap
TVFILT	Bandpass filter 25-30-120-130 Hz
GATHER	Sort data into common-depth-point maximum fold 3600%
SMUTE	Surgical mute to remove first arrival and refractions
NMO	Normal moveout correction 25% stretch mute
CDPSTAT	Non surface consistent statics 20 ms maximum shift
STATIC	Elevation static Sea-level datum
STACK	Stack 3600% maximum fold
DECONW	Deconvolution 70 msec operator 14 msec gap
AGC	Automatic gain 400 ms window

DISPLAY PARAMETERS

Horizontal scale : 6.06 traces/cm
Vertical scale : 25.00 cm/s
Bias : 2 %

HARDWARE : VAX 11/750-FPS 5105
SOFTWARE : DSIR

DSIR,GEOPHYSICS DIVISION
PO BOX 1320,WELLINGTON

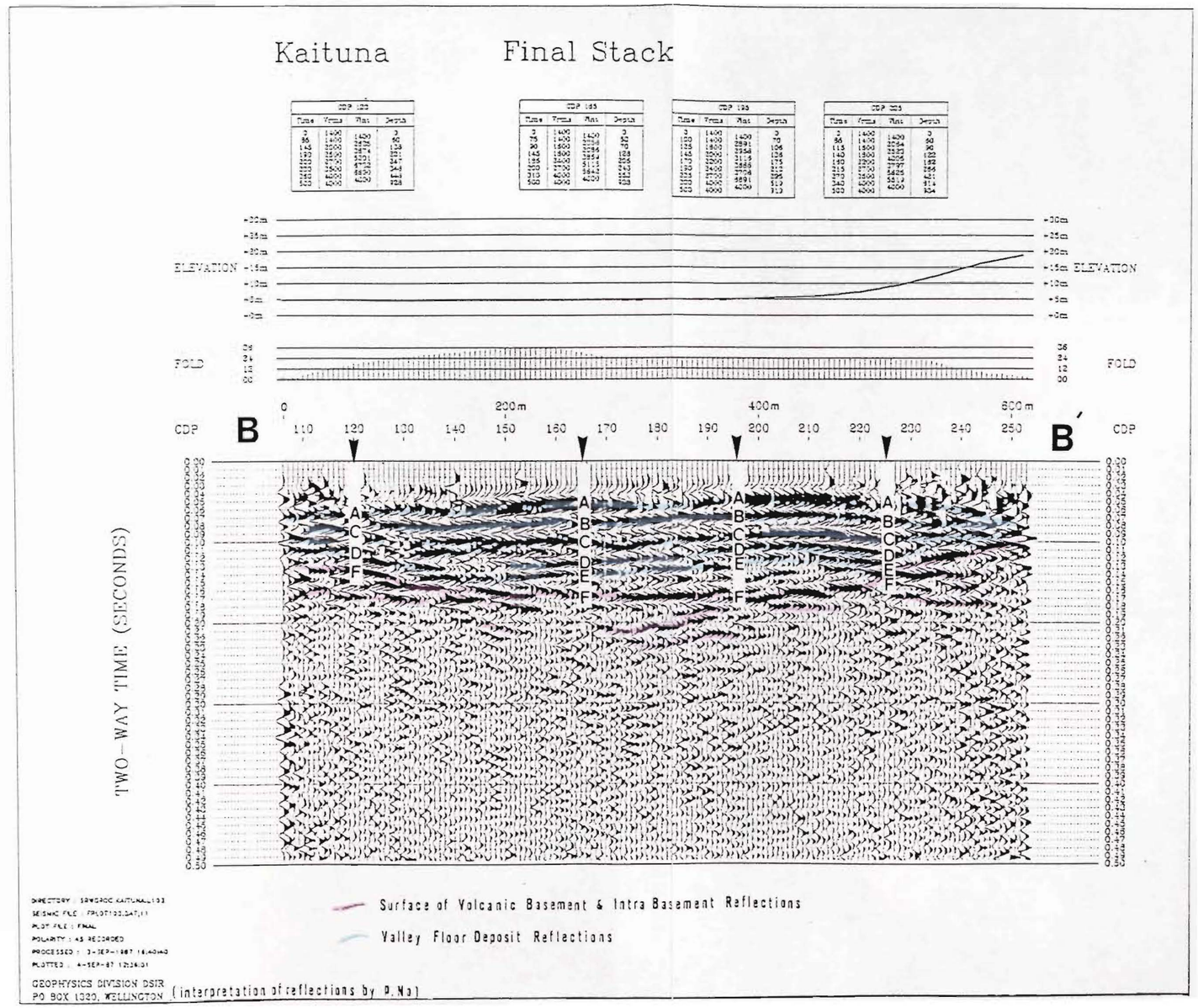

Figure 3.13 Seismic Reflection Line B-B′ (Time Distance)

Kaituna Line CC´ Final Stack

PROJECT NAME : KAITUNA

EAST

RECORDING PARAMETERS

Source type/weight : MINISOSIE	Spread : Off end
Shot spacing : 20 m	Receiver pattern : 6 in-line, 1.6 m int
Number of channels : 48	Geophone response : 28 Hz OYO
Near offset : 32 m	Receiver spacing : 8 m
Far offset : 408 m	Sampling rate : 1 msec
Equipment : SERCEL 338-HR	Record length : 3 sec
Date shot : March 1987	Filters: 25 Hz lowcut

PROCESSING SEQUENCE

DEMUX	Demultiplex shot gathers
GTGEOM	Geometry inserted into headers
DEBIAS	
FILTER	Bandpass filter 30-200 Hz
RESAMPLE	2 ms sampling rate
TRMUTE	Bad trace edit
STATIC	Correct for inconsistent surface velocites, Sea Level Datum
AGC	Automatic gain 400 ms window
FKTIME	To remove groundroll
DECONW	Deconvolution 70 msec operator 14 msec gap
GATHER	Sort data into common-depth-point maximum fold 1800%
TVFILT	Bandpass filter 30-35-120-130 Hz
SMUTE	Surgical mute to remove first arrival and refractions
NMO	Normal moveout correction 25% stretch mute with 10 ms taper
CDPSTAT	Non-Surface consistent static correction, 20 ms maximum shift
STACK	Stack 1800% maximum fold
DECONW	Deconvolution 70 msec operator 14 msec gap
AGC	Automatic gain 400 ms window

DISPLAY PARAMETERS

Horizontal scale : 6.06 traces/cm
Vertical scale : 25.00 cm/s
Bias : 2 %

HARDWARE : VAX 11/750-FPS 5105
SOFTWARE : DSIR

DSIR,GEOPHYSICS DIVISION
PO BOX 1320,WELLINGTON

CDP 125			
Time	Vrms	Vint	Depth
0	1400	1400	0
20	1400	1400	21
68	1600	1742	54
90	1800	2211	80
110	2000	2724	107
170	2400	3998	197
205	2600	3795	256
250	3000	4282	418
365	3500	4282	804
540	4000	4851	1022

CDP 185			
Time	Vrms	Vint	Depth
0	1400	1500	0
50	1600	2053	46
85	1800	2370	76
125	2000	2770	123
180	2400	4508	209
210	2800	3500	277
285	3000	5120	438
480	4000	4000	907
500	4000		947

CDP 225			
Time	Vrms	Vint	Depth
0	1300	1400	0
55	1400	1945	39
82	1600	2744	85
96	1800	2825	85
120	2000	2864	123
150	2200	3538	158
200	2600	3987	247
265	3000	4216	375
400	3500	4667	668
595	4000		1142

CDP 275			
Time	Vrms	Vint	Depth
0	1200	1200	0
90	1200	1855	18
50	1400	2015	56
70	1600	2771	56
90	1800	2506	78
120	2000	2871	116
205	2400	3624	238
300	2700	3624	393
365	3000	4110	526
485	3500	4628	837
690	4000	5052	1319

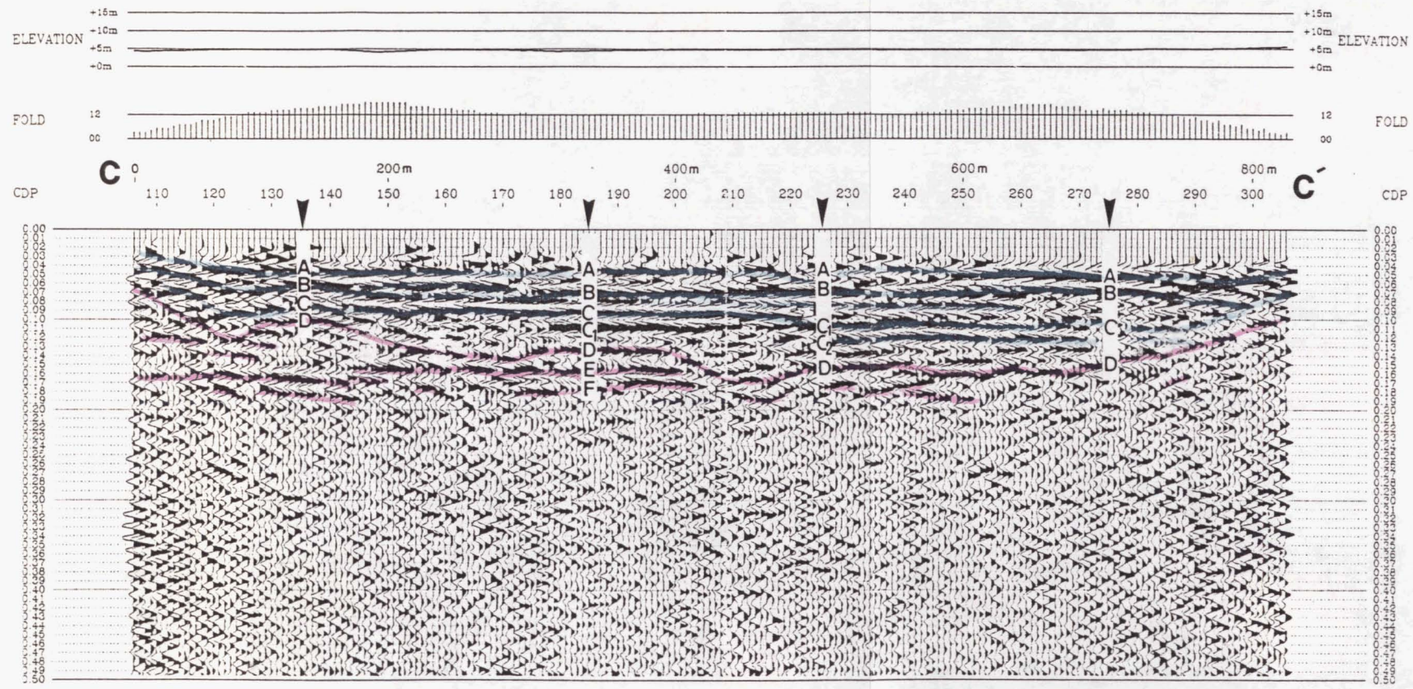

DIRECTORY : SRWGROC KAITUNA:L101
SEISMIC FILE : FPLOT101.DAT;13
PLOT FILE : FINSTACK
POLARITY : AS RECORDED
PROCESSED : 4-SEP-1987 16:43:13
PLOTTED : 4-SEP-87 19:07:11

GEOPHYSICS DIVISION DSIR
PO BOX 1320, WELLINGTON NZ.

(interpretation of reflections by P.Na)

Figure 3.14 Seismic Reflection Line C-C′ (Time Distance)

3) Reflection amplitude is controlled by the degree of velocity-density contrast along unit surfaces.

4) reflection termination or lateral change is controlled by lateral change and termination of the seismic facies.

5) Interval velocity is a critical factor in seismic data processing and provides information on lithology and composition of subsurface layers. It represents the uniform velocity within a homogeneous geological unit or the average velocity over a depth interval containing more than one unit. If two reflectors at depth z_1 and z_2 give reflections with one-way time of t_1 and t_2 the interval velocity V_{int} between z_1 and z_2 is defined as $(z_2 - z_1)/(t_2 - t_1)$. Interval velocities are presented in App. 7.5. for each reflection layer (Figs. 3.13 and 3.14).

Except for interval velocity, these factor were evaluated visually on the seismic reflection records.

2) Basement Interpretation

The volcanic bedrock surface is interpretated as a reflector with variable amplitude and continuity. The discontinuous nature of this reflector is mainly due to the presence of basal breccia and rubble top which scatters the seismic energy.

Line CC'(Fig. 3.15) shows volcanic basement dipping toward the east and flattening out after 450 m. The maximum depth to the volcanic basement is 175 m (Reduced Level, RL -170.2 m) at a distance of 457.5 m (Fig. 3.15). At a distance of 737.5 m the basement slopes upwards to form the eastern valley wall.

Line BB'(Fig. 3.15) has a similar basement configuration except that the dip towards the east is more gentle and uniform than in line CC'. The maximum depth to the basement is 165 m (RL -160 m) at a distance of 367 m. It slopes steeply to the west at distance of 388 m.

The volcanic bedrock has a weak reflectivity and amplitude (Figs 3.13 and 3.14. but some intra-basement reflectors have been resolved for both sections. These reflectors could represent surfaces of weathered and permeable basal breccia.

3) Depositional Sequence Interpretation

Geologic interpretation of the seismic facies indicates the existence of two distinct depositional environments.

1) Variable amplitude/Low continuity reflection response
2) High amplitude/high continuity reflection response

The former reflections commonly occur in response to alluvial plain facies from high-energy (rapidly degrading) fluvial channels and meander-belts (Brown 1984). On both lines these facies are interpreted as being deposited directly on basement. They occur at a depth of 100 m (RL -95.2 m) to 175 m (RL -170.2 m) on line CC′ and from 100 m (RL -95 m) to 165 m (RL -160 m) on line BB′(Fig. 3.15). The average interval velocity of layers is 2700 m/sec, indicating that coarser particles (gravels & sands) are more dominant. Discontinuous reflectors and their patterns and the general trend of the interval velocities (App. 7.5) indicate an occurrence of a old river channels interfingering with finer deposits (Fig 3.15)

The later reflections are more common in tectonically stable depositional setting (Brown 1984). Intercalating of marine and terrestrial deposits is the main cause of the impedance contrasts in these reflectors. The first major reflector is located at a depth of 20 to 40 m (RL -15.2 to -35.2 for line CC′ and RL -15 m to -35 m for line BB′, Fig. 3.15). The interval velocity for this unit is between 1733 and 1913 m/sec (App. 7.5) on the line CC′and between 1368 and 2066 m/sec on the line BB′. These velocities and downhole logging data from the wells in this part of the valley were used to interpret this layer as a clay unit that is the main confining layer (Fig. 3.15). This overlies a higher interval velocity unit which ranges between 2100 and 2421 m/sec on line CC′ and between 2148 and 2933 m/sec on line BB′(App. 7.5). The high interval velocities and downhole logging indicate the occurrence of gravels which is assumed to be an aquifer. The maximum thickness of this layer is 50 m (at a distance of 242.5 m on line CC′) and 44 m (at distance of 175 m on line BB′). Within this zone the pattern and continuity of the reflectors was used to locate river channels (Fig. 3.15). Although these channels are considered to have the capacity to transmit greater volumes of water but they are interpreted as a part of the whole aquifer layer.

In most clastic formation the velocity increases continuously with depth because of different compaction effect (Dobrin, 1981) Therefore the high amplitude reflector below the gravel layer is considered to be a clay layer although its interval velocity is higher (average of 2500 m/sec) than that of the clay layer closer to the surface. This interpretation is

also supported by the increase in natural gamma response below the same gravel layer.

Erosional unconformities were identified from the divergent pattern of reflections and their lack of the lateral persistence on both seismic sections (Fig. 3.15).

3.4.3 Seismic Refraction Surveys.

The interpreted refraction sections (AA', BB', CC'and the velocity spreads) are shown in App. 7.6.

1) Velocity Spread Line(V V')

Velocity Spreads were made to determine the velocity of the volcanic basement. The arrival times show the seismic P-wave refractor velocity is about 3900 m/sec for the volcanic basement. This is in good agreement with the refraction velocity (3000 to 4000 m/sec) found by Broadbent and Haines, (1976) for Akaroa Volcanics at Birdlings Flat (GR M37 871 92).

2) Line AA'

Line AA'is 350 m long and only four shots were fired, with no off-set shots. As a result the volcanic bedrock velocity was not detected.

A velocity of 200 m/sec was interpreted as an unsaturated silty clay layer with a thickness of 1-2 m. The next unit, with an average velocity of 1700 m/sec, is underlain by a layer with a higher average velocity (2100 m/sec). At the ends of the 2100 m/sec layer, a higher velocity of 3000 m/sec was calculated. However these higher velocities are based on one-way measurements at two ends of the profile, and the lack of overlap means no calculation of the true velocity was possible. The 3000 m/sec velocity is due to a 4 degree updip component at each end of the line (Fig. 3.15).

3) Line BB

The silty clay at top is thicker than the other two profiles with a higher seismic velocity (400 m/sec). There are two wedge-shaped layers one with a velocities of 600 m/sec interpreted as unsaturated loess colluvium (using auger hole) under the rising ground to the SE (Fig. 3.15) and one

A

B

Plate 3.3 Preparing Seismic Refraction Shot Point (using Gelignite).

A - Shot Hole (average depth 1 m).

B - Placing Gelegnite.

with a velocity of 1000 m/sec near the river, interpreted as silty clay above the watertable (Fig. 3.15).

Below the watertable two layers with the velocities of 1600 m/sec (saturated silt and silty clay) and 2000 m/sec (gravels) are interpreted. The layer with velocity of 2000 m/sec is underlain by a layer with a higher velocity (2800 m/sec) but it was not possible to determine the boundary accurately.

The velocity of the basement on this line is about 3900 m/sec. which is consistent with the basement velocity recorded by the velocity spread line. The interpreted basement boundary is slightly domed and is located at depth of about 150 m (RL -145 m)near the centre of the line (Fig. 3.23).

4) Line CC′

Line CC′ (the southern most seismic section across the valley) shows the first surface layer having a velocity averaging about 1000 m/sec, indicating the presence of an silty clay. This layer is slightly thinner (2 - 3 m) here than in line BB′ and has a lower velocity (100 m/sec) when compared with the section BB′. It is underlain by a saturated silty clay layer with a depth that correlates with the watertable (3 to 5 m in this section) with an average velocity of 1600 m/sec (ranging from 800 to 1900 m/sec). The next velocity zone (2800 m/sec) indicates the occurrence of the gravelly layer below a depth of 60 m (RL -55.2 m). Depth determination of this layer was not clear, partly due to the variable velocity in the overlying layer and partly due to lack of sufficient offset of the shots from the end of the geophone line. The presence of the gravelly layer is not identified in the first 130 m of the section, and for the next 80 m its presence is not certain.

Volcanic basement velocity measured in this line (3900 m/sec) agrees with the velocity of the basements found in the velocity spread line. It is level under the centre of the section (Fig. 3.15). bedrock with a velocity of 3900 m/sec being identified. The top of the volcanic basements is approximately flat under the centre of the section (Fig. 3.15).

3.4.4 Comparison of Reflection and Refraction surveys.

The two seismic methods (reflection and refraction)were in good

agreement about the depth of basement, with maximum depths of 160 m 175 m. The reflection survey indicates a maximum depth of 175 m for line CC,'while the refraction survey shows a depth of 160 m to bedrock. Layer boundary figures for the refraction survey should be considered with more caution since the narrow valley floor prevented the use of wide offset shots across the valley, which would have allowed a more detailed interpretation of the basement and the sediments above. Both surveys indicate volcanic basement dips steeply down the flanks of the valley and is flat in the middle.

The occurrence of coarser deposits nearer the basement was proved by both techniques. The seismic reflection method proved to be the more useful because it provides more detailed information as to the sedimentation environment and lithology of the overburden deposits. The configuration of the confining layer and the gravelly layer underneath (gravel), were only distinguished by the reflection survey.

The refraction survey provided a more detailed picture of the thickness and the velocities of the near-surface silt and silt and silty clay.

In general the seismic reflection survey is to be highly recommended for investigations of valley floor sediments and water bearing potential zones in similar valleys.

3.5 Aquifer Modeling

Two main aquifer zone have been identified.

3.5.1 Lower Aquifer

The Lower Aquifer overlies volcanic basement and consists of gravel and volcanic colluvium which is confined by marine clay deposits.

Geophysical Investigations employed in this study have identified the most suitable areas in which to conduct any future drilling phase of the groundwater exploration within Kaituna Valley.

Its thickness depends on volcanic bedrock topography, being greatest in the old river channels (15 m at electrical sounding site KB2 and 60 m at, 463 m along seismic line CC') and thinnest thickness at the edge of the channels, typically not more than 2 m thickness. From resistivity results geoelectric section AA' BB' CC' and seismic data it has been

assumed that the maximum thickness of water bearing gravel will be found over the deepest parts of the volcanic basement. Contours of depth to basement below ground level (using geological and geophysical data) are shown in (Fig. 3.16). Seismic data defines the thickness of the base gravel in the lower part of the valley. In the upper part of the valley depth contours were derived mainly from resistivity surveys which proved to be in good agreement with available geological and geophysical data.

3.5.2 Upper Aquifer

The upper aquifer lies within the valley floor deposits. The boundary of this gravelly layer is identified by downhole logging and seismic reflection survey. It is confined at the top by marine clay deposits (with 20 to 43 m thickness) and overlies the fine sediments. The aquifer occurs in the lower part of the valley with an average thickness of 24 m (Fig 3.15).

3.6 Synthesis

Correlation of geophysical logs between different holes was useful for recognizing lithological continuity and variation. The increased natural gamma count rate in logs (M36/1437, M36/1421, and M36,727), compared to logs that are located at higher elevation was considered to be due to an increase in clay component. The natural gamma activity for the water bearing gravel in wells M36/843, and M36/1344 was about 16 c/sec whereas in wells at the bottom of the valley was ranged between 20 to 35 c/sec.

The result obtained from the resistivity surveys indicates that the method is useful for the detection and delineation where the relative thickness is sufficient, of the near-surface gravelly zone (eg. section AA'). This technique also was successful for the outlining of the courses of buried channels above the volcanic rock where the depth to the bed rock is less than 40 m. Results was also quite satisfactory below 40 m depth for locating the basement which underlies the lowest aquifer system in the area.

The two seismic methods (reflection and refraction)were in good agreement about the depth of basement, with maximum depths of 160 m 175 m. The reflection survey indicates a maximum depth of 175 m for line CC,'while the refraction survey shows a depth of 160 m to bedrock. The two methods were in good agreement about the depth of basement, with maximum

depths of 160 m 175 m. The seismic reflection method proved to be of more use because it provide more detailed information on the sedimentation environment and lithology of the overburden deposits.

Two main aquifer zone have been identified by the geophysical investigation. The Lower Aquifer overlies volcanic basement and consists of gravel and volcanic colluvium which is confined by a marine clay deposits. The upper aquifer lies within the valley floor deposits. The boundary of It is confined at the top by marine clay deposits. Its thickness is about 24 m and occur in the lower part of the valley.

CHAPTER FOUR

SURFACE HYDROLOGY

4.1 Introduction and objectives

Information on surface hydrology is an important part of the geohydrology of the Kaituna catchment. Besides providing basic descriptive information, such documentation has been used to identify possible interactions between the surface and subsurface hydrological systems.

The monitored catchment covers an area of 38 km^2 (Fig. 4.1). and is oriented in a NE - SW direction. The head waters of most tributaries are located at the north and north east side of the valley (Fig. 4.1), where the catchment boundary has a higher elevation (Mt Bradley, 855 m and Mt Herbert 920 m).

The width of the catchment increases upstream, with tributary divergence occurring at low elevation (Okana stream) and continuing into the head water region. The catchment geometry is therefore classified as an equilibrium/concave-convex basin with a dendritic drainage pattern (Bannister, 1982).

The head waters of all the tributary streams are springs originating from volcanic and colluvial deposits (Figs, 1.6 and 1.7). The catchment geology and vegetation has been outlined in chapter 1.

In order to identify and describe the surface water resources of the catchment the following investigation program was undertaken.

1) Precipitation and evaporation monitoring.
2) Water flow analysis of the main river and major tributary streams in the investigation area.

Stream flow data has been obtained for three reasons:

a) continuous data was required for a general description of the flow rate characteristics, and analysis of extreme low and high flows in the Kaituna catchment;
b) estimates of stream flow were required for an analysis of water balance components in the catchment; and
c) to permit detection of any possible interaction between groundwater and stream flow.

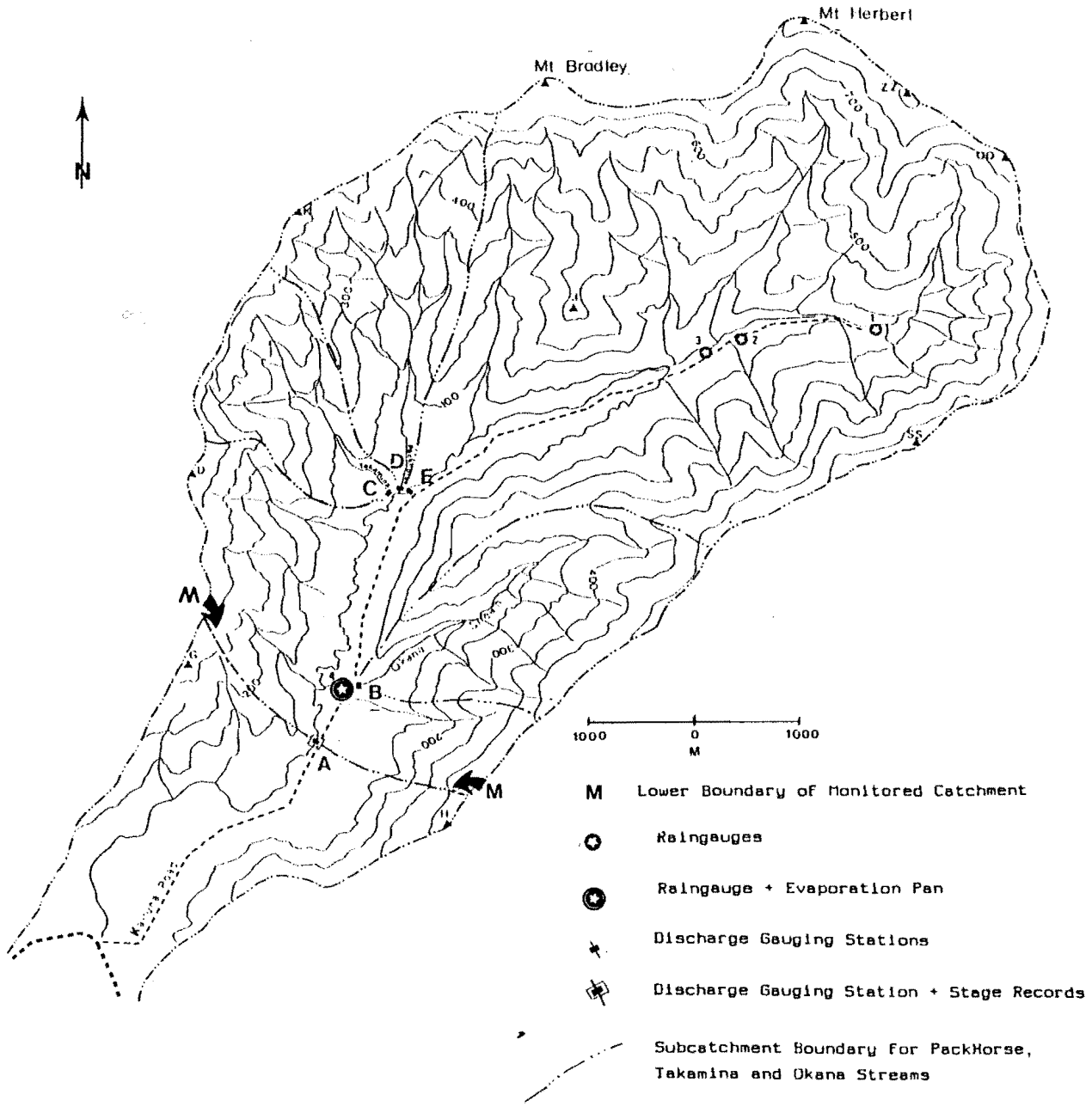

4.1 Surface Hydrological Data Points and Monitored Catchment Boundary

4.2 Precipitation

Precipitation monitoring is the main element of all hydrogeological studies.

4.2.1 Raingauge Sites and Installation

Rainfall monitoring was conducted using three existing raingauges (Fig. 4.1, stations 1, 2, 3). These three gauges were not spaced evenly throughout the valley, therefore a fourth rain gauge was installed in the middle of the valley (station 4). The main factor in choosing a raingauge site is the exposure effect; i.e. no obstruction should be closer to the raingauge than twice (preferably four times) the height of the obstructions. Obstructions, for example trees, either prevent water from entering, or add water to the raingauge.

Four funnel type (nonrecording) raingauges, which consist of a circular standard cylinder 20.3 cm in diameter (which serves as an overflow can), and a funnel-shaped receiver of the same diameter, were used to measure rainfall. Raingauges were installed so as to project 30 cm above the ground to avoid the effect of wind, which may produce turbulent eddies preventing water from entering the gauge, and to have sufficient height to avoid splash effects. Evaporation in the measuring tube might occur, but it is not possible to avoid this and the amount of is negligible in total precipitation values.

4.2.2 Data Collection and Rainfall Pattern

Rain data for each site was collected by the author and local farm owners on a daily basis (9 am) for a 12 month period (June 1986 -May 1987). Rainfall data is presented in App. 8.1, and comparison of rainfall at all four raingauge sites is presented in Fig. 4.2. The data suggests a relationship with height above sea-level; rainfall increasing with increase in elevation. This is because areas of high elevation area are more exposed to southwesterly airstreams. For the same reason seasonal rainfall variation is more pronounced at higher elevations (Fig. 4.2).

The maximum monthly mean recorded rainfall is 442 mm at station 1 for August, 1986 (Fig. 4.2) and the minimum is 8.9 mm at station 4 in January, 1987. The percentage of rainfall for each month is shown in Fig 4.3, and it is apparent that 19.6% of the total rainfall monitored

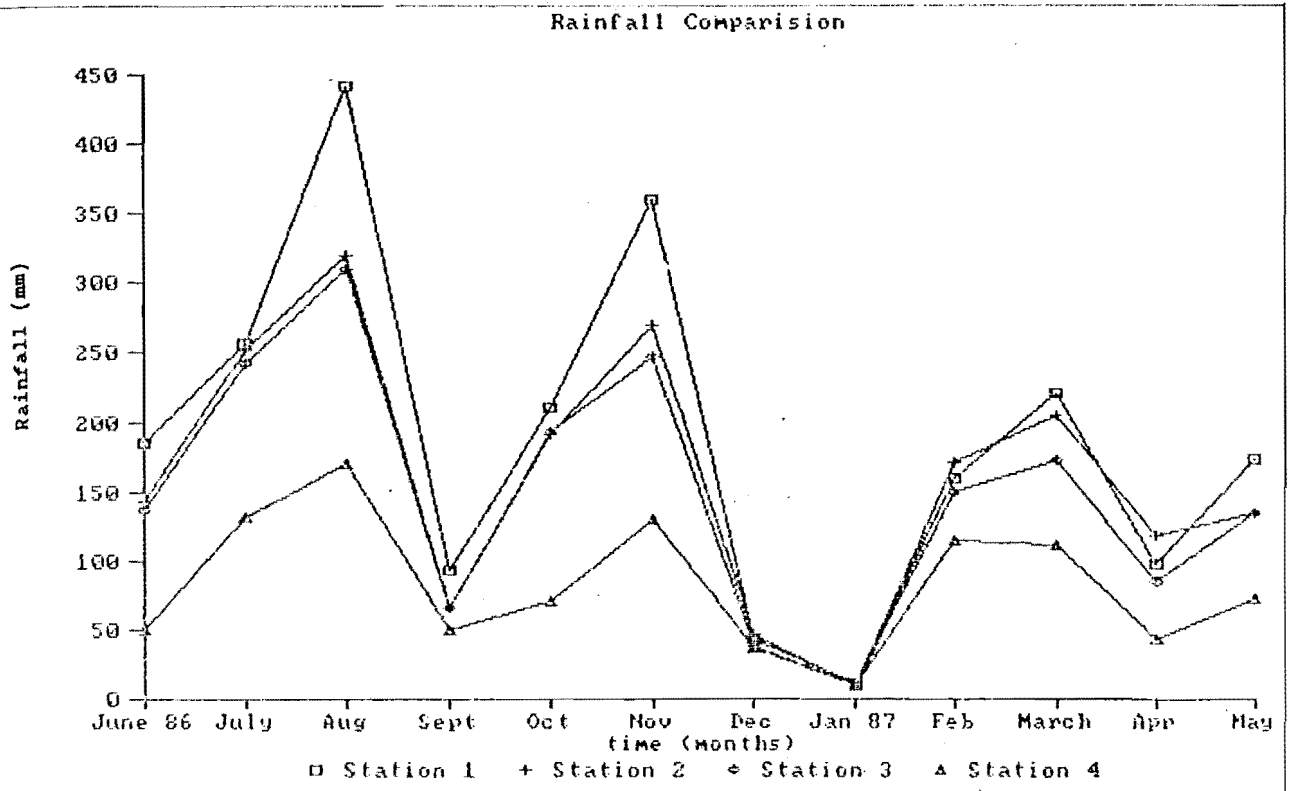

Figure 4.2 Rainfall Comparison For Monitored Water Year

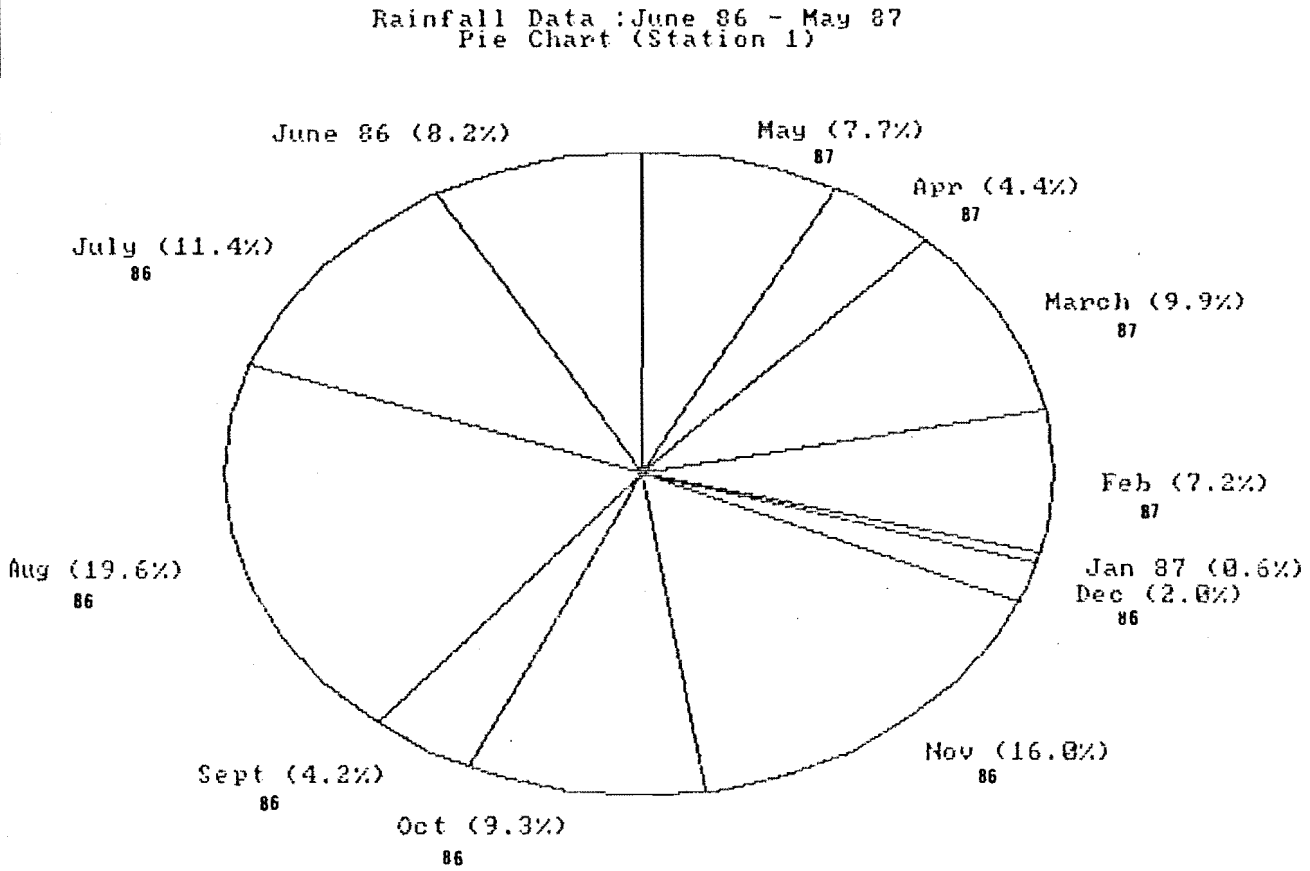

Figure 4.3 Rainfall Data: June 1986-May 1987 (Station 1)

(June 1986 to May 1987) occurred in August 1986.

4.2.3 Areal Precipitation Analysis

1) Analytical Techniques

For hydrological analysis, it is important to know the areal distribution of precipitation (Viessman et al 1977), and three methods are commonly used to assess this. The most direct approach is to use the arithmetic average of gauged quantities, however this technique is satisfactory only when gauges are uniformly distributed and the topography is flat. In the Thiessen method, the area is subdivided into polygonal subareas using raingauges as centers. The subareas are then weighted and used in estimating the average depth of the watershed. However the Thiessen method is not suitable for mountainous areas because of orographic influences (Viessman et al 1977). The most suitable technique for areal precipitation analysis in Kaituna Valley therefore is considered to be the Isohyetal method.

2) Isohyetal Method

The Isohetal method can be used for any area (flat or mountainous) to compute areal rainfall values. The annual mean rainfall for each station is plotted on Fig. 4.4, interpolation between gauges has been performed, and rainfall amounts at selected increments identified. Identical depths from each interpolation are then connected to form isohyets-lines of equal rainfall depth (Fig. 4.4). The isohyetal pattern was determined from data collected in this study, and from raingauge data compiled (from a period 1950 to 1985) by Jayet (1986) which covered the catchment and surrounding area. This was undertaken in order to produce a more realistic representation of isohyet patterns in relation to regional topography and adjacent raingauge sites. The area between adjacent isohyets was determined with a planimeter, the equivalent uniform depth of precipation between isohyets is assumed to be equal to the median value of the two isohyets (App. 8.2). The resultant isohyet map is given in Fig. 4.4.

3) Annual Rainfall

The average annual precipation depth within the catchment monitoring

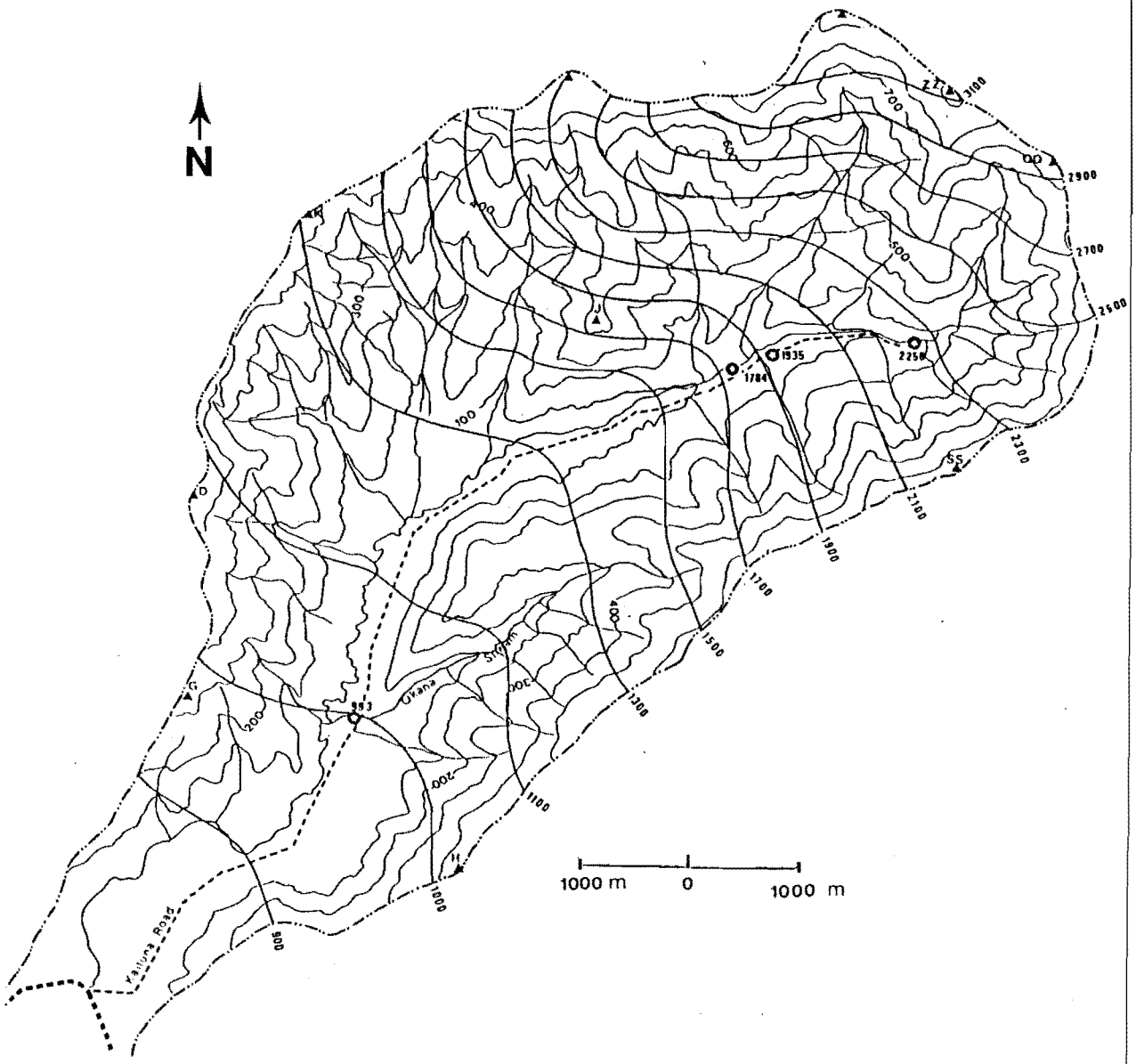

Figure 4.4 Isohyets Contour and Mean Annual Rainfall for each Station (June 86 - May 87)

«Rainfall in mm»

area has been computed at 1900 mm (as a result of isohyet interpretation), which means 722 x 10^5 m^3 of rainfall over the monitored catchment area (38 km^2) during the water year (June 1986 - May 1987).

4.3 Evaporation

Evaporation is a critical consideration when evaluating the potential for water resource development, and in water supply studies.

4.3.1 Evaporimeter Installation

A raised pan evaporimeter, identical with the U.S Weather Bureau class A pan evaporimeter, was used. The pan is a cylindrical tank of 120.65 cm inside diameter, and 25.4 cm inside depth set on wooden timber supports (100 mm 50 mm), so that the bottom was about 15 cm above the ground. The top of the stand was leveled and anchored by soil fill. A summary of the main parts of the evaporimeter is given in App. 8.3.

The raised pan evaporimeter was installed adjacent to raingauge station 4, close to the Okana stream (Fig 4.1). The site was chosen because it was flat, turfed, free from obstructions such as trees, shrubs and buildings,) and close to a water source (Okana stream). Availability of water to bring the level up to the fixed point after each measurement (App. 8.3) was an important factor in choosing the evaporation site.

4.3.2 Data Collection and Analysis

The quantity of water required to restore the water surface in the pan to a fixed level was measured by the author and a local farmer every day at 9 am, and the operation technique is presented in App. 8.3. The evaporation pan (Plate 4.1) became available in September 1986, and data collection was initiated from 27/9/1986. As the water year for this study started in June, correlation was made between data at Kaituna and the data from Lincoln college evaporation station. This provided a continuous evaporation record for the catchment (App. 8.4) over the study period. The correlation factor was in a satisfactory range (0.86), and therefore a regression equation was used to complete data for the Kaituna site for the water year (June 1986 - May 1987). The computed regression equation was;

Plate 4.1 Evaporation Pan. (G.R. 847 173).

Plate 4.2 Stage Gauging Site. (G.R. 844 165).

$C_1 = 0.307 + 0.931\ C_2$

where:

C_1 = Evaporation at Kaituna station
C_2 = Evaporation at Lincoln station.

Actual open water evaporation is less than measured evaporation by a specific factor, and a value of 0.69 was given as the reduction factor to be used for estimating actual reservoir evaporation (Finkelstein 1973).

Seasonal variation in evaporation (actual evaporation) is shown in Figure 4.5. Minimum monthly evaporation during July and August 1986 (wet conditions) was 23.4 and 23.5 mm respectively, and maximum monthly evaporation was 164 mm during January 1987. The annual evaporation (June 1986 - May 1987) for the Kaituna Valley was 860 mm. The surface area of the monitored catchment is 38 Km^2, therefore, assuming an areally uniform evaporation rate, approximately 326.8 x 10^5 m^3 of water evaporated from the monitored catchment during the water year.

4.4 Stream Flow

4.4.1 Stream Gauging Sites

In choosing the best site for stream gauging the following criteria were considered.

1) location the gauge in as uniform a reach as possible, and away from obstructions in the channel (e g. bridge, large boulders), to ensure that the velocity vectors are parallel.

2) avoidance of back water from downstream (due to tidal effects).

3) availability of a well-defined stream cross section where good discharge measurements could be made.

4) a uniform streambed to avoid continually changing stage-discharge relations due to changes in the vertical velocity component.

On the basis of these criteria, five stage-discharge stations were located within the monitored catchment (Fig. 4.1).

4.4.2 Stage and Discharge Monitoring.

The stage of stream is the height of water above an established datum plane (usually mean sea level). Gauge data was collected using an automatic stage recorder (3 m range Foxboro pressure bulb water level recorder) (Plate 4.2), at the gauging site located on the main stream

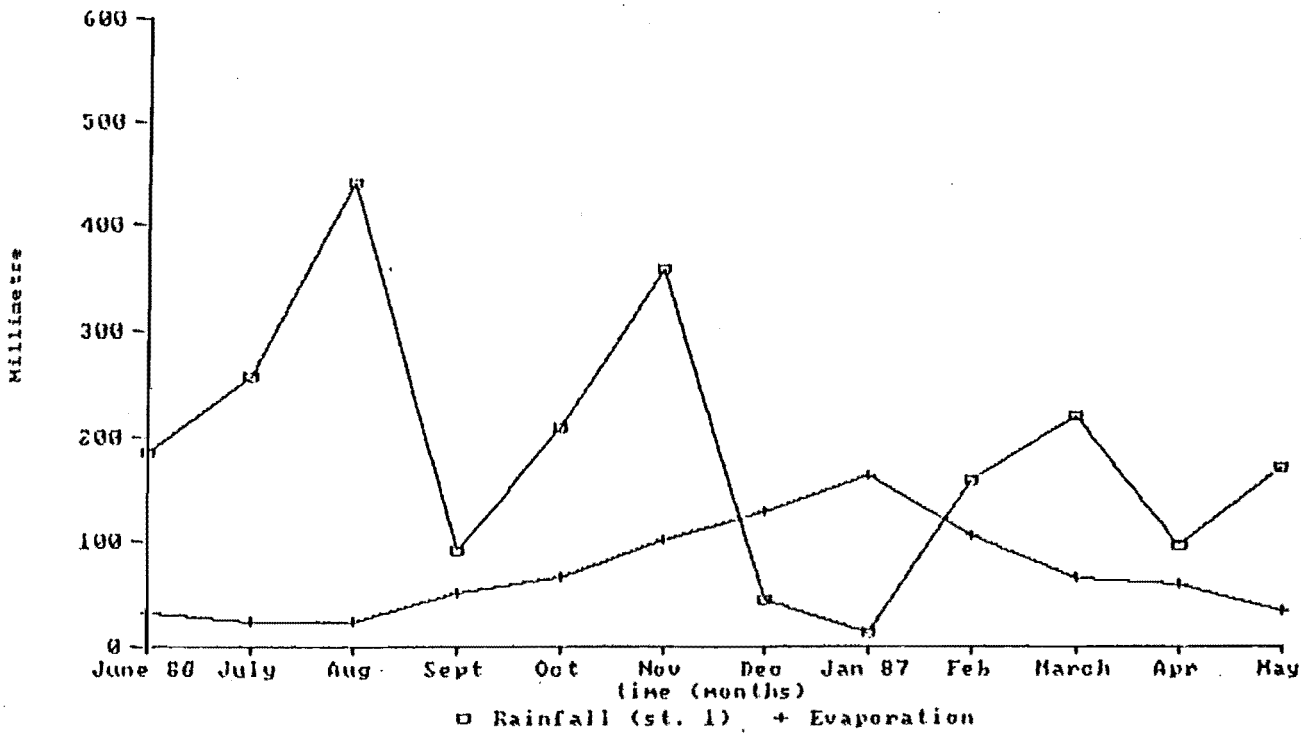

Figure 4.5 Evaporation and Rainfall Variation for June 1986 to May 1987

(Figs, 4.1 and 1.6). A Staff was used as an outside reference gauge for calibration of the stage recorder. The recorder supplied a continuous trace of the water stage with respect to time.

The monthly mean stage value for the water year (June 1986 - May 1987) indicates that the stage pattern is similar to the rainfall pattern. The result is presented in App. 9.1.

Discharge monitoring requires the determination of the cross-sectional area of a stream, and a sufficient number of velocity measurements across the station to permit determination of the average velocity perpendicular to the section. The technique used for measurement is described in App. 9.2.1. Measurements were undertaken using a Pygmy meter attached to a 1.5 mm wading rod. Velocities were measured using the one-depth method (0.6 x depth from the water surface) which is a standard technique for shallow water. Discharge monitoring was carried out at five stations (Fig 4.1) on a monthly basis during the water year (June 1986 -May 1987). Discharge and velocity measurements for the main station (Station A), and other streams is presented in App. 9.2.2. The resulting discharge and stage measurements were used to produce a rating curve and hydrographs for the monitored streams in the area.

4.4.3 Rating Curve

The relation of stage to discharge is a function of both section and channel controls. Section control is effective if a critical flow section exists a short distance downstream or upstream from the gauging site (eg. occurrence of pools), but this control is only effective at low discharge. At medium and high discharge, section control is submerged by channel control, which consists of all the physical features of the channel that determine the stage of the river. These control elements can be the size, roughness, alignment, stability of the streambed and banks, and the shape of the channel.

Stage-discharge relations are developed by plotting the stage against the discharge on rectangular-coordinate paper. The rating curve for a period of one year is presented in Fig. 4.6. The curve indicates that stage-discharge relations are relatively uniform. However, both control elements are effective over a particular range of stage (ie. compound controls). At low stage height (below 60 cm) the section controls are dominant (e.g. an existence of pools with higher water-level or weed growth). By increasing the stage, low water controlling elements

Figure 4.6 Rating Curves and their Periods

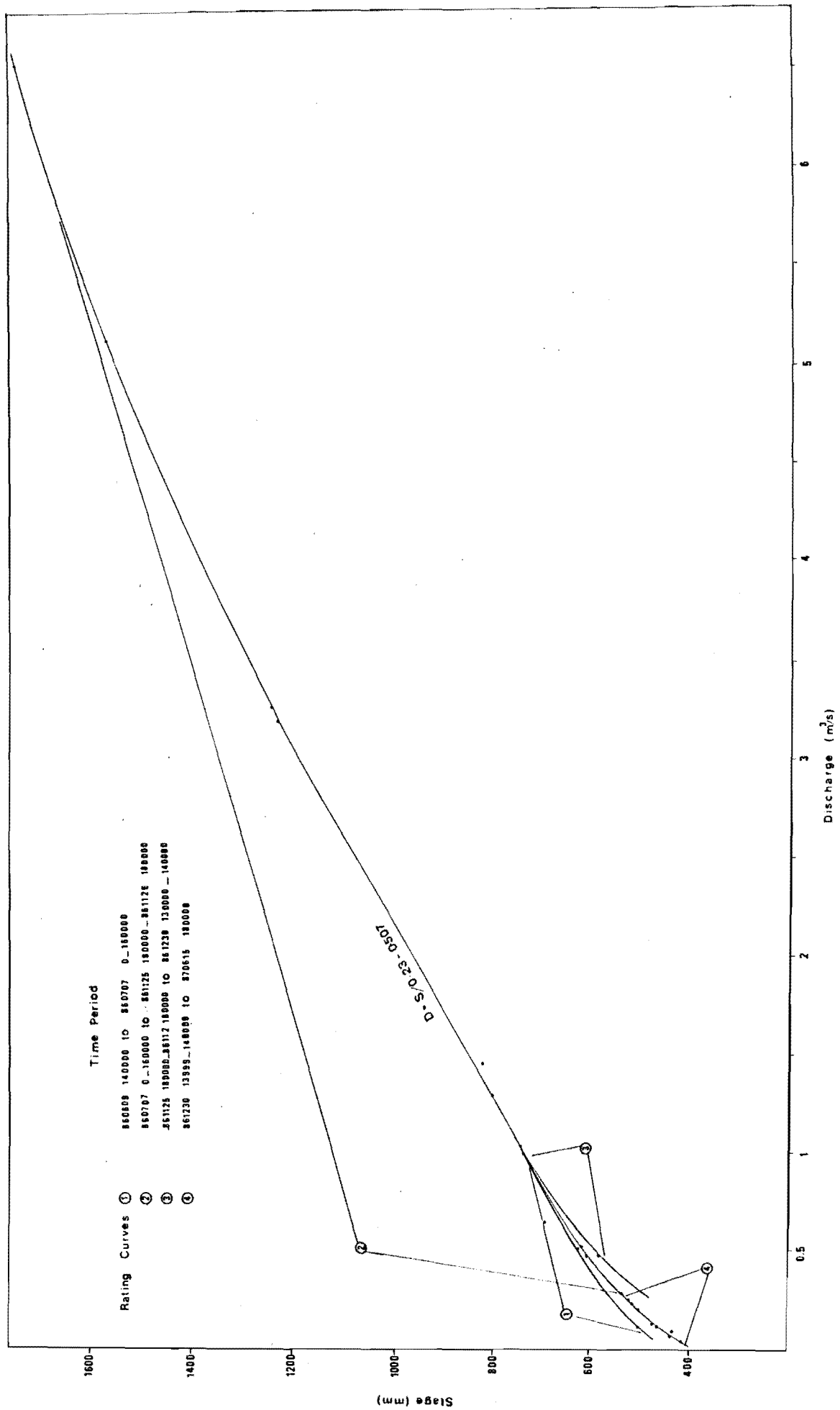

(section controls) are covered by higher level controlling elements (channel controls). This is the cause of a more uniform rating, as well as a straightening out of the typical parabolic curvature of the rating curve at the stages above 60 cm.

Any change in the stream bed during a period with a high stage, and high discharge will cause a more significant change in rating curve during a lower stage period (Fig. 4.6) with a lower discharge due to a higher flow sensitivity in the lower stage. Four different changes in rating were identified during monitoring over a 12 month period. The channel control is stable longer during rating curve no.2 ,identified between 860707 till 861126. 860707 till 861126), where the stage is higher than 60 cm. A change in the stream bed during this period resulted in a different rating at lower stage periods. Another factor which causes a change in rating during low stage periods, is the growth of weed. Weed growth is able to decrease the stream energy when the flow and discharge are at a lower rate - the stage for a given discharge shows an increase (e.g. rating no. 3 and 4 in Fig 4.6). In general the rating curve of the Kaituna River is indicative of relatively stable control elements.

4.4.4 Hydrographs

1) Hydrograph Sites.

A hydrograph is a chronological representation of the discharge of a river. It provides a convenient means of visualizing the behaviour of a stream under different climatic (hydrometeorological) conditions.

A hydrograph was established for each site (Fig. 4.1). Two sites were located on the main stream (discharge stations A and E)) and three were located on Okana stream (discharge station B), Takamina stream (discharge station C), and Packhorse stream (discharge station D).

2) Discharge Prediction.

Continuous discharge measurements were obtained by using a computer program (micro-TIDEA). This program is designed to carry out an interpolation procedure until the best straight line between stage and discharge coordinates is obtained. This procedure is carried out for each new rating period. Four different ratings were analyzed using this technique during the water year (June 1986 - May 1987), to obtain a continuous

record of discharge for the study period.

The stage - discharge relation also may be expressed by the following equation (Herschy 1985).

D = S/n - C (Linear equation)

where:

D = Discharge
S = Stage
n = gradient
C = the intersection of the line on the y axis.

For a linear portion of rating (No. 2);

D = S/0.23 - 0.507

The computer technique is preferred, as more consistent results are obtained using the interpolation procedure.

3) Hydrograph Correlations

To obtain a continuous discharge record for all gauging sites, results of discharge were correlated to the main gauging station which had a continuous stage recorder. This was undertaken to determine hydrographs for each site. Correlation factors ranged between .857 to .994, suggesting very good correlation. The computed regression equation is presented in Table 4.1 and the resulting hydrographs for each station are shown in App. 9.3.

Station No	Correlation Factor	Regression Equation
St. B (Okana)	.982	- 6.11 + 0.903 x A
St. C (Takmina)	.857	- 7.73 + .0452 x A
St. D (Packhorse)	.916	- 13.4 + .0986 x A
St. E (Kaituna at Packhorse)	.994	+ 23.9 + .650 x A

Table 4.1 Correlation Factors and Regression Equations For stream flow measurements.

4) Hydrograph Components and Separation

The two major hydrograph components are:

1) The direct surface run off component (quick flow), which consists of water that flows overland until a stream channel is reached. During storms this is the most significant hydrograph component.

2) The base flow component (delayed flow), which consists of the water that percolates downward until it reaches the aquifer, and then flows to the surface as groundwater discharge. In order to relate the direct runoff portion of a hydrograph to corresponding rainfall it is necessary to estimate the base flow and subtract it from total runoff (mean flow). The hydrograph separation was made with a straight line from the beginning of the rise of the hydrograph to the intersection with the hydrograph recession, which is the point where direct run off ceases. The separation for the major events during, the water year are presented in App. 9.4

5) Base Flow and Direct Run off Measurement Techniques.

There are several techniques which may be used to compute direct and base flows. Most of these methods are based on analyses of groundwater recession or depletion curves. If there is no direct flow and if all groundwater discharge from the upstream area is intercepted at the stream - gauging, then base flow can be measured by the following equation.

$$qt = q_0 K^t$$

where:

q_0 = a specified initial discharge (flow at the beginning of selected time interval)
q_t = the discharge at any time t after flow q_0
K = q_1/q_0 = a recession constant
q_1 = flow at the end of each intervals

For the purposes of this study a computer program (micro-TIDEA) was used to define the base flow and direct run off. First a hydrograph for each event was constructed, and the base flow separated graphically (App. 9.5). The base flow at the beginning (q_0) and the end of each event interval (q_1), together with their related time, was then used to compute the base and direct flow for the whole year, and for the eight major events determined during the water year (Table 4.2). The quantity of flow components for each event (Station A) is also illustrated in App. 9.5.

Using the correlation and regression equation shown in Table 4.1, base, quick, and mean flow was determined for other stations (Table 4.3).

Computed daily base and mean flow for the Kaituna Stream (Station A) is presented in App. 9.6 and 9.7.

Table 4.2: Flow Components for the Main Events

Event No.	Event period (yr/mon/day)	Mean flow (lit/sec)	Base flow (lit/sec)	Quick Flow (lit/sec)
1	860626-960717	2938	504	2434
2	860807-860817	2836	634	2202
3	860821-860915	5455	736	4719
4	861004-861024	2145	611	1534
5	861125-861206	5371	430	4941
6	870303-870307	2730	364	2366
7	870311-870316	2108	412	1696
8	870518-870527	2763	379	2389

Table 4.3: The Spatial Distribution of Mean, Quick and Base Annual (June 1986 — May 1985) Discharge For Streams

Stream Names	Mean flow		Quick flow		Base flow	
	lit/sec	mm/y	lit/sec	mm/y	lit/sec	mm/y
Kaituna (Stn.A)	1131	939	748	621	383	318
Okana (Stn.B)	96.02	79.7	61.43	50.1	28.5	23.6
Takamina (Stn.C)	43.4	36	26.1	21.6	9.58	7.95
Packhorse (Stn D)	98.11	81.4	60.35	50	24.36	20
Kaituna Stream at Packhorse (Stn.E)	759	630	510	423	272.8	226

4.4.5 Discussion of Results

1) Surface Water Resource Availability

The monthly minimum, mean and maximum values of base, quick, and total flow (mean flow) for the main stream are presented in Table 4.3. The daily flow value is also given in App 9.6. The total base, quick, and mean flows for each station are shown in Table 4.4.

The total available mean flow is 1131 l/Sec, 68% consisting of quick flow and the remaining 32% base flow. Mean annual specific yield from the basin is 938 mm y^{-1} for the water year over the monitored catchment area (38 km^2). This runoff (total flow) drains from the catchment via a network of smaller streams to the main stream outlet. Despite the relatively large water resource potentially available for allocation in the Kaituna Catchment, it is not distributed uniformly throughout the catchment. For example Packhorse stream (Fig. 4.1), has the highest flow rate of any tributary (102 l/sec), while Takamina stream to the west of Packhorse has the lowest discharge (45 Lit/Sec) with a smaller subcatchment area (Fig. 4.1).

2) Runoff - Rainfall Relationship

The spatial distribution of annual discharge is similar to the spatial distribution of rainfall; a lower response of mean flow to rainfall during dry season being due to higher evaporation. Daily and monthly mean rainfall and discharge are compared in Fig. 4.7.

The prediction of the percentage of rainfall appearing as runoff depends on the degree of seasonal climatic variation as well as the uniformity of the stream control elements (Sect. 4.4.3).

The precipation - runoff relationship is shown in Fig. 4.8. This relationship is more constant in a flow rate higher than 1100 l/sec or 75 mm over the monitored catchment (38 km^2) in a one month period. The relationship is estimated using the following equation.

$$Q = (1/s)\ (P - P_b)$$

where:

Q = mean flow (mm/month for monitored catchment area)
P = rainfall value (mm)
s= the slope of the line
P_b = a base precipation value below which Q is zero

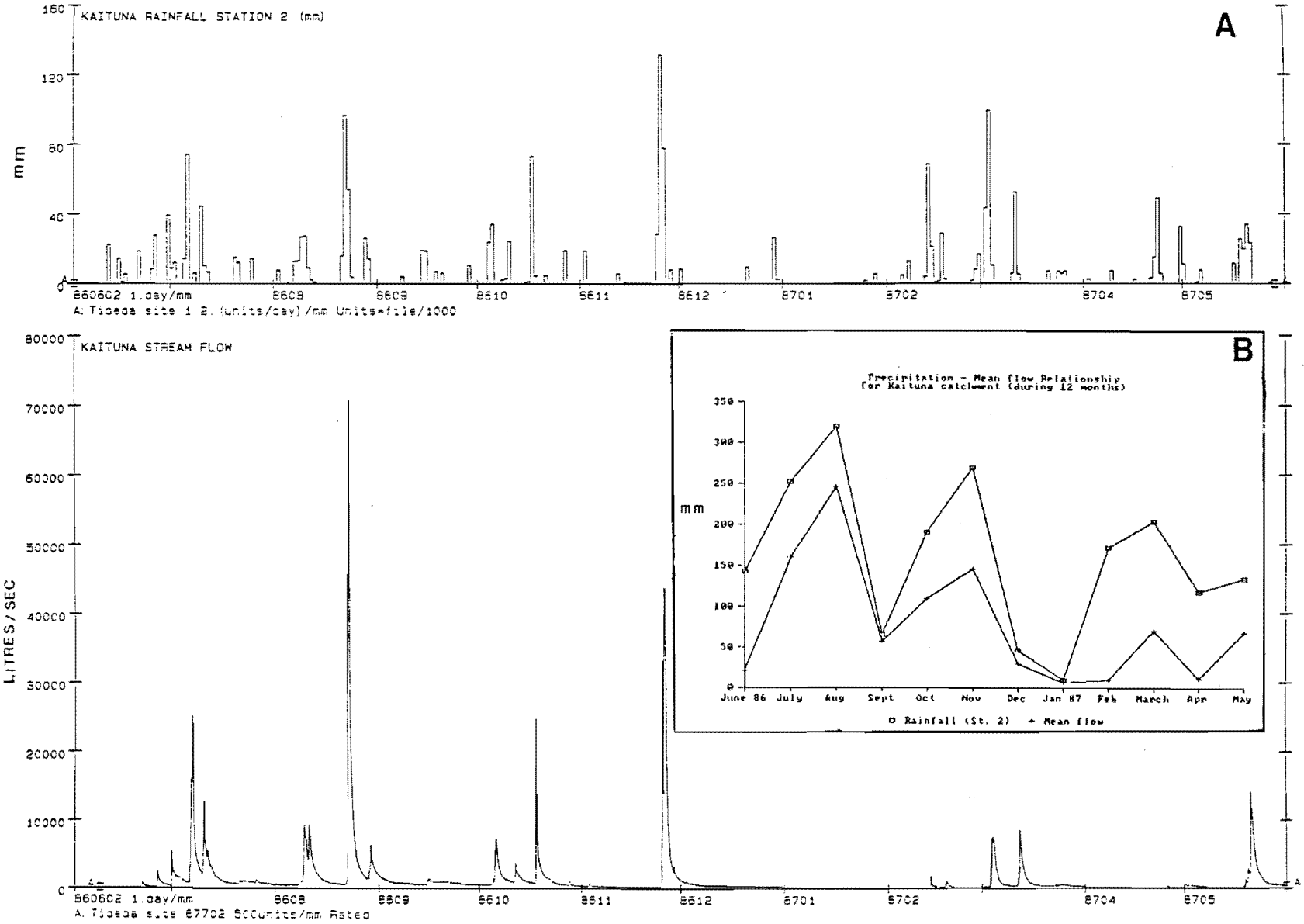

Figure 4.7 Preciptation-Mean Flow Comparison
A) Daily Comparison B) Monthly Comparison

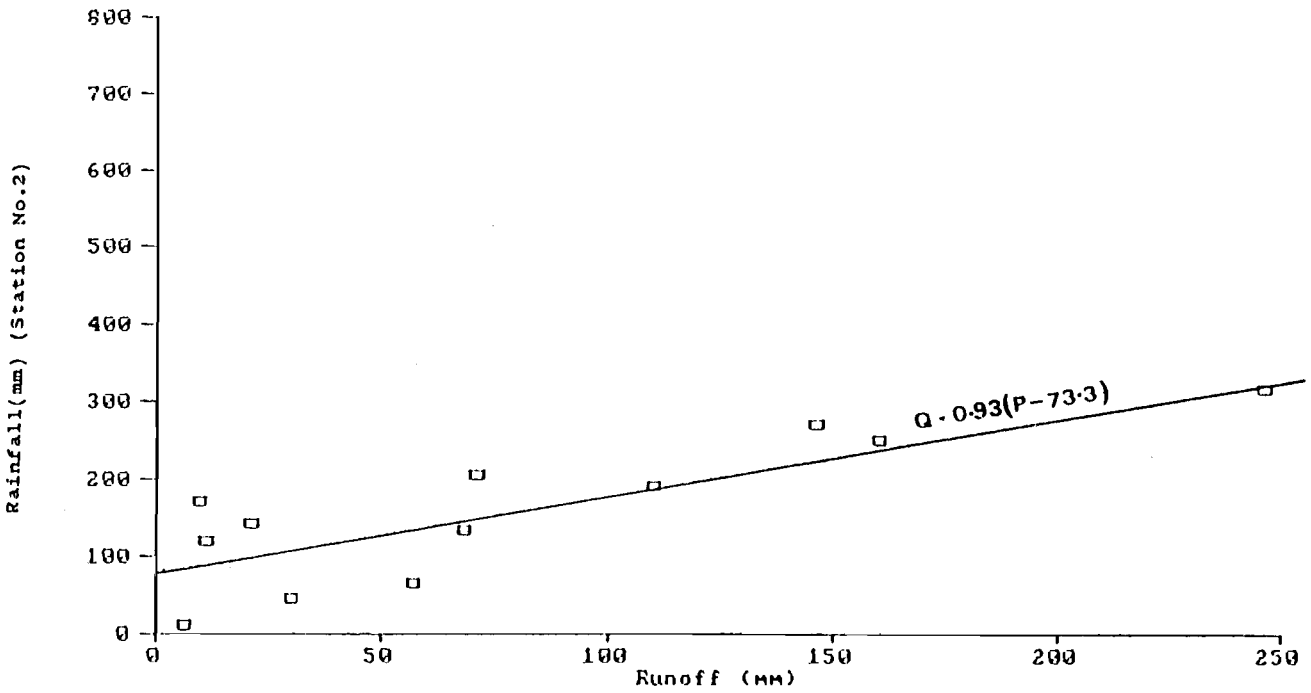

Figure 4.8 Precipitation Mean Flow Relationship for Kaituna Catchment (June 1986-May 1987)

Table 4.4: Ground Variation of Mean and Base Flow for the Main Stream (KaitunaSt A)

Monitored Period	Mean Flow (l/s)			Base Flow(l/s)		
	Min	Mean	Max	Min	Mean	Max
Jun 86	90	320	1190	86	205	566
Jly 86	550	2270	1600	342	687	1055
Aug 86	450	3620	4286	450	633	794
Sep 86	550	850	1710	551	789	1222
Nov 86	210	2140	31920	206	306	551
Dec 86	220	430	1080	209	379	531
Jan 87	28	87	162	28	85	153
Feb 87	21	150	597	21	83	191
Mar 87	220	1007	6394	220	379	538
Apr 87	104	106	306	104	161	306
May 87	138	971	9966	138	306	548

For the monitored catchment, the prediction of runoff for any given rainfall can be estimated using the equation.

$$Q = (1/1.07)(P - 73.3)$$

and therefore

$$Q = 0.93\ (P - 73.3)$$

3) Seasonal Variation of Flow

The seasonal variation of maximum, minimum and mean monthly total flows for the Kaituna River station is shown in Figs. 4.9 and 4.10. Table 4.4 shows the variation the variation of monthly mean and base flow (for station A). Seasonal variations in flow are highly pronounced, with the maximum flow showing a variation of up to 91% higher than mean monthly flow (August, 1986), and the minimum flow up to 87% lower than mean monthly flow (August, 1986). The smallest variation in flow occurs during summer (25% of the mean flow in February 1987). This indicates that low discharge is independent of storm rainfall and is sustained by groundwater derived from springs. The maximum river flow occurred on 23rd August 1986 (42810 l/sec), while the minimum discharge occurred on 7th February 1987 (21 l/sec). August (1986) has the highest mean flow (3620 l/sec), while the lowest mean flow of the river occurs in January 1987.

4) Data Analysis in Term of Infiltration

All 5 hydrographs (each with eight major events) from the Kaituna River and other tributary streams demonstrate a similar response to rainfall. During storm run off, quick flow is very high (Figs. 4.12 to 4.17), while base flow increases only fractionally (eg. 13.7% of total mean flow during the eighth event, App. 9.4). In addition, comparison of the daily and monthly mean rainfall intensity and the hydrograph from the main streams (Fig. 4.7), indicates that the time lag between the peak of the rising limb and the maximum rainfall is almost instantaneous. These two phenomenon indicate that the rate of infiltration through the stream bed during flood events is negligible (Sect. 5.5.1).

4.5 Synthesis

The head waters of all tributary streams are fed by springs originating from volcanic and colluvial deposits. The rainfall data for the

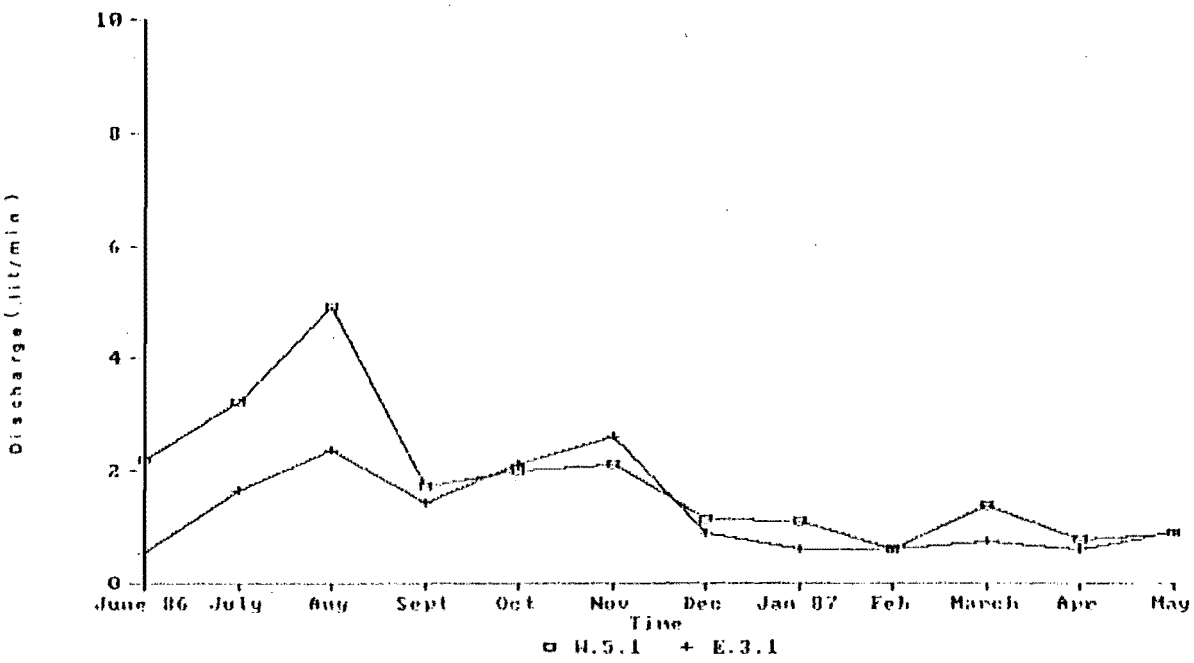

Figure 5.14 Spring Discharge (W.5.1 and E.3.1)

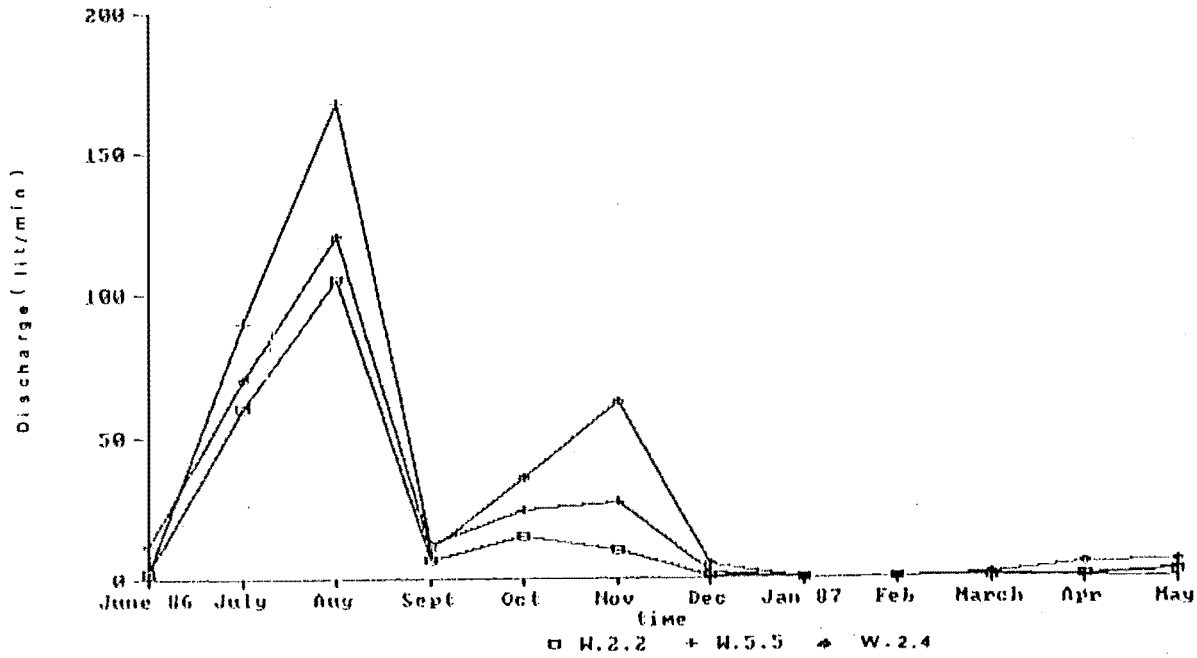

Figure 5.15 Spring Discharge (W.2.2, W.5.4, and W.5.5)

catchment suggests a positive relationship with height above sea-level (rainfall increases with increasing elevation).

Total average rainfall is 1900 mm and total evaporation over the monitored catchment is 860 mm.

The total potential surface water resource is 429.8 x 10^5 m^3 (1131 l/sec mean flow or 938 mm of water for whole monitored catchment). Of this, 68% is quick flow and the remaining 32% base flow.

The spatial distribution of annual discharge is similar to the spatial distribution of rainfall, and seasonal variation of flow is highly pronounced in the area. Small flow variations occur during summer, which indicates that low discharge is independent of storm rainfall, and is sustained by groundwater derived springs during the dry season.

CHAPTER FIVE

GROUNDWATER HYDROLOGY

5.1 Introduction and Objectives

Proper groundwater resource evaluation requires a knowledge of aquifer characteristics, piezometric fluctuations, discharge and recharge mechanisms, hydrogeological model and water balance components. Data regarding aquifer distribution and the hydrologic components of surface water are therefore essential for conducting the investigation.

The objectives for the groundwater investigation are given below:

1) The hydraulic characteristics of aquifers are determined to provide a measure of their productive capacity. The hydraulic parameters determine the rate at which water may be extracted, and also the effect which any production bore will have on either the aquifer or on another bore intersecting the same aquifer.

2) Piezometric fluctuations were carried out in order to: a) further define aquifers according to their piezometric grouping; b) describe the responses of the aquifers to seasonal hydrological inputs; and, c) determine groundwater flow patterns and movements.

3) Spring monitoring was undertaken in order to determine the groundwater discharge mechanism.

4) Two possible recharge models were investigated in order to define the best model suited for recharge of the groundwater system in Kaituna Valley: a) stream - aquifer interaction model; and b) fracture infiltration model.

5) The water balance component was identified in order to evaluate the groundwater resource.

6) The results of this investigation is used to generate a hydrogeological model for the groundwater system in Kaituna valley.

5.2 Aquifer Hydraulic Characteristics

5.2.1 Aquifer Parameters

The most important aquifer parameters are hydraulic conductivity,

transmissivity, storage coefficient and safe yield. These parameters are determined by a pumping test, slug tests and free flow tests in the boreholes shown in Fig. 5.1. The definitions of hydraulic properties are given in App. 10.1.

5.2.2 Base Aquifer Hydraulic Properties

1) The Step Drawdown Pumping Test on Bore M36/1344

a) Interpretation of Aquifer Properties

In step drawdown tests the drawdown of a well is observed while the discharge rate from the well is increased in steps. The test was carried out on well M36/1344 by Ministry of Agriculture and Fisheries on 3rd of May 1985. Field data is presented in App. 10.2. The test was interpretated by North Canterbury Catchment Board (Talbot and Callander, 1986), and reproduced by author, using new computer inputs to obtain a more accurate estimation of aquifer characteristics. The computer programme used for data interpretation is called THOM1 (App. 10.3). The programme is based on Theis's equation (Clark, 1977);

$$s = \frac{QW(u)}{4\pi T} + C\,Q^2 \qquad \text{and} \qquad u = \frac{r^2 S}{4Tt}$$

Where

Q = the constant pumping rate
s = drawdown
r = effective radius of the pumping bore
T = the aquifer transmissivity
S = Storage Coefficient
t = time since pumping started
W(u) = The well function of u
C = well loss coefficient

The equation parameters and step drawdown test technique are described in detail by Clark (1977), Hazel (1975) and Walton (1970).

A trial and error approach was adopted in this study to define a set of aquifer properties which would reproduce the drawdown measured during the test. Due to the number of parameters to be defined, the operation was highly complex and time consuming. The main parameter change from the previous interpretation was the lateral aquifer boundary. The resistivity data indicates a larger groundwater channel in the well site (KC4, resistivity sounding site), and therefore the lateral boundary parameter in the computer model was extended. The new

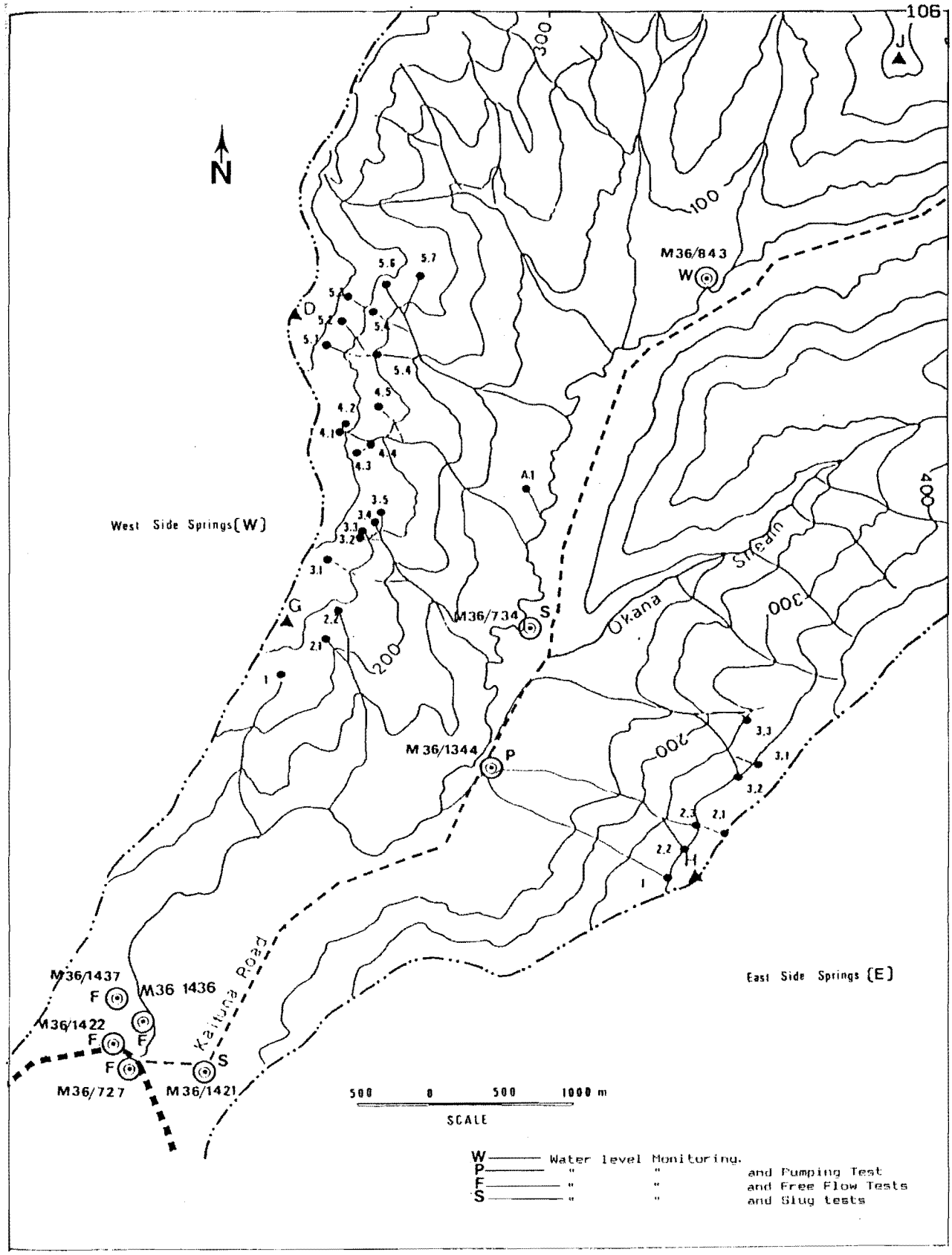

Figure 5.1 Location of Monitored Boreholes and Springs

set of aquifer parameter give a more accurate reproduction of the water level measured in the step drawdown test. The parameters used in the programme to give the model shown in Fig. 5.3 are presented in App. 10.3. The model was constructed using a transmissivity value of 0.0048 $m^2\ s^{-1}$ and a storage coefficient of 0.0025. Specific Storage therefore is $1.25 \times 10^{-3}\ m^{-1}$.

It should be noted that in a single well drawdown test, that during the first few minutes, the outlet pipes are still empty and the pump works against a very small pressure, and therefore its actual discharge is much larger than the rated discharge (Mandel 1981). The initial part of the test during which the main portion of the drawdown occurs does not match the computer model (Fig 5.2).

b) Safe Yield and Drawdown Prediction

The safe quantity of water available for extraction is dependent on the amount of water seepage into the aquifer from the volcanic bedrock, and this varies throughout the year. In dry conditions (water level at depth of 10 m) the computer model indicates that the maximum continuous pumping rate for 24 hours would be about 12 litres per second. The aquifer cannot sustain spray irrigation for more than this period and pumping should be stopped to allow aquifer recovery.

The computer program thomXX (App. 10.4) was used in this study to predict drawdown around the pumping well. The recharge to the aquifer due to pumping was decreased in the model to enable prediction of drawdown in drier climatic conditions.

The amount of drawdown after 24 hours at a pumping rate of 14 l/sec at 100 m distance from the pumped bore is shown in Fig. 5.3. As shown, drawdown at this imaginary site will start after 5 minutes pumping with the highest drawdown rate in the first 155 min.

The rate of drawdown after 12 hours at different distances from the bore was estimated using the same method. The drawdown prediction model is illustrated in Fig 5.4, from which it can be seen that at 1000 m from the pumping bore M36/1344 (eg. at M36/734), the first measurable drawdown occurs after 12 hours pumping (Q=14 l/sec).

2) Slug Test on Bore M36/734

The hydraulic conductivity and transmissivity values for the

Figure 5.2 Pump Test Measurements and Model Prediction (M36/1344)

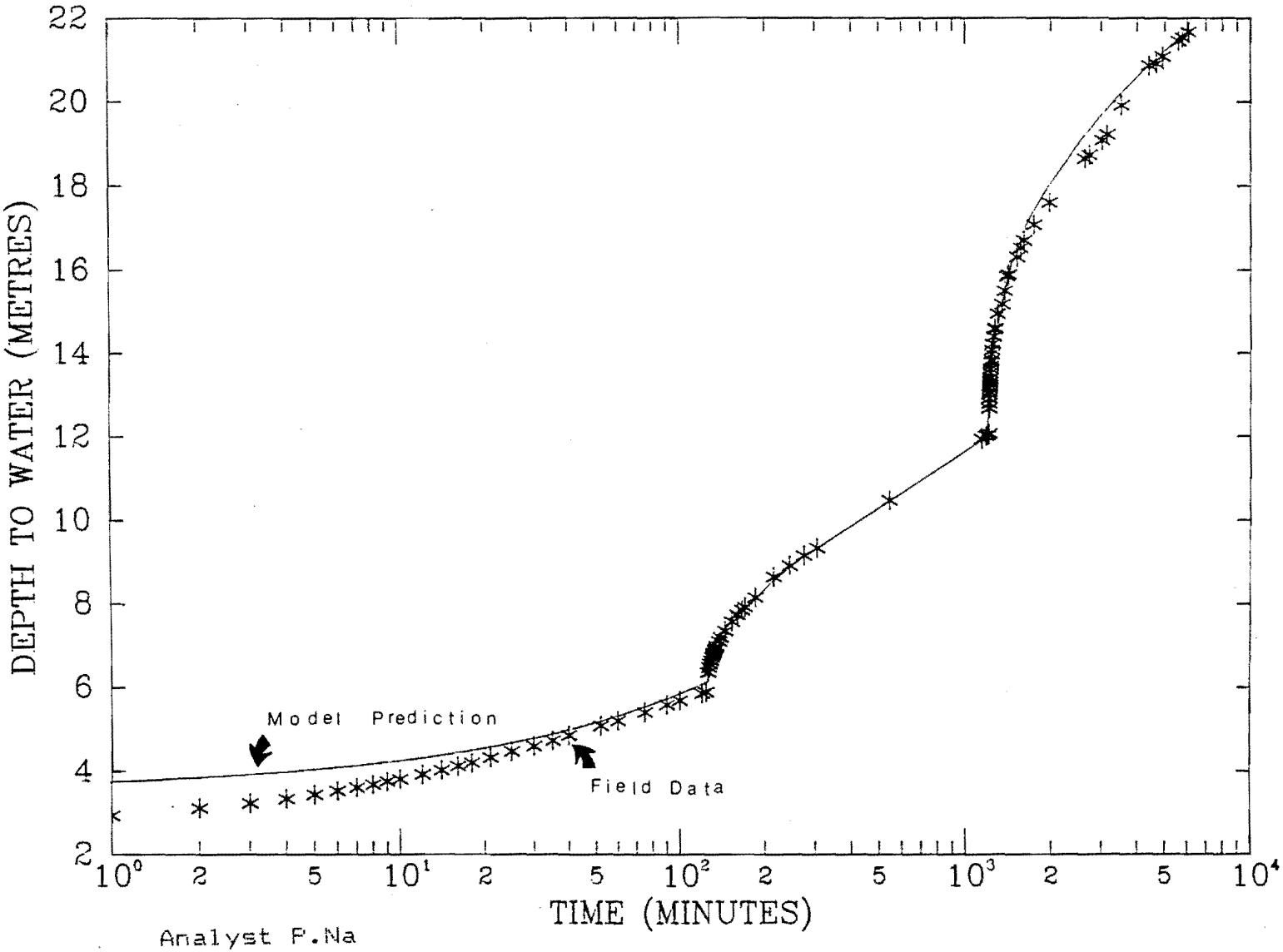

Figure 5.3 Predicted Drawdown due to Pumping (Q = 14l/s) from Bore M36/1344« at 100 m distance »

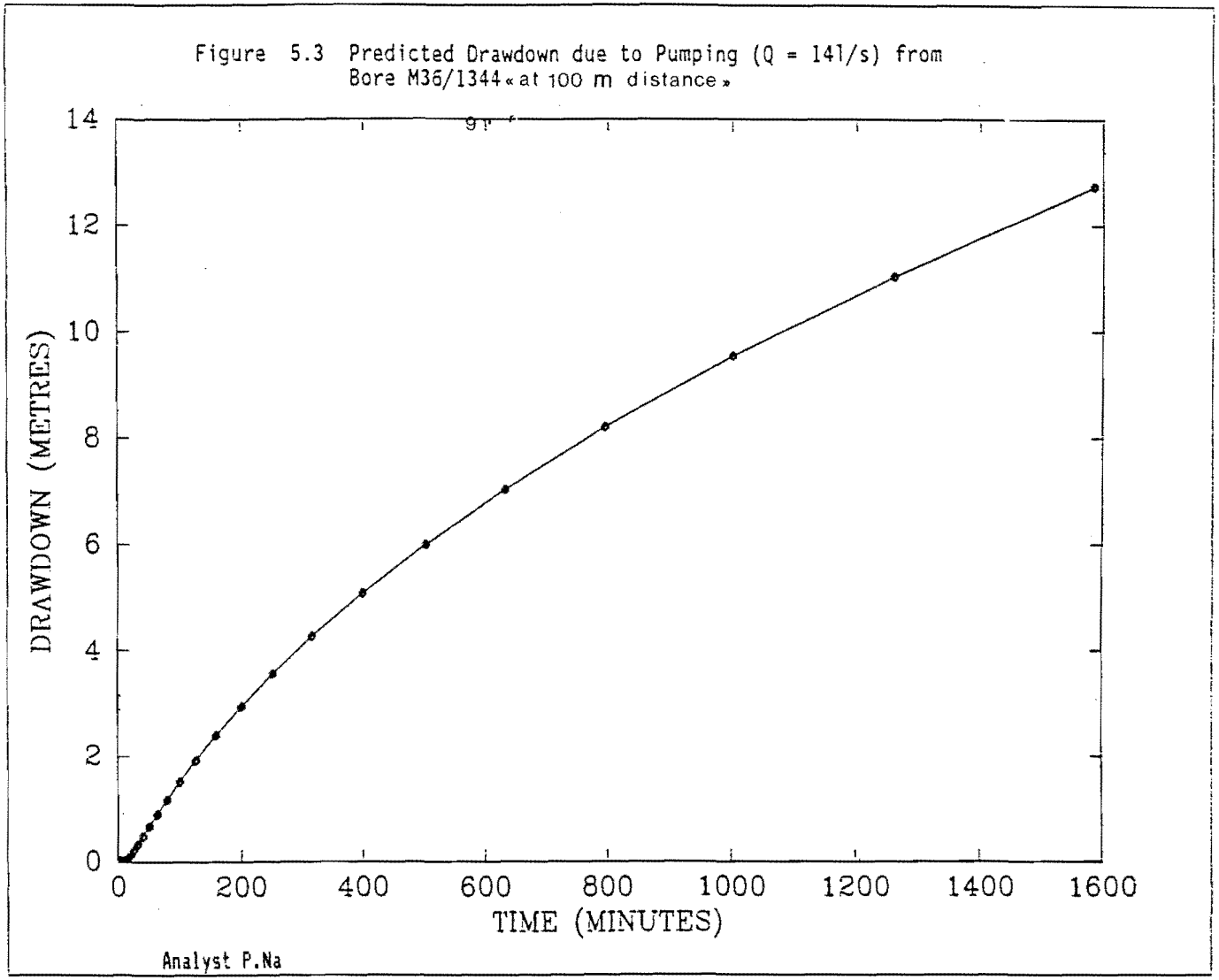

Figure 5.4 Drawdown Around Bore M36/1344 after 12 Hours Pumping at 14l/s

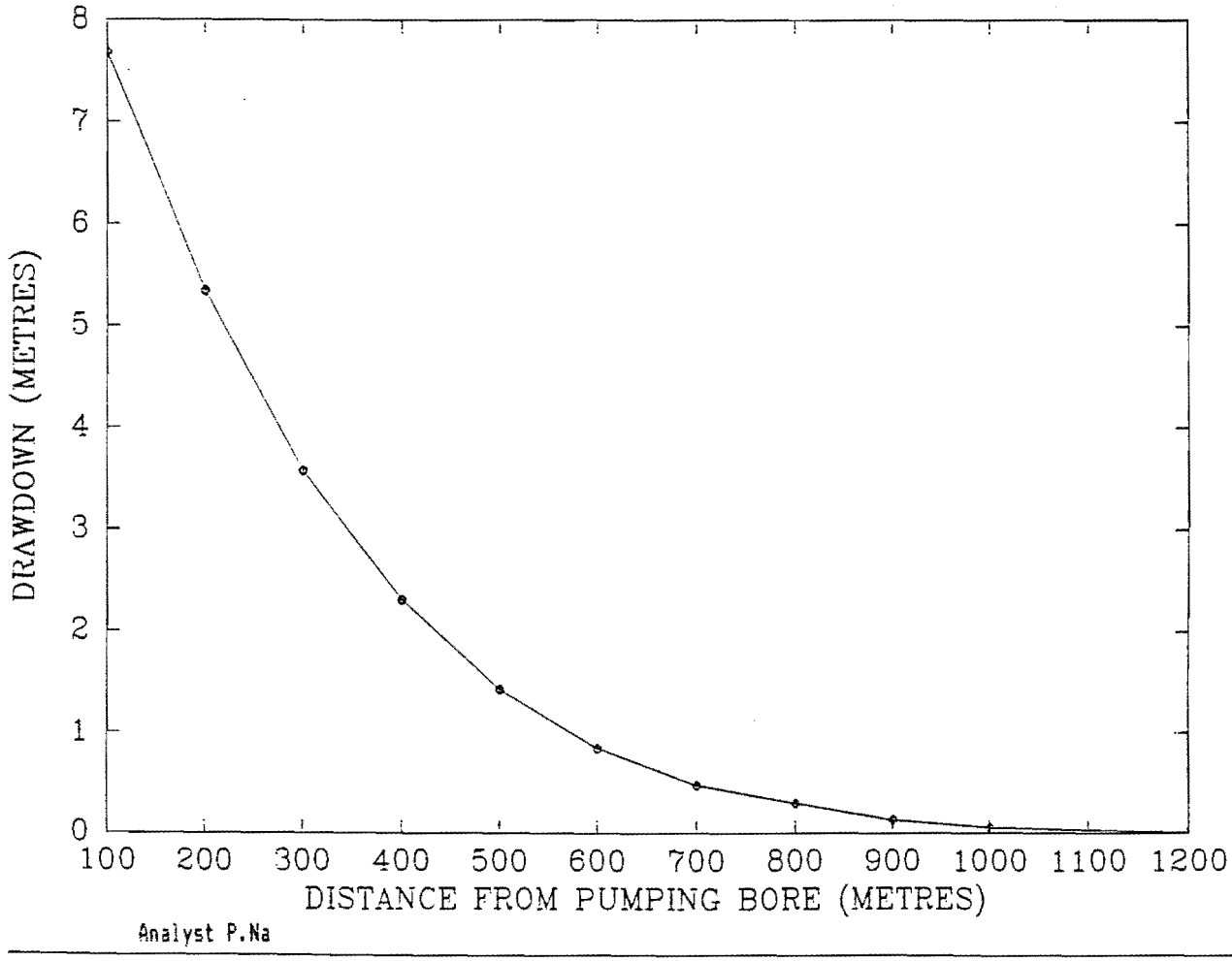

lower aquifer at bore site M36/734 were also determined using a Slug test. Tests were initiated by causing an instantaneous change in water level in the bore through a sudden introduction of water (using a water pump with a 500 litre capacity). The recovery of the water level with time was then monitored. The method, water level recovery, and test calculations are presented in App. 11 (A.11.3, A.11.4, A.11.5). As is shown in table 5.1, the hydraulic properties of this bore and bore M36/1344 are identical.

5.2.3 Upper Aquifer Hydraulic Properties

The hydraulic properties of the upper aquifer are identified using free flow and slug tests. Although a free flowing well (artesian well) is not pumped, the method of calculating the transmissivity is closely related to the analysis of pumping tests, and the test procedure is described in App. 11.1. Free flow tests were conducted on artesian wells in the lower part of the valley (M36/1436, M36/1437, M36/727, M36/1422) and slug tests on well 1421. The free flow calculations are shown in App. 11.2, and the result are presented in Table 5.1. During the tests on wells M36/1421 and M36/727 the steady state was not quite achieved as the rate of head fluctuation was more than 0.05 m per hour, which is an undesirable rate (Lee, 1984). The reliability of the resulting permeability values of 1.02×10^{-2} m/s and 7.74×10^{-3}m/s for upper aquifer is therefore questionable and is omitted from future analysis.

The problems associated with air entrapment in boreholes is a major limitation to the slug tests. The reliability of slug tests are also strongly dependent on the condition of the bore intake, and corroded or clogged wells may cause inaccuracies in measured values.

The transmissivity values (Table 5.1) are higher for the upper aquifer than for the base aquifer, due to their different thickness. The hydraulic conductivity of both aquifers are comparable, ranging from 1.03×10^{-3} m/s to 2.04×10^{-4} m/s for upper aquifer, and from 2.4×10^{-3} m/s to 9.6×10^{-4} m/s for lower aquifer (low to medium permeability, App. 3.2).

Table 5.1: Groundwater Transmissivity

Aquifer	Lower Aquifer		Upper Aquifer		
Bore no.	M36– 734	M36–1344	M36–1437	M36–1436	M36–1421
Grid.Ref. M36—	647 175	844 165	822 1522	823 150	827 146
Depth (m) (G.L)	21.2	29.6	70.3	90.72	48.58
Depth (m) (R.L)	10.49	6.45	3.25	2.93	2.85
Diameter (mm)	75	200	55	55	75
Test Type	Slug Test	Step Drawdown (Pumping)	Free Flow	Free Flow	Slug Test
Hydraulic Conductivity (m/s)	9.6×10^{-4}	2.4×10^{-3}	2.04×10^{-4}	7.75×10^{-4}	1.03×10^{-3}
Transmissivity (m^2/s)	4.3×10^{-3}	4.8×10^{-3}	4.9×10^{-3}	1.86×10^{-2}	2×10^{-2}

5.3. Piezometric Survey

5.3.1 The Piezometric Monitoring

Piezometers in eight bores were monitored from June 1986 to May 1897. Monitoring was carried out manually on a one week basis by staff of North Canterbury Catchment Board. Water levels in the bore were monitored using a standard W/A twin-cable electronic probe with an estimated accuracy of $\leq$2% The weekly data is presented in App. 12, and the monthly mean values are shown in Table 5.2.

5.3.2 Piezometric Data Interpretation

1) Vertical Distribution of Piezometric Head.

Vertical distributions of piezometric heads are presented in Figs 5.5 and 5.6. Seasonal and short term piezometric fluctuations indicate a significant drop in water level during dry conditions between November 1986 and March 1987 (eg. from 5.12 m in August 1986 to -1.6 m in January in well M36/1344). A sharp drop in piezometric level in January (1.63 m in December to -1.6 m in January, in well M36/1344) could be due to greater extraction of water by pumping

Deeper wells (M36/1436, and M36/1437) are less affected by the seasonal variations of rainfall and this is considered to be mainly due to a longer distance from the recharge area (see section 5.5).

Vertical differences in mean piezometric pressure with bore depth are shown in Figs. 5.7 and 5.8. The plots for the bores within the upper aquifer demonstrate a general trend toward higher piezometric pressure with increase in bore depth except for bore M36/1422 (45.85 m depth) which has a slightly higher piezometric head than expected (compare with bore M36/1421 with a 48.6 m depth). However, the sensitivity of measuring piezometric head is less than the variation expected for a 2.5 m difference in bore depth. On the basis of this data, it is inferred that the underlying deeper parts of the upper aquifer are generally acting as recharge sources for upper parts of the aquifer. The bores within the lower aquifer are located in different elevations, and the plots (Fig. 5.7) demonstrate a decline in piezometric pressure with increasing bore depth (decrease in aquifer elevation), indicating that recharge potential zones have a direct relationship with altitude.

Table 5.2: Water Level Monthly and Annual Mean Values

Year	1986						
Month / Well No.	June	July	Aug	Sept	Oct	Nov	Dec
727	3.40	3.52	3.65	3.56	3.89	3.62	3.83
734	6.35	7.16	7.09	6.56	6.04	5.87	5.10
843	24.6	25.1	25.1	25.0	24.9	24.8	24.8
1344	5.12	5.53	3.31	5.22	5.19	5.02	1.63
1421	3.21	3.48	3.56	3.56	3.34	3.2	2.39
1422	—	—	4.06	4.07	3.99	3.69	3.18
1436	6.30	6.3	6.36	6.34	6.61	6.5	6.34
1427	6.35	5.98	6	6.15	6.22	6.04	5.92

Year	1987					
Month / Well No.	Jan	Feb	March	Apr	May	Annual Mean Value
727	3.44	2.7	3.41	3.45	3.93	3.5
734	1.14	3.09	6.21	6.69	6.9	5.68
843	24.4	24.4	24.5	24.4	24.6	24.71
1344	-1.6(P)	1.5	4.79	5.15	5.21	4.27
1421	0.56	1.27	3.19	3.27	3.37	2.86
1422	p	p	3.76	3.91	3.92	3.4
1436	6.5	6.66	6.39	6.46	6.47	6.31
1427	5.6	5.18	5.83	5.86	6.26	5.94

Note: p means pumping,
— means no reading

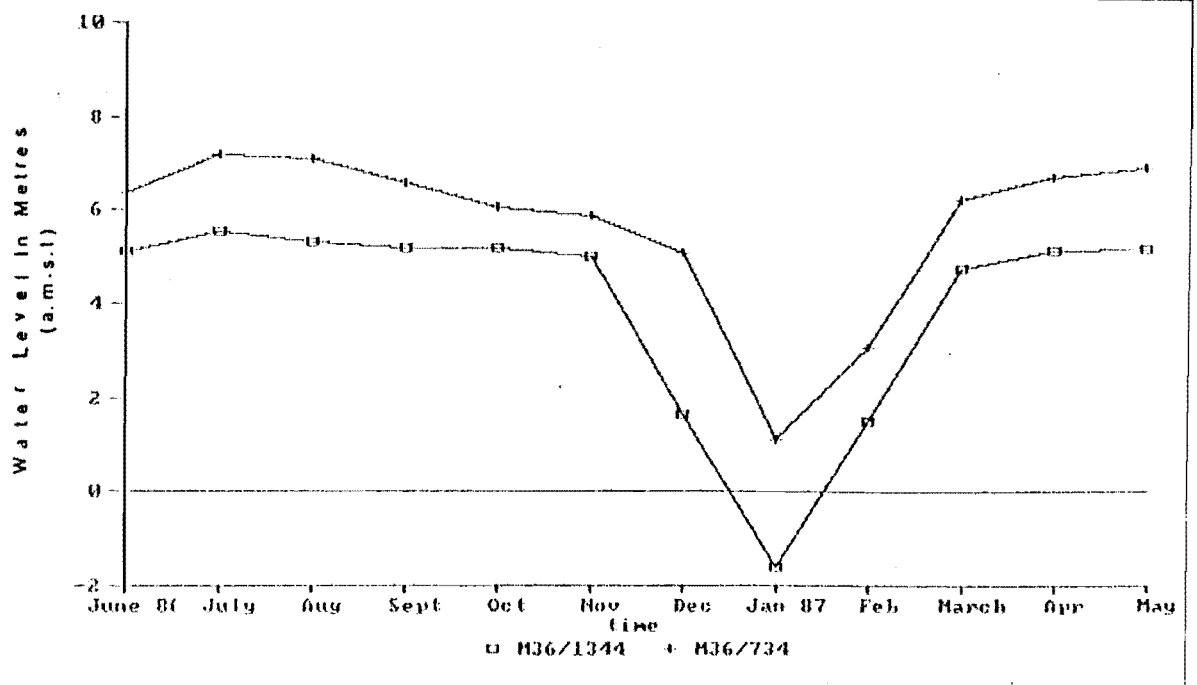

Figure 5.5 Water Level Fluctuations in Wells M36/1344 and M36/734

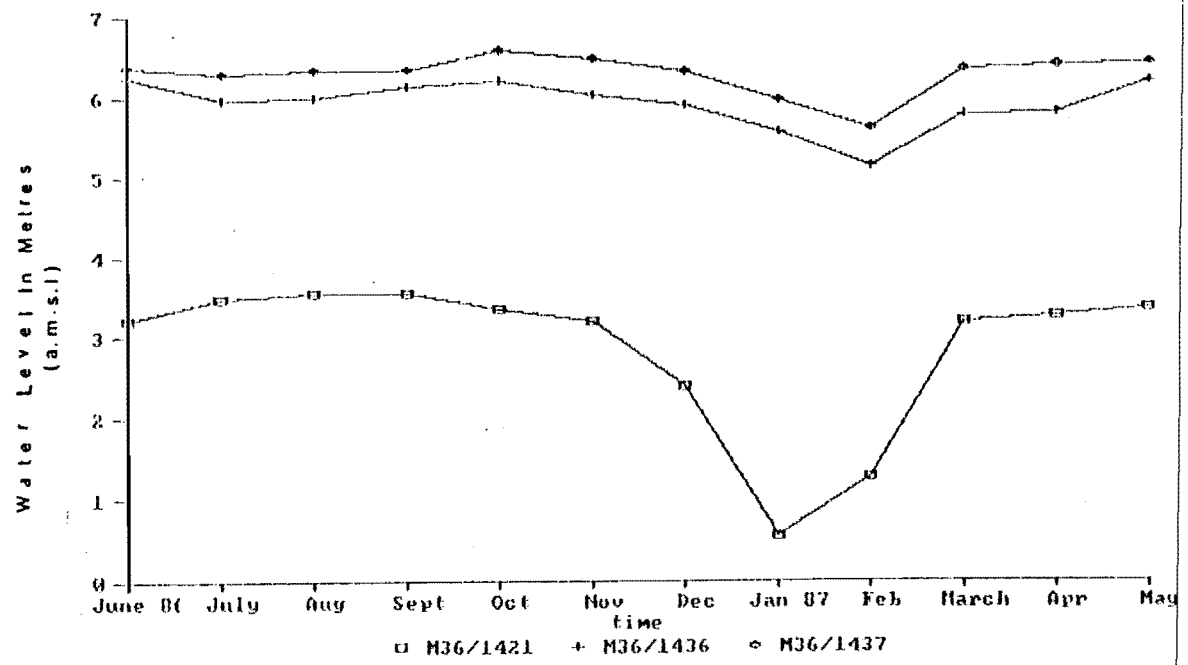

Figure 5.6 Water Level Fluctuations in Wells M36/1421, M36/1436 and M36/1437.

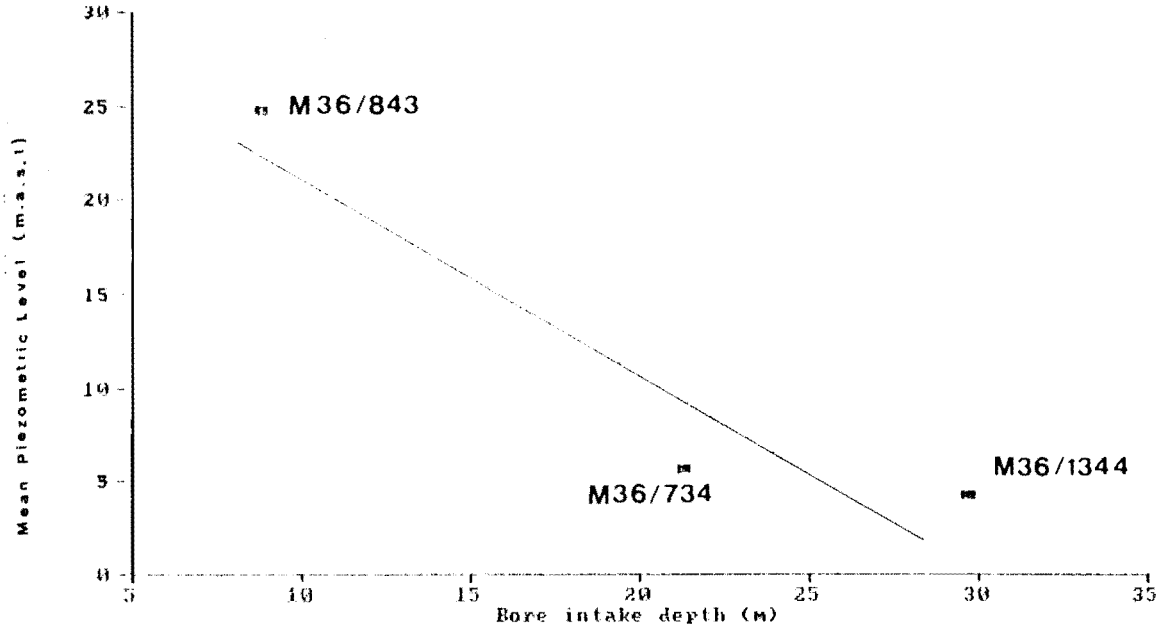

Figure 5.7 Mean Piezometric Level v Well depth for Lower Aquifer

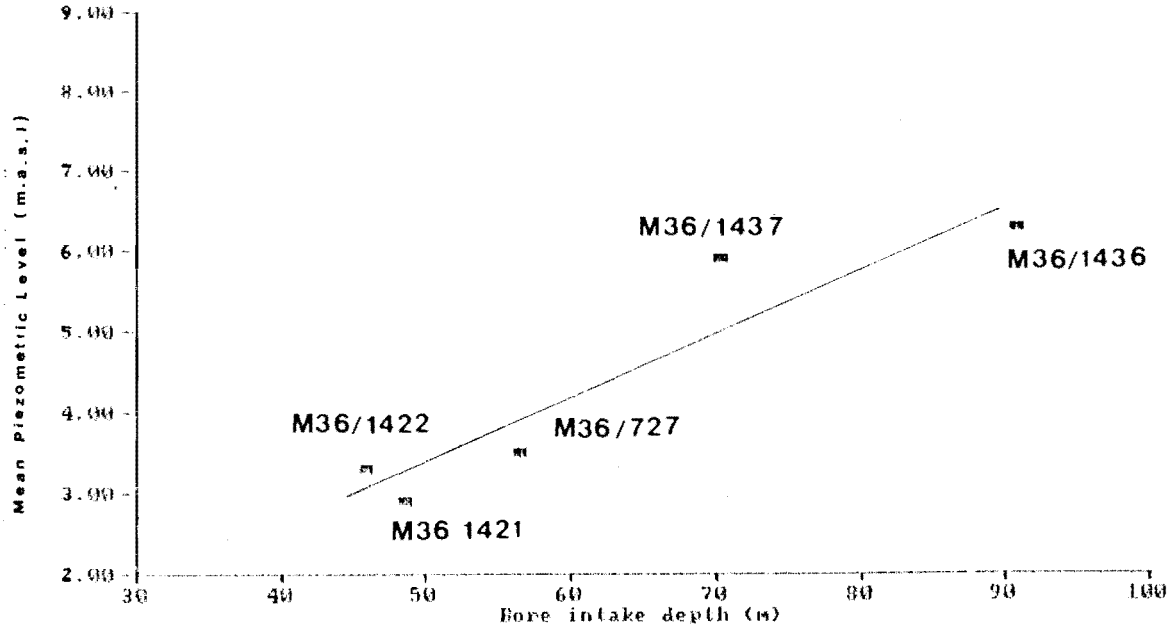

Figure 5.8 Mean Piezometric Level v Well Depth for Upper Aquifer

By comparing the resultant piezometric contour to contours for the south side of the lake (Mandel, 1974) and the lake level, it appears that Lake Ellesmere is in hydraulic connection with groundwater because piezometric levels around the lake are higher than water level in the lake (Fig. 5.9). However water fluctuations in the lake and in the adjacent wells differ, and do not show a direct interaction between the two.

2) Piezometric Contour Analysis

The distribution of piezometric head, as shown in Figs, 5.10, 5.11, 5.12, 5.13, provides a better understanding of the direction of groundwater movement, and hence of groundwater discharge and recharge patterns. Piezometric contour maps were constructed for summer and winter conditions using piezometric data from all bores monitored in the area. Piezometric gradients are lower for the section within the lower aquifer (Fig. 5.10, 5.11), and indicate that groundwater flow is likely to be slower in this section, with wide contour intervals. Piezometric levels drop for all bores during summer, with a small decrease for the wells within the upper aquifer (Fig, 5.12, 5.13) in the lower part of the valley close to the Lake Ellesmere.

Overall, flow patterns in wet and dry conditions are the same. The piezometric gradients and hence flow rates are clearly lower for the lower aquifer in summer conditions (Fig. 5.10). There is no distinct seasonal change in piezometric gradient for the upper aquifer (Figs. 5.12, and, 5.13), which is attributed to a longer flow path for the water in the upper aquifer.

5.4 Spring Discharge Variations

The springs and the groundwater systems feeding them are closely related to each other. The characteristics and variations of groundwater discharge were identified by the monitoring of 27 springs for a 12 month period (June 86 - May 87). The locations of the monitored springs are shown in Fig 5.1. Springs are named according to their location in the valley side (east,E or west,W) and their subcatchments. For example spring "E.3.1" indicates an east side spring, subcatchment 3, and spring number 1. The discharge values are given in App. 13.2.

Figure 5.9 Mean Piezometric Level Compared with Lake Ellesmere Water Level

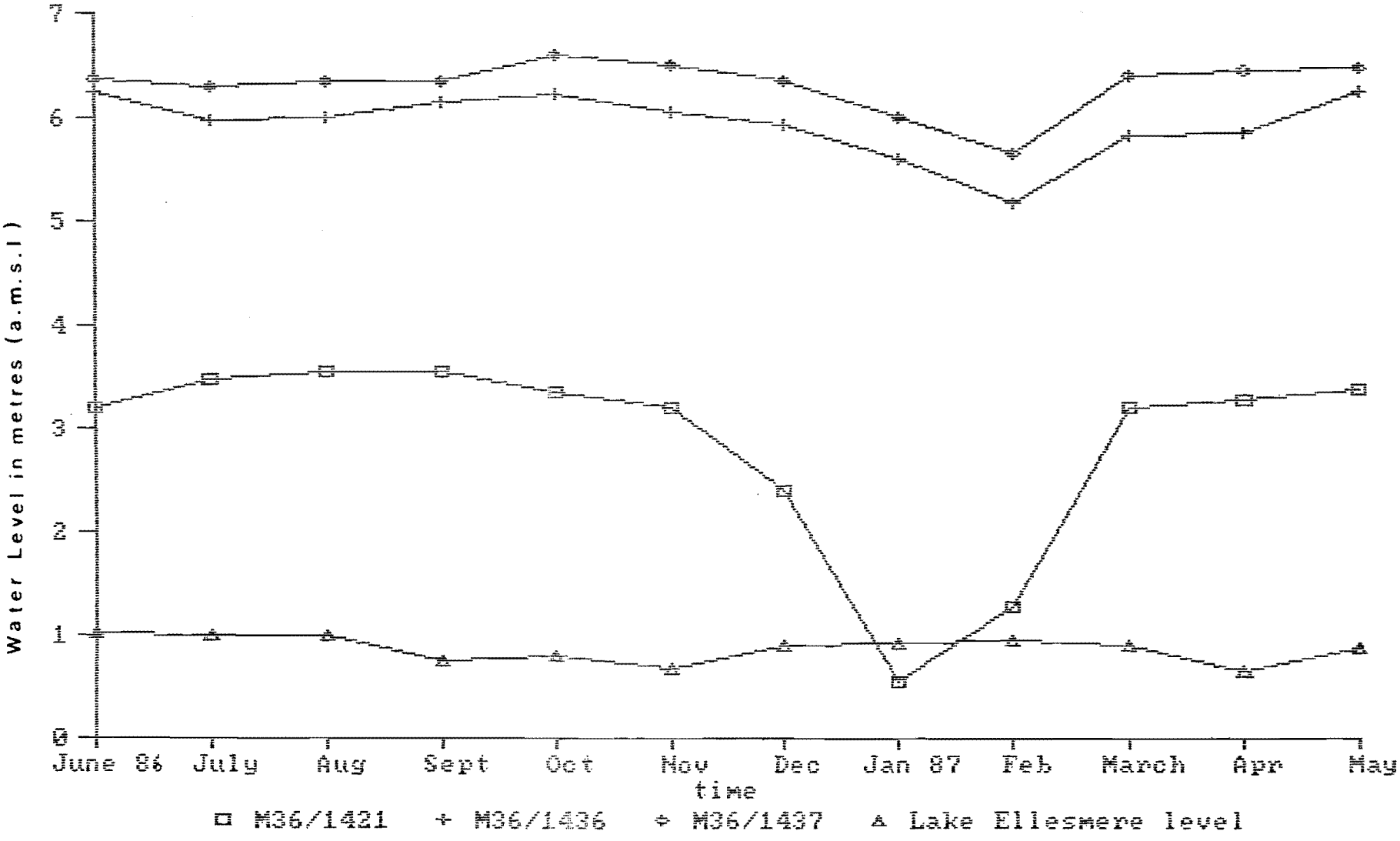

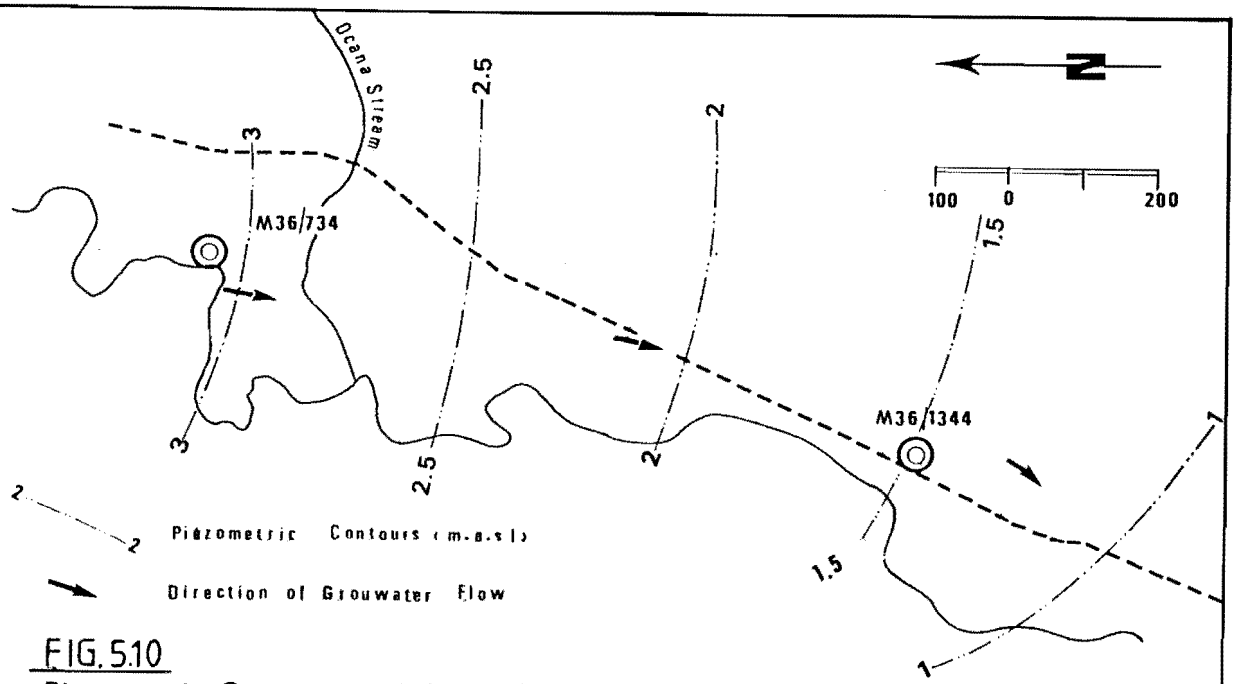

FIG. 5.10
Piezometric Contours and Groundwater Flow Direction for Lower Aquifer (Feb. 1987)

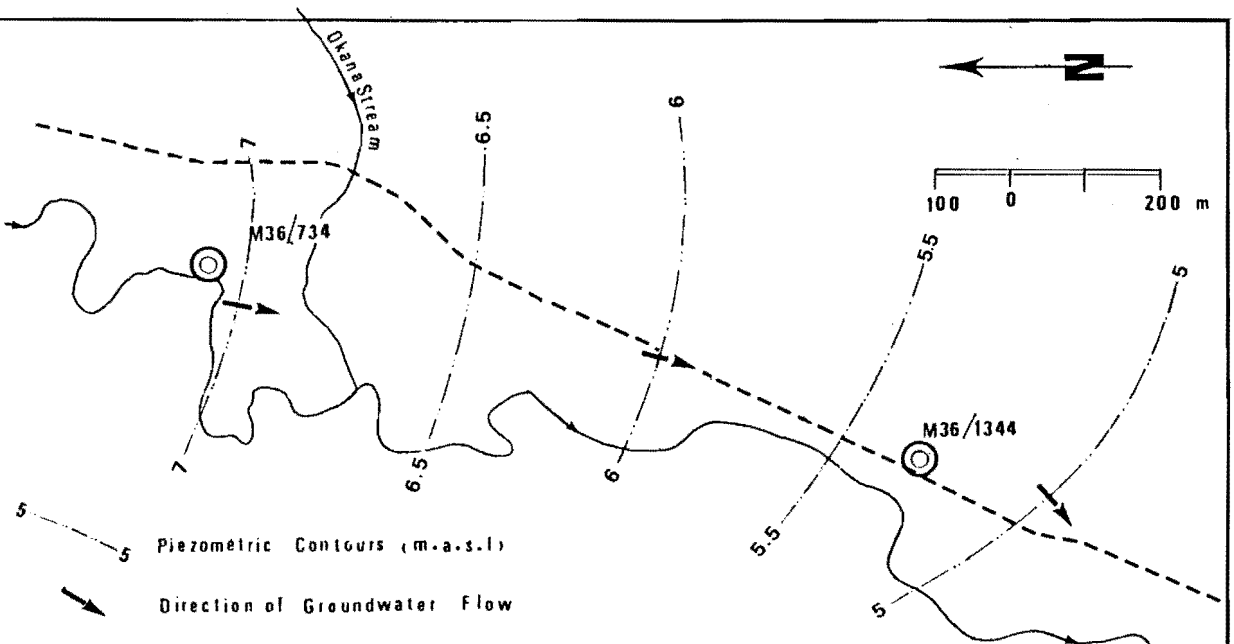

FIG. 5.11
Piezometric Contours and Groundwater Flow Direction for Lower Aquifer (Aug. 1986)

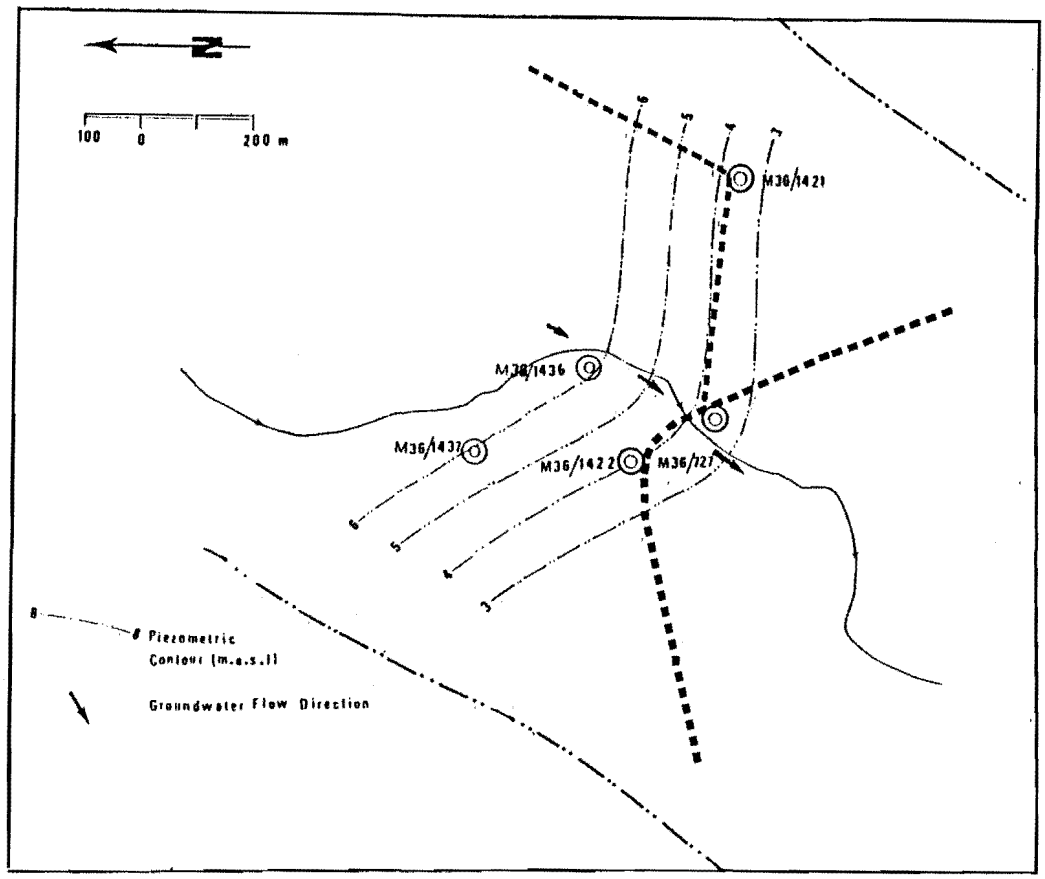

Figure 5.12 Piezometric Contours and Groundwater Flow Direction for Upper Aquifer (Aug. 1986)

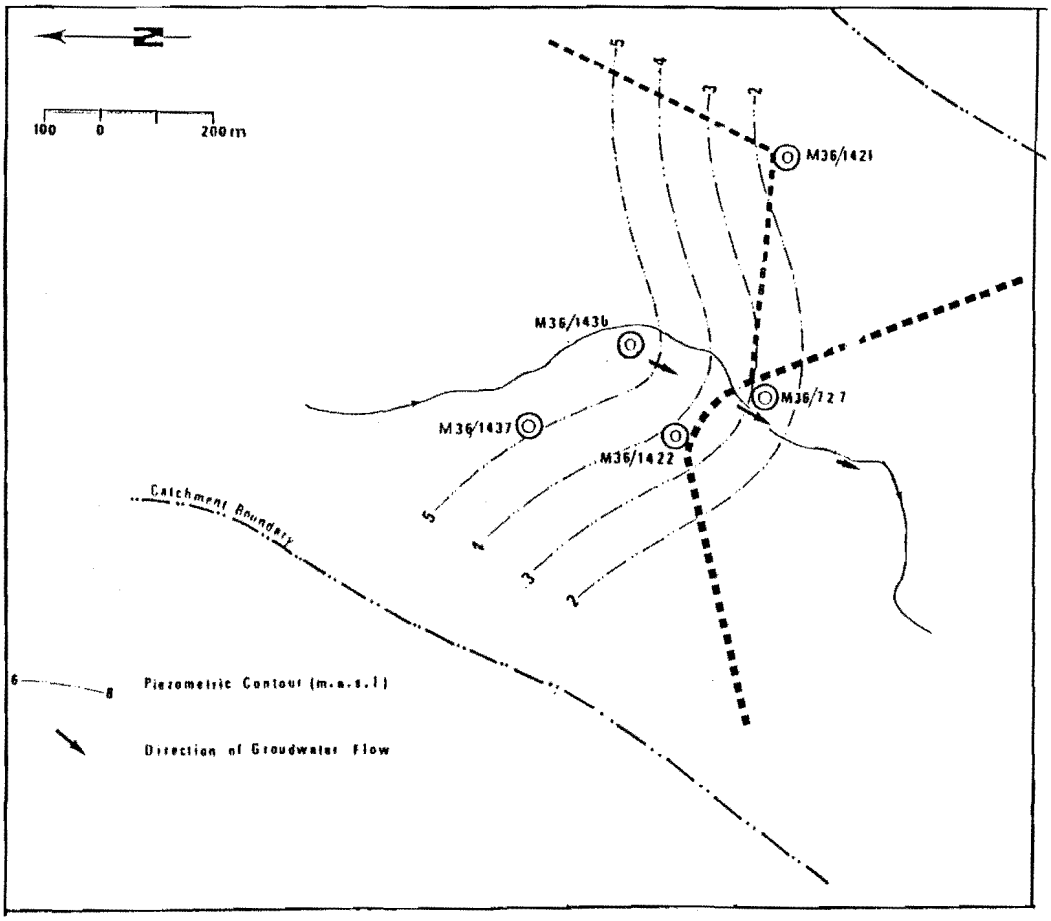

Figure 5.13 Piezometric Contours and Groundwater Flow Direction for Upper Aquifer (Feb. 1987)

5.4.1 Discharge Magnitude

The magnitude of discharge can be divided into three categories.

1) Low (less than 2.5 $lmin^{-1}$
2) Medium (between 2.5 and 15 $lmin^{-1}$)
3) High (more than 15 $lmin^{-1}$)

Most of the monitored and mapped springs, fall into the first of these categories (App. 13.2, and Figs 1.6 and 1.7). Eight of the monitored springs outlet from volcanic bedrock, 17 from volcanic colluvium, one from mixed colluvium , one from loess, and one from alluvium (App. 13.2). In general, the magnitude of discharge increases with increasing elevation and proximity to the upstream area (due to the higher rainfall in these areas). For example springs from subcatchment 5 with an elevation of 400 m to 500 m have the highest discharge among the monitoring springs (App. 13.2).

5.4.2 Seasonal Variation

The seasonal discharge trend of the monitored springs is shown in App. 13.3, and clearly indicates a decline in discharge between November 1986 and May 1987. In all monitored springs the maximum flow was observed in August 1986 and the minimum in February 1987.

The controlling factor for spring variability is the flow path and storage volume. The seasonal variation observed for springs E.3.1 and W.5.1 (Fig. 5.14) is highly uniform compared with the other springs (eg. springs W.2.2 and, W.5.5 in Fig. 5.14). The discharge of these two springs (E.3.1 and W.5.1) is continuous even in summer, due to their longer flow path and larger storage volume. The long flow path for the springs with a more continuous flow also has been confirmed by chemical and isotopic studies (see chapter 7).

Spring variability (Va) was computed using the following equation (Davis and Deweist, 1966).

$$Va\% = \frac{(Qmax - Qmin)}{(Qmed)} \times 100$$

where

Q max = maximum discharge
Q min = minimum discharge
Q med = median discharge

The spring variability for the monitored springs at different altitude is presented in APP. 13.2 Spring E.3.1 and W.5.1 show a minimum variability (228% and 277% respectively) while spring W.1 has a maximum variability of 5870 %. Data does not indicate any relationship between altitude and spring variability.

5.4.3 Discharge Component

Field observation indicates the presence of two spring discharge components, direct and indirect. Rapid infiltration of storm water in the small area close to the spring outlet increases the discharge rate, and this is a minor component of the discharge water because of the size of the recharge area.

An increase in the spring discharge is also a result of the increase in piezometric head due to infiltrating rainwater. This is the major component contributing to increased discharge. Larger and deeper volumes of older water will have less response to an increase in pressure, hence, their outflow fluctuations are smoother and their magnitude, less than shallower and smaller volumes of water within volcanic fractures.

As shown in Figs.A.13.3 the warm, dry period (January to May 1987) resulted in very little recharge of the groundwater system. The response to rainfall during the summer period is minimal due to high evapotranspiration.

5.5 Recharge Models

5.5.1 Stream - Aquifer Interaction Model

The possibility of groundwater recharge through the stream bed via the valley floor deposits was investigated using the following methods:

1) Flow gaugings
2) Piezometric level and stage comparisons
3) Geophysical and geological data.

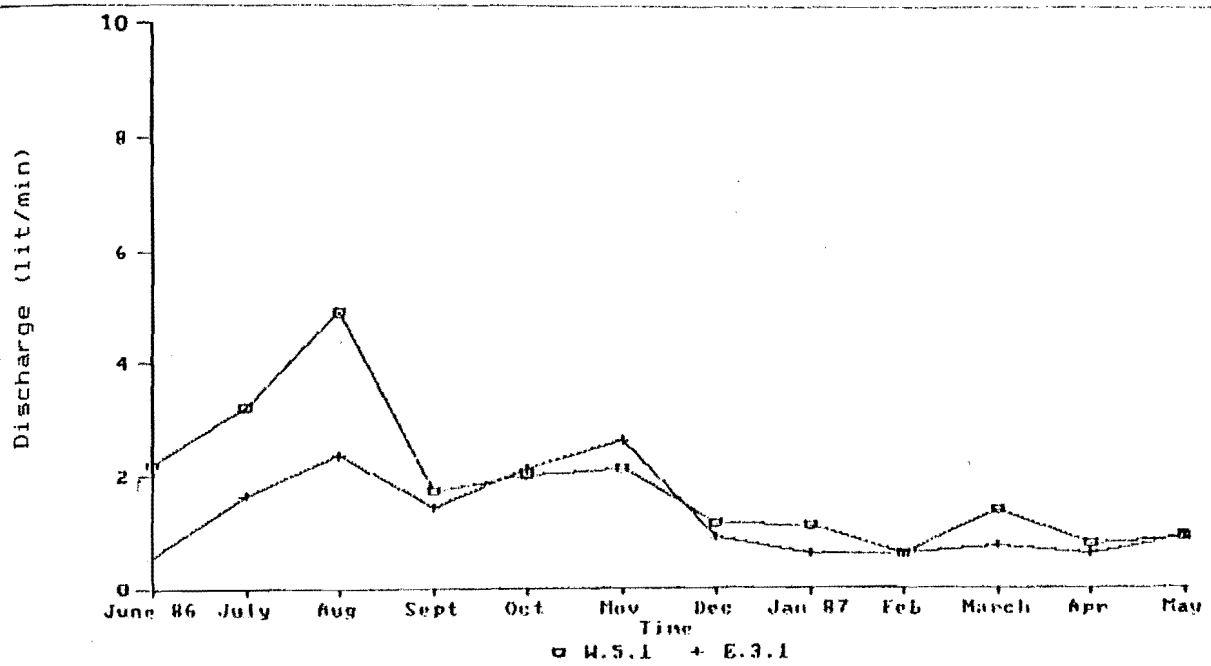

Figure 5.14 Springs Discharge (W.5.1 and E.3.1)

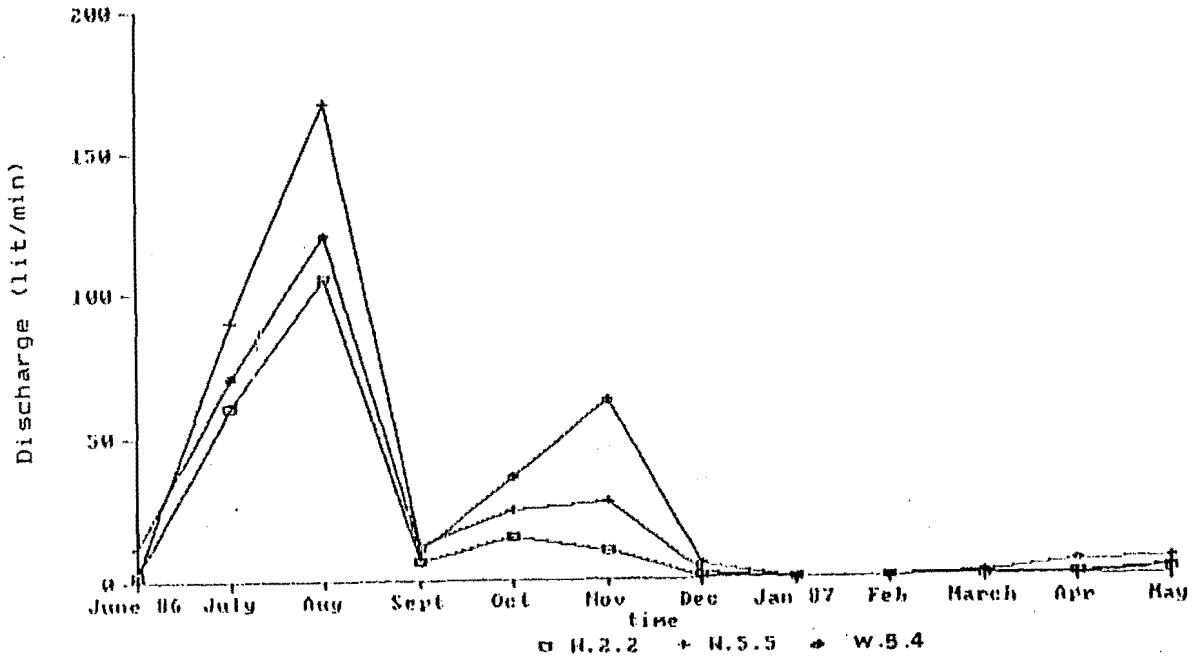

Figure 5.15 Springs Discharge (W.2.2, W.5.4, and W.5.5)

1) Flow Gauging

A direct method of determining possible recharge from the stream ıed through the valley floor deposits, is flow gauging of the main :tream and tributary streams. The spring runoff to the Kaituna River :egment between each gauging site was also measured at the end of each ıonth (this was possible for a flow rate less than 10 l/sec). 'hese flow rates were correlated to the Kaituna Stream hydrograph, and .he resulting regression equation (App. 9.8) was used to estimate the 'ate of the total base flow for spring runoff into the Kaituna river.

The base flow comparison for streams during the water year (June 986 - May 1987) is shown in table 5.3.

Base Flow (l/Sec)					
A	B	C	D	E	F
390	29	26	277	10	3.84

Table 5.3 Base flow comparison for the streams during the water year (June 1986 - May 1987).

A = base flow at Kaituna stream (main station)
B = " " " Okana stream
A = " " " Kaituna stream at Packhorse
C = " " " Packhorse stream
D = " " " Takamina stream
E = " " " Springs run off

Recharge = input - outflow = (B + C + D + E + F) - A
= 335.8 - 390 = - 54.2 l/sec

The gaining water is considered to be representative of under- round water flow to the stream channel, through volcanic rocks. Some f these flows outlet before reaching the stream channel, for example pring A.1, Fig. 2.7. The results suggest that there is no loss from alley floor deposits into the aquifer system in the monitored section.

2) Piezometric level and Stage Comparison

Comparison of piezometric levels within boreholes and river stage nd mean flow data have provided some understanding of the stream- roundwater interaction. The monthly mean value of the Kaituna Stream tage, and rainfall are compared with groundwater level in Figs, 5.16 \ and B. Although both stream and piezometric data show a response to ainfall and seasonal variations (Fig. 5.17) no direct response between

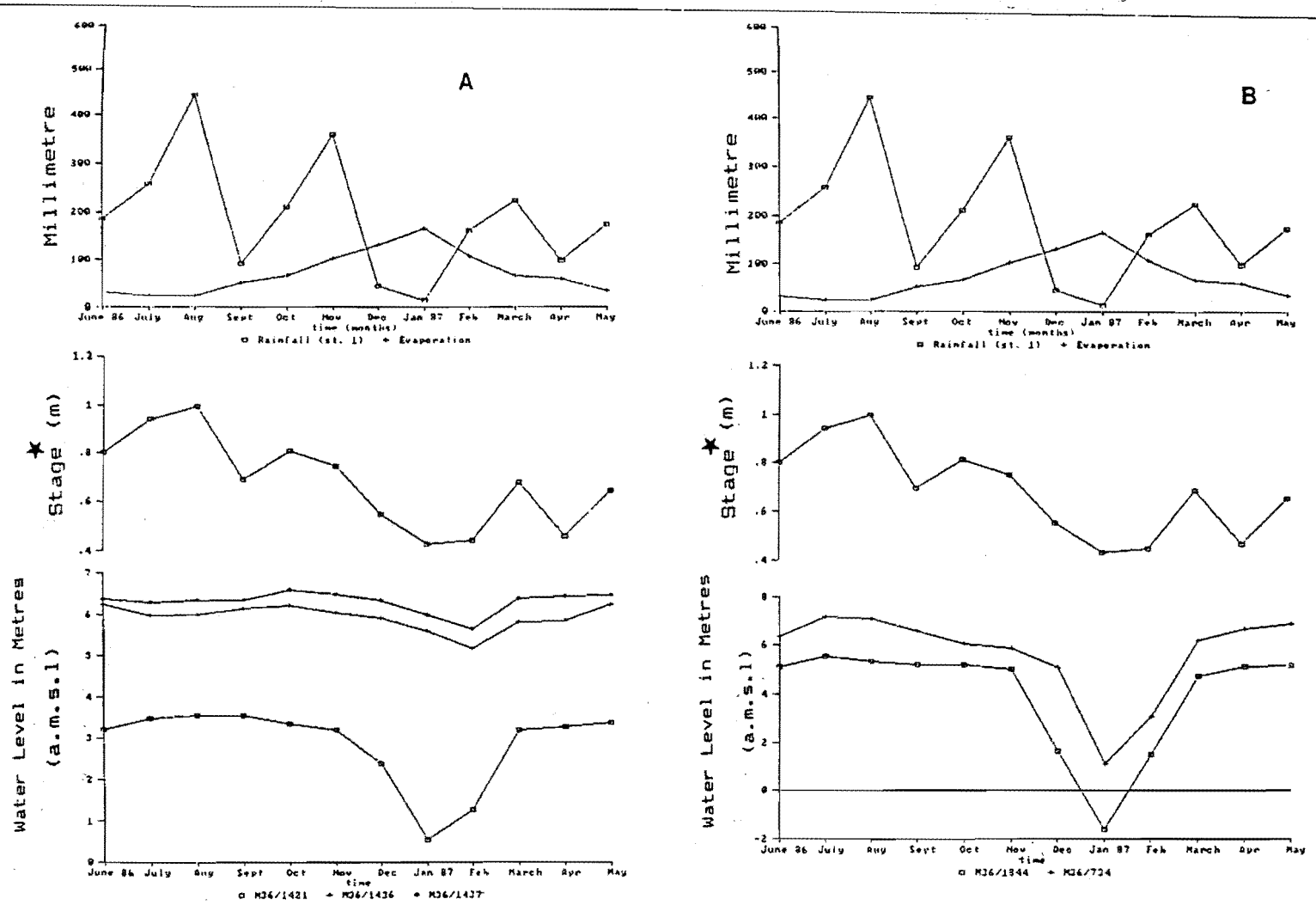

✱ Stage Height + 3.9 = metres above mean sea level

Figure 5.16 Comparison of Piezometric Changes, Rainfall and Evaporation A) Well M36/1421, M36/1436, M36/1437 B) Well M36/1344 and M36/734

stream stage and piezometric level is indicated.

3) Geophysical and Geological Data

Both geological and geophysical data suggest the presence of a clay confining layer above the upper and basal aquifer as discussed in chapter 3. Laboratory permeability results (presented in table 2.3) on samples from a 6 m auger hole in the valley floor deposits also indicates the occurrence of very low permeability materials. Although in the up stream area of alluvium (ie. above well M36/1344) downhole loggings and auger holes suggest the existence of a thin gravelly layer close to the surface, both geological and geophysical date indicate that this layer is not continuous and is underlain by a clayey layer.

4) Summary

The above investigations strongly suggest that a continuous aquiclude of marine clay exists beneath the full river width channel within the monitored area, and separates the underlying aquifers from streams flowing on the alluvial deposits. Therefore, the stream-aquifer interaction model has been proved invalid as the recharge model for aquifers in the valley floor sediments.

5.5.2 Fracture Infiltration Model

The possibility of groundwater recharge by direct infiltration (rainfall) through volcanic fractures was investigated using:

a) environmental isotopes and water chemistry analysis.
b) spring discharge and piezometric level changes

Results of the environmental isotope and water chemistry analysis are presented in detail in chapter 6. The three monitored springs and water samples from both aquifers have $\delta^{18}O$ values consistent with rainfall $\delta^{18}O$ values at moderate altitudes (section 6.4.2). This confirms that local precipitation on Banks Peninsula is the source of recharge for both aquifers.

The Tritium concentration (TR values) in the monitored springs is close to current rainfall (section 6.4.3), again indicating infiltra-

tion of rainfall through volcanic fractures.

Chemical analysis of spring water and groundwater indicates that the water flowpath recharging the aquifer system is through volcanic rocks. These results are different to those from the Canterbury Plains groundwater systems, which are recharged by direct precipitation and river flow.

Spring water are interpreted as rejected recharge due to the local occurrence of perched layers (tuff or ash). Study of the discharge of the springs with respect to climatic factors was undertaken to refine the recharge model for the groundwater system. The groundwater level and spring discharge show a similar overall response to seasonal variations in rainfall (Fig 5.17). This is further evidence for the direct precipitation-infiltration model suggested for groundwater recharge.

The continuous discharge of two of the springs even in the dry season (E.3.1 and W.5.1) is due to longer flow paths and larger groundwater storage. Both aquifer systems are therefore considered to be fed by the same type of springs (but by underwater flow), with a longer flowpath, more continuous flow, and greater storage volumes.

5.6 Water Balance Model

5.6.1 Hydrometeorological Equation

The evaluation of the groundwater resource is strongly dependent on the estimated natural groundwater balance. Water balance (water budget) method was therefore used to determine groundwater recharge. An advantage of the water balance method is that the aquifer does not have to be in dynamic equilibrium in order to use it. Many of the parameters used for a hydrologic water balance were measured directly; precipitation, stream flow, evaporation. The water balance of the catchment is defined by

$$R = P - (E + Q_q) - Q_b - \Delta SMD$$

where

R = net recharge
P = total precipitation
E = actual evaporation
Q_q = quick flow
Q_b = base flow
ΔSMD = change in unsaturated soil moisture deficit

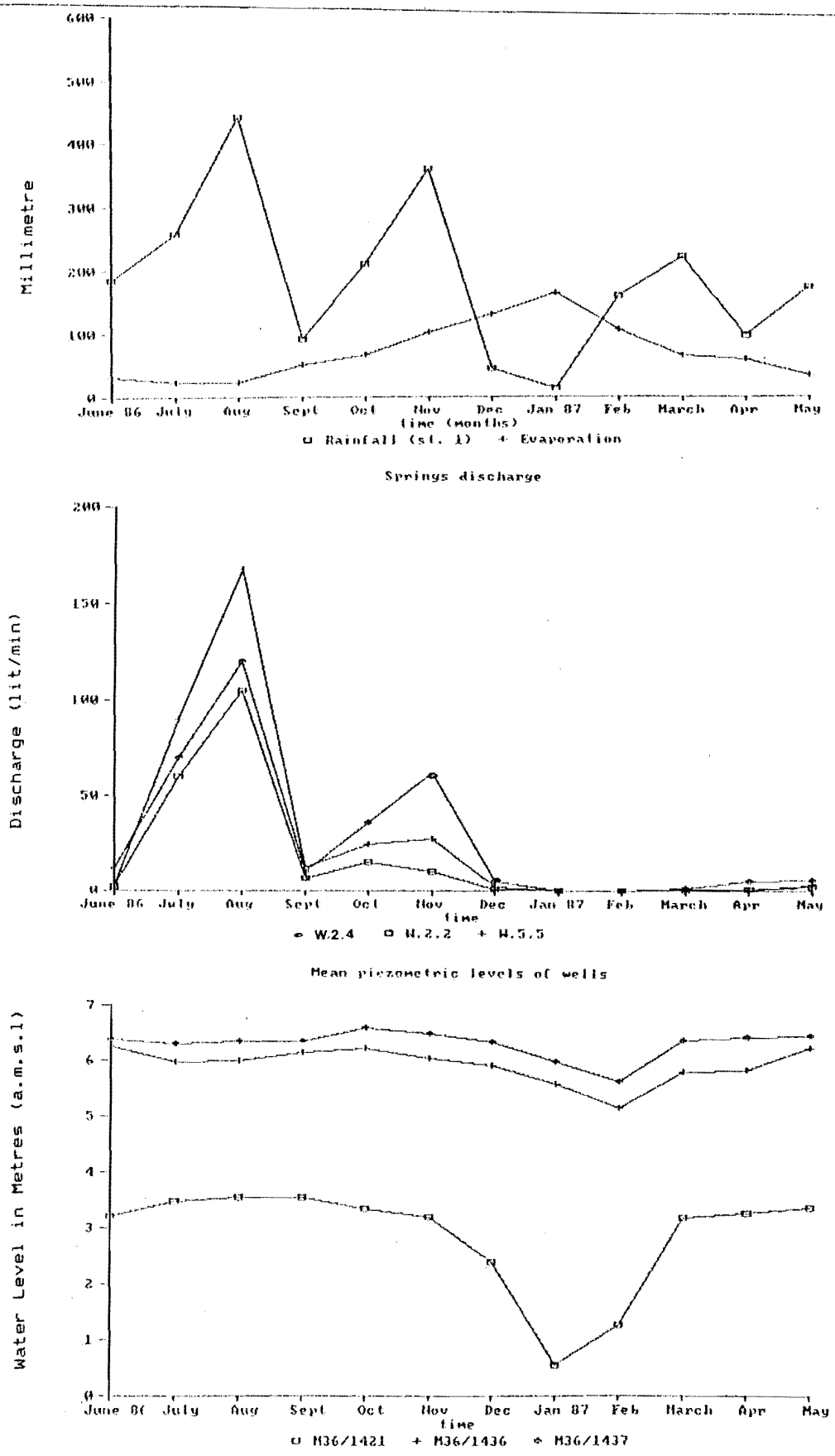

Figure 5.17 Comparison of Rainfall, Springs and Water Levels

The precipitation, actual evaporation, quick flow, and base flow components are summarized below and the relationships between water balance components are shown in Fig. 5.18:

1) Precipitation

The average depth of precipitation over the drainage basin was computed using isohyetal techniques (Section 4.2). The precipitation value for the monitored catchment (38 km^2) is equal to 1900 mm.

2) Evaporation

A total value of 860. mm actual evaporation (Sect. 4.3) is computed for the catchment.

3) Quick flow (Q_q) and base flow (Q_b)

Total base flow for the Kaituna Stream station (Stn. A, Fig 4.1) is equal to 383 l/sec or 318 mm (Sect. 4.4) for the water year (June 1986 - May 1987) over the monitored catchment (38 km^2).

Therefore;

quick flow (Q_q) = mean flow (Q) - base flow (Q_b) = 1131 - 383 = 748 l/sec

The quick flow (Q_q) during the water year for the monitored catchment for one year is equivalent to 621 mm (Sect. 4.4).

5.6.2 Available Water Capacity and Soil Moisture Deficit

1) Terminology

When all the water that plants are able to extract from the soil has been removed, the soil reservoir is said to be at the "Wilting point". At the other extreme, when a soil is holding the maximum possible amount of water the soil is said to be at "Field Capacity". The difference between these amounts is called the "Available Water Capacity" (AWC). AWC depends on the depth of the soil containing the roots and the soil type factor or (Moisture Volume Percent).

AWC = Moisture Volume Percent x Depth (mm)/100

If a soil at field capacity loses some of its water through evapotranspiration, then the amount of water needed to fill the soil reservoir back to full capacity again is called the "Soil Moisture Deficit"

(SMD). Typical "Available Water Capacities" are in the range 88 mm to 146 mm of water for silt loams and loessial deposits with soil profiles 0 to 76cm deep (Gradwell, 1976).

2) Change in Soil Moisture Deficit (ΔSWD).

When the soil is at field capacity, any additional rain (surplus water) that falls will cause runoff or recharge of the groundwater system. This results in zero values for the soil moisture deficit, and therefore the soil moisture deficit will be most significant in dry conditions. Since the study water year commenced in June, any changes in the soil deficit for the previous year could not be identified, and it was necessary to extend the water balance parameters (residual water) back to the previous winter to gain a zero value for soil moisture deficit.

3) Data Collection

Precipitation data was available for station 2, and data was collected from May 1985. The station is located in the area (Fig. 4.1) where rainfall data is more representative of the change in stream discharge rates measured at the Kaituna gauging station. Evaporation for this period was estimated using the regression equation determined between the Lincoln evaporation station and Kaituna (Sect. 4.4). Quick flow from May 1985 till June 1986 was estimated using the correlation between rainfall and known quick flow (App. 9.5).

4) Data Interpretation

The total residual water (P - (E + Qq)) during the winter of 1985 is higher (226 mm) than any type of the maximum AWC for the soil in the area (88 mm to 146 mm). Therefore the soil deficit will be zero at the end of the winter 1985, and this means that all residual water is percolating through the groundwater system. The first negative residual value occurs in September, 1985 (-10.4mm), and this builds up the soil deficit. For the next month (October 1985) the soil deficit is [(-10.4-(-2.65)] = -7.25mm. A high residual water value (37 mm) during November 1985 reduced the soil deficit back to zero (=field capacity). Using the same procedure the soil deficit at the beginning of the June

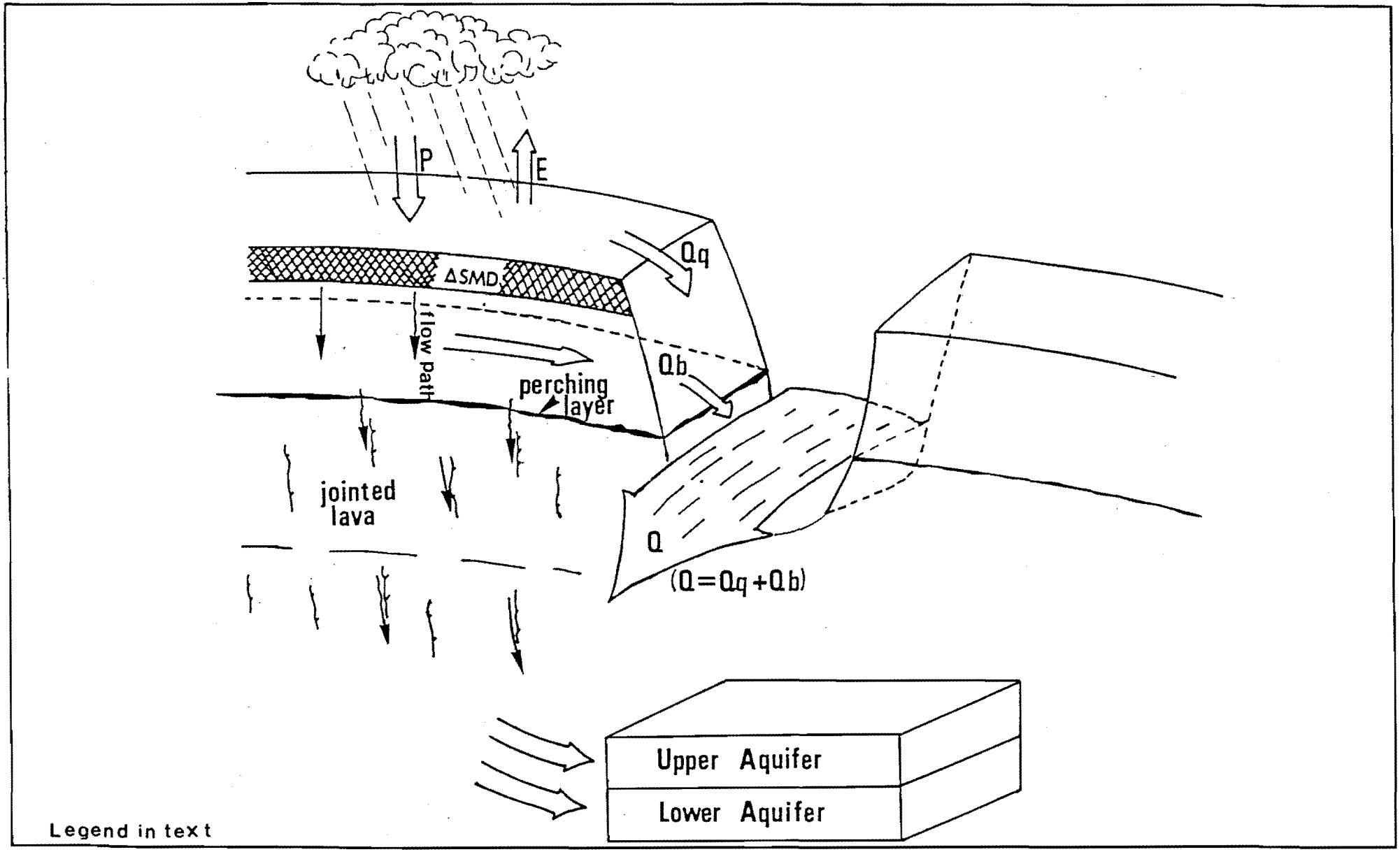

Figure 5.18 Water Balance Model

86 is computed to be 15 mm (Table 5.4).

In January 1987 the soil deficit is - 240 mm. This is lower than any possible value for the AWC (88 to 146 mm). Any value chosen within this range will cause a zero deficit value at the end of May 1987. Therefore the change in soil moisture deficit is equal to 15 mm (15 - 0). Even if the soil was able to hold 240 mm of water (which is not realistic) the soil deficit will be increased by just 5 mm at the end of the study year.

5.6.3 Recharge Volume to the Groundwater System

Computed water balance components are used to estimate the value of recharge to the groundwater system according to;

$$R = P - (E + Q_q) - Q_b - \Delta SMD$$

whence,

$$R = 1900 - (860 + 621) - 318 - 15 = 86 \text{ mm}$$

Therefore 86 mm of water has been added to the groundwater storage system during the study water year from June 1986 till May 1987.

The proposed water balance model is illustrated in Fig. 5.18

5.6.4 Assessment of Recharge using Aquifer Properties.

The groundwater resource was assessed by hydrodynamic analysis on the upper aquifer and lower aquifers:

1) Upper Aquifer

For this aquifer contour maps showing equipotential lines of the groundwater levels were produced, and the stream lines of water flow drawn, to give a flow net (Fig. 5.19). The piezometric level was based on the mean value for each month from June 1986 till May 1987. The transmissivity for each section is derived from the measured transmissivity value from the well closest to the section.

Calculation of total volumetric outflow was based on the following equation:

Table 5.4: Calculation of Change in Soil Moisture Dificit Δ S M D

Year	Month	Soil Moisture Deficit (mm) †	Residual (mm)	Evaporation (mm)	Quick Flow (mm)	Rain Stn.2 (mm)
1985	May	0	41.4	31.32	8.3	81
	June	0	23.4	16.5	3.12	43
	July	0	129.4	16.5	67.08	213
	Aug	0	31.4	38.5	7.3	77.25
	Sept	−10.4	−10.4	69.5	4.16	63.25
	Oct	−77	2.56	83	10.6	96.25
	Nov	0	37	92.7	37.6	167.25
	Dec	0	7.3	97	18.7	123
1986	Jan	−14.7	−14.7	131.4	26	142,7
	Feb	0	26.7	107	44.8	178.5
	Mar	0	70.5	73	110	2535
	Apr	−42.45	−42.45	66.7	0	24.25
	May	−15	27.55	35	6.25	68.8
	Jun	0	102.5	32.4	7.64	142.7
	July	0	121.4	23.4	107.9	252.7
	Aug	0	93.3	23.5	203.7	32.05
	Sept	0	11.23	50.9	4.16	66.3
	Oct	0	56.22	65.68	69.6	1915
	Nov	0	46.4	102.9	121	207.3
	Dec	-86.5	-86.52	129.65	3.6	46.73
1987	Jan	−240 * −140	−153.84	164.08	0.14	10.38
	Feb	−218	22.04	107.3	42.6	1719
	Mar	−124	93.9	66.82	44.6	204.75
	Apr	−62	61.9	60.26	0	122.2
	May	−5	56.9	33.36	45.2	135.62

Note

* : The minimum average soil moisture capacity is estimated to be −146 mm.

†: Soil moisture deficit at the end of each month.

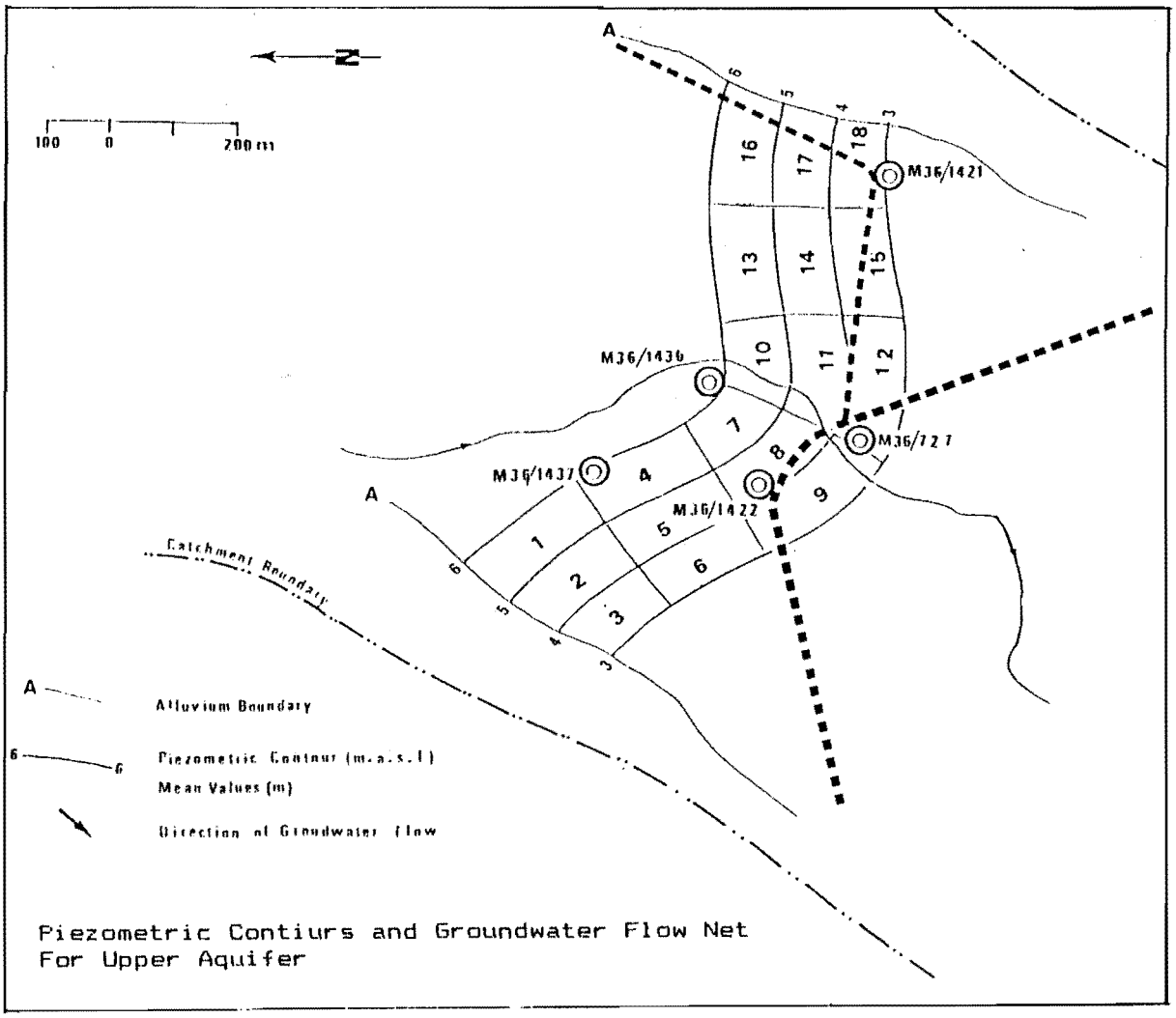

Figure 5.19 Sketch of Equipotential Lines and Patterns of Stream Lines for the Upper Aquifer

$$Q = q \times L$$

Where

Q = total volumetric outflow rate
q = outflow per unit length = T x I
T = transmissivity = K x d
K = coefficient of permeability
I = hydraulic gradient
d = aquifer thickness (m)
L = flow width (m)

The individual parameters for calculation are given in Table 5.5. The total outflow of the upper aquifer which occurs within a catchment of 47.6 km^2 is 1.07 x 10^{-1} m^3/sec (47.6 km^2 used as a catchment area due to location of the wells at the bottom part of the valley). Thus the annual (June 1986 - May 1987) outflow for the catchment area of 47.6 Km^2 will be equal to 71 mm, and this represents a water column 71 mm, over the catchment.

The amount of water which was lost through flow net area is

D = Outflow - inflow = 17 mm (Table 5.5).

2) Lower Aquifer

Due to an insufficient number of boreholes, flow net techniques could not be applied. The outflow was measured using the oscillation of the water level and storage coefficient in bore M36/1344, and calculation was based on the following equation

$$Q = F\ u\ h$$

where

Q = outflow of underground water
F = alluvium area,
h = amplitude of water level oscillation in well
u = storage coefficient

The quantity of water contained between the highest water level and the lowest was

$$Q = 4.3 \times 10^6 \times 0.0025 \times 7.13 = 76647\ m^3/year$$

Not all of this quantity of water appears as underground water outflow. Different authors have established different percentages of this storage, depending on the character of region. Roslonski (1947) accepted 50% of full storage as a free outflow, but Wiezysty (1970) accepted 78.5% as an average based on experiments. Using Wiezysty's data, the

Table 5.5: Estimated Values of outflow Q for the Upper Aquifer

Flow net no.	T (m^2/s)	I	q (m^3/s)	L (m)	Q (m^3/s)	D = outflow − inflow (m^3/s)
1				200	9.8×10^{-3}	—
2	4.9×10^{-3}	0.01	4.9×10^{-5}	170	8.33×10^{-3}	-1.47×10^{-3}
3				130	6.37×10^{-3}	-1.96×10^{-3}
4				185	9.06×10^{-3}	—
5	4.9×10^{-2}	0.01	4.9×10^{-5}	180	8.82×10^{-3}	0.24×10^{-3}
6				170	8.33×10^{-3}	4.9×10^{-3}
7				140	2.6×10^{-2}	—
8	1.86×10^{-2}	0.01	1.86×10^{-4}	180	3.5×10^{-2}	9×10^{-3}
9				170	4.2×10^{-2}	7×10^{-3}
10				150	2.7×10^{-2}	—
11	1.86×10^{-2}	0.01	1.86×10^{-4}	180	3.3×10^{-2}	6×10^{-3}
12				220	4.1×10^{-2}	8×10^{-3}
13	1.86×10^{-2}		1.86×10^{-4}	180	3.6×10^{-2}	—
14	2×10^{-2}	0.01	2×10^{-4}	180	3.6×10^{-2}	3×10^{-3}
15	2×10^{-2}		2×10^{-4}	180	3.6×10^{-2}	4×10^{-4}
16				170	3.1×10^{-2}	—
17	2×10^{-2}	0.01	2×10^{-4}	150	3×10^{-2}	-10^{-3}
18				130	2.6×10^{-3}	-4×10^{-3}

result obtained was 14 mm for the alluvium section, as the total outflow for the water year (June 86 - May 87).

5.6.5 Summary

The results of the assessment indicate variability in the rate of recharge to different groundwater systems over the catchment area. For the monitored water year the total rate of recharge to the groundwater system was equal to 86 mm using the water balance technique. For the lower aquifer, the specific outflow was computed to be 14 mm for the water year, and 71 for the upper aquifer.

The results indicate a close relationship between the total recharge value obtained from water balance techniques and the total specific outflow value (mm/y over the catchment) using hydrodynamic properties of the aquifers. However, due to the change in transmissivity value with saturated thickness, a more extensive investigation needed to better quantify the results.

5.7 Hydrogeological Model

5.7.1 Recharge Component of the Model

The fracture infiltration model proved to be the only possible recharge model for the groundwater system. In this model, groundwater is recharged by the infiltration of precipitation through shrinkage fractures of volcanic rocks (isotopic and chemical studies, chapter 6). The water bearing properties of volcanic materials indicate (section 2.2) that lava with a high concentration of shrinkage fractures are the main hydrogeological units for the vertical transmission of water. Basal brecciated lava is found to be the main unit for horizontal water flow.

Rainfall distribution as discussed in Sect. 4.2, shows a steep increase with altitude. Therefore, there is a higher potential for recharge in summit region, where the highly fractured volcanic rocks are exposed (or covered with volcanic colluvium).

5.7.2 Discharge Model

Discharge takes the form of spring flow, seepage into the Kaituna

stream river, and subsurface drainage into Lake Ellesmere. Monitoring of spring discharge indicates a direct relationship between the climatic factors and the rate of discharge. The rate of discharge increases with increasing rainfall.

The impermeable layers (tuff and ash) between lava flows and subvertical dikes (Sect. 2.2), divide the subsurface volcanic rocks into a number of groundwater compartments (Fig 5.20), each with its own water level and outlets. The outlet will be into an adjacent lower compartment or into a spring. As a result the groundwater passes through a number of steps down the hillside (Fig 5.20) into the zone adjacent to the valley floor sediments. The outlet through the gravelly layer in this zone (within the base and upper aquifer), is the main mechanism of groundwater replenishment within the valley floor deposits.

5.7.3 Lower Aquifer Model

Replenishment in the lower aquifer occurs through a gravelly layer of variable thickness. The thickness of this layer is up to 17 m in the upper part of the valley and 65 m in the lower part. The aquifer is confined by a 2 to 25 m clay layer (Fig. 3.10). Average transmissivity of the aquifer in both well M36/1344 and M36/734 is 4.5 x 10^{-3} m^2/s. The aquifer model derived from pumping tests predict a safe yield limit of 12 l/sec when pumped for 24 hours. The total specific discharge from this aquifer (Sect. 5.6.4) is computed to be 14 mm/y over the whole alluvium area for the water year.

5.7.4. Upper Aquifer Model

Replenishment in the upper aquifer occurs through a gravelly layer with an average thickness of 24 m. The aquifer is developed only in the lower part of the valley (Fig 5.20) due to a change in basement topography (perhaps as a result of the emplacement of the Stoddart Volcanics, Fig 1.3). The transmissivity value for this is more variable (due to changes in its thickness and degree of saturation), and ranges between 4.9 x 10^{-3} m^2/s and 1.86 x 10^{-2} m^2/s. Therefore, a larger amount of water could be extracted from this aquifer, but a pumping test is necessary to define a safe yield. The total discharge from the upper aquifer over the catchment area was calculated 71 mm for the

water year.

5.8 Synthesis

The study has defined the general characteristics of the Kaituna Valley groundwater system, and has provided an initial estimate of the groundwater resources in this area. The maximum continuous pumping rate for 24 hours would be about 12 l/sec (safe yield of the well). This figure shows that the lower aquifer can sustain spray irrigation yield for only short periods of time and then the pumping should stop for aquifer recovery.

Results indicate a higher transmissivity value for the upper aquifer compared with the lower aquifer. Seasonal and short term piezometric fluctuations are greater at bores drawing on the lower aquifer compared with those drawing on the upper aquifer because of a difference in hydraulic conductivity and the distance from the recharge area.

Piezometric levels increase with depth in the upper aquifer, indicating that an upward flow component is dominant in this aquifer. Therefore, it is inferred that the underlying deeper upper aquifer zones are generally acting as water feeding sources for upper parts of the aquifer. The bores within the lower aquifer show a decline in piezometric pressure with increasing bore depth (ie. a decrease in aquifer elevation). This indicates that recharge potential zones have a direct relationship with altitude.

Increase in the discharge component of springs is mainly a result of an increase in piezometric head due to infiltrating rainwater. The spatial variation for spring E.3.1 and W.5.1 is highly uniform compared with the other springs, and their discharge is continuous even in the summer. This is due to their longer flow path and larger storage volume.

The groundwater recharge from direct infiltration through the volcanic fractures was proved to be the main recharge mechanism. Using the hydrological budget model for the monitored water year, the total rate of recharge to the groundwater system was 86 mm/y (applying the water balance technique). For the lower aquifer specific outflow was computed to be 14 mm/y. The upper aquifer shows a specific outflow of 71 mm, over the whole catchment for the water year.

CHAPTER SIX

HYDROCHEMISTRY AND ENVIRONMENTAL ISOTOPE STUDIES

6.1 Introduction

Hydrochemistry and environmental isotope studies were undertaken to help understand the groundwater type and its history, water quality, and groundwater recharge source and ages. Water samples for chemical analysis were collected from a total of five groundwater wells, three springs and one surface water site. The collected samples were analysed by the North Canterbury Catchment Board on 24/11/86. Water samples from three boreholes and three springs were also forwarded to the Institute of Nuclear Science for analysis for the stable isotope Oxygen-18, and the radio-active isotope Tritium. Sampling techniques for both chemical and isotope analysis are presented in App. 14.1 and the water sampling sites are shown in Fig. 6.1.

6.2 Groundwater Origin

6.2.1 General

Study of the spatial distribution of chemical constituents in groundwater is valuable in understanding the sources of recharge and flow paths. Without chemical analysis it is impossible to deduce whether Kaituna groundwater is recharged through volcanic rocks or if any mixing occurs with marine water or Canterbury Plains aquifers (Canterbury Plains groundwater flow direction is towards Banks Peninsula, Talbot et al, 1986) especially in the area close to the Lake Ellesmere.

Samples for the hydrochemical analysis of groundwater were collected from the lower aquifer (M36/843, M36/734, M36/1344), upper aquifer (M36/1421, and M36/1436), and springs W.5.3, W.3.4, E.3.1 (Fig. 6.1).

Chemical analyses of water samples which were run by the North Canterbury Catchment Board on 24/11/86 are summarized in Table 6.1 and 6.2.

6.2.2 Groundwater Composition

Groundwater classification is based on the percentage of dissolved

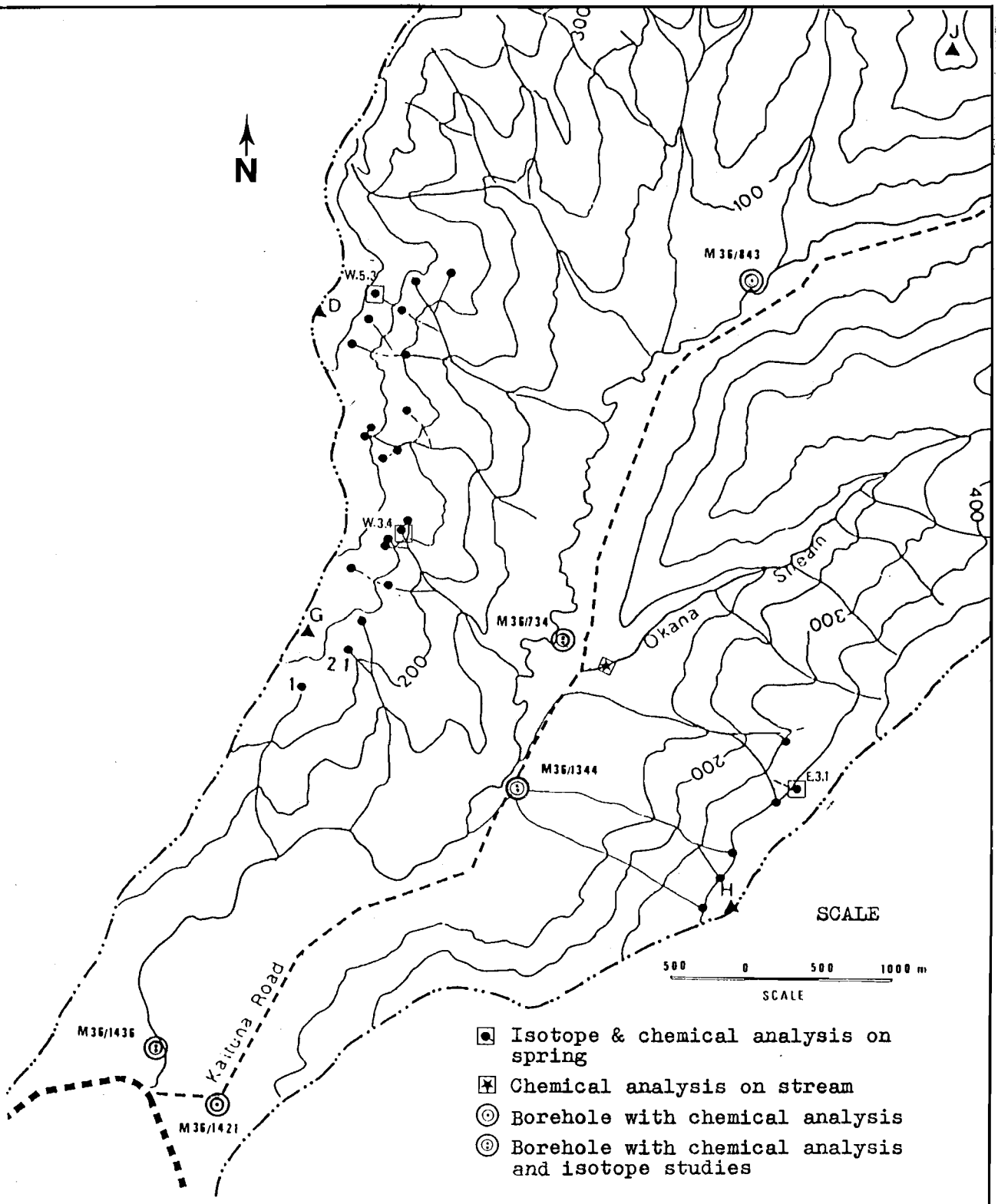

Figure 6.1 Sampling Sites for Hydrochemical and Environmental Isotope Analysis

Table 6.1: Chemical Analysis of Groundwater Samples

Chemical Analysis	M36/834	M36/734	M36/1344	M36/1421	M36/1436
Temperature (^{0}C)	14.7	14.6	14.5	16	14
pH	7.2	7.34	7.6	8.0	8.3
Conductivity at 25 ^{0}C (mS/m)	31.4	55.6	73.7	48.9	47.9
Biocarbonate Alkalinity (as HCO_3^-)	—	190	269	205	129
Nitrate Nitrogen	4.6	0.015	0.007	★	0.1
Chloride	34.0	130	110.0	58.0	83.0
Sulphate	10	7	9.0	6.0	10.0
Total Hardness (as CO_3Ca)	77	150	228	95	71
Calcium	15	27	40.0	15.0	14.0
Magnesium	9.7	20	31.0	14.0	8.8
Sodium	33	60	76.00	72.00	63.00
Potassium	2.2	2.5	2.00	2.10	1.90
Reactive Sillica (As SiO_2)	27.3	22	27.0	19.0	19.0
Iron	0.05 0.82 uf	0.24	2.50	0.30	0.18
Manganese	0.6	<0.05	1.10	0.10	★
Dissolved Reactive Phosphorous	<0.005	0.130	0.128	1.03	0.40
Total Phosphorous	0.031	0 182	0.750	1.1	0.46
Total Organic Nitrogen	0.05	2.05	—	—	—
Carbon Dioxide	—	10	11	3.0	—

Note: Units in g/m^3, ★= less than detectable limit
uf=unfiltered sample, Analyst: N.C.C.B.(24/11/86)

Table 6.2: Chamical Analysis of Stream Water Samples

Chemical Analysis	Spring W.5.3	Spring E.3.1	Spring W.3.4	Okana Stream
Temperature (^{0}C)	10.4	12.2	10.8	10
pH	6.2	6.2	6.12	7.5
Conductivity at 25 ^{0}C (mS/m)	10.1	11.6	10.1	11.3
Biocarbonate Alkalinity (as HCO_3^-)	22	25	25	34
Nitrate Nitrogen	0.36	0.26	0.13	0.11
Chloride	16.0	18.0	16.0	18.0
Sulphate	<5	<5	<5	<5
Total Hardness (as CO_3Ca)	10	17	11	17
Calcium	1.8	3.5	1.6	3.1
Magnesium	1.3	2.0	1.6	2.2
Sodium	14	17	17	17
Potassium	0.5	0.75	0.44	0.76
Reactive Sillica (As SiO_2)	16	28	18	19.0
Iron	0.09	0.29	0.60	0.15
Manganese	,0.05	<0.05	<0.05	<0.05
Dissolved Reactive Phosphorous	<0.005	0.130	0.128	1.03
Total Phosphorous	0.065	0.102	0.091	0.039
Total Organic Nitrogen	0.16	0.08	0.35	0.11
Carbon Dioxide	37	25	28	2

Note: 1. Units in

Analyst: N.C.C.B. (24/11/1986)

ions. The triangular diagram of major-ion composition is presented in Fig 6.2 and 6.3. For this classification, concentration in g/m^3 are converted to milliequivalents per litre (meq/l) using the conversion factors presented in App. 14.6.

Chemical analyses of groundwater from four bores and three springs were used for the classification. The triangular diagram indicates that the anions and cations are fairly consistent throughout the area. Sodium is the dominant cation and HCO^-_3, and Cl^- are the dominant anions.

6.2.3 Groundwater flow path and origin

1) Background

The minerals occurring in volcanic rocks (eg. plagioclase) are dynamically unstable and tend to dissolve when in contact with water. The dissolution process, which is strongly related to CO_2 concentration causes the water to acquire dissolved constituents (ions) of the host rock. This alteration results in production of clay minerals such as kaolinite, illite and montmorillonite. Major cations released to the water by this process are Na^+, K^+, Mg^{2+}, and Ca^{2+}. Another consequence of the process is a rise in pH and in HCO^-_3 concentration. Based on these trends, the ionic composition of groundwater can be used to define the groundwater origin and flowpath.

It should be noted, however, that the concentration of dissolution products, also depends the water flow rate within the volcanic rock. (ie. the solute concentration will be smaller at a greater flow rate).

2) Calcium (Ca^{2+})

Ca^{2+}concentration ranges between 1.8 and 3.5 g/m^3 for springs, and between 14 and 27 g/m^3 for groundwater from the boreholes (Table 6.1 and 6.2). Calcium concentration values from borehole water are higher than those obtained from Canterbury Plains aquifers, whereas spring water calcium concentration is less than for the Plains (Fig. 6.6). According to Matthess the calcium concentration in volcanic rocks is mainly held in plagioclase feldspar. In clay minerals (montmorillonite) calcium occurs as absorbed ions on mineral surfaces (Matthess, 1982). Bores M36/1344 and M36/1421 (within the lower aquifer and upper aquifer respectively) have a higher concentration of calcium which also suggests longer flow paths

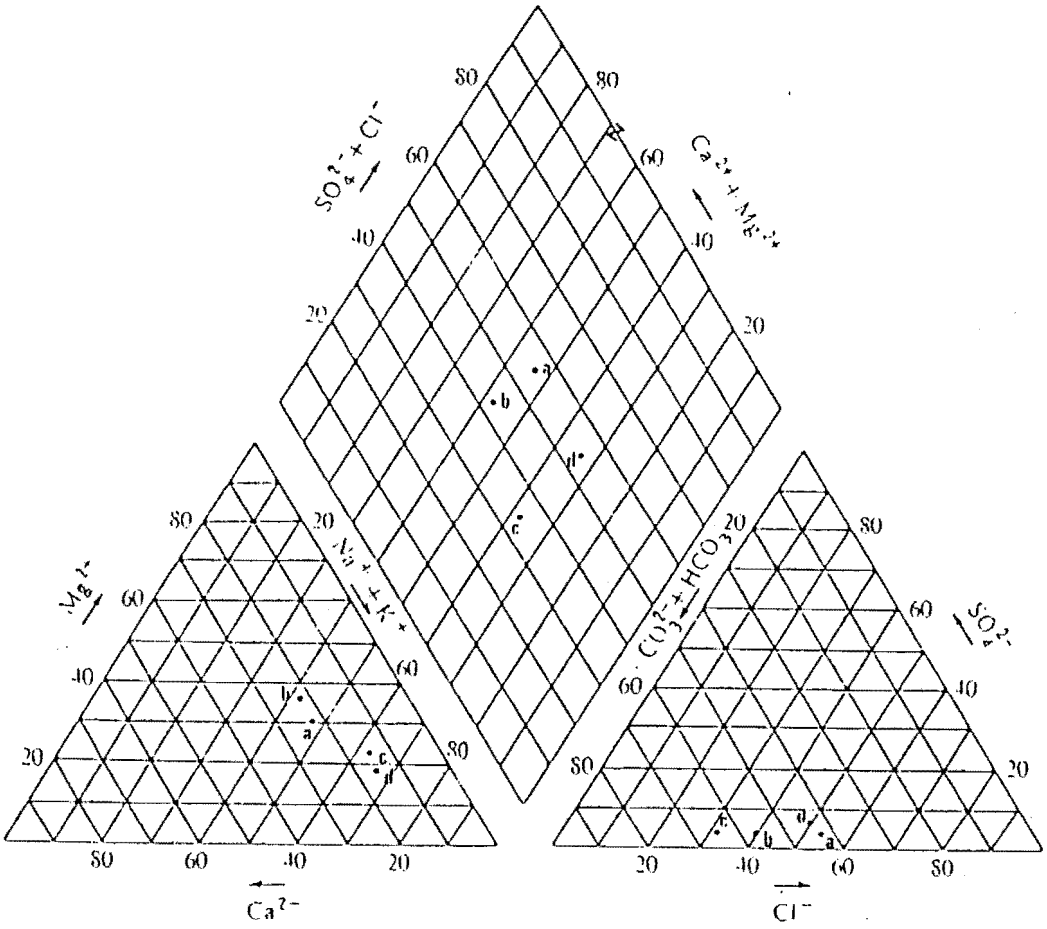

a: M36/734
b: M36/1344
c: M36/1421
d: M36/1436

Figure 6.2 Triangular Classification of Borehole Groundwater (ion concentration in meq/l)

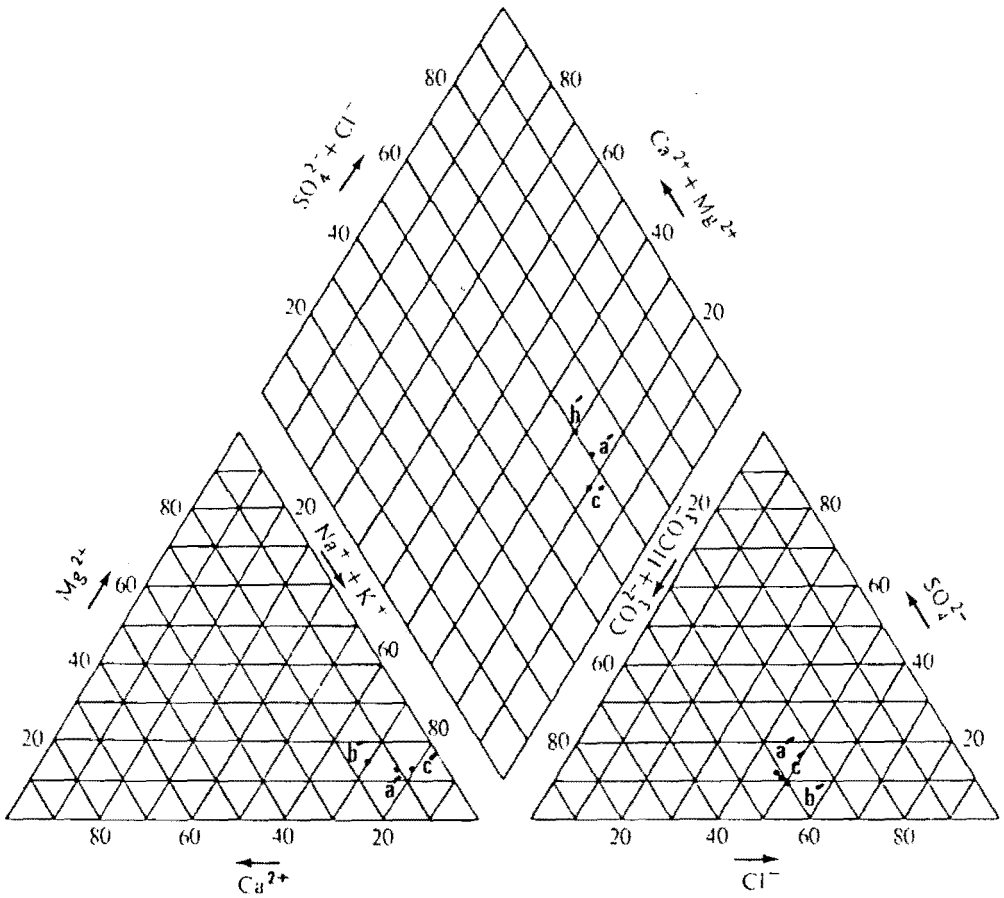

a': spring E.3.1
b': spring W.5.3
c': spring W.3.4

Figure 6.3 Triangular Classification of Spring Water (ion Concentration in meq/l)

(Fig. 6.7). Spring E.3.1 also shows a higher calcium concentration indicating a longer flowpath (Fig. 6.8)

3) Magnesium (Mg^{2+})

Mg^{2+} concentration ranges between 8.8 and 31.0 g/m^3 for waters from the wells, and between 1.3 and 2.2 for the springs. The main source of the magnesium is olivine-basalts rocks. Sea water is not considered as the source for Mg^{2+}due to the piezometric gradient of the groundwater system (sect. 5.3) in both aquifers. In spite of the higher solubility of most of its compounds compared with calcium, magnesium content is generally lower than calcium. This is due to the lower geochemical abundance of magnesium (Matthess 1982). Spatial distribution of magnesium (Fig. 6.9) and (Fig. 6.10) is similar to that of calcium.

4) Sodium (Na^{+})

Na^{+} concentrations for groundwater samples are presented in Fig. 6.4 and 6.5, and range from 14 to 17 g/m^3 where the source is springs, and from 33 to 72 g/m^3 from boreholes. The range is distinctly higher in comparison to results obtained from the Canterbury Plain aquifers (Fig. 6.6), indicating a different recharge zone and origin.

Three sources may be considered for high sodium concentration (maximum 76 g/m^3 in well M36/1344) in the area;

1) sodium could enter the groundwater system as a result of ion exchange with Ca^{2+} along the flow path.

2) sodium may occur as a part of the terrestrial dust in precipitation especially in coastal area, however the amount will be small, 0.2 to a few g/m^3 per day (Matthess, 1982).

3) A maximum sodium concentration can occur in association with Cl^{-1} ions (marine origin). Sea water dilution has increased the sodium concentration in the coastal areas. The volcanic rocks in the Kaituna Valley have been analysed by Sewell (1985). The volcanic rock is rich in calcium and sodium-plagioclase feldspar, which will increase the probability of these rocks being a source for sodium concentration.

However the pattern which was developed from the concentration of other ions remains the same (Fig. 6.4) indicating a longer flow path for water from well M36/1344 and M36/1421 (within the lower and upper aquifer respectively).

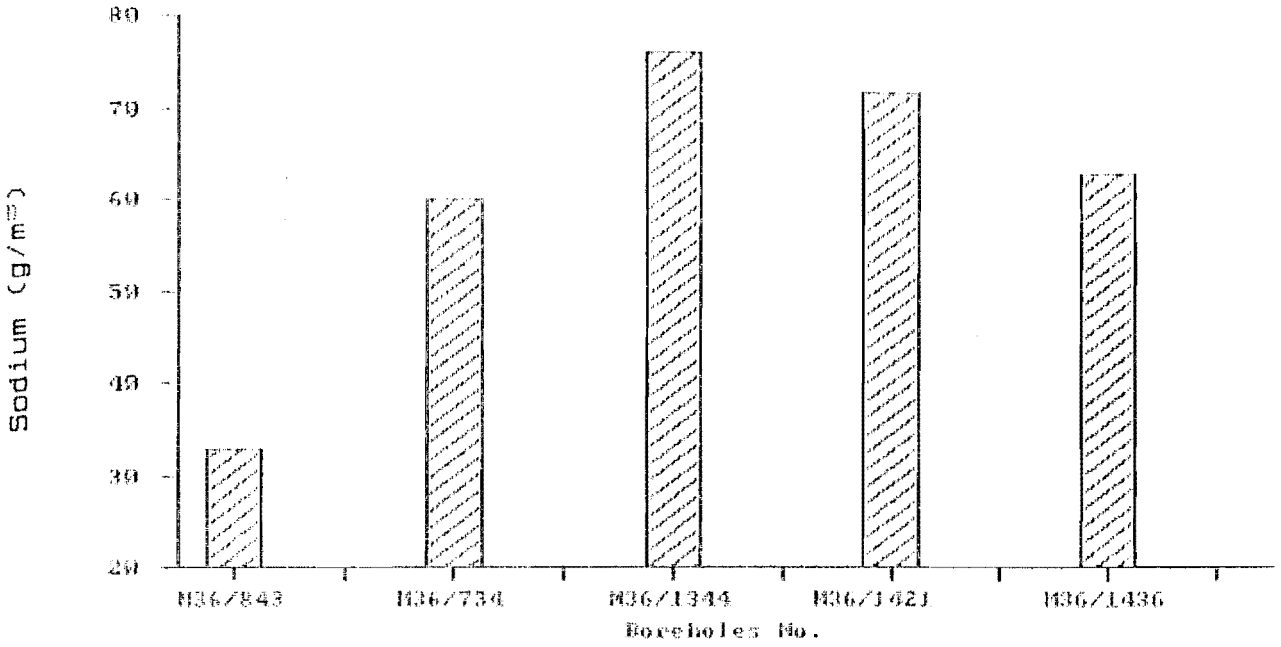

Figure 6.4 Comparison of Groundwater Sodium Data

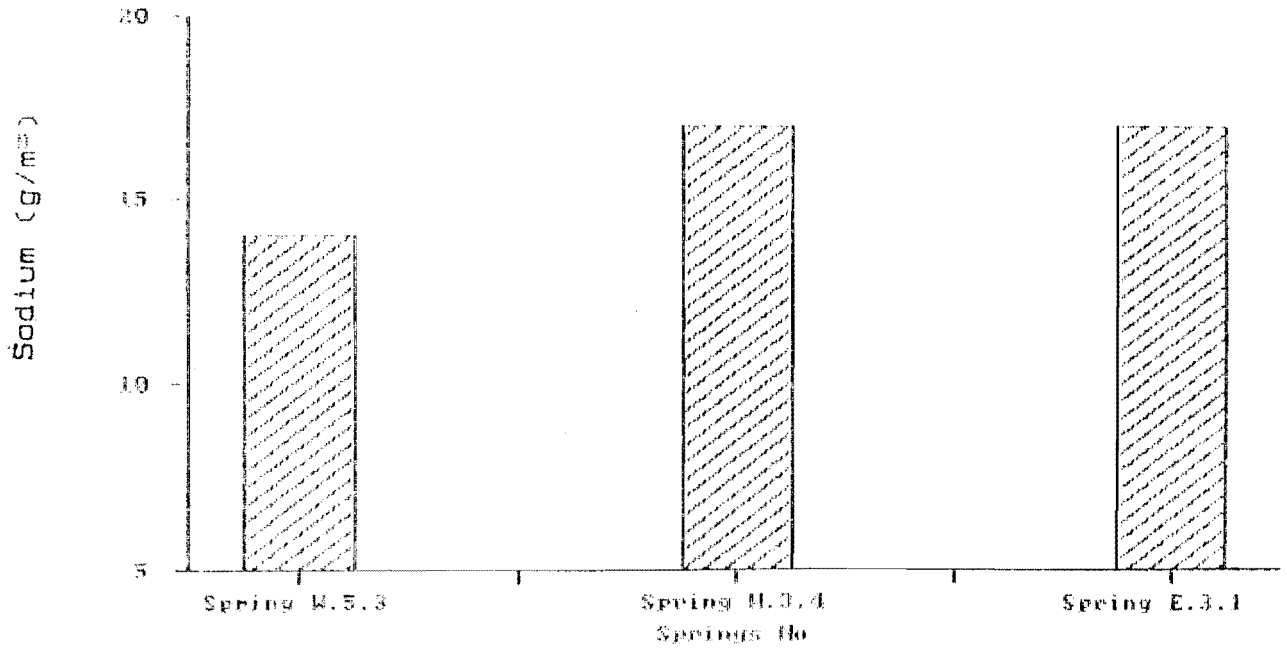

Figure 6.5 Comparison of Springs Sodium Data

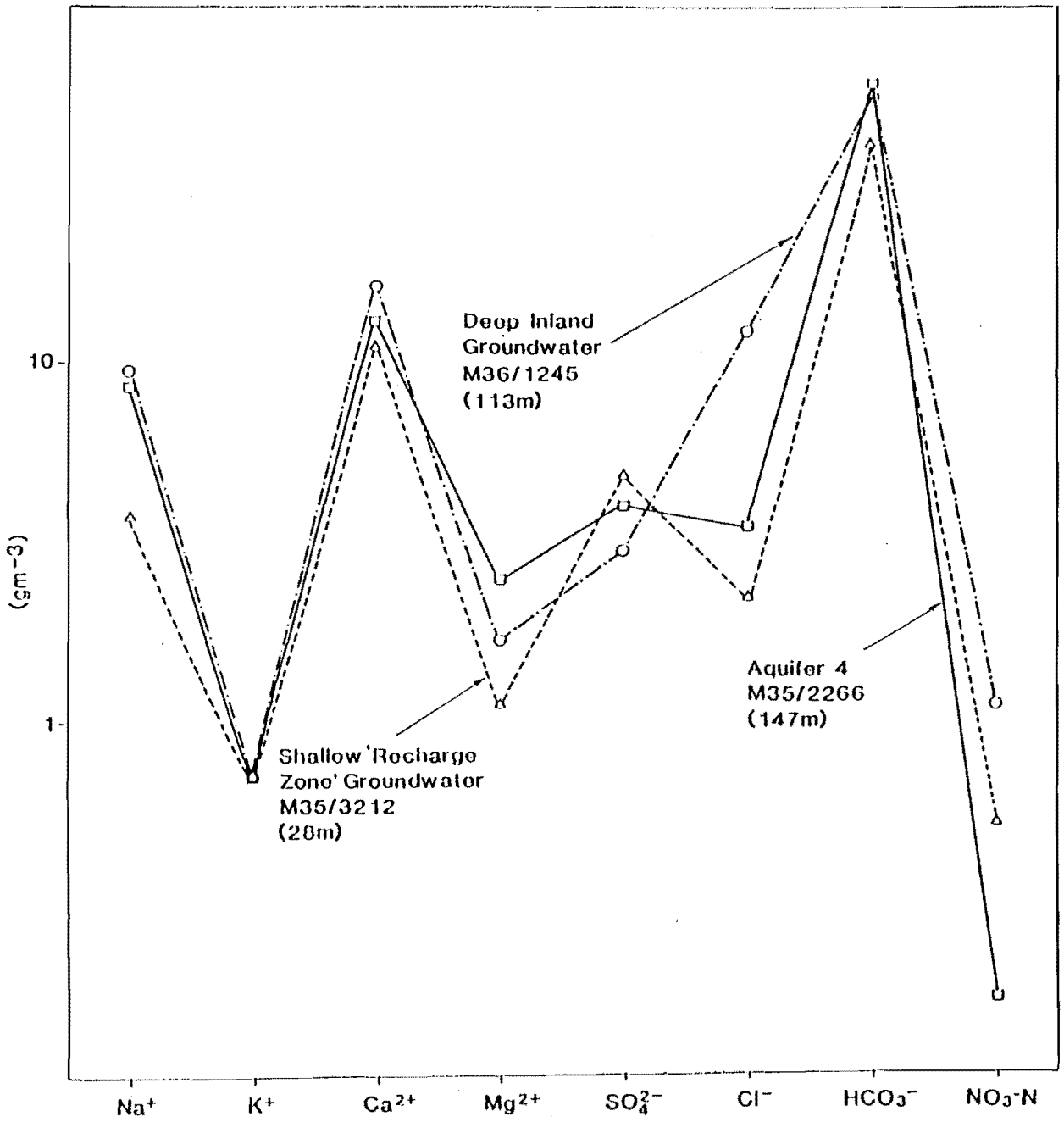

Figure 6.6 Chemical Profiles of Groundwater from Different Sources within the Canterbury Plains (after Talbot et al, 1986)

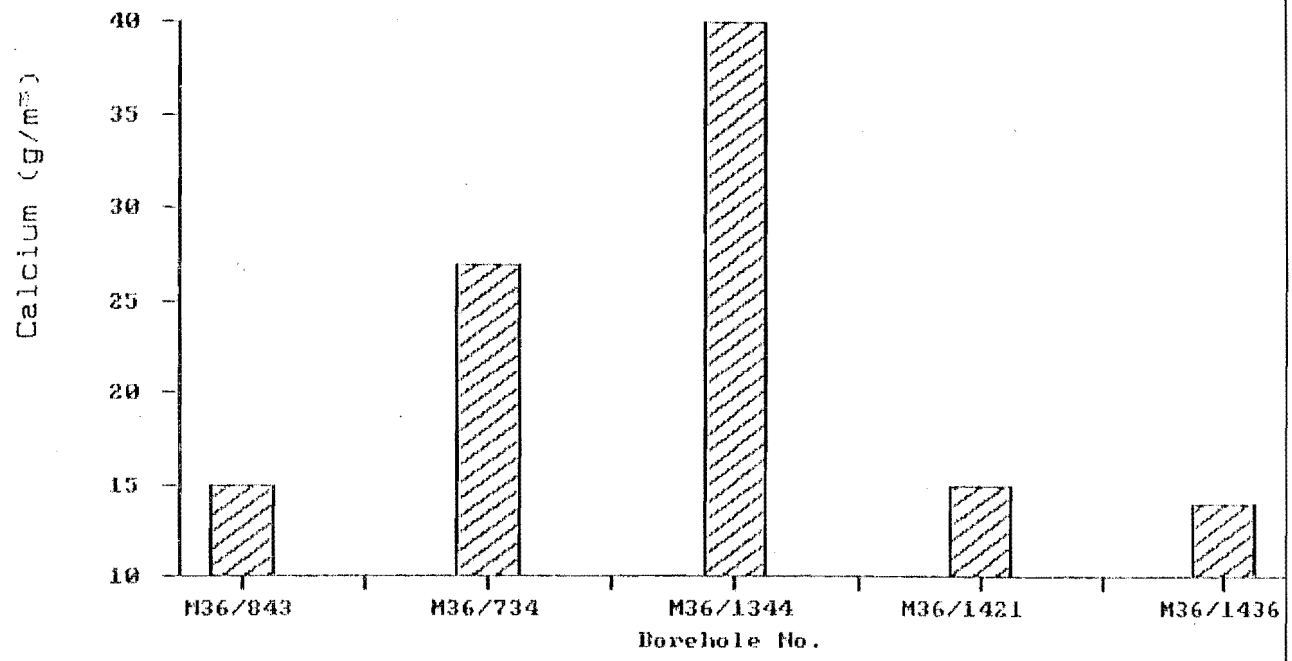

Figure 6.7 Comparison of Groundwater Calcium Data

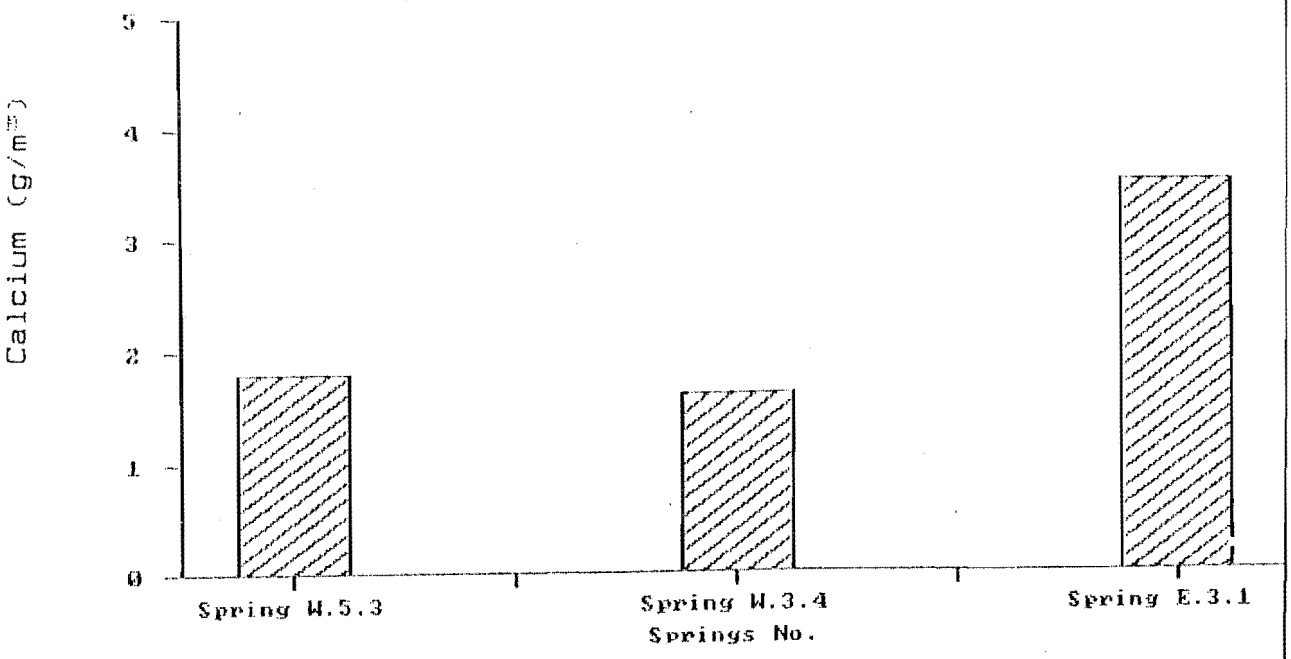

Figure 6.8 Comparison of Springs Calcium Data

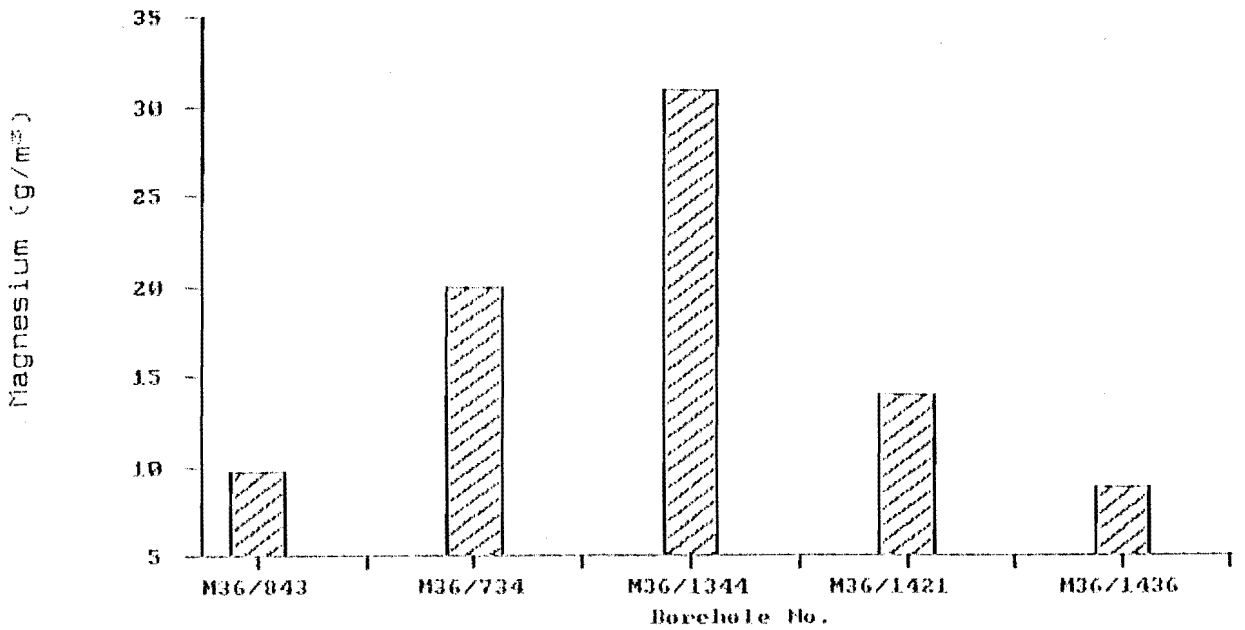

Figure 6.9 Comparison of Groundwater Magnesium Data

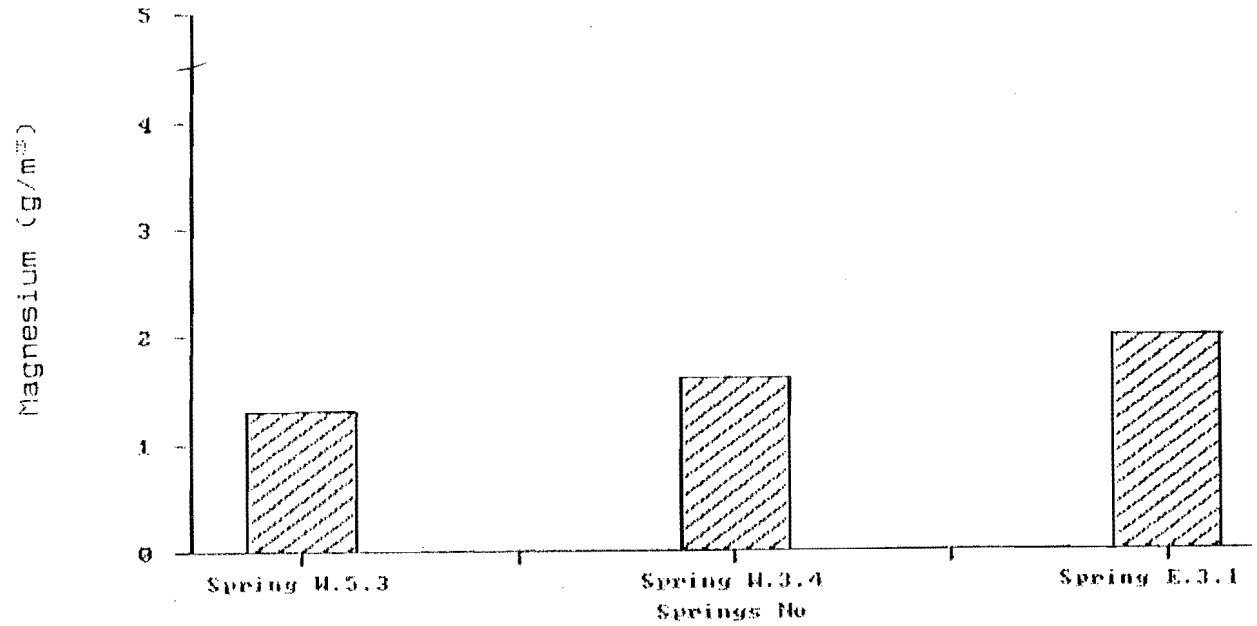

Figure 6.10 Comparison of Springs Magnesium Data

The higher concentration of sodium for spring E.3.1 compared with the other spring analyses also indicates a longer flow path. This is also supported by spring discharge monitoring (spring E.3.1 has a minimum response to rainfall variation, Sect. 5.4).

5) Iron (Fe^{2+})

Fe^{2+} concentration in groundwater from boreholes ranges between 0.18 and 2.5 g/m^3, and from springs between 0.09 and 0.29 g/m^3 (Table 6.1 and 6.2). Within volcanic rock, preferential sources of iron are the dark coloured minerals, such as pyroxenes, biotite and olivine. Iron content within groundwater samples from Kaituna Valley, are higher than values obtained from the Canterbury plain aquifers (Fig. 6.6). Bore M36/1344 shows an unusually high iron content in comparison to other wells sampled (Fig. 6.11). When drilled on 21/June/83, this bore was screened with stainless steel, excluding the possibility that an iron casing is responsible for the higher content in this well. Instead the high value in bore M36/1344 is considered to be partly due to the longer water flow path, and partly due to deoxygenated waters caused by high microbial activity in the confining clay.

The spatial pattern of iron is similar to that of previous cations for spring W.5.3 and E.3.1, and spring W.3.4 shows a higher iron content (0.60 g/m^3) compared with the other two springs (Fig. 6.12). This is considered to be due to a local change in chemistry of water (eg. a change in composition of volcanic rock along the flow path) rather than flow path length since it is not consistent with the previous results.

6) pH and Bicarbonate (HCO^-_3)

The incongruent dissolution of volcanic derived feldspars (eg. albit) involves the consumption of H^+ (Increase in pH).

As an example the reaction for dissolution of albite-kaolinite is given here.

$$NaAlSi_3O_8 + H^+ + 9/2\ H_2O = 1/2\ Al_2Si_2O_5(OH)_4 + Na^+ + 2S\ (OH)_4.$$

Production of CO_2 in the soil zone (due to decay of organic matter and respiration of plant roots) is considered to be the main source of H^+.

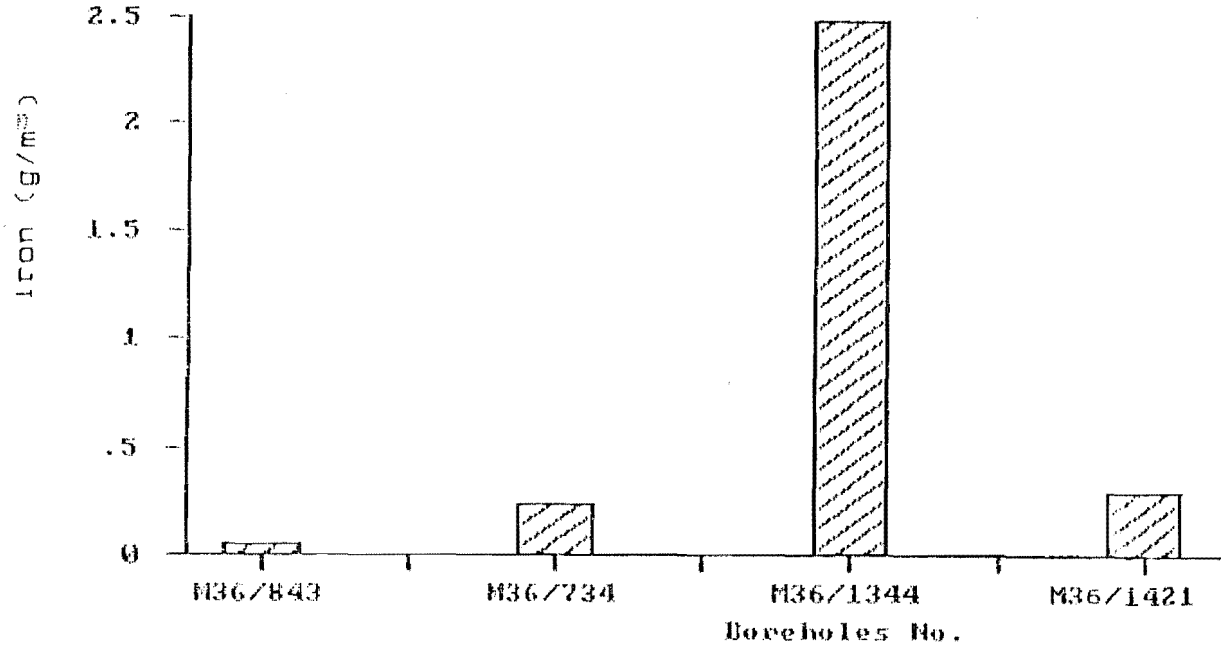

Figure 6.11 Comparison of Groundwater Iron Data

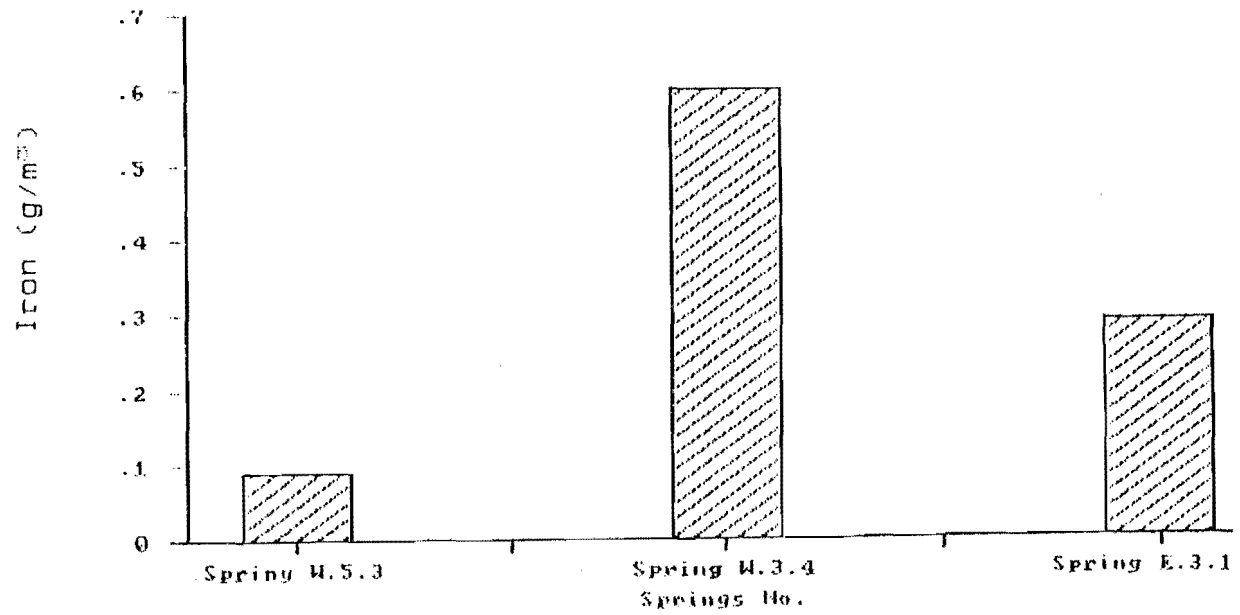

Figure 6.12 Comparison of Springs Iron Data

As this action proceeds, there is a progressive increase in pH and Biocarbonate alkalinity of water (Table 6.1 and 6.2). Therefore groundwater with a higher pH and $HCO3^-$ values would be expected to have a longer flow path.

The pH values for groundwater from the boreholes and springs are presented in Fig. 6.13 and 6.14. Flow path interpretation using pH is consistent overall with the previous results obtained from cations. The pH value for well M36/1421 (within the upper aquifer) is slightly lower than that from well M36/1436, however the difference is not sufficient to alter the previous consistent assumptions regarding the flow paths in this aquifer.

7) Chloride (Cl^-) and Sulphate (SO_4^{2-})

Cl^- and SO_4^{2-} are not significant constituents in basalt, hence there is no increase in concentration of these anions due to pathflow along volcanic rocks. An increase in Cl^- can be due to the chemical evolution of groundwater towards the composition of seawater with increasing age;

$$HCO^-_3 \text{ ----> } HCO^-_3 + SO_4^{2-} \text{ ----> } cl^-$$

As a result all water samples from bores show a higher concentration of Cl^- compared with spring water (Tables, 6.1 and 6.2).

No direct seawater intrusion was detected in any of the groundwater samples. (the concentration value for sea water in coastal area of Canterbury Plains is 19000 g/m^3, Talbot et al, 1986). However sea water dilution of groundwater recharged through the volcanic rocks is possible.

6.2.4 Summary

Study of the spatial distribution of chemical constituents in groundwater indicates a volcanic flow path and origin for water in both aquifers in Kaituna Valley. No evidence of mixing of Kaituna groundwater with marine water or Canterbury Plain aquifers was determined. The hydrochemical analyses on groundwater water from boreholes M36 1344 (within the lower aquifer), and M36/1421 (within the upper aquifer) indicate a longer flow path compared with other wells.

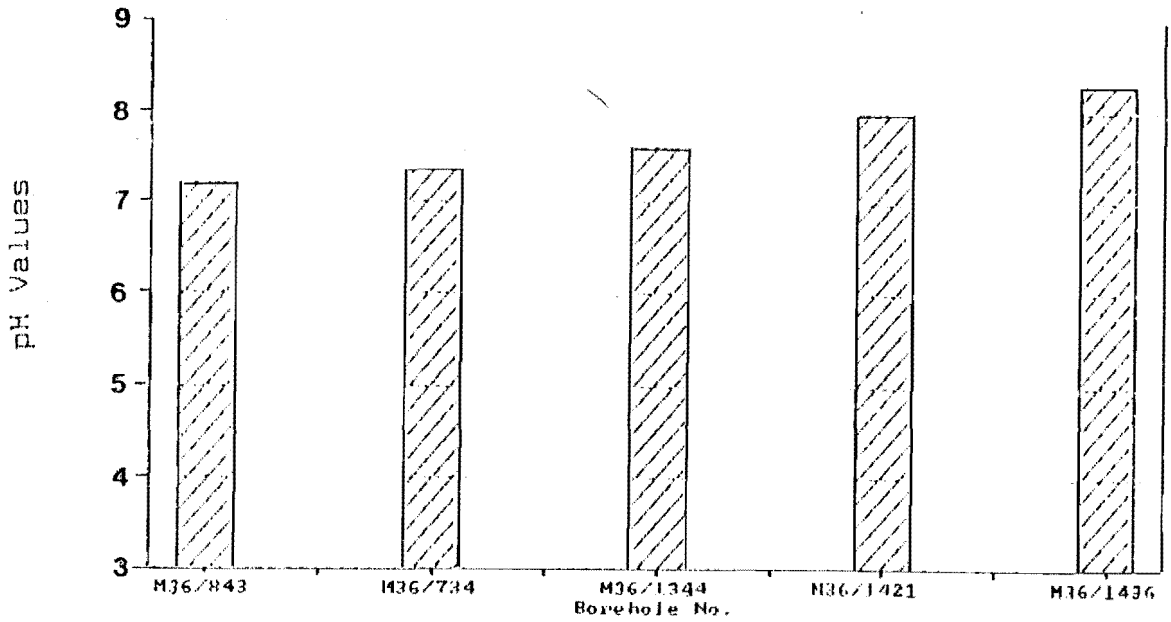

Figure 6.13 Comparison of Groundwater pH Data

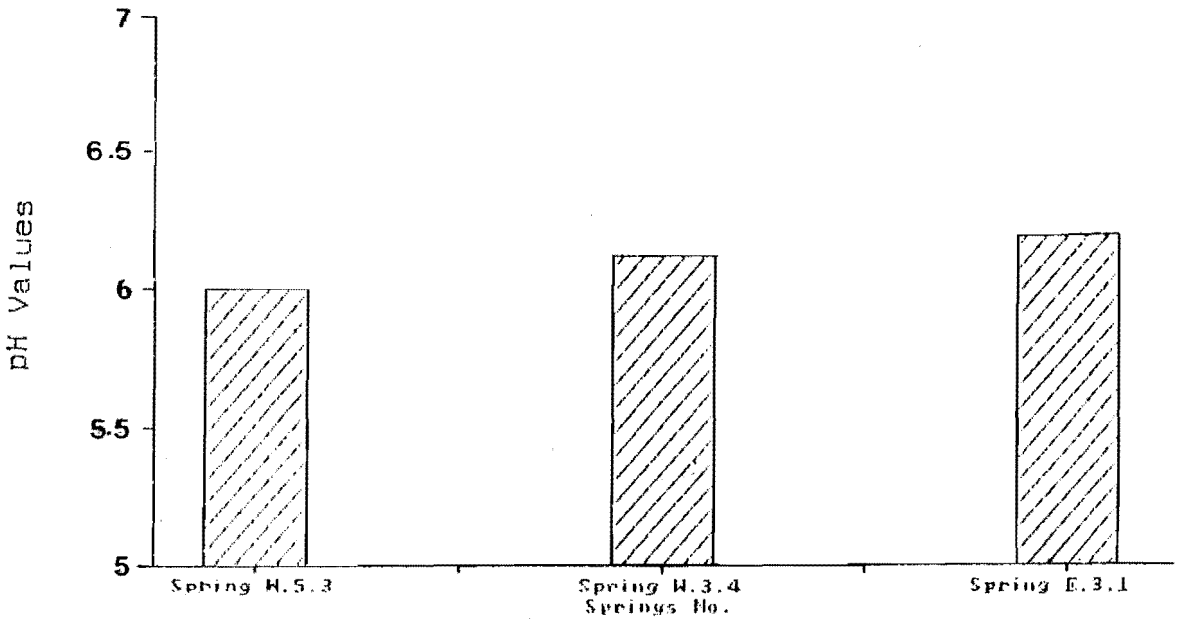

Figure 6.14 Comparison of Springs pH Data

6.3 Hydrochemistry and Water Quality

6.3.1 Water Quality Parameters.

The hydrochemical analysis of water is of great importance in determining the suitability of a particular groundwater or surface water for a specific use (eg. public water supply, and/or irrigation application). The more important chemical constituents and the defined quality parameters for their use as drinking water and for irrigation purposes are reviewed in this section. Water sampling sites are shown in Fig. 6.1.

Surface water from Okana stream is used mainly as drinking water and its suitability for this purpose are also evaluated. Quality parameters for drinking water are mostly taken from "Drinking-Water Standard for New Zealand" (N.Z.D.W.S 1984)(APP. 14.2), which is based on World Health Organization Standards (APP. 14.3) with consideration given to New Zealand's local conditions of topography, land use, natural water quality and other relevant factors.

In this classification "highest desirable" refers to water which would be generally accepted to consumers. Concentration of solutes higher than "excessive value" markedly impair the potability of the water.

Irrigation water quality requirements differ between crop type, soil type and climatic variations, therefore the standards for irrigation water cannot be formulated precisely for different areas. However general guidelines are given by Ayers (1975), National Academy of Sciences (N.A.S), and the National Academy of Engineering (N.A.E)(1972) are considered for evaluation of water for irrigation proposes in this study. Guidelines tables are given in App. 14.4 and 14.5.

6.3.2 Nitrogen

Although some volcanic rocks contain nitrogen, most nitrogen found in groundwater is derived from the biosphere. The inorganic salts of the nitrogen cycle include nitrate (NO_3^{2-}) and nitrite (NO_2^-). In addition, ammonical nitrogen can exist as a gas (NH_3), which is highly soluble in water.

Nitrate has been proven to be a health hazard when occurring in water at concentrations in excess of 10 g/m^3 (N.Z.D.W.S). At higher nitrate level, young infants (less than 4 months old) are affected by

metahaemoglobinemia. In all water samples the nitrate content is less than the undesirable limit of 10 g/m^3.

All water samples from the wells show a low nitrate nitrogen concentration (<1 g/m^3) except that from M36/843 where the concentration is significantly higher (4.6 g/m^3). This uncapped well is located in grazing land with no cap and hasn't been used for about one year due to pump failure. The high nitrate nitrogen value here is assumed to be due to urine "spotting", a local change in chemistry of the groundwater unrelated to the recharge zone. It is still, however, satisfactory as drinking water, the nitrate nitrogen being less than the 10 g/m^3 maximum given by the Drinking Water Standards for N.Z.

Ammonia nitrogen is undesirable in water due to its taste and odour. The recommended upper limit for ammonia nitrogen in drinking water is 0.5 mg/l, according to World Health Org. 1963, (App 14.3). For irrigation water, ammonia nitrogen in excess of (>5 g/m^3) may delay harvest time and adversely affect the quality of several types of fruits (eg. apricots).

Water from boreholes and springs sampled in this study have an acceptable concentration of ammonia nitrogen for use as drinking water, except boreholes M36/734 (0.58 g/m^3), M36/1344 (0.95 g/m^3) and M36/1421 (0.55 g/m^3). These are however in acceptable range for irrigation purposes.

6.3.3 Hardness as ($CaCO_3$)

The reaction of soap with calcium, and also magnesium, iron, manganese, copper, barium, and zinc has led to the concept of water hardness. In general this property is attributed only to calcium and magnesium dissolved in water [Ca & Mg $(H\ CO_3)_2^-$], but it is usual to calculate it on the basis of calcium alone (Matthess, 1982). Water Hardness is specifically classified according to calcium carbonate content, with a highest desirable hardness level set at 80 g/m^3 $CaCo_3$ for domestic user (N.Z.D.W.S).

Hem (1970) defines the following water types with reference to $CaCO_3$;

soft 0-60 g/m^3
moderately hard 61-120 g/m^3
hard 121-180 g/m^3
very hard >180 g/m^3

Using this classification, all springs sampled consisted of soft water (below "highest desirable" values), while bores M36/843, M36/1421 and M36/1436 have a moderately hardness (Tables, 6.1 and 6.2). Bore M36/734 contained hard water (150 g/m^3) and water from well M36/1344 is very hard at 228 g/m^3 which is higher than the "excessive " limit (200 g/m^3) (Drinking Water Standards for N.Z, Fig. 6.15 and 6.16).

6.3.4 Iron as Fe^{2+}

The soluble ferrous ion Fe^{2+} is the common form of iron found in groundwater. When exposed to the atmosphere, Fe^{2+} is oxidized to the Fe^{3+} state which is insoluble and causes a brown discoloration of the water. Both corrosion of well casings and bacterial activity can also affect the concentration of iron in groundwater. The "highest desirable" value (according to N.Z.D.W.S) is 0.1 g/m^3 with "excessive" content set at 1.0 g/m^3, as shown in Fig. 6.17 and 6.18. Iron concentration is more than the "Highest desirable" value in all water samples. Well M36/1344 (Fig. 6.19) exceeds the "excessive" values.

Undesirable effects of excessive iron include taste, turbidity, deposits, and growth of iron bacteria. Recommended maximum limits of iron for permanent irrigation is 5 mg/l (N.A.S and N.A.E, 1972), and all groundwater samples tested therefore fall within the desirable range for irrigation purposes.

6.3.5 Manganese (Mn^{2+})

Soluble Mn^{2+} is oxidized to much less-soluble hydrated oxides upon exposure to the atmosphere, and forms black stains in pipes. The maximum desirable values of manganese for supply water is set at 0.05 g/m^3 with, an "excessive" limit of 0.5 (N.Z.D.W.S). At these high levels manganese contributes undesirable taste, turbidity, and discolouration to the water. Springs and surface water from Okana stream have values less than the "highest desirable" limit. Manganese concentrations are greater than this desirable value in all boreholes, except for well M36/734 (Fig. 6.17). Bores M36/843 and M36/1344 contain manganese in concentration higher than the excessive level. The manganese concentration in groundwater from wells M36/843 and M36/1344 (Fig. 6.17) is also higher than the maximum recommended limit for water (0.2 g/m^3) for permanent irrigation (App.

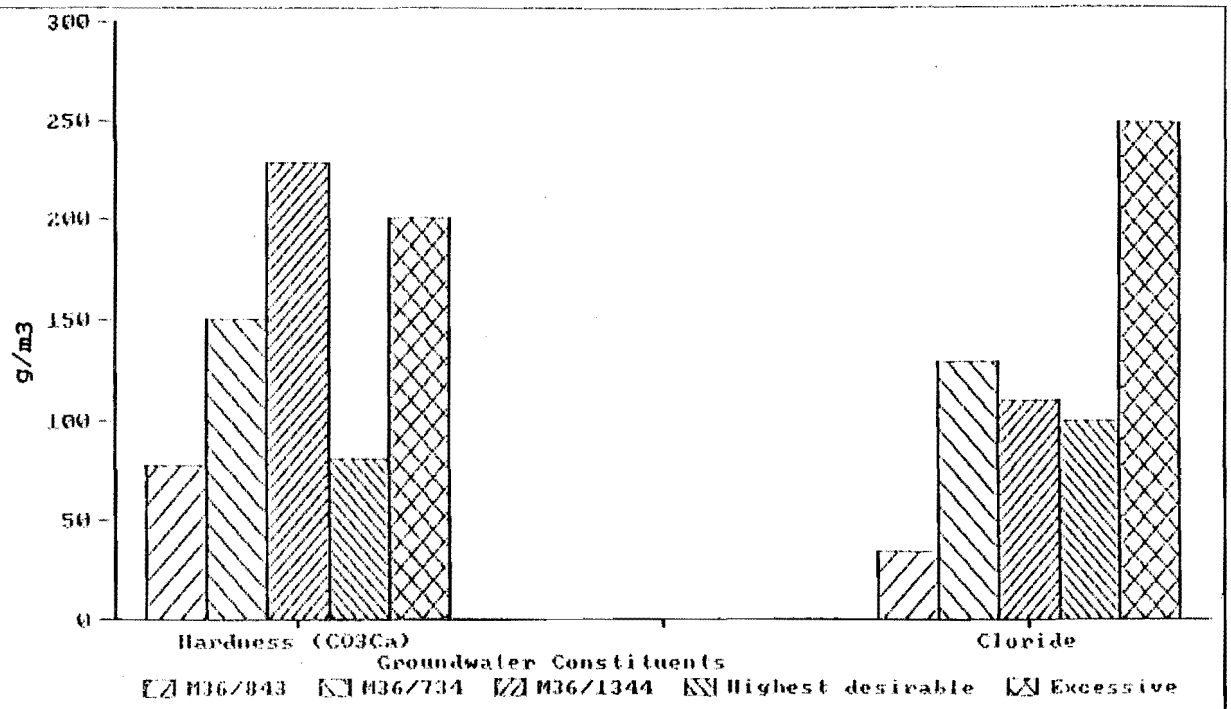

Figure 6.15 Comparison of Cl^{1} and $CaCo_{3}$ constituents and N.Z Standard Guideline Values for wells M36/843, M36/734, and M36/1344 (lower aquifer)

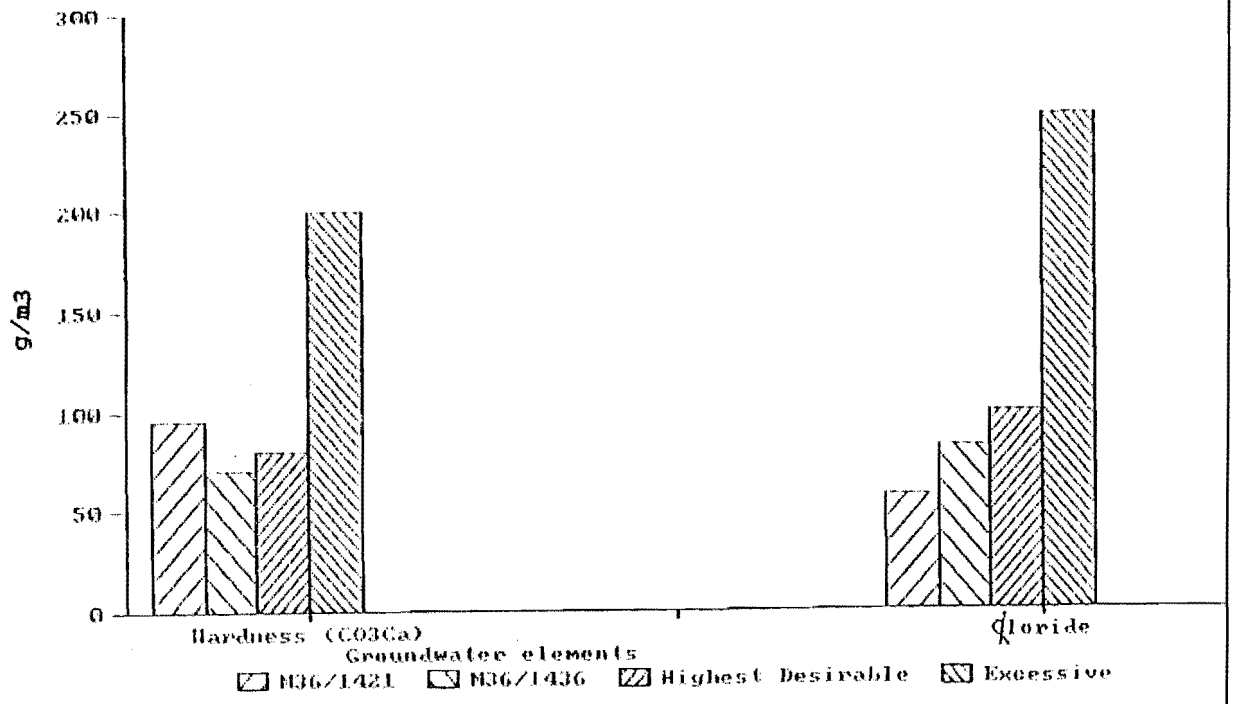

Figure 6.16 Comparison of Cl and $CaCo_{3}$ Values for wells M36/1421, M36/1436, (upperr aquifer)

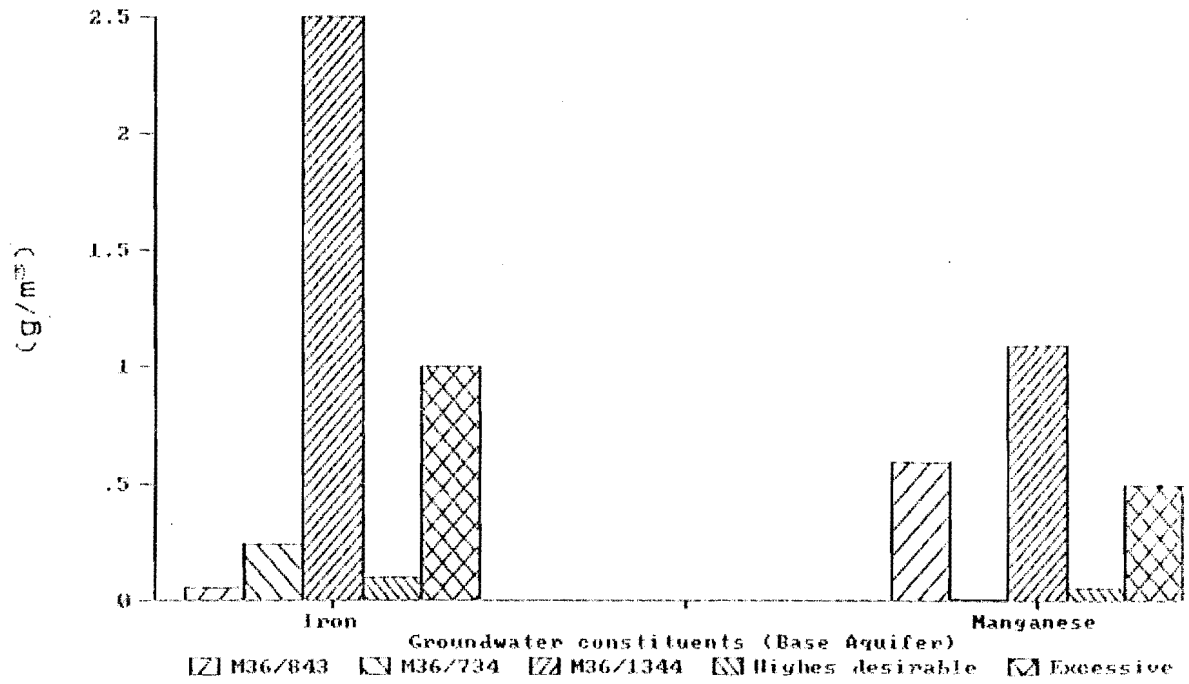

Figure 6.17 Comparison of Fe^{2+} and Mn^{2+} constituents and N.Z Standard Guideline Values for wells M36/843, M36/734, and M36/1344 (lower aquifer)

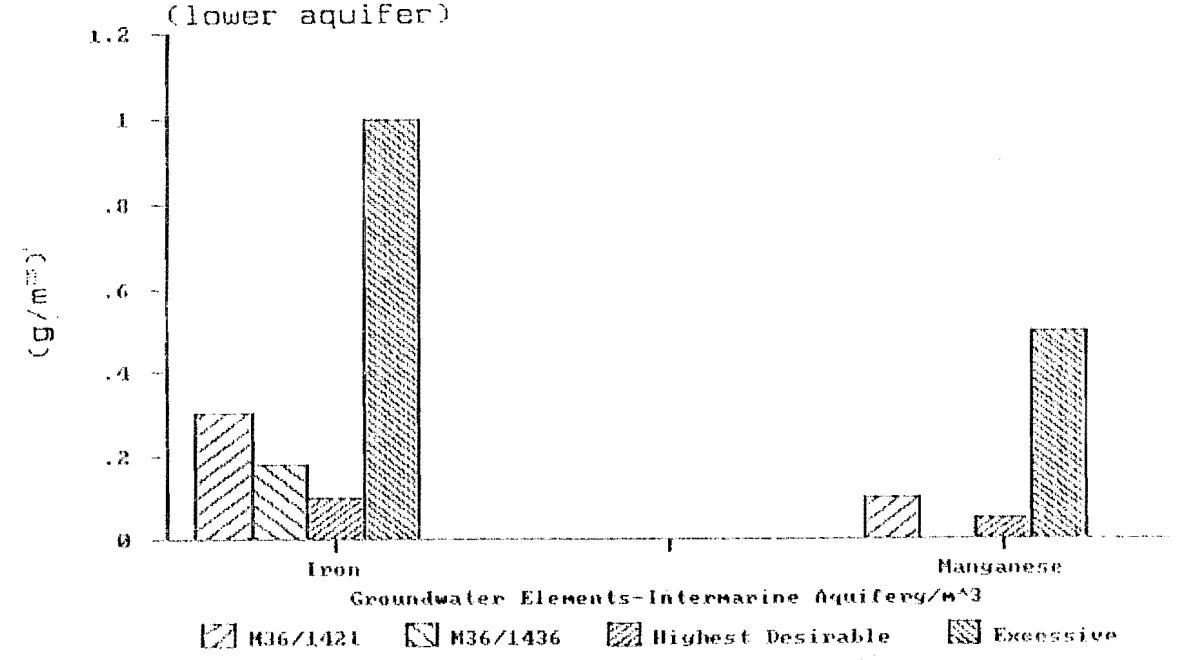

Figure 6.18 Comparison of Fe^{2+} and Mn^{2+} Values for wells M36/1421, M36/1436, (upperr aquifer)

14.5).

6.3.6 Magnesium (Mg^{2+}), Sodium (Na^{+}), Calcium (Ca^{2+})

Magnesium concentration in groundwater is relatively low compared with other cations (eg. Na^{2+}, Ca^{2+}). In all water samples tested, magnesium concentration is less than the maximum acceptable limit (50 g/m^3) set by the World Health Organization App. 14.3.

Sodium content for all water samples tested are lower than the "highest desirable" value (100 g/m^3) recommended for drinking water quality (N.Z.D.W.S). Water with a sodium concentration higher than 69 g/m^3 is not suitable for irrigation especially if the water is absorbed by the leaves of crops (Ayers, 1975). Water from all wells except M36/843 shows a sodium concentration which is unsuitable for irrigation purposes (Table 6.1).

Calcium concentration values within groundwater samples and surface water fall below maximum acceptable values (75 g/m^3) adopted by the World Health Organization (App. 14.3) for drinking water.

6.3.7 pH

The pH of groundwater samples and surface water falls below the "Highest desirable" limit (7.4 to 8.5) set by N.Z.D.W.S Corrective pH treatment is therefore not necessary.

6.3.8 Sulphate (SO_4^{2-}), Chloride (Cl^{-}), and Bicarbonate (HCO_3^{-})

Sulphate is a non toxic substance, however high sulphate water may have a laxative effect. Groundwater and surface water tested show a sulphate value which is less than the highest desirable limit (50 g/m^3)(Tables, 6.1 and 6.2). Cloride concentration is above the "Highest desirable" values in water samples from bores, M36/734 and M36/1344 (Fig. 6.15). The taste threshold is reached at concentrations between 200 and 250 g/m^3 and corrosion of metal well casings may also result.

Excessive bicarbonate content is defined as a range between 90 and 520 g/m^3 in water, making it unsuitable for irrigation and possibility causing white carbonate deposition on fruits and leaves (when applied with sprinklers). In all tested boreholes the groundwater had values within

the above range (Table 6.1), hence rendering it unsatisfactory for irrigation, although it is at present being utilized for this purpose.

6.4 Environmental isotopic Study

6.4.1 Methodology

In addition to the standard chemistry of the groundwater and surface water, representative samples have been analyzed for environmental Isotopes. The term of "environmental isotopes" in hydrology is used to describe isotopes that occur naturally in the hydrological cycle (Lloyd, 1981). The main hydrogeological objectives of this part of the study were; 1) to define the groundwater sources, and 2) to provide age information about groundwater

Due to lack of finance only Oxygen-18 (^{18}O) and Tritium (^{3}H or TR) were used for these purposes and Deuterium (^{2}H) measurements were omitted. Water was sampled from three boreholes (M36/734, M36/1344, and M36/1437) and three springs (E.3.1, W.5.3, W.3.4) the locations of which are shown in Fig. 6.1. and date is summarized in Tables, 6.3 and 6.4.

6.4.2 Oxygen-18 (^{18}O) and Recharge Altitude

1) Oxygen-18 (^{18}O)

Oxygen-18 measurements are expressed as δ-values, representing parts per thousand difference between measured $^{18}O/^{16}O$ and that of an arbitrary standard, the Standard Mean Ocean Water, SMOW.

$$\delta^{18}O^{o}/_{oo} = \frac{R(\text{samples}) - R(\text{SMOW})}{R(\text{SMOW})} \times 1000$$

where

R is isotope ratio of $^{18}O/^{16}O$

Precipitation falling at a high elevation is generated at colder temperatues and is more depleted in ^{18}O than precipitation falling at lower elevations. This produces marked vertical concentration gradients in the atmosphere (ie. altitude effect). The $\delta^{18}O$ of high altitude precipitation near the Southern Alps ranges between δ-9.0, and δ-9.8 (Talbot and et al 1986), whilst for predominantly low altitude the $\delta^{18}O$ is range between δ-6.6 and δ-7.4. Values of δ-7.8 to δ-8.6 are from moderate alti-

Table 6.3: Isotope Measurements of Groundwater

Grid. Ref.	Bore No.	Bore hole (Sample) depth (m)	Bore hole elevation (m)	Tritium (TR)	$\delta^{18}O$ ($O^0/_{00}$)
M36 47 175	M36/734	21.3	10.5	0.90 ± 0.11	-7.32
M36 844 165	M36/1344	30.0	6.45	0.03 ± 0.09	-7.21
M36 823 150	M36/1436	90.7	3.25	0.01 ±0.08	-7.87

δ values with respect to SMOW (for ^{18}O)

E.g. $\delta\ ^{18}O^0/_{00} = [(^{18}O/^{16}O)_{Sample} / (^{18}O/^{16}O)_{SMOW} - 1] \times 1000$

Analyst: Institute of Nuclear Science. Date: 24/11/86.

Table 6.4: Isotope Measurements of Springs

Grid. Ref.	Spring number	Elevation (approx.) (m)	Tritium (TR)	$\delta^{18}O$ ($O^0/_{00}$)
M36 836 196	W.5.3	500	4.27 ± 0.27	-7.91
M36 859 165	E.3.1	400	3.98 ± 0.26	-8.01
M36 837 181	W.3.4	300	4.41 ± 0.29	-7.64

δ values with respect to SMOW (for ^{18}O)

E g. $\delta\ ^{18}O^0/_{00} = [(^{18}O/^{16}O)Sample/(^{18}O/^{16}O)_{SMOW} - 1]\times 1000$

Analyst: Institute of Nuclear Science. Date: 24/11/86.

tude or water of mixed origin, therefore ^{18}O values can be indicators of the recharging water altitude.

2) Recharge Altitude

During 1970-73 a number of groundwater sites which couldn't have derived in any other way but precipitation, were sampled within the Kaikoura, Wairau and Waimea Plains and the Tumarina Valley (Taylor et al. 1978). On the basis of temperature correlations, results indicated a very uniform isotopic composition. It was deduced that the isotopic composition $\delta^{18}O=-6.2$ would approximate closely to the mean precipitant-derived groundwater within the Canterbury Plains (Taylor et al 1978)

In Kaituna Valley isotope measurement of spring W.5.3, which is located at an altitude of 475 m showed an oxygen-18 concentration of -7.91 (Tables, 6.3 and 6.4). Chemical analysis revealed that the spring has the shortest flow path compared with the other springs sampled, therefore its oxygen-18 concentration is assumed to be the same for precipitation in this altitude.

The relationship between the two measurements δ -6.2 for precipitation on the Canterbury Plains and the δ -7.95 for precipitation at elevation 475 m on Banks Peninsula gave an approximate altitude gradient of $-0.35^{o}/_{oo}$ per 100 m for ^{18}O (or $\delta^{18}O=-0.0035H$ -6.2) where H is elevation above mean sea level (Fig. 6.19).

The computed elevation interpretation for springs water recharge altitude is presented in Table 6.5

Boreholes No.	$\delta^{18}O$	R.L (m)	Springs No.	$\delta^{18}O$	R.L (m)
M36/734	-7.32	320	W.5.3	-7.91	475
M36/1344	-7.21	288	W.3.4	-7.64	480
M36/1436	-7.87	477	E.3.1	-8.01	517

Table 6.5 Computed recharge elevation (R.L) for groundwater and springs

The Oxygen-18 concentration of groundwater from bore M36/734 and M36/1344 are less negative than the value obtained from bore M36/1436. This indicates water in wells M36/734, M36/1344 has originated from higher elevations compared with water from bore M36/1436 (Table. 6.5). According to Table 6.5 the spring E.3.1 is recharged from a higher elevation (517 m) compare with the other tested springs indicating a longer

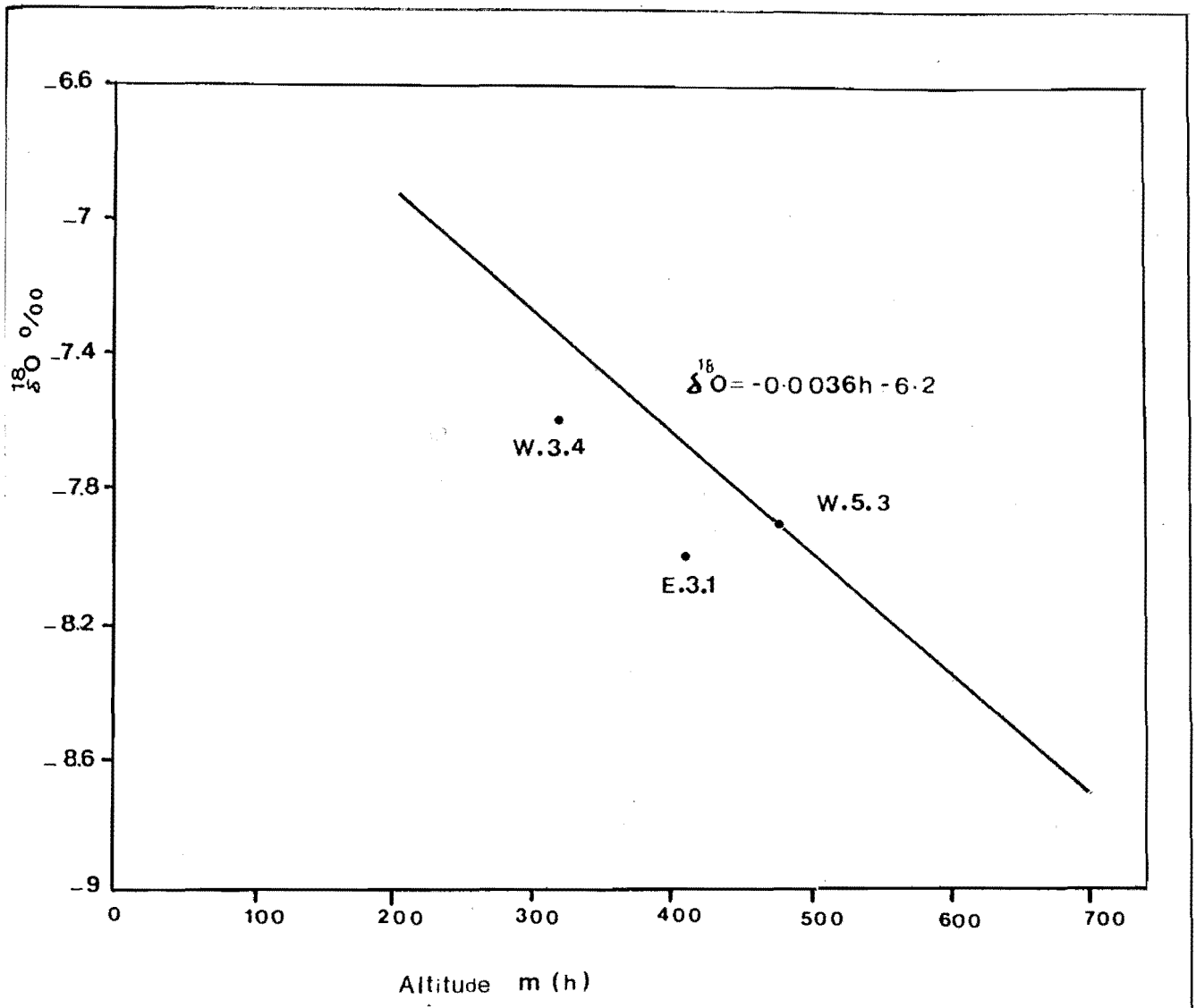

Figure 6.19 Oxygen-18 Values of Springs Plotted Against the Outlet Altitude and Computed Recharge - Elevation Line

flow path. The longer flow path for the spring was also supported by the water chemistry data (sect. 6.2) and springs discharge monitoring (sect. 5.4).

6.4.3 Tritium (^3H) and Groundwater Dating

1) Tritium (^3H)

Tritium is produced in the atmosphere as a result of cosmic high energy radiation, and enters the hydrological cycle in precipitation. Natural levels of tritium have been significantly disturbed since 1952 following the detonation of thermonuclear devices. The hydrogen bomb was found to introduce tritium of such an extent that it totally changed any natural background level. The tritium ratio in precipitation in the southern hemisphere, rose from 1.5 - 2.0 to a peak of about 40 in 1965 at Kaitoke near Wellington (Stewart and taylor, 1981).

2) Groundwater Dating

The TR (^3H) concentration data from Kaituna valley is presented in Table 6.3 and 6.4 and are measured in units of TR where (TR= one atom of ^3H per 10^{18} atom of ^1H). Mean annual tritium ratio values at Kaitoke, are presented in Fig. 6.20. The TR value for all boreholes indicates that the groundwater was formed earlier than 1955 (30 to 35 years). Tritium values of the two wells (M36/1436 and M36/1344) lie beyond the detected age rang indicating that it has a mean residence time greater than 50 years (Table 6.4), therefore bore M36/734 is relatively younger than the two other wells.

The value of tritium for those springs tested are presented in Table 6.4. All springs have tritium concentration close to the current rainfall concentration (Fig 6.20). Considering the mean annual tritium ratio, recharge for groundwater derived springs has been occurring within the last five years.

6.5 Synthesis

The comparison between the chemistry of groundwater in Kaituna and adjacent Canterbury Plains (Fig. 6.6) indicates a volcanic recharge path for the groundwater system in Kaituna Valley. The spatial pattern of ion

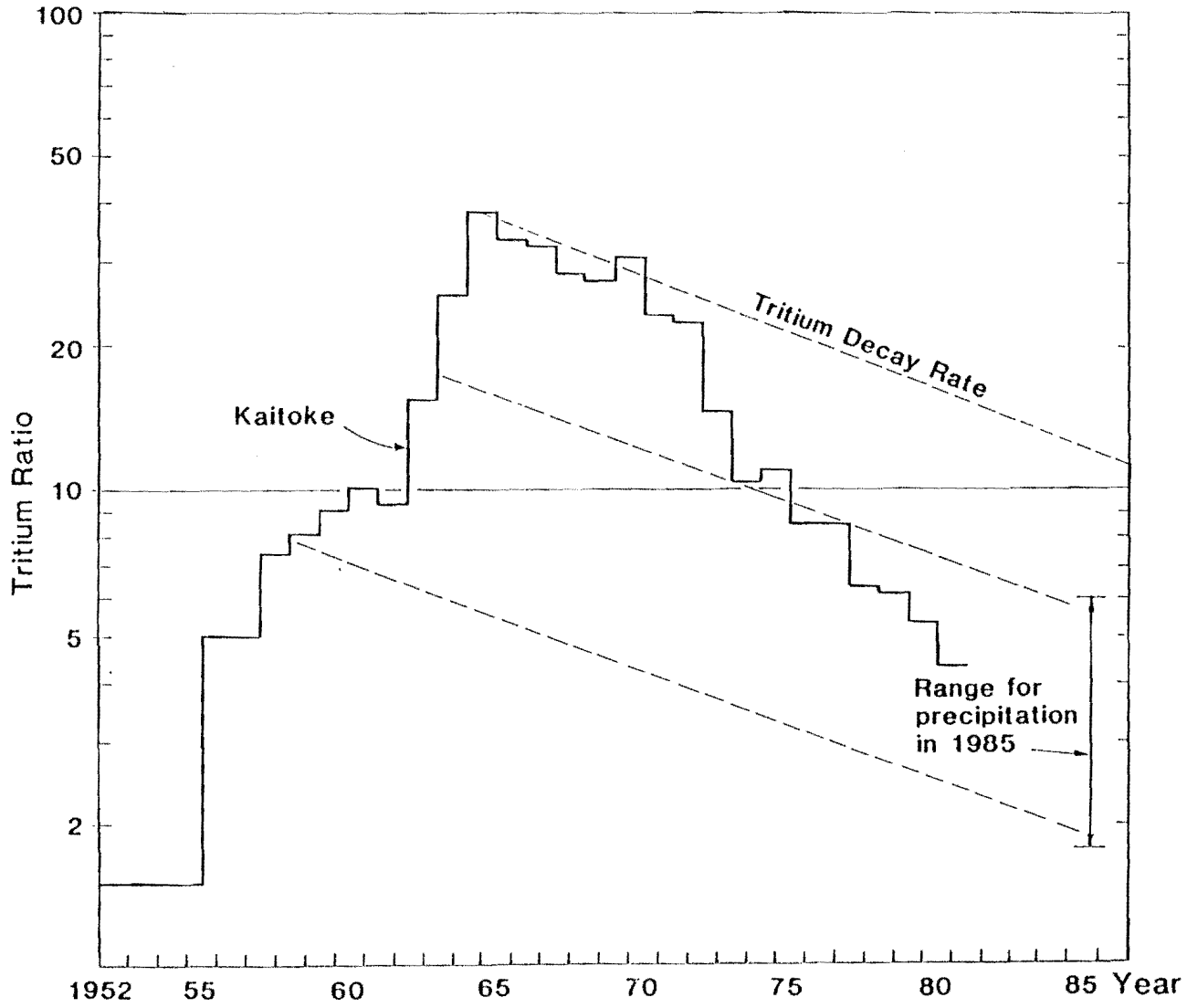

Figure 6.20;

Mean Annual Tritium Ratio Values at Kaitoke, Near Wellington (after Taylor and Stewart, 1981)

concentrations in groundwater derived from the lower and upper aquifers is different, due either to volcanic composition being different along the flow paths or to residual seawater in the lower aquifer. A longer flow path is find in bore M36/1344 related to the lower aquifer and bore M36/1421 related to upper aquifer.

With respect to water use, if ground water is to be used for drinking, it must be treated for excessive iron in well M36/1344, and excessive manganese in wells M36/843 and M36/1344. The sodium concentration in all bores (except M36/843) and bicarbonate content in all wells are too high for drinking water and not well suited for irrigation.

$\delta^{18}O$ values from aquifers and springs indicates that the predominant source of water in Kaituna Valley is from elevations between 320 m and 550 m. Tritium measurements indicates that base and upper aquifer waters have an age greater than 30 years while springs indicate a water age formed within the last five years.

CHAPTER SEVEN

SUMMARY AND CONCLUSION

7.1 Project Background

In the Kaituna Valley in recent years there has been a steady change in land use from traditional pastoral farming to more intensive forms of land use, including horticulture, market gardening and dairying. These changes have produced an increased demand for water, particularly groundwater. The present study was undertaken in order to provide an adequate data base to assess and delineate the groundwater system, and in order to provide an adequate data base to develop appropriate water management strategies for the Kaituna Catchment, and for other similar tributary catchments in an the Banks Peninsula.

7.2 Hydrogeological Characterization

Hydrogeological characterisation was mainly undertaken to define the geological controls on groundwater movement. The geologic frame work in the study area consists of volcanic lava flows and intrusive rocks, pyroclastic materials, regolith deposits and alluvial and coastal sediments.

Two types of water flow were distinguished within the lava flows. Horizontal water flow occurs predominantly within the basal breccias and rubbly tops of the lava flows. Water flows to the south due to the gentle (6°-20°)dip of the lava. Vertical water flow occurs within vertical shrinkage cracks within the lava.

The main perching layer within the rock mass is ash and tuff. Volcanic colluvium which consists of poorly sorted volcanic fragments with less than 10% loess, is the most suitable medium for water flow among the regoliths.

The alluvial and coastal terrain in the Kaituna Valley floor consist of a wedge of sediments resting on a lake ward inclined (southward) volcanic basement surface. Marine and terrestrial sediments within the area are related to transgressions and regressions of the sea level during the Pleistocene.

Permeability tests revealed that the silty layers which cover the top part of the alluvial plain have a very low hydraulic conductivity from 1.13×10^{-6} to 1.15×10^{-8} m/s.

7.3 Engineering Geophysical Investigation

Geophysical investigation consisted of, electrical resistivity, geophysical logging, and seismic refraction and reflection surveys. Profiles were carried out to complement geological observation in defining aquifer distribution.

Correlation of geophysical logs between different holes defined lithological continuity and variation of valley floor sediments. The results obtained from the resistivity surveys indicate that the method is useful for the detection and delineation of near-surface gravelly zones.

The technique was also successful for outlining courses of buried channels above the volcanic rock, where the depth to the bed rock is less than 40 m. Results were also quite satisfactory for locating the basement which underlies the lowest aquifer system in the area, at depths of less than 40 m.

The two seismic methods (reflection and refraction) were in good agreement about depth to basement, with the reflection survey indicating a maximum depth of 175 m for line CC′, and the refraction survey suggesting a depth of 160 m to bedrock. The seismic reflection method proved to be of more use because it provides more detailed information on the sedimentation environment and lithology of the overburden deposits.

Two main aquifer zones have been identified by the geophysical investigation. The Lower Aquifer overlies volcanic basement and consists of gravel and volcanic colluvium with thickness ranging from 2m (bore M36/1344) to 60 m in the bottom part of the valley (Geophysical logging and seismic lines AA′ and CC′). The upper aquifer lies within the valley floor deposits. Consisting predominantly of gravels it has a uniform thickness (average 24 m from geophysical logging). Both aquifers are confined by marine clay .

7.4 Surface Hydrology Investigations.

Stream discharge monitoring and catchment meteorological studies (evaporation and rainfall monitoring) were undertaken to detect any possible interaction between groundwater and stream flow and to assess

the inputs and outputs of the groundwater system.

The head waters of all tributary streams are fed by springs originating from volcanic and colluvial deposits. The rainfall data for the catchment suggests a positive relationship with height above sea-level (eg rainfall increases with increasing height above sea level). The total average rainfall during the monitoring period (June 1986 till May 1987) was 1900 mm and total evaporation over the monitored catchment was 860 mm.

The total potential surface water resource is 429.8 x 10^5 m^3 (1131 Lit/Sec mean flow or 938 mm of water for the whole monitored catchment). 68% of this is quick flow and the remaining 32% base flow. The spatial distribution of annual discharge is similar to the spatial distribution of rainfall and seasonal variation of flow is highly pronounced in the area. Small flow variations occur during summer, which indicates that low discharge is independent of storm rainfall, and is sustained by groundwater derived water (springs) during the dry season.

7.5 Groundwater Investigations and Water Budget.

Hydrological parameters of both aquifers were identified using pumping, slug and free flow tests. The study has defined the general characteristics of the Kaituna Valley groundwater system, and has provided an initial estimate of the groundwater resources in the area. The maximum continuous pumping rate for 24 hours would be about 12 litres per second which suggests that the aquifer can sustain spray irrigation yield for only short periods of time, and then the pumping should stop to allow aquifer recovery.

The lower aquifer has transmissivity values ranging between 4.8 x 10^{-3} m^2/s and 4.3 x 10^{-3} m^2/s with an average of 4.45 x 10^{-3} m^2/s. The upper aquifer has higher transmisivity values ranging between 2 x 10^{-2} and 4.9 x 10^{-3} m^2/s and with an average of 14.5 x 10^{-3} m^2/s. Results indicate a higher transmissivity value for the upper aquifer compared with the base aquifer.

Seasonal and short term piezometric fluctuations are greater at bores drawing on the lower aquifer compared with those drawing on the upper aquifer because of the differences in hydraulic conductivity and distance from the recharge area.

Piezometric levels increase with depth in the upper aquifer, indicating that an upward flow component is dominant there. The bores

within the lower aquifer show a decline in piezometric pressure with increasing bore depth (decrease in aquifer elevation) indicating that recharge potential zones have a direct relationship with altitude.

Increase in the discharge component of a spring is mainly a result of an increase in piezometric head due to infiltrating rainwater. The spatial variation for springs E.3.1 and W.5.1 is highly uniform compared with the other springs and their discharge is continuous even in the summer. This is due to their longer flow path and larger storage volume.

The groundwater recharge from direct infiltration through the volcanic fractures was proved to be the main recharge mechanism.

Using the hydrological budget model for the monitored water year, the total rate of recharge to the groundwater system was 86 mm(using the water balance technique). For the lower aquifer specific outflow was computed to be 14 mm. The upper aquifer shows 71 mm total specific outflow over the whole catchment for the water year.

The hydrogeological model proposed for the groundwater system (with a direct precipitation and infiltration recharge mechanism) precisely reflects the investigation results obtained in this study.

7.6 Recommendation for Further Investigation

The following points should be taken into account If future investigation in similar valleys on BanksPeninsula to be carried out.

1) The monitoring of springs discharge should be undertaken throughout the catchment to locate those with a minimum seasonal variation (a larger water storage capacity). These springs may then can be used as reliable water sources in the area.

2) In future investigation cost effectiveness will be maximized if the following program is undertaken in conjunction with drilling.

a) Constant head permeability tests should be undertaken when the drilling rig is still in position. The test should be carry out where a significant change in water hydraulic conductivity is observed by drillers (occurrence or loss of water) or where the available hydrogeological data suggest the existence of an aquifer zone.

b) The presence of a engineering geologist on site during drilling is essential to obtain reliable geological and hydrogeological data. Core samples from a selected depth should be tested for laboratory analyses such as permeability and porosity. The laboratory results can then be compare to field permeability test for more accurate

quantification of lithological units in terms of aquifer, aquifuge, and aquitard.

c) Resistivity logging should be performed before casing installation. This enables the measurement of a formation's resistivity which in turn can be used for better interpretation of surface resistivity measurements.

3) It is recommended that stream gaging be extended to upstream areas where the water flows on volcanic basement, and volcanic colluvium which would enable more accurate documentation of the loss of water through joints and fractures within lava flows.

4) Quantitative work, such as aquifer calibration, requires reliable water level contour maps. Where there is not a uniform distribution of exploited wells, explorative boreholes with a small diameter (eg. 50 mm) casing and screen, can be used for monitoring water level observations. On the basis of one year's records the observation network can be reduced by eliminating redundant observation points as well as boreholes that are unsuitable or uncharacteristic. The maximum distance between observation points should be smaller than the distance over which geologic aquifer characteristics can be reliably interpolated. The observation network should be located in order to be used as an observation well for future pumping tests.

5) Pumping tests in this study proved to be of more use for defining the hydrological characteristics of aquifers. Free flow and slug tests should be used to estimate the highest hydraulic conductivity of different aquifers. The wells with maximum hydraulic conductivity should then be tested by pumping tests to gather accurate data on transmissivity, storage coefficient, and safe yield of any aquifers.

6) The monitoring of water quality by hydrochemical analyses of water samples taken from springs and exploited wells should be repeated at least twice per year to identify significant changes of chemical composition along the flow path, with time.

REFERENCES

AYERS, R.S. 1975: Quality of Water for Irrigation. Proc. Irrig. Drain. Div., Speciality Conf., Am. Soc. Civ. Eng. Logan, Utah.

BARRY, M. 1967: Delay Time and its Application to Refraction Profile Interpretation. Seismic Refraction Prospecting: 348-361. A.W. Musgrave (ed). Society of Exploration Geophysicists, Tulsa, USA.

BANNISTER, E.N. 1982: in Larimore, A.E. Studies in Geomorphology and Morphometry: the Collected Papers of Everette N. Bannister. Michigan Geographical Geographical Publication No 27.

BELL, D.H. and TRANGMAR, B.B. 1987: Regolith Materials and Erosion Processes on the Port Hills, Christchurch, New Zealand. Fifth Int. Conf. and Field Workshop on Landslides, Part 2: pp 93-105.

BROADBENT, M. and HAINES, A.J. 1976: Birdlings Flat Seismic Refraction Survey. Geophysics Division Report No 116.

BROWN, L.F. and FISHER, W.L. 1979: Principles of Seismic Stratigraphic Interpretation. Austin , Texas.

BRUCE, J.P. and CLARK, R.H. 1966: Introduction to Hydrometeorology. Permagon Press, London.

BUCHANAN, T. J. and SOMERS, W. P. 1969: Discharge Measurements at Gauging Stations. U.S Geol. Survey Techniques of Water-Resources Inv., Book 3, Chapter A8. pp 1-10.

CEDERGREN, H.R. 1967: Seepage, Drainage and Flow Nets. John Wiley & Sons, Inc.

CLARK, L. 1977: The Analysis and Planning of Step Drawdown Tests. Q. Jl. Engng. Geol. Vol. 10 pp 125-143.

DAVIS, S.N. and DeWEIST, R.J.M. 1966: Hydrology. John Wiley and Sons.

DAWSON, G.B. and THOMPSON, G.E.K. 1981: Ground Water Survey at Taupo - Part 1 Physical Data and Hydrology. DSIR Geophysics Division Report No 153.

DOBRIN, M.B. 1982: Introduction to Geophysical Prospecting. McGraw-Hill,

FINKELSTEIN, J. 1973: Survey of New Zealand Tank Evaporation. Jl. of Hydrol. (NZ). Vol 12 No 2.

FOLK, R.L. 1968: Petrology of Sedimentary rocks. Austin, Tex. Hemphill

FREEZE, R.A. and CHEERY, J.A. 1979: Ground Water. Prentice-Hall, Englewood Cliffs, N.J.

GRADWELL, M.W. 1976: Available-Water Capacities of some Intrazonal Soils of New Zealand. N.Z. Jl. Agric. Research. Vol 19. pp 69-78.

GRIFFITHS, E. 1973: Loess of Banks Peninsula. N.Z. Jl. Geol. Geophy. 16. (3)6 pp 657-675.

HAGEDOORN, J.C. 1959: The Plus-minus Method of Interpreting Seismic Refraction Sections. Geophysical Prospecting 7: 158-182.

HAZEL, C.P. 1975: Groundwater Hydraulics. Lectures Presented to the Australian Water Resources Councils Groundwater School, Adelaide,

HEM, J.D. 1970: Study and Interpretation of the Chemical Characteristics of Natural Water, Second ed. U.S. Geol. Survey Water Supply Paper 1473,

HERSCHY, R.W. 1985: Streamflow Measurement. Elsevier

JAYET, D.F. 1986: An Examination of Observed Climatic Trends/Changes Over Banks Peninsula and the Surrounding Plains Area, and their Synoptic Climatology. Unpublished M.Sc Thesis, University of Canterbury.

LAMBE, T. W., and WHITMAN, R. V. 1979. Soil Mechanics, SI Version. Wiley, NY. USA.

LANDS and SURVEY DEPARTMENT 1982: Coastal Reserves Investigation - Mount Herbet County Part 1. Lands and Survery Department Publication.

LANDS AND SURVEY DEPARTMENT 1984: Kaitorete Spit Scientific Reserve Management Plan. Management Plan No SCR 4.

LEE, J. 1984: Requirements of Free Flow Test. Unpublished Report - Civil Engineering Department, University of Canterbury.

LIOYD, J. W. 1981: Environmental Isotopes in Groundwater. In Case-studies in Groundwater resources evaluation (ed, Lioyd J.W) pp. 112-113. Oxford Science Publishers, Oxford.

MACDONALD, G.A. 1972: Volcanoes. Prentice-Hall Inc.

MANDEL, S. 1974: The Groundwater Resources of the Canterbury Plains. N.Z. Agric. Eng. Inst., Lincoln College , Canterbury, New Zealand.

MANDEL, S. and SHIFTAN, Z.L. 1981: Groundwater Resources - Investigation and Development. Academic Press. N.Y.

MATTHESS, G. 1982: The Properties of Groundwater. John Wiley and Sons.

MERRICK, N.P. 1977: A Computer Program for the Inversion of Schlumberger Sounding Curves in the Apparent Resistivity Domain. Water Resources Commission (NSW) Hydrogeological Report No 1977/5.

MOODY, L. F. 1944: Friction Factor for Pipe Flow, Trans. ASME.

NATIONAL ACADEMY OF SCIENCE and NATIONAL ACADEMY OF ENGINEERING 1972: Water Quality Criteria. Report prepared by Committee of Water Quality Criteria at request of U.S. Environmental Protection Agency, Washington D.C.

NEW ZEALAND BOARD OF HEALTH 1984: Drinking Water Standards for New Zealand, N.Z Board of Health Publication.

NWASCO 1975: N.Z Land Resource Inventory Worksheet, Sheets S84, S94.

PALMER, J.D. 1982: Ellesmere; A Critical area Coastal Resource Investigation. Dept. Lands and Survey. Christchurch.

RAHN, P.H. 1986: Engineering Geology, An Environmental Approach. Elsevier.

RIDER, M.H. 1986: The Geological Interpretation of well Logs. John Wiley and Sons. N.Y.

ROSLONSKI, R. 1947: Water Balance in the Catchment Area, and Method to Calculate it. Bull. Hydologic and Meterologic Service Vol 1 No 2. Warsaw.

SANDERS, R. 1986: Hydrogeological studies of Springs in the Akaroa County, Banks Peninsula. Unpublished Engineering Geology MSc. Thesis, University of Canterbury, Christchurch.

SCOTT KEYS, W. and MacCARY, L.M. 1972: Application of Borehole Geophysics to Water-Resources Investigations. U.S Geol. Survey Techniques of Water-Resources Investigations Book 2 Collection of Environmental Data.

SEWELL, R.J. 1985: The Volcanic Geology and Geochemistry of Central Banks Peninsula and Relationships to Lyttelton and Akaroa Volcanoes. PhD Thesis, University of Canterbury.

SIMPSON M.J. 1987: The Geophysical Logging of Demonstration Bores at Canterbury University. MOW. Report No WS 1280.

TALBOT, J.D. and CALLANDER, P.F. 1986: Water Right Investigation. 1985/0001 M. Marriot, Kaituna Valley. North Canterbury Catchment Board, Water Right Investigation Report.

TALBOT, J.D. et al 1986: The Christchurch Artesian Aquifers. Report by the Resources Division - North Canterbury Catchment Board and Regional Water Board.

TAYLOR, C.B. and STEWART, M.K. 1981: Environmental Isotopes in New Zealand Hydrology. 1 Introduction: The Role of Oxygen - 18, Detrium, and Tritium in Hydrology. New Zealand Journal of Science 24: pp 295 - 311.

TAYLOR, C.B. and STEWART, M.K. 1978: Isotopic Identification of Sources of Groundwater in Canterbury: Present Status of Programme. in, Noonan M.J. (ed): Groundwater. Sym. on Current Research in N.Z. Lincoln University College.

TELFORD, W.M., GELDART, L.P., SHERIFF, R.E. and KEYS, D.A. 1976: Applied Geophysics. Cambridge University Press.

VIESSMAN, W., KNAPP, J.W., LEWIS, G.L. and HARBAUGH, T.E. 1977: Introduction to Hydrology. 2nd ed. IEP. N.Y.

WALTON, W.C. 1970: Groundwater Resource Evaluation. McGraw-Hill.

WATER AND SOIL DIVISION, MINISTRY OF WORK AND DEVELOPMENT, 1979: Our Land Resources. Water and Soil Divisn, Ministry of Work and Developmentr

WEAVER, S. SEWELL, R. DORSEY, C. 1985: Extinct Volcanoes. Geol. Soc. N.Z. Guidebook no. 7.

WHITE, P.A. 1982: Resistivity Calculation and Analysis Programs for the PDP 11. MOW Report WS 0872.

WHITE, P. 1985: Lower Wairarapa Valley Geophysical Logging - Part 1 A Comparison of geophysical Logs and Lithology. MOW report 973.

WIECZYSTY, A. 1970: Hydrogeological Engineering. Warsaw.

WILSON, H.D. et al 1987: The Banks Peninsula Landscape Report. Queen Elizabeth the II National Trust.

ZOHDY A. A. R. 1980: Electrical Methods. U.S Geol. Survey Techniques Water-Resources Inv., Book 2, Chapter D1.

APPENDIX 1

WEATHER SUMMARY FOR LINCOLN STATION

A.1 : Weather Summary For Lincoln Station (May – December 1986)

Totals	
Rainfall	613.7 mm
Pan Evaporation	699.8 mm
Solar Radiation	2941.8 MJ/m^2
Wind Run	81050.0 km
Penman	735.3 mm
Potential Deficit	238.5 mm
Temperature Sum	292.6 Day degrees C
Mean Temperatures (T)	
Maximum (T)	14.3° deg C
Mean (T)	9.4° deg C
Minimum (T)	4.4° deg C
Grass Minimum (T)	2.1° deg C
Mean Wind Run	330.8 km/day
Mean VP	7.5 mb
Highest Daily Maximum (T)	28.1° on 20 December 1986
Lowest Daily Minimum (T)	–5.4° on 14 June 1986
Lowest Grass Minimum (T)	–8.6° on July 1986
Number of Ground Frosts	85
Number of Screen Frosts	52
Number of Rain Days	98
Highest Daily Rainfall (mm)	41.5 on 25 November 1986

A.1 continued on next page

A.1 continued: Weather Summary For Lincoln Station (January – June 1987)

Totals	
Rainfall	414.6 mm
Pan Evaporation	697.1 mm
Solar Radiation	2114.2 MJ/m^2
Wind Run	62803.0 km
Penman	548.8 mm
Potential Deficit	134.2 mm
Temperature Sum	2002.9 Day degrees C
Mean Temperatures (T)	
Maximum(T)	15.8 deg C
Mean(T)	11.1 deg C
Minimum(T)	6.3 deg C
Grass Minimum(T)	5.5 deg C
Mean Wind Run	347.0 km/day
Mean VP	8.9 mb
Highest Daily Maximum(T)	30.0° on 15 January 1987
Lowest Daily Minimum(T)	–3.2° on 10 June 1987
Lowest Grass Minimum(T)	–5.0° on 3 May 1987
Number of Ground Frosts	29
Number of Screen Frosts	18
Number of Rain Days	69
Highest Daily Rainfall	33.0 mm on 15 June 1987

APPENDIX 2

ENGINEERING GEOLOGICAL FIELD DESCRIPTION SHEETS FOR ROCK AND SOIL

A.2.1 Description Sheet for Rock Material

A.2.2 Description Sheet for Soil Material

A.2.3 Terminology for Rock Mass Description

Table A.2

ENGINEERING GEOLOGICAL FIELD DESCRIPTION FOR ROCK MATERIAL

WEATHERING

	TERM	GRADE	ROCK DESCRIPTION
6.	* residual soil (RW)	VI	discolouration and complete transformation to soil, original fabric destroyed
5.	completely weathered (CW)	V	discolouration and transformation to soil, original fabric largely preserved
4.	highly weathered (HW)	IV	material pervasively altered with discolouration and loss of strength; fabric preserved; lithorelicts
3.	moderately weathered (MW)	III	penetrative discolouration and alteration of rock material, with some loss of strength
2.	slightly weathered (SW)	II	slight discolouration of rock fabric; no loss of material strength
1.	unweathered (UW)	I	no discolouration or loss of strength, or any other effects due to weathering

STRENGTH

	TERM	POINT LOAD STRENGTH INDEX Is(50)	FIELD ESTIMATION OF STRENGTH
1.	extremely strong (ES)	more than 10	can only be chipped with geological hammer
2.	very strong (VS)	3 to 10	several hard blows required to break hand specimen
3.	strong (S)	1 to 3	few firm blows of hammer required to break specimen
4.	moderately strong (MS)	0·3 to 1	breaks readily with one blow of hammer
5.	moderately weak (MWk)	0·1 to 0·3	broken by hand only with difficulty; small thin pieces broken by finger pressure
6.	weak (Wk)	0·03 to 0·1	broken by hand, pieces 25 mm or more broken by finger pressure
7.	* very weak (VWk)	less than 0·03	crushed or remoulded by hand (grades into soil materials)

* may require description as soil material

GEOLOGICAL CLASSIFICATION

CRYSTAL OR GRAIN SIZE	SEDIMENTARY (T)		IGNEOUS (T)				METAMORPHIC (T)	
	CLASTIC	CHEM/ORGANIC	Mode of Occurrence	Silicic	Intermed.	Mafic	Ultramaf.	FOLIATED	MASSIVE
very coarse 64	CONGLOMERATE (1)		INTRUSIVE	(27) GRANITE GRANODIORITE	(29) SYENITE DIORITE	(31) GABBRO	(32) PERIDOTITE DUNITE (33)	GNEISS (34)	HORNFELS (39)
coarse 2	AGGLOMERATE (2) BRECCIA (3)							SCHIST (35)	MARBLE (40)
medium 0·06	SANDSTONE (4)	Calcareous LIMESTONE (9) Siliceous CHERT (10) OTHER (11)						PHYLLITE (36)	QUARTZITE (41)
fine	SILTSTONE (5)	Carbonaceous COAL (12) OTHER (13)	EXTRUSIVE	(19) RHYOLITE OBSIDIAN DACITE (20) (21)	(22) TRACHYTE ANDESITE (23)	(24) DOLERITE BASALT (25)	SERPENTINITE (26)	SLATE (37)	AMPHIBOLITE (42)
TUFFS (7)	MUDSTONE (6)	Ferruginous LATERITE (14) OTHER (15)						MYLONITE (38)	
very fine 0·002 (mm)	CLAYSTONE (8)	Saline ROCK SALT (16) GYPSITE (17) OTHER (18)							(T) OTHERS Specify (43)

WEATHERING TERM | STRENGTH TERM | COLOUR | FABRIC & ROCK NAME

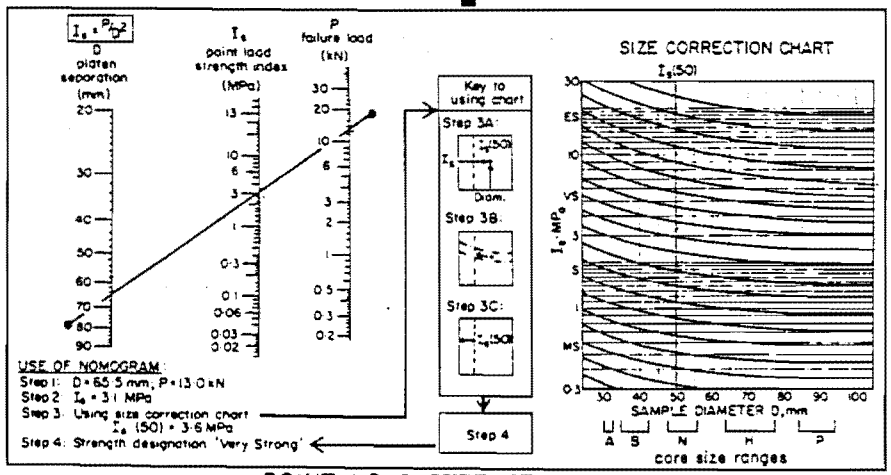

POINT LOAD STRENGTH INDEX

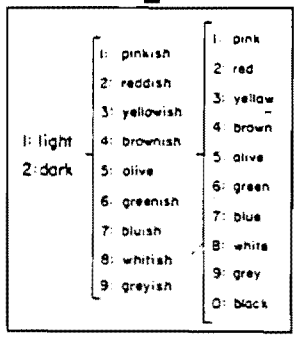

COLOUR

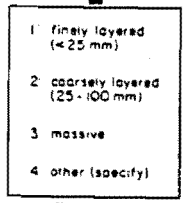

FABRIC

Table A.2

ENGINEERING GEOLOGICAL FIELD DESCRIPTION FOR SOIL MATERIAL

WEATHERING

	TERM	GRADE	SOIL DESCRIPTION
5	Completely Weathered (CW)	V	completely discoloured and altered, no trace of original fabric
4	Highly Weathered (HW)	IV	mostly altered and weakened, little trace of original fabric
3	Moderately Weathered (MW)	III	large discoloured portions of original soil separated by more altered material, significantly weakened
2	Slightly Weathered (SW)	II	minor discolouration of some parts of the original soil, no loss of strength
1	Unweathered (UW)	I	original soil with NO discolouration, loss of strength or other effects due to weathering
0	NOTE: in coarse-grained soils record weathering grade of DOMINANT fraction here and quality weathering grade of subordinate and/or minor fractions if appropriate		

STRENGTH

	TERM	FIELD CRITERIA
1	loose	can be removed from exposure in disaggregated form by hand
2	compact	only removed from exposure by implement, material readily disaggregated by physical means
3	* cemented	only removed from exposure by implement, material does not disaggregate
4	hard	may be removed from exposure with difficulty by implement or hand, softened on immersion in water and may be remoulded
5	stiff	indented by thumb pressure, but not moulded by fingers; softened on immersion in water, and may be remoulded
6	firm	moulded or indented only by strong finger pressure, easily moulded after immersion in water
7	soft	easily indented or moulded by finger pressure
8	very soft	exudes between fingers when squeezed
9	spongy	readily compressed by finger pressure, but cannot be remoulded

* may require description as rock material

UNIFIED SOIL CLASSIFICATION SYSTEM

			FIELD IDENTIFICATION	GROUP SYMBOL	TYPICAL NAMES
COARSE-GRAINED SOILS	GRAVELS (>50% larger than 2mm)	clean gravels	wide range in grain size and substantial amounts of all interm. sizes	GW	well graded GRAVELS
			predom. one size or a range of sizes with some interm. sizes missing	GP	poorly graded GRAVELS
		gravels with fines	non-plastic fines (see ML below)	GM	poorly graded SILTY-GRAVELS
			plastic fines (see CL below)	GC	poorly graded CLAYEY-GRAVELS
	SANDS (<50% smaller than 2mm)	clean sands	wide range in grain sizes and substantial amounts of all interm. sizes	SW	well graded SANDS
			predom. one size or a range of sizes with some interm. sizes missing	SP	poorly graded SANDS
		sands with fines	non-plastic fines (see ML below)	SM	poorly graded SILTY-SANDS
			plastic fines (see CL below)	SC	poorly graded CLAYEY-SANDS

			SHINE	DILATANCY (1)	TOUGHNESS (1)		
FINE-GRAINED SOILS: SILTS AND CLAYS	LIQUID LIMIT <50		none to very dull	quick to slow	none	ML	INORGANIC SILTS with slight plasticity
			moderate	none to very slow	medium	CL	INORGANIC CLAYS of low to medium plasticity
			none to very dull	slow	slight	OL	ORGANIC SILTS & CLAYS of low plasticity
	LIQUID LIMIT >50		dull	slow to none	slight to medium	MH	INORGANIC SILTS of high plasticity
			very glossy	none	high	CH	INORGANIC CLAYS of high plasticity
			moderate to v. glossy	none to very slow	slight to medium	OH	ORGANIC CLAYS of medium to high plasticity
HIGHLY ORGANIC SOILS			identified by colour, odour, spongy feel and fibrous texture			Pt	PEAT and other highly organic soils

PROCEDURES FOR FINE-GRAINED SOILS OR FRACTIONS (1)

DILATANCY (reaction to shaking) -
1) Prepare pat of moist soil, adding water to make soft - but not sticky.
2) Place pat in palm of hand, shake horizontally by striking vigorously against other hand.
Positive Reaction: appearance of water on surface of pat, which becomes glossy. When squeezed between fingers, water and gloss disappear, pat stiffens and may crumble.

TOUGHNESS: (consistency near plastic limit) -
1) Mould sample to consistency of putty, adding water or air drying as required.
2) Roll to thin (3 mm) thread, fold and re-roll repeatedly until thread crumbles at plastic limit.
3) Knead together and continue until lump crumbles.
Dry/Silty: a tough thread and stiff lump indicate high plasticity, a weak thread and lump low plasticity clays.

GROUP SYMBOL CODINGS FOR USCS

COLUMN 1		COLUMN 2	
G=1	C=4	W=1	C=4
S=2	O=5	P=2	L=5
M=3	Pt=6	M=3	H=6

BOUNDARY CLASSIFICATIONS specify, enter 0.0

WEATHERING TERM | WATER CONTENT TERM | STRENGTH TERM | COLOUR | FABRIC | SOIL NAME | USCS SYMBOL

WATER CONTENT

	TERM	FIELD CRITERIA
1	Dry	looks and feels dry, fine-grained soils usually hard, powdery or friable, coarse-grained soils may run freely through hands
2	Moist	soil feels cool and may be darkened in colour, particles tend to adhere in coarse-grained materials, fine-grained soils may be softened
3	Wet	soils feel cold and are darkened in colour, free water forms on hands when sample is disturbed
4	Saturated	restricted to wet soils below the water table or the static water level in excavations or drill holes

COLOUR

1: light
2: dark

1	pinkish	1	pink
2	reddish	2	red
3	yellowish	3	yellow
4	brownish	4	brown
5	olive	5	olive
6	greenish	6	green
7	bluish	7	blue
8	whitish	8	white
9	greyish	9	grey
		0	black

FABRIC

1: finely layered (< 25 mm)
2: coarsely layered (25-100 mm)
3: massive
4: other (specify)

SOIL NAME

*SUBORDINATE FRACTION: 20-50% volume visual estimate

DOMINANT FRACTION: >50% volume visual estimate

* MINOR FRACTION: < 20% volume visual estimate

1	coarse	gravelly
2	medium	
3	fine	
4	coarse	sandy
5	medium	
6	fine	
7	silty	
8	clayey	
9	peaty	

PARTICLE SIZE

	SOIL TYPE TERM		PARTICLE SIZE (mm)	GRAPHIC LOG
1	coarse	gravel	> 60	
2	medium		20-60	
3	fine		2-20	
4	coarse	sand	0.6-2.0	
5	medium		0.2-0.6	
6	fine		0.06-0.2	
7	silt		0.002-0.06	
8	clay		< 0.002	
9	peat		NA	

WITHSOM

1	coarse	gravel
2	medium	
3	fine	
4	coarse	sand
5	medium	
6	fine	
7	silt	
8	clay	
9	peat	

Table A.2

ENGINEERING GEOLOGICAL FIELD DESCRIPTION FOR ROCK MASS

FIELD SKETCH OR ANNOTATED PHOTOGRAPH

SCALE: ORIGINAL SCALE: 1 SKETCH ORIENTATION:

GENERAL INFORMATION

PROJECT/AREA

LOCALITY

REFERENCE MAP

COORDINATES

ELEVATION

GEOLOGY BY

DATE

CHECKED

Sheet No: of

SHEET REFERENCE

ADDITIONAL DATA

GRAPHIC SYMBOL	ROCK UNIT No	ROCK MATERIAL DESCRIPTION				
		WEATHERING	STRENGTH	COLOUR	FABRIC	ROCK NAME
	1					
	2					
	3					
	4					
	5					
	6					
		OTHER MATERIAL DESCRIPTIONS (specify)				
	7					
	8					
	9					

TERMINOLOGY FOR COMMON DEFECTS IN ROCK MASS

DEFECT TYPE	LAYERING (1)			FRACTURES AND FRACTURE ZONES (1)		WEAK SEAMS OR ZONES (1)		
	BEDDING (1)	FOLIATION (2)	CLEAVAGE (3)	JOINT / FAULT (4)	SHEARED ZONE (5)	CRUSHED (6)	DECOMPOSED (7)	INFILLED (8)
DESCRIPTION	i) Arrangement in layers of mineral grains or crystals of similar size or composition ii) Arrangement of elongated or platy minerals near parallel to one another and/or to the layers			Smooth fracture across which rock has little tensile strength, planar, curved, or irregular; open, closed or occupied; surface rough, smooth or slicken-sided	Zone of multiple closely spaced (< 100 mm) fracture planes, with roughly parallel planar boundaries, blocks of intact material within zone typically lenticular or wedge shaped, fractures closed, open, weakly cemented or soil-coated	Zone with roughly parallel planar boundaries - i) Composed of disoriented, usually angular, rock fragments of variable size in a soil matrix ii) Some weathering of fragments possible, with soils either cohesive or non-cohesive iii) Lowest shear strength parallel to zone boundaries, which are commonly slickensided	Zone of any shape, but commonly with roughly parallel planar boundaries - i) Within zone rock moderately to completely weathered ii) At margins gradation into fresher rock NOTE materials forming zone require separate description as soil or weak rock	Zone of any shape, but commonly with roughly parallel planar boundaries - i) Composed of soil materials which may show layering roughly parallel to zone boundaries ii) Rock fabric not present in infill zone
MAP SYMBOLS with strike and dip				'open' 'closed'	★ Record width of zone as required			

(1) OTHERS: Specify (9)

DEFECT DATA SUMMARY TABLE

ROCK UNIT No	DEFECT SET No	DEFECT TYPE	DEFECT SPACING	DEFECT PERSISTENCE	AV. UNIT BLOCK SIZE	DEFECT ORIENTATION DIP	DEFECT ORIENTATION DIRECTION	INF. VALUE	GROUND WATER	REMARKS

DEFECT ORIENTATION DIAGRAM

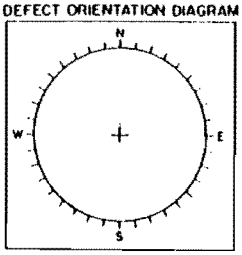

DEFECT SPACING

	TERM	SPACING (mm)
1	extremely wide	> 2000
2	very wide	500 – 2000
3	wide	200 – 500
4	moderate	100 – 200
5	close	25 – 100
6	very close	5 – 25
7	extremely close	< 5

DEFECT PERSISTENCE

	TERM	LENGTH (m)
1	very high	> 10
2	high	5 – 10
3	moderate	2 – 5
4	low	0.5 – 2
5	very low	< 0.5

AVERAGE UNIT BLOCK SIZE

	TERM	EQUIVALENT CUBE SIDE	AVERAGE BLOCK VOLUME (m^3)
1	very large	> 1000 mm	> 1.0
2	large	500 mm – 1000 mm	0.1 – 1.0
3	medium	100 mm – 500 mm	0.001 – 0.1
4	small	10 mm – 100 mm	< 0.001
5	very small		

GROUNDWATER

	TERM	FLOW RATE
1	dry	
2	seepage	< 1 ml s^{-1}
3	very low flow	1 – 10 ml s^{-1}
4	low flow	10 – 100 ml s^{-1}
5	moderate flow	0.1 – 1 l s^{-1}
6	large flow	1 – 10 l s^{-1}
7	very large flow	> 10 l s^{-1}

APPENDIX 3

FALLING HEAD PERMEABILITY TESTS

A.3.1 Test Procedure

A.3.2 Permeability Conversion Chart

A.3.1: Falling Head Permeameter Test Procedure

To obtain the coefficient of permeability of fine grained soils a falling head permeameter is used.

This apparatus consists of a cylinder of 76 or 102 mms diameter, having a head and baseplate clamped on. The baseplate is drilled to pass water, and a piece of wire screen cloth is placed on top of this under the soil specimen. The head is fitted with a glass standpipe, and the underside of the head is formed to a conical shape to facilitate displacement of air from the cylinder.

Special techniques are needed to measure the coefficient of permeability of an undisturbed soil in the laboratory. For the purposes of this laboratory experiment, moist soil will be compacted into the cylinder using standard Proctor compaction; the coefficient of permeability obtained will therefore be for remoulded recompacted soil.

The soil is compacted into the cylinder and screeded off level inside, and the height of the soil is measured. The cylinder is filled with water, the head is placed in and tightened down, then the apparatus is topped up with water through a small-bore plastic inserted down the standpipe into the cylinder. The plastic tube is withdrawn leaving the standpipe filled with water.

The height of the water above the baseplate is noted, together with the time. At some later time the height of water is again read. The normal temperature for the test is 20^0C.

If a is the internal area of the standpipe in sq. mms,
l is the thickness of the specimen in mms,
A is the area of the sample is sq. mms,
t is the time interval in seconds,
H_1 is the initial height of the water in the standpipe above the bottom of the sample in mms,
H_2 is the final height of the water in the standpipe above the bottom of the sample in mms,
and k is the coefficient of permeability, then

$$k = (al/At) \log_e(H_1/H_2)$$
$$= 2.3\ (al/At) \log_{10}(H_1/H_2) \text{ mm/sec.}$$

Table. A.3.2 Permeability Conversion Chart

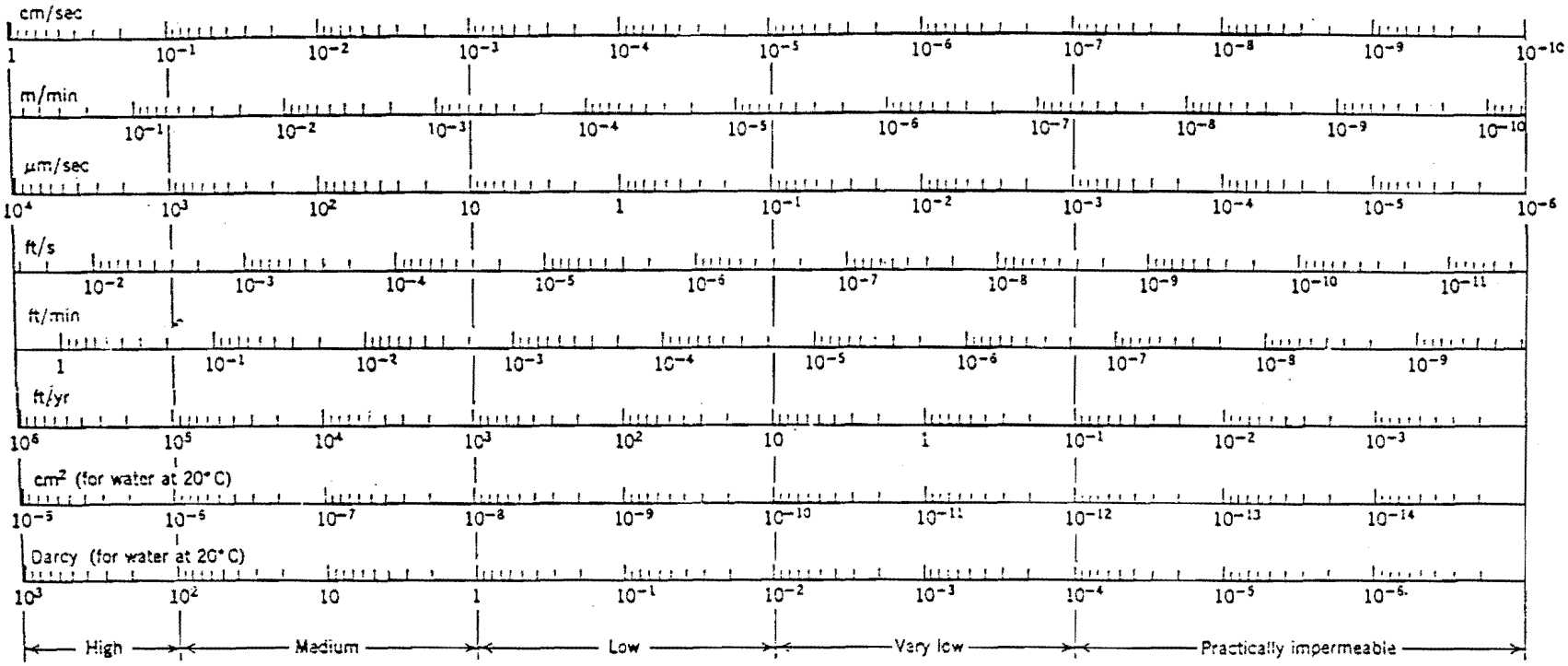

*For water at 20°C

To convert from cm/sec to:	m/min	μm/sec	ft/sec	ft/min	ft/yr	cm²*	Darcy*
Multiply by:	0.600	10^4	0.0328	1.968	1.034×10^6	1.031×10^{-5}	1.045×10^3

AFTER LAMBE AND WHITMAN (1979)

APPENDIX 4

GRAIN SIZE ANALYSIS

A.4.1 Methodology

A.4.2 Results

A.4.3 Textural Terminology

A.4.1: Methodology For Grain Size Analysis

1. Methodology

The analysis of samples passing -3 phi seive were carried out. Gravel and sand fractions were determined by dry sieving using 1/2 phi sieves from -3 phi to 4 phi. Silt and clay fractions were determined by hydrometer analysis.

There was a tendency for aggregates and partially weathered material to break down with continued sieving; therefore in order to avoid bias all samples were mechanically sieved for a standard period of fifteen minutes.

Disaggregation for hydrometer analyses was done by hand in a solution of distilled water and deflocculent (calgon). The silt/clay boundary was taken as 0.002mm (9 phi) rather than the traditional sedimentary boundry of 0.0039 (8 phi).

A4.2: Results

Grain size distribution curves for soil materials analysed are included in the following pages. The results are summarised in table.

UNIVERSITY OF CANTERBURY

DEPARTMENT OF GEOLOGY

A.4.2 PARTICLE SIZE DISTRIBUTION – LOG PROBABILITY PLOT

PROJECT ..Kaituna..... SAMPLE NO .. ...A..... SAMPLED BY ..P. Na..... ANALYSED BY ..P. Na.....

..... LOCATION ....AH1 (Fig 1.6) DATE .Sept. 1986. DATE .Sept. 1986....

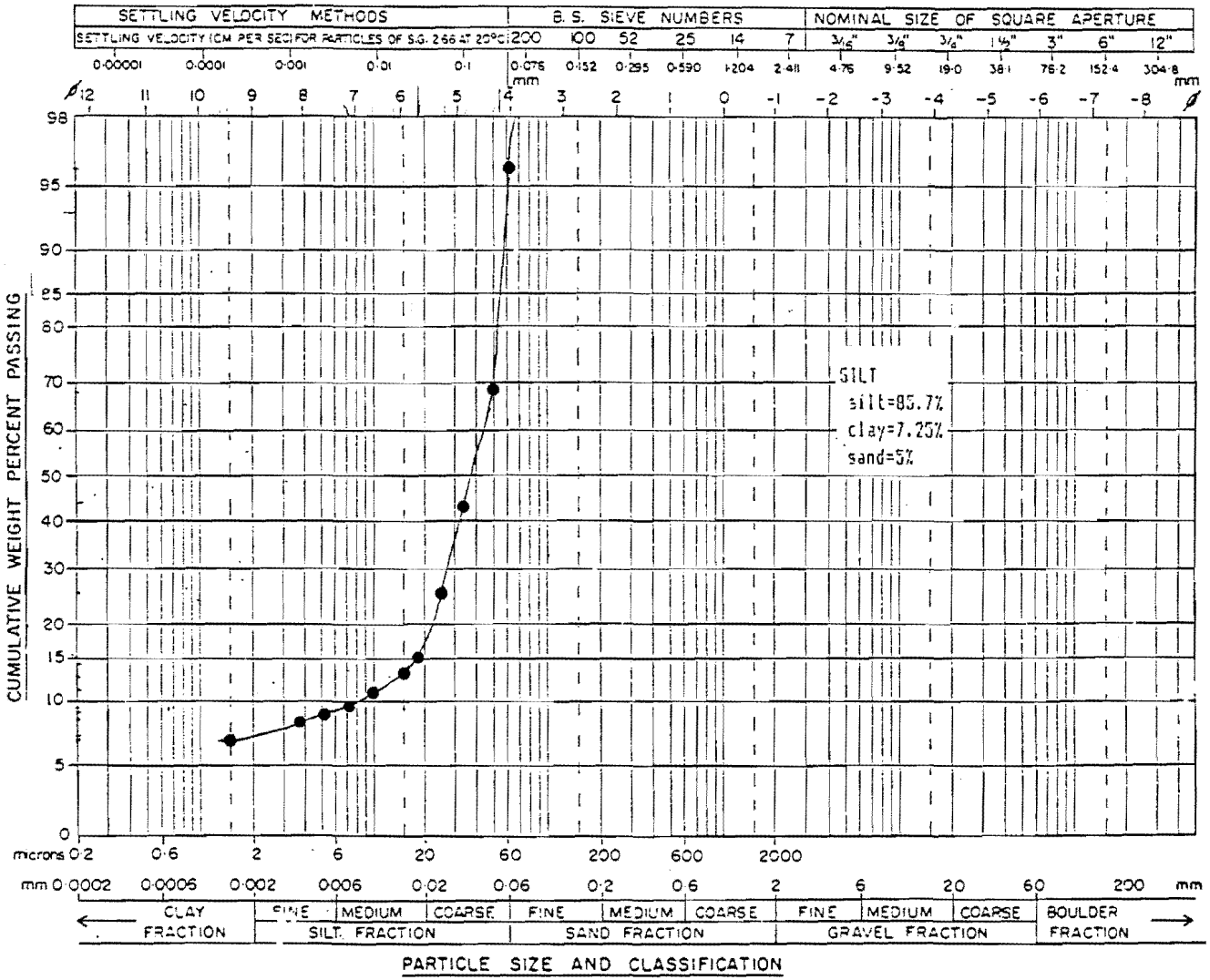

PARTICLE SIZE AND CLASSIFICATION

UNIVERSITY OF CANTERBURY

DEPARTMENT OF GEOLOGY

A.4.2 PARTICLE SIZE DISTRIBUTION – LOG PROBABILITY PLOT

PROJECT ..Kaituna..... SAMPLE NO ..B ..... SAMPLED BY ..P..Na..... ANALYSED BY..P..Na.....

..... LOCATION ....AH1 (Fig 1.6) DATE .Sept..1986. DATE .Sept..1986....

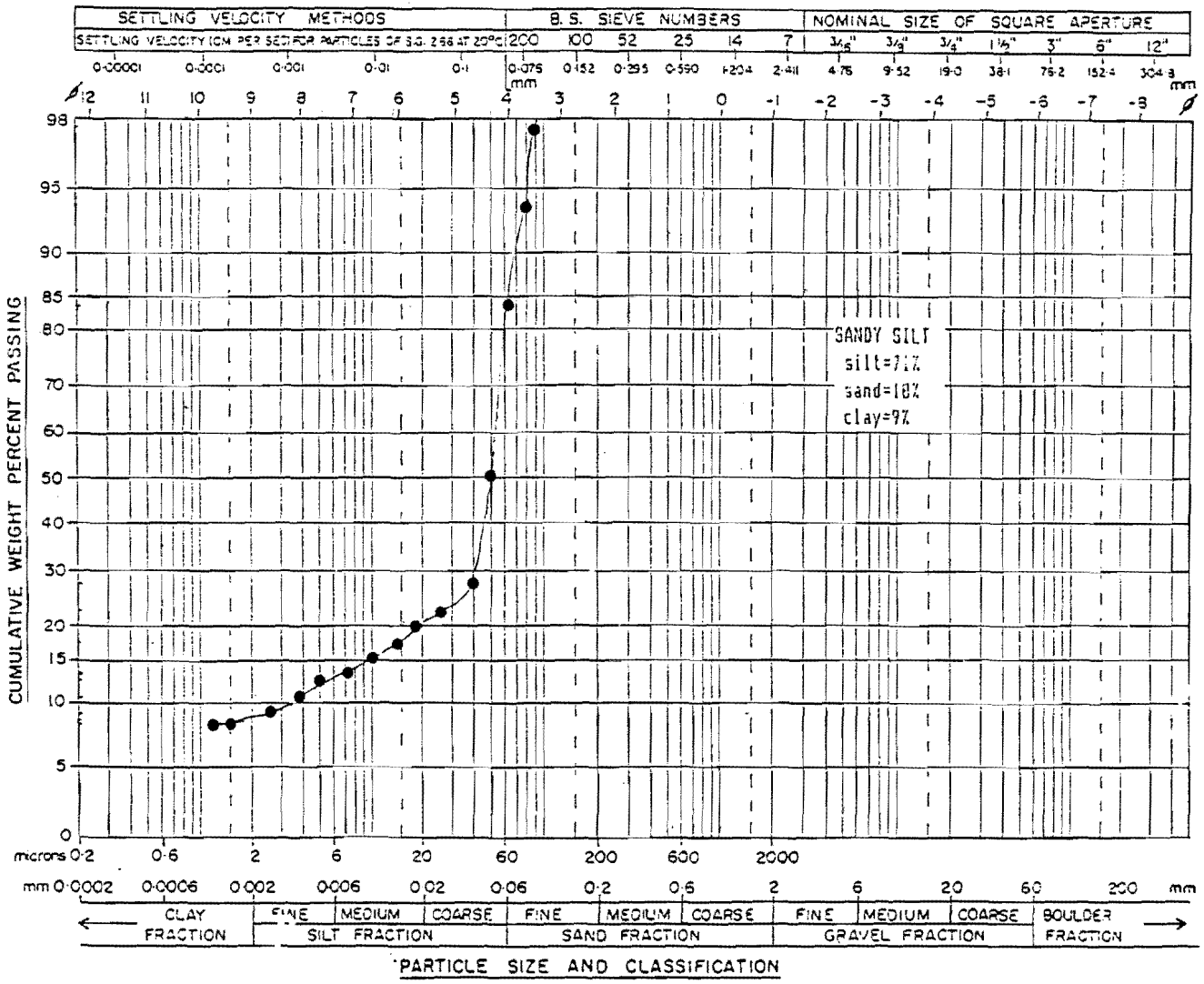

PARTICLE SIZE AND CLASSIFICATION

UNIVERSITY OF CANTERBURY

DEPARTMENT OF GEOLOGY

A.4.2 PARTICLE SIZE DISTRIBUTION – LOG PROBABILITY PLOT

PROJECT ..Kaituna..... SAMPLE NO .. C .. .. SAMPLED BY ..P. Na..... ANALYSED BY ..P. Na.....

..... LOCATION ....AH1 (Fig 1.6) DATE .Sept..1986. DATE .Sept..1986....

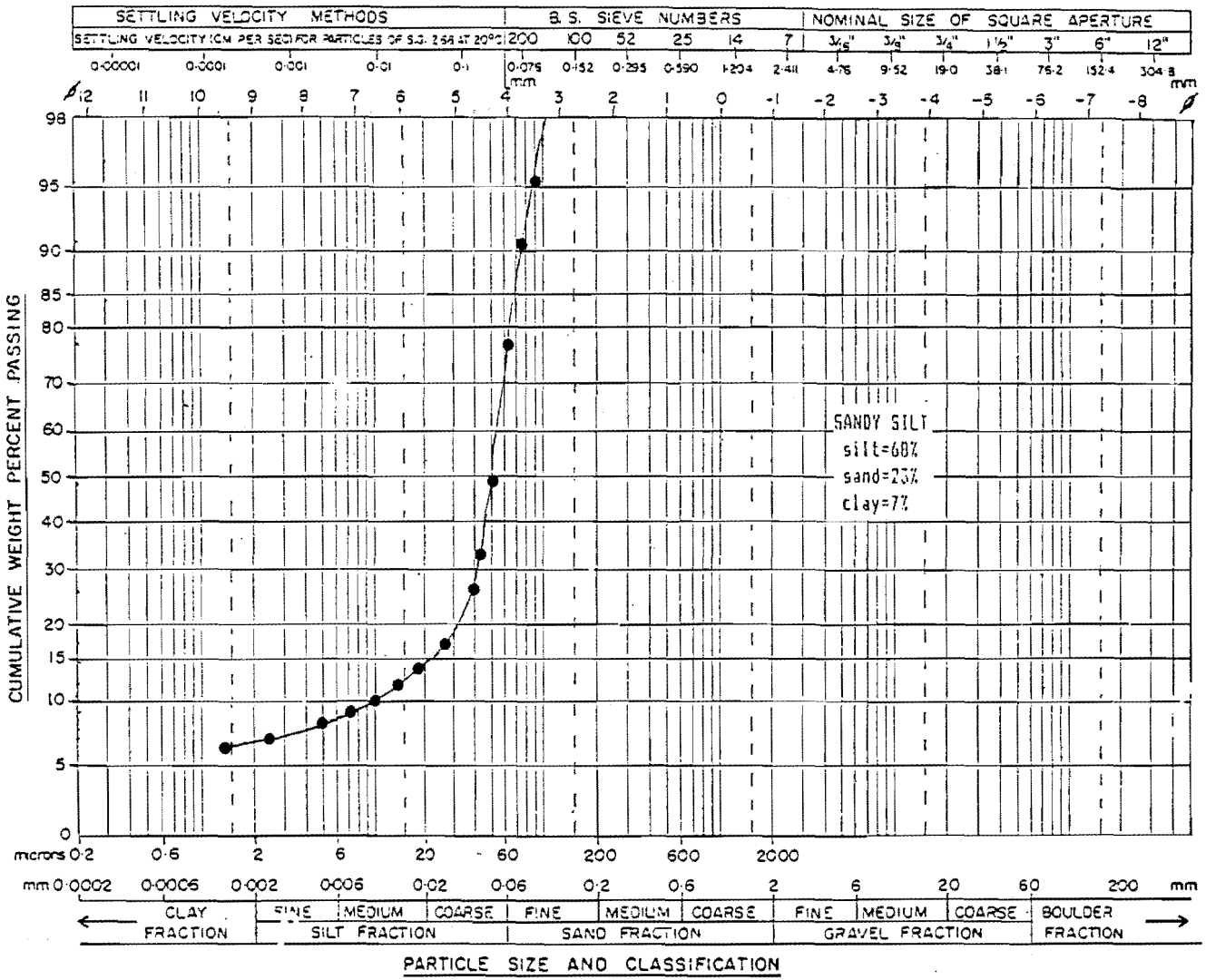

PARTICLE SIZE AND CLASSIFICATION

UNIVERSITY OF CANTERBURY

DEPARTMENT OF GEOLOGY

PARTICLE SIZE DISTRIBUTION – LOG PROBABILITY PLOT

PROJECT ..Kaituna..... SAMPLE NO .. D ..... SAMPLED BY ..P. Na..... ANALYSED BY ..P. Na.....

..... LOCATION ....AH1 (Fig 1.6) DATE .Sept..1986. DATE .Sept..1986....

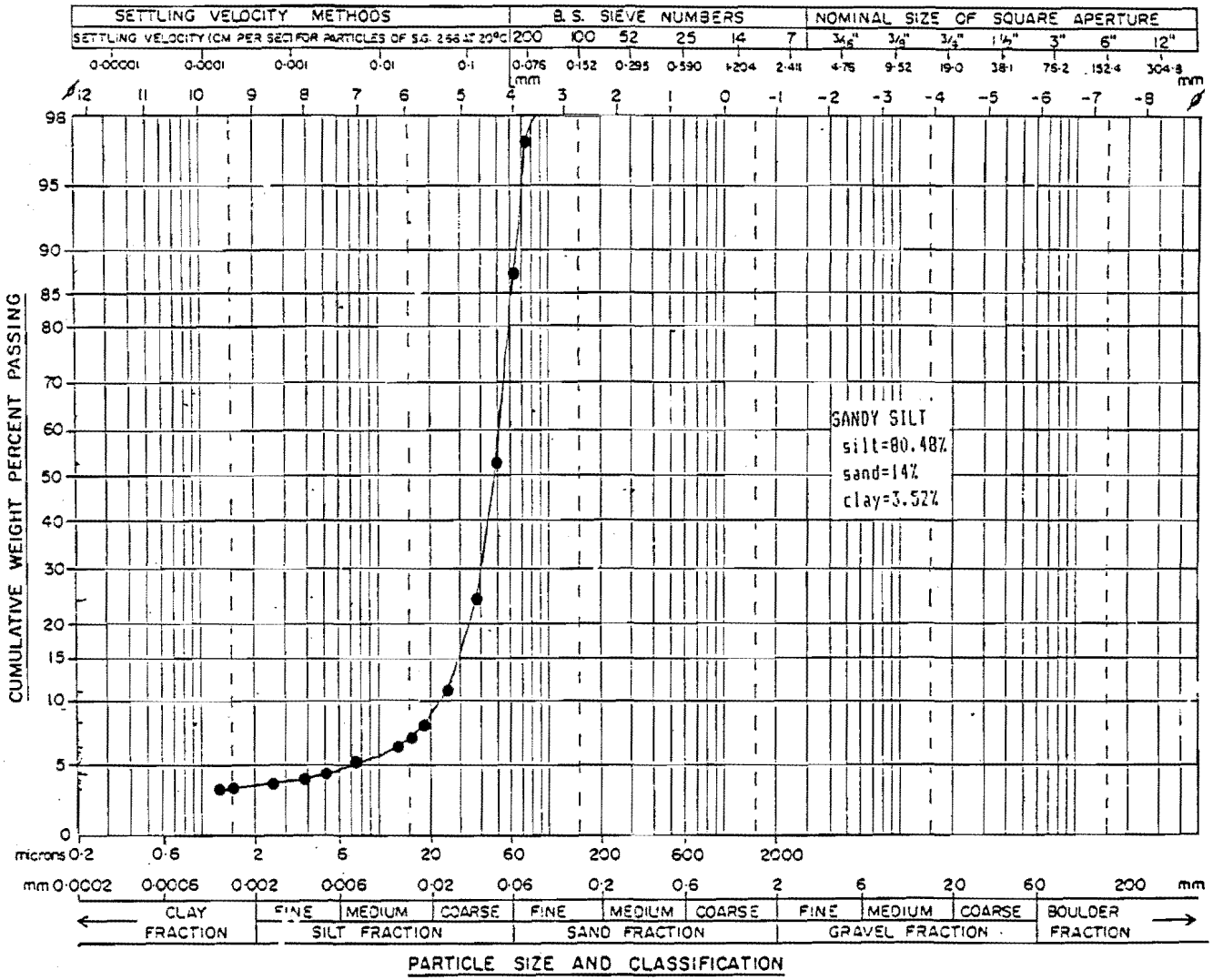

PARTICLE SIZE AND CLASSIFICATION

UNIVERSITY OF CANTERBURY

DEPARTMENT OF GEOLOGY

A.4.2 PARTICLE SIZE DISTRIBUTION – LOG PROBABILITY PLOT

PROJECT ..Kaituna..... SAMPLE NO .. E ..... SAMPLED BY ..P..Na..... ANALYSED BY..P..Na.....

..... LOCATION ....AH1 (Fig 1.6) DATE .Sept..1986. DATE .Sept..1986....

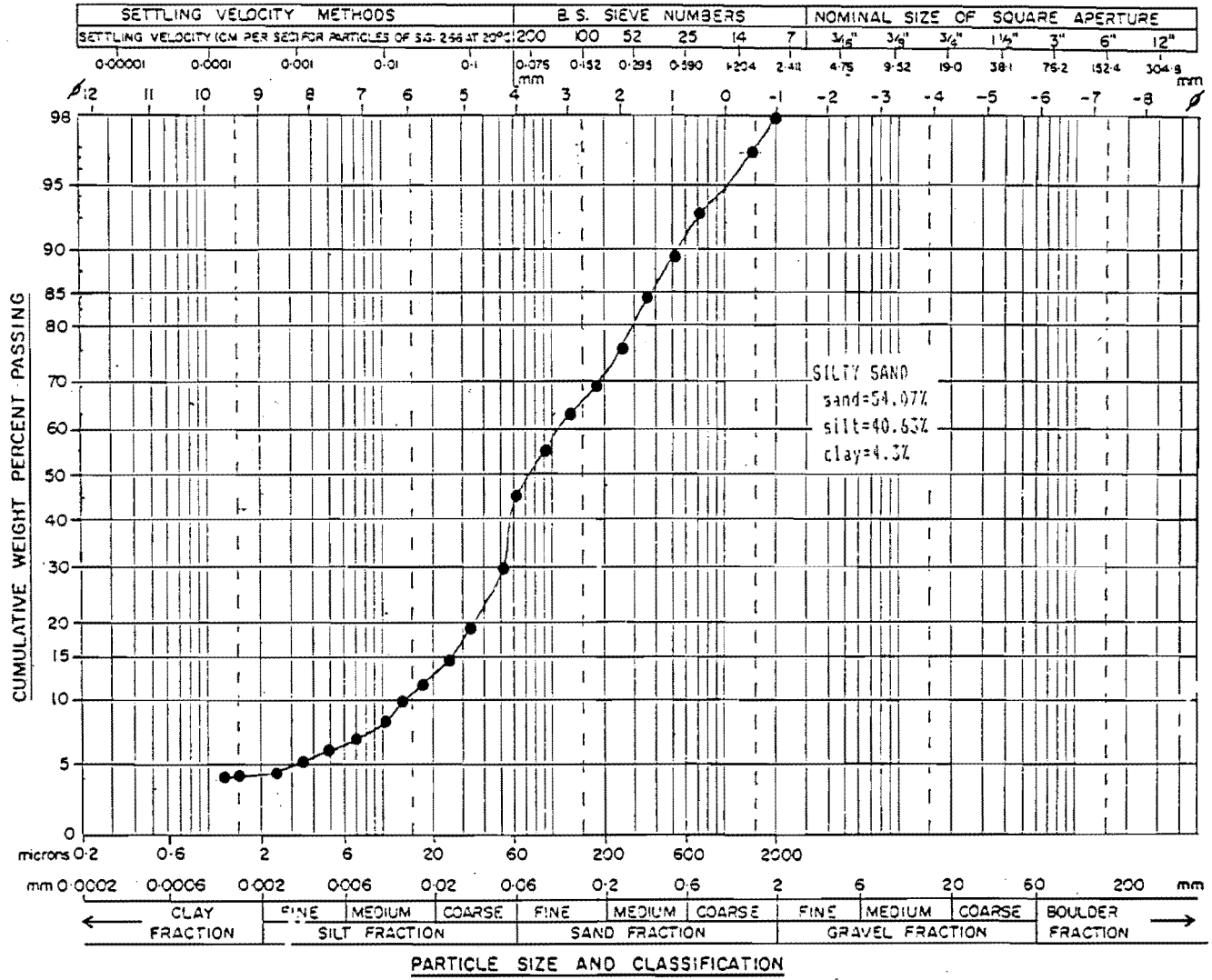

PARTICLE SIZE AND CLASSIFICATION

UNIVERSITY OF CANTERBURY

DEPARTMENT OF GEOLOGY

A.4.2 PARTICLE SIZE DISTRIBUTION – LOG PROBABILITY PLOT

PROJECT ..Kaituna..... SAMPLE NO .. F ..... SAMPLED BY ..P..Na..... ANALYSED BY ..P..Na.....

..... LOCATION ....AH1 (Fig 1.6) DATE .Sept..1986. DATE .Sept..1986....

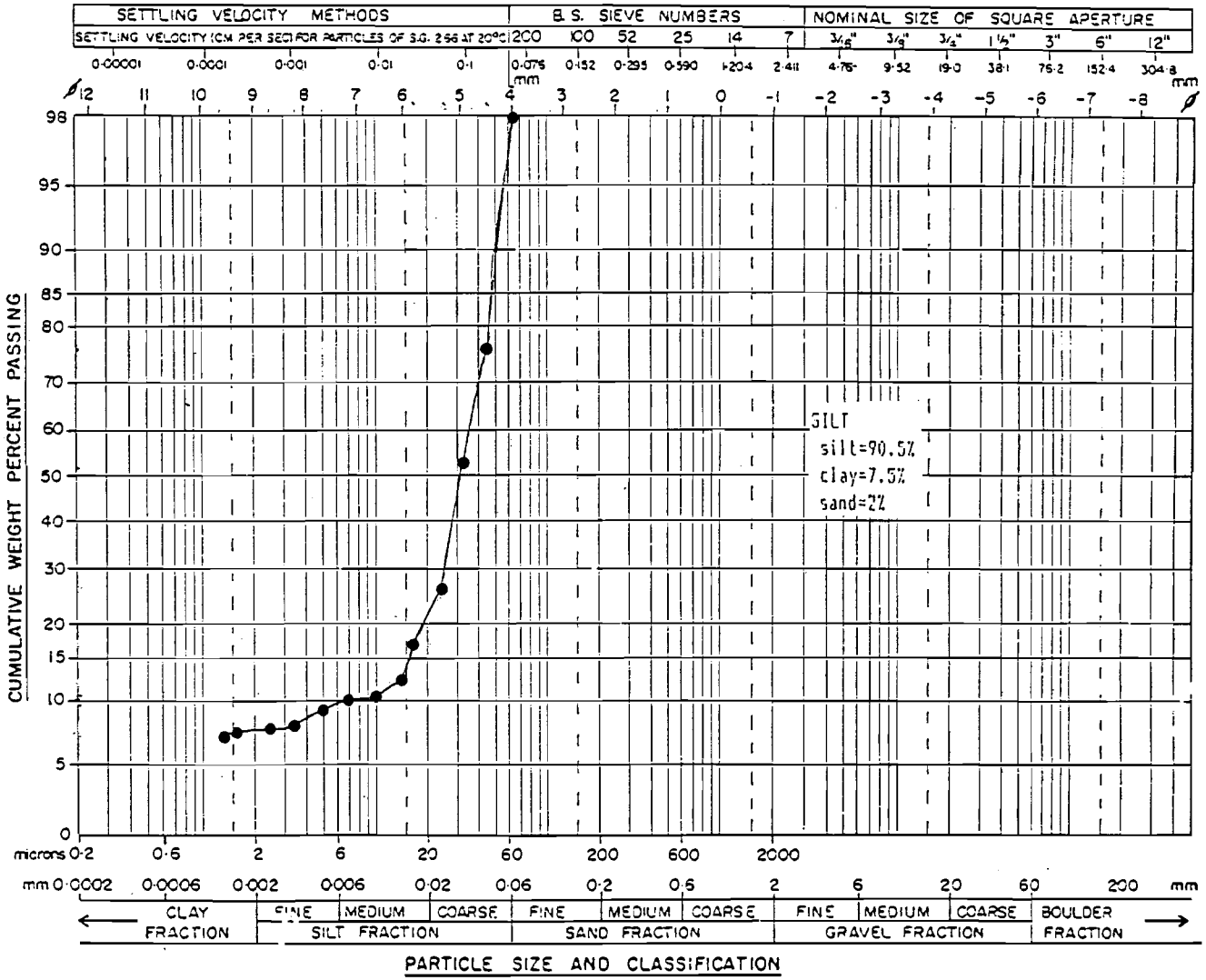

UNIVERSITY OF CANTERBURY

DEPARTMENT OF GEOLOGY

A.4.2 PARTICLE SIZE DISTRIBUTION – LOG PROBABILITY PLOT

PROJECT ..Kaituna..... SAMPLE NO .. G ..... SAMPLED BY .P. Na..... ANALYSED BY .P. Na.....

..... LOCATION ....AH1 (Fig 1.6) DATE .Sept. 1986. DATE .Sept. 1986....

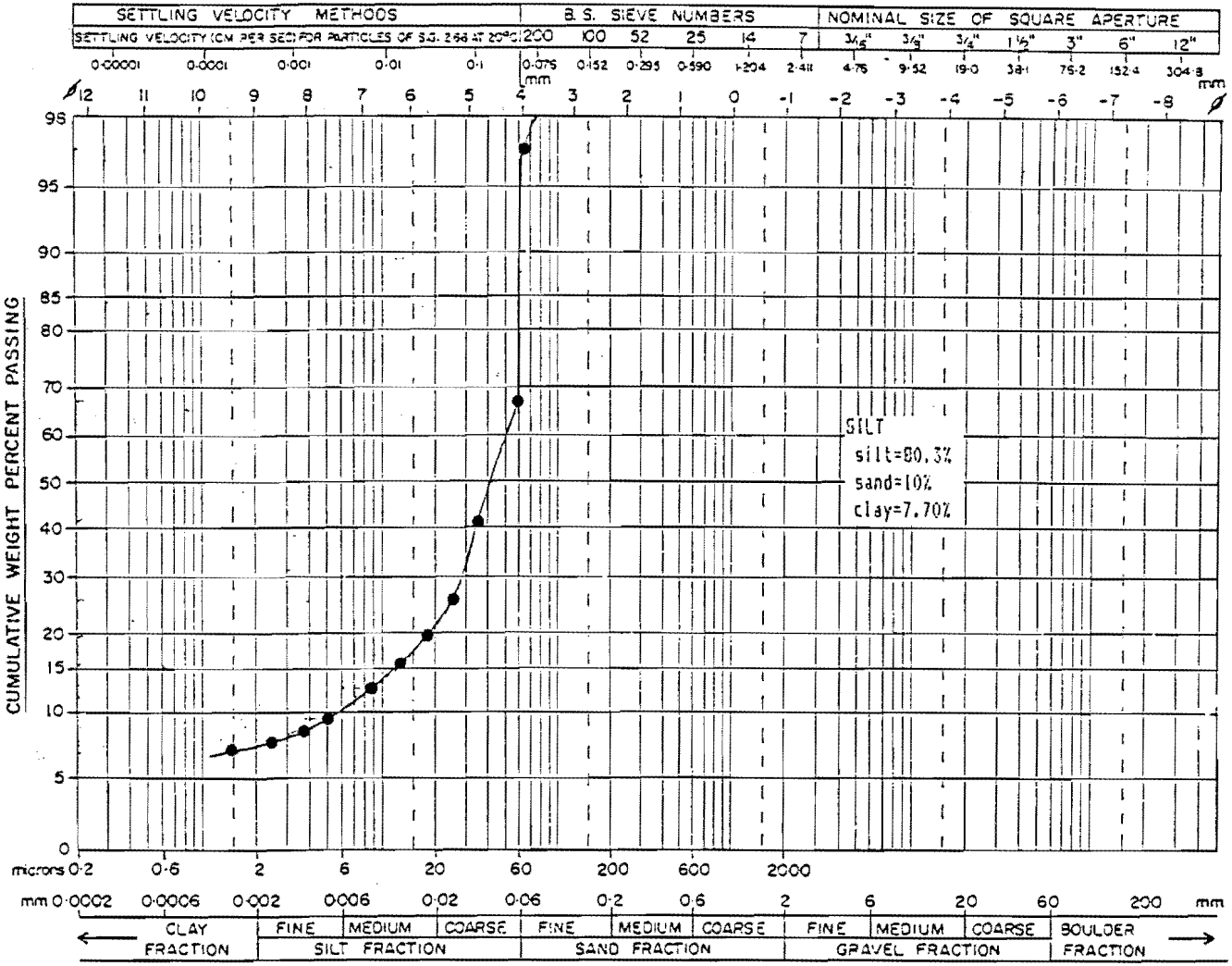

PARTICLE SIZE AND CLASSIFICATION

UNIVERSITY OF CANTERBURY

DEPARTMENT OF GEOLOGY

A.4.2 PARTICLE SIZE DISTRIBUTION – LOG PROBABILITY PLOT

PROJECT ..Kaituna..... SAMPLE NO .. H..... SAMPLED BY ..P..Na..... ANALYSED BY..P..Na.....

..... LOCATION ....AH1 (Fig 1.6) DATE .Sept..1986. DATE .Sept..1986....

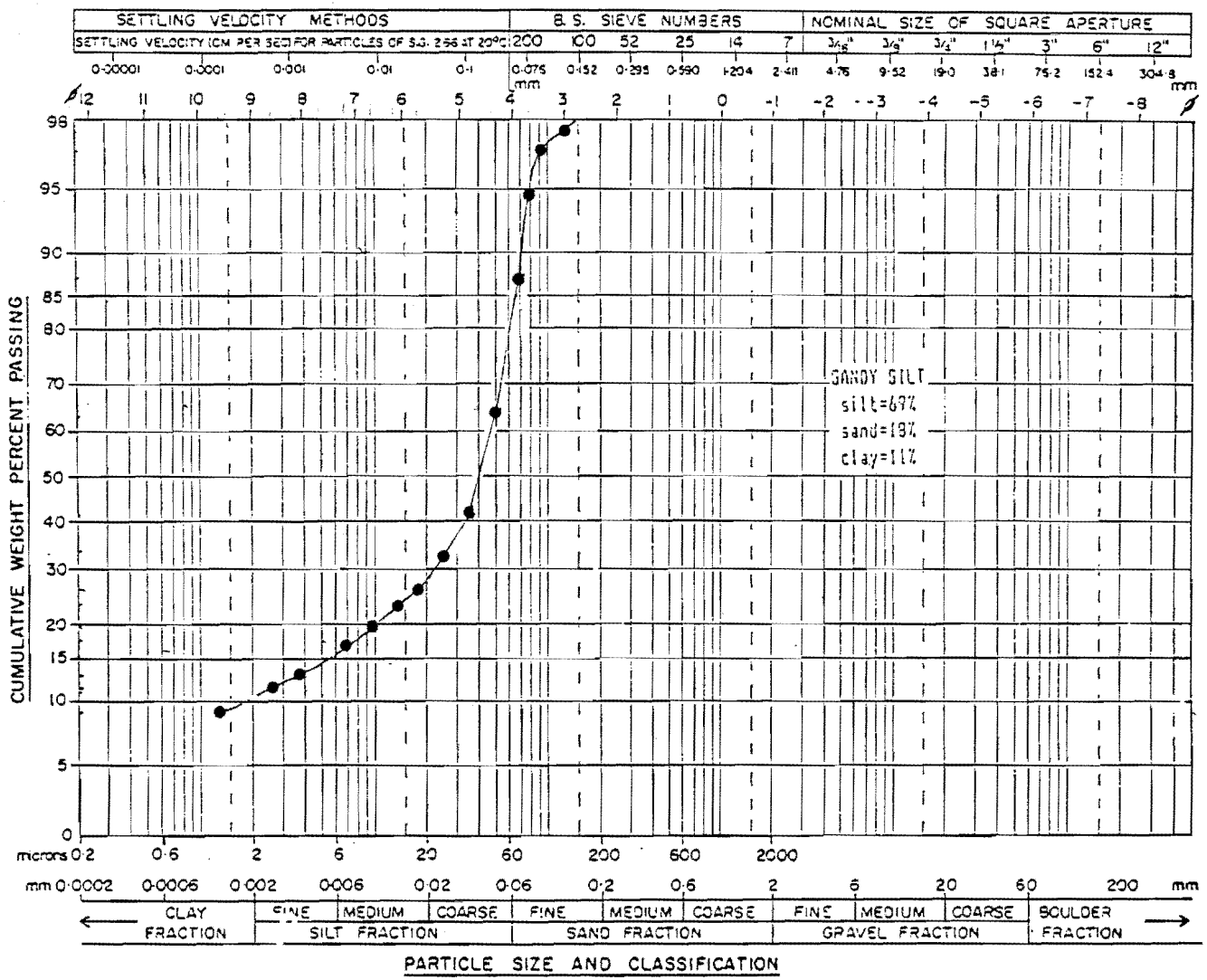

PARTICLE SIZE AND CLASSIFICATION

A4.3

TEXTURAL TERMINOLOGY FOR GRAVEL - FREE DETRITAL SEDIMENTS
(Folk, Andrews, Lewis, 1968)

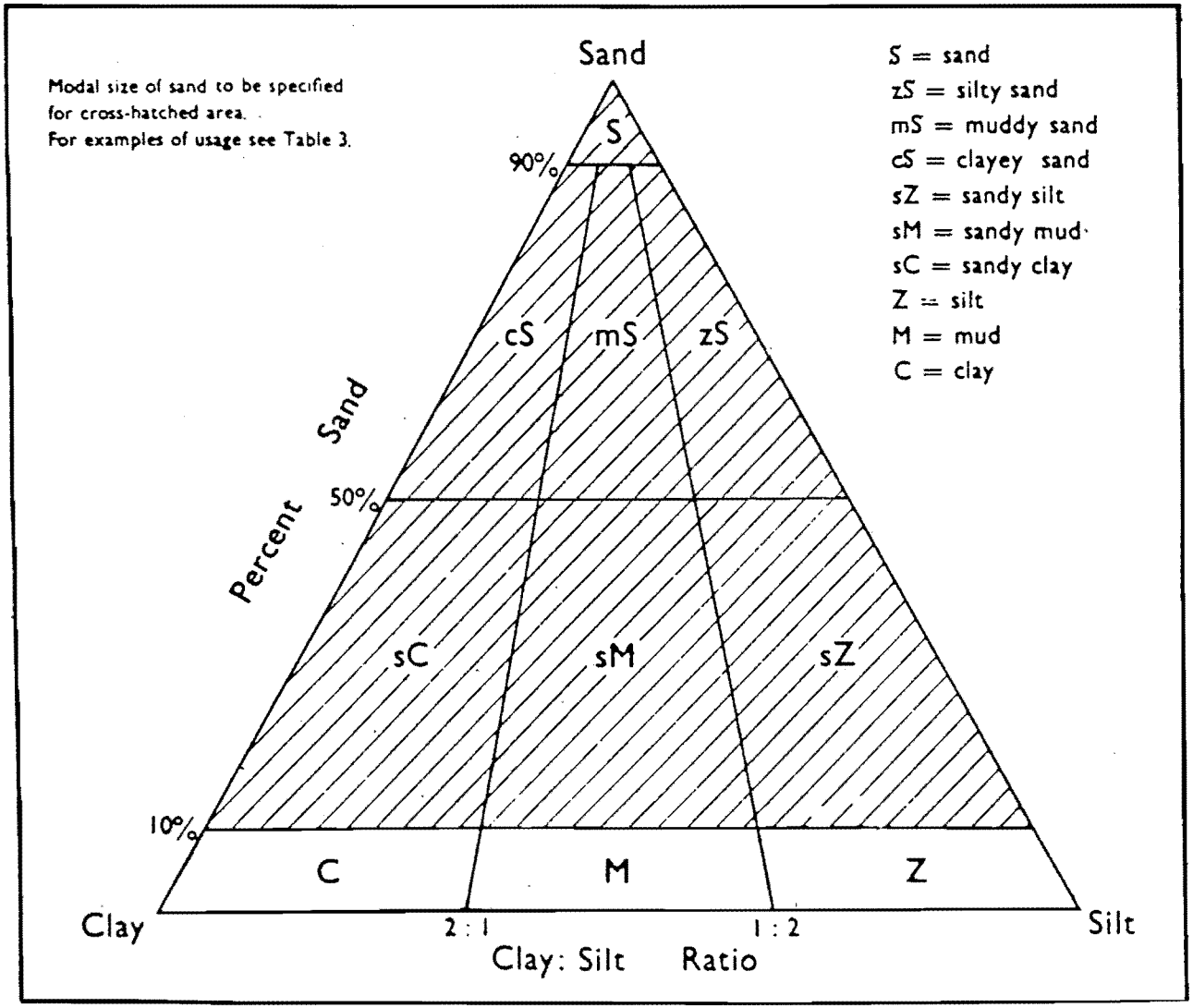

APPENDIX 5

GEOPHYSICAL LOGGING

A.5.1 Caliper

A.5.2 Natural Gamma

A.5.3 Gamma-Gamma (Density)

A.5.4 Neutron

A.5.1 Caliper Log

The Caliper Sonde is a tool about two metres long with three spring tensioned feelers at one end. These feelers move in and out as the tool is raised in a borehole and the bore diameter is recorded on the chart recorder above. The sensitivity of the tool can be adjusted to suit the bore size and to show smaller features such as welds in the casing if required (Simpson, 1987).

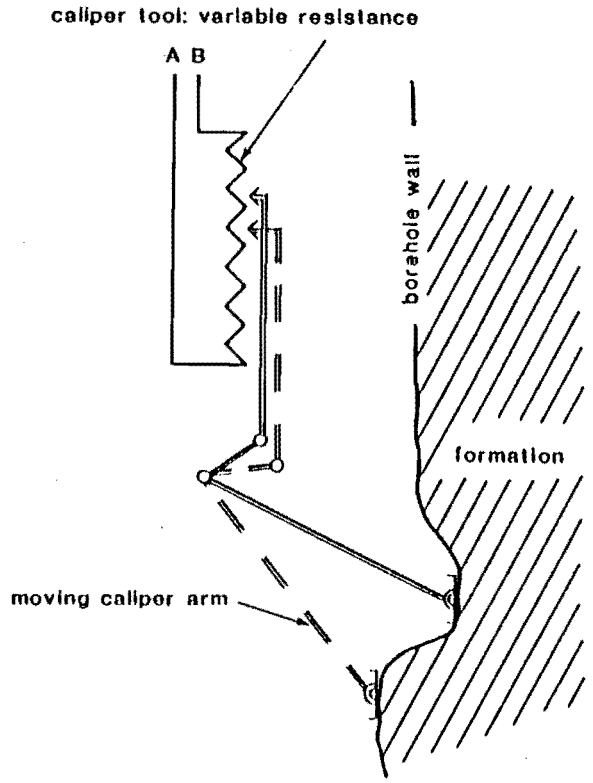

Fig: A.5.1, Schematic caliper tool showing the conversion of a mechanical movement to an electrical signal using a variable resistance (after Rider 1986)

A.5.2 Natural Gamma

Natural Gamma radiation in rocks comes essentially from only three elemental sources: the radioactive elements of the thorium family, of the uranium-radium family and of the radioactive isotope of potassium ^{40}K (Rider, 1986).

A.5.2.1 Tool

Gamma ray tools consist essentially of a sensitive gamma ray detector, generally a scintillation counter made with a large sodium iodide crystal. When a gamma ray penetrates the crystal it produces a flash of light, which is then converted to an electric pulse by a photoelectric cell. The tool literally "counts" the gamma rays (Rider, 1986).

A.5.3 Gamma-Gamma (Density)

The density log is a continuous record of a formation's bulk density. This is the overall density of a rock including solid matrix and the fluid enclosed in the pores. Geologically, bulk density is a function of the density of the minerals forming the rock (ie. matrix) and the volume of free fluids which it encloses (ie. porosity) (Rider, 1986)(Fig. A.5.3)

A.5.3.1 Source

The density tool had a collimated sodium iodide (thallium activated) gamma ray source.

A.5.4 Neutron

The neutron log provides a continuous record of a formation's reaction to fast neutron bombardment. It is quoted in terms of neutron porosity units, which are related to a formation's hydrogen index, an indication of its richness in hydrogen.

Formations absorb neutrons rapidly when they contain abundant hydrogen nuclei, which are supplied by water. The log is therefore principally a measure of a formation's water content, be it bound water, water of crystallisation or free pore water (Rider, 1986)(Fig. A.5.4)

A.5.4.1 Tools

The neutron consists of a fast neutron source and the two detectors. The source bombards the formation's with fast neutrons, and the detectors register the degradation in energy of the neutrons as they pass through the formation.

The source used was plutonium-beryllium (PuBe) or americium-beryllium (Am-Be) (Rider, 1986).

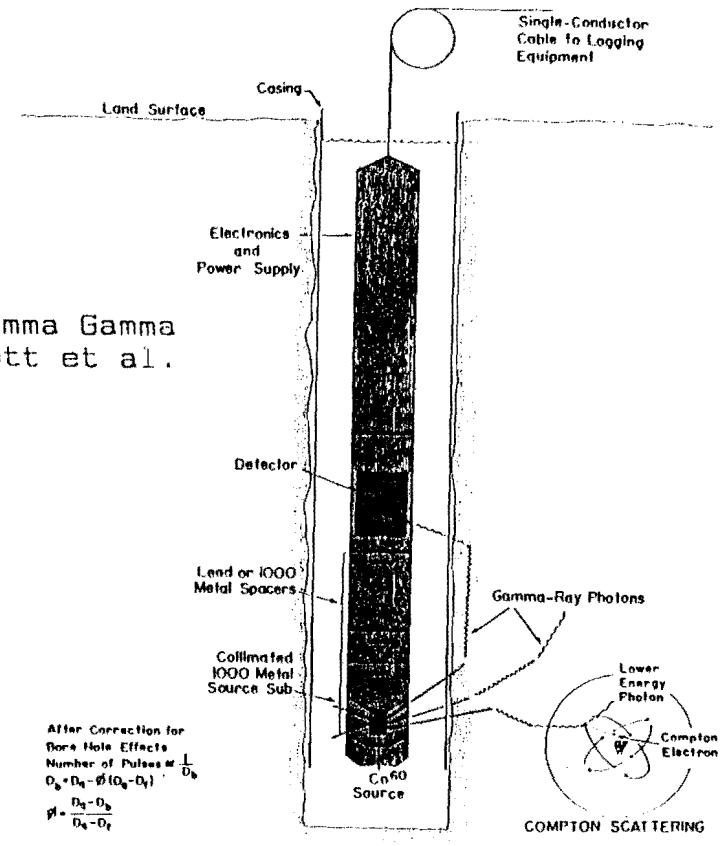

Fig A.5.3;
The Principle of Gamma Gamma Equipment (from Scott et al. 1971).

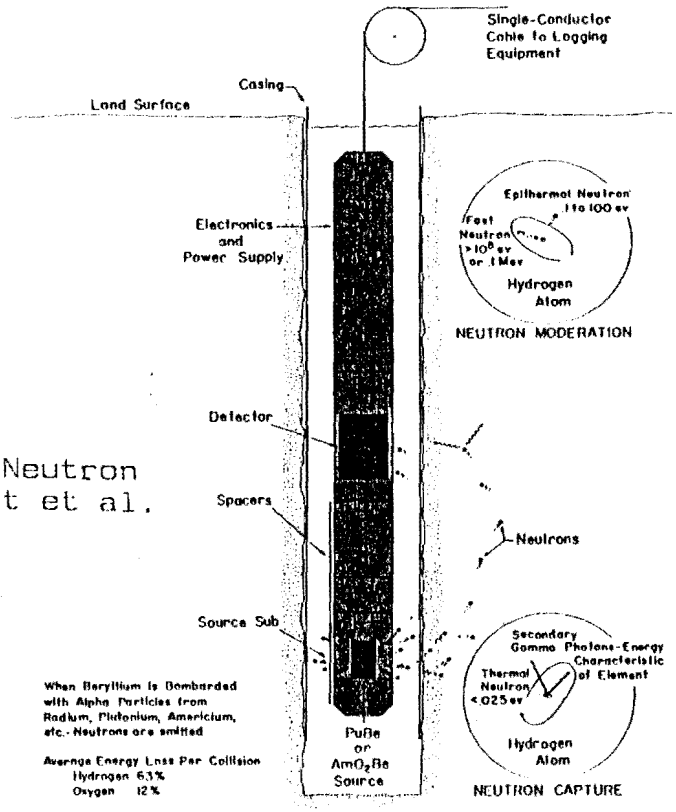

Fig A.5.4;
The Principle of Neutron Equipment (from Scott et al. 1971).

APPENDIX 6

RESISTIVITY SURVEY

A.6.1 Resistivity Equipment

A.6.2 Electrode Arrangements
- A.6.2.1 Wenner Array
- A.6.2.2 Schlumberger Array

A.6.3 Resistivity Sounding Curves

A.6.4 Resistivity Standard Curves

A.6.5 Curve Matching Technique

A.6.6 Tables of Measured Apparent Resistivity and Electrode Spacing used for the Schlumberger and Wenner Soundings

A.6.7 Modified Computer Resistivity Models

A.6.1: Resistivity Equipment Specifications

This section presents specifications for the Terrameter SAS 300, Terrameter SAS 2000 Booster, Terrameter SAS LOG 200 and UBC Universal Battery Charger.

Terrameter SAS 300 – Specifications

Transmitter:	Selectable currents	0.2, 0.5, 1, 2, 5, 10,20 mA Voltage, max 160 V (320 V p–p)
Receiver, voltage measurement	Input impedance	10 MΩ, min
	Input ranges	1, 10, 100, 500 V
	Precision	± 0.00001 V (1 V range)
	Noise rejection	95 dB at 50–60 Hz 85 dB at 16–20 Hz
Receiver, resistivity measurement:		
	ΔV/I range	1 Ω, 100 Ω, 10 kΩ, 1 MΩ
	ΔV/I	0.0005 Ω (1 Ω range 20 mA, one reading)
System data:	Selectable cycle times	3.6, 7.2, 14.4 seconds
	Selectable total averaging period (1–64 readings)	3.6–920 seconds
	Accuracy	±2% ±precision
Temperature range	Within specification	0.....+60^{0}C Operating–10^0... +70^{0}C
Power supply:		Rachargeable 12 V battery
Battery capacity		3500–5000 single cycle measurements per charge
Weight:		5.6 kg incl battery
Dimensions:		W×L×H 10×325×300 mm

A .6.1 Continued:

Terrameter SAS 2000 Booster – Specifications

Transmitter:	Selectable currents	0.2, 0.5, 1, 2, 5,10, 20, 50, 100, 200, 500 mA
	Voltage, max	400 V (800 V p–p)
System data	ΔV/I precision	0.00002 Ω, (1 Ω range, 500 mA, one reading)
	ΔV/I accuracy	±2% ±precision
Temperature range:	Within specification	0^0...+60^0C
		Operating –10^0... +70^0C
Power supply:		Rachargeable 12 V battery
Battery capacity		800–3500 single cycle measurements per charge
Weight:		6.3 kg incl battery
Dimensions:		W×L×H 105×325×300 mm

Terrameter SAS LOG 200 – specifications

«Not used»

Cable length:		200 m
Logging probe diameter, max		35 mm
Survey modes:	–16" short normal	0.05–100,000 m
	–64" long normal	0.5 –100,000 m
	–18' lateral	0.5 –100,000 m
	–Fluid resistivity cell	0.05–100,000 m
	Self potential	0.05–100 mV
	Temperature, range	0^0 +50^0C
	Temperature, precision	±0.01^{0}C (0^0...+20^0C)
	Temperature, precision	±0.1^{0}C (+20^0...+50^0C)
	Temperature, accuracy	±1^{0}C
Weight:		14.0 kg
Dimensions:		W×L×H 880×440×230 mm

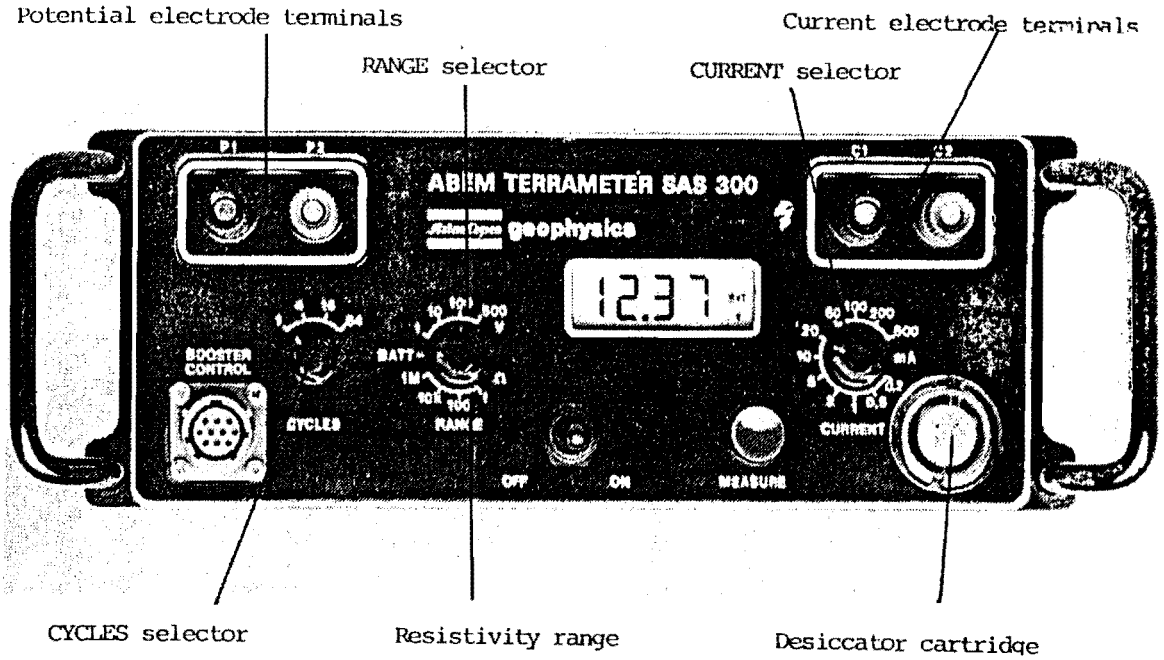

Fig A6.1a SAS 300 controls and terminals

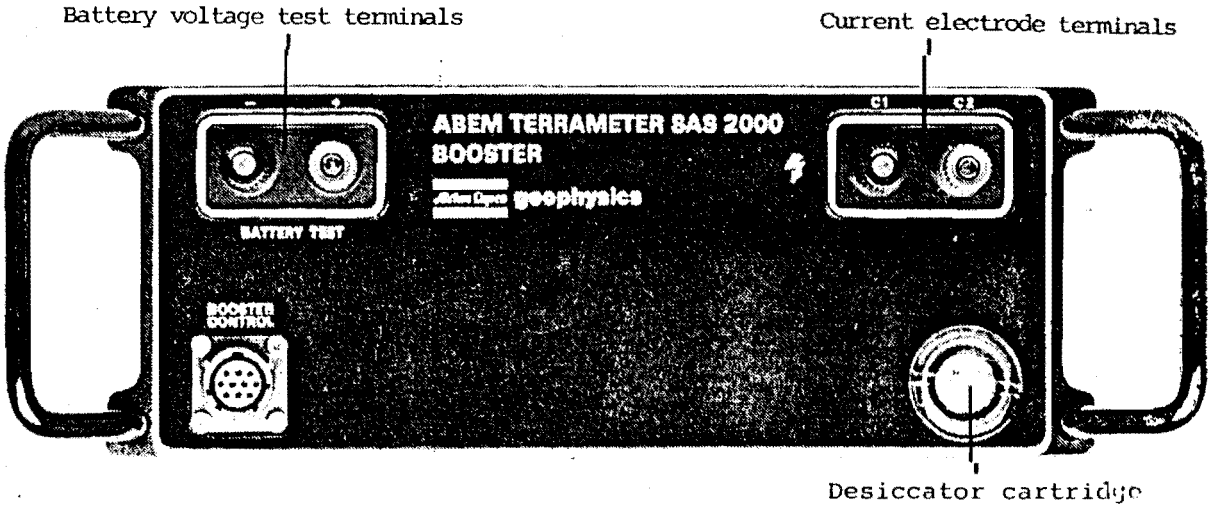

Fig A6.1b SAS 2000 Booster controls and terminals

A.6.1 continued:

UBC Universal Battery Charger – specifications

Input	10–30 DC, from any battery or other DC supply **Or,** 100–240 V AC, 47–63 Hz, from mains
Output	Two seperate charging circuits (outputs A and B), each of which provides provides 400 mA ± 5% at a maximum output voltage of 15 V **Or,** Single charging circuit (output A) which provides 400 mA ± 5% at a maximum output voltage of 36 V
Cell temperature	0 to +65^{0}C
Overheating protection:	Internal protector cuts off input current
Fuses	15 mA fuse for AC input 2.5 mA fuse for DC input
Two indicator lamps when charging	One LED for each output lights up when charging current exceeds 280 mA
Dimensions:	W×L×H 125×80×220 mm
Weight:	2.4 kg

A.6.2 Arrangements

A.6.2.1 Wenner Configuration

The Wenner arangement uses four electrodes equally spaced along a straight line. It is designed to measure the potential difference (V) between M and N, with spacing between adjacent electrodes designated "A".

$$\text{(apparent resistivity) } p = 2\pi A(V/I) = 2\pi AR \text{ (R=resistance)}$$

The Wenner Configuration has the disadvantage that lateral sub-surface variations can be misinterpreted as depth variations. Some protection against this possibilty can be obtained by taking measurements along two perpendicular lines.

In a Wenner Electrode Configuration, the outer electrodes serve as the current electrodes and the two inner electrodes serve as the potential recieving electrodes. In use, a theoretical ellipsoid-shaped electric field is induced between the current electrodes while bowl shaped equipotential surfaces are induced around each current electrode.

Measured from the centre position, each potential electrode (P_1, P_2) is at a distance A/2 and each current electrode (C_1, C_2) is at a distance 3A/2 (Fig A.6.2).

A.6.2.2 Schlumberger Configuration

The Schlumberger Configuration is symmetric, colinier, and uses four electrodes A, M, N, and B. The two measuring electrodes are closely placed, midway between the two widely spaced current electrodes. The arrangement is designed to measure approximately the potential gradient at the mid-point of the current spread. A current I is passed through the ground (A and B), and the voltage drop $\triangle$ V between M and N associated with the electric field driving the current is measured (Fig. A.6.2). The apparent resistivity, p_a given by the following equation is calculated for each set of four electrodes.

$$p_a = \pi/MN \left((AB/2)^2 - (MN/2)^2\right) \triangle V/I$$

The advantages of this configuration lie in the fact that only the current electrodes are moved. The potential electrodes remain in their original positions, or at least are moved a minimum number of times during a given electrical sounding. The ratio L/MN is kept within the limits 5/1 and 30/1. The potential electrodes are moved only when this ratio becomes toohigh. Use of the configuration is fast, economical and accurate.

Fig. A.6.2 Electrode Arrangements
(From Zohdy, 1980)

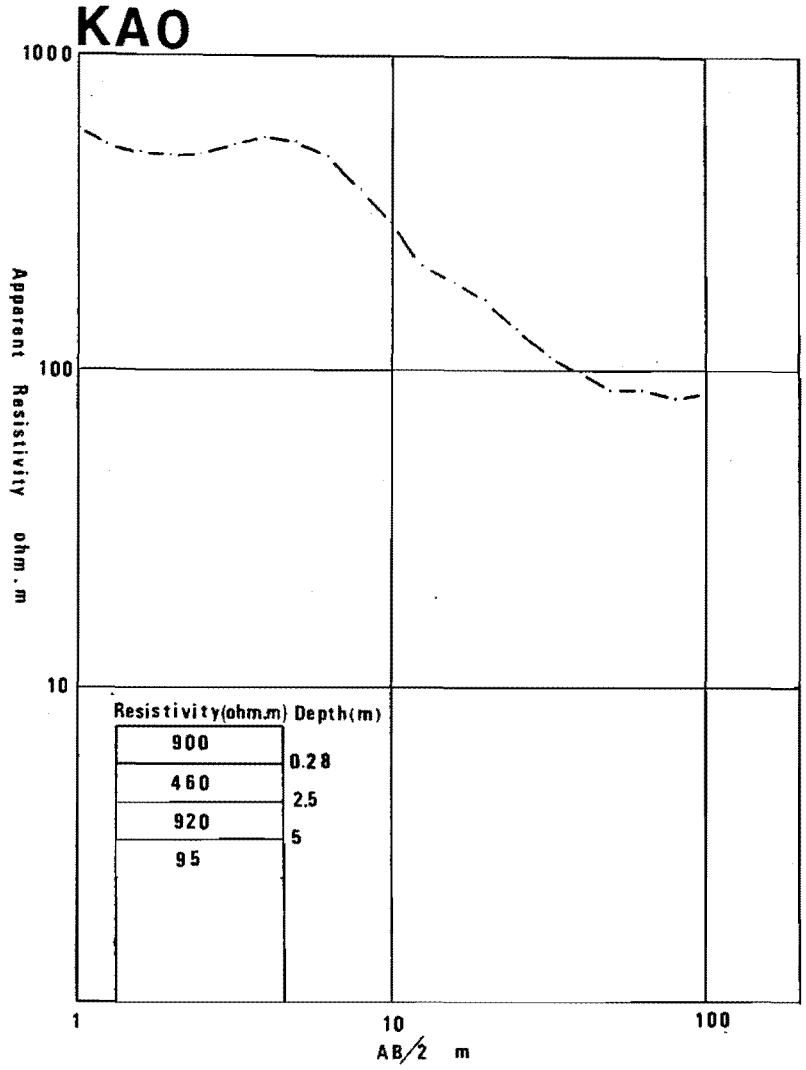

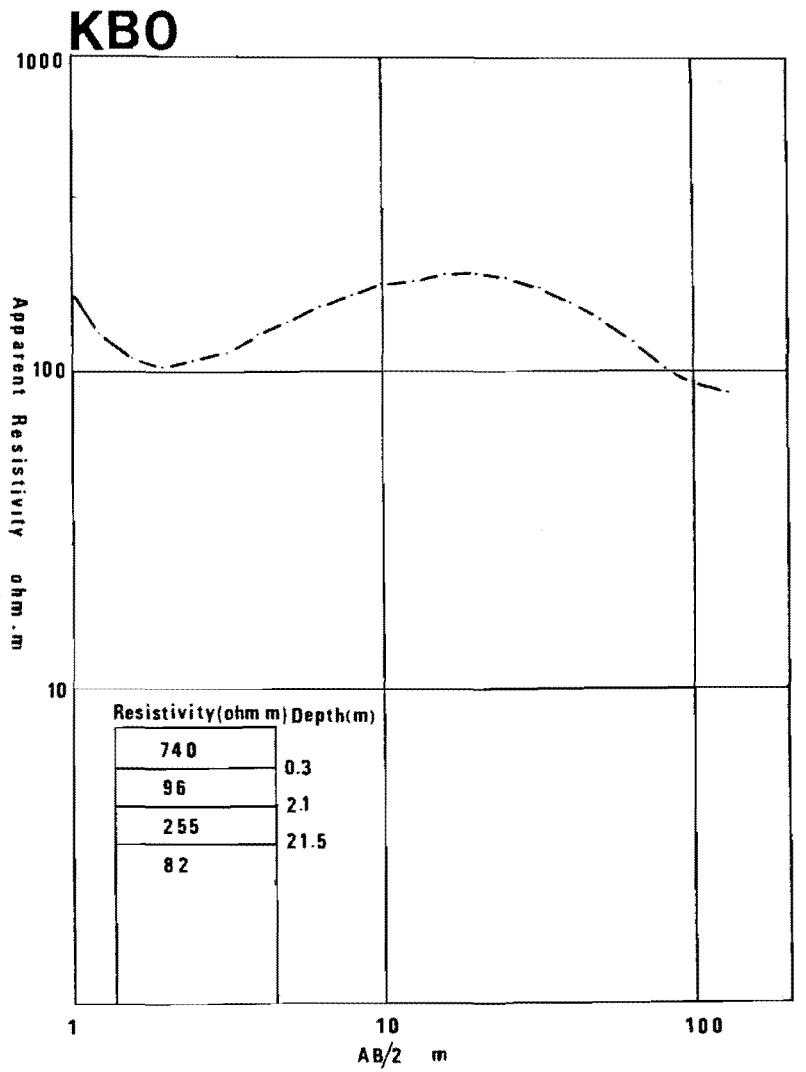

A.6.3 Resistivity Sounding Curves

&

Input Models

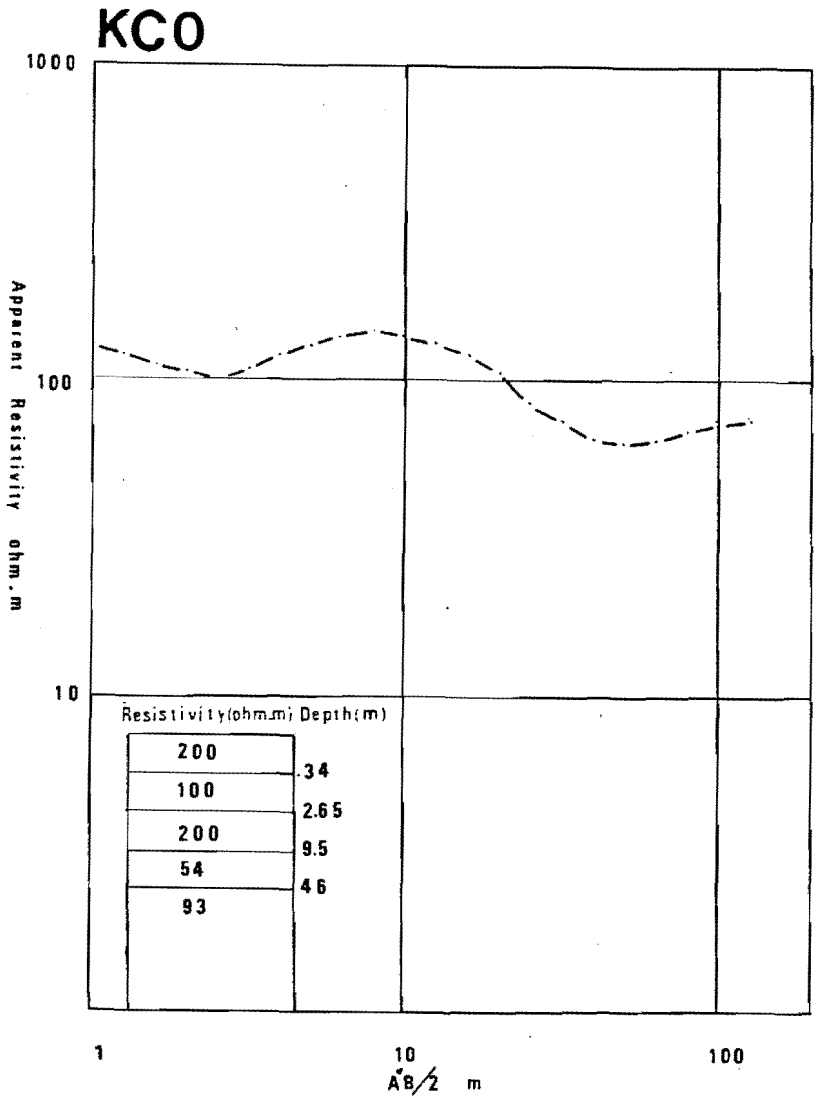

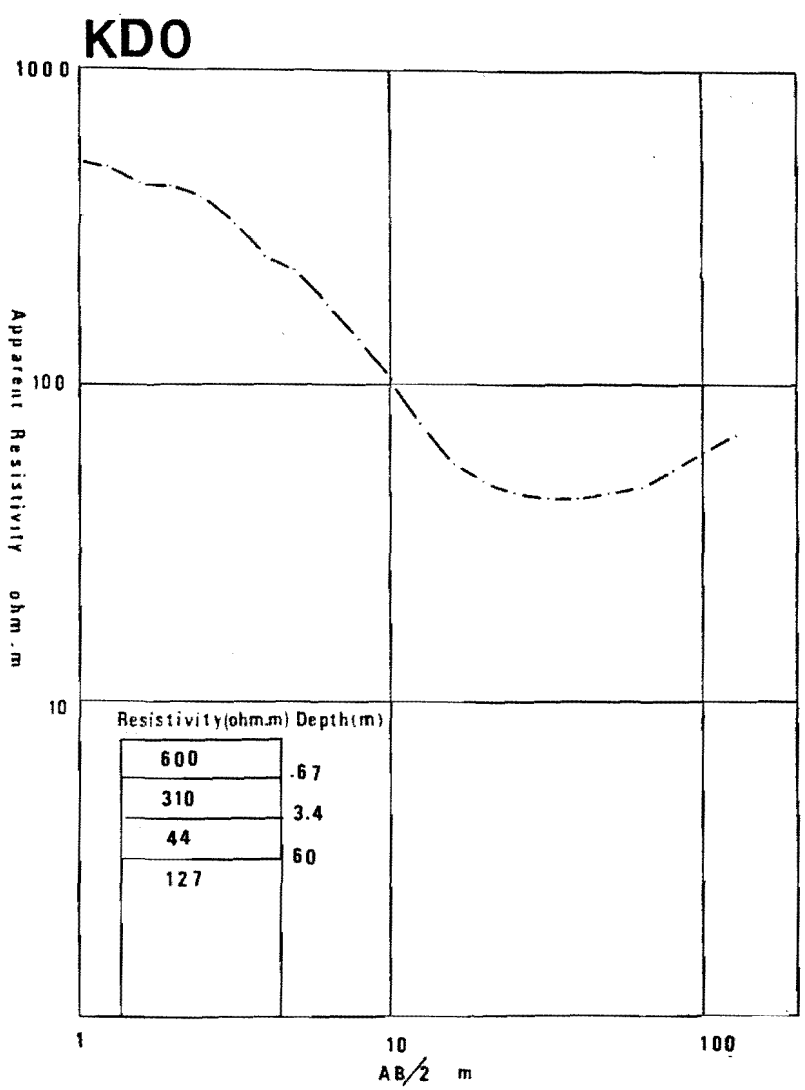

A.6.3 Resistivity Sounding Curves

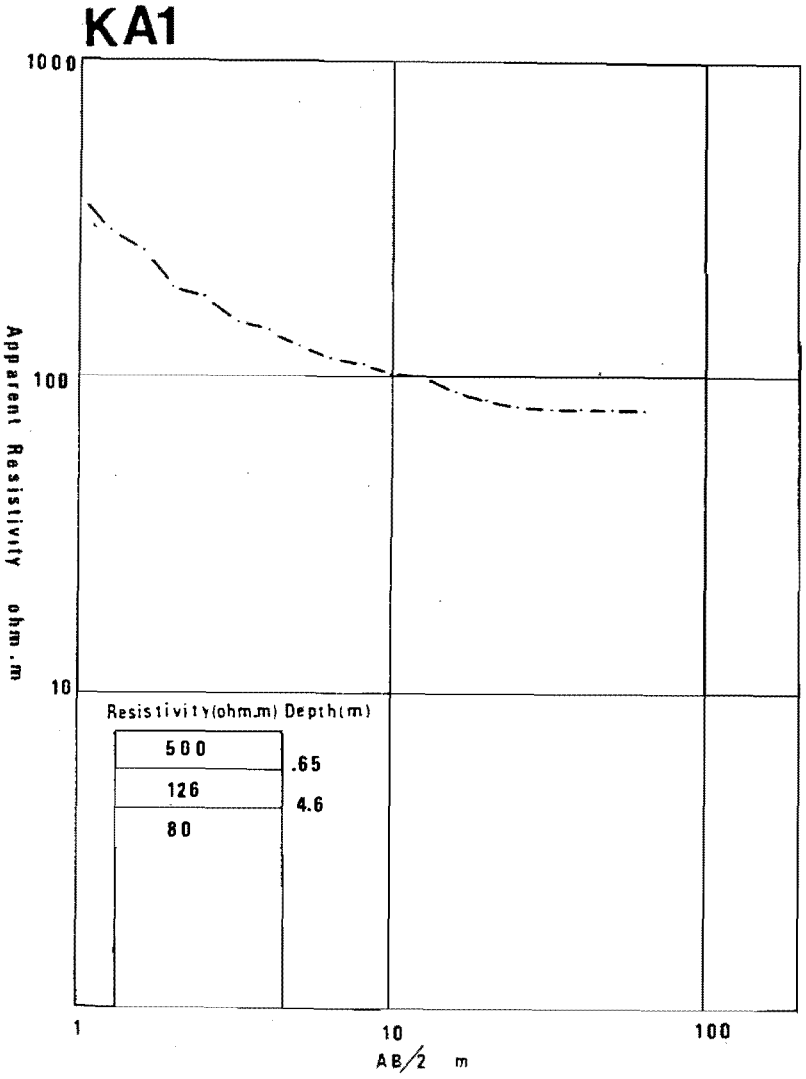

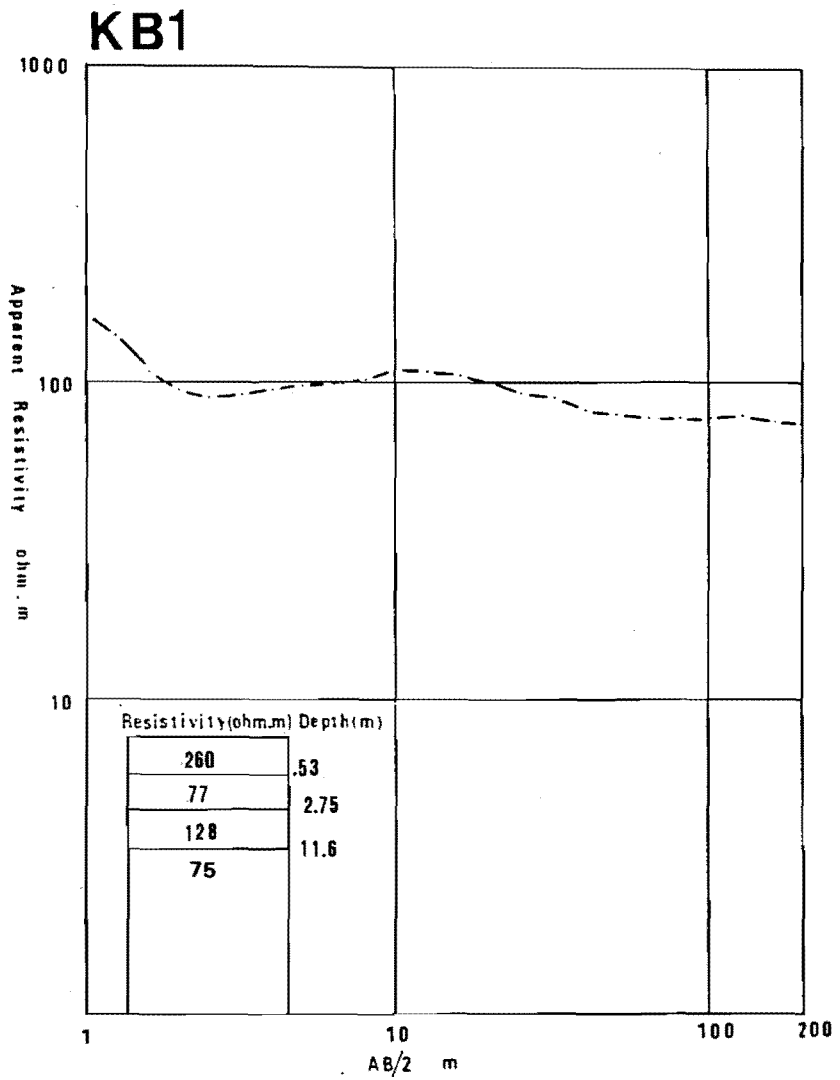

A.6.3 Resistivity Sounding Curves

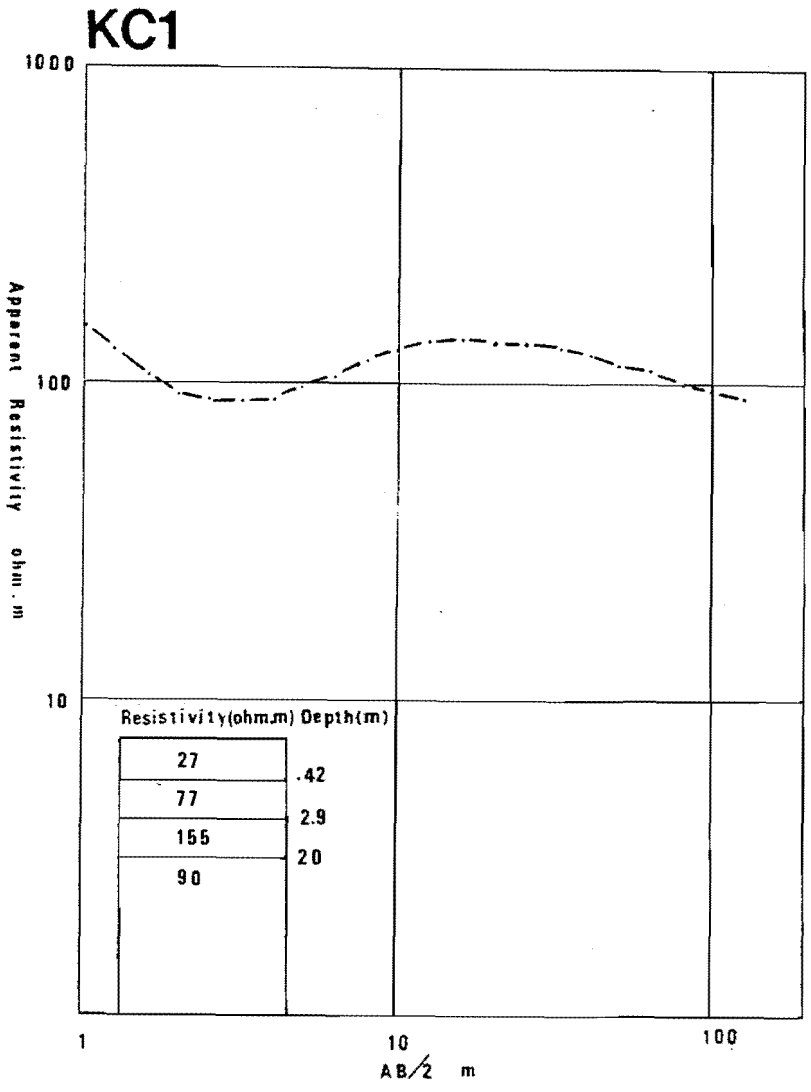

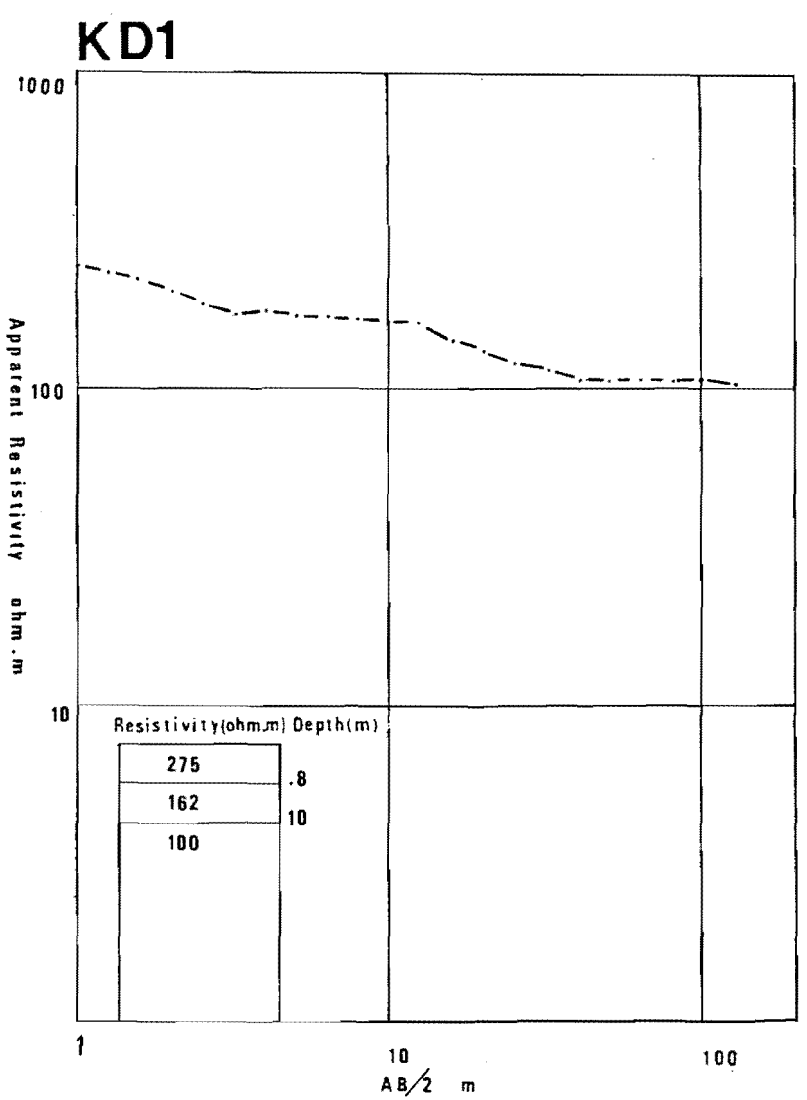

A.6.3 Resistivity Sounding Curves

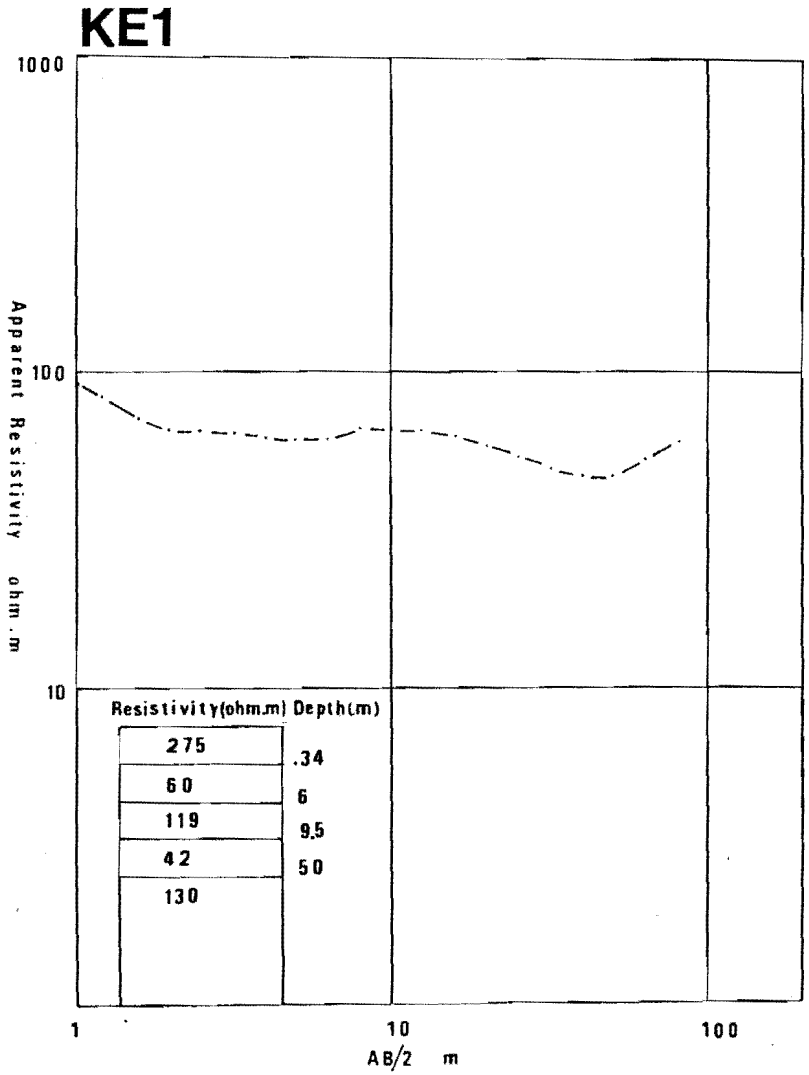

A.6.3 Resistivity Sounding Curve

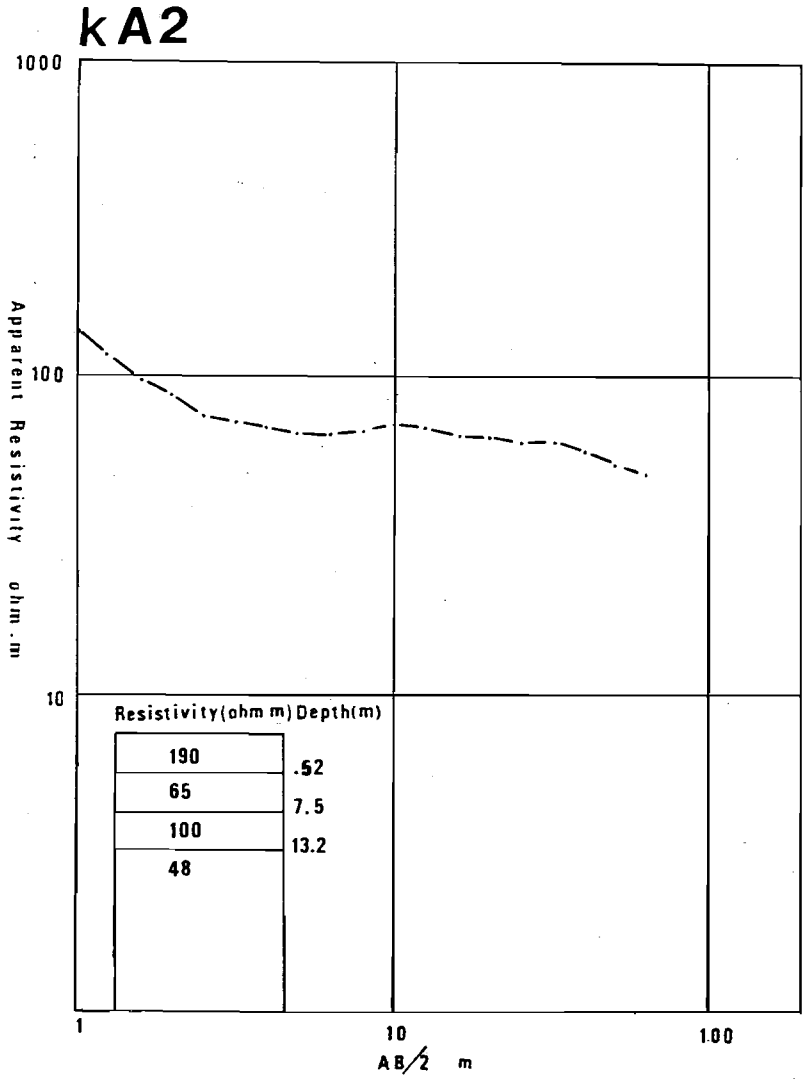

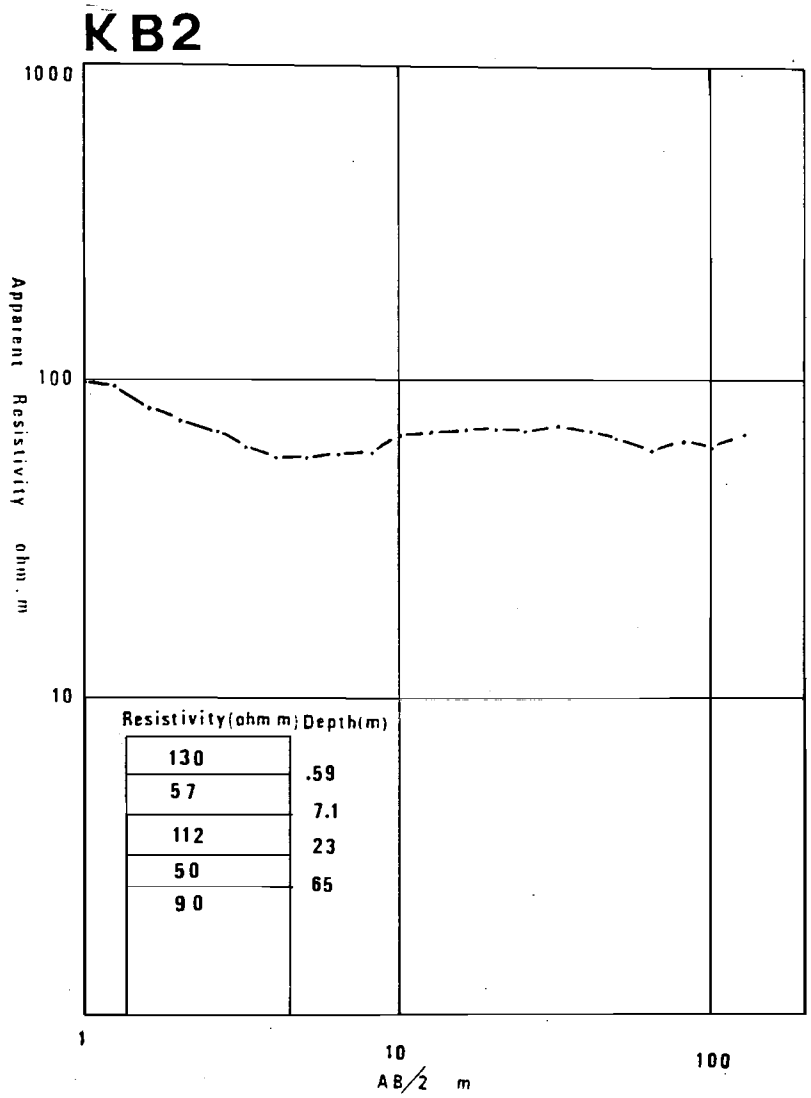

A.6.3 Resistivity Sounding Curves

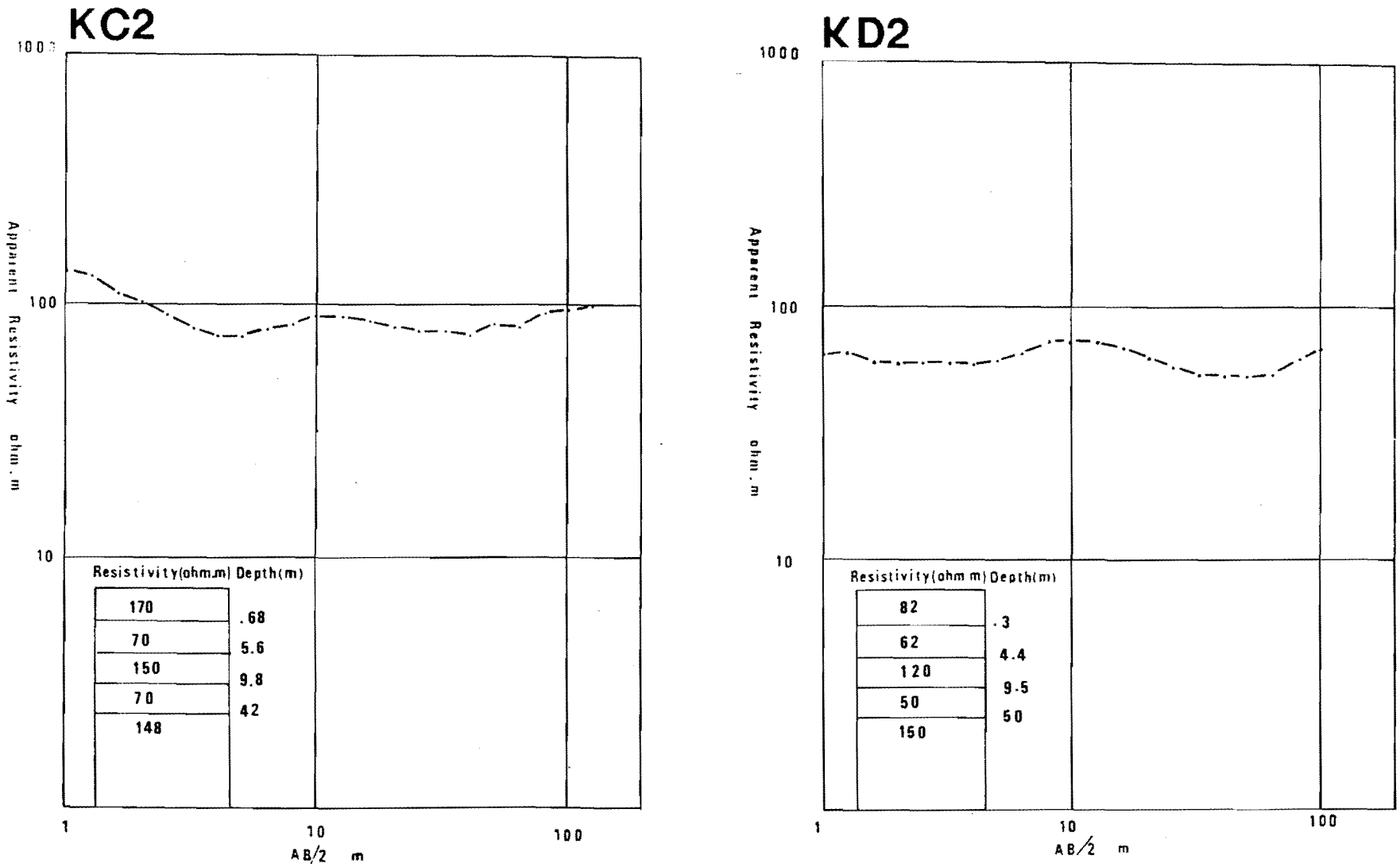

A.6.3 Resistivity Sounding Curves

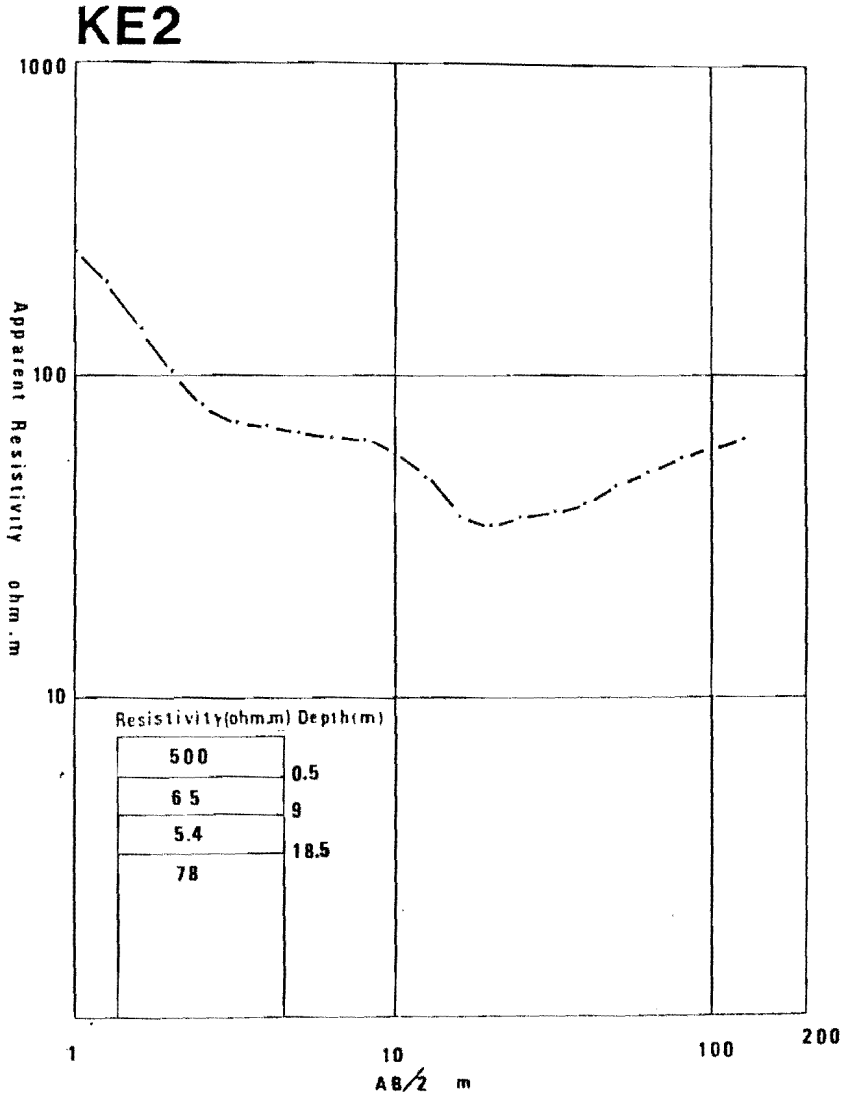

A.6.3 Resistivity Sounding Curve

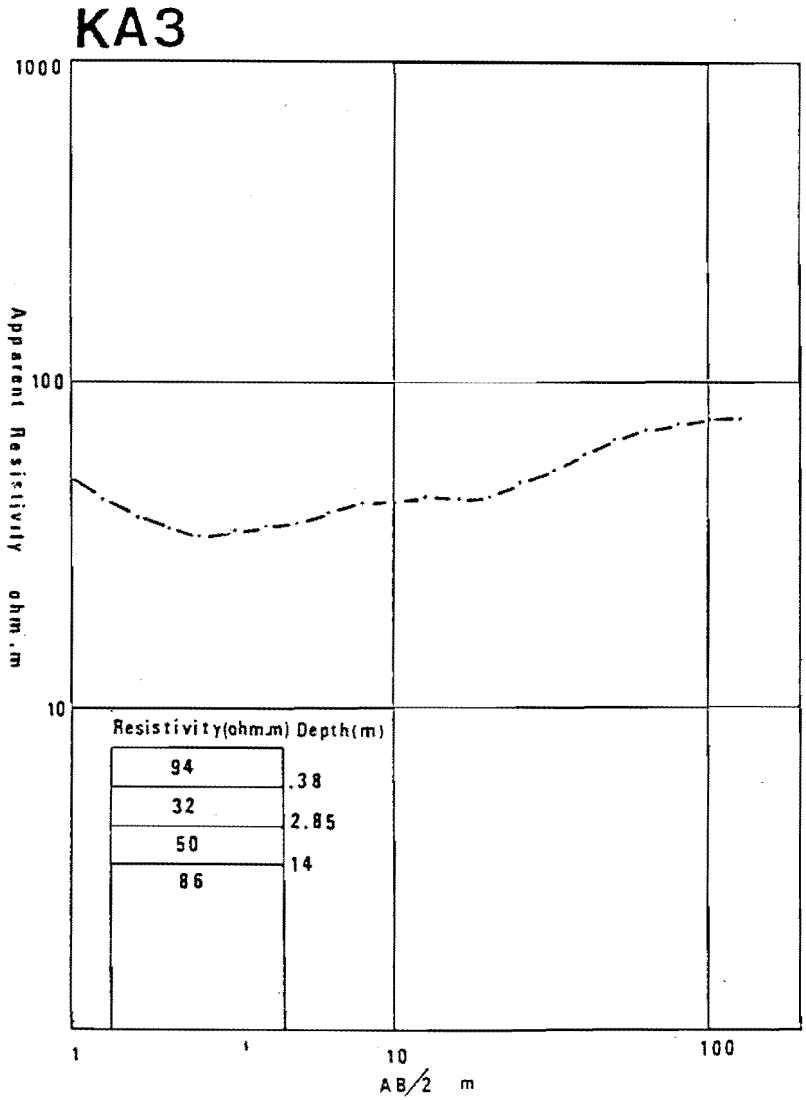

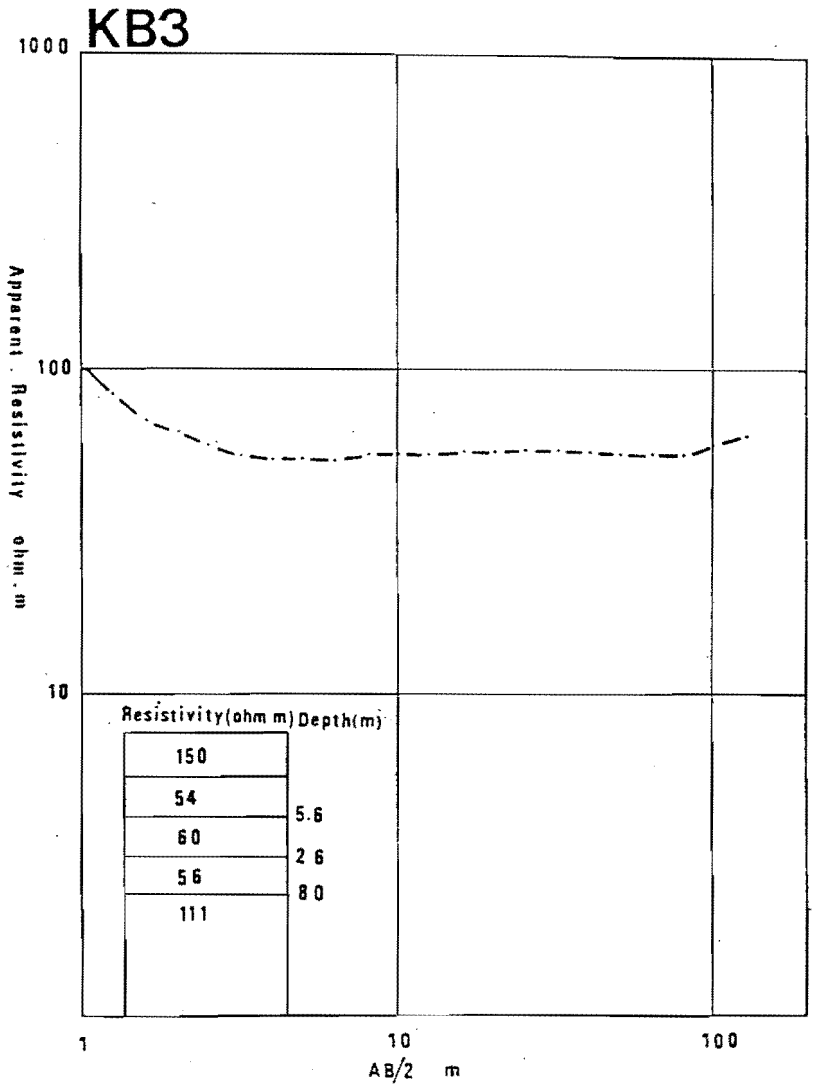

A.6.3 Resistivity Sounding Curves

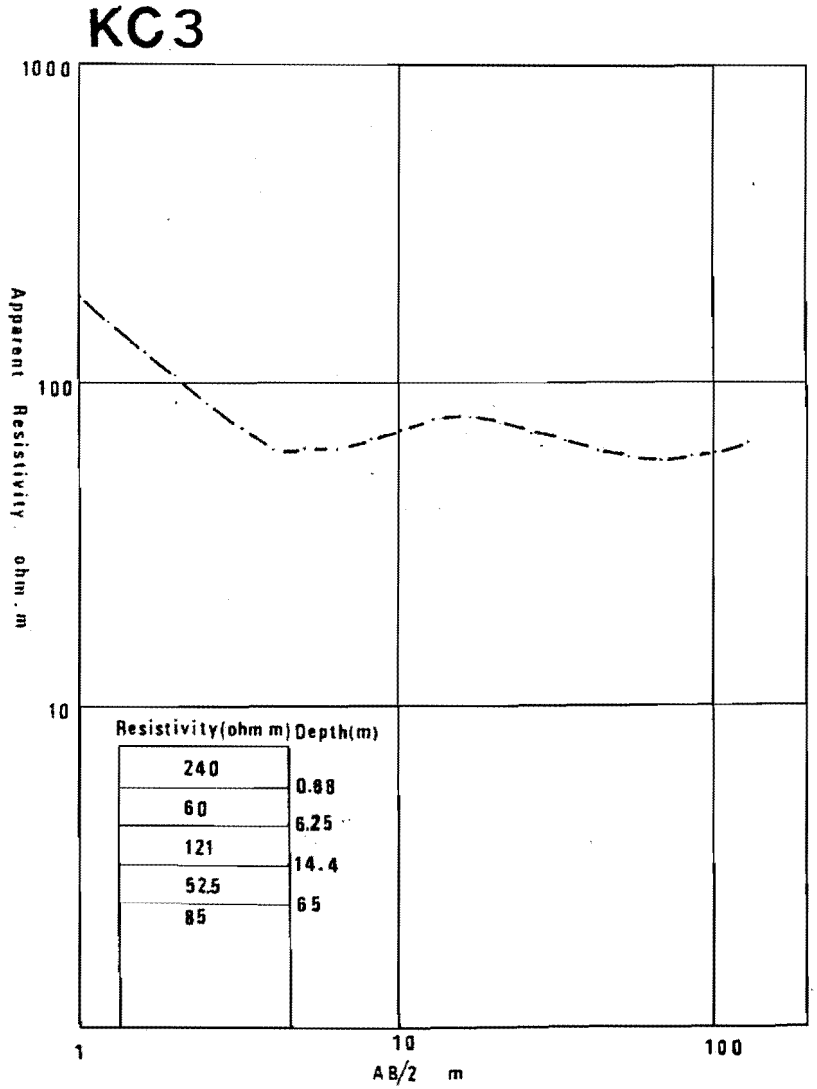

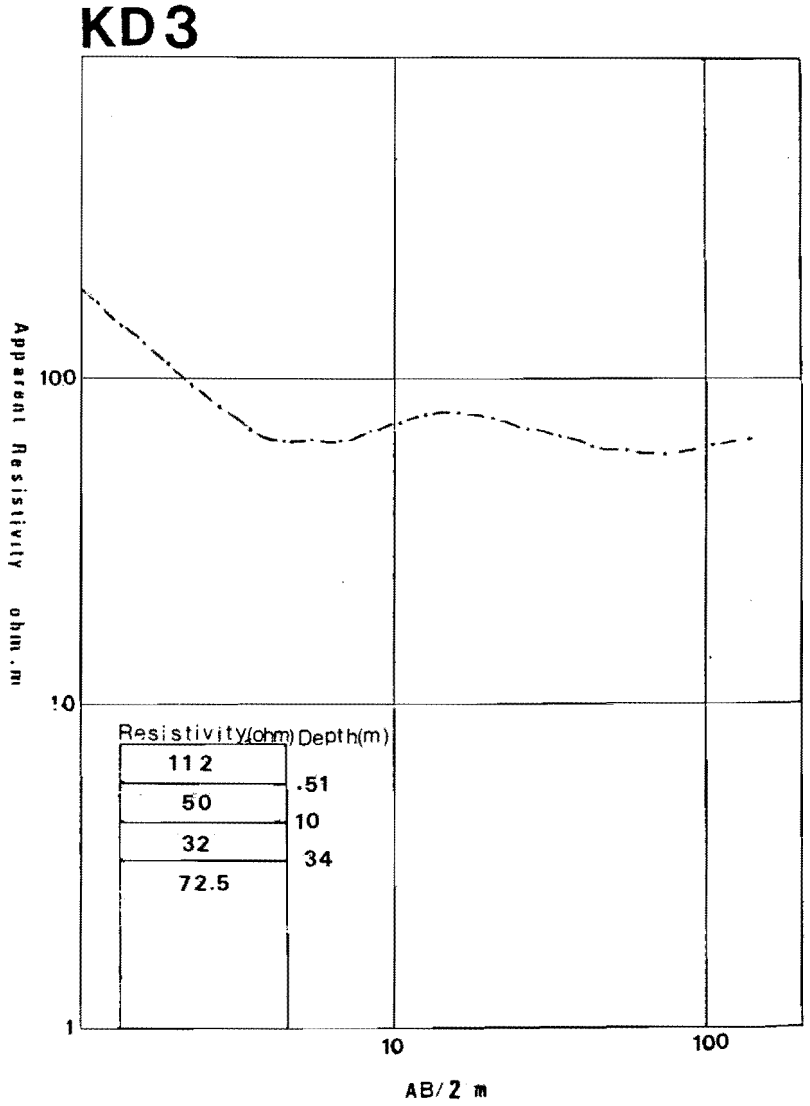

A.6.3 Resistivity Sounding Curves

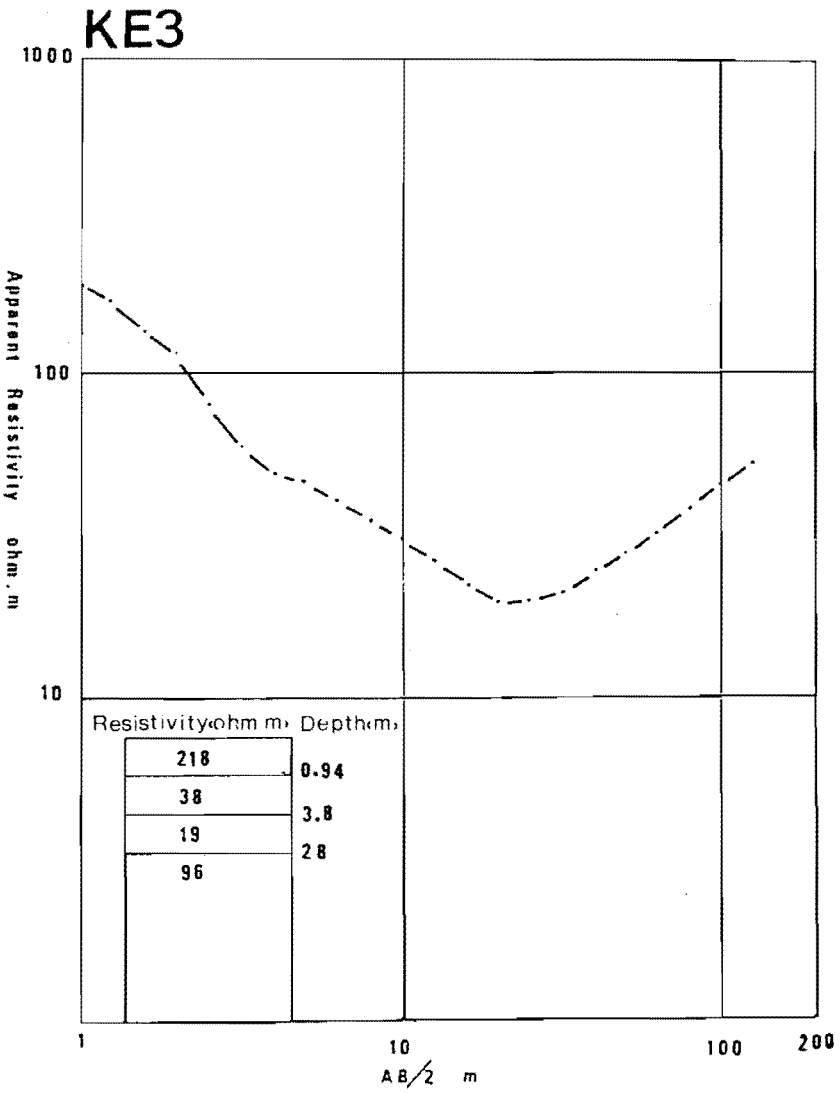

A.6.3 Resistivity Sounding Curve

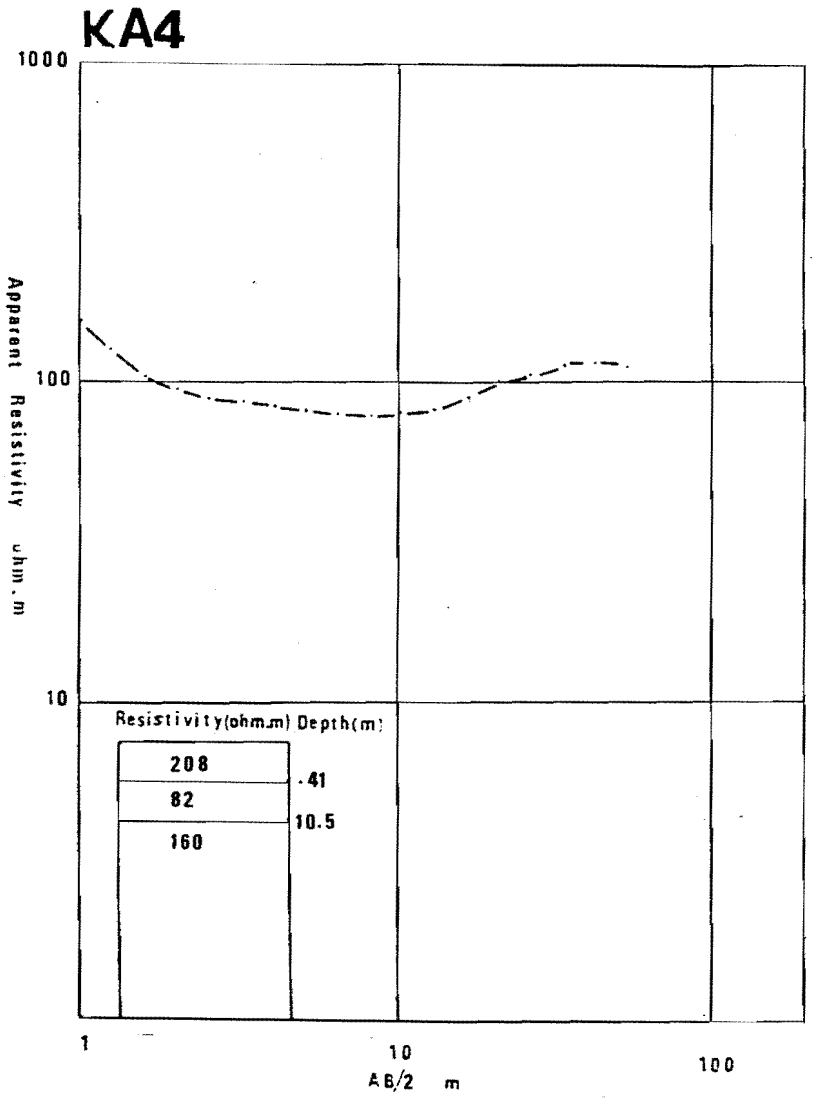

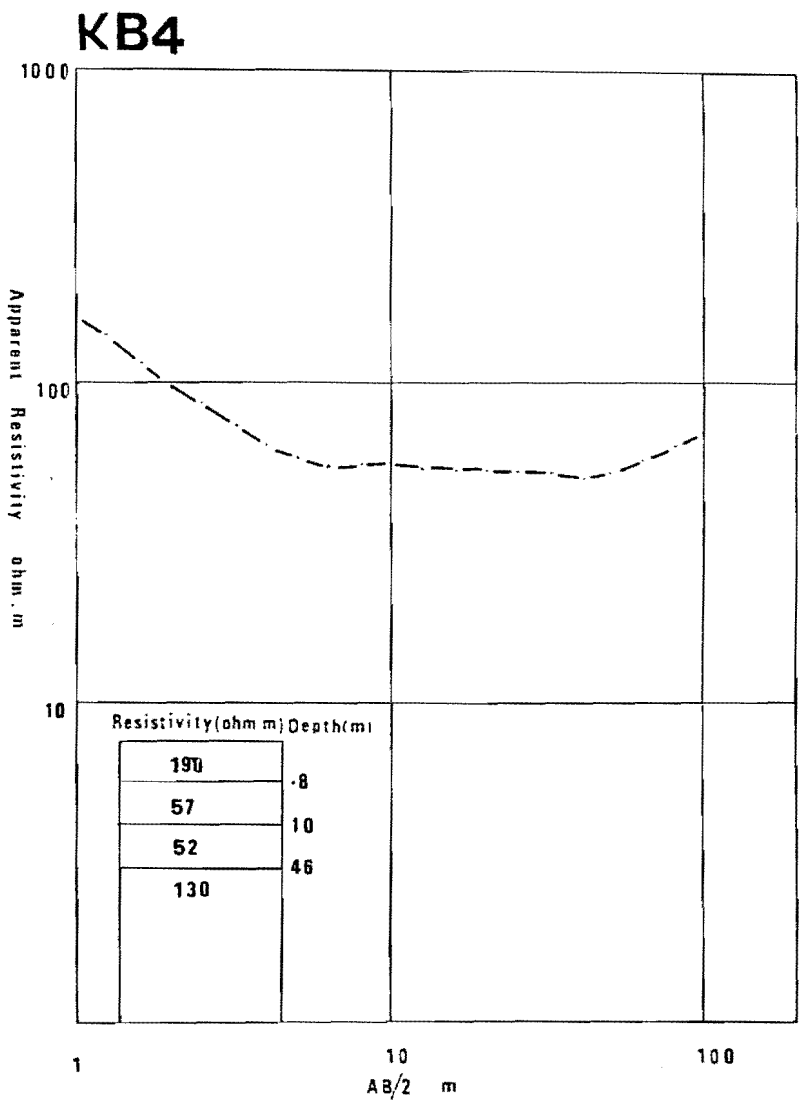

A.6.3 Resistivity Sounding Curves

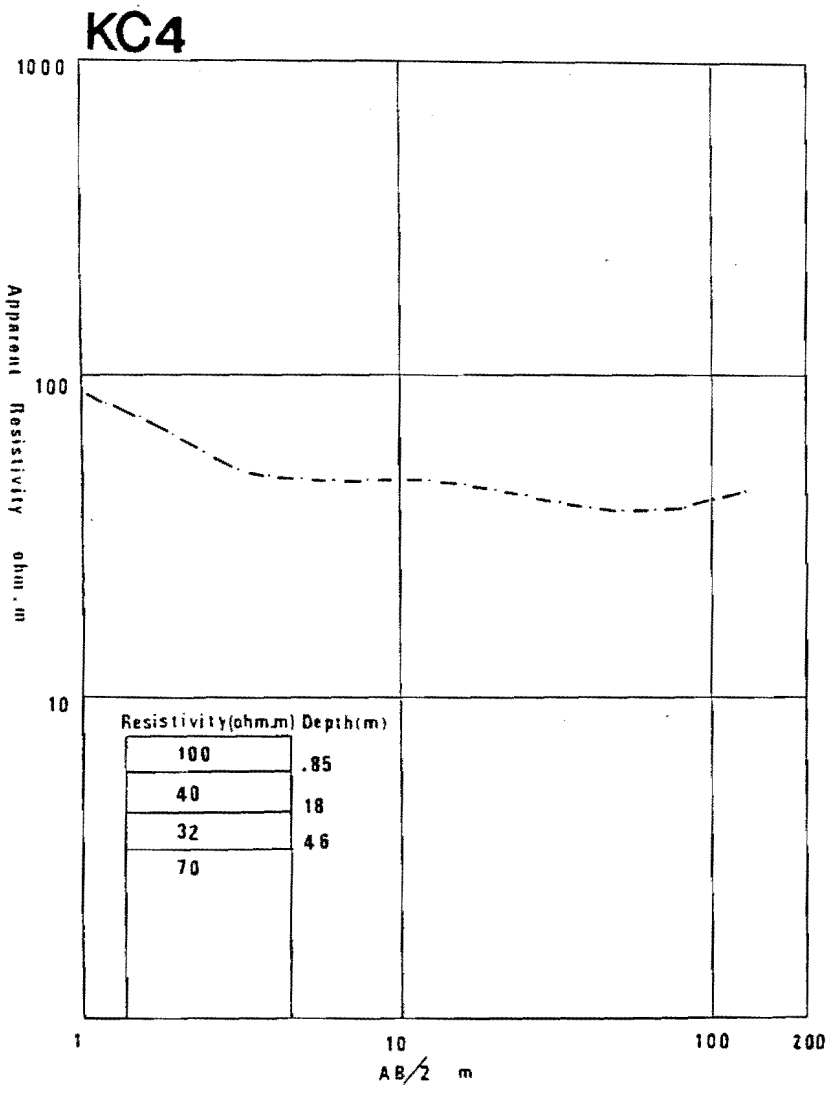

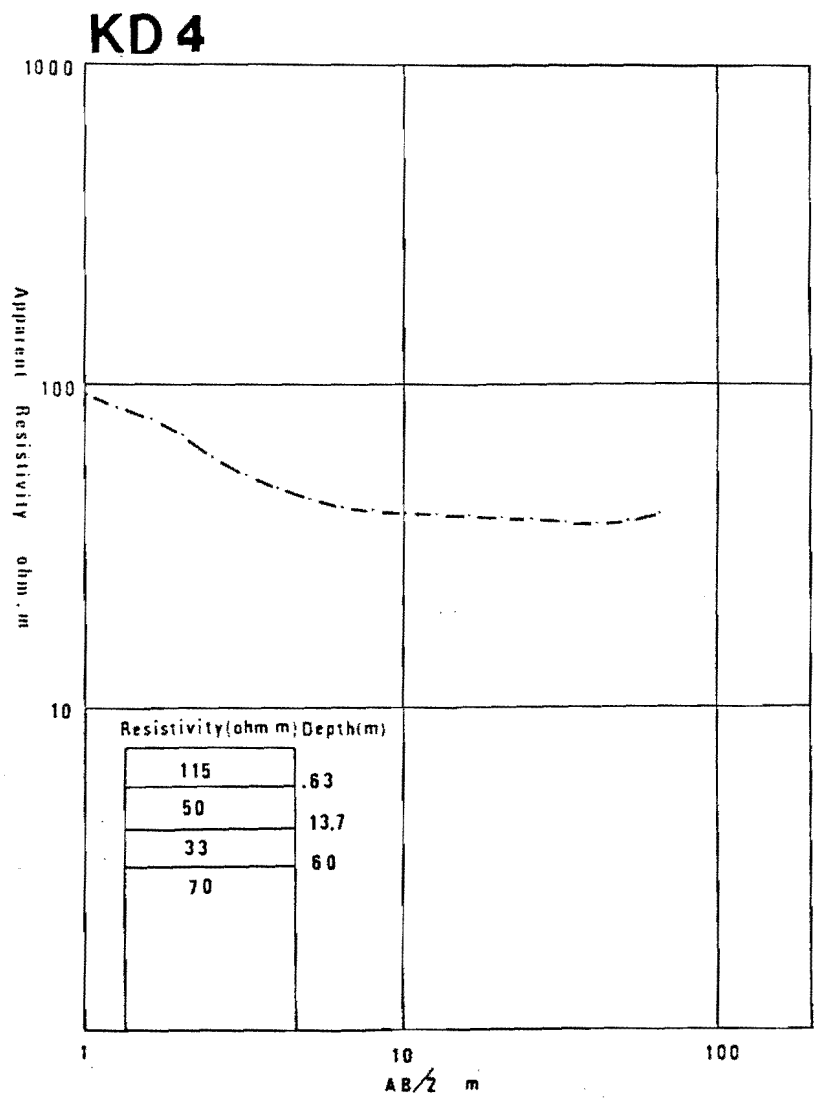

A.6.3 Resistivity Sounding Curves

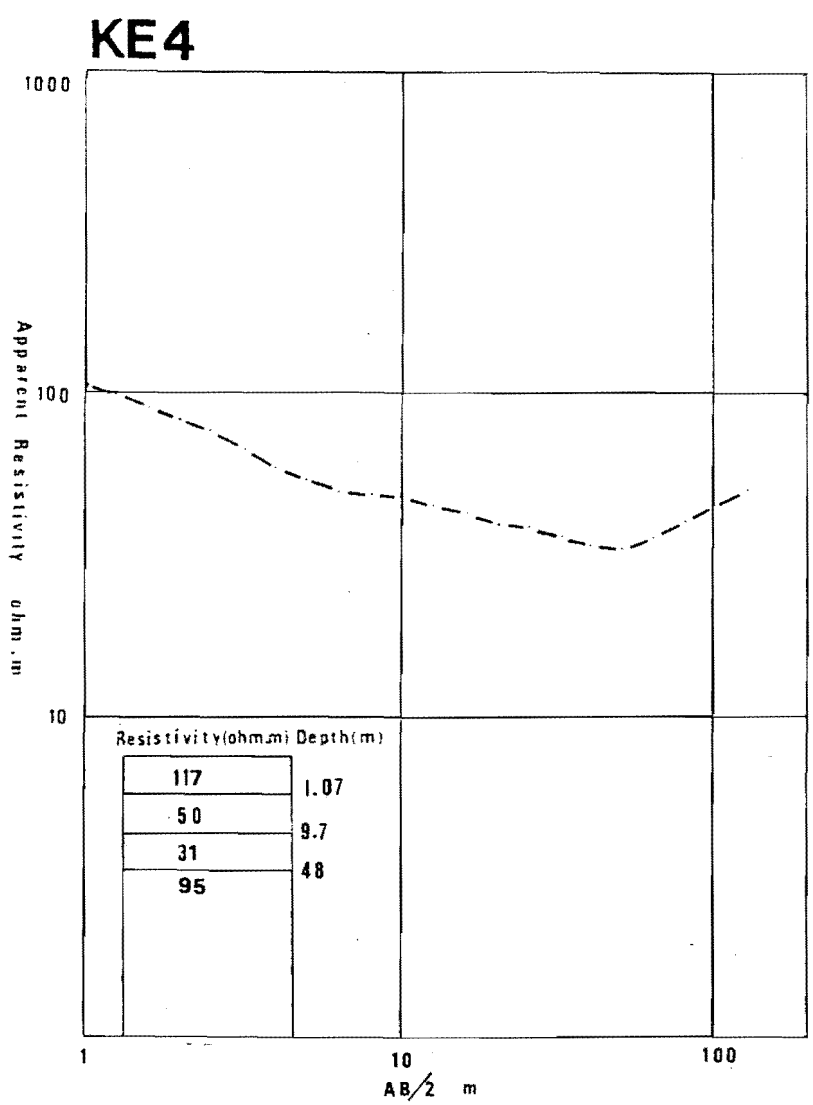

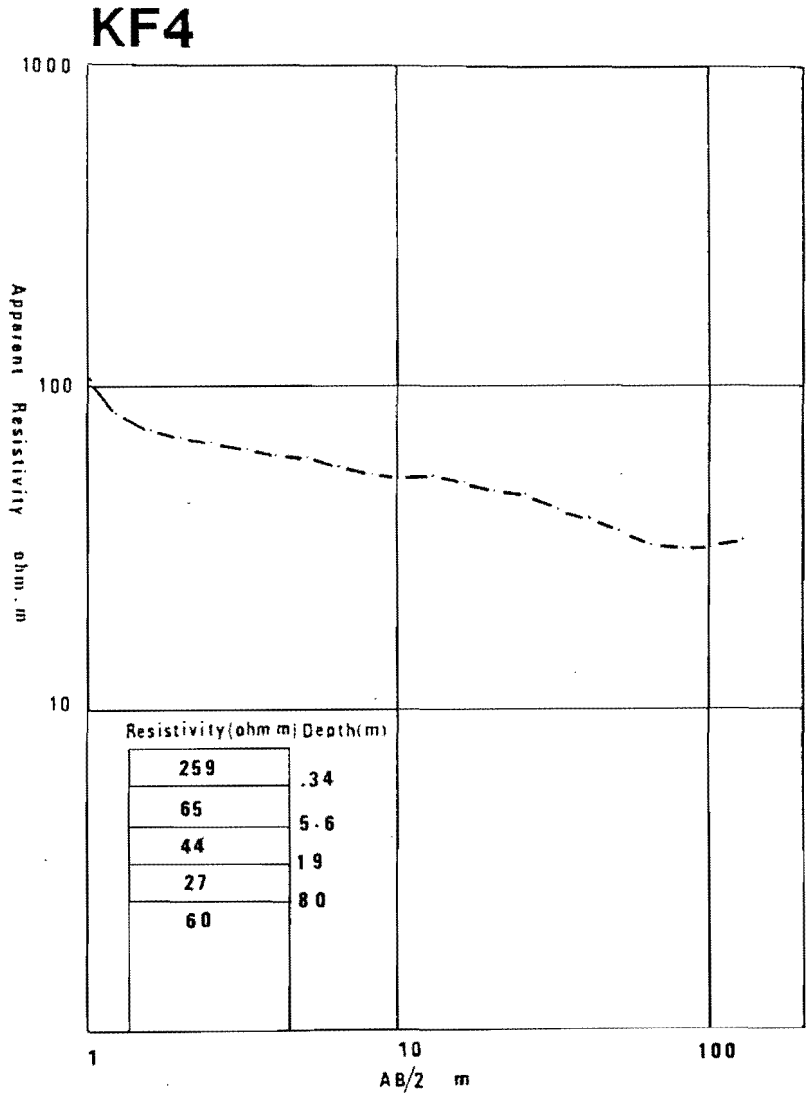

A.6.3 Resistivity Sounding Curves

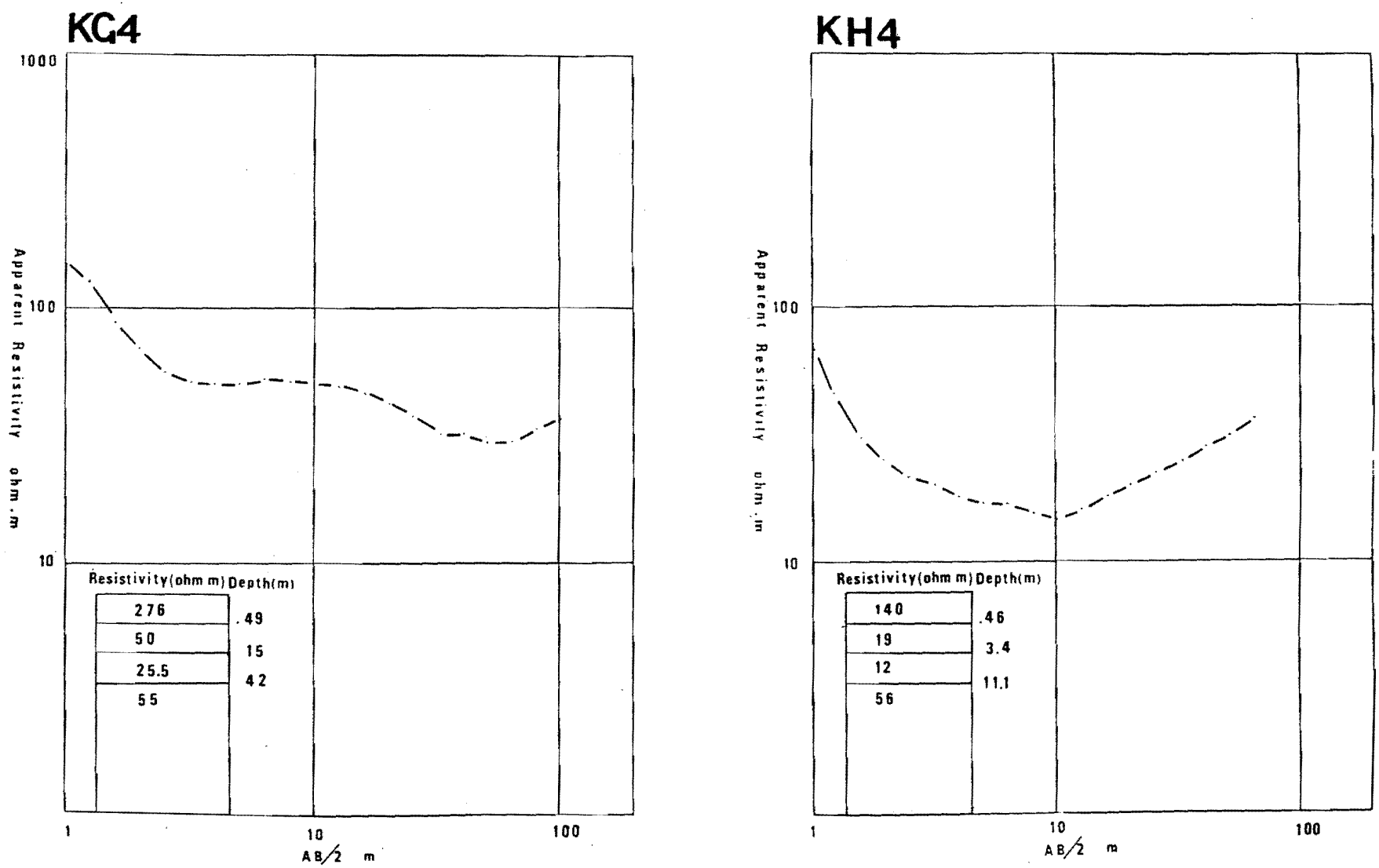

A.6.3 Resistivity Sounding Curves

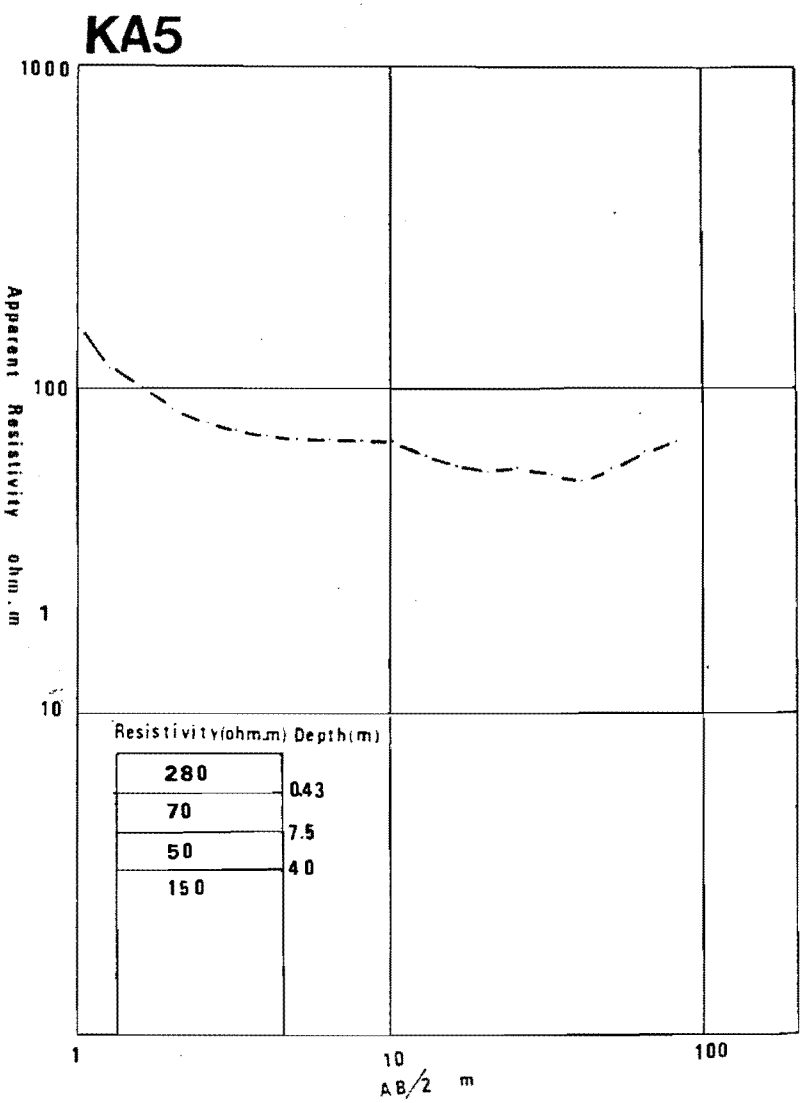

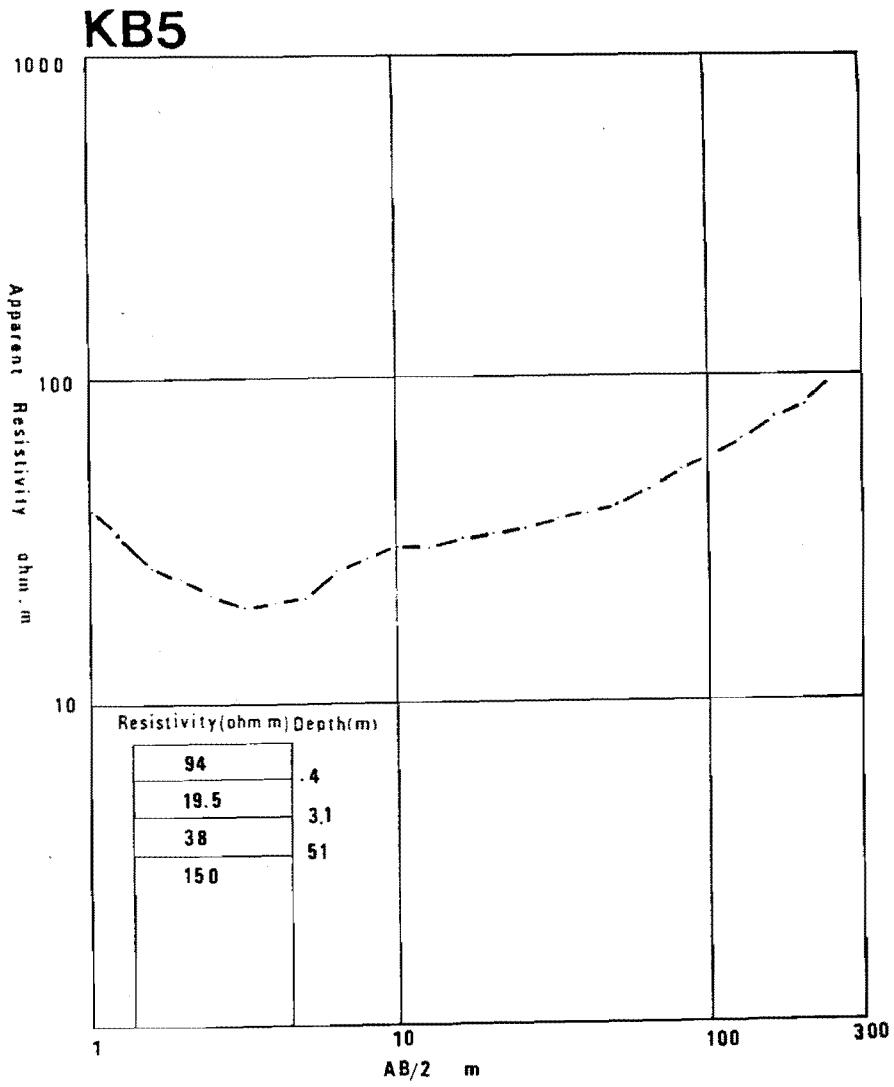

A.6.3 Resistivity Sounding Curves

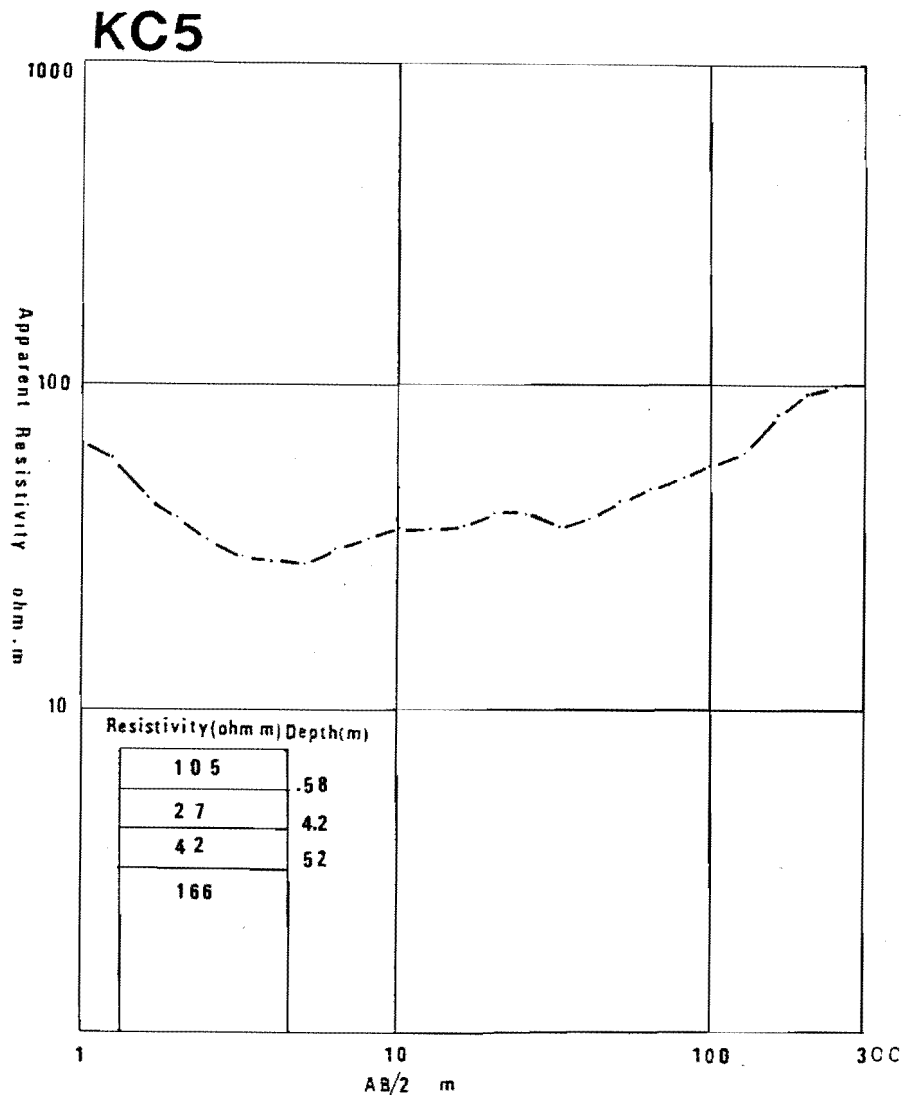

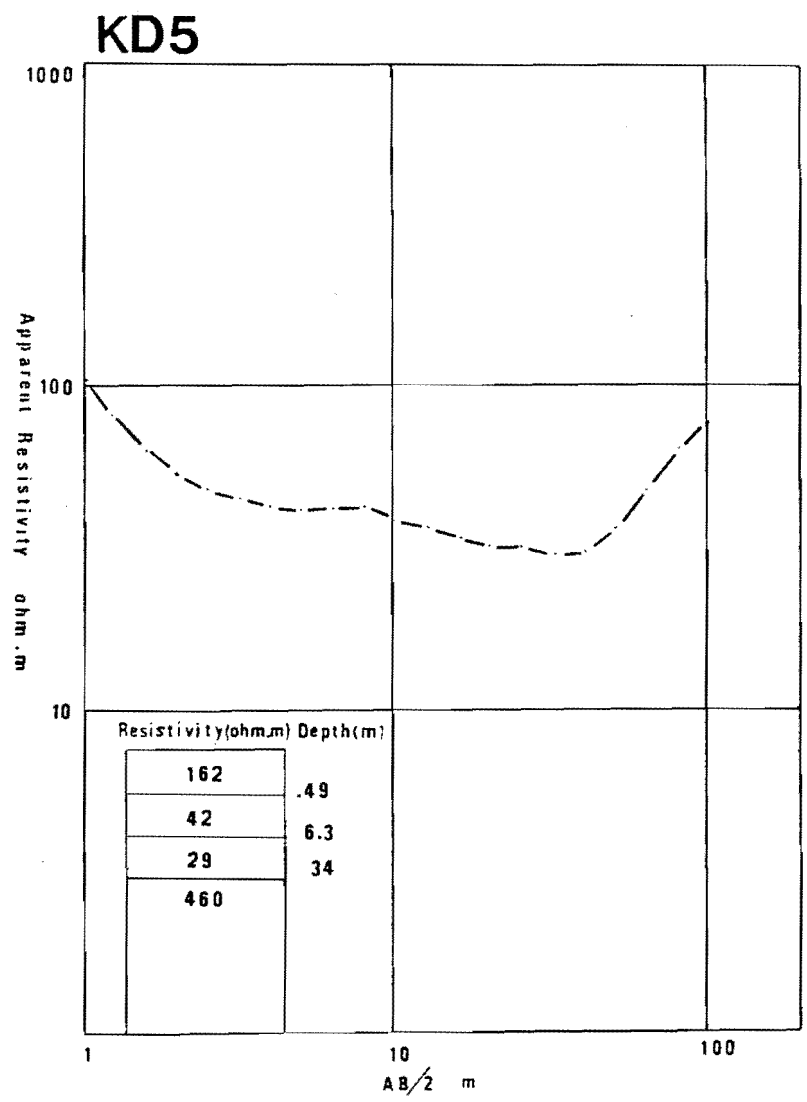

A.6.3 Resistivity Sounding Curves

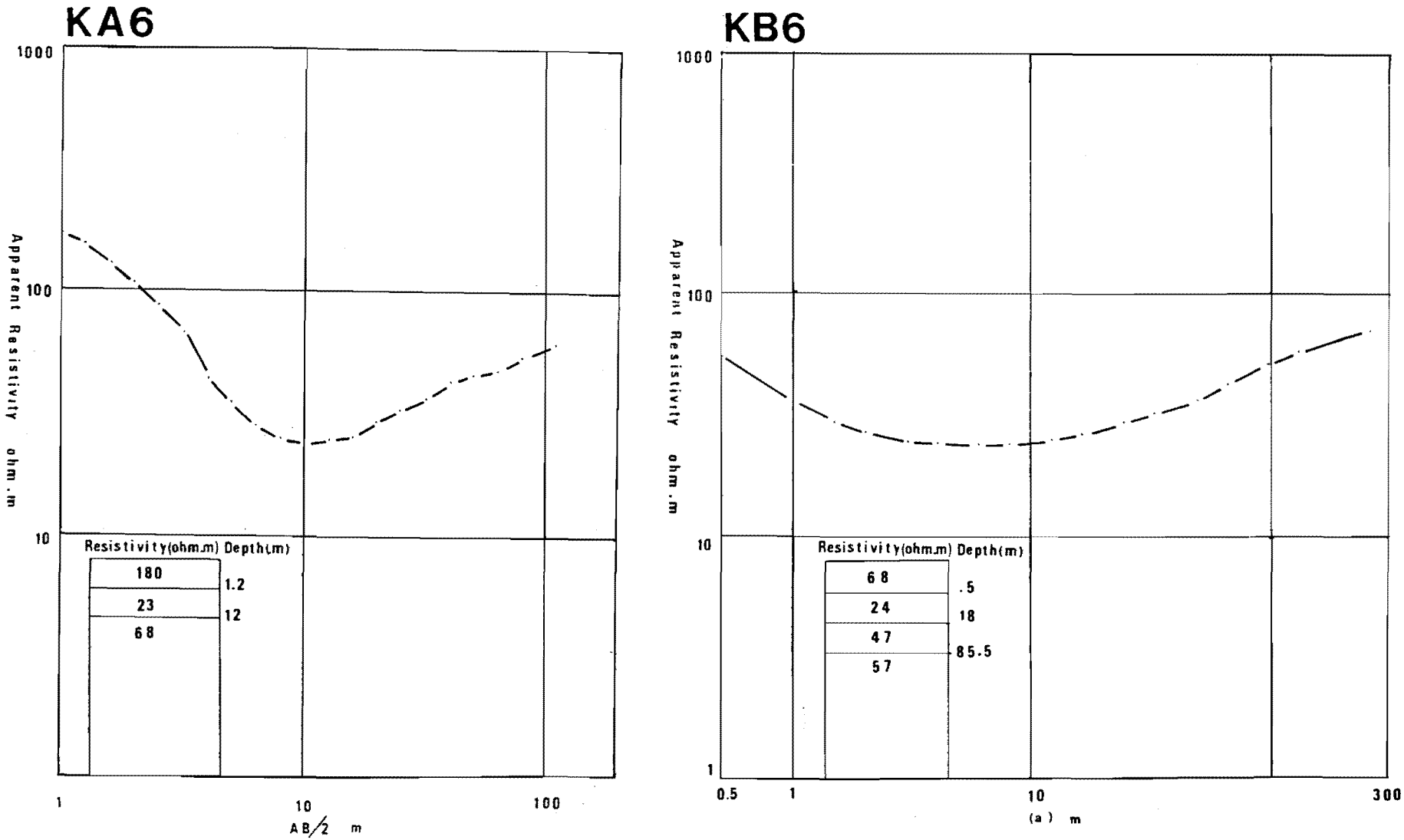

A.6.3 Resistivity Sounding Curves

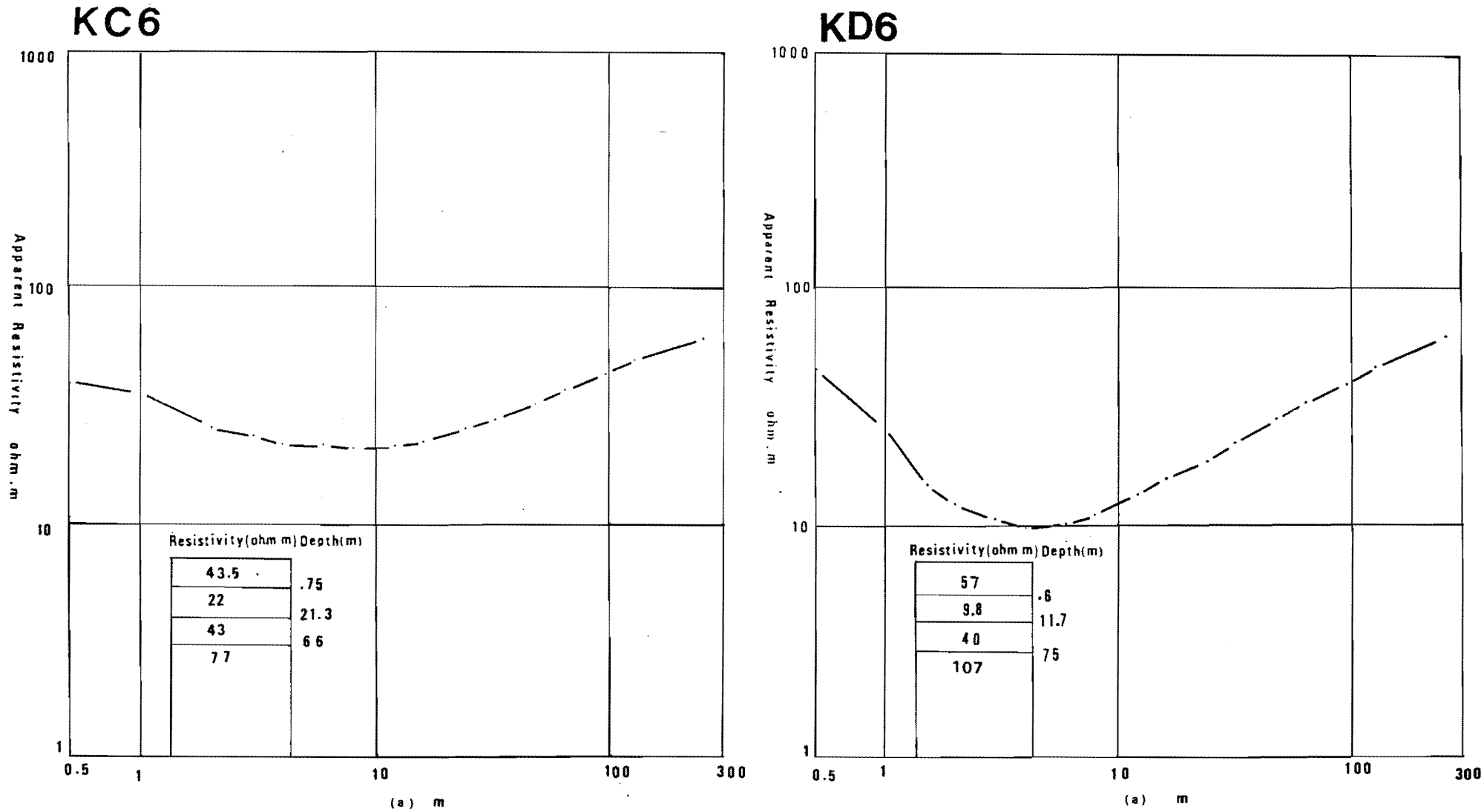

A.6.3 Resistivity Sounding Curves

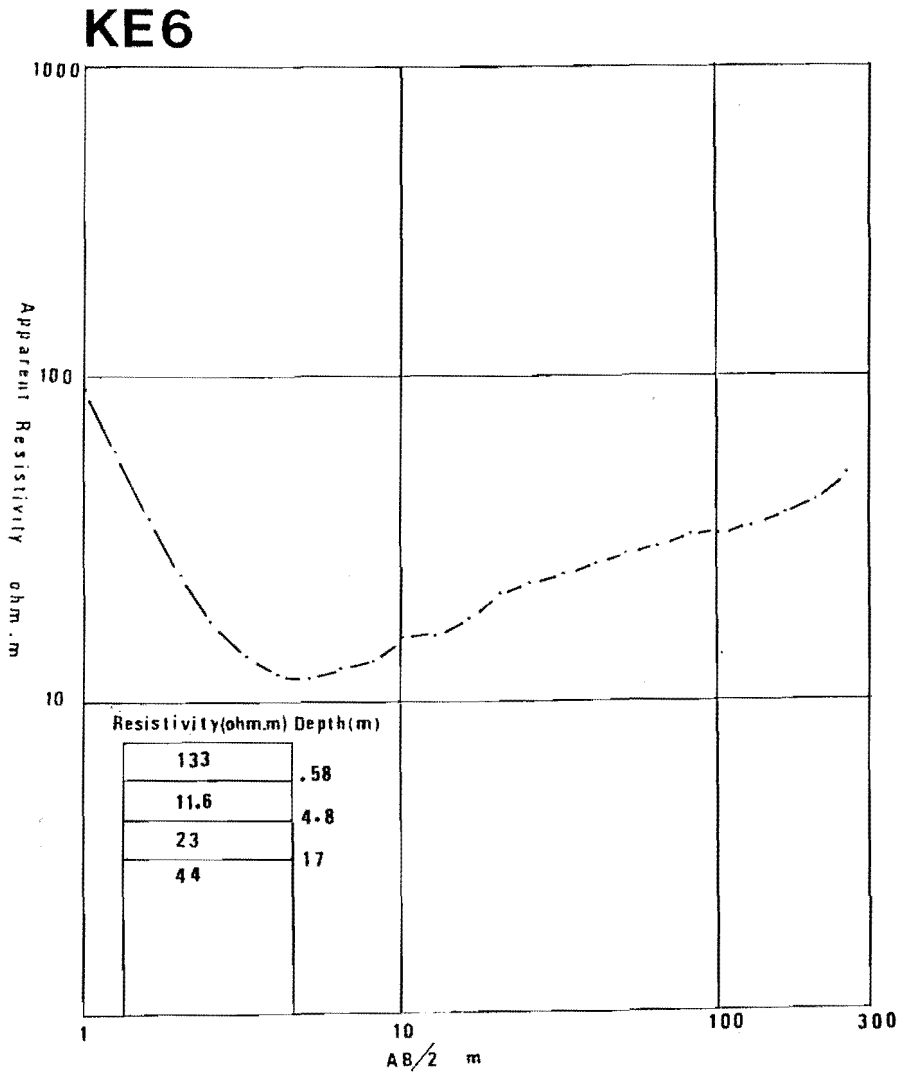

A.6.3 Resistivity Sounding Curve

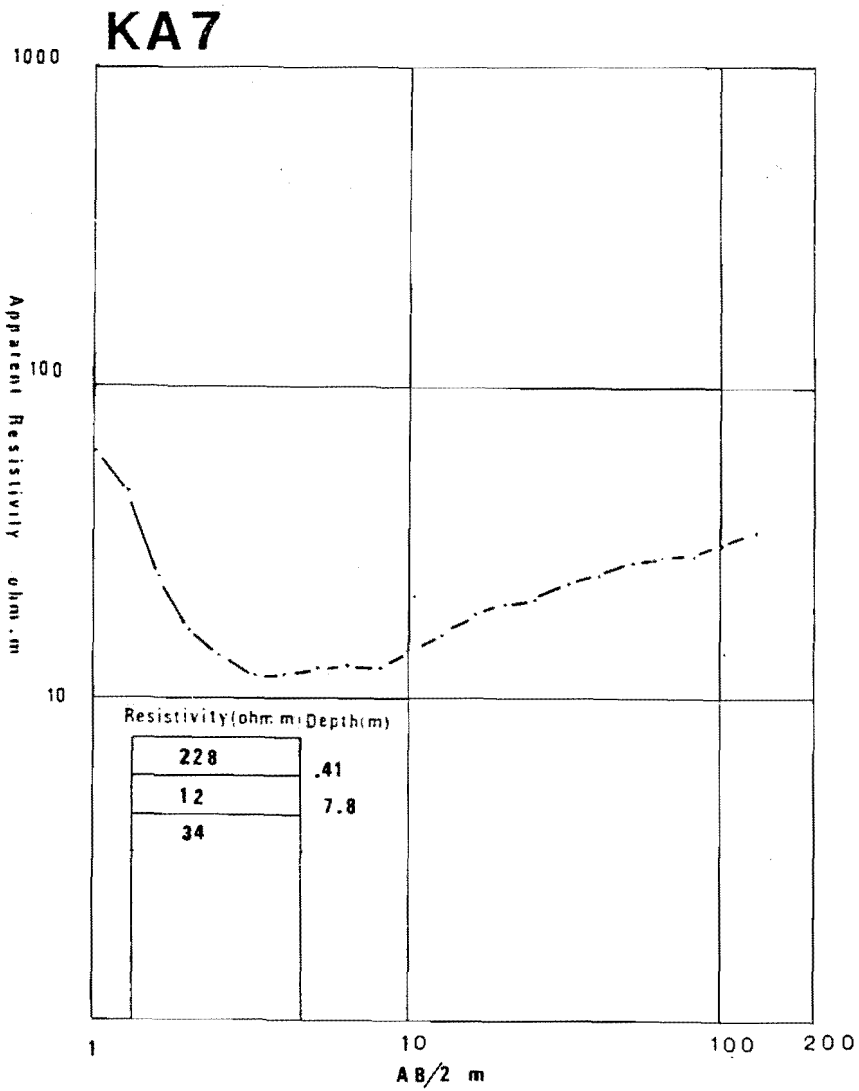

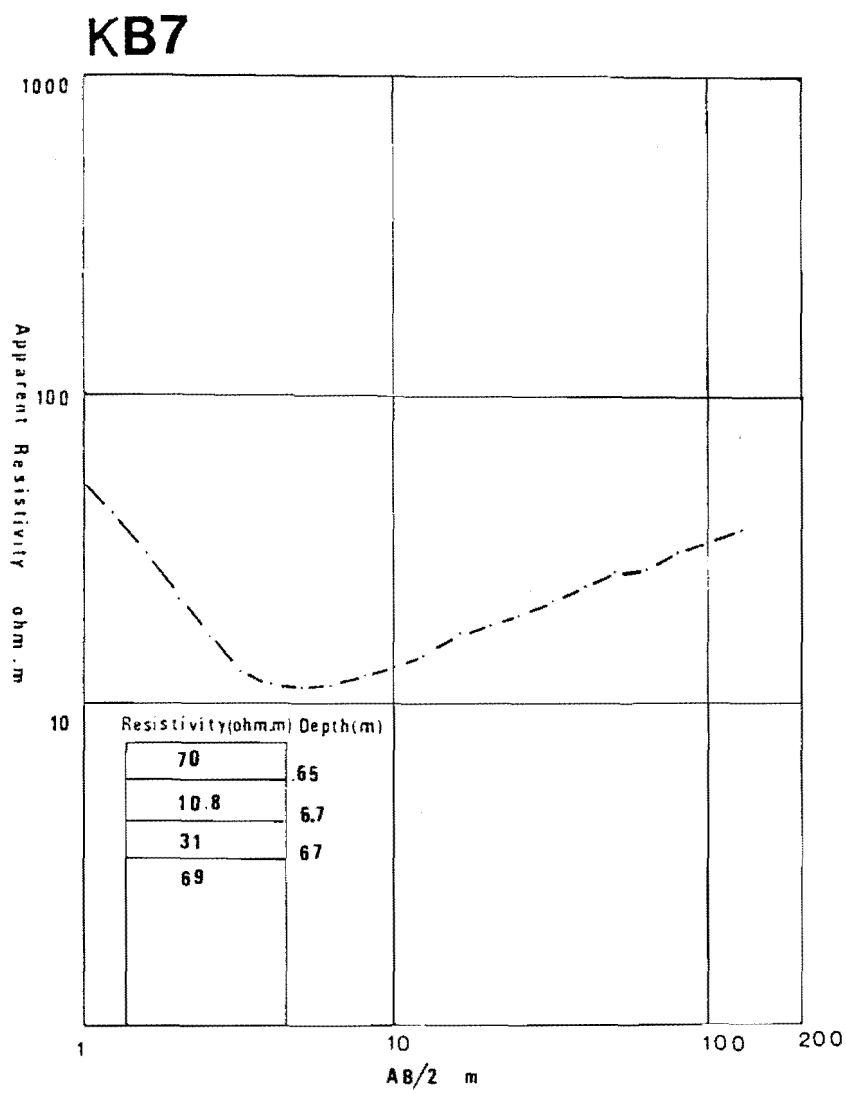

A.6.3 Resistivity Sounding Curves

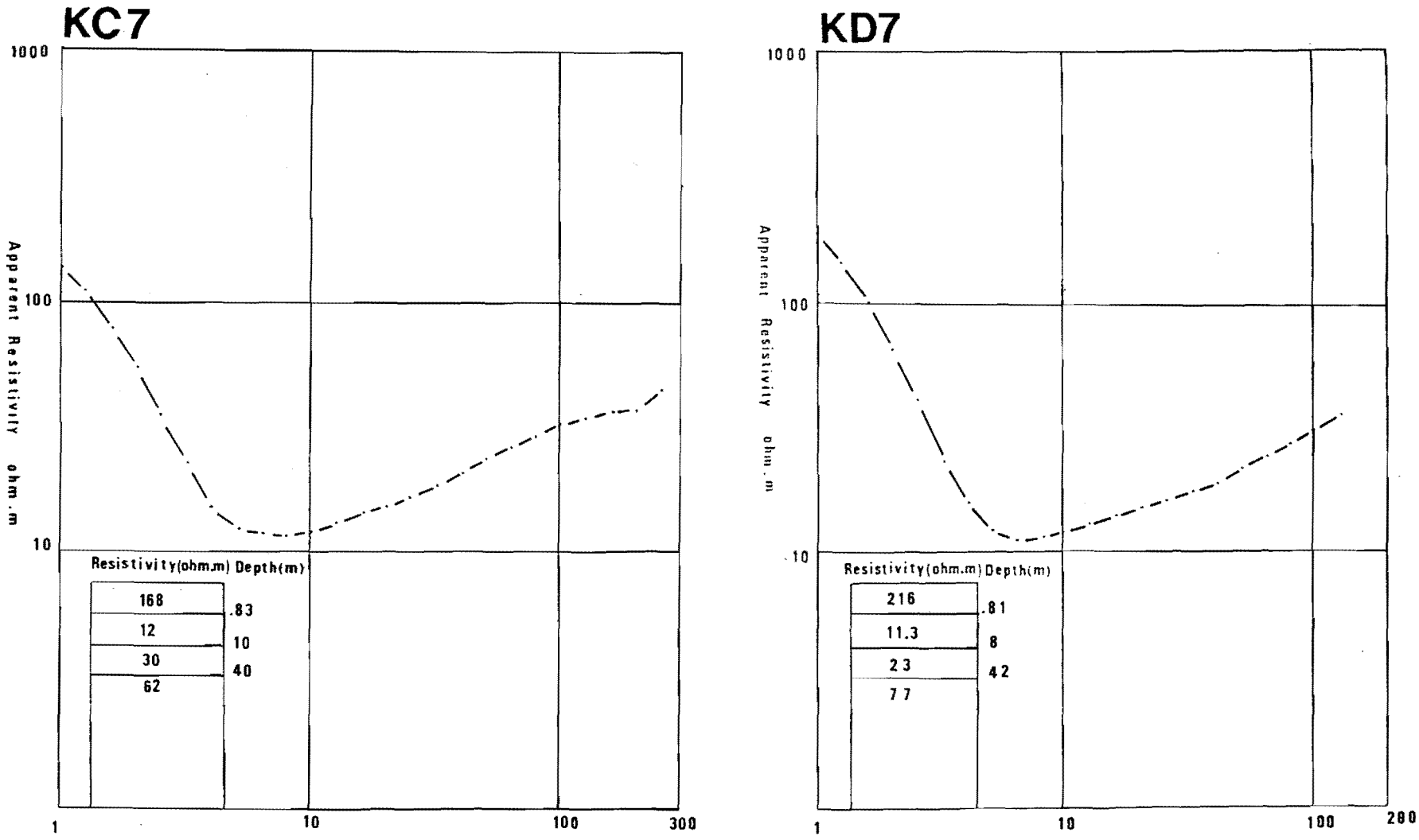

A.6.3 Resistivity Sounding Curves

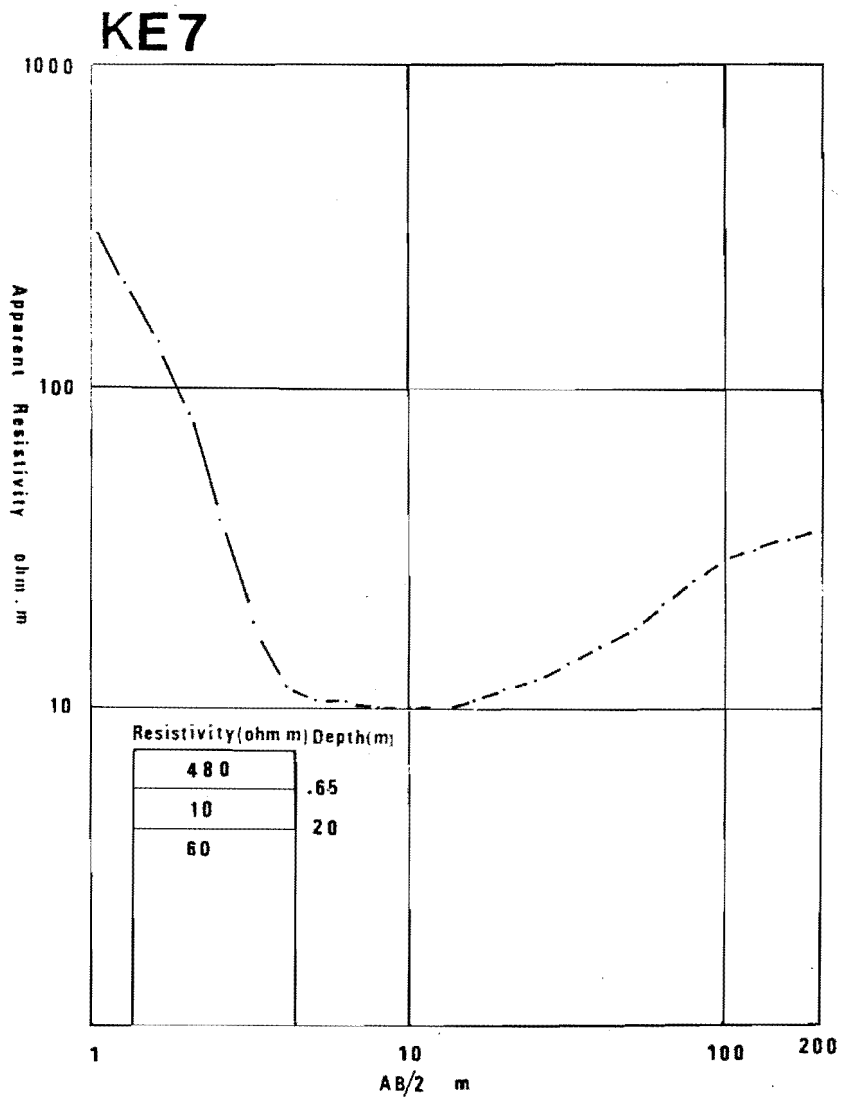

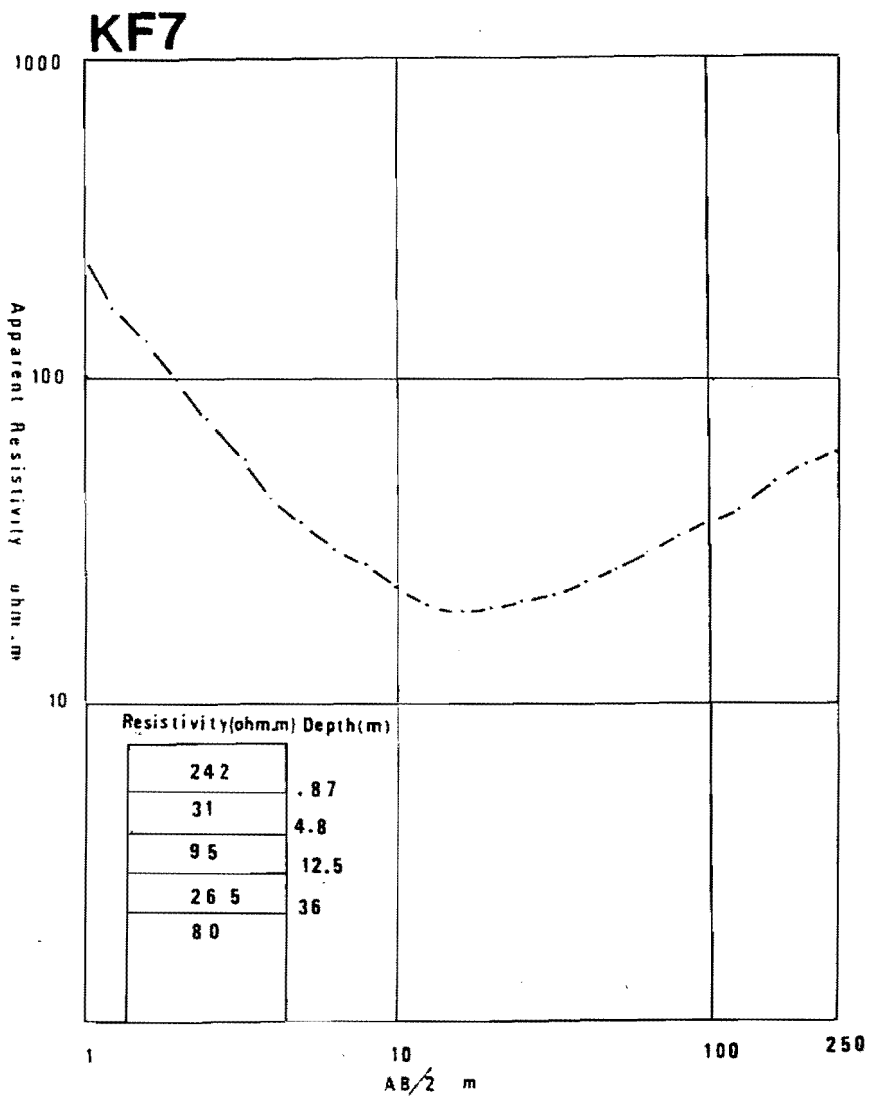

A.6.3 Resistivity Sounding Curves

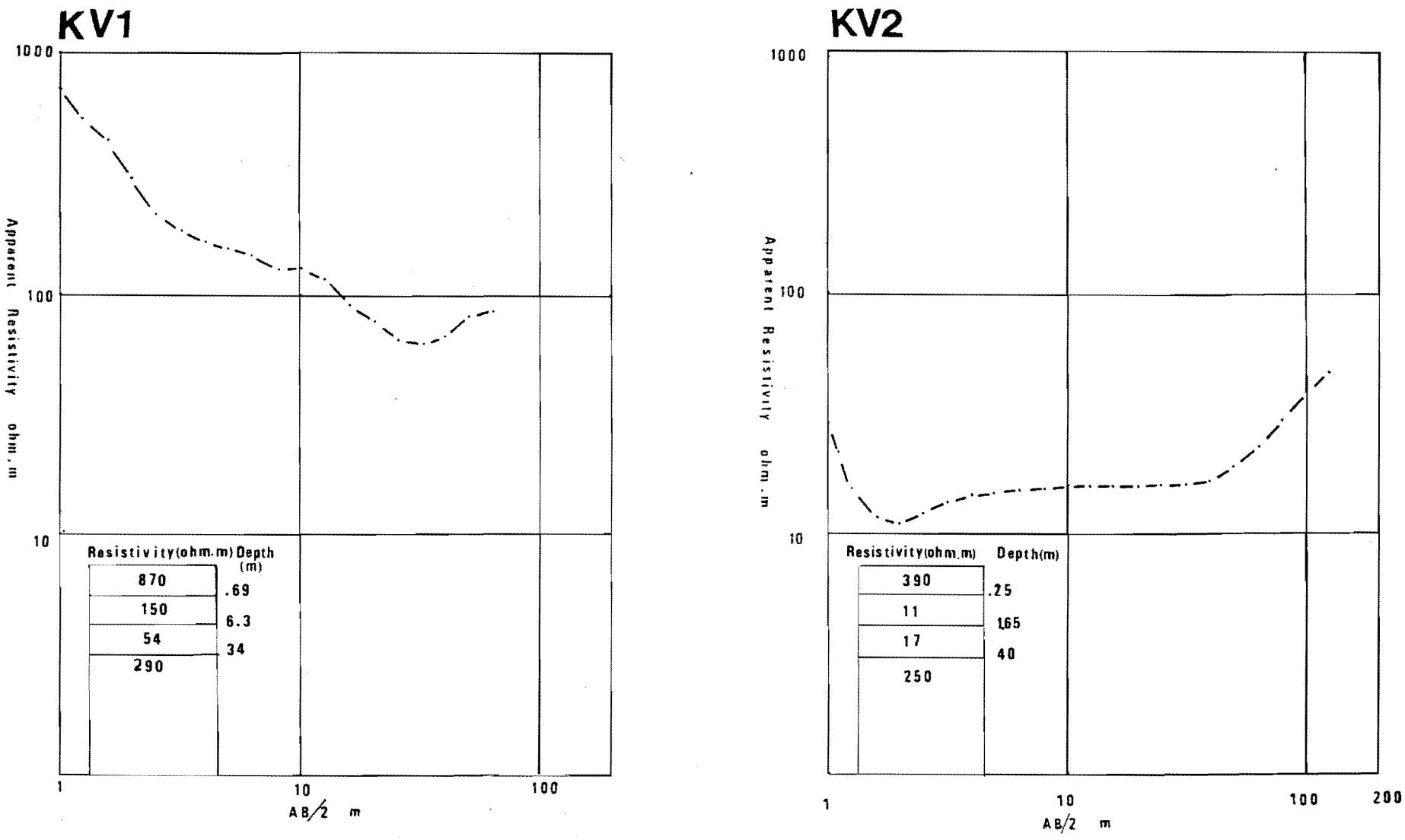

A.6.3 Resistivity Sounding Curves

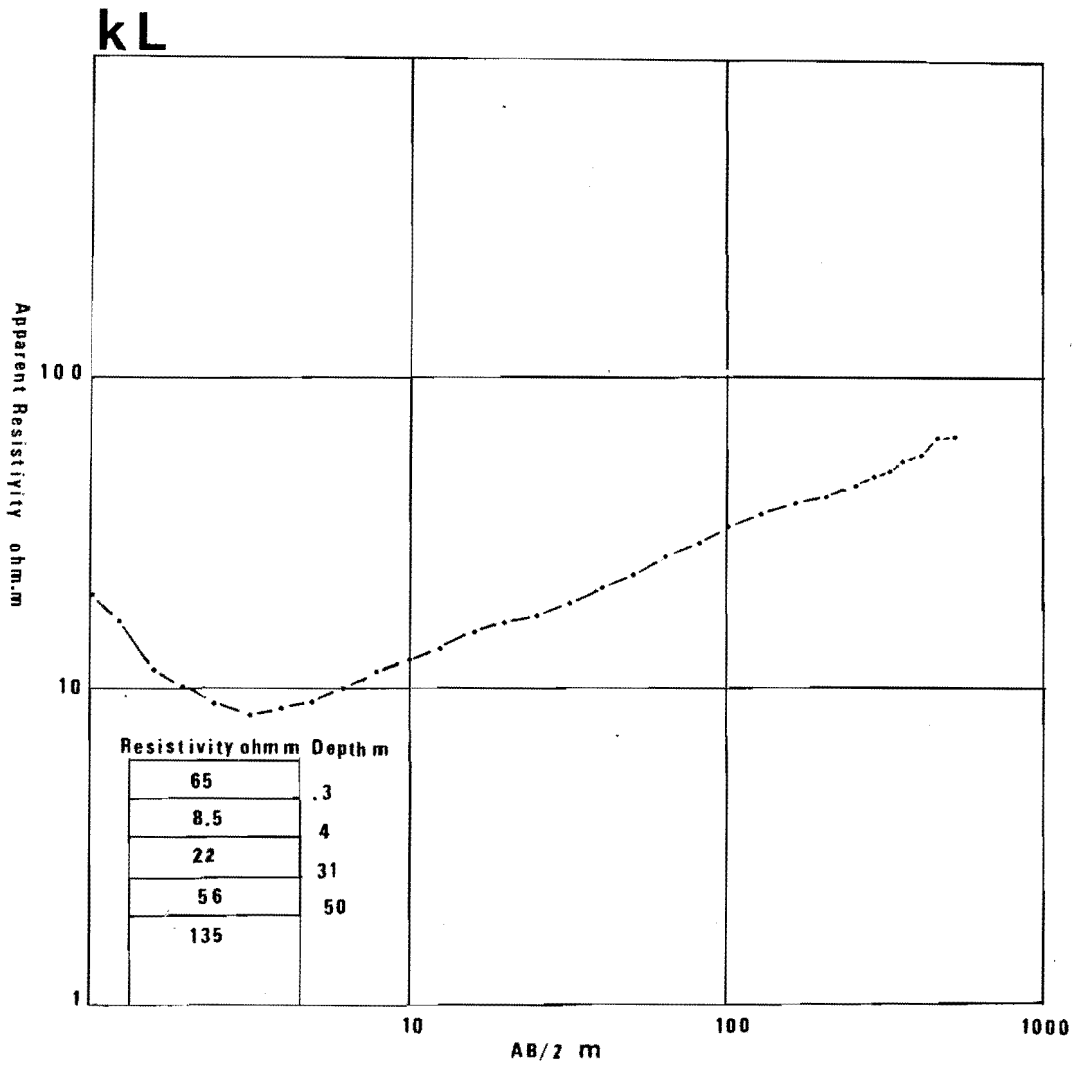

A.6.3 Resistivity Sounding Curve

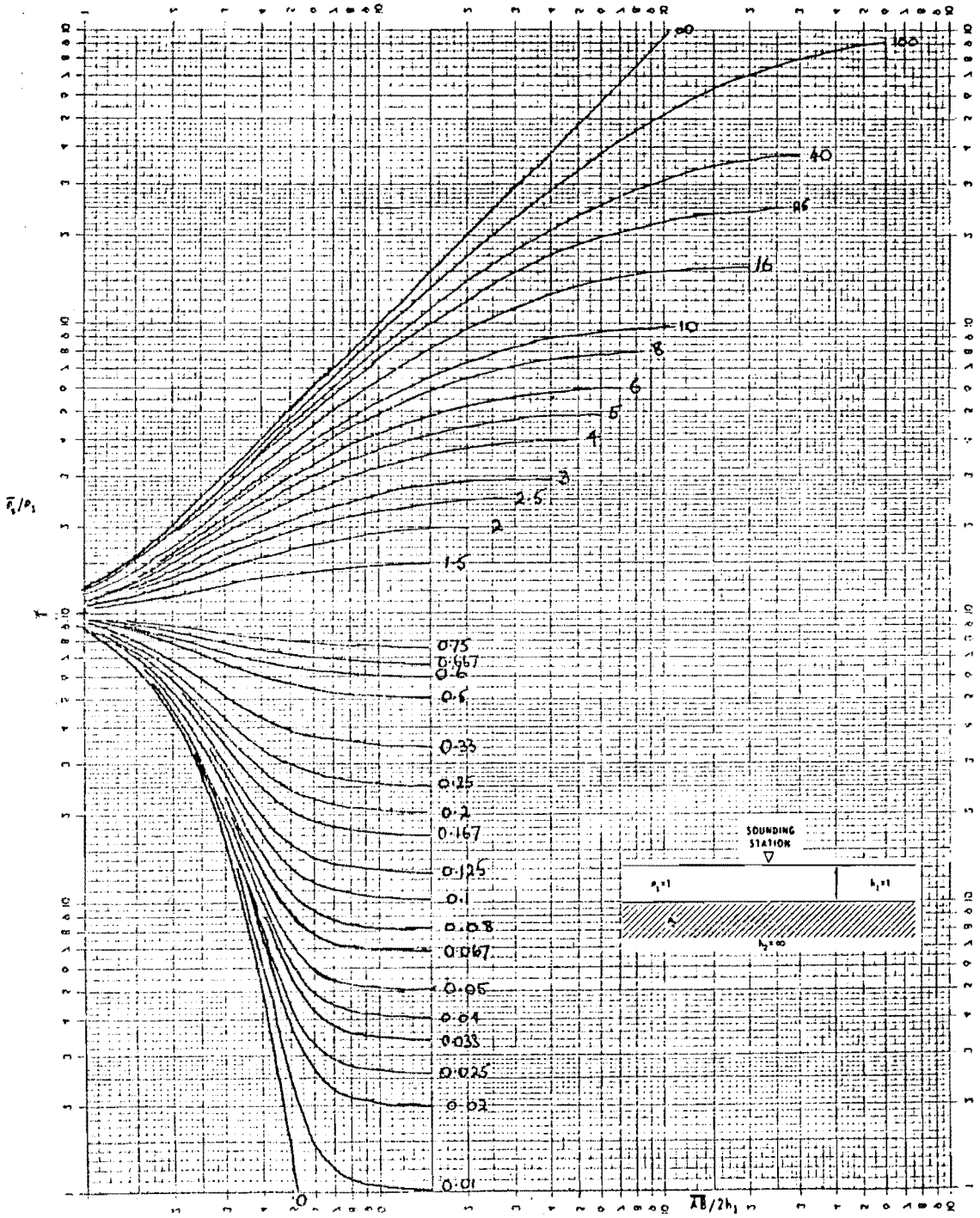

Fig A.6.4 Resistivity Standard Curves (two layer master set for the schlumberger array).($\bar{\rho}_s$ = Schlumberger apparent resistivity)

A.6.5 Curve Matching Techniques

The first method for quantitative interpration is called curve matching. A graph of the field readings is matched against a theoretical graph which has been computed for particular layer resistivities. If a match can be obtained, then the subsurface structure is assumed to be identical with the theoretical structure.

The process can be best carried out using double-logrithmic paper. The reason is that the shape and size of the theoretical curves become independent of the units of measurement for this type of paper, so that any one theoretical curve can be used for interpreting many different sub-surface structures.

A set of theoretical curves is shown figure A.6.4 for a two layer structure.

A two layer structure means that a uniform surface layer of resistivity p_1, overlies a large thickness of material with resisivity p_2. Interpretation is carried out as follows:

STEP 1: Plot the field data (apparent resistivity against electrode separation A or AB/2) on the same size of double logarithmic paper that has been used for the theoretical curves.

A different size of paper or a paper with a different number of logarithmic cycles may be used if the logarithmic cycles are identical in size on the theoretical and field sheets.

STEP 2: Superimpose a sheet with field data onto the sheet with the theoretical curves. It may be convenient to use a window or a light table.

STEP 3: Slide the top sheet over the bottom sheet until the field curve matches one of the theoretical curves. Keep the axes of the graph paper parallel. Often, it will be possible to match only that portion of the field curve corresponding to the smaller electrode separations. This means that the subsurface structure includes more than two layers, and that more complicated theoretical curves will be required. The two layer interpretation will give useful information on the shallower sub-surface materials, however.

STEP 4: On the graph of the field data, read the number along the vertical axis which overlies the horizontal heavy black line on the graph of theoretical data. This equals surface-layer resistivity, p_1.

STEP 5: On the graph of the field data, read the number along the horizontal axis which overlies the vertical heavy black line on the graph of theoretical data. This gives the best estimate as to thickness of the surface layer.

STEP 6: Make a note of which theoretical curve provided the best match. Each curve is identified by a number which specifies the quantity

$$(p_2 - p_1)/(p_2 + p_1)$$

Since p_1 is now known, p_2 may now be computed. This gives the resistivity of the material beneath the surface layer.

A.6.6 TABLES OF MEASURED APPARENT RESISTIVITIES AND ELECTRODE SPACINGS USED FOR THE SCHLUMBERGER SOUNDINGS

Electrode spacing, AB/2, m	Apparent Resistivities, ohm.m — Sounding Numbers					
	KA0	KB0	KC0	KD0	KA1	KB0
MN=0.3m						
1	563.0	228.3	132.8	582.2	383.3	184.3
1.25	502.0	165.4	124.8	552.4	298.0	155.2
1.6	475.0	137.9	114.9	490.9	258.8	119.5
2	463.4	130.2	110.4	484.2	197.9	104.1
2.5	481.0	135.3	104.7	441.0	185.9	99.5
3.2	508.3	143.1	112.4	363.8	155.2	101.6
4	527.0	162.1	123.4	287.8	145.4	104.6
5	523.2	176.1	134.1	261.6	131.5	106.0
6.3	462.1	197.3	141.0	198.9	120.7	108.0
8	369.3	217.8	147.1	155.4	115.6	11.4
10	293.2	232.9	138.7	112.6	104.7	121.7
12.5	212.7	240.5	135.0	86.9	106.3	118.6
MN=3.2m						
10	289.4	205.7	138.5	110.0	104.0	105.8
12.5	211.2	210.7	129.2	79.2	102.1	105.4
16	186.6	223.9	119.3	59.6	91.9	102.0
20	163.4	224.8	105.4	52.5	86.4	970.2
25	135.8	216.6	84.0	48.1	82.2	89.2
32	107.8	200.6	74.0	47.0	50.1	87.1
40	98.0	181.9	66.0	45.9	50.0	78.4
MN=10m						
32	114.6	188.3	75.3	44.7	81.6	89.4
40	99.0	168.2	65.8	44.5	82.8	83.2
50	87.5	149.7	64.2	46.2	81.6	79.3
63	88.3	128.6	65.3	48.2	80.5	77.0
80	83.9	104.1	70.1	55.1		78.1
100	86.2	94.0	73.6	62.7		76.8
125		87.7	75.9	70.5		79.6
MN=32m						
100						73.5
125						74.2
160						71.9
200						71.2
250						70.3

A.6.6 TABLES OF MEASURED APPARENT RESISTIVITIES AND ELECTRODE SPACINGS USED FOR THE SCHLUMBERGER SOUNDINGS

Electrode spacing, AB/2, m	Apparent Resistivities, ohm.m — Sounding Numbers					
	KC1	KD1	KE1	KA2	KB2	KC2
MN=0.3m						
1	93.3	240.3	102.4	158.7	131.8	136.9
1.25	80.4	225.8	94.8	132.0	129.0	130.0
1.6	66.3	215.9	79.6	110.1	108.3	109.0
2	57.3	200.5	76.0	97.9	97.9	102.0
2.5	55.6	182.3	73.8	84.9	90.0	89.7
3.2	54.7	170.9	72.1	81.6	80.4	79.8
4	56.1	176.1	70.3	77.2	76.0	73.9
5	60.3	169.7	70.5	75.6	75.9	74.6
6.3	65.4	166.0	70.8	75.6	76.9	78.9
8	73.7	162.5	76.2	76.5	78.7	82.1
10	81.0	157.0	76.2	79.8	90.2	89.0
12.5	85.3	157.3	73.6	78.7	90.4	88.6
MN=3.2m						
10	131.5	162.6	69.4	75.3	75.3	98.1
12.5	141.5	154.5	68.3	73.9	77.3	98.5
16	143.1	137.2	65.3	69.7	78.4	94.6
20	140.3	128.8	60.5	69.3	78.5	90.0
25	137.5	117.6	56.5	67.2	76.5	84.8
32	130.4	110.9	51.4	67.7	82.7	85.0
40	129.6	102.9	49.2	62.7	78.4	84.3
MN=10m						
32	131.8	113.0	49.0	62.8	73.0	78.3
40	124.7	107.4	46.5	59.1	69.3	76.7
50	116.6	104.8	46.7	53.4	65.5	85.5
63	111.5	110.0	51.9	49.6	60.1	81.8
80	100.1	104.1	59.0	50.1	64.1	94.1
100	95.6	109.5			62.7	97.0
125	90.7	102.9			68.6	98.0

A.6.6 TABLES OF MEASURED APPARENT RESISTIVITIES AND ELECTRODE SPACINGS USED FOR THE SCHLUMBERGER SOUNDINGS

Electrode spacing, AB/2, m	Apparent Resistivities, ohm.m — Sounding Numbers					
	KD2	KE2	KA3	KB3	KC3	KD3
MN=0.3m						
1	61.3	230.3	54.8	115.4	222.4	80.1
1.25	62.9	183.4	46.0	94.5	185.3	76.8
1.6	58.5	132.2	40.5	79.3	149.5	67.8
2	58.6	95.6	38.4	73.5	125.0	61.1
2.5	58.6	75.8	35.9	66.5	101.9	54.3
3.2	58.6	66.7	36.9	61.1	85.9	50.8
4	58.0	64.8	38.2	60.2	75.2	48.9
5	59.6	61.5	38.7	60.7	76.5	48.7
6.3	63.3	59.0	43.6	59.1	75.3	47.8
8	69.3	57.8	45.6	62.2	80.4	48.5
10	70.7	52.4	46.1	62.8	88.3	48.3
12.5	68.8	44.9	47.2	61.8	92.0	46.8
MN=3.2m						
10	76.4	61.9	43.6	58.6	76.4	47.1
12.5	75.6	51.7	44.9	58.8	79.6	45.7
16	72.0	39.9	44.2	59.7	79.7	43.7
20	65.6	37.6	45.8	58.9	78.0	41.4
25	60.7	39.9	50.4	61.0	73.3	38.9
32	56.0	40.1	54.1	60.2	70.8	37.4
40	56.7	43.7	62.7	60.4	64.5	37.0
MN=10m						
32	56.6	38.7	55.2	57.9	67.5	38.2
40	55.4	40.8	61.6	57.4	63.9	37.6
50	55.1	46.8	68.4	56.3	59.9	40.4
63	57.2	50.7	73.1	56.7	58.2	42.8
80	65.1	57.1	76.3	56.1	60.1	47.3
100	72.5	61.1	76.8	61.1	62.6	50.9
125		65.3	79.6	63.9	66.8	54.9

A.6.6 TABLES OF MEASURED APPARENT RESISTIVITIES AND ELECTRODE SPACINGS USED FOR THE SCHLUMBERGER SOUNDINGS

Electrode spacing, AB/2, m	Apparent Resistivities, ohm.m — Sounding Numbers					
	KE3	KA4	KB4	KC4	KD4	KE4
MN=0.3m						
1	212.4	156.1	174.0	87.8	92.3	1520.0
1.25	185.3	125.0	149.2	80.5	83.6	119.9
1.6	147.8	103.6	122.2	73.6	76.3	111.5
2	125.6	94.8	103.1	65.3	67.1	101.6
2.5	79.9	89.0	92.8	57.2	59.8	93.7
3.2	64.8	85.6	78.9	50.0	52.5	81.6
4	51.9	83.7	68.6	45.5	49.9	72.6
5	51.0	81.1	62.1	42.2	49.0	65.4
6.3	44.1	80.0	58.1	39.8	48.9	61.1
8	37.7	77.1	59.5	39.0	49.0	59.6
10	33.0	81.1	58.8	38.5	49.2	57.7
12.5	28.5	81.8	57.7	38.1	48.3	54.8
MN=3.2m						
10	34.3	79.5	56.2	39.1	49.1	53.9
12.5	29.0	83.4	54.8	39.2	48.6	51.3
16	24.4	90.0	54.7	38.9	47.1	48.3
20	21.8	101.4	53.7	37.9	45.5	44.0
25	21.9	107.3	83.7	37.6	43.7	44.3
32	23.1	113.3	52.0	36.6	42.1	40.6
40	27.2	116.1	51.8	35.9	39.7	38.4
MN=10m						
32	22.0	114.6	52.7	38.1	42.1	37.7
40	25.1	118.8	52.5	38.0	40.7	35.1
50	28.8	113.5	54.4	38.8	40.0	34.2
63	33.4	111.5	59.5	41.4	40.4	37.2
80	39.4	108.2	66.1		41.1	42.0
100	46.8		72.1		43.5	47.0
125	55.1				46.2	53.7

A.6.6 TABLES OF MEASURED APPARENT RESISTIVITIES AND ELECTRODE SPACINGS USED FOR THE SCHLUMBERGER SOUNDINGS

Electrode spacing, AB/2, m	Apparent Resistivities, ohm.m — Sounding Numbers					
	KF4	KG4	KH4	KA5	KB5	KC5
MN=0.3m						
1	110.0	153.5	82.5	148.4	62.7	76.8
1.25	85.7	129.0	54.8	112.9	51.8	69.3
1.6	74.8	90.4	36.5	98.1	40.2	51.2
2	71.3	71.9	29.7	83.3	37.3	44.8
2.5	68.9	57.5	25.4	80.3	33.4	37.8
3.2	65.4	53.4	23.5	73.6	30.0	33.7
4	62.9	51.9	20.9	70.3	31.5	32.2
5	61.5	52.3	19.8	68.7	32.4	31.6
6.3	57.6	54.0	19.7	69.3	39.5	35.3
8	54.4	53.6	18.1	67.0	43.6	37.7
10	53.1	50.3	17.2	66.7	46.9	41.9
12.5	54.0	51.1	18.8	61.4	46.6	40.5
MN=3.2m						
10	58.8	58.0	14.6	73.5	32.4	38.7
12.5	58.1	55.9	16.0	67.1	31.7	37.7
16	56.0	53.5	18.0	62.3	34.3	39.2
20	52.6	48.8	20.0	59.5	35.1	42.9
25	51.3	47.0	22.3	61.9	36.1	42.7
32	46.1	38.6	25.1	58.0	39.1	38.2
40	42.3	36.1	28.6	56.9	40.7	42.0
MN=10m						
32	43.9	30.6	25.3	54.9	37.4	37.7
40	40.9	34.1	29.2	53.2	38.6	38.6
50	37.0	30.3	32.0	57.5	40.4	44.7
63	34.1	30.0	37.5	65.5	44.6	48.6
80	33.0	34.0		70.1	51.9	53.1
100	33.3	37.6			58.8	59.5
125	35.3	35.5			64.0	64.5
MN=32m						
100					52.9	54.4
125					60.4	59.1
160					69.7	78.4
200					76.1	90.7
250					97.5	97.8

A.6.6 TABLES OF MEASURED APPARENT RESISTIVITIES AND ELECTRODE SPACINGS USED FOR THE SCHLUMBERGER SOUNDINGS

Electrode spacing, AB/2, m	Apparent Resistivities, ohm.m — Sounding Numbers					
	KD5	KA6	KE6	KA7	KB7	KC7
MN=0.3m						
1	97.2	179.1	94.4	78.1	51.1	142.2
1.25	76.4	164.5	58.9	58.1	41.9	113.4
1.6	58.5	152.8	37.3	30.9	30.9	78.9
2	49.8	114.5	25.0	20.8	21.8	57.4
2.5	44.4	91.3	17.9	17.6	17.0	36.7
3.2	41.6	70.2	13.9	15.0	12.8	23.4
4	39.3	46.9	12.1	14.9	11.7	15.9
5	38.5	37.6	11.8	16.0	11.5	13.1
6.3	39.5	30.4	12.8	16.1	11.7	12.5
8	39.4	27.1	13.4	15.9	12.7	12.3
10	35.3	25.7	16.8	17.9	13.6	12.7
12.5	34.0	26.6	15.2	20.5	14.7	13.5
MN=3.2m						
10	30.6	24.3	15.0	17.5	12.9	12.5
12.5	30.1	24.1	16.9	19.2	14.3	13.6
16	27.3	25.2	18.0	22.3	16.5	14.8
20	25.9	29.2	21.7	24.4	17.6	15.9
25	26.0	32.4	25.7	25.1	19.0	17.2
32	25.1	36.6	25.1	28.6	21.1	19.4
40	25.1	43.2	27.1	30.7	23.5	21.6
MN=10m						
32	30.1	37.7	25.1	24.3	21.9	19.5
40	32.3	44.5	26.6	24.7	24.1	21.9
50	37.2	47.0	29.2	27.2	27.2	24.7
63	48.9	49.6	31.0	28.5	27.4	28.0
80	76.5	55.9	33.0	28.5	31.0	31.0
100	77.9	62.7	33.7	31.3	33.1	34.5
125			35.5	34.3	36.9	36.1
MN=32m						
100			34.0		34.3	33.5
125			65.5		36.6	35.6
160			38.3		39.8	38.2
200			42.8		44.9	37.1
250			51.2		52.3	45.8

A.6.6 TABLES OF MEASURED APPARENT RESISTIVITIES AND ELECTRODE SPACINGS USED FOR THE SCHLUMBERGER SOUNDINGS

Electrode spacing, AB/2, m	Apparent Resistivities, ohm.m — Sounding Numbers					
	KD7	KE7	KF7	KL	KV1	KV2
MN=0.3m						
1	149.0	209.9	209.8	20.8	622.2	27.1
1.25	115.0	138.1	153.8	16.8	470.4	14.0
1.6	80.0	87.4	122.9	11.6	392.0	10.4
2	52.1	51.6	93.7	10.3	265.5	10.0
2.5	32.8	24.4	70.1	9.0	205.9	10.9
3.2	18.9	11.7	53.5	8.2	163.2	12.3
4	12.9	7.4	41.0	8.7	145.4	13.0
5	10.0	6.8	33.0	9.2	139.0	15.2
6.3	9.4	6.6	28.0	10.1	129.7	13.7
8	9.5	6.5	25.1	11.3	128.1	13.8
10	10.0	6.3	20.9	12.6	112.6	14.7
12.5	10.6	6.3	18.8	13.5	102.3	14.3
MN=3.2m						
10	12.1	8.5	22.8	12.5	140.3	15.7
12.5	13.1	9.2	20.0	13.7	124.5	15.1
16	14.0	9.4	19.3	15.9	101.4	15.2
20	14.9	10.2	19.8	16.9	87.8	15.2
25	16.1	10.8	20.6	17.8	74.9	15.3
32	17.7	12.2	21.8	19.2	70.2	15.3
40	19.0	13.8	23.5	21.8	76.5	15.7
MN=10m						
32	17.9	14.0	21.5	19.1	64.3	16.2
40	19.9	15.7	23.5	21.3	66.4	16.7
50	22.8	17.7	25.7	23.7	81.6	19.4
63	25.2	21.5	28.7	27.4	86.7	23.2
80	28.5	25.8	32.2	30.4	76.1	30.0
100	32.1	29.8	35.9	34.3		39.2
125	36.8	31.9	40.2	37.6		48.4
MN=32m						
100		30.9	32.5	33.3		
125		34.0	34.7	36.7		
160		36.3	43.5	39.3		
200		38.5	47.8	41.2		
250			52.3	44.7		
MN=64m						
200				42.4		
250				45.9		
282				51.8		
320				54.4		
360				57.6		
400				60.5		
450				69.2		
500				69.4		

A.6.6

TABLES OF MEASURED APPARENT RESISTIVITIES AND ELECTRODE SPACINGS USED FOR THE WENNER SOUNDINGS

Electrode spacing, (a), m	Apparent Resistivities, ohm.m Sounding Numbers		
	KB6	KC6	KD6
0.5	55.9	38.9	45.4
1	35.9	35.6	25.2
1.5	29.7	26.7	14.7
2	27.2	25.7	12.3
3	24.4	23.8	10.4
4	24.5	21.8	9.7
6	24.0	21.6	10.0
8	24.5	21.4	11.0
12	25.3	21.6	13.2
16	26.6	22.6	15.3
24	29.9	25.5	18.4
32	32.3	27.9	22.1
48	36.5	32.6	28.4
64	42.7	37.4	33.2
96	51.8	43.1	39.4
128	58.1	50.3	47.5
256	71.1	50.3	64.0

A.6.7 Computer Resistivity Model

SCHLUMBERGER INTERPRETATION: 6PT/DECADE

● KA0

RMS P/C CUTOFF : 0.10
NUMBER OF LAYERS = 4

INITIAL MODEL... * : FIXED PARAMETER

	«ohm.m»	DEPTH «m»	T=THICK*RES	S=THICK/RES
		0.00		
THICK = 0.20	RES = 900.00		252.00	0.000
		0.20		
THICK = 2.22	RES = 460.00		1021.20	0.005
		2.50		
THICK = 2.50	RES = 920.00		2300.00	0.003
		5.00		
RES = 95.00				

INTERPRETED MODEL... * : FIXED PARAMETER

		DEPTH	T=THICK*RES	S=THICK/RES
		0.00		
THICK = 0.34	RES = 1013.91		345.00	0.000
		0.34		
THICK = 0.40	RES = 329.57		133.45	0.001
		0.75		
THICK = 4.49	RES = 568.03		2528.47	0.008
		5.24		
RES = 92.39				

I	L	RA-FIELD	RA-MODEL	P/C ERROR
1	1.000	577.540	570.896	-1.150
2	1.250	515.350	519.146	0.737
3	1.600	487.270	496.863	1.969
4	2.000	475.360	494.915	4.114
5	2.500	493.330	499.960	1.334
6	3.200	521.390	504.977	-3.148
7	4.000	540.660	501.330	-7.274
8	5.000	536.730	485.663	-9.514
9	6.300	474.080	452.965	-4.454
10	8.000	378.880	398.676	5.225
11	10.000	300.270	334.446	11.382
12	12.500	218.510	262.495	20.131
13	16.000	193.350	123.788	-0.226
14	20.000	169.290	147.430	-12.754
15	25.000	138.650	120.403	-13.157
16	32.000	113.120	104.573	-7.556
17	40.000	100.250	98.589	-1.667
18	50.000	87.470	96.025	9.791
19	63.000	88.230	94.592	7.150
20	80.000	83.860	93.963	12.047
21	100.000	86.170	93.340	8.321

RMS P/C ERROR = 7.63

SCHLUMBERGER INTERPRETATION: 6PT/DECADE

● KB0

RMS P/C CUTOFF : 0.10
NUMBER OF LAYERS = 4

INITIAL MODEL... * : FIXED PARAMETER

		DEPTH	T=THICK*RES	S=THICK/RES
		0.00		
THICK = 0.30	RES = 740.00		222.00	0.000
		0.30		
THICK = 1.80	RES = 96.00		172.80	0.017
		2.10		
THICK = 19.40	RES = 255.00		4947.00	0.076
		21.50		
RES = 82.00				

INTERPRETED MODEL... * : FIXED PARAMETER

		DEPTH	T=THICK*RES	S=THICK/RES
		0.00		
THICK = 0.31	RES = 667.21		209.12	0.000
		0.31		
THICK = 1.59	RES = 83.85		133.50	0.019
		1.91		
THICK = 17.42	RES = 252.13		4392.05	0.069
		19.33		
RES = 78.14				

I	L	RA-FIELD	RA-MODEL	P/C ERROR
1	1.000	137.060	136.976	-0.045
2	1.250	135.470	136.512	0.769
3	1.600	112.970	112.821	-0.132
4	2.000	106.670	106.433	-0.222
5	2.500	110.930	109.034	-1.709
6	3.200	117.200	119.024	1.487
7	4.000	132.630	131.252	-1.038
8	5.000	144.700	145.613	0.631
9	6.300	161.700	161.063	-0.394
10	8.000	178.450	176.542	-1.069
11	10.000	191.270	189.436	-0.958
12	12.500	196.700	199.874	1.614
13	16.000	208.070	207.094	-0.469
14	20.000	209.510	208.390	-0.540
15	25.000	201.850	203.246	0.692
16	32.000	187.590	189.682	1.115
17	40.000	169.870	170.483	0.355
18	50.000	149.680	148.305	-0.919
19	63.000	128.050	125.556	-2.321
20	80.000	104.140	106.879	2.630
21	100.000	94.010	94.446	0.464
22	125.000	87.670	86.726	-1.077

RMS P/C ERROR = 0.71

SCHLUMBERGER INTERPRETATION: 6PT/DECADE

● KCO

RMS P/C CUTOFF : 0.10
NUMBER OF LAYERS = 5

INITIAL MODEL... * : FIXED PARAMETER

		DEPTH	T=THICK*RES	S=THICK/RES
		0.00		
THICK = 0.34	RES = 200.00		68.00	0.002
		0.34		
THICK = 2.31	RES = 100.00		231.00	0.023
		2.65		
THICK = 6.85	RES = 200.00		1370.00	0.034
		9.50		
THICK = 36.50	RES = 54.00		1971.00	0.676
		46.00		
	RES = 93.00			

INTERPRETED MODEL... * : FIXED PARAMETER

		DEPTH	T=THICK*RES	S=THICK/RES
		0.00		
THICK = 0.75	RES = 151.40		112.33	0.005
		0.75		
THICK = 0.58	RES = 45.73		26.42	0.013
		1.32		
THICK = 5.64	RES = 204.01		1149.99	0.028
		6.96		
THICK = 35.80	RES = 52.31		1072.62	0.684
		42.76		
	RES = 107.43			

I	L	RA-FIELD	RA-MODEL	P/C ERROR
1	1.000	130.870	131.293	0.323
2	1.250	122.980	122.203	-0.632
3	1.600	113.250	112.932	-0.281
4	2.000	103.770	107.397	-1.262
5	2.500	103.140	107.172	3.910
6	3.200	110.700	112.358	1.498
7	4.000	121.600	120.793	-0.664
8	5.000	132.120	130.099	-1.530
9	6.300	138.960	137.936	-0.737
10	8.000	144.900	142.078	-1.948
11	10.000	138.130	140.764	1.907
12	12.500	131.600	133.364	1.340
13	16.000	120.240	119.240	-0.832
14	20.000	106.180	103.345	-2.670
15	25.000	84.700	87.884	3.759
16	32.000	74.900	74.387	-0.685
17	40.000	66.140	67.421	1.937
18	50.000	64.150	64.515	0.569
19	63.000	65.300	65.407	0.164
20	80.000	70.100	68.901	-1.710
21	100.000	73.640	73.729	0.121
22	125.000	75.900	79.212	4.364

RMS P/C ERROR = 0.95

SCHLUMBERGER INTERPRETATION: 6PT/DECADE

● L00

RMS P/C CUTOFF : 0.10
NUMBER OF LAYERS = 4

INITIAL MODEL... * : FIXED PARAMETER

		DEPTH	T=THICK*RES	S=THICK/RES
		0.00		
THICK = 0.67	RES = 600.00		402.00	0.001
		0.67		
THICK = 2.73	RES = 310.00		846.30	0.009
		3.40		
THICK = 56.60	RES = 44.00		2490.40	1.286
		60.00		
	RES = 127.00			

INTERPRETED MODEL... * : FIXED PARAMETER

		DEPTH	T=THICK*RES	S=THICK/RES
		0.00		
THICK = 1.28	RES = 536.05		688.77	0.002
		1.28		
THICK = 3.10	RES = 219.02		677.94	0.014
		4.38		
THICK = 65.38	RES = 41.59		2719.12	1.572
		69.76		
	RES = 397.28			

I	L	RA-FIELD	RA-MODEL	P/C ERROR
1	1.000	528.370	515.235	-2.486
2	1.250	501.300	499.955	-0.268
3	1.600	445.570	471.594	5.841
4	2.000	439.450	435.333	-0.937
5	2.500	400.250	389.173	-2.768
6	3.200	330.180	331.743	0.473
7	4.000	251.170	279.293	6.939
8	5.000	237.420	229.452	-3.356
9	6.300	180.490	182.373	1.043
10	8.000	141.070	137.766	-2.342
11	10.000	103.930	103.356	-0.553
12	12.500	77.500	76.765	-0.949
13	16.000	57.270	58.554	2.243
14	20.000	50.430	50.004	-0.785
15	25.000	46.240	46.045	-0.421
16	32.000	44.950	44.791	-0.354
17	40.000	44.310	44.860	1.241
18	50.000	46.170	46.199	0.063
19	63.000	48.150	49.031	1.767
20	80.000	56.070	54.309	-1.381
21	100.000	62.670	61.898	-1.232
22	125.000	70.450	72.619	3.070

RMS P/C ERROR = 1.62

SCHLUMBERGER INTERPRETATION: 6PT/DECADE

● KA1

RMS P/C CUTOFF : 0.10
NUMBER OF LAYERS = 3

INITIAL MODEL... * : FIXED PARAMETER

			DEPTH	T=THICK*RES	S=THICK/RES
			0.00		
THICK = 0.65	RES = 500.00			325.00	0.001
			0.65		
THICK = 3.95	RES = 126.00			497.70	0.031
			4.60		
	RES = 80.00				

INTERPRETED MODEL... * : FIXED PARAMETER

			DEPTH	T=THICK*RES	S=THICK/RES
			0.00		
THICK = 0.55	RES = 548.22			304.13	0.001
			0.55		
THICK = 3.51	RES = 136.48			479.74	0.026
			4.07		
	RES = 80.51				

KA1

I	L	RA-FIELD	RA-MODEL	P/C ERROR
1	1.000	374.400	373.310	-0.291
2	1.250	291.010	310.683	6.760
3	1.600	252.730	246.256	-2.562
4	2.000	193.740	200.441	3.724
5	2.500	191.030	179.191	-6.247
6	3.200	151.540	149.377	-1.236
7	4.000	141.970	138.574	-2.392
8	5.000	128.390	130.040	1.292
9	6.300	117.700	121.411	2.978
10	8.000	112.880	112.174	-0.625
11	10.000	103.120	103.843	0.701
12	12.500	102.990	96.641	-6.165
13	16.000	91.360	90.532	-1.446
14	20.000	86.430	86.826	0.459
15	25.000	82.230	84.432	2.678
16	32.000	81.940	82.871	1.136
17	40.000	82.410	82.015	-0.480
18	50.000	81.640	81.519	-0.149
19	63.000	80.540	81.191	0.808

RMS P/C ERROR = 1.42

SCHLUMBERGER INTERPRETATION: 6PT/DECADE

● KB1

RMS P/C CUTOFF : 0.10
NUMBER OF LAYERS = 4

INITIAL MODEL... * : FIXED PARAMETER

			DEPTH	T=THICK*RES	S=THICK/RES
			0.00		
THICK = 0.53	RES = 260.00			137.80	0.002
			0.53		
THICK = 2.22	RES = 77.00			170.94	0.029
			2.75		
THICK = 8.85	RES = 128.00			1132.80	0.069
			11.60		
	RES = 75.00				

INTERPRETED MODEL... * : FIXED PARAMETER

			DEPTH	T=THICK*RES	S=THICK/RES
			0.00		
THICK = 0.39	RES = 345.51			134.25	0.001
			0.39		
THICK = 2.68	RES = 81.70			219.18	0.033
			3.07		
THICK = 5.07	RES = 150.18			761.39	0.034
			8.14		
	RES = 74.00				

I	L	RA-FIELD	RA-MODEL	P/C ERROR
1	1.000	169.100	169.686	0.346
2	1.250	142.430	135.206	-5.072
3	1.600	109.700	111.239	1.403
4	2.000	90.550	93.467	3.053
5	2.500	91.260	92.584	1.451
6	3.200	93.270	91.477	-1.922
7	4.000	95.960	93.233	-2.842
8	5.000	97.220	96.796	-0.436
9	6.300	99.110	101.438	2.349
10	8.000	102.220	103.956	0.655
11	10.000	111.100	108.826	-2.047
12	12.500	109.440	109.124	-0.289
13	16.000	106.500	106.411	-0.083
14	20.000	101.410	101.502	0.091
15	25.000	93.130	95.442	2.483
16	32.000	90.200	88.744	-1.615
17	40.000	92.530	93.871	1.449
18	50.000	79.300	80.232	1.175
19	63.000	77.000	77.820	1.065
20	80.000	78.100	76.281	-2.329
21	100.000	75.770	75.445	-0.429
22	125.000	79.600	74.944	-5.849

RMS P/C ERROR = 1.62

SCHLUMBERGER INTERPRETATION: 6PT/DECADE

● KC1

RMS P/C CUTOFF : 0.10
NUMBER OF LAYERS = 4

INITIAL MODEL... * : FIXED PARAMETER

		DEPTH	T=THICK*RES	S=THICK/RES
		0.00		
THICK = 0.43	RES = 270.00		114.75	0.002
		0.43		
THICK = 2.48	RES = 77.00		190.08	0.032
		2.90		
THICK = 17.10	RES = 155.00		2650.50	0.110
		20.00		
	RES = 90.00			

INTERPRETED MODEL... * : FIXED PARAMETER

		DEPTH	T=THICK*RES	S=THICK/RES
		0.00		
THICK = 0.51	RES = 222.46		112.95	0.002
		0.51		
THICK = 2.10	RES = 69.00		144.92	0.030
		2.61		
THICK = 11.64	RES = 178.69		2079.69	0.065
		14.25		
	RES = 91.30			

I	L	RA-FIELD	RA-MODEL	P/C ERROR
1	1.000	131.090	131.190	0.066
2	1.250	130.250	128.612	-1.258
3	1.600	107.360	107.931	0.532
4	2.000	92.740	94.787	2.207
5	2.500	90.040	88.337	-1.892
6	3.200	88.600	87.560	-1.173
7	4.000	90.760	91.706	1.042
8	5.000	97.650	98.850	1.229
9	6.300	105.940	108.157	2.093
10	8.000	119.350	118.374	-0.818
11	10.000	130.500	127.371	-2.398
12	12.500	138.950	134.717	-2.976
13	16.000	141.130	139.949	-0.851
14	20.000	138.400	141.245	2.056
15	25.000	135.650	138.770	2.293
16	32.000	130.200	132.330	1.636
17	40.000	126.300	124.065	-1.770
18	50.000	116.630	115.473	-0.990
19	63.000	111.510	107.545	-3.556
20	80.000	100.138	[illegible].429	1.289
21	100.000	95.600	97.527	2.016
22	125.000	90.660	95.027	4.817

RMS P/C ERROR = 1.63

SCHLUMBERGER INTERPRETATION: 6PT/DECADE

● KD1

RMS P/C CUTOFF : 0.10
NUMBER OF LAYERS = 3

INITIAL MODEL... * : FIXED PARAMETER

		DEPTH	T=THICK*RES	S=THICK/RES
		0.00		
THICK = 0.80	RES = 275.00		220.00	0.00
		0.80		
THICK = 9.20	RES = 162.00		1490.40	0.05
		10.00		
	RES = 100.00			

INTERPRETED MODEL... * : FIXED PARAMETER

		DEPTH	T=THICK*RES	S=THI
		0.00		
THICK = 0.54	RES = 296.86		161.50	0.002
		0.54		
THICK = 6.97	RES = 175.68		1223.63	0.040
		7.51		
	RES = 104.09			

I	L	RA-FIELD	RA-MODEL	P/C ERROR
1	1.000	249.900	252.295	0.958
2	1.250	234.300	235.686	0.577
3	1.600	224.600	218.155	-2.869
4	2.000	208.500	204.413	1.960
5	2.500	189.600	194.026	2.334
6	3.200	177.800	185.931	4.573
7	4.000	183.170	180.998	-1.186
8	5.000	176.500	177.044	0.308
9	6.300	172.620	172.975	0.206
10	8.000	169.000	167.698	-0.770
11	10.000	165.480	161.258	-2.551
12	12.500	161.400	152.790	-5.335
13	16.000	141.400	142.166	0.542
14	20.000	132.730	132.323	-0.307
15	25.000	121.260	123.738	2.044
16	32.000	113.670	116.283	2.298
17	40.000	106.700	111.816	4.795
18	50.000	104.770	108.864	3.907
19	63.000	109.960	107.020	-2.674
20	80.000	104.140	105.872	1.663
21	100.000	109.520	105.239	-3.909
22	125.000	102.900	104.857	1.902

RMS P/C ERROR = 2.48

A.6.7 Computer Resistivity Model

SCHLUMBERGER INTERPRETATION: SPT/DECADE

● KK1

RMS P/C CUTOFF = 0.10
NUMBER OF LAYERS = 5

INITIAL MODEL... * = FIXED PARAMETER

		DEPTH	T=THICK/RES	S=THICK/RES
		0.00		
THICK = 0.34	RES = 275.00	0.34	93.50	0.001
THICK = 5.66	RES = 60.00	6.00	339.60	0.094
THICK = 3.50	RES = 119.00	9.50	416.50	0.029
THICK = 40.50	RES = 42.00	50.00	1701.00	0.964
	RES = 130.00			

INTERPRETED MODEL... * = FIXED PARAMETER

		DEPTH	T=THICK/RES	S=THICK/RES
		0.00		
THICK = 0.39	RES = 134.12	0.39	52.82	0.003
THICK = 4.85	RES = 56.82	5.24	265.32	0.082
THICK = 2.72	RES = 141.41	7.96	384.57	0.019
THICK = 32.70	RES = 32.17	40.66	1052.01	1.016
	RES = 255.01			

I	L	RA-FIELD	RA-MODEL	P/C ERROR
1	1.000	89.000	89.632	-0.122
2	1.250	82.400	79.005	-4.120
3	1.600	69.200	71.170	2.847
4	2.000	66.080	66.364	0.430
5	2.500	64.140	63.513	-0.978
6	3.200	62.700	62.046	-1.043
7	4.000	61.120	61.694	0.939
8	5.000	61.300	62.092	1.297
9	6.300	61.550	63.057	2.448
10	8.000	66.260	64.325	-2.920
11	10.000	66.140	65.101	-1.601
12	12.500	64.000	64.613	0.958
13	16.000	61.930	62.029	0.159
14	20.000	57.300	57.701	0.701
15	25.000	53.600	58.000	-1.104
16	32.000	48.050	48.429	-0.067
17	40.000	46.600	46.585	-0.033
18	50.000	46.730	47.483	1.611
19	63.000	51.900	51.946	0.089
20	80.000	59.000	59.786	1.333

RMS P/C ERROR = 0.83

● KA2

RMS P/C CUTOFF = 0.10
NUMBER OF LAYERS = 4

INITIAL MODEL... * = FIXED PARAMETER

		DEPTH	T=THICK/RES	S=THICK/RES
		0.00		
THICK = 0.52	RES = 150.00	0.52	78.80	0.003
THICK = 6.98	RES = 65.00	7.50	453.70	0.107
THICK = 5.70	RES = 100.00	13.20	570.00	0.057
	RES = 48.00			

INTERPRETED MODEL... * = FIXED PARAMETER

		DEPTH	T=THICK/RES	S=THICK/RES
		0.00		
THICK = 0.51	RES = 204.29	0.51	103.29	0.002
THICK = 5.98	RES = 64.59	6.48	386.19	0.093
THICK = 1.28	RES = 170.34	7.76	218.23	0.008
	RES = 52.17			

I	L	RA-FIELD	RA-MODEL	P/C ERROR
1	1.000	139.570	138.698	-0.625
2	1.250	116.160	117.711	1.335
3	1.600	96.870	97.984	1.129
4	2.000	86.100	84.479	-1.887
5	2.500	74.720	75.908	1.589
6	3.200	71.770	70.660	-1.547
7	4.000	67.920	68.485	0.739
8	5.000	66.510	67.575	1.602
9	6.300	66.230	67.445	1.834
10	8.000	67.330	67.828	0.739
11	10.000	70.310	68.239	-2.945
12	12.500	69.170	68.241	-1.343
13	16.000	65.100	67.305	3.388
14	20.000	64.730	65.424	1.087
15	25.000	62.820	62.899	0.126
16	32.000	63.010	59.881	-4.965
17	40.000	58.050	57.537	-2.202
18	50.000	53.350	55.693	4.391
19	63.000	49.560	54.398	9.763
20	80.000	50.069	53.524	6.901

RMS P/C ERROR = 4.09

A.6.7 Computer Resistivity Model

SCHLUMBERGER INTERPRETATION: APT/DECADE

● 102

RMS P/C CUTOFF = 0.10
NUMBER OF LAYERS = 5

INITIAL MODEL... * = FIXED PARAMETER

			DEPTH	T=THICK/RES	S=THICK/RES
			0.00		
THICK = 0.59	RES =	130.00		76.70	0.005
			0.59		
THICK = 6.51	RES =	57.00		371.07	0.114
			7.10		
THICK = 15.90	RES =	112.00		1780.80	0.142
			23.00		
THICK = 42.00	RES =	50.00		2100.00	0.840
			65.00		
	RES =	90.00			

INTERPRETED MODEL... * = FIXED PARAMETER

			DEPTH	T=THICK/RES	S=THICK/RES
			0.00		
THICK = 0.96	RES =	108.79		96.06	0.009
			0.96		
THICK = 2.30	RES =	44.20		102.02	0.052
			3.20		
THICK = 26.93	RES =	78.76		2120.94	0.342
			30.13		
THICK = 18.75	RES =	23.49		440.51	0.799
			48.88		
	RES =	123.70			

I	L	RA-FIELD	RA-MODEL	P/C ERROR
1	1.000	98.340	98.149	-0.198
2	1.250	96.270	92.205	-4.222
3	1.600	80.810	82.947	2.649
4	2.000	73.040	74.136	1.501
5	2.500	67.150	66.171	-1.457
6	3.200	60.000	59.626	-0.623
7	4.000	56.740	56.863	0.217
8	5.000	54.610	54.450	-0.292
9	6.300	52.350	53.203	1.631
10	8.000	50.740	51.145	4.005
11	10.000	46.800	48.307	+3.216
12	12.500	47.050	47.143	-1.042
13	16.000	49.170	49.679	0.735
14	20.000	69.300	71.113	2.616
15	25.000	67.560	71.527	5.871
16	32.000	72.970	70.646	-3.212
17	40.000	59.210	60.467	-1.117
18	50.000	65.500	65.576	0.115
19	63.000	60.070	62.573	4.133
20	80.000	64.000	61.287	-4.378
21	100.000	62.070	62.300	-0.091
22	125.000	68.610	65.901	-3.949

RMS P/C ERROR = 1.92

● 102

RMS P/C CUTOFF = 0.10
NUMBER OF LAYERS = 5

INITIAL MODEL... * = FIXED PARAMETER

			DEPTH	T=THICK/RES	S=THICK/RES
			0.00		
THICK = 0.68	RES =	170.00		115.60	0.004
			0.68		
THICK = 4.92	RES =	70.00		344.40	0.070
			5.60		
THICK = 4.20	RES =	150.00		630.00	0.028
			9.80		
THICK = 32.20	RES =	70.00		2254.00	0.460
			42.00		
	RES =	140.00			

INITIAL MODEL... RMS P/C = 5.82

INTERPRETED MODEL... * = FIXED PARAMETER

			DEPTH	T=THICK/RES	S=THICK/RES
			0.00		
THICK = 0.95	RES =	150.04		142.28	0.006
			0.95		
THICK = 2.38	RES =	52.20		124.04	0.046
			3.32		
THICK = 2.89	RES =	209.55		605.46	0.014
			6.21		
THICK = 10.89	RES =	47.33		515.67	0.230
			17.10		
	RES =	109.89			

I	L	RA-FIELD	RA-MODEL	P/C ERROR
1	1.000	138.730	136.635	-1.510
2	1.250	131.760	128.780	-2.255
3	1.600	110.400	115.614	4.723
4	2.000	103.400	102.615	-0.759
5	2.500	90.870	90.339	-0.584
6	3.200	80.900	80.150	-0.927
7	4.000	74.850	76.213	1.821
8	5.000	75.530	76.256	0.935
9	6.300	79.970	79.970	-0.001
10	8.000	83.160	84.676	1.823
11	10.000	89.970	88.205	-1.962
12	12.500	85.930	88.653	+1.197
13	16.000	86.570	86.708	0.252
14	20.000	82.430	83.110	0.835
15	25.000	77.640	79.733	2.696
16	32.000	78.050	77.697	-0.453
17	40.000	76.940	78.871	2.509
18	50.000	85.530	81.941	-4.196
19	63.000	81.770	86.569	5.869
20	80.000	94.130	91.550	-2.741
21	100.000	96.980	95.858	-1.157
22	125.000	98.020	99.553	1.564

RMS P/C ERROR = 1.72

SCHLUMBERGER INTERPRETATION: 6PT/DECADE

● KD2

RMS P/C CUTOFF : 0.10
NUMBER OF LAYERS = 5

INITIAL MODEL... * : FIXED PARAMETER

		DEPTH	T=THICK*RES	S=THICK/RES
		0.00		
THICK = 0.30	RES = 82.00	0.30	24.60	0.004
THICK = 4.10	RES = 62.00	4.40	254.20	0.066
THICK = 5.10	RES = 120.00	9.50	612.00	0.042
THICK = 40.50	RES = 50.00	50.00	2025.00	0.810
	RES = 150.00			

INTERPRETED MODEL... * : FIXED PARAMETER

		DEPTH	T=THICK*RES	S=THICK/RES
		0.00		
THICK = 1.55	RES = 67.06	1.55	103.97	0.023
THICK = 1.00	RES = 34.97	2.55	34.97	0.029
THICK = 3.57	RES = 140.76	6.12	502.60	0.025
THICK = 36.25	RES = 43.43	42.38	1574.05	0.835
	RES = 145.27			

I	L	RA-FIELD	RA-MODEL	P/C ERROR
1	1.000	66.440	66.373	-0.100
2	1.250	68.170	65.937	-3.276
3	1.600	63.430	64.969	2.426
4	2.000	63.530	63.956	0.670
5	2.500	63.520	62.997	-0.823
6	3.200	63.510	62.615	-1.409
7	4.000	62.960	63.701	1.139
8	5.000	64.590	66.100	2.330
9	6.300	68.600	69.788	1.731
10	8.000	75.110	73.280	-2.436
11	10.000	76.300	75.160	-1.495
12	12.500	74.860	74.414	-0.596
13	16.000	71.600	70.923	-0.946
14	20.000	65.230	66.008	1.193
15	25.000	60.380	60.832	0.760
16	32.000	55.890	56.276	0.691
17	40.000	56.130	54.447	-2.999
18	50.000	55.120	54.947	-0.314
19	63.000	57.240	58.211	1.697
20	80.000	65.080	63.993	-1.670
21	100.000	72.540	71.455	-1.495

RMS P/C ERROR = 1.11

● KE2

RMS P/C CUTOFF : 0.10
NUMBER OF LAYERS = 4

INITIAL MODEL... * : FIXED PARAMETER

		DEPTH	T=THICK*RES	S=THICK/RES
		0.00		
THICK = 0.50	RES = 500.00	0.50	250.00	0.001
THICK = 8.50	RES = 65.00	9.00	552.50	0.131
THICK = 9.50	RES = 5.40	18.50	51.30	1.759
	RES = 78.00			

INTERPRETED MODEL... * : FIXED PARAMETER

		DEPTH	T=THICK*RES	S=THICK/RES
		0.00		
THICK = 0.51	RES = 458.58	0.51	232.20	0.001
THICK = 7.10	RES = 69.12	7.63	496.00	0.104
THICK = 0.61	RES = 1.30	8.27	0.79	0.468
	RES = 81.28			

I	L	RA-FIELD	RA-MODEL	P/C ERROR
1	1.000	254.360	258.621	1.675
2	1.250	202.390	197.782	-2.278
3	1.600	146.000	141.846	-2.845
4	2.000	105.370	106.802	1.358
5	2.500	93.720	87.128	4.071
6	3.200	73.710	76.072	3.205
7	4.000	71.600	71.426	-0.243
8	5.000	67.900	68.423	0.770
9	6.300	65.200	65.031	-0.257
10	8.000	63.820	60.344	-5.447
11	10.000	58.220	54.780	-5.909
12	12.500	49.250	47.905	-2.731
13	16.000	37.300	41.120	9.783
14	20.000	35.540	36.770	3.483
15	25.000	37.730	35.654	-5.503
16	32.000	38.200	37.538	-1.733
17	40.000	41.080	41.455	0.912
18	50.000	46.750	46.454	-0.632
19	63.000	50.740	51.702	2.054
20	80.000	57.000	57.105	0.183
21	100.000	61.110	61.877	1.255
22	125.000	65.300	66.103	1.230

RMS P/C ERROR = 2.76

SCHLUMBERGER INTERPRETATION: 6PT/DECADE

● KA3

RMS P/C CUTOFF : 0.10
NUMBER OF LAYERS = 4

INITIAL MODEL... * : FIXED PARAMETER

		DEPTH	T=THICK*RES	S=THICK/RES
		0.00		
THICK = 0.39	RES = 94.00	0.39	36.19	0.004
THICK = 2.47	RES = 32.00	2.85	78.88	0.077
THICK = 11.15	RES = 50.00	14.00	557.50	0.223
	RES = 86.00			

INTERPRETED MODEL... * : FIXED PARAMETER

		DEPTH	T=THICK*RES	S=THICK/RES
		0.00		
THICK = 0.43	RES = 84.73	0.43	36.13	0.005
THICK = 1.14	RES = 27.28	1.57	31.14	0.042
THICK = 14.32	RES = 44.13	15.89	632.04	0.325
	RES = 93.02			

I	L	RA-FIELD	RA-MODEL	P/C ERROR
1	1.000	51.970	51.870	-0.192
2	1.250	43.590	44.105	1.182
3	1.600	38.430	38.477	0.123
4	2.000	36.440	35.552	-2.436
5	2.500	34.920	34.658	-0.674
6	3.200	35.000	35.313	0.894
7	4.000	36.100	36.600	1.161
8	5.000	36.650	38.168	4.142
9	6.300	41.370	39.725	-3.976
10	8.000	43.300	41.220	-4.803
11	10.000	43.630	42.567	-2.436
12	12.500	44.870	43.977	-1.980
13	16.000	44.230	45.906	3.799
14	20.000	45.870	48.220	5.124
15	25.000	50.490	51.329	1.661
16	32.000	54.680	55.690	1.847
17	40.000	62.170	60.359	-2.944
18	50.000	68.420	65.359	-4.474
19	63.000	73.100	70.499	-3.558
20	80.000	76.300	75.432	-1.137
21	100.000	76.770	79.499	3.555
22	125.000	79.640	82.942	4.146

RMS P/C ERROR = 2.90

SCHLUMBERGER INTERPRETATION: 6PT/DECADE

● KB3

RMS P/C CUTOFF : 0.10
NUMBER OF LAYERS = 5

INITIAL MODEL... * : FIXED PARAMETER

		DEPTH	T=THICK*RES	S=THICK/RES
		0.00		
THICK = 0.50	RES = 150.00	0.50	75.00	0.003
THICK = 5.10	RES = 54.00	5.60	275.40	0.094
THICK = 20.40	RES = 60.00	26.00	1224.00	0.340
THICK = 54.00	RES = 56.00	80.00	3024.00	0.964
	RES = 111.00			

THICKNESSES : 0.441 4.479 25.501 26.800

INTERPRETED MODEL... * : FIXED PARAMETER

		DEPTH	T=THICK*RES	S=THICK/RES
		0.00		
THICK = 0.44	RES = 168.31	0.44	74.26	0.003
THICK = 4.48	RES = 52.55	4.92	235.38	0.086
THICK = 25.50	RES = 59.99	30.42	1529.83	0.425
THICK = 26.80	RES = 36.07	57.22	966.76	0.743
	RES = 131.23			

I	L	RA-FIELD	RA-MODEL	P/C ERROR
1	1.000	104.020	103.307	-0.686
2	1.250	85.140	84.553	1.669
3	1.600	71.500	72.777	1.786
4	2.000	66.260	64.121	-3.229
5	2.500	59.950	58.994	-1.595
6	3.200	55.100	54.128	1.865
7	4.000	54.300	54.910	1.123
8	5.000	54.700	54.495	-0.375
9	6.300	53.300	54.523	2.295
10	8.000	56.000	54.948	-2.018
11	10.000	56.330	55.572	-1.346
12	12.500	56.020	56.291	0.484
13	16.000	57.100	57.022	-0.136
14	20.000	56.400	57.483	1.919
15	25.000	58.300	57.635	-1.140
16	32.000	57.740	57.440	-0.520
17	40.000	57.600	56.904	-1.200
18	50.000	56.300	56.434	0.237
19	63.000	56.700	56.444	-0.451
20	80.000	56.070	57.988	3.420
21	100.000	61.110	61.151	0.068
22	125.000	63.900	66.207	3.611

RMS P/C ERROR = 1.39

A.6.7 Computer Resistivity Model

SCHLUMBERGER INTERPRETATION ZPT/DECADE

● KQ3

RMS P/C CUTOFF : 0.10
NUMBER OF LAYERS = 5

INITIAL MODEL... * : FIXED PARAMETER

			DEPTH	T=THICK*RES	S=THICK/RES
			0.00		
THICK = 0.68	RES = 240.00		0.68	163.20	0.003
THICK = 5.57	RES = 60.00		6.25	334.20	0.093
THICK = 8.15	RES = 121.00		14.40	986.15	0.067
THICK = 50.60	RES = 52.50		65.00	2656.50	0.964
	RES = 85.00				

INTERPRETED MODEL... * : FIXED PARAMETER

			DEPTH	T=THICK*RES	S=THICK/RES
			0.00		
THICK = 0.71	RES = 231.48		0.71	163.79	0.003
THICK = 4.55	RES = 54.47		5.25	247.55	0.083
THICK = 3.50	RES = 184.15		8.75	644.38	0.019
THICK = 39.91	RES = 47.08		48.66	1878.93	0.848
	RES = 92.14				

I	L	RA-FIELD	RA-MODEL	P/C ERROR
1	1.000	185.600	181.997	-1.941
2	1.250	154.600	158.389	2.697
3	1.600	124.730	128.388	2.930
4	2.000	104.270	103.374	-0.859
5	2.500	85.030	84.251	0.916
6	3.200	71.660	70.484	-1.642
7	4.000	62.750	64.965	3.531
8	5.000	63.850	63.366	-0.758
9	6.300	62.840	64.740	3.023
10	8.000	67.090	68.058	1.443
11	10.000	73.710	71.865	-2.503
12	12.500	78.600	75.067	-2.256
13	16.000	76.920	76.705	-0.279
14	20.000	75.270	75.667	0.528
15	25.000	70.740	72.369	2.303
16	32.000	67.900	67.356	-0.801
17	40.000	62.600	62.863	0.420
18	50.000	59.870	59.715	-0.259
19	63.000	58.230	58.560	0.566
20	80.000	60.000	59.721	-0.397
21	100.000	62.600	62.574	-0.042
22	125.000	66.770	66.495	-0.412

RMS P/C ERROR = 1.73

● KD3

RMS P/C CUTOFF : 0.10
NUMBER OF LAYERS = 4

INITIAL MODEL... * : FIXED PARAMETER

			DEPTH	T=THICK*RES	S=THICK/RES
			0.00		
THICK = 0.51	RES = 112.00		0.51	57.12	0.005
THICK = 9.49	RES = 50.00		10.00	474.50	0.190
THICK = 24.00	RES = 32.00		34.00	768.00	0.750
	RES = 72.50				

INTERPRETED MODEL... * : FIXED PARAMETER

			DEPTH	T=THICK*RES	S=THICK/RES
			0.00		
THICK = 0.54	RES = 111.42		0.54	59.72	0.005
THICK = 14.39	RES = 47.48		14.92	683.13	0.303
THICK = 7.72	RES = 14.05		22.65	108.53	0.550
	RES = 73.83				

I	L	RA-FIELD	RA-MODEL	P/C ERROR
1	1.000	85.000	85.374	0.440
2	1.250	76.290	76.119	-0.224
3	1.600	67.340	66.722	-0.918
4	2.000	60.770	59.766	-1.651
5	2.500	53.920	54.914	1.843
6	3.200	50.510	51.537	2.034
7	4.000	48.550	49.820	2.616
8	5.000	48.380	48.790	0.848
9	6.300	47.480	48.059	1.219
10	8.000	48.210	47.408	-1.663
11	10.000	47.950	46.695	-2.618
12	12.500	46.540	45.697	-1.812
13	16.000	44.540	44.100	-0.989
14	20.000	42.120	42.229	0.259
15	25.000	39.640	40.196	1.404
16	32.000	38.130	38.512	1.001
17	40.000	37.640	38.369	1.936
18	50.000	40.430	39.702	-1.802
19	63.000	42.750	42.806	0.131
20	80.000	47.270	46.994	-0.584
21	100.000	50.930	51.357	0.839
22	125.000	54.090	55.657	1.397

RMS P/C ERROR = 1.17

A.6.7 Computer Resistivity Model

SCHLUMBERGER INTERPRETATION: 6PT/DECADE

● KE3

RMS P/C CUTOFF : 0.10
NUMBER OF LAYERS = 4

INITIAL MODEL... * : FIXED PARAMETER

		DEPTH	T=THICK/RES	S=THICK/RES
		0.00		
THICK = 0.94	RES = 218.00		204.92	0.004
		0.94		
THICK = 2.86	RES = 38.00		108.68	0.075
		3.80		
THICK = 24.20	RES = 13.00		459.80	1.274
		28.00		
	RES = 96.00			

INTERPRETED MODEL... * : FIXED PARAMETER

		DEPTH	T=THICK/RES	S=THICK/RES
		0.00		
THICK = 0.78	RES = 254.77		199.01	0.003
		0.78		
THICK = 4.94	RES = 45.66		225.49	0.108
		5.72		
THICK = 17.70	RES = 13.80		244.22	1.282
		23.42		
	RES = 109.59			

I	L	RA-FIELD	RA-MODEL	P/C ERROR
1	1.000	204.250	204.975	0.012
2	1.250	178.760	179.759	0.559
3	1.600	142.600	143.233	0.444
4	2.000	121.170	111.393	-8.064
5	2.500	77.080	84.877	10.115
6	3.200	62.200	64.083	3.027
7	4.000	50.040	53.461	6.835
8	5.000	49.220	46.684	-5.153
9	6.300	42.400	41.859	-1.739
10	8.000	36.350	36.829	1.428
11	10.000	32.000	32.136	0.424
12	12.500	27.020	27.226	0.600
13	16.000	23.000	23.041	0.179
14	20.000	20.420	20.766	1.694
15	25.000	20.600	20.341	-1.276
16	32.000	21.800	21.765	-0.162
17	40.000	25.330	24.643	-2.711
18	50.000	28.770	28.724	-0.162
19	63.000	33.360	33.909	1.645
20	80.000	39.550	40.092	1.370
21	100.000	46.840	46.462	-0.806
22	125.000	55.130	53.281	-3.354

RMS P/C ERROR = 1.49

SCHLUMBERGER INTERPRETATION: 6PT/DECADE

● KA4

RMS P/C CUTOFF : 0.10
NUMBER OF LAYERS = 3

INITIAL MODEL... * : FIXED PARAMETER

		DEPTH	T=THICK/RES	S=THICK/RES
		0.00		
THICK = 0.41	RES = 208.00		85.28	0.002
		0.41		
THICK = 10.07	RES = 82.00		827.38	0.123
		10.50		
	RES = 160.00			

		DEPTH	T=THICK/RES	S=THICK/RES
		0.00		
THICK = 0.41	RES = 283.45		116.16	0.001
		0.41		
THICK = 11.32	RES = 79.02		902.15	0.143
		11.80		
	RES = 176.16			

I	L	RA-FIELD	RA-MODEL	P/C ERROR
1	1.000	130.760	157.303	-0.867
2	1.250	127.110	129.230	1.672
3	1.600	105.400	107.087	2.050
4	2.000	96.370	95.270	-1.142
5	2.500	90.540	88.138	-2.653
6	3.200	87.060	84.365	-3.096
7	4.000	85.070	82.673	-2.810
8	5.000	82.500	82.021	-0.560
9	6.300	81.320	81.973	0.803
10	8.000	78.360	82.689	5.524
11	10.000	81.710	84.275	3.140
12	12.500	84.000	87.127	3.723
13	16.000	91.540	92.130	0.644
14	20.000	103.160	98.596	-4.434
15	25.000	107.130	106.678	-2.247
16	32.000	114.900	117.010	1.807
17	40.000	118.400	126.773	7.072

RMS P/C ERROR = 2.52

SCHLUMBERGER INTERPRETATION: 6PT/DECADE

● KB4

RMS P/C CUTOFF : 0.10
NUMBER OF LAYERS = 4

INITIAL MODEL... * : FIXED PARAMETER

		DEPTH	T=THICK*RES	S=THICK/RES
		0.00		
THICK = 0.80	RES = 190.00		152.00	0.004
		0.80		
THICK = 9.20	RES = 57.00		524.40	0.161
		10.00		
THICK = 36.00	RES = 52.00		1872.00	0.692
		46.00		
	RES = 130.00			

INTERPRETED MODEL... * : FIXED PARAMETER

		DEPTH	T=THICK*RES	S=THICK/RES
		0.00		
THICK = 0.77	RES = 194.04		150.01	0.004
		0.77		
THICK = 19.66	RES = 55.93		1099.29	0.351
		20.43		
THICK = 10.31	RES = 22.47		231.59	0.459
		30.74		
	RES = 143.61			

I	L	RA-FIELD	RA-MODEL	P/C ERROR
1	1.000	167.750	162.677	-3.140
2	1.250	144.000	146.661	1.848
3	1.600	117.270	123.789	4.933
4	2.000	99.500	103.470	3.990
5	2.500	89.540	86.266	-3.656
6	3.200	76.160	72.294	-5.077
7	4.000	66.210	65.001	-1.826
8	5.000	59.570	60.745	1.972
9	6.300	56.030	58.556	4.509
10	8.000	57.000	57.310	0.545
11	10.000	56.810	56.584	-0.397
12	12.500	56.370	55.933	0.653
13	16.000	55.440	55.166	-0.495
14	20.000	54.320	54.339	0.016
15	25.000	54.320	53.375	-1.758
16	32.000	52.480	52.663	-0.037
17	40.000	52.420	52.941	0.774
18	50.000	54.430	54.909	0.880
19	63.000	59.470	59.373	-0.164
20	80.000	66.020	66.264	0.264
21	100.000	72.070	74.023	3.820

RMS P/C ERROR = 2.44

● KC4

RMS P/C CUTOFF : 0.10
NUMBER OF LAYERS = 4

INITIAL MODEL... * : FIXED PARAMETER

		DEPTH	T=THICK*RES	S=THICK/RES
		0.00		
THICK = 0.85	RES = 100.00		85.00	0.009
		0.85		
THICK = 17.15	RES = 40.00		686.00	0.429
		18.00		
THICK = 28.00	RES = 32.00		896.00	0.875
		46.00		
	RES = 70.00			

INTERPRETED MODEL... * : FIXED PARAMETER

		DEPTH	T=THICK*RES	S=THICK/RES
		0.00		
THICK = 0.90	RES = 103.19		92.58	0.009
		0.90		
THICK = 19.50	RES = 40.72		793.81	0.479
		20.39		
THICK = 15.35	RES = 23.25		356.82	0.660
		35.74		
	RES = 76.99			

I	L	RA-FIELD	RA-MODEL	P/C ERROR
1	1.000	94.120	93.531	-0.625
2	1.250	86.320	87.927	1.861
3	1.600	78.930	78.991	0.078
4	2.000	70.040	70.069	0.041
5	2.500	61.330	61.407	0.125
6	3.200	53.590	53.368	-0.413
7	4.000	48.810	48.378	-0.884
8	5.000	45.260	45.091	-0.374
9	6.300	42.730	43.182	1.058
10	8.000	41.810	42.048	0.569
11	10.000	41.180	41.417	0.575
12	12.500	41.020	40.909	-0.272
13	16.000	40.770	40.368	-0.987
14	20.000	39.710	39.799	0.224
15	25.000	39.490	39.103	-0.979
16	32.000	38.250	38.418	0.440
17	40.000	37.840	38.130	0.767
18	50.000	38.800	38.591	-0.539
19	63.000	41.380	40.317	-2.569

RMS P/C ERROR = 0.61

A.6.7 Computer Resistivity Model

● KD4

RMS P/C CUTOFF : 0.10
NUMBER OF LAYERS = 4

INITIAL MODEL... * : FIXED PARAMETER

		DEPTH	T=THICK*RES	S=THICK/RES
		0.00		
THICK = 0.63	RES = 115.00			
		0.63	72.45	0.005
THICK = 13.07	RES = 50.00			
		13.70	653.50	0.261
THICK = 46.30	RES = 33.00			
		60.00	1527.90	1.403
	RES = 70.00			

INTERPRETED MODEL... * : FIXED PARAMETER

		DEPTH	T=THICK*RES	S=THICK/RES
		0.00		
THICK = 0.65	RES = 114.17			
		0.65	73.83	0.006
THICK = 19.04	RES = 48.47			
		19.69	923.05	0.393
THICK = 12.02	RES = 21.04			
		31.71	252.93	0.571
	RES = 55.71			

I	L	RA-FIELD	RA-MODEL	P/C ERROR
1	1.000	93.640	94.619	1.045
2	1.250	84.800	85.969	1.379
3	1.600	77.400	75.515	-2.436
4	2.000	68.060	66.892	-1.716
5	2.500	60.690	60.192	-0.821
6	3.200	53.320	55.024	3.196
7	4.000	50.600	52.319	3.396
8	5.000	49.700	50.699	2.009
9	6.300	49.580	49.722	0.287
10	8.000	49.770	49.068	-1.411
11	10.000	49.820	48.567	-2.515
12	12.500	49.100	48.017	-2.207
13	16.000	47.710	47.174	-1.124
14	20.000	46.130	46.078	-0.113
15	25.000	44.250	44.542	0.659
16	32.000	42.380	42.608	0.538
17	40.000	40.450	40.927	1.178
18	50.000	40.040	39.971	-0.172
19	63.000	40.390	40.110	-0.692
20	80.000	41.060	41.472	1.003
21	100.000	43.470	43.551	0.187
22	125.000	46.220	45.899	-0.695

RMS P/C ERROR = 1.53

SCHLUMBERGER INTERPRETATION: 6FT/DECADE

● KE4

RMS P/C CUTOFF : 0.10
NUMBER OF LAYERS = 4

INITIAL MODEL... * : FIXED PARAMETER

		DEPTH	T=THICK*RES	S=THICK/RES
		0.00		
THICK = 1.07	RES = 117.00			
		1.07	125.19	0.009
THICK = 8.63	RES = 49.00			
		9.70	422.87	0.176
THICK = 38.30	RES = 31.00			
		48.00	1187.30	1.235
	RES = 95.00			

INTERPRETED MODEL... * : FIXED PARAMETER

		DEPTH	T=THICK*RES	S=THICK/RES
		0.00		
THICK = 1.09	RES = 115.03			
		1.09	125.93	0.010
THICK = 11.57	RES = 48.83			
		12.66	564.93	0.237
THICK = 33.43	RES = 25.46			
		46.09	851.69	1.312
	RES = 128.14			

I	L	RA-FIELD	RA-MODEL	P/C ERROR
1	1.000	110.120	108.748	-1.246
2	1.250	103.230	104.615	1.342
3	1.600	95.240	97.198	1.312
4	2.000	87.470	88.809	1.531
5	2.500	80.680	79.380	-1.611
6	3.200	70.230	69.391	-1.194
7	4.000	62.500	62.030	-0.721
8	5.000	56.300	56.642	0.607
9	6.300	51.750	53.034	2.481
10	8.000	51.320	50.590	-1.443
11	10.000	49.630	48.859	-1.554
12	12.500	47.210	47.087	-0.261
13	16.000	44.500	44.752	0.566
14	20.000	40.510	42.170	4.147
15	25.000	40.200	39.362	-3.524
16	32.000	37.530	36.619	-2.429
17	40.000	35.250	35.147	-0.292
18	50.000	34.210	35.179	2.831
19	63.000	37.200	37.213	0.035
20	80.000	42.000	41.405	-1.416
21	100.000	47.010	47.092	0.174
22	125.000	53.660	54.039	0.707

RMS P/C ERROR = 1.30

A.6.7 Computer Resistivity Model

SCHLUMBERGER INTERPRETATION: 6PT/DECADE

● KF4

RMS P/C CUTOFF : 0.10
NUMBER OF LAYERS = 5

INITIAL MODEL... * : FIXED PARAMETER

			DEPTH	T=THICK*RES	S=THICK/RES
			0.00		
THICK = 0.34	RES =	259.00		87.54	0.001
			0.34		
THICK = 5.26	RES =	65.00		342.03	0.081
			5.60		
THICK = 13.40	RES =	44.00		589.60	0.305
			19.00		
THICK = 61.00	RES =	27.00		1647.00	2.259
			80.00		
	RES =	60.00			

INTERPRETED MODEL... * : FIXED PARAMETER

			DEPTH	T=THICK*RES	S=THICK/RES
			0.00		
THICK = 0.25	RES =	558.48		140.74	0.000
			0.25		
THICK = 1.98	RES =	71.63		142.17	0.028
			2.24		
THICK = 16.39	RES =	54.27		889.46	0.302
			18.63		
THICK = 59.94	RES =	25.79		1545.69	2.324
			78.56		
	RES =	68.51			

I	L	RA-FIELD	RA-MODEL	P/C ERROR
1	1.000	115.240	114.614	-0.543
2	1.250	89.750	90.984	1.375
3	1.600	78.330	78.947	0.787
4	2.000	74.700	74.184	-0.691
5	2.500	72.120	71.232	-1.243
6	3.200	68.500	68.557	0.083
7	4.000	65.870	65.910	0.061
8	5.000	64.300	63.305	-1.670
9	6.300	60.360	60.726	0.606
10	8.000	57.010	58.445	2.516
11	10.000	56.040	56.614	1.023
12	12.500	56.140	55.020	-1.994
13	16.000	53.740	53.117	-1.159
14	20.000	50.480	51.000	1.029
15	25.000	49.130	48.168	-2.018
16	32.000	44.100	44.403	0.687
17	40.000	40.780	40.503	-0.679
18	50.000	37.030	36.782	-0.128
19	63.000	34.070	34.230	0.471
20	80.000	33.040	32.990	-0.151
21	100.000	33.300	33.288	-0.037
22	125.000	35.300	34.940	-1.020

RMS P/C ERROR = 0.90

SCHLUMBERGER INTERPRETATION: 6PT/DECADE

● KG4

RMS P/C CUTOFF : 0.10
NUMBER OF LAYERS = 4

INITIAL MODEL... * : FIXED PARAMETER

			DEPTH	T=THICK*RES	S=THICK/RES
			0.00		
THICK = 0.49	RES =	276.00		135.24	0.002
			0.49		
THICK = 14.51	RES =	50.00		725.50	0.290
			15.00		
THICK = 27.00	RES =	25.50		688.50	1.059
			42.00		
	RES =	35.00			

INTERPRETED MODEL... * : FIXED PARAMETER

			DEPTH	T=THICK*RES	S=THICK/RES
			0.00		
THICK = 0.47	RES =	280.11		131.74	0.002
			0.47		
THICK = 14.86	RES =	50.46		749.71	0.294
			15.33		
THICK = 10.02	RES =	9.69		97.10	1.034
			25.35		
	RES =	39.39			

I	L	RA-FIELD	RA-MODEL	P/C ERROR
1	1.000	149.950	152.338	1.593
2	1.250	126.000	117.260	-6.937
3	1.600	88.240	87.812	-0.485
4	2.000	70.170	69.804	-0.521
5	2.500	56.130	60.006	6.906
6	3.200	52.120	54.802	5.146
7	4.000	50.660	52.686	3.990
8	5.000	51.030	51.675	1.263
9	6.300	52.710	50.883	-3.467
10	8.000	52.350	50.107	-4.284
11	10.000	49.730	49.126	-1.214
12	12.500	48.260	47.675	-1.217
13	16.000	46.470	45.151	-2.832
14	20.000	42.370	41.934	-0.581
15	25.000	38.210	37.947	-0.689
16	32.000	32.070	33.682	5.027
17	40.000	32.770	30.920	-5.646
18	50.000	30.520	29.940	-1.953
19	63.000	30.040	31.130	3.629
20	80.000	34.000	33.895	-0.306
21	100.000	37.600	37.417	-0.486
22	125.000	35.900	41.163	15.952

RMS P/C ERROR = 3.11

SCHLUMBERGER INTERPRETATION: 6PT/DECADE

● LH4

RMS P/C CUTOFF = 0.10
NUMBER OF LAYERS = 4

INITIAL MODEL... * = FIXED PARAMETER

		DEPTH	T=THICK*RES	S=THICK/RES
		0.00		
THICK = 0.46	RES = 140.00		64.40	0.003
		0.46		
THICK = 2.91	RES = 19.00		55.29	0.153
		3.37		
THICK = 7.73	RES = 12.00		92.76	0.644
		11.10		
RES = 56.00				

INTERPRETED MODEL... * = FIXED PARAMETER

		DEPTH	T=THICK*RES	S=THICK/RES
		0.00		
THICK = 0.36	RES = 239.29		85.12	0.001
		0.36		
THICK = 2.14	RES = 21.65		46.33	0.099
		2.50		
THICK = 7.04	RES = 11.81		83.20	0.596
		9.54		
RES = 46.48				

I	L	RA-FIELD	RA-MODEL	P/C ERROR
1	1.000	71.310	71.211	-0.139
2	1.250	47.310	46.249	-2.243
3	1.400	31.570	32.114	1.723
4	2.000	25.640	25.412	-0.890
5	2.500	21.970	22.116	0.665
6	3.200	20.330	20.280	-0.219
7	4.000	18.070	18.736	3.686
8	5.000	17.110	17.375	1.548
9	6.300	17.020	16.159	-5.056
10	8.000	15.630	15.470	-1.027
11	10.000	14.830	15.447	4.157
12	12.500	16.260	16.233	-0.167
13	16.000	18.300	17.893	-2.225
14	20.000	20.300	20.067	-1.146
15	25.000	22.640	22.779	0.613
16	32.000	25.380	25.840	1.811
17	40.000	29.130	28.774	-1.221
18	50.000	32.000	31.688	-0.975
19	63.000	37.500	34.537	-7.901

RMS P/C ERROR = 2.26

● LA5
0

RMS P/C CUTOFF = 0.10
NUMBER OF LAYERS = 4

INITIAL MODEL... * = FIXED PARAMETER

		DEPTH	T=THICK*RES	S=THICK/RES
		0.00		
THICK = 0.43	RES = 280.00		120.40	0.002
		0.43		
THICK = 7.07	RES = 70.00		494.90	0.101
		7.50		
THICK = 32.50	RES = 50.00		1625.00	0.650
		40.00		
RES = 150.00				

INTERPRETED MODEL... * = FIXED PARAMETER

		DEPTH	T=THICK*RES	S=THICK/RES
		0.00		
THICK = 0.40	RES = 295.51		119.48	0.001
		0.40		
THICK = 7.96	RES = 72.26		575.11	0.110
		8.36		
THICK = 7.53	RES = 35.45		266.85	0.212
		15.89		
RES = 70.25				

	L	RA-FIELD	RA-MODEL	P/C ERROR
1	1.000	153.230	152.801	-0.313
2	1.250	116.590	122.180	4.802
3	1.600	101.260	99.732	-1.509
4	2.000	86.030	86.813	0.910
5	2.500	82.900	79.695	-3.866
6	3.700	75.970	75.926	-0.057
7	4.000	72.570	73.979	1.942
8	5.000	70.920	72.646	2.434
9	6.300	71.540	71.200	-0.475
10	8.000	69.190	69.269	0.114
11	10.000	69.060	66.891	-3.141
12	12.500	63.230	63.723	0.779
13	16.000	58.650	60.021	2.337
14	20.000	55.980	57.039	1.891
15	25.000	58.210	55.394	-4.857
16	32.000	54.760	55.238	0.879
17	40.000	53.340	56.698	6.295
18	50.000	57.540	58.881	2.331
19	63.000	65.540	61.340	-6.408
20	80.000	70.010	63.750	-8.934

RMS P/C ERROR = 3.26

SCHLUMBERGER INTERPRETATION: 6PT/DECADE

● KNS

RMS P/C CUTOFF : 0.10
NUMBER OF LAYERS = 4

INITIAL MODEL... * : FIXED PARAMETER

			DEPTH	T=THICK*RES	S=THICK/RES
			0.00		
THICK = 0.40	RES = 94.00			37.60	0.004
			0.40		
THICK = 2.70	RES = 19.50			52.65	0.138
			3.10		
THICK = 47.90	RES = 38.00			1820.20	1.261
			51.00		
	RES = 150.00				

INTERPRETED MODEL... * : FIXED PARAMETER

			DEPTH	T=THICK*RES	S=THICK/RE
			0.00		
THICK = 0.63	RES = 54.11			33.95	0.012
			0.63		
THICK = 1.43	RES = 12.87			18.35	0.111
			2.05		
THICK = 42.51	RES = 36.89			1568.03	1.152
			44.56		
	RES = 147.24				

KNS

I	L	RA-FIELD	RA-MODEL	P/C ERROR
1	1.000	40.930	40.022	-2.218
2	1.250	33.810	34.321	1.512
3	1.600	26.240	27.875	6.232
4	2.000	24.370	23.342	-4.217
5	2.500	21.810	20.835	-4.473
6	3.200	19.560	20.029	2.393
7	4.000	20.530	20.962	2.105
8	5.000	21.150	22.704	7.348
9	6.300	25.760	24.854	-3.515
10	8.000	28.430	27.125	-4.592
11	10.000	30.720	29.124	-5.196
12	12.500	30.300	30.916	2.033
13	16.000	32.670	32.671	0.002
14	20.000	33.420	34.076	1.963
15	25.000	34.310	35.401	3.150
16	32.000	37.280	36.998	-0.756
17	40.000	38.670	38.832	0.420
18	50.000	40.430	41.406	2.413
19	63.000	44.600	45.232	1.417
20	80.000	51.900	50.765	-2.187
21	100.000	58.080	57.429	-1.120
22	125.000	64.730	65.382	0.930
23	160.000	73.610	73.127	-0.638
24	200.000	82.580	84.440	2.252
25	250.000	105.700	93.885	-11.245

RMS P/C ERROR = 3.39

SCHLUMBERGER INTERPRETATION: 6PT/DECADE

● KES

RMS P/C CUTOFF : 0.10
NUMBER OF LAYERS = 4

INITIAL MODEL... * : FIXED PARAMETER

			DEPTH	T=THICK*RES	S=THICK/RES
			0.00		
THICK = 0.58	RES = 105.00			60.90	0.006
			0.58		
THICK = 3.62	RES = 27.00			97.74	0.134
			4.20		
THICK = 47.80	RES = 42.00			2007.60	1.138
			52.00		
	RES = 166.00				

INTERPRETED MODEL... * : FIXED PARAMETER

			DEPTH	T=THICK*RES	S=THICK/RES
			0.00		
THICK = 0.72	RES = 84.29			61.04	0.009
			0.72		
THICK = 1.43	RES = 19.00			27.19	0.075
			2.16		
THICK = 56.20	RES = 40.15			2256.24	1.400
			58.35		
	RES = 200.61				

I	L	RA-FIELD	RA-MODEL	P/C ERROR
1	1.000	68.000	66.998	-1.474
2	1.250	61.300	58.907	-3.903
3	1.600	45.300	48.023	6.010
4	2.000	39.630	39.333	-0.750
5	2.500	33.500	33.165	-0.999
6	3.200	27.830	29.326	5.380
7	4.000	28.510	28.803	1.029
8	5.000	28.000	29.679	5.997
9	6.300	31.250	31.383	0.427
10	8.000	33.370	33.275	-0.285
11	10.000	37.000	34.905	-5.662
12	12.500	35.910	36.276	1.019
13	16.000	37.370	37.548	0.476
14	20.000	40.920	38.513	-5.882
15	25.000	40.710	39.394	-3.232
16	32.000	37.020	40.483	9.354
17	40.000	39.300	41.795	6.348
18	50.000	44.700	43.825	-1.958
19	63.000	48.600	47.133	-3.019
20	80.000	53.070	52.527	-1.024
21	100.000	59.400	59.731	0.422
22	125.000	64.510	69.091	7.566
23	160.000	85.600	82.713	-3.373
24	200.000	99.050	96.833	-2.238
25	250.000	106.750	112.689	5.563

RMS P/C ERROR = 3.62

SCHLUMBERGER INTERPRETATION: APT/DECCAN

● KD3

RMS P/C CUTOFF : 0.10
NUMBER OF LAYERS = 4

INITIAL MODEL... * : FIXED PARAMETER

		DEPTH	T=THICK*RES	S=THICK/RES
		0.00		
THICK = 0.42	RES = 162.00		79.08	0.003
		0.42		
THICK = 5.81	RES = 42.00		244.02	0.138
		6.30		
THICK = 27.70	RES = 29.00		803.30	0.955
		34.00		
RES = 460.00				

INTERPRETED MODEL... * : FIXED PARAMETER

		DEPTH	T=THICK*RES	S=THICK/RES
		0.00		
THICK = 0.44	RES = 197.12		87.03	0.002
		0.44		
THICK = 10.26	RES = 42.11		432.11	0.244
		10.70		
THICK = 12.11	RES = 12.40		150.23	0.977
		22.82		
RES = 608.44				

I	L	RA-FIELD	RA-MODEL	P/C ERROR
1	1.000	106.020	105.680	-0.307
2	1.250	83.350	82.643	-0.609
3	1.600	63.780	64.926	1.643
4	2.000	54.300	54.057	-0.448
5	2.500	48.470	48.101	-0.761
6	3.200	45.350	44.957	-0.867
7	4.000	42.090	43.516	3.389
8	5.000	42.030	42.674	1.533
9	6.300	43.050	41.851	-2.785
10	8.000	42.940	40.815	-4.948
11	10.000	38.320	39.459	2.972
12	12.500	37.250	37.480	0.617
13	16.000	34.000	34.756	2.223
14	20.000	32.180	32.212	0.101
15	25.000	32.230	30.522	-5.083
16	32.000	30.670	30.681	0.034
17	40.000	31.770	33.750	6.233
18	50.000	37.240	39.340	5.637
19	63.000	48.940	48.018	-1.885
20	80.000	65.090	59.926	-7.933
21	100.000	77.870	72.964	-6.300

RMS P/C ERROR = 2.97

SCHLUMBERGER INTERPRETATION: APT/DECCAN

● KA6

RMS P/C CUTOFF : 0.10
NUMBER OF LAYERS = 3

INITIAL MODEL... * : FIXED PARAMETER

		DEPTH	T=THICK*RES	S=THICK/RES
		0.00		
THICK = 1.20	RES = 180.00		216.00	0.007
		1.20		
THICK = 10.80	RES = 23.00		248.40	0.470
		12.00		
RES = 68.00				

		DEPTH	T=THICK*RES	S=THICK/RES
		0.00		
THICK = 1.19	RES = 183.20		218.60	0.007
		1.19		
THICK = 11.98	RES = 22.54		269.94	0.531
		13.17		
RES = 73.51				

I	L	RA-FIELD	RA-MODEL	P/C ERROR
1	1.000	171.170	168.280	-1.684
2	1.250	157.180	157.896	0.456
3	1.600	146.000	139.485	-4.462
4	2.000	109.450	117.623	7.467
5	2.500	87.240	92.083	5.557
6	3.200	67.100	65.715	-2.064
7	4.000	44.770	46.605	4.098
8	5.000	35.930	34.629	-3.621
9	6.300	29.020	28.193	-2.876
10	8.000	25.720	25.497	-1.631
11	10.000	24.770	25.152	1.542
12	12.500	25.120	25.711	2.353
13	16.000	25.950	27.378	5.579
14	20.000	30.110	29.804	-1.016
15	25.000	33.370	33.046	-0.971
16	32.000	37.690	37.454	-0.625
17	40.000	44.560	41.053	-5.949
18	50.000	47.030	46.441	-1.252
19	63.000	49.560	51.101	3.110
20	80.000	55.800	55.641	-0.292
21	100.000	62.670	59.463	-5.117

RMS P/C ERROR = 3.50

```
WENNER INTERPRETATION, 4PT/DECADE, NE
WENNER ARRAY RESISTIVITIES..
   55.200    38.940    29.740    27.210    24.370    24.480    24.010    24.480
   25.260    26.500    29.860    32.240    36.490    42.700    51.840    56.860
CALCULATED 4PT RESISTIVITIES..
   50.300    38.402    29.204    24.648    24.179    24.629    26.511    31.138
   37.250    50.199    58.679
```

● KD6

```
                RMS P/C  CUTOFF  = 0.10
                NUMBER OF LAYERS =  4

 INITIAL    MODEL...                          * : FIXED PARAMETER

                                          DEPTH          T=THICK*RES     S=THICK/RES
                                          0.00
 THICK =   0.49     RES =    68.00
                                          0.49            33.32           0.007
 THICK =  17.51     RES =    24.00
                                         18.00           420.24           0.730
 THICK =  39.00     RES =    47.00
                                         57.00          1833.00           0.830
                    RES =    85.00

 INTERPRETED MODEL...                    * : FIXED PARAMETER

                                          DEPTH          T=THICK*RES     S=THICK/RES
                                          0.00
 THICK =   0.44     RES =    70.42
                                          0.44            30.95           0.006
 THICK =  14.26     RES =    23.03
                                         14.70           329.84           0.599
 THICK =  63.98     RES =    38.54
                                         78.69          2466.03           1.660
                    RES =   235.66
```

```
BEST FIT 4PT RESISTIVITIES..
   55.414    39.280    28.268    24.914    24.285    24.692    26.635    30.821
   37.472    49.814    72.923
    I          L          RA-FIELD        RA-MODEL        P/C ERROR

    1        0.500        55.200          55.414           -0.369
    2        1.000        38.940          38.466            1.463
    3        1.500        29.740          28.990           -2.523
    4        2.000        27.210          26.362           -3.115
    5        3.000        24.370          24.743            1.533
    6        4.000        24.480          24.325           -0.633
    7        6.000        24.010          24.282            1.134
    8        8.000        24.480          24.520            0.163
    9       12.000        25.260          25.479            0.866
   10       16.000        26.500          26.698            0.748
   11       24.000        29.860          29.436           -1.419
   12       32.000        32.240          32.022           -0.676
   13       48.000        36.490          36.872            1.047
   14       64.000        42.700          41.065           -3.824
   15       96.000        51.840          52.108            0.517
   16      128.000        56.860          62.666           10.210

        RMS P/C ERROR =  2.91
1
WENNER INTERPRETATION, 4PT/DECADE, NE
WENNER ARRAY RESISTIVITIES..
   23.830    35.560    26.700    25.720    23.830    21.840    21.600    21.390
   21.600    22.670    25.480    27.920    32.570    37.400    43.130    50.340
CALCULATED 4PT RESISTIVITIES..
   38.690    30.730    26.370    24.195    21.544    21.354    22.611    26.759
   33.212    41.878    60.627
```

● KC6

```
                RMS P/C  CUTOFF  = 0.10
                NUMBER OF LAYERS =  4

 INITIAL    MODEL...                          * : FIXED PARAMETER

                                          DEPTH          T=THICK*RES     S=THICK/RES
                                          0.00
 THICK =   0.75     RES =    43.50
                                          0.75            32.63           0.017
 THICK =  20.25     RES =    22.00
                                         21.00           445.50           0.920
 THICK =  45.00     RES =    43.00
                                         66.00          1935.00           1.047
                    RES =    77.00

 INTERPRETED MODEL...                    * : FIXED PARAMETER

                                          DEPTH          T=THICK*RES     S=THICK/RES
                                          0.00
 THICK =   0.74     RES =    42.70
                                          0.74            31.80           0.017
 THICK =  20.32     RES =    20.83
                                         21.06           423.23           0.975
 THICK =  94.65     RES =    46.40
                                        115.72          4391.43           2.040
                    RES =   116.94
```

```
BEST FIT 4PT RESISTIVITIES..
   40.404    35.631    28.346    23.303    21.591    21.456    22.730    26.607
   33.287    41.839    59.703
    I          L          RA-FIELD        RA-MODEL        P/C ERROR

    1        0.500        38.690          40.404            4.428
    2        1.000        35.560          34.136           -4.003
    3        1.500        26.700          28.965            8.482
    4        2.000        25.720          25.936            0.840
    5        3.000        23.830          22.987           -3.537
    6        4.000        21.840          21.995            0.709
    7        6.000        21.600          21.391           -0.956
    8        8.000        21.390          21.374           -0.075
    9       12.000        21.600          21.885            1.319
   10       16.000        22.670          22.784            0.502
   11       24.000        25.480          25.277           -0.798
   12       32.000        27.920          27.882           -0.136
   13       48.000        32.570          32.734            0.504
   14       64.000        37.400          36.661           -1.977
   15       96.000        43.130          43.186            0.129
   16      128.000        50.340          48.831           -2.998

        RMS P/C ERROR =  2.91
```

```
WENNER INTERPRETATION, 4PT/DECADE, NE
WENNER ARRAY RESISTIVITIES..
   45.350    25.200    14.650    12.300    10.320     9.680    10.030    10.590
   13.230    15.260    18.400    22.110    28.440    33.150    37.390    47.930
CALCULATED 4PT RESISTIVITIES..
   45.350    29.911    14.061    10.614     9.711    11.473    15.171    20.311
   29.106    37.983    59.200
```

● KD6

```
                  RMS P/C  CUTOFF  : 0.10
                  NUMBER OF LAYERS =  4

 INITIAL    MODEL...                          * : FIXED PARAMETER

                                                DEPTH      T=THICK*RES      S=THICK/RES
                                                 0.00
 THICK =    0.60      RES =     57.00                          34.20            0.011
                                                 0.60
 THICK =   10.77      RES =      9.80                         105.55            1.099
                                                11.37
 THICK =   63.63      RES =     40.00                        2545.20            1.591
                                                75.00
                      RES =    107.00

 INTERPRETED MODEL...                          * : FIXED PARAMETER

                                                DEPTH      T=THICK*RES      S=THICK/RES
                                                 0.00
 THICK =    0.53      RES =     58.53                          31.18            0.009
                                                 0.53
 THICK =    9.69      RES =      9.29                          90.06            1.043
                                                10.23
 THICK =   92.39      RES =     37.79                        3491.81            2.443
                                               102.62
                      RES =    539.72
```

```
RMSE FIT 4PT RESISTIVITIES..
   46.090    28.827    14.561    10.242     9.983    11.349    15.029    20.084
   28.210    38.603    58.435
    I          L          RA-FIELD          RA-MODEL          P/C ERROR

    1        0.500            45.350            46.090             1.632
    2        1.000            25.200            25.066            -0.532
    3        1.500            14.650            15.415             5.221
    4        2.000            12.300            12.122            -1.449
    5        3.000            10.320            10.080            -2.327
    6        4.000             9.680             9.807             1.314
    7        6.000            10.030            10.226             1.955
    8        8.000            10.980            10.959            -0.193
    9       12.000            13.230            12.975            -1.931
   10       16.000            15.260            15.128            -0.865
   11       24.000            18.400            17.069            -7.230
   12       32.000            22.110            22.365             1.152
   13       48.000            28.440            27.615            -2.899
   14       64.000            33.150            32.087            -3.205
   15       96.000            39.390            40.568             2.990
   16      128.000            47.930            49.407             3.049

      RMS P/C ERROR =  2.61
```

SCHLUMBERGER INTERPRETATION: 6PT/DECADE

● KD6

```
                  RMS P/C  CUTOFF  : 0.10
                  NUMBER OF LAYERS =  4

 INITIAL    MODEL...                          * : FIXED PARAMETER

                                                DEPTH      T=THICK*RES      S=THICK/RES
                                                 0.00
 THICK =    0.50      RES =    130.00                          77.14            0.004
                                                 0.50
 THICK =    3.72      RES =     11.60                          43.15            0.321
                                                 4.30
 THICK =    6.70      RES =     27.40                         183.58            0.245
                                                11.00
                      RES =     41.00

 INTERPRETED MODEL...                          * : FIXED PARAMETER

                                                DEPTH      T=THICK*RES      S=THICK/RES
                                                 0.00
 THICK =    0.52      RES =    176.57                          91.60            0.003
                                                 0.52
 THICK =    5.91      RES =     11.31                          66.82            0.522
                                                 6.42
 THICK =   80.54      RES =     34.97                        2816.73            2.303
                                                86.96
                      RES =     51.12
```

```
    I          L          RA-FIELD          RA-MODEL          P/C ERROR

    1        1.000            24.050            20.161            -4.135
    2        1.250            18.630            64.424             9.092
    3        1.600            37.120            38.957             4.948
    4        2.000            24.090            24.054            -2.153
    5        2.500            17.860            16.970            -4.904
    6        3.200            13.050            13.322            -3.811
    7        4.000            12.080            12.450             3.060
    8        5.000            11.720            12.471             6.410
    9        6.300            12.720            12.872             1.125
   10        8.000            13.380            13.736             2.662
   11       10.000            15.000            14.934            -5.483
   12       12.500            15.950            16.538             3.690
   13       16.000            17.090            18.666             4.339
   14       20.000            21.510            20.784            -3.373
   15       25.000            23.480            22.954            -2.240
   16       32.000            25.000            25.305             1.221
   17       40.000            26.700            27.293             2.221
   18       50.000            29.160            29.125            -0.121
   19       63.000            30.920            30.843            -0.442
   20       80.000            33.040            32.480            -1.694
   21      100.000            33.750            33.968             0.630
   22      125.000            35.460            35.527             0.189
   23      160.000            38.100            37.396            -1.847
   24      200.000            42.660            39.282            -7.919

      RMS P/C ERROR =  4.11
```

SCHLUMBERGER INTERPRETATION: 6PT/DECADE

● KA7

RMS P/C CUTOFF : 0.10
NUMBER OF LAYERS = 3

INITIAL MODEL... * : FIXED PARAMETER

		DEPTH	T=THICK*RES	S=THICK/RES
		0.00		
THICK = 0.41	RES = 228.00		92.34	0.002
		0.41		
THICK = 7.35	RES = 12.00		88.14	0.612
		7.75		
	RES = 34.00			

INTERPRETED MODEL... * : FIXED PARAMETER

		DEPTH	T=THICK*RES	S=THICK/RES
		0.00		
THICK = 0.44	RES = 152.61		67.34	0.003
		0.44		
THICK = 5.84	RES = 11.05		64.51	0.529
		6.28		
	RES = 32.42			

I	L	RA-FIELD	RA-MODEL	P/C ERROR
1	1.000	61.970	62.399	0.692
2	1.250	46.100	41.510	-9.956
3	1.600	24.520	25.587	4.350
4	2.000	16.940	17.330	4.777
5	2.500	13.980	13.635	-2.466
6	3.200	11.890	12.188	2.508
7	4.000	11.650	11.672	0.182
8	5.000	12.720	12.052	-5.253
9	6.300	12.770	12.490	-2.175
10	8.000	12.630	13.330	5.546
11	10.000	14.340	14.476	0.950
12	12.500	16.080	15.951	-0.850
13	16.000	18.540	17.976	-3.042
14	20.000	20.190	19.928	-1.299
15	25.000	20.740	21.902	5.602
16	32.000	23.990	24.003	0.055
17	40.000	25.090	25.735	2.572
18	50.000	27.210	27.267	0.209
19	63.000	28.500	28.602	0.352
20	80.000	28.540	29.708	4.093
21	100.000	31.330	30.503	-2.640
22	125.000	34.310	31.076	-9.367

RMS P/C ERROR = 1.80

SCHLUMBERGER INTERPRETATION: 6PT/DECADE

● KD7

RMS P/C CUTOFF : 0.10
NUMBER OF LAYERS = 4

INITIAL MODEL... * : FIXED PARAMETER

		DEPTH	T=THICK*RES	S=THICK/RES
		0.00		
THICK = 0.65	RES = 70.00		45.50	0.009
		0.65		
THICK = 6.05	RES = 10.80		65.34	0.560
		6.70		
THICK = 60.30	RES = 31.00		1869.30	1.945
		67.00		
	RES = 69.00			

INTERPRETED MODEL... * : FIXED PARAMETER

		DEPTH	T=THICK*RES	S=THICK/RES
		0.00		
THICK = 0.64	RES = 74.02		47.30	0.009
		0.64		
THICK = 5.66	RES = 10.08		57.00	0.561
		6.30		
THICK = 54.78	RES = 29.57		1619.94	1.852
		61.07		
	RES = 72.95			

I	L	RA-FIELD	RA-MODEL	P/C ERROR
1	1.000	50.700	51.046	0.683
2	1.250	41.640	41.707	0.161
3	1.600	30.680	30.276	-1.317
4	2.000	21.610	21.972	1.676
5	2.500	16.830	16.420	-2.435
6	3.200	12.750	12.889	1.093
7	4.000	11.630	11.678	0.414
8	5.000	11.400	11.357	-0.378
9	6.300	11.600	11.607	0.057
10	8.000	12.570	12.330	-1.906
11	10.000	13.430	13.376	-0.400
12	12.500	14.710	14.770	0.408
13	16.000	17.030	16.609	-2.471
14	20.000	18.150	18.420	1.531
15	25.000	19.630	20.292	3.374
16	32.000	21.850	22.351	2.293
17	40.000	24.210	24.174	-0.150
18	50.000	27.210	26.028	-4.345
19	63.000	27.440	28.071	2.300
20	80.000	31.040	30.523	-1.665
21	100.000	33.900	33.250	-1.916
22	125.000	36.660	36.578	-0.223
23	160.000	39.640	40.828	2.996
24	200.000	44.680	45.054	0.838
25	250.000	52.030	49.416	-5.024

RMS P/C ERROR = 1.65

SCHLUMBERGER INTERPRETATION: GPT/DELUADE

● PC7

RMS P/C CUTOFF = 0.10
NUMBER OF LAYERS = 4

INITIAL MODEL... * : FIXED PARAMETER

		DEPTH	T=THICK*RES	S=THICK/RES
		0.00		
THICK = 0.83	RES = 160.00		139.44	0.005
		0.83		
THICK = 9.17	RES = 12.00		110.04	0.764
		10.00		
THICK = 30.00	RES = 30.00		900.00	1.000
		40.00		
RES = 62.00				

INTERPRETED MODEL... * : FIXED PARAMETER

		DEPTH	T=THICK*RES	S=THICK/RES
		0.00		
THICK = 0.79	RES = 176.90		140.29	0.004
		0.79		
THICK = 6.88	RES = 11.41		78.53	0.603
		7.68		
THICK = 9.45	RES = 16.70		157.86	**0.566**
		17.13		
RES = 44.80				

I	L	RA-FIELD	RA-MODEL	P/C ERROR
1	1.000	142.600	135.655	-4.870
2	1.250	113.690	114.816	0.990
3	1.600	79.120	84.466	6.756
4	2.000	57.500	58.510	1.757
5	2.500	36.750	37.215	1.265
6	3.200	23.490	22.465	-4.365
7	4.000	15.930	16.135	1.284
8	5.000	13.110	13.248	1.049
9	6.300	12.490	12.500	0.080
10	8.000	12.260	12.485	1.835
11	10.000	12.630	12.856	1.786
12	12.500	13.630	13.482	-1.087
13	16.000	14.990	14.544	-2.974
14	20.000	16.050	15.866	-1.144
15	25.000	17.350	17.563	1.229
16	32.000	19.570	19.872	1.543
17	40.000	21.860	22.307	2.046
18	50.000	24.720	24.977	1.039
19	63.000	28.000	27.853	-0.527
20	80.000	31.040	30.801	-0.770
21	100.000	34.340	33.420	-2.679
22	125.000	36.250	35.802	-1.236
23	160.000	39.070	38.090	-2.487
24	200.000	37.880	39.821	5.125
25	250.000	46.830	41.211	-11.992

RMS P/C ERROR = 2.80

● KD7

RMS P/C CUTOFF = 0.10
NUMBER OF LAYERS = 4

INITIAL MODEL... * : FIXED PARAMETER

		DEPTH	T=THICK*RES	S=THICK/RES
		0.00		
THICK = 0.81	RES = 216.00		174.96	0.004
		0.81		
THICK = 7.19	RES = 11.30		81.25	0.636
		8.00		
THICK = 34.00	RES = 23.00		782.00	1.478
		42.00		
RES = 77.00				

INTERPRETED MODEL... * : FIXED PARAMETER

		DEPTH	T=THICK*RES	S=THICK/RES
		0.00		
THICK = 0.75	RES = 245.57		185.29	0.003
		0.75		
THICK = 8.12	RES = 11.16		90.62	0.727
		8.87		
THICK = 35.90	RES = 22.43		805.32	1.600
		44.77		
RES = 91.78				

I	L	RA-FIELD	RA-MODEL	P/C ERROR
1	1.000	187.870	180.042	-4.167
2	1.250	145.000	148.571	2.463
3	1.600	100.880	104.54	3.629
4	2.000	65.690	68.652	4.509
5	2.500	41.360	40.743	-1.492
6	3.200	23.830	22.814	-4.263
7	4.000	16.260	15.794	-2.863
8	5.000	12.600	12.790	1.511
9	6.300	11.790	12.131	2.894
10	8.000	11.930	12.181	2.103
11	10.000	12.540	12.567	0.214
12	12.500	13.470	13.198	-2.016
13	16.000	14.440	14.205	-1.626
14	20.000	15.400	15.372	-0.180
15	25.000	16.630	16.715	0.514
16	32.000	18.060	18.410	1.937
17	40.000	19.760	20.146	1.953
18	50.000	22.700	22.228	-2.421
19	63.000	25.150	24.912	-0.947
20	80.000	28.540	28.451	-0.310
21	100.000	32.120	32.525	1.260
22	125.000	36.760	37.299	1.466

RMS P/C ERROR = 2.50

SCHLUMBERGER INTERPRETATION: 6PT/DECADE

● KE7

RMS P/C CUTOFF : 0.10
NUMBER OF LAYERS = 4

INITIAL MODEL... * : FIXED PARAMETER

		DEPTH	T=THICK*RES	S=THICK/RES
		0.00		
THICK = 0.65	RES = 480.00		312.00	0.001
		0.65		
THICK = 12.35	RES = 10.00		123.50	1.235
		13.00		
THICK = 18.00	RES = 20.00		360.00	0.900
		31.00		

RES = 70.00

INTERPRETED MODEL... * : FIXED PARAMETER

		DEPTH	T=THICK*RES	S=THICK/RES
		0.00		
THICK = 0.63	RES = 525.51		330.86	0.001
		0.63		
THICK = 16.94	RES = 9.80		165.99	1.729
		17.57		
THICK = 2.49	RES = 8.34		20.75	0.299
		20.06		

RES = 54.89

I	L	RA-FIELD	RA-MODEL	P/C ERROR
1	1.000	334.820	319.850	-4.471
2	1.250	220.300	240.667	9.243
3	1.600	139.400	144.316	3.526
4	2.000	82.310	79.579	-3.317
5	2.500	38.900	38.898	-0.005
6	3.200	18.610	19.388	4.181
7	4.000	11.820	12.629	6.843
8	5.000	10.000	10.539	5.443
9	6.300	10.550	10.192	-3.370
10	8.000	10.320	10.183	-1.307
11	10.000	9.900	10.246	3.491
12	12.500	10.250	10.388	1.346
13	16.000	10.740	10.754	0.131
14	20.000	11.020	11.352	2.991
15	25.000	12.360	12.330	-0.240
16	32.000	13.970	13.938	-0.227
17	40.000	15.750	15.960	1.333
18	50.000	17.730	18.465	4.147
19	63.000	21.520	21.492	-0.128
20	80.000	25.750	24.961	-3.178
21	100.000	29.520	28.410	-3.775
22	125.000	32.060	31.945	-0.360
23	160.000	34.530	35.844	3.804

RMS P/C ERROR = 3.04

● KE7

RMS P/C CUTOFF : 0.10
NUMBER OF LAYERS = 5

INITIAL MODEL... * : FIXED PARAMETER

		DEPTH	T=THICK*RES	S=THICK/RES
		0.00		
THICK = 0.87	RES = 242.00		210.54	0.004
		0.87		
THICK = 3.93	RES = 31.00		121.83	0.127
		4.80		
THICK = 7.70	RES = 9.50		73.15	0.811
		12.50		
THICK = 23.50	RES = 26.50		622.75	0.887
		36.00		

RES = 80.00

INTERPRETED MODEL... * : FIXED PARAMETER

		DEPTH	T=THICK*RES	S=THICK/RES
		0.00		
THICK = 0.61	RES = 322.29		195.37	0.002
		0.61		
THICK = 2.00	RES = 55.56		111.26	0.036
		2.61		
THICK = 23.76	RES = 17.94		429.82	1.335
		26.37		
THICK = 97.37	RES = 52.03		5066.22	1.871
		123.74		

RES = 187.03

I	L	RA-FIELD	RA-MODEL	P/C ERROR
1	1.000	223.890	219.114	-2.133
2	1.250	164.110	178.554	8.801
3	1.600	131.130	132.230	0.844
4	2.000	99.990	97.937	-2.053
5	2.500	74.790	73.735	-1.410
6	3.200	57.080	55.771	-2.293
7	4.000	43.730	45.115	3.167
8	5.000	35.240	36.915	4.752
9	6.300	29.920	30.071	0.506
10	8.000	26.800	25.047	-6.540
11	10.000	22.480	21.969	-2.275
12	12.500	19.940	20.382	2.218
13	16.000	19.120	19.652	2.782
14	20.000	19.580	19.660	0.408
15	25.000	20.440	20.195	-1.198
16	32.000	21.540	21.417	-0.573
17	40.000	23.410	23.207	-0.866
18	50.000	25.660	25.621	-0.151
19	63.000	28.680	28.766	0.299
20	80.000	32.240	32.561	0.996
21	100.000	36.320	36.615	0.813
22	125.000	39.700	41.189	3.750
23	160.000	49.230	47.139	-4.207
24	200.000	54.030	53.645	-0.705
25	250.000	59.070	61.360	3.877

RMS P/C ERROR = 2.32

● KV1

RMS P/C CUTOFF : 0.10
NUMBER OF LAYERS = 4

INITIAL MODEL... * : FIXED PARAMETER

		DEPTH	T=THICK*RES	S=THICK/RES
		0.00		
THICK = 0.69	RES = 870.00		600.30	0.001
		0.69		
THICK = 5.61	RES = 150.00		841.50	0.037
		6.30		
THICK = 27.70	RES = 54.00		1495.80	0.513
		34.00		
RES = 270.00				

INTERPRETED MODEL... * : FIXED PARAMETER

		DEPTH	T=THICK*RES	S=THICK/RES
		0.00		
THICK = 0.66	RES = 922.99		610.06	0.001
		0.66		
THICK = 8.08	RES = 150.11		1212.78	0.054
		8.74		
THICK = 1.26	RES = 3.30		4.15	0.381
		10.00		
RES = 356.30				

I	L	RA-FIELD	RA-MODEL	P/C ERROR
1	1.000	703.900	665.795	-5.413
2	1.250	582.140	555.969	4.462
3	1.600	443.420	418.173	-5.693
4	2.000	300.400	313.385	4.323
5	2.500	233.000	239.326	2.715
6	3.200	184.600	188.482	2.103
7	4.000	164.440	166.851	1.466
8	5.000	157.270	154.680	-1.615
9	6.300	146.730	145.964	-0.522
10	8.000	128.050	136.024	6.202
11	10.000	129.840	124.134	-4.395
12	12.500	113.320	108.449	-4.297
13	16.000	90.520	90.351	-0.186
14	20.000	78.400	76.203	-2.802
15	25.000	66.830	69.071	3.354
16	32.000	63.500	68.971	8.616
17	40.000	67.340	77.173	14.610
18	50.000	81.640	90.747	11.155

RMS P/C ERROR = 7.80

SCHLUMBERGER INTERPRETATION: 6PT/DECADE

● KV2

RMS P/C CUTOFF : 0.10
NUMBER OF LAYERS = 4

INITIAL MODEL... * : FIXED PARAMETER

		DEPTH	T=THICK*RES	S=THICK/RES
		0.00		
THICK = 0.25	RES = 370.00		97.50	0.001
		0.25		
THICK = 1.40	RES = 11.00		15.40	0.127
		1.65		
THICK = 38.35	RES = 17.00		651.95	2.256
		40.00		
RES = 250.00				

INTERPRETED MODEL... * : FIXED PARAMETER

		DEPTH	T=THICK*RES	S=THICK/RES
		0.00		
THICK = 0.26	RES = 350.00		92.40	0.001
		0.26		
THICK = 0.28	RES = 4.08		1.13	0.069
		0.54		
THICK = 39.19	RES = 15.96		625.55	2.455
		39.72		
RES = 256.19				

I	L	RA-FIELD	RA-MODEL	P/C ERROR
1	1.000	30.410	30.165	-0.805
2	1.250	15.670	15.859	1.209
3	1.600	11.710	11.997	2.452
4	2.000	11.230	11.697	5.096
5	2.500	12.260	12.573	2.554
6	3.200	13.810	13.498	-2.261
7	4.000	14.610	14.124	-3.329
8	5.000	17.020	14.647	-13.945
9	6.300	15.430	15.071	-2.329
10	8.000	15.320	15.407	+0.730
11	10.000	16.500	15.653	-5.135
12	12.500	16.040	15.859	-1.131
13	16.000	16.130	16.095	-0.217
14	20.000	16.100	16.380	1.736
15	25.000	16.220	16.824	3.726
16	32.000	16.200	17.677	9.118
17	40.000	18.460	19.006	14.095
18	50.000	19.440	21.108	8.579
19	63.000	23.230	24.406	5.062
20	80.000	30.040	29.210	-2.762
21	100.000	39.170	35.130	-10.313
22	125.000	48.400	42.437	-12.319

RMS P/C ERROR = 6.29

A.6.7 Computer Resistivity Model

KL

INTERPRETED MODEL... * : FIXED PARAMETER

		DEPTH	T=THICK*RES	S=THICK/RES
		0.00		
THICK = 0.48	RES = 36.29		17.55	0.013
		0.48		
THICK = 2.68	RES = 6.97		18.67	0.385
		3.16		
THICK = 20.86	RES = 18.89		393.92	1.104
		24.02		
THICK = 331.11	RES = 52.26		17303.80	6.336
		355.13		
	RES = 294.01			

INTERPRETED MODEL... * : FIXED PARAMETER

		DEPTH	T=THICK*RES	S=THICK/RES
		0.00		
THICK = 0.48	RES = 36.27		17.35	0.013
		0.48		
THICK = 2.67	RES = 6.96		18.61	0.384
		3.16		
THICK = 20.55	RES = 18.84		387.24	1.091
		23.71		
THICK = 298.22	RES = 51.62		15395.21	5.777
		321.93		
	RES = 246.38			

I	L	RA-FIELD	RA-MODEL	P/C ERROR
1	1.000	20.910	20.683	-1.086
2	1.250	16.890	16.211	-4.021
3	1.600	11.650	12.349	6.003
4	2.000	10.310	10.013	-2.874
5	2.500	9.050	8.834	-2.391
6	3.200	8.250	8.459	2.530
7	4.000	8.770	8.704	-0.752
8	5.000	9.210	9.323	1.222
9	6.300	10.200	10.236	0.354
10	8.000	11.360	11.374	0.121
11	10.000	12.580	12.549	-0.248
12	12.500	13.630	13.743	0.832
13	16.000	15.710	15.104	-3.858
14	20.000	16.640	16.382	-1.553
15	25.000	17.540	17.789	1.419
16	32.000	19.020	19.604	3.067
17	40.000	21.400	21.629	1.070
18	50.000	23.710	24.039	1.389
19	63.000	27.380	26.957	-1.546
20	80.000	30.400	30.273	-0.419
21	100.000	34.230	33.539	-2.022
22	125.000	37.650	36.797	-2.260
23	160.000	40.511	40.386	-0.309
24	200.000	42.400	43.629	2.897
25	250.000	45.880	47.042	2.532
26	320.000	51.790	51.390	-0.772
27	400.000	57.580	56.345	-2.144

RMS P/C ERROR = 1.97

APPENDIX 7

SEISMIC SURVEY

A.7.1 Refraction Method

A.7.2 Reflection Method

A.7.3 Seismic Configurations (Geometry)

A.7.4 Seismic Specifications

A.7.5 Seismic Reflection Velocity Intervals

A.7.6 Seismic Refraction Time-Distance Curves

A.7.1: Refraction Method

(Based on Rahn 1986)

Seismic method are widely used in petroleum exploration where dynamic explosions are commonly used. In engineering geology, a simple blasting cap, sledge hammer, or small explosive charge can be used to generate the seismic wave. Hand–held sledge hammers rarely provide ebnough energy to determine subsurface information for depths greater than 10 m, however.

The theory of refraction stems from the fact that any ray bends (refracts) upon entering a different velocity medium. Consider the expanding hemispherical shells of P waves radiating from a source, simplified in two dimensions as rays (Fig.1) The ray strikes the boundary at some angle of incidence (i), measured from a line perpendicular to the boundary. The angle of incidence changes to a refracted angle (r) when the wave travels through the new velocity medium. The larger the velocity differential between the two mediums, the larger angle r becomes with respect to angle i.

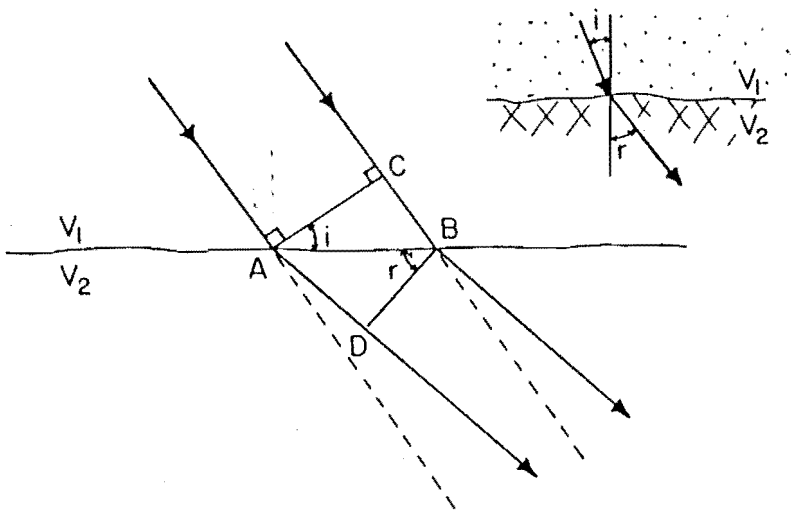

Fig 1: Refraction of elastic waves across an Interface

The precise relationship between refraction and velocity differential can be established using simple trigonometry. Consider Fig.1, where V_1 is the velocity of the first medium and V_2 is the velocity of the second medium. Two parallel rays are drawn as well as orthogonals AC and DB from the two rays. Consider the right triangle ACB and ADB:

$$BC = AB \sin i$$
$$AD = AB \sin r$$

The time for a wave to travel distance AD is the same as a wave traveling the distance BC:

$$t_{AD} = t_{CB}$$

Since time equals $\frac{\text{distance}}{\text{velocity}}$,

$$\frac{AD}{V_1} = \frac{BC}{V_2}$$

Substitute from above:

$$\frac{AB \sin r}{V_2} = \frac{AB \sin i}{V_1}$$

or

$$\frac{\sin i}{\sin r} = \frac{V_1}{V_2} \qquad (1)$$

Equation (1) is called Snell's law.

The depth (z) to some buried horizontal interface can be determined using Snell's law and the following theory. As a ray strikes the V_1 interface at increasingly smaller angles (i.e. angle i increases), there eventually will be a refracted ray which travels along the interface (i.e. angle $r = 90^0$). This angle of incidence is called the critical angle (i_c). Because $\sin 90^0 = 1$, from (1),

$$\sin i_c = \frac{V_1}{V_2} \qquad (2)$$

As waves travel along the boundary at velocity V_2, they continuously emit new disturbances into the upper medium, also at the critical angle. Consider geophones stationed at various distances (x) away from the seismic source (Fig.2). A short distance away, geophones pick up both the direct wave and the refracted wave. Geophones nearest the seismic source receive the direct wave first, traveling at velocity V_1. But, because the refracted wave travels along the interface at the faster velocity V_2, there will be a critical distance (x_c) beyond which the refracted wave reaches geophones before the direct wave. The relationship between x_c and depth (z) of a buried boundary can be derived as follows. The time–distance plot for the direct wave passed through the origin so that:

$$T = \frac{x}{V_1}$$

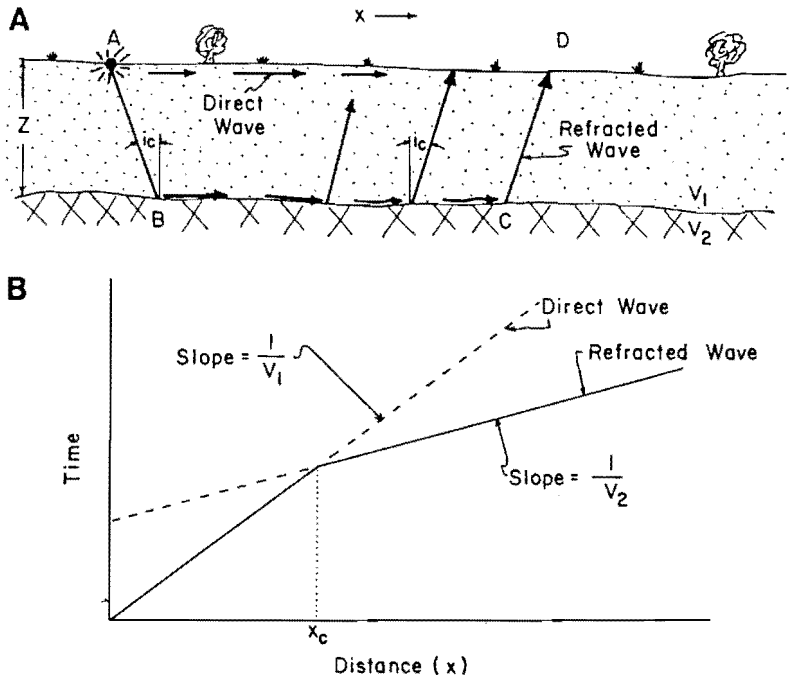

Figure 2: Ray paths for two layers seperated by a horizontal interface.

A. Geological cross section. B. Time–distance plot.

The refracted wave must traverse three legs in order to reach the geophone: distance AB,BC, and CD. Three trigonometric relations involving these legs are necessary for the folllwing derivation of the formula which determines the depth (z) to a buried interface:

$$\sin i_c = \frac{V_1}{V_2} \tag{2}$$

$$\cos i_c = (1-\sin^2 i_c)^{0.5} = (1 - V_1^2/V_2^2)^{0.5}$$

$$\tan i_c = \sin i_c/\cos i_c = V_1/(/V_2^2 - V_1^2)^{0.5}$$

The total time along refraction path ABCD is:

$$T = T_{AB} + T_{BC} + T_{CD}$$

For a thickness z, since time = $\frac{\text{distance}}{\text{velocity}}$, the above equation can be written as:

$$T = \frac{AB}{V_1} + \frac{BC}{V_2} + \frac{CD}{V_1}$$

From Fig 2,

$$T = \frac{z/\cos i_c}{V_1} + \frac{x - 2(z \tan i_c)}{V_2} + \frac{z/\cos i_c}{V_1}$$

Substituting trigonometric relationships yields:

$$T = \frac{2z}{V \cos i_c} - \frac{2 z \sin i_c/\cos i_c}{V_2} + \frac{x}{V_2}$$

$$T = \frac{2z}{V \cos i_c} \cdot (1 - \sin^2 i_c) + \frac{x}{V_2}$$

$$T = \frac{x}{V_2} + \frac{2z(V_2^2 - V_1^2)^{0.5}}{V_1 V_2}$$

At the critical distance, boh direct and refracted waves arrives at the same time so that:

$$T_{direct} = T_{refracted}$$

$$\frac{x_c}{V_1} = \frac{x_c}{V_2} + \frac{2z(V_2^2 - V_1^2)^{0.5}}{V_1 V_2},$$

which simplifies to

$$z = \frac{1}{2} \frac{V_1 V_2 \; x_c}{(V_2^2 - V_1^2)^{0.5}} \cdot \left(\frac{1}{V_1} - \frac{1}{V_2}\right),$$

$$z = \frac{x_c}{2} \frac{(V_2 - V_1)^{0.5}}{(V_2 + V_1)}.$$

A.7.2 Reflection Method

(Based on Rahn 1986)

The reflection method is used extensively for petroleum exploration. It gives a detailed picture of the subsurface structure and interfaces with an accuracy that is exceeded only by test holes. The depths are determined by observing the travel times of P waves generated near the surface which are reflected back from deep formations. The method is comparable to that of echo sounding used to determine water depths. A unique advantage of the reflection method is that it permits the mapping of many horizons from each shot.

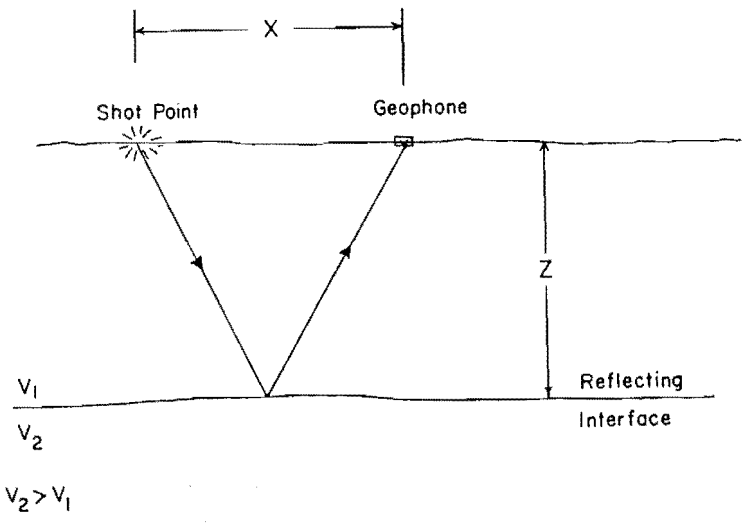

Figure 3 Wave reflected from a horizontal interface

If the seismic velocity of some overlying medium is a constant V_1, the wave will reflect from a horizontal interface at a depth z as shown in Fig.3. The total length (L) of the wave path to some distance(x) from the shot point is:

$$L = V_1T$$

where T is the total travel time.

$$L = 2\ (\frac{x^2}{2} + z^2)^{0.5}$$

Therefore,

$$z = 1/2\ ((V_1T)^2 - x^2)^{0.5}. \qquad (3)$$

When x = 0,

$$z = \frac{V_1T}{2} \qquad (4)$$

The reflection method also makes possible the calculation of depths to dipping interfaces, as well as the angle of dip (see Dobrin, 1982, for derivation of dip formula and examples).

In petroleum prospecting, multiple geophones are often used, giving continuous printout on tapes. When several closely spaced geophones are placed along a line and the resulting seismograms held together for continuous viewing, the waves themselves line up on the seismograms in a manner that allows the viewer to see the interfaces as if the seismograms were a geologic cross section. This is because the waves corresponding to a common reflection will all line up across the record in such a way that the crests or troughs on adjacent traces appear to fit together (CDP method) (see Dobrin, 1982).

A.7.3 Seismic Configuration

Recording parameters for Refraction line AA′

Source: Shallow dynamite
1 charge per source
1 m depth

Geophones: 28 Hz OYO strings – 6 phones per string

Geometry: No gap split spread

8 m group interval

geophone pattern – in line

32 m shot interval
each 3rd shot of 640 g of AN60
other shots 160 g of AN60

Spread Geometry:
No gap
Shots 2 m from nearest geophone
378 m maximum offset

Recording on at least 36 48 geophones
with as near even number of phones
on each side of the shot as possible

Typical layout

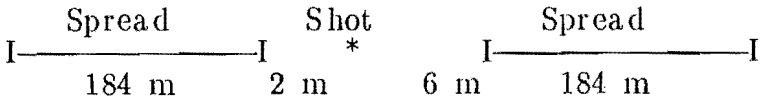

End shot

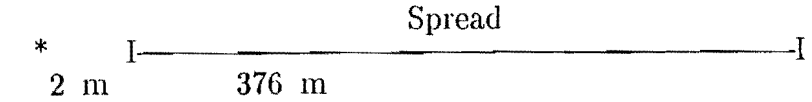

A.7.3 Continued

Recording parameters for Minisosie line BB'

Source	2 Minisosie tampers
Geophones	28 Hz OYO strings – 6 phones per string
Geometry:	Split spread

8 m group interval
geophone pattern – in line 1.6 m spacing

8 m shot interval
8 m ramming segment
1000 pops minimum
maximum RSF = 8

Spread geometry
32 m minimum of offset
(from center of ram segment to center of first geophone spread)
196 m maximum offset

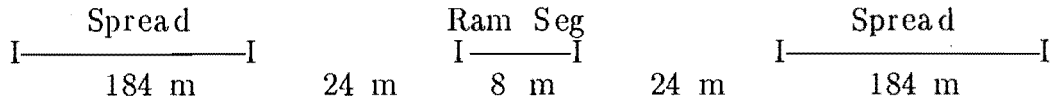

Recording	1 msec sample rate 1 second recording

Filters: Low – 25 Hz
Anti–Alias filter

2400% fold coverage

A.7.3 continued on nest page

A.7.3 Continued

Recording parameters for Minisosie line CC′

Source	2 Minisosie tampers
Geophones	28 Hz OYO strings – 6 phones per string
Geometry:	Split spread

8 m group interval
geophone pattern
– in line 1.6 m spacing

8 m shot interval
8 m ramming segment
1500 pops minimum
maximum RSF = 8

Spread geometry
32 m minimum of offset
(from center of ram segment to center of first geophone spread)
196 m maximum offset

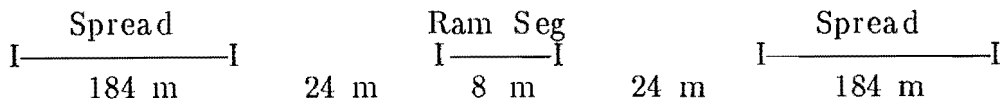

Recording	1 msec sample rate 1 second recording

Filters: Low – 25 Hz
Anti–Alias filter

1200% fold coverage

A.7.3 continued on next page

A.7.4: Technical Specifications of Geophysics Division's Special Seismic Equipment as at 17 February 1987

The specifications are:

Model	Sercel 338–HR	
Number of Channels		48/24
Sampling Rate	1/0.5 ms	
Transport	Truck mounted	
Seismic Sources	Explosives	
		Minisosie
Shot Timing	Radio/line	
Auxillary Channels		Up hole phone Confirmation Time break 2 spare
Amplifiers		
	Fixed gain	2**5 and 2**7 These are initial Actual gain increases during recording
	Variable gain	Floating point 84 dB in 12 dB steps
Input Impedence	1 MΩ	
Filters		
	anti–alias	yes (24 dB/Octave)
	hi–cut	anti–alias
	lo–cut	out–10–25 Hz
	notch	50 Hz
Digital Recording		
Digital format	floating point	
		15 bit manitsa 4 bit gain
Recording length	0–infinite	
Recording media	1200 foot mag tape	
Recording format	SEG–B	
Field Stacking	records up to 4 s at 1 ms sampling rate	
Monitor Recording		ERC–10C electrostatic camera
Playback filters		
	Hi–cut	80, 125 and 250 Hz
	Lo–cut	AGC, NON–AGC (gain is displayed)

A.7.4 Continued: Test Equipment

Line Test	for continuity	
		leakage
Equipment tests	for Amplifiers	
		A/D conversion
		cross talk
		noise

Auxiliary Equipment

	TRucks	Seismic truck – Stonefield
		Cable laying – Jeep J20
		Shot Firing – Jeep J20
	Radios	4 Tait FM mounted in trucks
		3 Tait FM hand held
		1 Tait FM radio repeater
		(All Tait radios operate on came two frequencies)
Cables	14×48 channel CDP cables with	
		12 taleouts at 12 m spacing
		2×100 m jumpers
		times 2 scrambler
		times 3 scrambler
Geophones	>100 14 Hz Metrix single geophones	
		>100 28 Hz OYO strings each with 6 geophones
		60 3 Hz refraction phones
Minisosie	2 road tampers and radios	
Explosive sources		2 hand–held motor augers
		loading poles
		shot firing equipment including radio repeater
Survey equipment	1 Wild tacheometer RDS–1	
		1 Wild automatic level
		3 staffs

The Division also has drill rigs which are available to drill deeper shot holes. The data from the equipment can be read on the Divisions VAX11/750 for display, and processing.

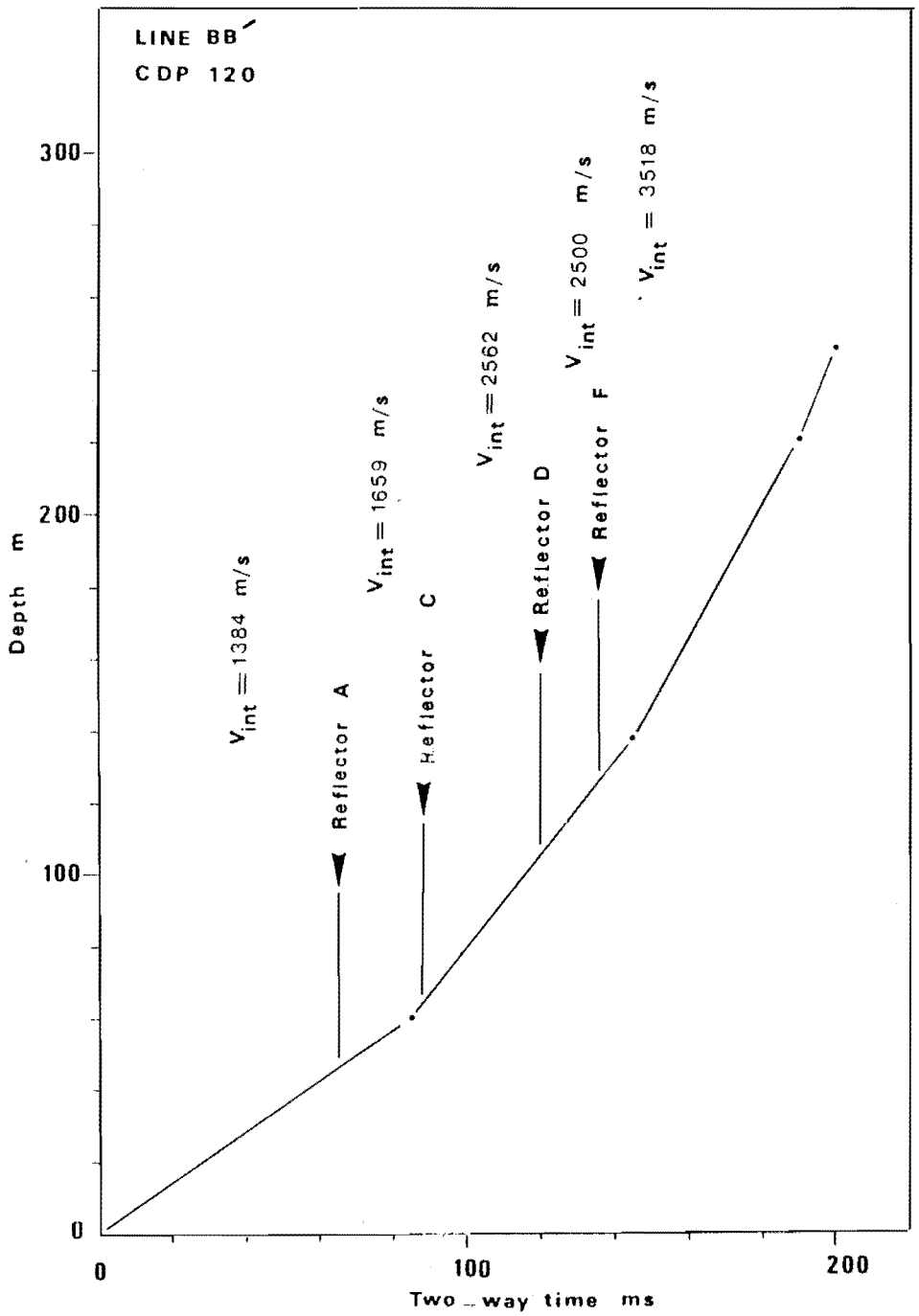

A.7.5 Seismic Reflection Velocity (Interval)

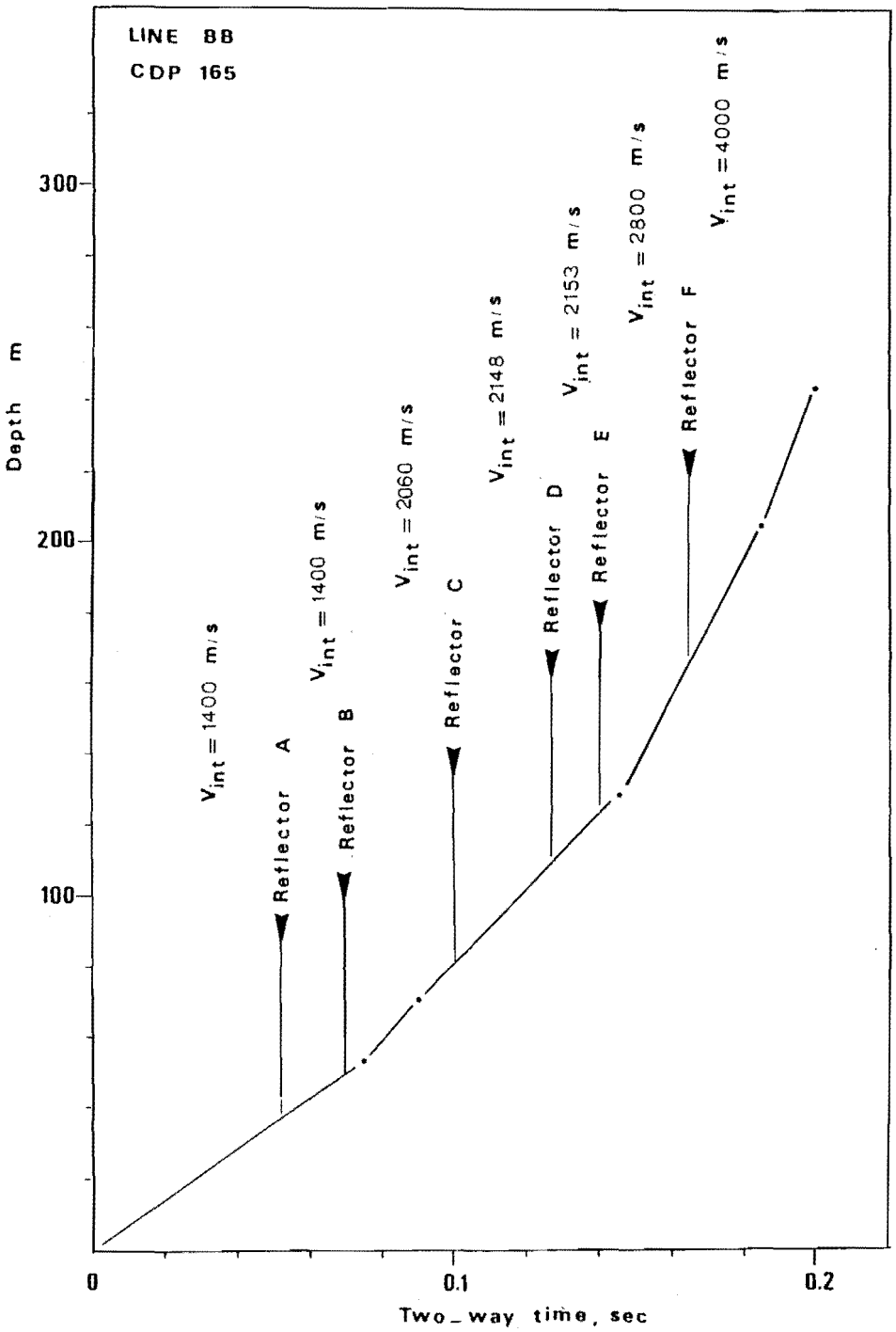

A.7.5 Seismic Reflection Velocity Interval

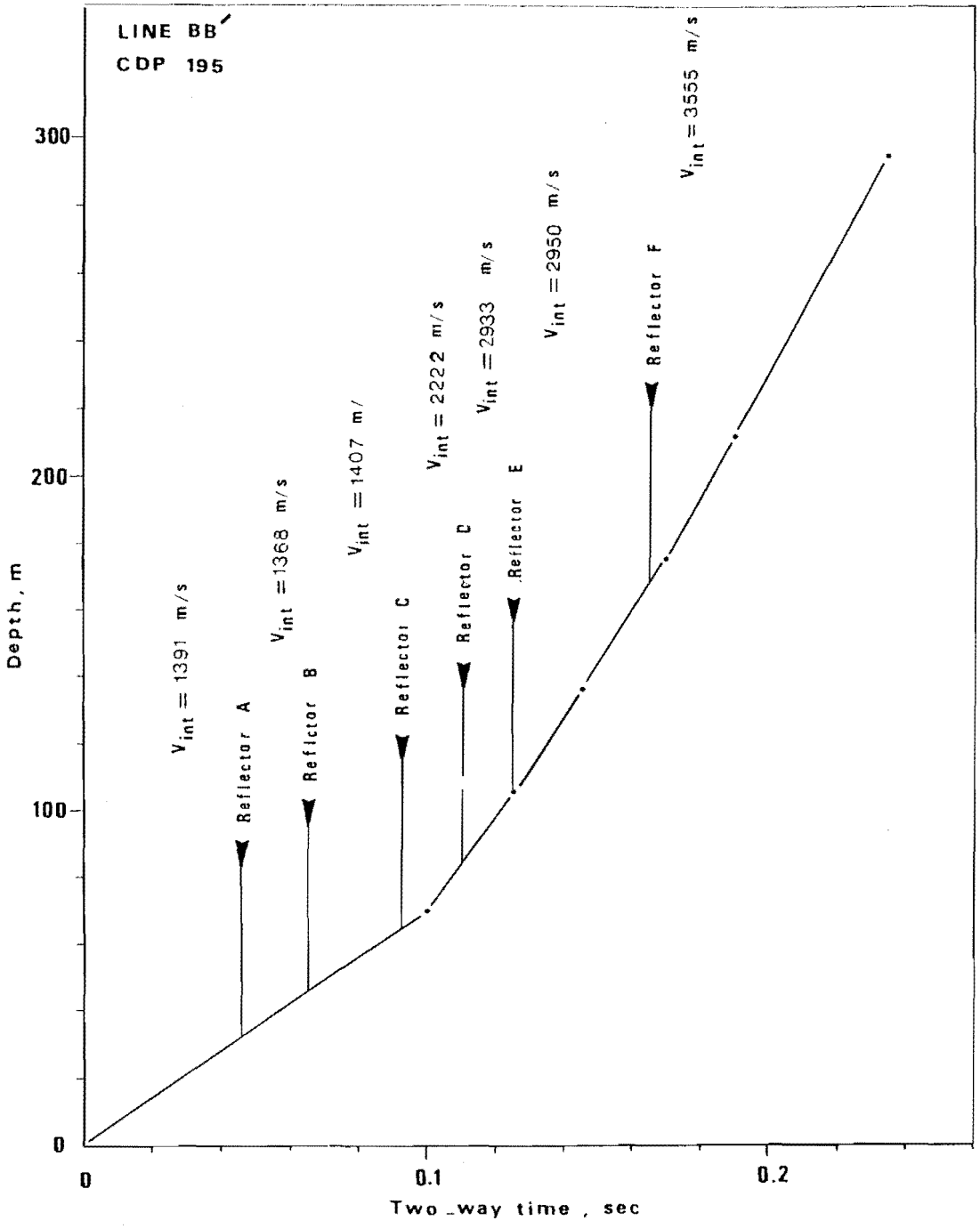

A.7.5 Seismic Reflection Velocity (Interval)

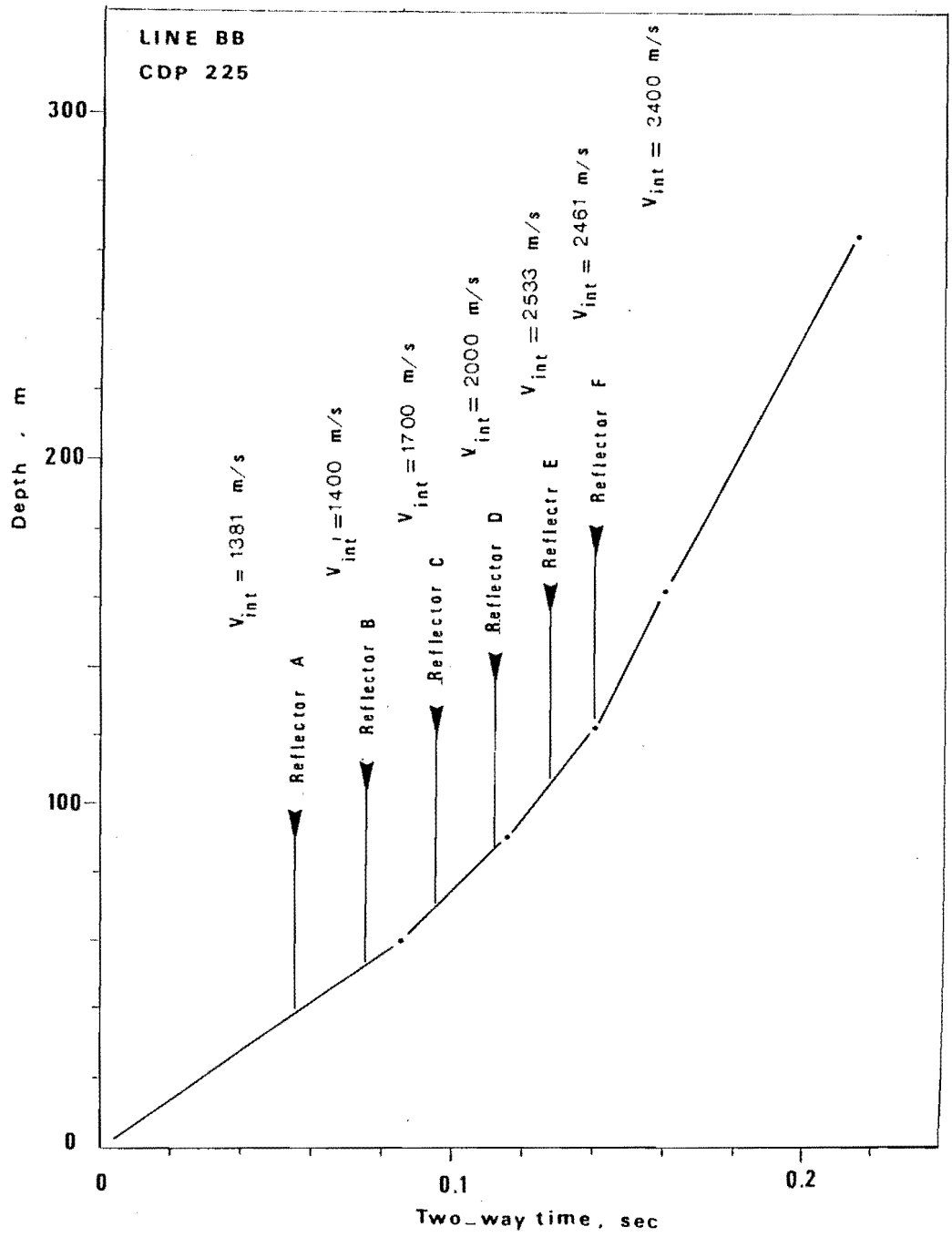

A.7.5 Seismic Reflection Velocity ‹Interval›

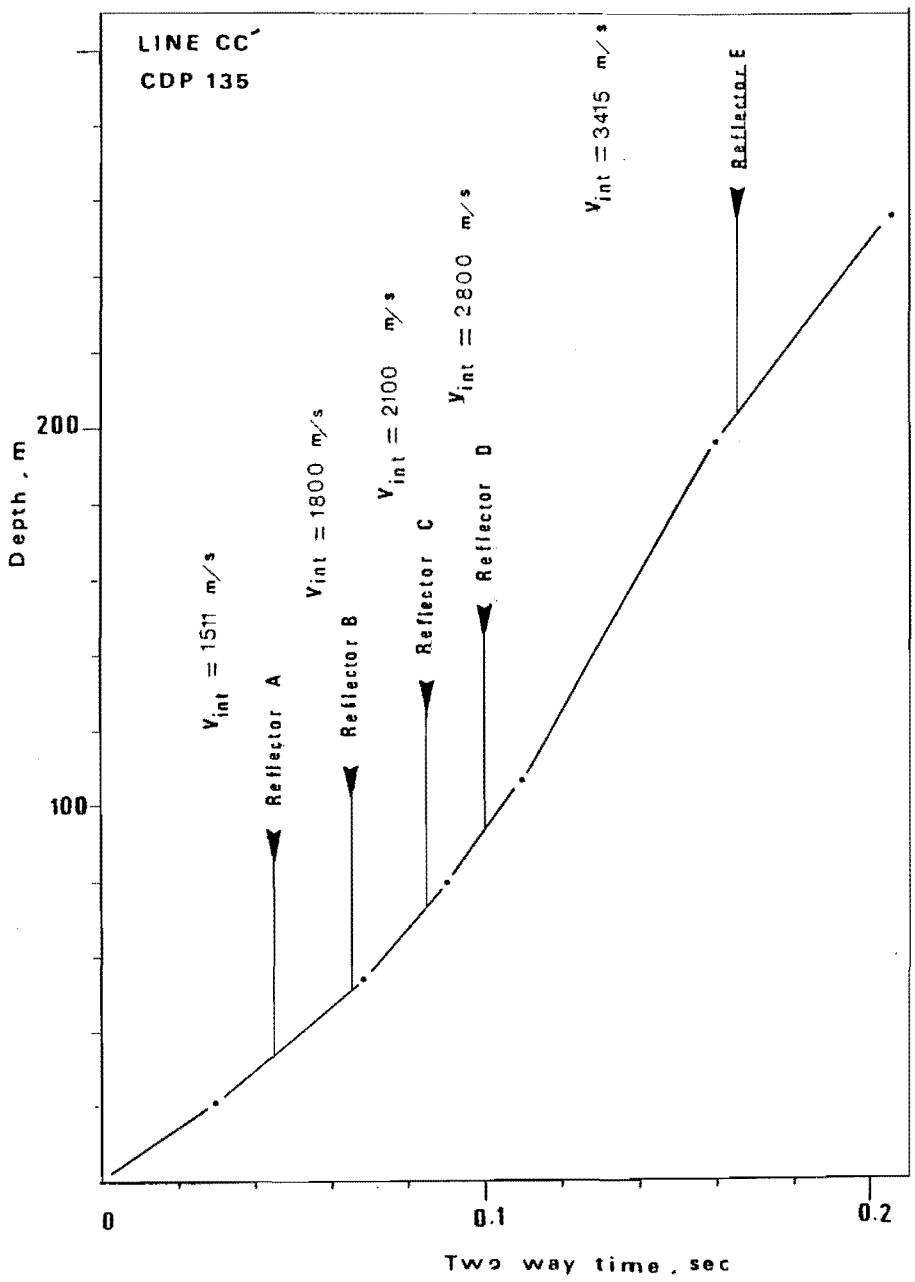

A.7.5 Seismic Reflection Velocity (Interval)

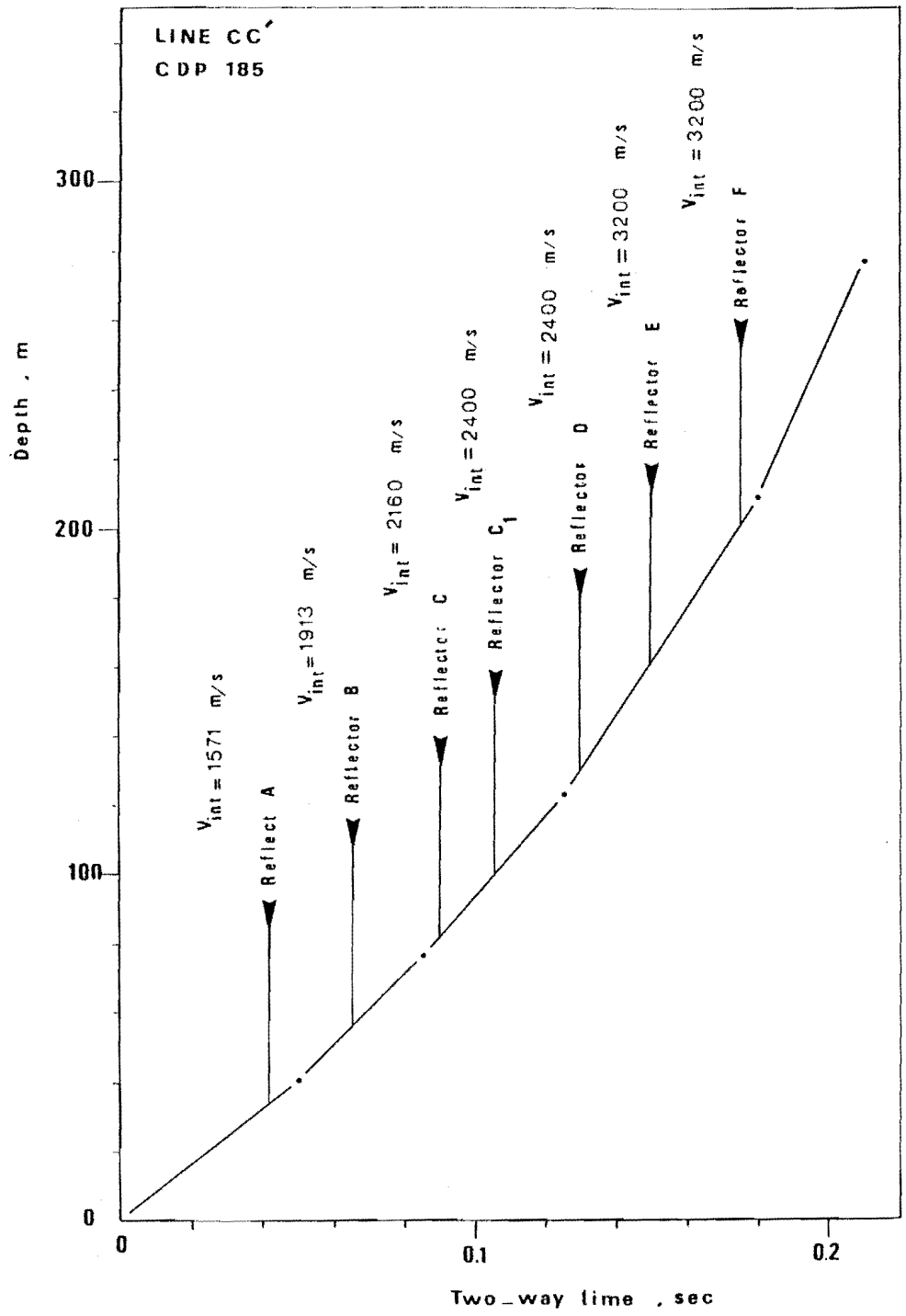

A.7.5 Seismic Reflection Velocity (Interval)

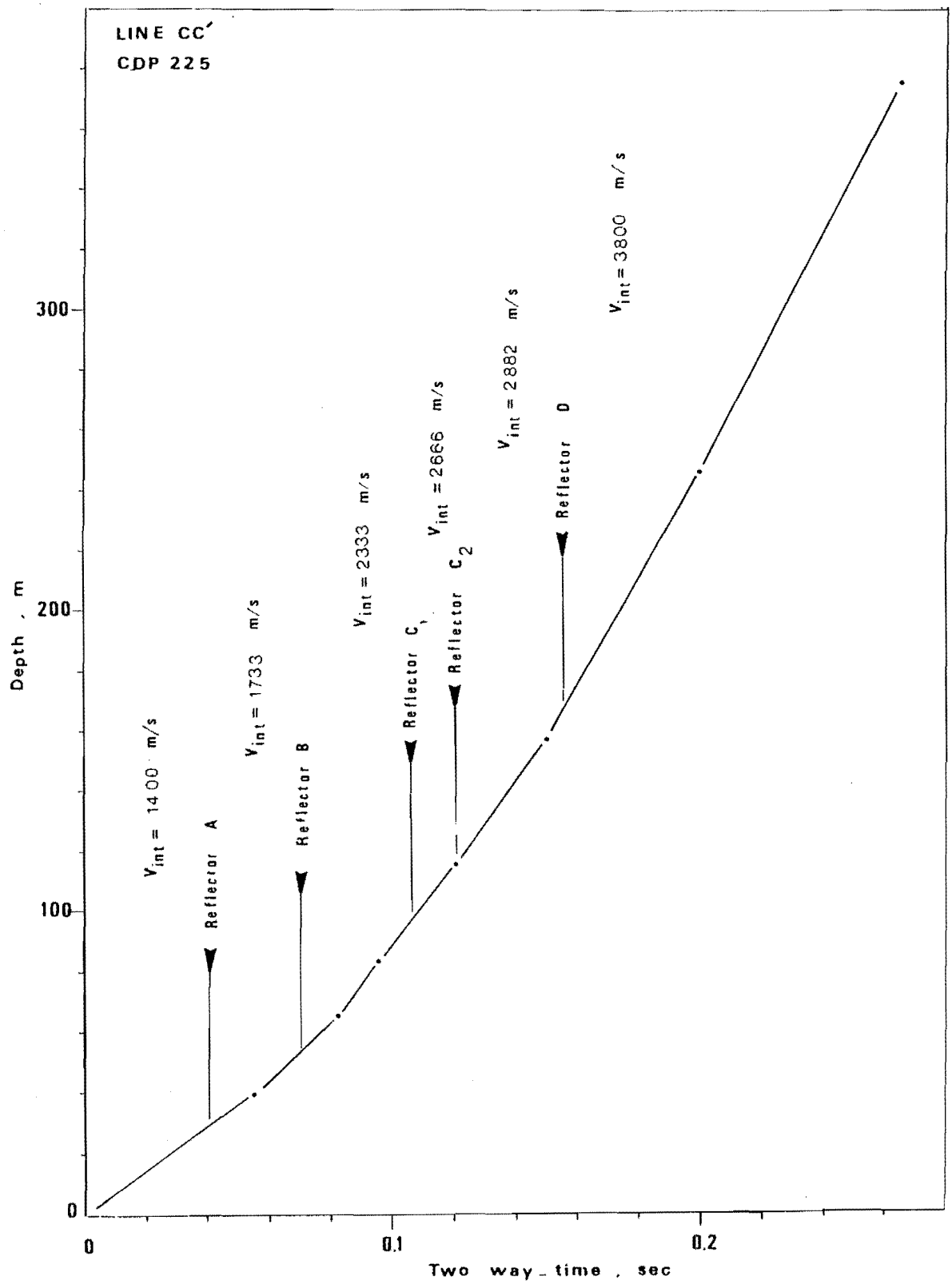

A.7.5 Seismic Reflection Velocity (Interval)

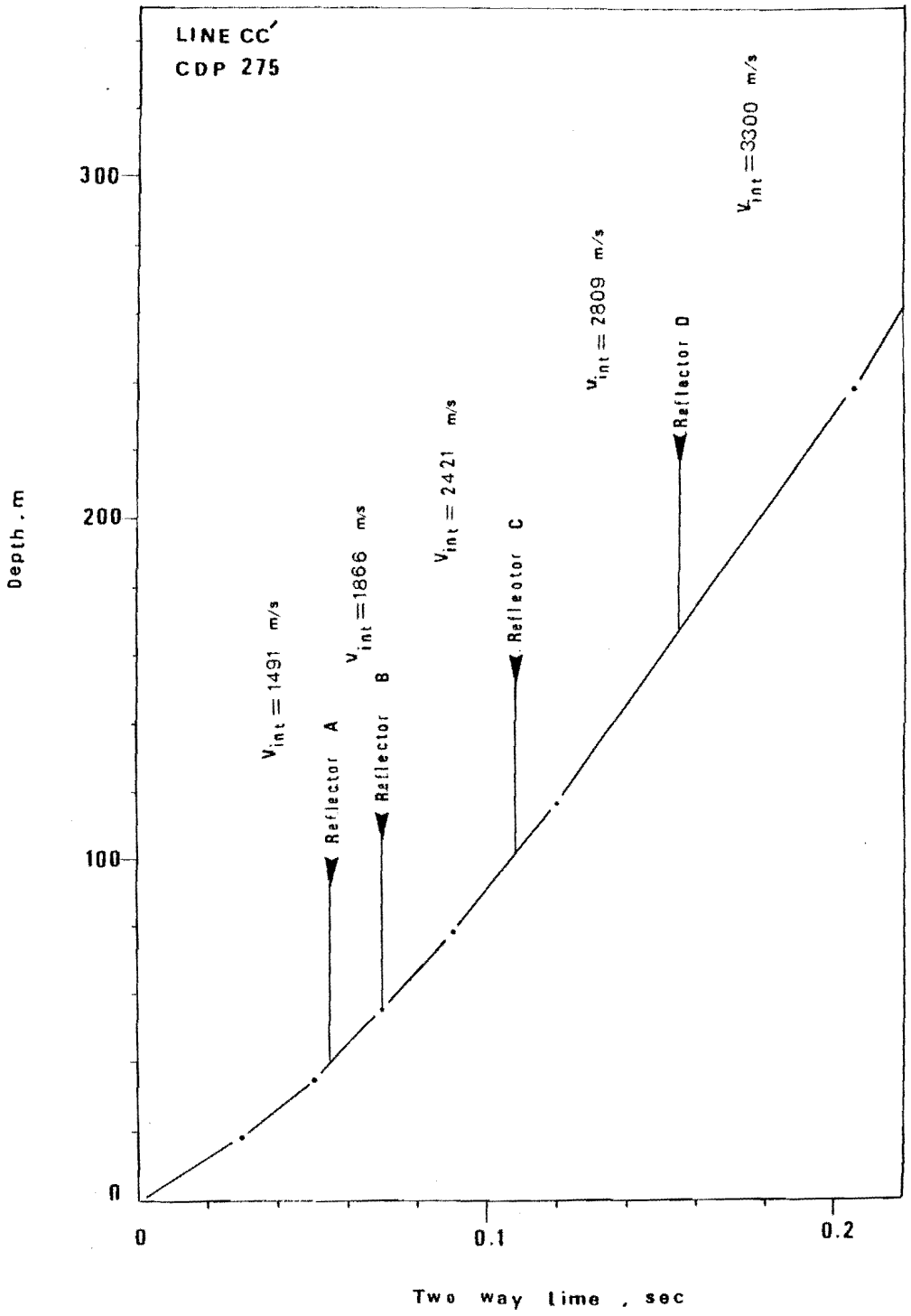

A.7.5 Seismic Reflection Velocity (Interval)

A .7.6 Seismic Refraction Time Distance Curves Line AA´

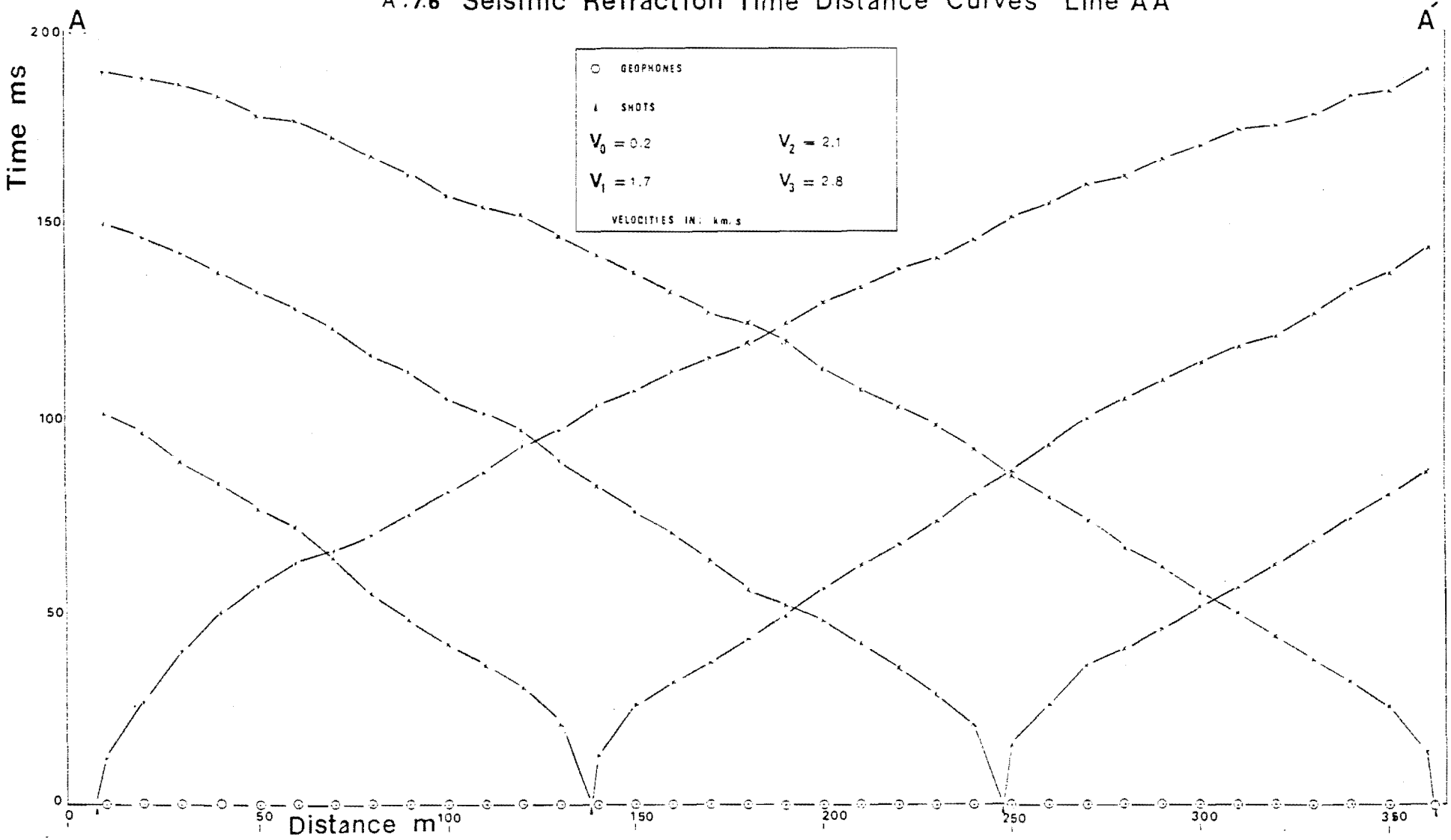

A.7.6 Seismic Refraction Time Distance Curves Line BB´

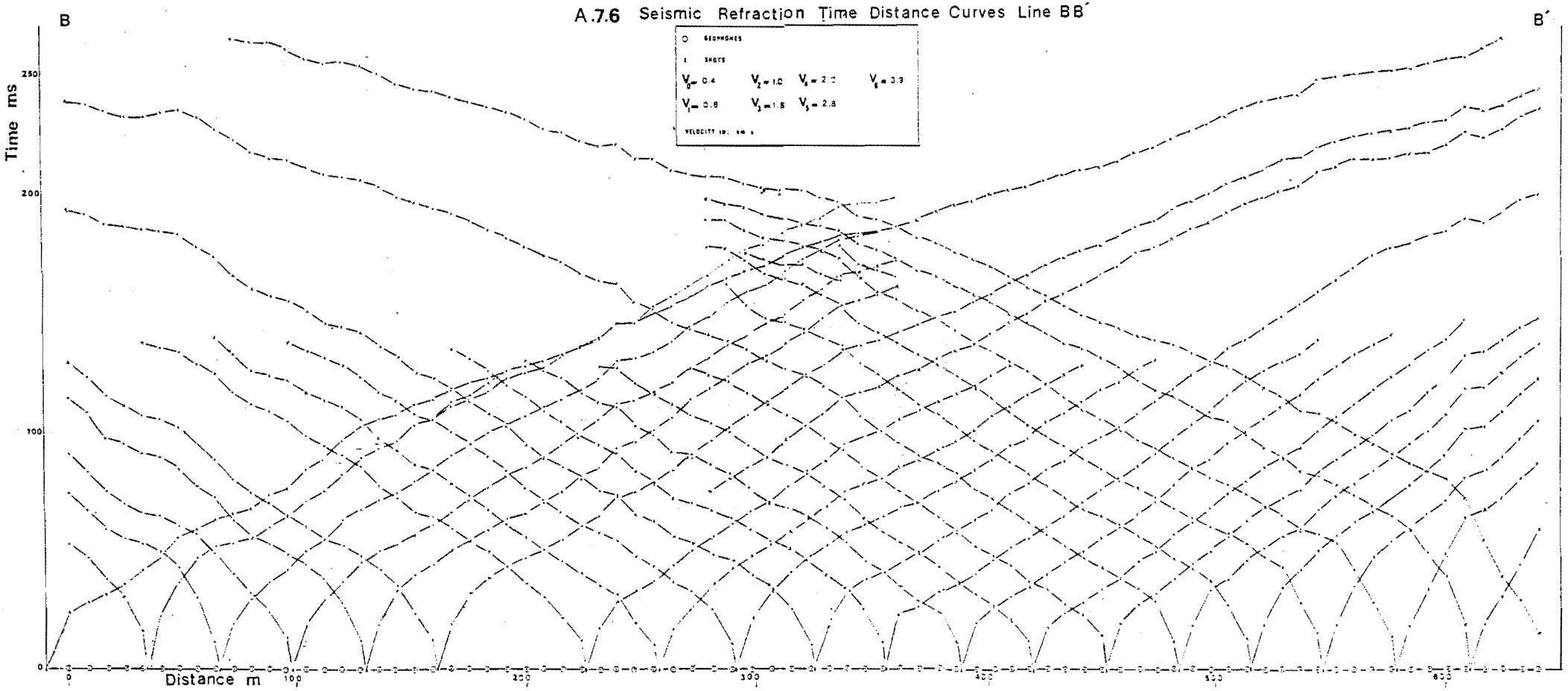

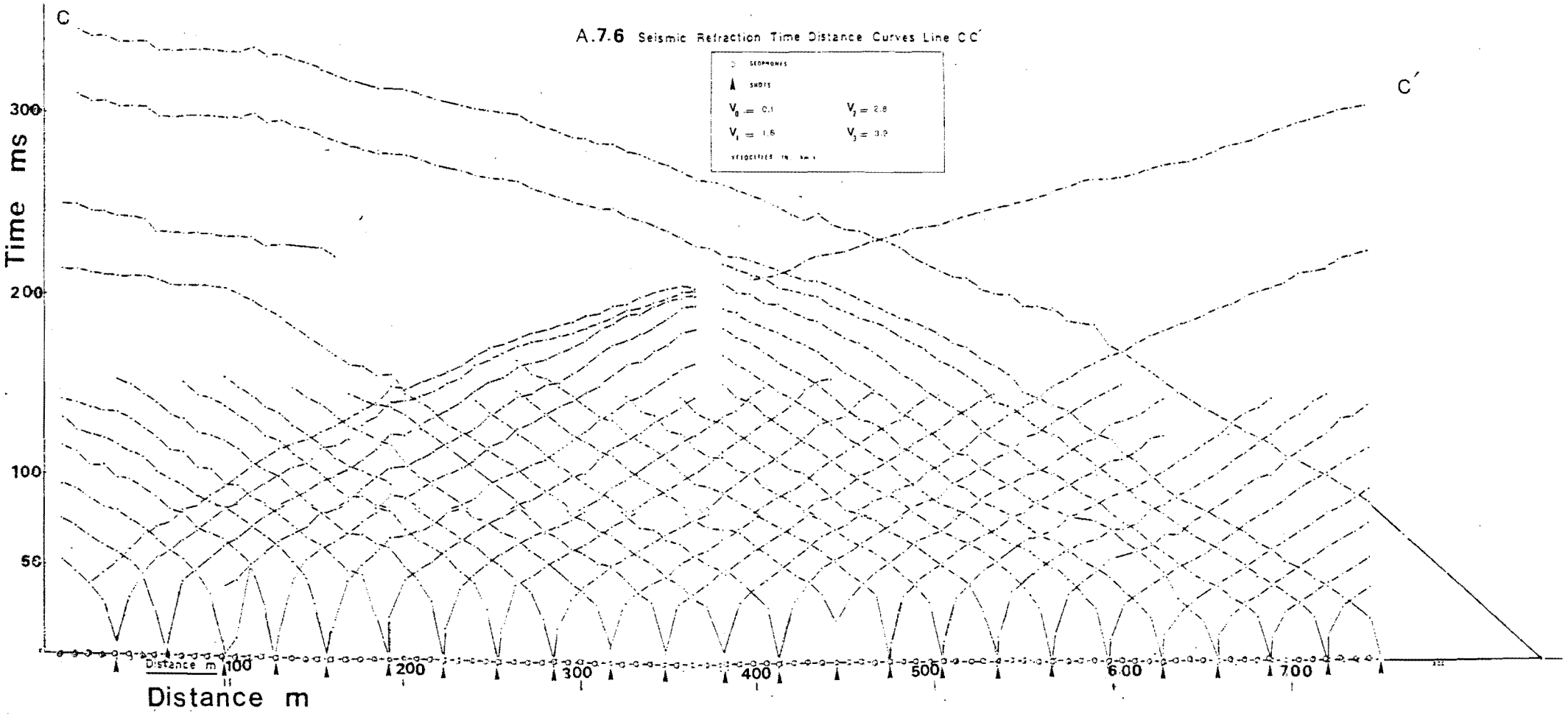
A.7.6 Seismic Refraction Time Distance Curves Line CC´
C
C´
GEOPHONES
SHOTS
V_0 = 0.3
V_1 = 1.6
V_2 = 2.8
V_3 = 3.9
VELOCITIES IN km/s
Time ms
300
200
100
50
Distance m
100
200
300
400
500
600
700
Distance m

A.7.6

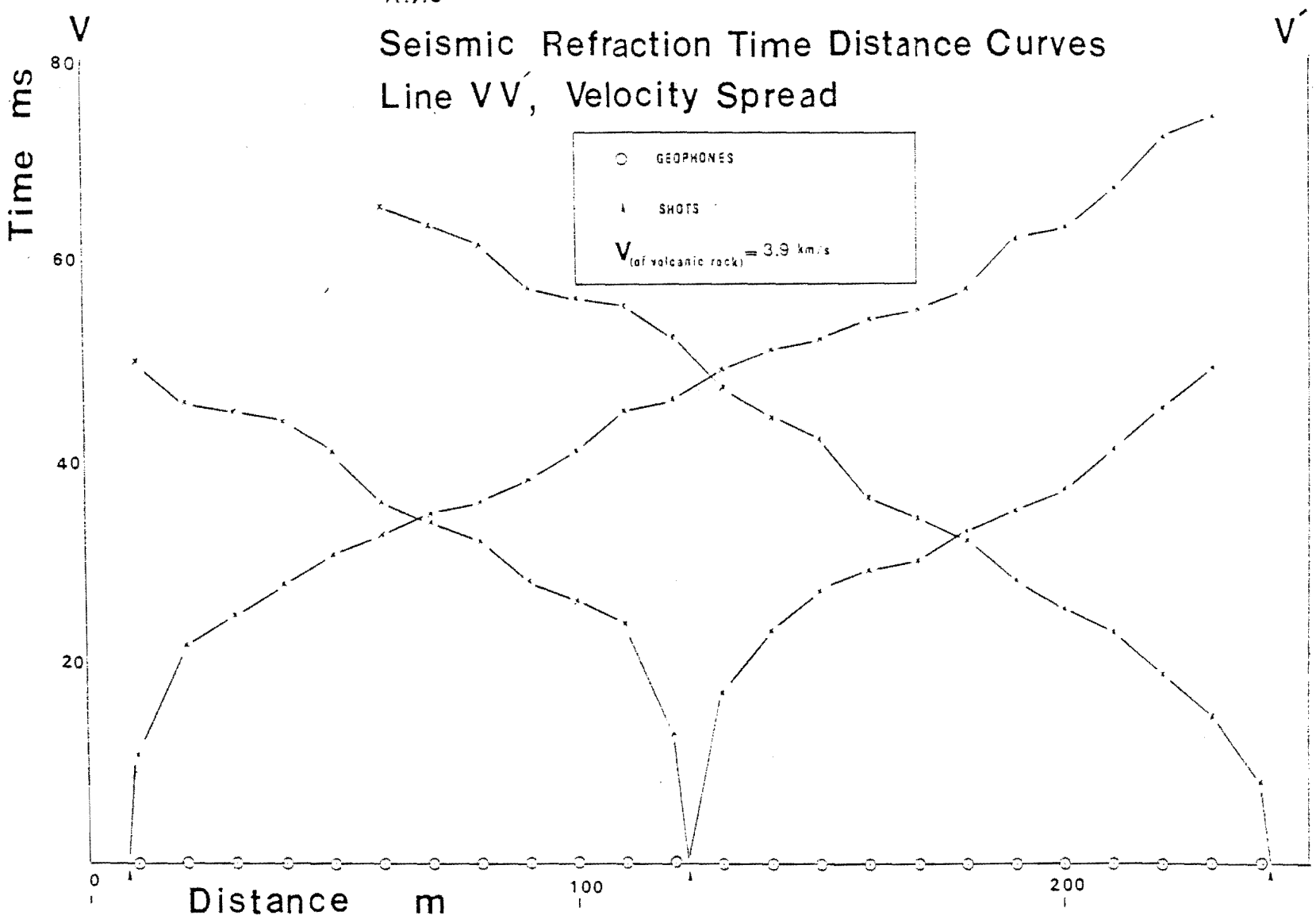
V
V´
Seismic Refraction Time Distance Curves
Line VV´, Velocity Spread
GEOPHONES
SHOTS
V(of volcanic rock) = 3.9 km/s
Time ms
80
60
40
20
0
100
200
Distance m

APPENDIX 8

RAINFALL AND EVAPORATION

A.8.1 Rainfall Data

A.8.2 Isohyetal Data

A.8.3 Procedure for Collection and Manipulation of Evaporation Data

A.8.4 Evaporation Data

A.8.5 Rainfall and Quickflow Correlation

A.8.1 Rainfall Data

Month	June 1986				July			
Station	1	2	3	4	1	2	3	4
Date	Rainfall (mm)							
1		1.78	2.54	0.7	12.4	8.89	8.89	3.4
2					*14.6	*12.19	*13.71	5.4
3								
4								
5					25	14.48		
6					52.6	74.42	82.04	38.1
7					32.6	32.51	27.18	14
8						6.36	5.33	1.4
9				0.6				
10	9		2.03	2.4	*47.4	*44.7	*42.67	23.3
11					*15.6	*10.41	*8.89	4.3
12	24.2	22.35	18.8	11.1	7.6	6.86	6.6	2.9
13								
14		3.05	3.3	1.2				
15	21	14.48	15.5	6.6				
16	12.2	1.01						
17		5.59	5.84	2				
18								
19								
20			3.81	1.7	*32.0	15.24	*15.75	14.6
21	6	18.79	13.97	2.2	2.0	12.19	12.44	8
22								
23								
24								
25	*27.8	*8.38			*16.6	14.47	16.51	12.5
26	*37.6	*27.94	*35.81	9.6				
27								
28								
29								
30	*47.2	*39.37	*35.56	*12.3				
31								
Toatl	185	142.74	137.16	50.4	442	320.49	310.12	170.3

* snow

A.8.1 Continued

Month	Aug				Sep			
Station	1	2	3	4	1	2	3	4
Date	(mm)			Rainfall	(mm)			
1								
2	*9.8	*7.87	*6.6	4.4				
3								
4								
5	*18.8	*9	*10.41	5.7				
6						0.25		0.5
7	*19.8	12.8	*12.70	14.6				
8	18.8	13.21	*15.24	7.6	6.2	4.06	3.81	0.6
9	*43.6	*26.92	*29.72	24.6				
10	36.6	27.43	25.4	6.2				
11	*16.4	9.14	7.62	1.3				
12	2.4	2.29	2.54					
13	*2.2	*1.02	1.27	2.5	49.8			
14	2.2			0.6		19.3	18.29	18.8
15						18.0	20.83	8.1
16								0.7
17							3.56	0.9
18					*10.6	7.11	3.81	4
19					*4.0			1.3
20					12.6	6.1	3.56	1.8
21	17.2	16					1.27	2.8
22	121.6	96.52	113.03	42.3				
23	64.6	54.1	51.81	35.2				
24	*5.4	*3.81	*3.3	0.7				
25	*1.8							
26								
27								
28	40	26.16	24.64	4.8	*9.4	10.67	8.89	10.3
29	20.8	14.22	12.44	8.6				
30								
31								
Toatl	442	320.49	310.12	170.3	92.6	66.29	65.32	49.7

* snow

A.8.1 Continued

Month		Oct				November		
Station	1	2	3	4	1	2	3	4
Date				Rainfall (mm)				
1								
2					21.8	18.8	18.03	16.3
3			4.3					
4	41.4	23.87	21.33	16.2				
5	31.8	34.3	40.13	18.6				
6			0.25					
7			0.51	0.3				
8	4.4	2.28	0.51					0.1
9	7	3.05	2.54					0.1
10	26	24.38	22.86	1.6				
11				11				
12				0.6	6	5.6	4.82	7.1
13								
14				0.7	0.76			
15	1.01							
16	4.6	1.27	2.29	0.8				
17	62.2	72.9	76.71					
18	5.6	4.57	4.06	3.4				
19								
20	2.8			1.1				
21		4.82	4.57	2.7				
22						0.51		0.6
23								
24					56.6	28.45	51.5	31.5
25					186.4	130.81	112.77	40
26					82.4	77.47	72.39	31
27	24	19.05	17.52	9				0.5
28					7.2	7.87	7.87	2
29								
30								
31								
Toatl	209.8	191.5	193.28	70.3	360.4	270.27	247.38	130.8

Month	December				January 1987			
Station	1	2	3	4	1	2	3	4
Date				Rainfall (mm)				
1	7.4	8.38	8.13	4.3				
2				0.4				
3								
4								
5								
6								
7								0.1
8								
9								
10								
11								
12								
13								
14								
15				0.4				
16				0.5				
17							0.76	1
18								
19								
20								
21	14.2	9.4	9.65	10				
22					6	3	4.32	4.7
23								
24								
25					0.8	1.78	1.01	1
26								
27								
28				2.1	5	5.6	3.3	2.1
29	20.4	26.41	18.8	17				
30	2	2.54	1.78	1.8				
31								
Toatl	44	46.73	38.36	36.5	11.8	10.38	9.39	8.9

A.8.1 continued on next page.

A.8.1 Continued.

Month	February				March			
Station	1	2	3	4	1	2	3	4
Date	Rainfall (mm)							
1						0.51		
2					57.4	4.32	6.6	2.8
3					55.2	99.06	73.66	43.7
4					15.6	10.41	8.9	
5	2.8	4.83	3.3	1.4				
6	1.6	0.76	0.51	0.6				
7	11	12.7	9.14	7.2				
8								6.7
9								
10						5.84	4.75	0.3
11					66.4	52.32	50.29	32
12		4.06		4.5	6	5.32	3.05	8.6
13	48	68.32	61.21	46			1.78	
14	26.8	21.08	19.81	17.5				
15		0.76	1.02					
16		1.52	1.78	1.7				
17	31	28.7	28.19	21.1				
18		2.54	1.27	0.7				
19								
20								
21					13	7.11	7.37	0.6
22								
23								
24						7.11	5.08	12.3
25					3.2	5.84	6.1	6
26		1.78	2.79	2.4	5.4	7.11	6.1	
27		8.13	7.37	2.6				
28	39.2	16.76	15.24	10				
29								
30								
31								
Total	161.4	171.94	151.63	115.7	222.2	204.95	173.5	113

A.8.1 continued

Month	April				May			
Station	1	2	3	4	1	2	3	4
Date	Rainfall (mm)							
1					15.2	11.17	11.17	7
2		2.79	2.54				10.16	
3				0.1				
4								
5						1.02		
6					8.4	7.87	7.11	3.5
7								
8								
9	19.2	7.36	8.9	0.32				
10								
11								
12								
13								
14								
15								
16	3.2	2.54	1.52	0.06	15.33	11.68	9.4	9
17			0.51				3.55	3
18		2.54	1.27	0.7	33.6.	25.65	21.33	15
19					25.96	19.81	18.03	10
20					44.59	34.03	31.75	9.5
21		3.3	2.28	1.9	30.62	23.37	22.6	13
22		15.24	1.27					
23	33.6	49.02	32.76	15				
24		5.89	5.08	3.5				
25								
26								
27						1.02		
28								
29								
30	42.8	32.76	30.73	23				
31								
Toatl	98.8	122.2	85.59	43.88	173.7	135.62	135.1	72

A.8.2: Isohyetal Data

A Isohyet (mm)	B Estimated EDU* (mm)	C Net Area (km^2)	D Weighted precipitation (mm) = BC/total area
900	985	0.79	20.5
1000	1050	3.48	96.23
1100	1200	6.54	206.7
1300	1400	4.08	150.43
1500	1600	1.98	83.43
1700	1800	2.18	103.34
1900	2000	2.98	156.96
2100	2200	3.48	201.6
2300	2400	3.95	249.7
2500	2600	3.4	232.8
2700	2800	2.68	197.63
2900	3000	1.78	140.64
3100	3200	0.65	54.78
Total		37.97	1894.7

Note: EUD = the effective uniform depth.

A.8.3 Procedure for Collection and Manipulation of Evaporation Data

The following discussion is based on Bruce, 1966.

The Class A pan (Fig. A.8.1) is 122cm in diameter, 25cm deep and is mounted near the ground on supports which permit a free flow of air around and under the pan. Measurements of water loss are made by either determining the water level on successive days by means of a micrometer hook gauge, adjusting the point of the hook until it touches the water, or by filling the from a graduated measure until it just covers the point of a thin rod fixed to the pan bottom or the bottom of the stilling well which is set in the pan. The latter method has the advantages of being cheaper, providing a magnification of the water loss by means of a graduated measure of much smaller diameter than the pan, and of forcing the observer to keep the water level in the pan nearly the same distance below the rim each day. If the water level in the pan drops, major decreases in water loss result and the observations become difficult to interpret.

On rainy days, the amount of rain collected in a standard raingauge near the pan must be subtracted from the water loss observed from the pan, if the rainfall is less than the evaporation. If greater, the water loss is determined by measuring the amount of water that must be taken from the pan to reduce the water level to that of the fixed point, and then subtracting this amount from the rain observed in the nearby raingauge.

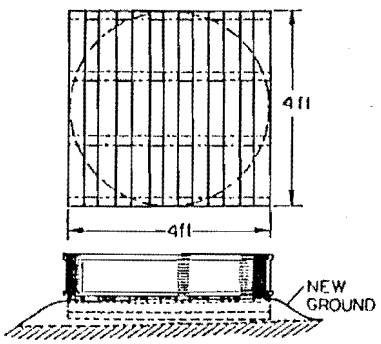

Figure A.8.3 a
Class A pan and
support.

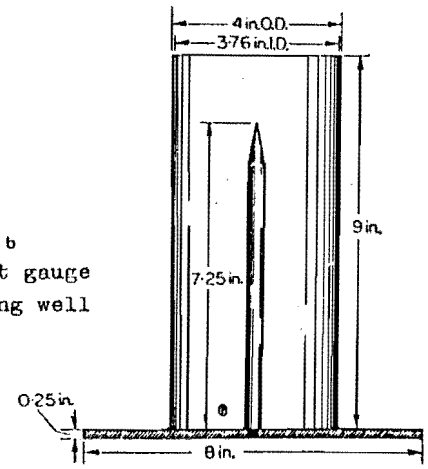

Figure A.8.3 b
fixed point gauge
and stilling well

A.8.4: Kaituna Evaporation Data

Year			1986				
Month	Jun	Jly	Aug	Sep	Oct	Nov	Dec
Date			Evaporation (mm)				
1	3.85	0.31	1.24	1.89	4.40	5.89	3.30
2	0.68	0.31	2.73	2.26	5.61	2.36	3.60
3	0.87	1.05	1.05	2.17	3.10	4.03	4.00
4	2.17	0.31	1.42	2.36	0.77	4.22	6.65
5	1.61	1.24	1.33	4.03	0.31	4.50	6.00
6	1.52	0.31	1.61	4.22	3.19	4.03	6.00
7	1.42	0.31	1.05	4.22	1.61	5.89	6.00
8	2.54	1.05	0.49	3.29	1.80	2.10	2.90
9	3.10	1.24	0.77	2.26	3.10	6.70	6.00
10	2.73	0.31	0.31	2.36	1.70	6.00	5.05
11	3.57	0.59	1.98	2.82	0.31	8.00	4.00
12	2.08	2.45	0.96	4.03	2.91	1.65	2.00
13	1.42	3.10	1.05	1.61	2.64	4.03	6.00
14	1.33	0.96	1.33	3.10	3.47	1.89	12.0
15	2.64	0.96	1.98	2.26	4.40	1.10	6.40
16	1.42	1.61	0.31	1.33	3.85	6.00	4.00
17	1.05	1.52	1.89	2.17	1.24	6.00	9.50
18	1.31	2.17	2.54	1.52	2.64	5.60	10.0
19	2.17	0.31	1.89	1.24	5.23	6.00	7.70
20	1.98	0.77	2.26	2.82	5.06	6.00	10.55
21	3.94	1.24	0.68	3.94	3.01	8.00	9.25
22	2.64	1.15	0.37	2.64	4.40	10.4	4.00
23	0.77	1.15	0.31	1.61	5.33	8.00	6.00
24	1.05	3.19	1.52	2.17	1.80	7.50	7.76
25	1.70	1.05	1.71	4.03	4.03	4.00	9.62
26	1.42	2.73	1.42	2.17	5.33	1.00	4.03
27	1.80	1.05	1.05	5.43	3.29	8.50	4.03
28	2.17	2.73	0.96	1.42	4.68	6.00	9.06
29	0.307	3.47	1.61	3.85	3.10	5.75	9.06
30	0.59	3.1	2.64	3.57	5.06	6.36	5.00
31	–	2.26	2.82	–	4.03	–	7.40

A.8.4 continued on next page.

A.8.4 continued

Year	1987				
Month	Jan	Feb	Mar	Apr	May
Date	Evaporation (mm)				
1	5.89	10.00	3.29	3.57	3.00
2	7.76	2.00	2.17	3.29	0.60
3	7.76	11.95	0.77	2.17	2.40
4	5.89	13.34	2.82	5.24	3.60
5	7.38	6.45	2.82	2.17	2.00
6	7.76	4.03	4.03	2.54	0.00
7	7.29	3.38	5.89	4.22	2.00
8	4.03	5.80	4.59	6.36	1.10
9	6.00	3.57	4.59	3.10	0.90
10	8.00	4.78	1.33	1.61	0.00
11	6.70	6.73	3.19	2.17	1.30
12	6.00	8.69	2.64	4.59	2.00
13	10.00	4.03	2.73	2.36	0.35
14	14.00	0.77	5.89	1.52	1.20
15	13.06	3.57	2.91	3.57	1.40
16	7.76	4.96	2.54	1.89	0.00
17	9.62	5.23	2.91	1.60	0.00
18	10.18	5.52	2.17	1.30	7.20
19	7.60	4.50	4.03	0.90	0.00
20	9.10	4.03	2.17	6.00	0.00
21	10.00	5.89	2.17	3.70	0.25
22	8.70	12.78	4.87	3.57	0.70
23	4.00	3.47	1.80	3.29	0.70
24	9.00	5.61	2.17	5.89	1.10
25	7.80	5.89	2.17	4.03	1.40
26	6.00	4.68	3.10	5.52	3.30
27	10.00	11.01	2.17	2.00	3.70
28	4.60	0.96	4.03	4.00	6.90
29	9.10	–	7.66	2.00	3.66
30	5.89	–	6.64	0.00	3.38
31	9.62	–	5.80	–	1.24

Figure A.8.5

Quick Flow - Rainfall Correlation
for water balance calculations.

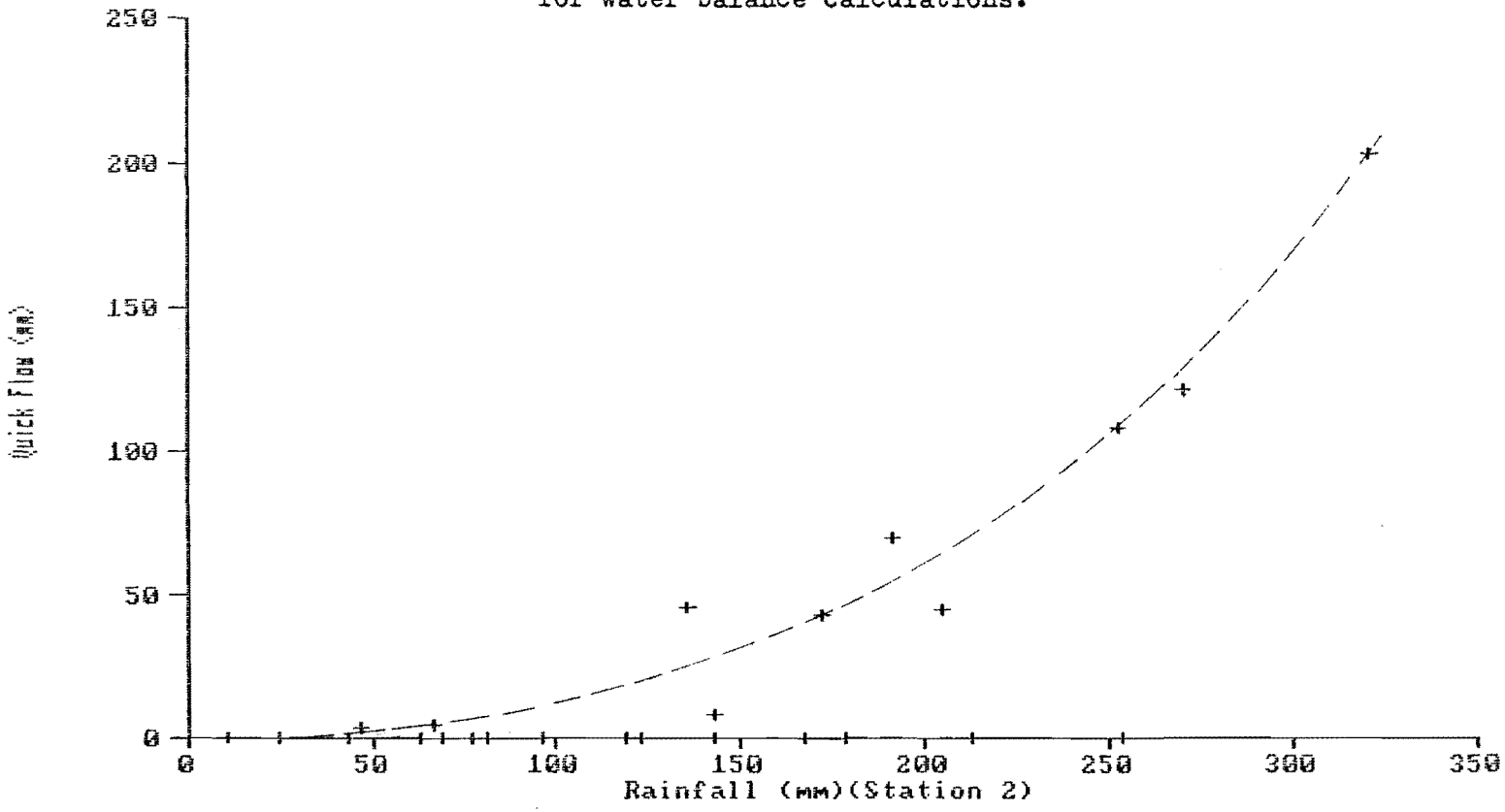

APPENDIX 9

STREAM-FLOW DATA

A.9.1 Kaituna Stream: Monthly Stage Data (Mean Value in mm)

A.9.2 Discharge and Stream Velocity
A.9.2.1 Measurment
A.9.2.2 Data

A.9.3 Stream Hydrographs

A.9.4 Hydrograph Separation

A.9.5 Hydrograph Components

A.9.6 Kaituna Stream Mean Flow (Station "A")

A.9.7 Kaituna Stream Daily Bsae Flow (Station "A)

A.9.8 Regression Equation for Run-off from Springs.

A.9.1: Kaituna Stream
Monthly Stage Data (Mean Value in mm)

Year	1986	1987	Min.	Mean	Max.
Jan	–	443	443	443	443
Feb	–	463	463	463	463
Mar	–	695	695	695	695
Apr	–	479	479	479	479
May	–	667	667	667	667
Jun	–	590	590	590	590
Jly	942	675	675	808	942
Aug	1044	–	1044	1044	1044
Sep	700	–	700	700	700
Oct	824	–	824	824	824
Nov	757	–	757	757	757
Dec	556	–	556	556	556

Note: values + 3189 = a.m.s.l.(mm)

Thus, for example, the discharge through partial section 4 (Fig. A.9.2) is

$$q_4 = v_4((b_5 - b_3)/2)d_4$$

The procedure is similar when "x" is at an end section. The "preceding location" at the begging of the cross-section is considered coincident with location 1; the "next location" at the end of the cross-section is considered coincident with location n. Thus

$$q_1 = v_1((b_2 - b_1)/2)d_1 \text{ and}$$
$$q_n = v_n((b_n - b_{(n-1)})/2)d_n$$

For the example shown in figure A.9.2, q_1 is zero because the depth at observation point 1 is zero. However, when the cross-section boundary is a vertical line at the edge of the water as at location n, the depth is not zero and velocity at the end section may or may not be zero. The formula for q_1 or q_n is used whenever there is water only on one side of an observation point such as at piers, abutments, and islands. It usually is necessary to estimate the velocity at an end section as some percentage of the adjacent section because it normally is impossible to measure the velocity accurately with the current meter close to a boundary.

Discharge is the product of the average of two mean velocities, the average depth (0.6 depth), and the distance between locations.

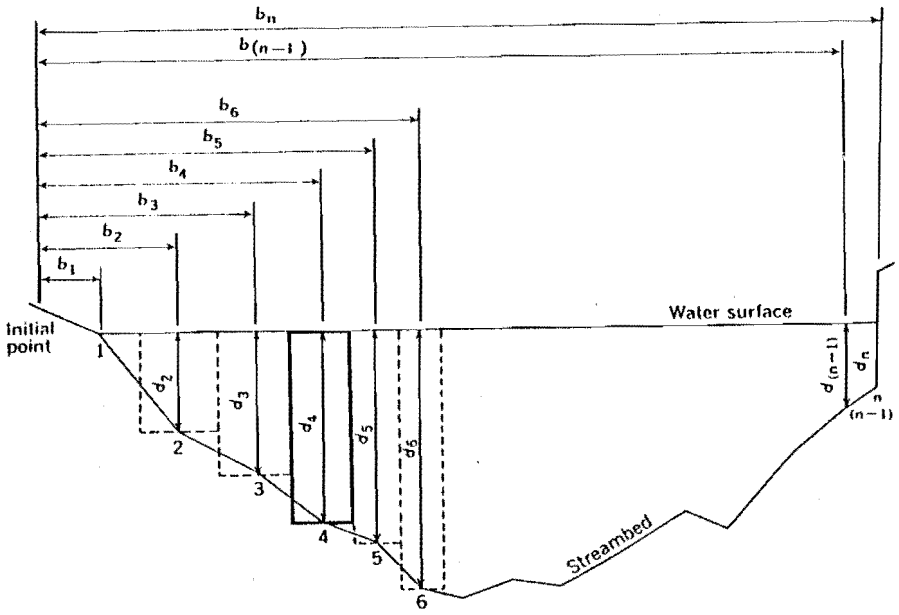

EXPLANATION

1, 2, 3, ... n	Observation points
$b_1, b_2, b_3, \ldots\ldots b_n$	Distance, in feet, from the initial point to the observation point
$d_1, d_2, d_3, \ldots\ldots d_n$	Depth of water, in feet, at the observation point
Dashed lines	Boundary of partial sections; one heavily outlined discussed in text

Fig. A.9.2 Definition sketch of midsection method of computing cross-section area for discharge measurements.

A.9.2 Discharge and Stream Velocity

A.9.2.1 Measurement (from Buchanan, T. and Somers, W. P. 1969).

Streamflow, or discharge, is defined as the volume rate of flow of the water including any sediment or other solids that may be dissolved or mixed with it.

A current meter measurement is the summation of the products of the partial areas of the stream cross section and their respective average velocities. The formula

$$Q = \Sigma(av) \qquad (1)$$

represents the computation where Q is total discharge, "a" is an individual partial cross-section area, and "v" is the corresponding mean velocity of the flow normal to the partial area.

In the mid-section method of making a current meter measurement it is assumed that the velocity sample at each location represents the mean velocity in a partial rectangular area. The area extends laterally from half the distance to the next and vertically, from the water surface to the sounded depth (Fig. A.9.2).

The cross-section is defined by depths at locations 1, 2, 3, 4, ... n. At each location the velocities are sampled by current meter to obtain the mean of the vertical distribution of velocity. The partial discharge is now computed for any partial section at location "x" as

$$q_x = v_x((b_x - b_{(x-1)}/2 + (b_{(x+1)} - b_x)/2)d_x$$

$$= v_x(b_{(x+1)} - b_{(x-1)})d_x$$

where:

q_x = discharge through partial section x
v_x = mean velocity at location x
b_x = distance from initial point to location x
$b_{(x-1)}$ = distance from initial point to preceding location x
$b_{(x+1)}$ = distance from initial point to next location
d_x = depth of water at location x

A.9.2.2:Discharge and Velocity Data for Streams

Station A: Kaituna Stream (main site)
Grid.Ref. M36 844 167

Date	Discharg (m^3/s)	Aeea (m^2)	Mean Velocity (m/s)
26-JUN-1985	0.261	0.441	0.591
30-JUL-1985	2.310	4.180	0.551
27-AUG-1985	0.258	0.516	0.499
24-SEP-1985	0.167	0.420	0.397
29-OCT-1985	0.240	0.341	0.704
19-DEC-1985	0.567	0.855	0.686
26-MAR-1986	0.398	1.130	0.352
14-MAY-1986	0.102	0.167	0.651
9-JUN-1986	0.110	0.152	0.728
23-JUN-1986	0.472	0.488	0.968
8-JUL-1986	5.130	8.280	0.620
09-JUL-1986	3.180	6.740	0.472
9-JUL-1986	3.260	6.850	0.477
23-JUL-1986	1.030	1.920	0.537
31-JUL-1986	0.508	1.440	0.353
7-AUG-1986	0.465	1.350	0.345
6-AUG-1986	0.511	1.490	0.343
23-SEP-1986	0.646	2.190	0.295
9-OCT-1986	1.290	2.940	0.439
12-NOV-1986	0.280	0.977	0.287
18-NOV-1986	0.200	1.180	0.170
25-NOV-1986	6.540	11.000	0.596
25-NOV-1986	6.510	11.200	0.583
26-NOV-1986	34.300	25.800	1.330
8-DEC-1986	0.475	0.690	0.689
5-JAN-1987	0.113	0.613	0.185
22-JAN-1987	0.040	0.106	0.374
20-FEB-1987	0.205	0.328	0.625
26-FEB-1987	0.063	0.171	0.367
29-APR-1987	0.122	0.255	0.480
29-MAY-1987	0.499	0.713	0.699
5-JUN-1987	0.257	0.447	0.576
2-JUL-1987	1.030	1.080	0.953
10-JUL-1987	0.570	0.457	0.589
13-JUL-1987	0.590	0.480	0.631
14-JUL-1987	0.620	0.655	0.810
31-JUL-1987	0.585	0.459	0.635
24-SEP-1987	0,470	0.157	0.301
4-NOV-1987	0.430	0.095	0.229
2-DEC-1987	-	-	-

A.9.2 continued on next page.

A.9.2.2 Continued

Station B: Okana Stream
Grid.Ref. M36 848 174

Date	Discharg (m^3/s)	Aeea (m^2)	Mean Velocity (m/s)
23-JUN-1986	0.023	0.225	0.143
23-JUN-1986	0.089	0.431	0.208
6-AUG-1986	0.040	0.351	0.114
23-SEP-1986	0.052	0.308	0.170
15-OCT-1986	0.098	0.368	0.268
12-NOV-1986	0.021	0.200	0.104
8-DEC-1986	0.028	0.237	0.119
5-JAN-1987	0.007	0.079	0.091
22-JAN-1987	0.003	0.023	0.128
20-FEB-1987	0.009	0.043	0.223
29-APR-1987	0.006	0.070	0.084
5-JUN-1987	0.019	0.128	0.149
2-JUL-1987	0.078	0.301	0.259

Station C: Takamina Streamm
Grid.Ref. M36 852 193

Date	Discharg (m^3/s)	Aeea (m^2)	Mean Velocity (m/s)
23-JUN-1986	0.008	0.054	0.142
23-JUN-1986	0.066	0.119	0.556
6-AUG-1986	0.014	0.067	0.208
23-SEP-1986	0.017	0.113	0.152
15-OCT-1986	0.034	0.120	0.283
12-NOV-1986	0.005	0.043	0.129
8-DEC-1986	0.009	0.027	0.322
5-JUN-1987	0.003	0.034	0.084
2-JUL-1987	0.023	0.076	0.309

A.9.2 Continued on next page

A.9.2.2 Continued

Station D: Packhorse Stream
Grid.Ref. M36 853 194

Date	Discharg (m^3/s)	Aeea (m^2)	Mean Velocity (m/s)
23-JUN-1986	0.020	0.108	0.183
23-JUN-1986	0.128	0.298	0.428
6-AUG-1986	0.034	0.422	0.081
23-SEP-1986	0.046	0.148	0.311
15-OCT-1986	0.064	0.157	0.410
12-NOV-1986	0.013	0.083	0.155
8-DEC-1986	0.018	0.066	0.273
5-JAN-1987	0.004	0.034	0.112
22-JAN-1987	0.002	0.019	0.083
20-FEB-1987	0.013	0.109	0.123
29-APR-1987	0.004	0.065	0.061
5-JUN-1987	0.012	0.100	0.117
2-JUL-1987	0.088	0.189	0.467

Station E: Kaituna at Packhorse
Grid. Ref. M36 845 195

Date	Discharg (m^3/s)	Aeea (m^2)	Mean Velocity (m/s)
23-JUN-1986	0.351	0.742	0.474
23-JUN-1986	0.698	0.872	0.801
6-AUG-1986	0.350	1.810	0.149
23-SEP-1986	0.509	0.848	0.600
15-OCT-1986	0.658	1.190	0.554
12-NOV-1986	0.193	0.456	0.424
8-DEC-1986	0.312	0.766	0.407
5-JAN-1987	0.084	0.568	0.148
22-JAN-1987	0.044	0.466	0.095
20-FEB-1987	0.139	0.593	0.235
29-APR-1987	0.103	0.549	0.187
5-JUN-1987	0.197	0.703	0.281
2-JUL-1987	0.660	1.130	0.585

A.9.3 STREAM HYDROGRAPHS

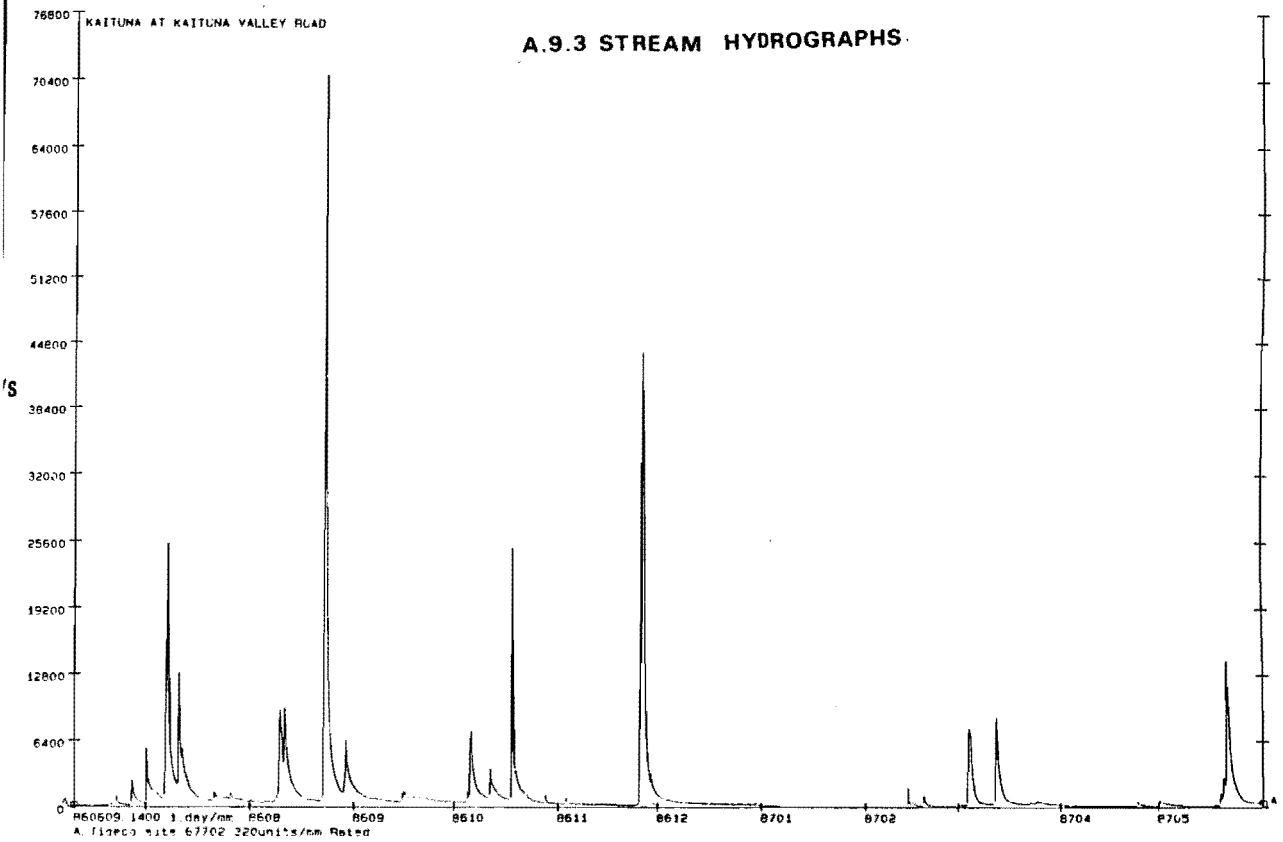

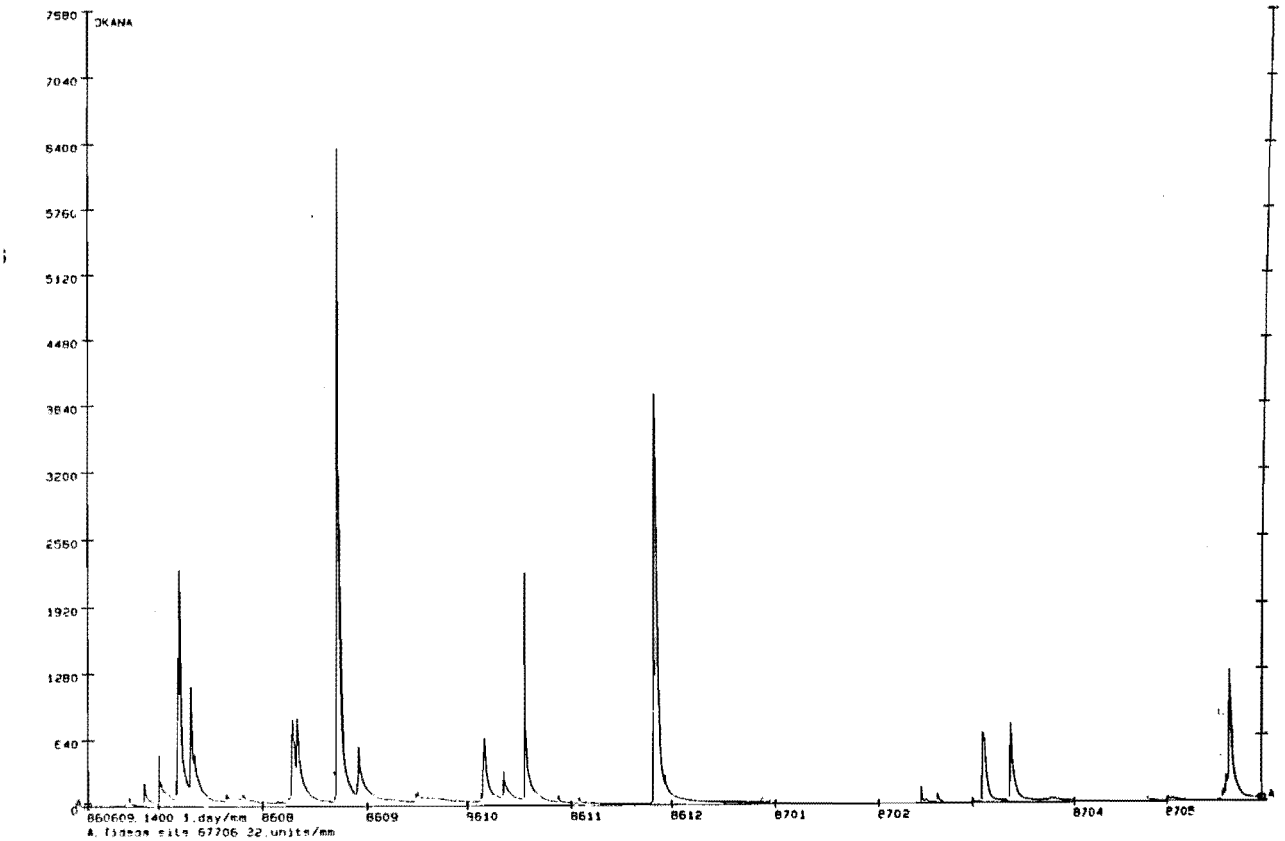

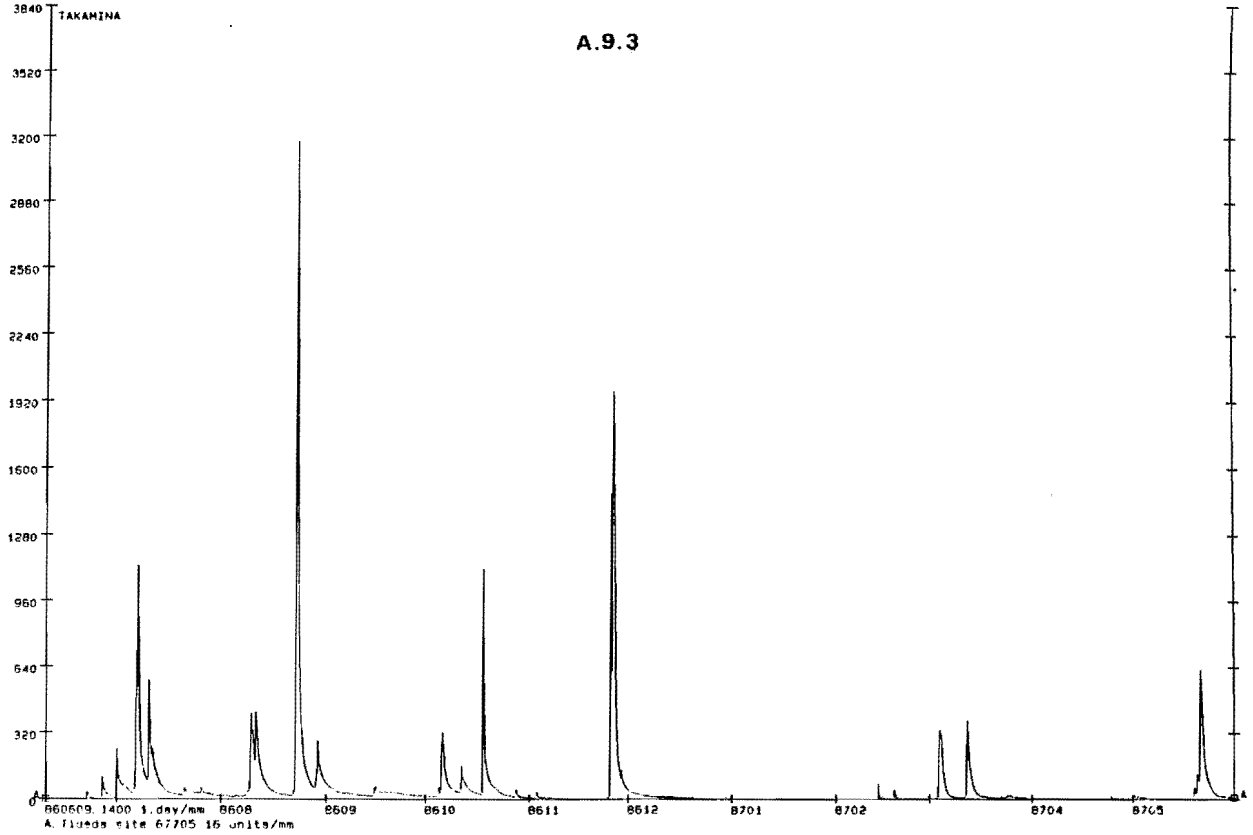
TAKAMINA
3840
3520
3200
2880
2560
2240
1920
1600
1280
960
640
320
0
860609. 1400 1.day/mm 8608
8609
8610
8611
8612
8701
8702
8704
8705
A. flieds site 67705 16.units/mm

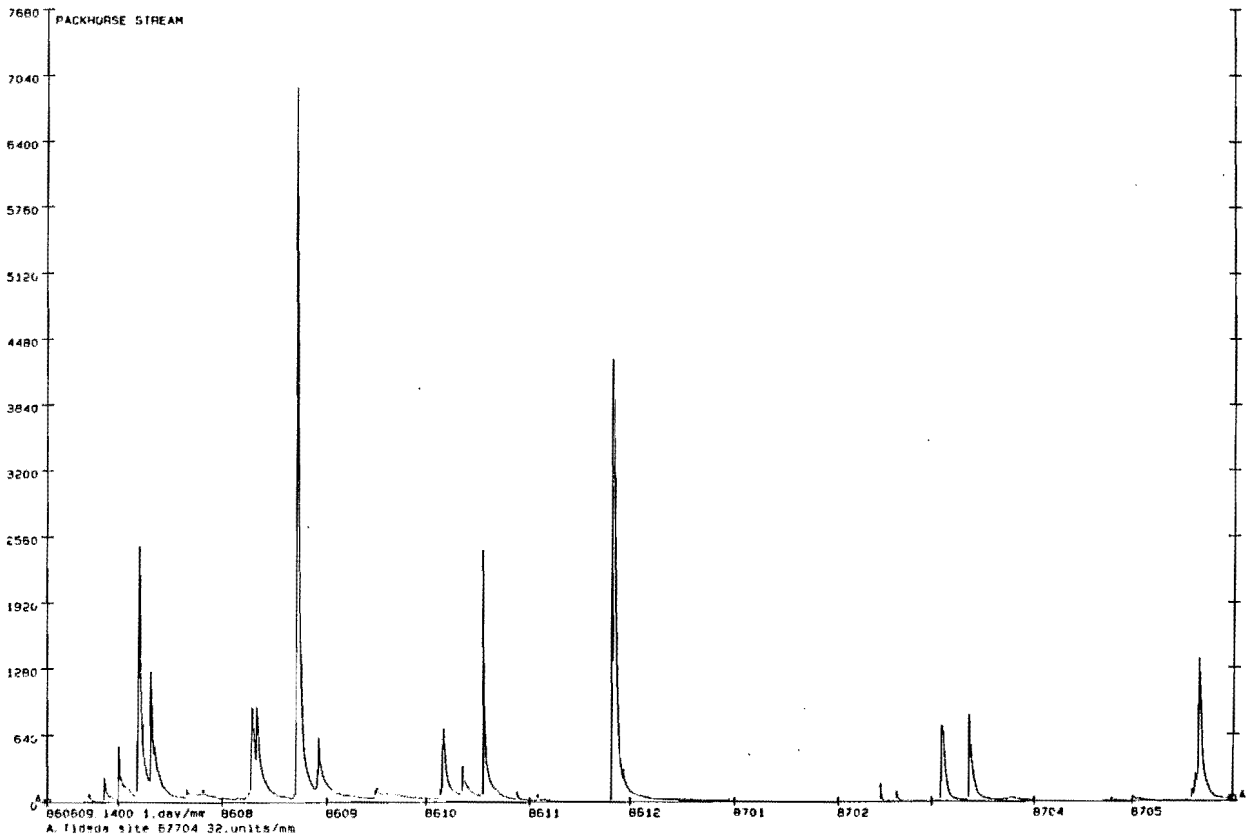
PACKHORSE STREAM
7680
7040
6400
5760
5120
4480
3840
3200
2560
1920
1280
640
0
860609 1400 1.day/mm 8608
8609
8610
8611
8612
8701
8702
8704
8705
A. flieds site 67704 32.units/mm

A.9.3

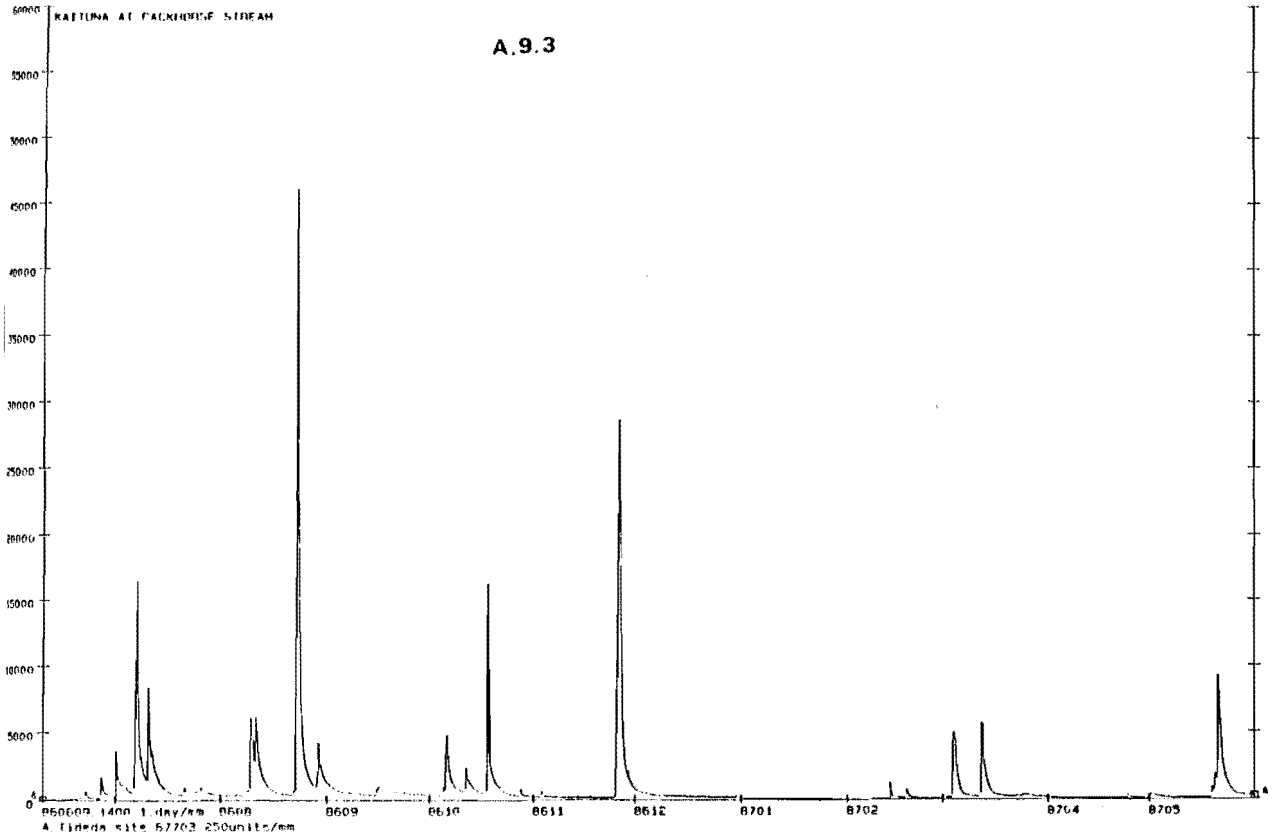
60000
55000
50000
45000
40000
35000
30000
25000
20000
15000
10000
5000
0
8609
8610
8611
8612
8701
8702
8704
8705

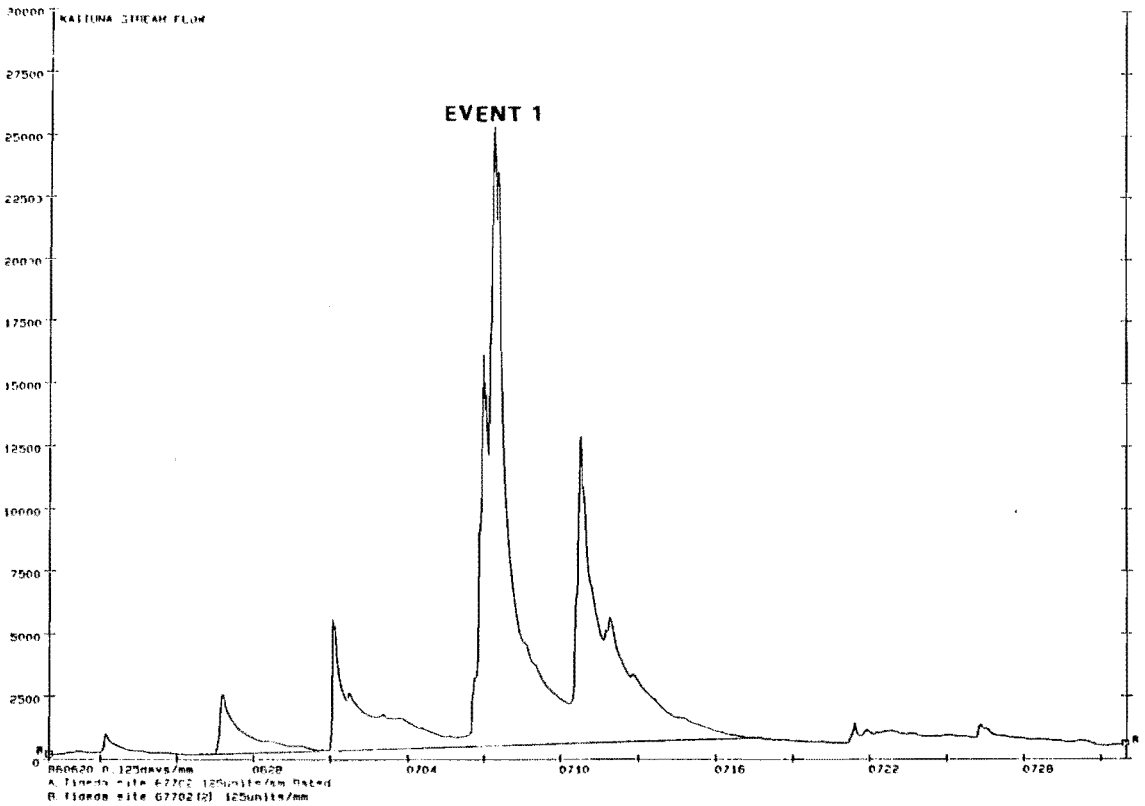
KAITUNA STREAM FLOW
EVENT 1
30000
27500
25000
22500
20000
17500
15000
12500
10000
7500
5000
2500
0
0628
0704
0710
0716
0722
0728

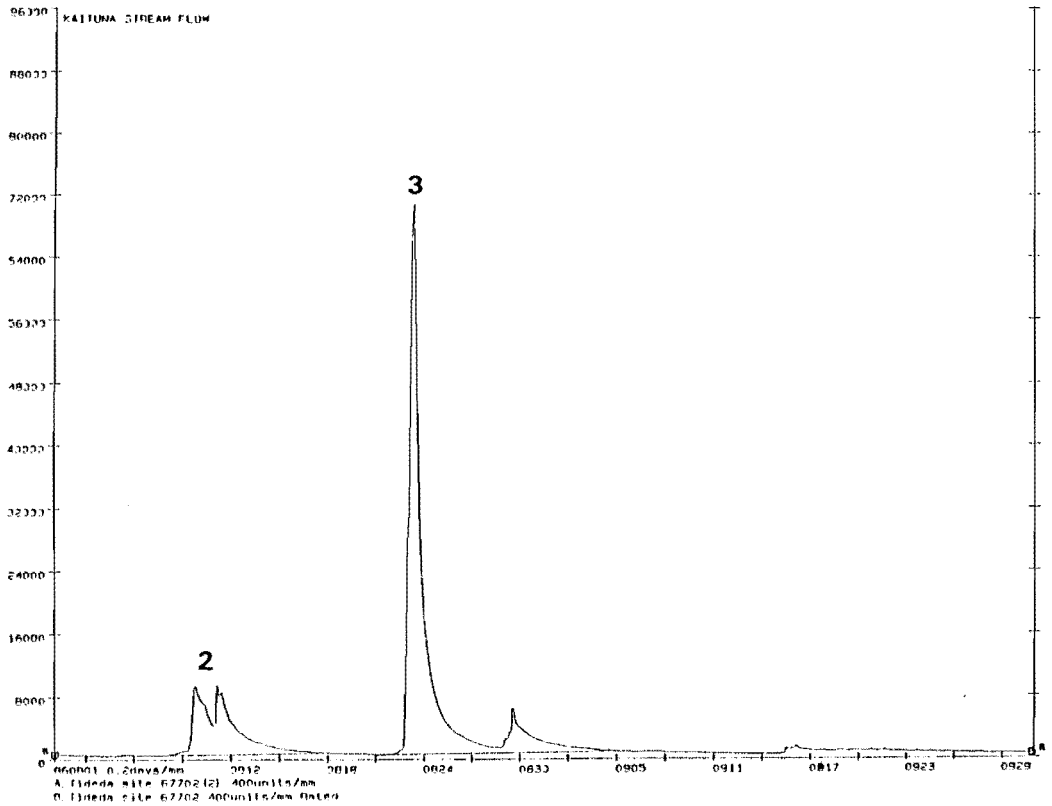
KAITUNA STREAM FLOW
3
2
88000
80000
72000
64000
56000
48000
40000
32000
24000
16000
8000
0
0824
0833
0905
0911
0917
0923
0929

A.9.4

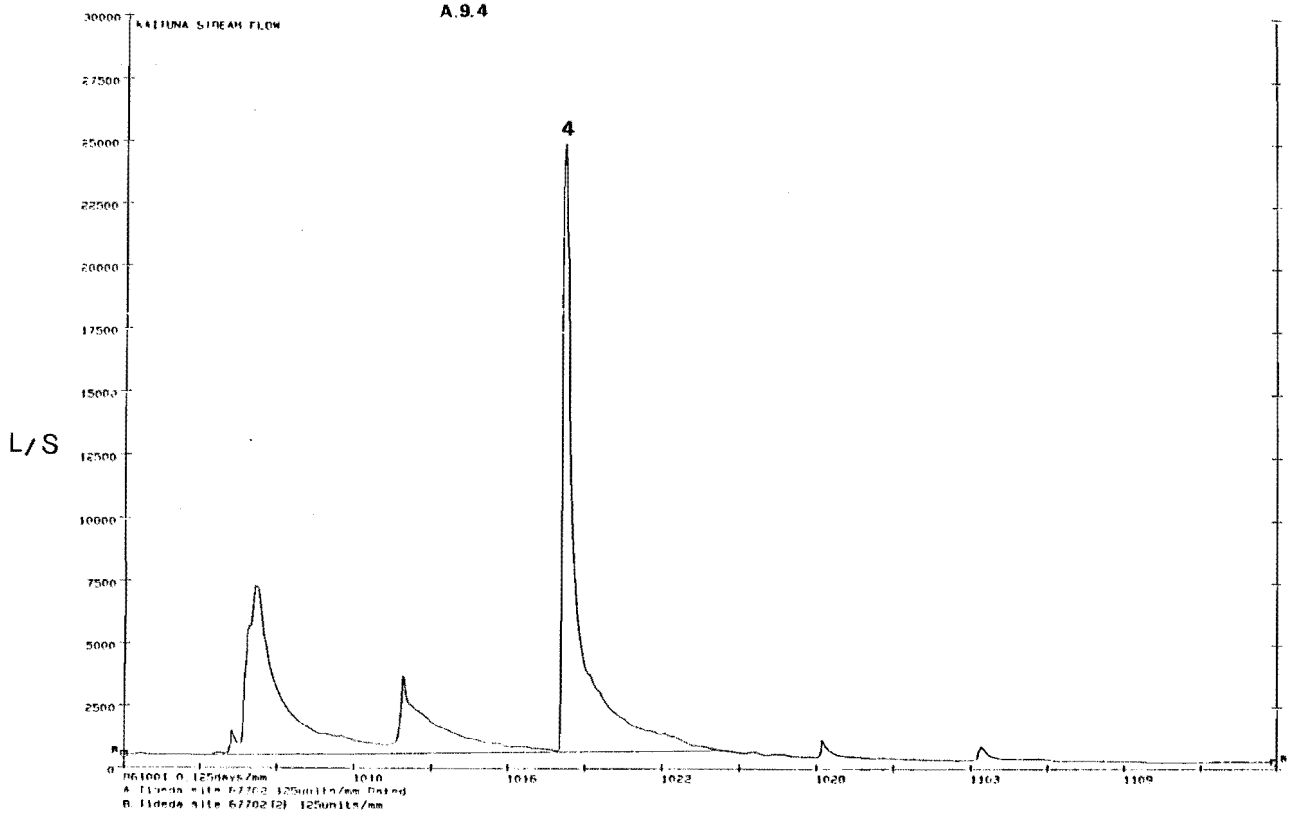
KAITUNA STREAM FLOW
4
L/S
30000
27500
25000
22500
20000
17500
15000
12500
10000
7500
5000
2500
0
1010
1016
1022
1028
1103
1109

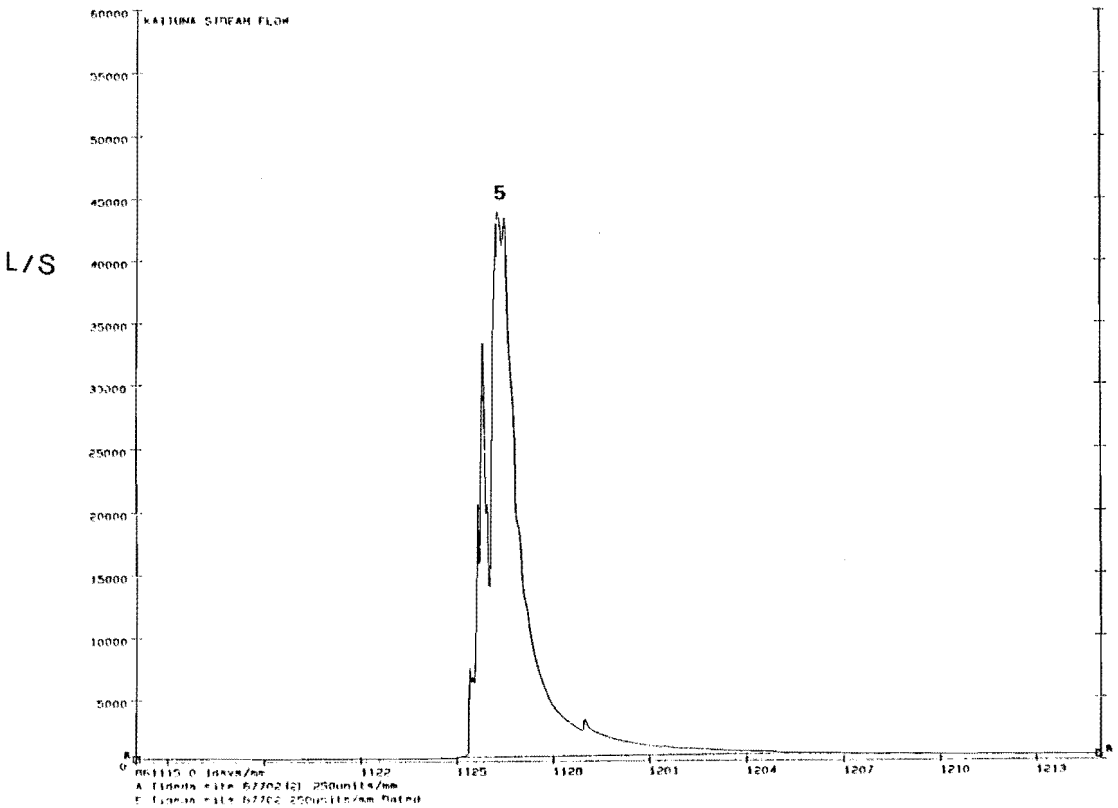
KAITUNA STREAM FLOW
5
L/S
60000
55000
50000
45000
40000
35000
30000
25000
20000
15000
10000
5000
0
1122
1125
1128
1201
1204
1207
1210
1213

A.9.4

L/S

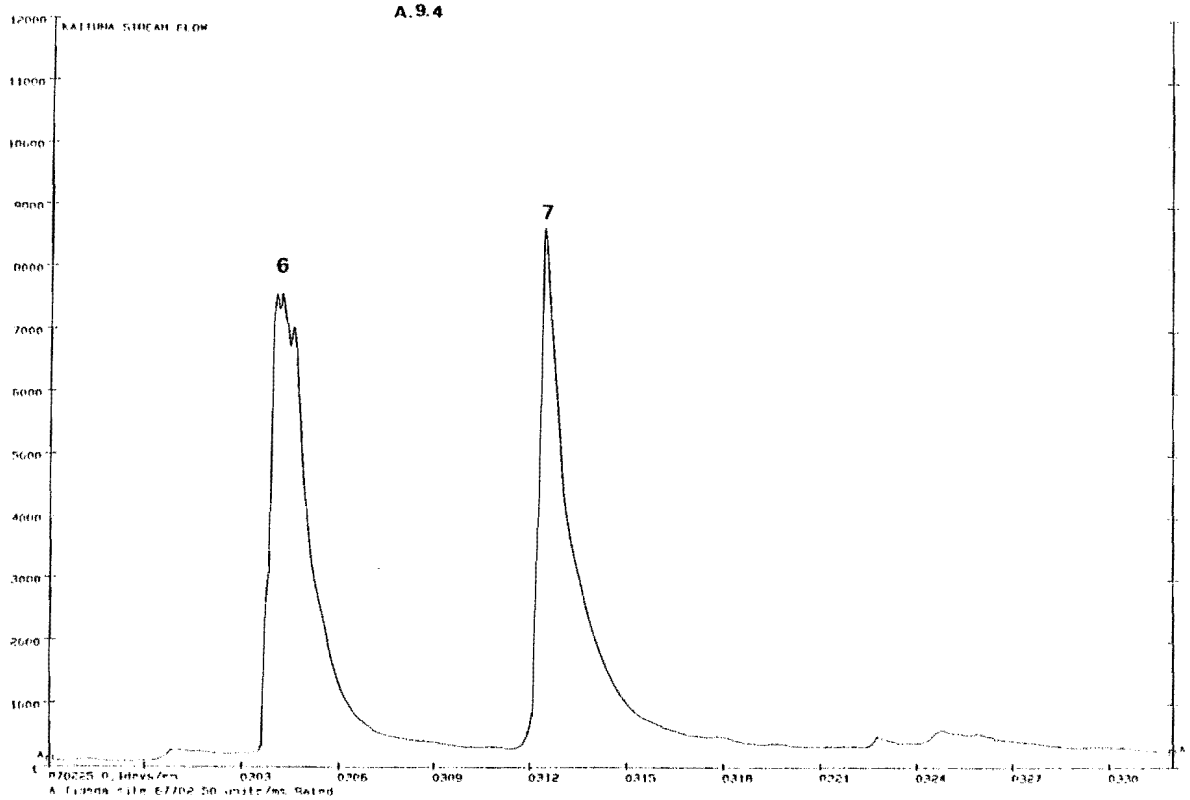
KATUNA STREAM FLOW
6
7
0303
0306
0309
0312
0315
0318
0321
0324
0327
0330

L/S

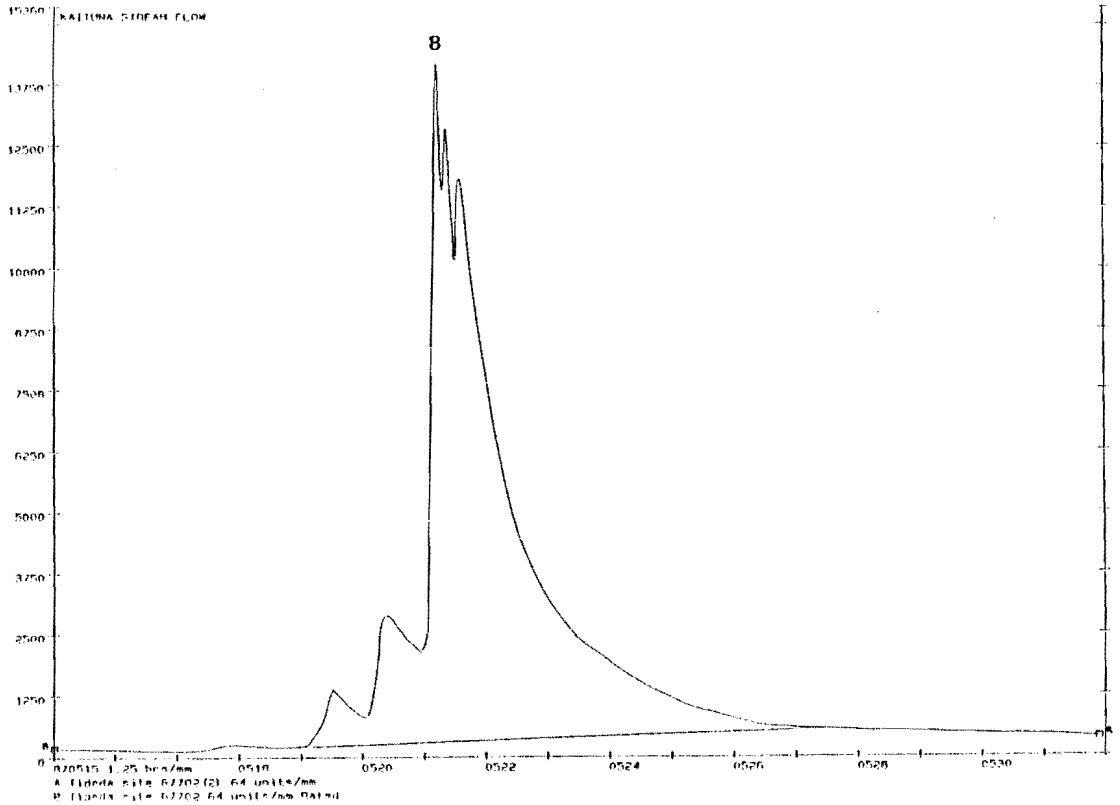
KATUNA STREAM FLOW
8
0510
0520
0522
0524
0526
0528
0530

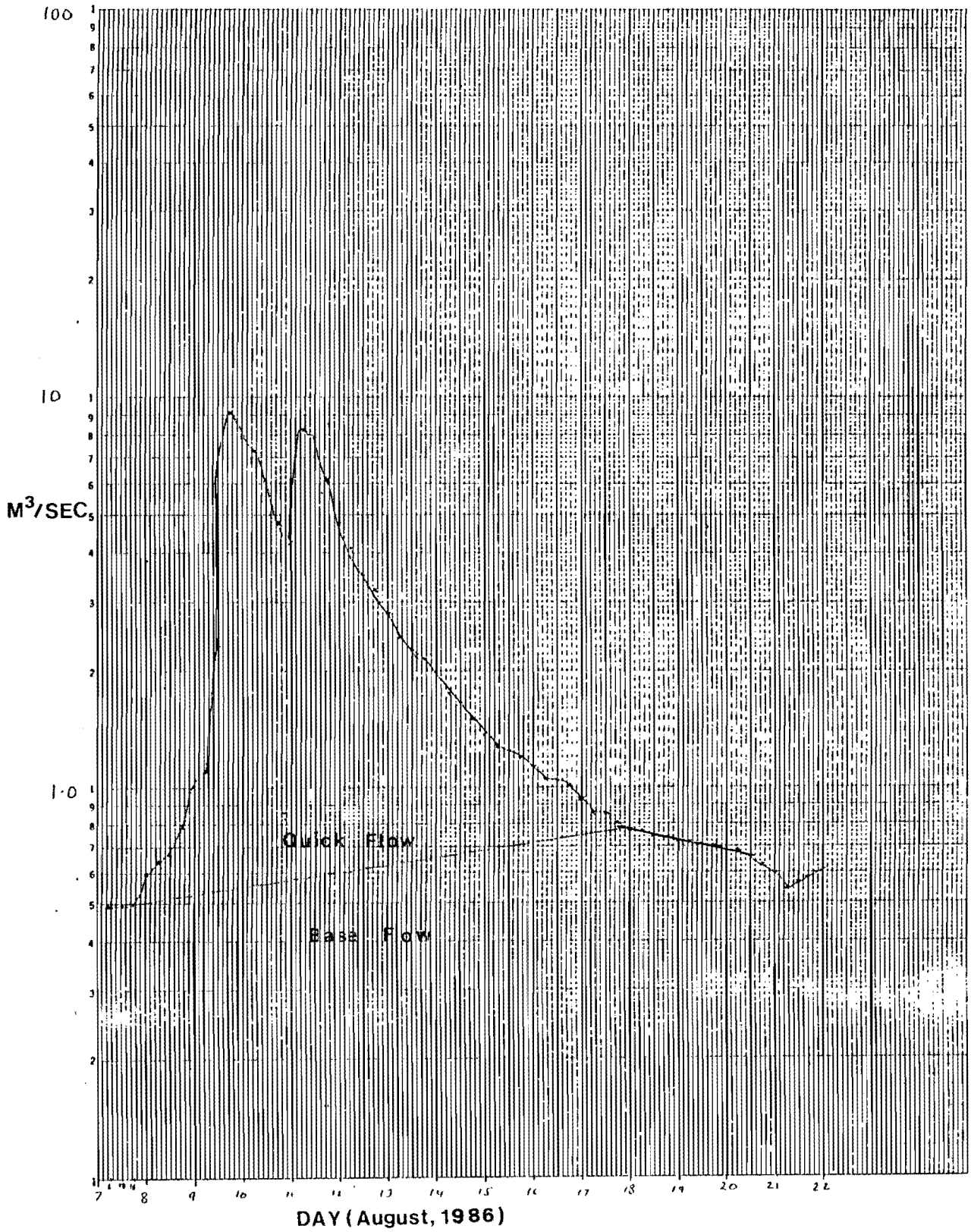

A.9.5 Example of Hydrograph Separation (Event 2)

A.9.6: Kaituna Stream Mean Flow (lit/sec)
at Station A (June 1986 – May 1987)

Day	Jun	1986– Jly	Aug	Sep	Oct	Nov	Dec	1987– Jan	Feb	Mar	Apr	May
1	–	2960	590	1710	530	350	1080	162	30	259	225	475
2	–	1810	520	1410	520	340	910	152	36	220	212	425
3		1620	490	1200	520	550	770	140	30	1775	199	384
4	–	1240	450	1010	540	390	700	120	38	6394	166	335
5	–	920	540	900	2130	380	600	114	32	2331	180	267
6	–	3960	530	830	5310	320	540	109	25	874	146	248
7	–	1600	510	840	2300	320	500	106	21	520	156	237
8	–	5050	750	770	1480	300	480	108	40	428	163	186
9	–	2910	4210	770	1240	290	460	115	44	363	160	140
10	110	5650	6110	690	1020	260	440	111	48	329	158	177
11	110	5750	6960	640	1190	260	440	105	44	364	157	168
12	110	3730	3700	600	2260	270	420	88	32	5536	161	158
13	140	2450	2330	580	1580	280	420	96	518	3042	128	160
14	90	1680	1670	550	1200	270	420	87	377	1435	127	160
15	90	1290	1250	950	980	260	390	103	389	804	114	165
16	120	990	1030	1220	860	250	340	91	207	581	104	138
17	130	830	850	970	760	250	350	94	176	495	120	179
18	180	750	750	930	10940	240	340	91	597	425	120	213
19	170	690	700	960	3140	210	340	93	325	380	119	833
20	210	640	650	960	1980	220	340	82	201	344	129	2165
21	280	940	570	960	1510	210	320	71	154	338	119	9966
22	570	1060	3390	890	1240	210	330	70	121	389	119	4962
23	310	990	4281	810	890	230	290	62	113	405	113	2466
24	240	900	1077	760	700	240	280	59	111	499	306	1510
25	180	890	4480	690	620	10510	300	58	103	538	296	949
26	860	1050	2800	650	550	31920	290	48	115	468	239	649
27	1190	860	1910	620	480	8230	290	42	96	402	164	557
28	710	760	148	580	680	320	280	37	170	342	139	510
29	540	690	390	590	470	2160	280	37	–	331	137	477
30	390	650	321	560	420	1410	310	30	–	318	141	441
31		550	220		380		220	28	–	274		400
Min	90	550	450	550	380	210	220	28	21	220	104	138
Mean	320	2270	3620	850	1570	2140	430	87	150	1007	161	971
Max	1190	1600	4280	1710	10940	31920	1080	62	597	6394	306	9966

A.9.7: Kaituna Base Flow (lit/scc) at Station A (June 1986 – May 1987)

	1986								1987			
Day	Jun	Jly	Aug	Sep	Oct	Nov	Dec	Jan	Feb	Mar	Apr	May
1	–	342	586	816	532	351	443	153	30	259	225	475
2	–	372	523	839	518	335	461	144	36	220	212	425
3	–	403	494	861	521	551	479	133	30	246	199	384
4	–	432	450	883	498	392	496	116	38	305	166	335
5	–	463	545	884	509	383	513	110	32	367	180	267
6	–	492	527	830	521	321	531	106	25	429	146	248
7	–	522	501	839	532	324	496	103	21	479	156	237
8	–	552	519	774	544	297	477	105	40	428	163	186
9	–	582	546	773	556	287	457	112	44	363	160	140
10	114	612	572	693	568	261	440	108	48	329	158	177
11	107	642	599	638	579	255	436	102	44	313	157	168
12	111	672	625	604	591	267	417	87	32	341	161	158
13	140	702	651	576	603	276	417	91	38	375	128	160
14	92	733	678	551	615	269	419	86	60	410	127	160
15	86	762	705	945	627	259	388	100	83	444	114	165
16	119	793	731	1222	638	245	339	90	106	479	104	138
17	125	813	757	971	650	247	352	92	128	494	120	179
18	182	754	747	928	662	236	344	90	151	425	120	211
19	168	687	703	962	674	207	342	91	174	380	119	228
20	215	643	654	959	685	221	344	82	191	344	129	269
21	277	938	575	959	697	215	320	71	154	338	119	311
22	566	1055	595	886	709	206	335	70	121	389	119	353
23	314	992	617	810	721	230	295	62	113	405	113	394
24	238	898	639	760	697	241	282	59	111	499	306	436
25	181	894	661	694	616	338	303	58	103	538	296	477
26	194	1048	684	648	551	355	286	48	115	468	239	519
27	222	856	706	620	477	373	289	42	96	402	164	548
28	253	764	728	584	680	391	278	37	170	342	139	510
29	283	694	750	589	467	408	278	37	–	331	137	477
30	313	648	772	564	420	426	292	30	–	318	141	441
31	–	547	794	–	379	–	209	–	28	274	–	–
Min	86	342	450	551	379	206	209	28	21	220	104	138
Mean	205	687	633	789	582	306	379	85	83	379	161	306
Max	566	1055	794	1222	721	551	531	153	191	538	306	548

A.9.8: Regression Equation for springs runoff to the Kaituna River, Total base flow for runoff from springs = -3.49 + 0.188 x Kaituna River toatl base flow.

APPENDIX 10

PUMP TESTS

A.10.1 Aquifer Parameter Definitions

A.10.2 Field Data

A.10.3 Programme THOM 1 (Computation of Transmissivity and Storage Coefficient)

A.10.4 Programme THOM XX (Drawdown Prediction)

A10.1 Aquifer Parameter Definitions.

The following definitions of hydraulic properties are based on Hazel, 1975.

Hydraulic Conductivity is the rate at which water at the prevailing viscosity can be transmitted through a unit area of an aquifer, normal to the direction of flow under a unit gradient

Transmissivity is the rate at which water at the prevailing viscosity can be transmitted through a unit of strip of aquifer under a unit gradient.

Storage Coefficient is the volume of the water which saturated column of aquifer released from or takes into storage per unit surface area per unit change in head.

Specific Storage is the volume of water released from or taken into storage per unit volume of aquifer per unit change in head.

Safe Yield is the amount of water which can be withdrawn from an aquifer without producing an undesirable result.

A.10.2: Step-Down Test on Bore M36-1344, Kaituna Valley

diameter = 200 mm, depth = 30.0 m,
Test commenced at 12.25 pm 30/5/1985

Step 1: Q_1 = 8.2 lit/sec.

Time t_1 (minutes)	Water level (metres)	Drawdown (metres)	Time t_1 (minutes)	Water level (metres)	Drawndown (mitres)
0	2.37	0.00	1	2.94	0.57
2	3,12	0.75	3	3.24	0.87
4	3.12	0.75	5	3.44	1.07
6	3.53	1.16	7	3.61	1.24
8	3.68	1.31	9	3.76	1.39
10	3.81	1.44	12	3.93	1.56
14	4.03	1.66	16	4.13	1.76
18	4.21	1.84	21	4.33	1.96
25	4.48	2.11	30	4.61	2.24
35	4.74	2.37	40	4.86	2.49
52	5.09	2.72	60	5.21	2.84
52	5.09	2.72	60	5.21	2.84
75	5.41	3.04	90	5.59	3.22
100	5.69	3.32	120	5.86	3.49
124	5.89	3.52			

Step 2: Q_2 = 12.1 lit/sec

Time t_1 (minutes)	Water level (metres)	Drawdown (metres)	Time t_1 (minutes)	Water level (metres)	Drawndown (mitres)
125	—	—	126	6.36	3.99
127	6.48	4.11	128	6.57	4.20
129	6.64	4.27	130	6.72	4.35
131	6.78	4.41	132	6.83	4.46
133	6.89	4.52	134	6.94	4.57
135	6.99	4.62	138	7.10	4.73
140	7.19	4.82	145	7.35	4.89
153	7.75	5.20	160	7.74	5.37
166	7.85	5.48	170	7.92	5.55
185	8.15	5.78	215	8.64	6.27
245	8.91	6.54	275	9.15	6.78
305	9.33	6.96	545	10.47	8.10
1140	11.93	9.56	1177	12.00	9.63
1194	12.03	9.66	12 08	12.07	9.70

A.10.2 continued on next page.

A.10.2 Continued

Step 3: Q_3 = 17.1 lit/sec

Time t_1 (minutes)	Water level (metres)	Drawdown (metres)	Time t_1 (minutes)	Water level (metres)	Drawndown (mitres)
1200	—	—	1210.5	12.67	10.30
12 11	12.79	10.42	1212	12.91	10.54
12 13	13.00	10.63	1214	13.07	10.70
12 15	13.16	10.79	12 16	13.22	10.85
12 17	13.28	10.91	12 18	13.32	10.95
12 19	13.38	11.01	1220	13.43	11.06
1222	13.52	11.15	1224	13.61	11.24
1226	13.69	11.32	1228	13.77	11.40
1230	13.83	11.46	1235	13.97	11.60
1239	14.07	11.70	1246	14.22	11.85
1256	14.40	12.03	1267	14.57	12.20
1270	14.61	12.24	1295	14.95	12.58
1345	15.18	12.81	13 73	15.50	13.13
1400	15.84	13.47	14 15	15.89	13.52
1520	16.30	13.93	1565	16.52	14.15
1607	16.70	14.33	1735	17.07	14.70
2630	18.64	16.27	2725	18.73	16.36
3030	19.08	16.71	3140	19.22	16.85
35 22	19.91	17.54	4408	20.86	18.49
4665	20.90	18.53	49 13	21.08	18.71
5595	21.45	19.08	5768	21.53	19.16
6060	21.67	19.30			

A.10.3 PROGRAM THOM1, PETER CALLANDER - AUGUST,1985

```
C
C  A PROGRAM TO MODEL THE THOMAS'S STEP DRAWDOWN TEST
C
C       THIS PROGRAM CALCULATES DRAWDOWNS USING THE THEIS EQUATION
C       FOR A POINT AT A SPECIFIED DISTANCE FROM A PUMPING WELL
C       AT A VARIETY OF TIMES IN A CHANNEL SHAPED AQUIFER.
C       THE AQUIFER IS MODELLED BY PAIRS OF IMAGE WELLS PUMPING
C       AT THE SAME RATE AS THE ONE REAL WELL.
C       THIS CREATES THE EFFECT OF A STRIP AQUIFER BOUNDED BY TWO
C       PARALLEL BARRIERS.
C       AS THE DRAWDOWN INCREASES RECHARGING SPRINGS OCCUR. THESE
C       ARE MODELLED BY RECHARGING IMAGE WELLS.
C       TOTAL DRAWDOWNS AT EACH TIME STEP ARE CALCULATED BY SUMMING
C       THE COMPONENT DRAWDOWNS FROM THE REAL WELL AND THE IMAGE WELLS.
C
C
C       THIS PROGRAM MUST BE LINKED WITH ,'FUNCTION THEIS'
C
C
C
      INTEGER IN,OUT,FILE,I,K,J,L,IPLOT,IREAD,J1,I1,I2,I3,ITEST
      REAL PI,T,S,DISTW,Q,Q2,Q3,DDOWN,TIME,TERMW,TERM1,VAR,SOME,DISTI
      REAL COEFF1,COEFF2,SW,SI,TIME1,TIME2,TIME3,TIMEA,COEFF3,COEFF4
      REAL COEFI,COEF3I,COEF4I,QI,QI2,QI3,C,WL1,WL2,WL3,TIMER,QR,QRR
      REAL TEST,TIMEX,DDX,SR,TERMR,QR2,TIMER2,TIMEX2,QRR2,SR2,QRLIM
      REAL QRR3,DTWI,DTW,TIME22,TIME33
      DIMENSION X(200),Y(200)
C
      IN=5
      OUT=6
      FILE=10
      IREAD=8
C
      OPEN(UNIT=FILE,NAME='THOM1.OUT',TYPE='NEW')
      OPEN(UNIT=IREAD,NAME='TIME.DAT',TYPE='OLD',READONLY)
C
C
      PI = 3.14159
C
C     INPUT DATA FROM TERMINAL
C
      WRITE(OUT,1000)
1000  FORMAT('  ENTER ALL VALUES IN S.I. UNITS  ',/
     1       ,'  ENTER TRANSMISSIVITY              : '$)
      READ (IN,1010) T
ccc      T = 0.005
1010  FORMAT(F10.0)
      WRITE(OUT,1020)
1020  FORMAT('  ENTER STORATIVITY                 : '$)
      READ (IN,1010) S
ccc      S = 0.005
C     WRITE(OUT,1025)
C1025 FORMAT('  ENTER WELL LOSS COEFFICIENT C     : '$)
C     READ (IN,1010) C
      C = 0.0
c     WRITE(OUT,1030)
c1030 FORMAT('  ENTER DISTANCE FROM PUMPING WELL : '$)
c     READ (IN,1010) DISTW
      DISTW = 0.1
      VAR = DISTW*DISTW
C     WRITE(OUT,1040)
C1040 FORMAT('  ENTER REAL PUMPING RATE STEP 1          : '$)
C     READ (IN,1010) Q
      Q = 0.0082
```

A.10.3

```
C       WRITE(OUT,1041)
C1041   FORMAT('  ENTER IMAGE  PUMPING RATE STEP 1        : '$)
C       READ (IN,1010) QI
        QI = 0.0082
C       WRITE(OUT,1042)
C1042   FORMAT('  ENTER INCREASE TO REAL PUMPING STEP 2   : '$)
C       READ (IN,1010) Q2
        Q2 = 0.0039
C       WRITE(OUT,1043)
C1043   FORMAT('  ENTER INCREASE TO IMAGE PUMPING STEP 2  : '$)
C       READ (IN,1010) QI2
        QI2 = 0.0039
C       WRITE(OUT,1044)
C1044   FORMAT('  ENTER INCREASE TO REAL PUMPING STEP 3   : '$)
C       READ (IN,1010) Q3
        Q3 = 0.005
C       WRITE(OUT,1045)
C1045   FORMAT('  ENTER INCREASE TO IMAGE PUMPING STEP 3  : '$)
C       READ (IN,1010) QI3
        QI3 = 0.005
        WRITE(OUT,1046)
1046    FORMAT('  ENTER DISTANCE BETWEEN PUMPING WELL ',/,
     1          ' AND NEAREST PAIR OF IMAGE WELLS         : '$)
        READ (IN,1010) SOME
CCC        SOME = 40.0
        WRITE(OUT,491)
491     FORMAT('  ENTER WATER DEPTH WHERE FIRST RECHARGE RATE OCCURS : '$)
        READ (IN,1010) REC1
ccc        REC1 = 9.0
        WRITE(OUT,1047)
1047    FORMAT('  ENTER FIRST RECHARGE RATE PER METRE DECLINE IN HEAD : '$)
        READ (IN,1010) QRR
ccc        QRR = -0.007
        WRITE(OUT,1048)
1048    FORMAT('  ENTER LIMIT OF FIRST RECHARGE RATE                  : '$)
        READ (IN,1010) QRLIM
ccc        QRLIM = -0.048
        WRITE(OUT,492)
492     FORMAT('  ENTER WATER DEPTH WHERE SECOND RECHARGE RATE OCCURS  : '$)
        READ (IN,1010) REC2
ccc        REC2 = 15.5
        WRITE(OUT,1049)
1049    FORMAT(' ENTER SECOND RECHARGE RATE PER METRE DECLINE IN HEAD : '$)
        READ (IN,1010) QRR2
ccc        QRR2 = -0.0068
        WRITE(OUT,493)
493     FORMAT('  ENTER LIMIT OF SECOND RECHARGE RATE                 : '$)
        READ (IN,1010) QRLIM2
ccc        QRLIM2 = -2.0
C       WRITE(OUT,494)
C494    FORMAT('  INPUT INITIAL DEPTH TO WATER                        : '$)
C       READ (IN,1010) DTWI
        DTWI = 2.37
C
C
C  INITIAL VARIABLES INPUTED
C  OUTPUT THEM TO A FILE
C
10      WRITE(FILE,1050) T,S,C,DISTW,SOME,Q,Q2,Q3,QI,QI2,QI3,REC1,QRR
     1         ,QRLIM,REC2,QRR2,QRLIM2,DTWI
1050    FORMAT(' INTIAL VALUES ENTERED USING S.I. UNITS : ',/,
     1   ' TRANSMISSIVITY                    = ',F15.7,/,
     2   ' STORATIVITY                       = ',F15.7,/,
     2   ' WELL LOSS COEFICIENT              = ',F15.7,/,
     3   ' DISTANCE FROM PUMPING WELL        = ',F15.7,/,
     4   ' DISTANCE BETWEEN PUMPING WELL ',/,
```

```
     5    ' AND NEAREST IMAGE WELL PAIR      = ',F15.7,/,
     7    ' PUMPING RATE                     = ',F15.7,/,
     8    ' PUMPING RATE INCREASE AT STEP 2  = ',F15.7,/,
     8    ' PUMPING RATE INCREASE AT STEP 3  = ',F15.7,/,
     7    ' IMAGE PUMPING RATE               = ',F15.7,/,
     8    ' IMAGE PUMPING RATE INCREASE AT STEP 2  = ',F15.7,/,
     8    ' IMAGE PUMPING RATE INCREASE AT STEP 3  = ',F15.7,/,
     8    ' WATER DEPTH AT START OF FIRST RECHARGE RATE ',F15.7,/,
     8    ' FIRST RECHARGE RATE PER METRE DECLINE IN HEAD= ',F15.7,/,
     8    ' LIMIT OF FIRST RECHARGE RATE                = ',F15.7,/,
     8    ' WATER DEPTH AT START OF SECOND RECHARGE RATE ',F15.7,/,
     8    ' SECOND RECHARGE RATE PER METRE DECLINE IN HEAD= ',F15.7,/,
     8    ' LIMIT OF SECOND RECHARGE RATE               = ',F15.7,/,
     8    ' INITIAL DEPTH TO WATER        = ',F15.7,/,
     8    '      TIME           DEPTH TO WATER  ',
     7      /,' (in minutes)           (in metres)',/)
C
C
C       CALCULATION OF DRAWDOWNS AT SET TIMES
C
        SR = 0.0
        COEFF1 = Q/(4.0*PI*T)
        WL1 = C*Q**2.0
        COEFI = QI/(4.0*PI*T)
        COEFF2  = S/(4.0*T*60.0)
        TERMW = DISTW*DISTW*COEFF2
C       INPUT TIMES FROM DATA FILE
        DO 20 I1 = 1,100
            READ(IREAD,1055) TIME
1055        FORMAT(F10.0)
            IF(TIME.EQ.-999) GOTO 25
            TIME1 = TIME
            SW = COEFFI*THEIS(TERMW/TIME)
            DDOWN = SW+WL1
            DTW = DTWI+SW+WL1
C           CALCULATE THE EFFECT OF THE IMAGE WELLS
            DO 15 L = 1,500
               DISTI = L*SOME
               DISTI = VAR+DISTI**2.0
               TERMI = DISTI*COEFF2
               SI = COEFI*THEIS(TERMI/TIME)
               DDOWN = DDOWN+2.0*SI
               DTW = DTW+2.0*SI
               IF(SI.LT.0.001) GOTO 22
15          CONTINUE
22          X(I1) = TIME
            Y(I1) = DTW
            J=I1
             WRITE(OUT,1060)TIME,DTW
C           WRITE(FILE,1060)TIME,DTW
1060        FORMAT(2X,F10.2,14X,F8.3)
20      CONTINUE
C
C
C    CALCULATE FOR STEP2
C
C
25      COEFF3 = Q2/(4.0*PI*T)
        WL2 = 0+Q2
        WL2 = C*WL2**2.0
        COEF3I = QI2/(4.0*PI*T)
        TERMR = VAR+SOME**2.0
        TERMR = TERMR*COEFF2
        TEST = 1.0
        ITEST = 1
C       INPUT TIME VALUES FROM DATA FILE
```

```
      DO 30 I2 = 1,100
          READ(IREAD,1055) TIME
          IF(TIME.EQ.-999) GOTO 35
          TIME2 = TIME-TIME1
          TIME22 = TIME
          SW = COEFF1*THEIS(TERMW/TIME)+COEFF3*THEIS(TERMW/TIME2)
          DDOWN = SW+WL2
          DTW = DTWI+SW+WL2
C         CALCULATE THE EFFECT OF THE IMAGE WELLS
          DO 26 L = 1,500
             DISTI = L*SOME
             DISTI = VAR+DISTI**2.0
             TERMI = DISTI*COEFF2
             SI = COEFI*THEIS(TERMI/TIME)+COEF3I*THEIS(TERMI/TIME2)
             DDOWN = DDOWN+2.0*SI
             DTW = DTW+2.0*SI
             IF(SI.GT.0.001) GOTO 26
C               CALCULATE THE EFFECT OF A RECHARGING SPRING
                IF(TEST.EQ.2.0) GOTO 9800
                   IF(DTW.GT.REC1) GOTO 9900
                   GO TO 27
9900               TIMEX = TIME
                   TEST = 2.0
9800               IF(ITEST.EQ.1) GOTO 28
                   TIMER = TIME-TIMEX
                   DDX = DTW-REC1
                   QR = QRR*DDX
                   SR = QR*THEIS(TERMR/TIMER)/(4.0*PI*T)
                   DDOWN = DDOWN+SR
                   DTW = DTW+SR
                   GO TO 27
26           CONTINUE
             GOTO 27
28           ITEST = 2
27           K = I2+J
             X(K) = TIME
             Y(K) = DTW
C             WRITE(OUT,1060)TIME,DTW
             WRITE(FILE,1060)TIME,DTW
30        CONTINUE
C
C
C     CALCULATE FOR THIRD TIME STEP
C
C
35        COEFF4 = 03/(4.0*PI*T)
C                 WRITE(OUT,93) DDOWN,SR,QR,TIME
C93               FORMAT(' DDOWN = ',F7.2,' SR = ',F7.2,
C     1             ' QR = ',F7.4,'TIME = ',F7.1,//)
          WL3 = 0+02403
          WL3 = C*WL3**2.0
          COEF4I = 013/(4.0*PI*T)
          TEST = 1.0
          ITEST = 1
          ATEST = 3.0
          IATEST = 3
C         INPUT TIME VALUES FROM DATA FILE
          DO 40 I3 = 1,100
              READ(IREAD,1055) TIME
              IF(TIME.EQ.-999) GOTO 45
              TIME3 = TIME-TIME22
              TIME33 = TIME
              TIMEA = TIME-TIME1
              SW = COEFF1*THEIS(TERMW/TIME)'COEFF3*THEIS(TERMW/TIMEA)
     1             +COEFF4*THEIS(TERMW/TIME3)
              DDOWN = SW+WL3
```

```
            DTW = DTWI+SW+WL3
C           CALCULATE THE EFFECT OF THE IMAGE WELLS
            DO 36 L = 1,500
               DISTI = L*SOME
               DISTI = VAR+DISTI**2.0
               TERMI = DISTI*COEFF2
               SI = COEFI*THEIS(TERMI/TIME)+COEF3I*THEIS(TERMI/TIMEA)
     1           +COEF4I*THEIS(TERMI/TIME3)
               DDOWN = DDOWN+2.0*SI
               DTW = DTW+2.0*SI
               IF(SI.GT.0.001) GOTO 36
C                 CALCULATE THE EFFECT OF A RECHARGING SPRING
                     TIMER = TIME-TIMEX
                     DDX = DTW-REC1
                     QR = QRR*DDX
                     IF(QR.GT.QRLIM) GOTO 91
                     QR = QRLIM
91                   SR = QR*THEIS(TERMR/TIMER)/(4.0*PI*T)
                     DDOWN = DDOWN+SR
                     DTW = DTW+SR
C             WRITE(OUT,92) SW,SI,SR
C92           FORMAT(' SW = ',F7.2,' SI = ',F7.2,' SR = ',F7.4)
C           CALCULATE THE EFFECT OF A SECOND RECHARGING SPRING
                  IF(TEST.EQ.2.0) GOTO 9880
                   IF(DTW.GT.REC2) GOTO 9990
                     GO TO 37
9990                 TIMEX2 = TIME
                     TEST = 2.0
9880                 IF(ITEST.EQ.1) GOTO 38
                     TIMER2 = TIME-TIMEX2
                     DDX2 = DTW-REC2
                     QR2 = QRR2*DDX2
                     IF(QR2.GT.QRLIM2) GO TO 906
                     QR2 = QRLIM2
906                  SR2 = QR2*THEIS(TERMR/TIMER2)/(4.0*PI*T)
                  DDOWN = DDOWN+SR2
                  DTW = DTW+SR2
            GO TO 37
36          CONTINUE
            GO TO 37
38          ITEST = 2
            GO TO 37
39          IATEST = 4
37          J = 13+K
            X(J) = TIME
            Y(J) = DTW
              SRT = SR+SR2
C              WRITE(OUT,944) SR2,QR2,TIME
C944            FORMAT(' SR2 = ',F7.2,' QR2 = ',F7.4,' TIME ',F7.1)
C             WRITE(OUT,1060)TIME,DTW
            WRITE(FILE,1060)TIME,DTW
40      CONTINUE
C
C
C
CC
C
C       CREATE OUTPUT FILE FOR PLOTTING
C
45      IPLOT = 9
        OPEN(UNIT=IPLOT,NAME='THOM1.PLO',TYPE='NEW')
        K = 1
        J1 = J/10
        DO 2000 I=1,J1
            WRITE(IPLOT,3000) (X(I1),I1=K,K+9)
            K = I*10+1
```

A.10.3

```
2000    CONTINUE
        IF(J1*10.EQ.J) GOTO 2010
        WRITE(IPLOT,3000) (X(I1),I1=K,J)
2010    CONTINUE
        K = 1
        DO 2020 I=1,J1
            WRITE(IPLOT,3010) (Y(I1),I1=K,K+9)
            K = I*10+1
2020    CONTINUE
        IF(J1*10.EQ.J) GOTO 2030
        WRITE(IPLOT,3010) (Y(I1),I1=K,J)
2030    CONTINUE
3000    FORMAT(<10>(F7.1))
3010    FORMAT(<10>(F7.2))
C
        CLOSE(UNIT=IPLOT,DISPOSE='SAVE')
C
C
        CLOSE(UNIT=FILE,DISPOSE='SAVE')
C
        CLOSE(UNIT=IREAD,DISPOSE='SAVE')
C
        END
```

A.10.3

```
INTIAL VALUES ENTERED USING S.I. UNITS :
TRANSMISSIVITY                    =       0.0048000
STORATIVITY                       =       0.0025000
WELL LOSS COEFICIENT              =       0.0000000
DISTANCE FROM PUMPING WELL        =       0.1000000
DISTANCE BETWEEN PUMPING WELL
AND NEAREST IMAGE WELL PAIR       =      44.5000000
PUMPING RATE                      =       0.0082000
PUMPING RATE INCREASE AT STEP 2   =       0.0039000
PUMPING RATE INCREASE AT STEP 3   =       0.0050000
IMAGE PUMPING RATE                =       0.0082000
IMAGE PUMPING RATE INCREASE AT STEP 2  =       0.0039000
IMAGE PUMPING RATE INCREASE AT STEP 3  =       0.0050000
WATER DEPTH AT START OF FIRST RECHARGE RATE       8.5000000
FIRST RECHARGE RATE PER METRE DECLINE IN HEAD=      -0.0064500
LIMIT OF FIRST RECHARGE RATE                =      -0.0488000
WATER DEPTH AT START OF SECOND RECHARGE RATE      16.0000000
SECOND RECHARGE RATE PER METRE DECLINE IN HEAD=      -0.0068300
LIMIT OF SECOND RECHARGE RATE               =      -2.0000000
INITIAL DEPTH TO WATER            =       2.3699999
    TIME            DEPTH TO WATER
(in minutes)           (in metres)

      1.00                3.752
      2.00                3.856
      3.00                3.931
      4.00                3.993
      5.00                4.048
      6.00                4.098
      7.00                4.143
      8.00                4.186
      9.00                4.226
     10.00                4.263
     12.00                4.334
     14.00                4.398
     16.00                4.458
     18.00                4.514
     21.00                4.594
     25.00                4.691
     30.00                4.801
     35.00                4.903
     40.00                4.998
     52.00                5.204
     60.00                5.328
     75.00                5.541
     90.00                5.733
    100.00                5.852
    120.00                6.074
    124.00                6.116
    125.00                6.784
    126.00                6.844
    127.00                6.890
    128.00                6.930
    129.00                6.966
    130.00                7.000
    131.00                7.032
    132.00                7.062
    133.00                7.091
    134.00                7.119
    135.00                7.146
    138.00                7.223
    140.00                7.271
    145.00                7.384
    153.00                7.549
    160.00                7.682
```

A.10.3

166.00	7.790
170.00	7.859
185.00	8.104
215.00	8.542
245.00	8.863
275.00	9.111
305.00	9.322
545.00	10.451
1140.00	11.883
1177.00	11.945
1194.00	11.973
1208.00	11.996
1210.00	12.770
1210.50	12.796
1211.00	12.819
1212.00	12.862
1213.00	12.899
1214.00	12.934
1215.00	12.966
1216.00	12.996
1217.00	13.024
1218.00	13.051
1219.00	13.078
1220.00	13.103
1222.00	13.150
1224.00	13.195
1226.00	13.238
1228.00	13.279
1230.00	13.318
1235.00	13.411
1239.00	13.480
1246.00	13.593
1256.00	13.743
1267.00	13.895
1270.00	13.935
1295.00	14.245
1345.00	14.784
1373.00	15.059
1400.00	15.310
1415.00	15.444
1520.00	16.319
1565.00	16.524
1607.00	16.702
1745.00	17.192
1975.00	17.819
2630.00	19.018
2725.00	19.151
3020.00	19.521
3140.00	19.656
3522.00	20.036
4408.00	20.711
4665.00	20.867
4913.00	21.005
5595.00	21.326
5768.00	21.397
6060.00	21.507

A.10.4

```
      PROGRAM THOMXX
C
C       PETER CALLANDER - AUGUST,1985
C
C  A PROGRAM TO MODEL THE THOMAS'S BORE (M36/1344) ABSTRACTING WATER
C     FROM THE BASAL AQUIFER IN THE KAITUNA VALLEY.
C
C  THIS PROGRAM CALCULATES DRAWDOWNS USING THE THEIS EQUATION
C     FOR A POINT AT A SPECIFIED DISTANCE FROM A PUMPING WELL
C     AT A VARIETY OF TIMES IN A CHANNEL SHAPED AQUIFER.
C    THE AQUIFER IS MODELLED BY PAIRS OF IMAGE WELLS PUMPING
C     AT THE SAME RATE AS THE ONE REAL WELL.
C    THIS CREATES THE EFFECT OF A STRIP AQUIFER BOUNDED BY TWO
C     PARALLEL IMPERMEABLE BOUNDARIES.
C    AS DRAWDOWN INCREASES SOME RECHARGING SPRINGS OCCUR. THESE
C     ARE MODELLED BY A RECHARGING IMAGE WELL.
C
C
C    THIS PROGRAM MUST BE LINKED WITH ,'FUNCTION THEIS'
C
C
C
      INTEGER FILE,IATEST,IN,IPLOT,ITEST,II,J,L,LIMT,OUT
      REAL ATEST,C,COEFI,COEFF1,COEFF2,DDOWN,DDX,DDX2,DISTI,DISTW
      REAL DTW,DTWI,EXP,PI,Q,QI,QR,QR2,QRLIM,QRLIM2,QRR,QRR2
      REAL REC1,REC2,S,SI,SOME,SR,SR2,SW,T,TERMI,TERMR,TERMW
      REAL TEST,TIME,TIMER,TIMER2,TIMEX,TIMEX2,VAR,WL1
      DIMENSION X(100),Y(100)
C
      IN=5
      OUT=6
      FILE=10
C
      OPEN(UNIT=FILE,NAME='THOMXX.OUT',TYPE='NEW')
C
C
      PI = 3.14159
C
C   INPUT DATA FROM TERMINAL
C
      WRITE(OUT,1111)
1111  FORMAT('  ENTER INITIAL DEPTH TO WATER     : '$)
      READ (IN,1010) DTWI
      WRITE(OUT,1000)
1000  FORMAT('  ENTER ALL VALUES IN S.I. UNITS  ',/
     1       ,'  ENTER TRANSMISSIVITY             : '$)
      READ (IN,1010) T
ccc      T = 0.005
1010  FORMAT(F10.0)
      WRITE(OUT,1020)
1020  FORMAT('  ENTER STORATIVITY                : '$)
      READ (IN,1010) S
ccc      S = 0.005
C     WRITE(OUT,1025)
C1025 FORMAT('  ENTER WELL LOSS COEFFICIENT C    : '$)
C     READ (IN,1010) C
      C = 0.0
      WRITE(OUT,1030)
1030  FORMAT('  ENTER DISTANCE FROM PUMPING WELL : '$)
      READ (IN,1010) DISTW
      VAR = DISTW*DISTW
      WRITE(OUT,1040)
1040  FORMAT('  ENTER PUMPING RATE               : '$)
      READ (IN,1010) Q
      QI = Q
```

A.10.4

```
      WRITE(OUT,1041)
1041  FORMAT('  ENTER 10xlog10 OF TIME LIMIT (in minutes)
     1   FOR CALCULATIONS : '$)
      READ (IN,1011) LIMT
1011  FORMAT(I4)
      WRITE(OUT,1046)
1046  FORMAT('  ENTER DISTANCE BETWEEN PUMPING WELL ',/,
     1          ' AND NEAREST PAIR OF IMAGE WELLS         : '$)
      READ (IN,1010) SOME
ccc      SOME = 30.0
      WRITE(OUT,941)
941   FORMAT('  ENTER WATER DEPTH WHERE FIRST RECHARGE RATE OCCURS : '$)
      READ (IN,1010) REC1
      WRITE(OUT,1047)
1047  FORMAT('  ENTER FIRST RECHARGE RATE PER METRE DECLINE IN HEAD : '$)
      READ (IN,1010) QRR
C      QRR = -0.007
      WRITE(OUT,1048)
1048  FORMAT('  ENTER LIMIT OF FIRST RECHARGE RATE                  : '$)
      READ (IN,1010) QRLIM
C      QRLIM = -0.05
      WRITE(OUT,942)
942   FORMAT('  ENTER WATER DEPTH WHERE SECOND RECHARGE RATE OCCURS : '$)
      READ (IN,1010) REC2
      WRITE(OUT,1049)
1049  FORMAT(' ENTER SECOND RECHARGE RATE PER METRE DECLINE IN HEAD : '$)
      READ (IN,1010) QRR2
C      QRR2 = -0.0068
      WRITE(OUT,943)
943   FORMAT('  ENTER LIMIT OF SECOND RECHARGE RATE                 : '$)
      READ (IN,1010) QRLIM2
C
C   INITIAL VARIABLES HAVE NOW BEEN ENTERED
C   OUTPUT THEM TO A FILE
C
10    WRITE(FILE,1050) T,S,C,DISTW,SOME,Q,QI,REC1,QRR,QRLIM
     1                 ,REC2,QRR2,QRLIM2,DTWI
1050  FORMAT(' INTIAL VALUES ENTERED USING S.I. UNITS : ',/,
     1   ' TRANSMISSIVITY                    = ',F15.7,/,
     2   ' STORATIVITY                       = ',F15.7,/,
     2   ' WELL LOSS COEFICIENT              = ',F15.7,/,
     3   ' DISTANCE FROM PUMPING WELL        = ',F15.7,/,
     4   ' DISTANCE BETWEEN PUMPING WELL ',/,
     5   ' AND NEAREST IMAGE WELL PAIR       = ',F15.7,/,
     7   ' PUMPING RATE                      = ',F15.7,/,
     7   ' IMAGE PUMPING RATE                = ',F15.7,//,
     8   ' WATER DEPTH WHERE FIRST RECHARGE RATE OCCURS = ',F15.7,/,
     8   ' FIRST RECHARGE RATE PER METRE DECLINE IN HEAD= ',F15.7,/,
     8   ' MAXIMUM FLOW OF FIRST RECHARGE RATE     ,    = ',F15.7,//,
     8   ' WATER DEPTH WHERE SECOND RECHARGE RATE OCCURS = ',F15.7,/,
     8   ' SECOND RECHARGE RATE PER METRE DECLINE IN HEAD= ',F15.7,/,
     8   ' MAXIMUM FLOW OF SECOND RECHARGE RATE          = ',F15.7,//,
     8   ' INITIAL DEPTH TO WATER = ',F7.3,////)
68     WRITE(FILE,69) Q
69     FORMAT(' AT PUMPING RATE Q = ',F8.5,/,
     9       '         TIME                  DRAWDOWN  ',/,
     9       '   (in minutes)                (in meters)',/)
C
C
C   COMMENCE CALCULATION OF DRAWDOWNS AT SET TIMES
C
      TEST = 1.0
      ITEST = 1
      ATEST = 1.0
      IATEST = 1
      COEFF1 = Q/(4.0*PI*T)
```

A.10.4

```
      WL1 = C*D**2.0
      COEFI = 01/(4.0*PI*T)
      COEFF2  = S/(4.0*T*60.0)
      TERMW = VAR*COEFF2
      TERMR = SOME*SOME*COEFF2
C   SET TIMES TO GIVE TEN POINTS PER LOG CYCLE
      DO 20 II = 1,LINT
          J=II
          EXP = 0.1*I1
          TIME = 10.0**EXP
          SW = COEFF1*THEIS(TERMW/TIME)
          DDOWN = SW+WL1
          DTW = DTWI+SW+WL1
C   CALCULATE THE EFFECT OF THE IMAGE WELLS
          DO 15 L = 1,100
             DISTI = L*SOME
             DISTI = VARIDISTI**2.0
             TERMI = DISTI*COEFF2
             SI = COEFI*THEIS(TERMI/TIME)
             DDOWN = DDOWN+2.0*SI
             DTW = DTW+2.0*SI
             IF(SI.GT.0.001) GOTO 15
C   AS THE WATER LEVEL IN THE PUMPING BORE DROPS BELOW REC1 METRES,
C     A RECHARGING SPRING OCCURS
                IF(ITEST.EQ.2.0) GOTO 9800
                   IF(DTW.GT.REC1) GOTO 9900
                   GO TO 22
9900               TIMEX = TIME
                   TEST = 2.0
9800               IF(ITEST.EQ.1) GOTO 38
                   TIMER = TIME-TIMEX
                   DDX = DTW-REC1
                   QR = QRR*DDX
                   SR = QR*THEIS(TERMR/TIMER)/(4.0*PI*T)
                   DDOWN = DDOWN+SR
                   DTW = DTW+SR
C   AS THE WATER LEVEL IN THE PUMPING BORE DROPS BELOW REC2 METRES,
C     A SECOND RECHARGING SPRING OCCURS
                IF(ATEST.EQ.2.0) GOTO 9880
                   IF(DTW.GT.REC2) GOTO 9990
                   GO TO 22
9990               TIMEX2 = TIME
                   ATEST = 2.0
9880                  IF(IATEST.EQ.1) GOTO 39
                TIMER2 = TIME-TIMEX2
                DDX2 = DTW-REC2
                QR2 = QRR2*DDX2
                SR2 = QR2*THEIS(TERMR/TIMER2)/(4.0*PI*T)
                DDOWN = DDOWN+SR2
                DTW = DTW+SR2
          GO TO 22
15        CONTINUE
          GO TO 22
38        ITEST = 2
          GO TO 22
39        IATEST = 4
C   STORE THE CALCULATED TIMES AND DEPTHS TO WATER IN AN ARRAY
C     FOR PLOTTING AND WRITE THEM TO THE OUTPUT FILE
22        X(I1) = TIME
          Y(I1) = DTW
          WRITE(FILE,1060)TIME,DTW
1060      FORMAT(4X,F8.0,14X,F8.3)
C   IF THE DRAWDOWNS CAUSE THE AQUIFER TO BECOME DE-WATERED WRITE
C     A MESSAGE TO THE OUTPUT FILE AND REDUCE THE PUMPING RATE BY
C     1.0 LITRES PER SECOND
          IF(DTW.GT.24.0) GOTO 44
```

A.10.4

```
            GO TO 20
66          WRITE(FILE,67) TIME,Q
67          FORMAT(' DEPTH TO WATER EXCEEDS 24.0 METRES AT TIME = '
     1             ,F8.1,' MINUTES ',/,
     1            ' FOR A PUMPING RATE OF ',F7.5,' M3/S ',///)
            Q = Q-0.001
            GO TO 68
20      CONTINUE
C
C
C
C   CREATE OUTPUT FILE FOR PLOTTING
C
45      IPLOT = 9
        OPEN(UNIT=IPLOT,NAME='THOMXX.PLO',TYPE='NEW')
        K = 1
        J1 = J/10
        DO 2000 I=1,J1
            WRITE(IPLOT,3000) (X(I1),I1=K,K+9)
            K = I*10+1
2000    CONTINUE
        IF(J1*10.EQ.J) GOTO 2010
        WRITE(IPLOT,3000) (X(I1),I1=K,J)
2010    CONTINUE
        K = 1
        DO 2020 I=1,J1
            WRITE(IPLOT,3010) (Y(I1),I1=K,K+9)
            K = I*10+1
2020    CONTINUE
        IF(J1*10.EQ.J) GOTO 2030
        WRITE(IPLOT,3010) (Y(I1),I1=K,J)
2030    CONTINUE
3000    FORMAT(<10>(F7.1))
3010    FORMAT(<10>(F7.2))
C
        CLOSE(UNIT=IPLOT,DISPOSE='SAVE')
C
C
        CLOSE(UNIT=FILE,DISPOSE='SAVE')
C
C
        END
```

A.10.4

```
INITIAL VALUES ENTERED USING S.I. UNITS :
TRANSMISSIVITY                          =        0.0048000
STORATIVITY                             =        0.0025000
WELL LOSS COEFFICIENT                   =        0.0000000
DISTANCE FROM PUMPING WELL              =      100.0000000
DISTANCE BETWEEN PUMPING WELL
AND NEAREST IMAGE WELL PAIR             =       44.5000000
PUMPING RATE                            =        0.0140000
IMAGE PUMPING RATE                      =        0.0140000

WATER DEPTH WHERE FIRST RECHARGE RATE OCCURS =       15.0000000
FIRST RECHARGE RATE PER METRE DECLINE IN HEAD=       -0.0030000
MAXIMUM FLOW OF FIRST RECHARGE RATE          =       -0.0300000

WATER DEPTH WHERE SECOND RECHARGE RATE OCCURS =      23.0000000
SECOND RECHARGE RATE PER METRE DECLINE IN HEAD=      -0.0030000
MAXIMUM FLOW OF SECOND RECHARGE RATE          =      -1.0000000

INITIAL DEPTH TO WATER =    0.000
```

AT PUMPING RATE Q = 0.01400

TIME (in minutes)	DRAWDOWN (in meters)
1.	0.000
2.	0.000
2.	0.000
3.	0.000
3.	0.000
4.	0.000
5.	0.001
6.	0.003
8.	0.009
10.	0.021
13.	0.044
16.	0.081
20.	0.138
25.	0.220
32.	0.332
40.	0.480
50.	0.668
63.	0.901
79.	1.185
100.	1.523
126.	1.922
158.	2.387
200.	2.927
251.	3.547
316.	4.258
398.	5.067
501.	5.988
631.	7.030
794.	8.209
1000.	9.542
1259.	11.042
1585.	12.733

APPENDIX 11

FREE FLOW AND SLUG TESTS

A.11.1 Free Flow Test

A.11.2 Free Flow Test Calculation

A.11.3 Slug Test

A.11.4 Slug Test Data

A.11.5 Slug Test Calculation

A.11.1: Free Flow Test
(Based on Lee 1984)

1. Measurement Required from Field Work:

   (1) Static head, h_0 (Read directly from the pressure gauge before commencement of free flow).
   (2) Free flow rate, Q at steady state (Steady state can be assumed achieved when the rate of head change is less than 0.05 m of water per hour).
   (3) Pressure head, h_2 at steady state (Read directly from the pressure gauge).
   (4) Length, L as shown in the figure 1.

2. Additional Information Required (from well record):

   (1) Screen Length, $2l$
   (2) Internal pipe diameter of well, D
   (3) Pipe roughness. ϵ of well
   (4) Location of well screen with respect to aquifer stratification.

3. Determination of Transmissivity, T

   At steady rate the principle of conservation of energy gives

$$h_1 = h_2 + fLv^2/D2g \qquad (1)$$

where v = flow velocity in well = $4Q/\pi D^2$ and f is the friction factor of the well pipe. The second term on the right hand side of Eq. (1) is the friction loss for flow through a length L. The frictin factor f can be determined from Moody diagram for known Reynolds Number, R = vD/γ and relative roughness, ϵ/D.

The steady state drawdown,

$$S_0 = h_0 - h_1 \qquad (2)$$

$$K = Q/4\pi l S_0 \sinh^{-1}(l/r_0) \qquad (3)$$

Finally, transmissivity

$T = KB$ where B = aquifer thickness

If $l/r_0 < 1$,

$$S_0 = Q/4\pi K r_0 \qquad (4)$$

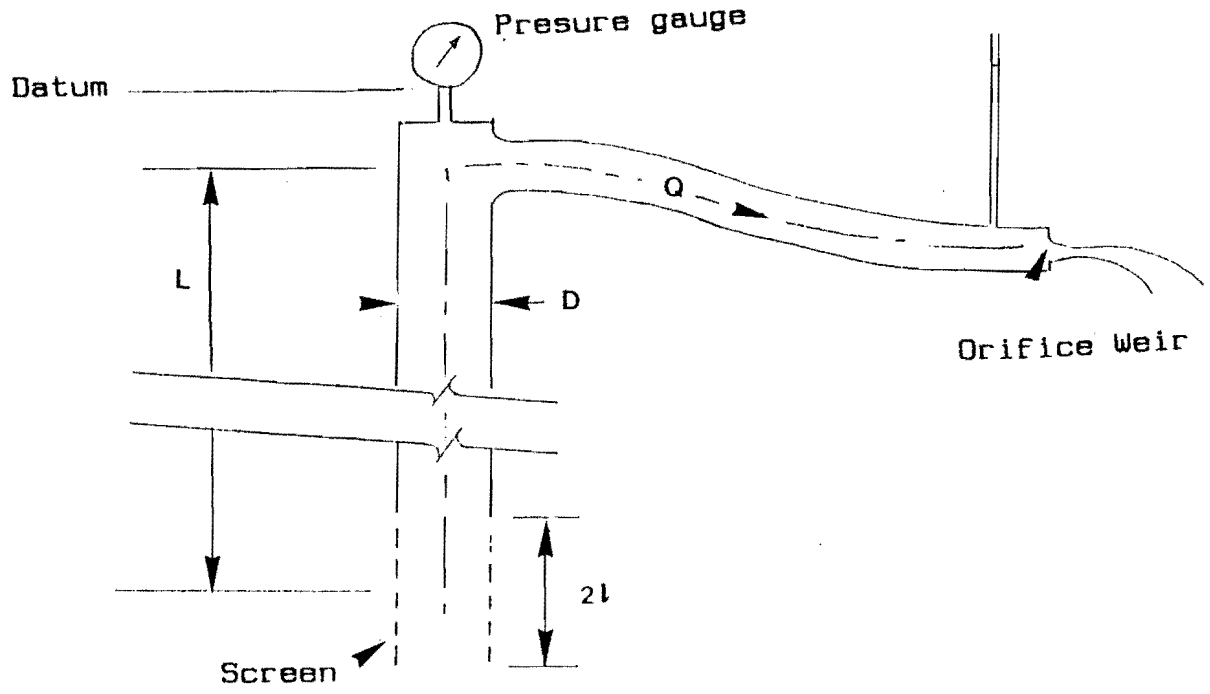

Fig 1 (A.11.1), Set up of Free Flow Test.

A.11.2: Free Flow Test Calculations for Well M36–1437 and Well M361–1436

For Well M36–1437:

$D = 0.055$ m

$Q = 107.3\times10^{-3}$lit/sec $= 107.3\times10^{-6}$m^3/s

$L = 71.2$ m

$h_0 = 2.11$ m

$h_2 = 0.555$ m

velocity $v = 4Q/rD^2$

$= (4 \times 107.3 \times 10^{-6})/\pi(0.055)^2$

$= 0.045$ m/s

Assume the viscosity at the amblent temperature to be $\gamma = 1.13\times10^{-6}$ m^2/s

$R = vD/\gamma$

$= 0.045 \times 0.055/1.31\times10^{-6}$

$= 1889.31$

Assume pipe's roughness $\epsilon = 0.046$ mm,

Relative roughness

$\epsilon/D = 0.046\times10^{-3}/0.055$

$= 8.36\times10^{-5}$

From Moody diagram, $F = 0.051$ (Fig 2)

$h_1 = h_2 + FLv^2/D2g$

$= 0.555 + 0.051\times71.2\times(0.045)^2/0.055\times2\times9.81$

$= 0.56$ m

and $S_0 = h_0 - h_1$

$= 2.11 - 0.56$

$= 1.55$ m

Since $S_0 = Q/4\pi Kr_0$ we obtain

$K = 107.3\times10^{-6}/(4\pi \times 1.55 \times 0.027)$

$= 2.04 \times 10^{-4}$ m/s

and $T = KB$, B = aquifer thickness

$= 2.04 \times 10^{-4} \times 24$

$= 4.9 \times 10^{-3}$ m^2/s

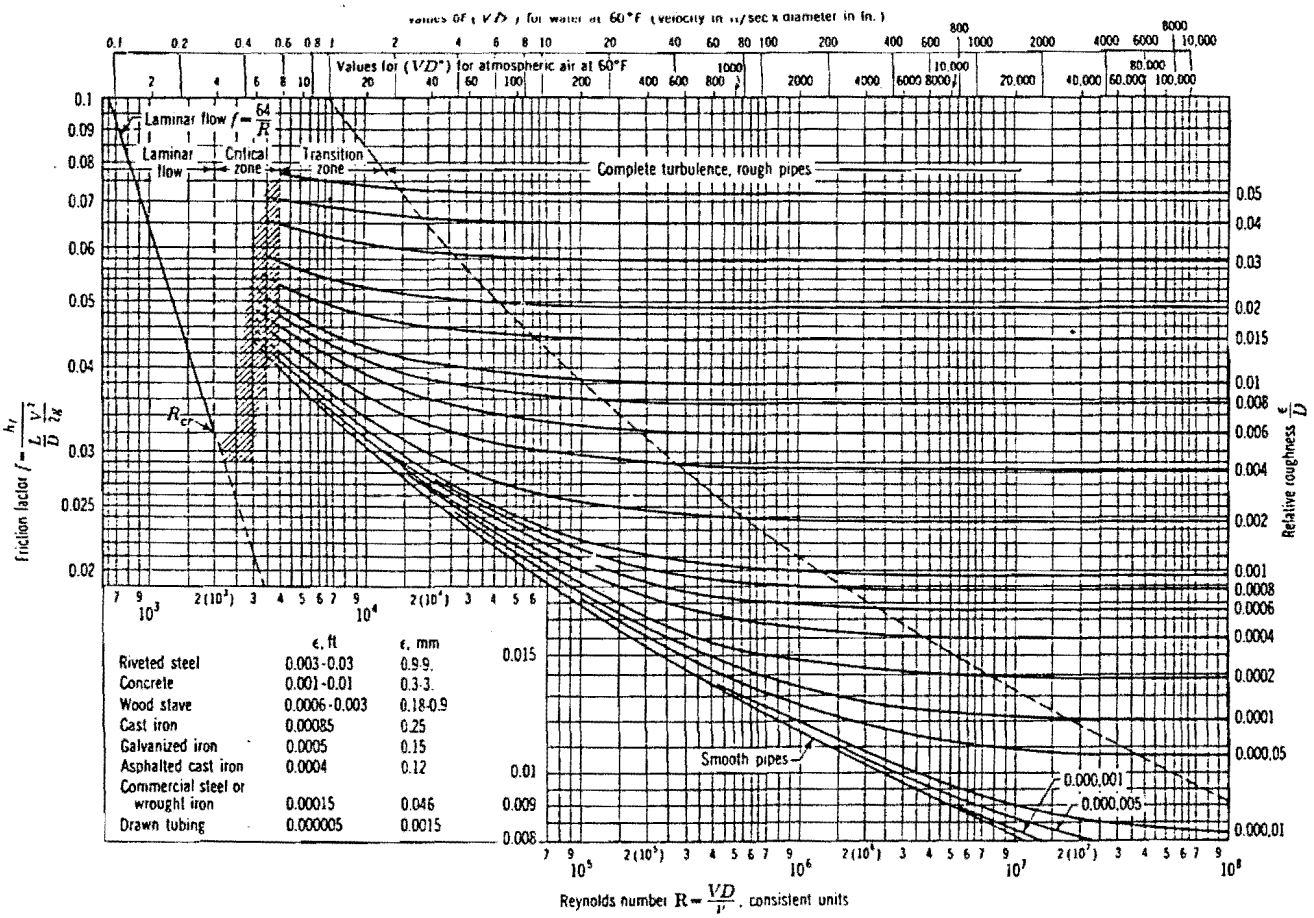

Fig 2 (A.11.2), Moody Diagram For Calculating the Relative Pipe Roughness. (From Moody, 1944).

A.11.3: Slug Test

For interpretation of slug tests Hvorslev, 1951 defined the following procedures. He reasoned that the rate of inflow, q, at the piezometer at any time t is proportional to the hydraulic conductivity, K, of the soil and to the unrecovered head difference, H – h, so that

$$q(t) = \pi r^2 \frac{dh}{dt} = FK(H - h) \qquad (1)$$

where F is a factor that depends on the shape and dimensions of the piezometer intake. If $q = q_0$ at $t = 0$, it is clear that q(t) will decrease asymptotically toward zero as time goes on.

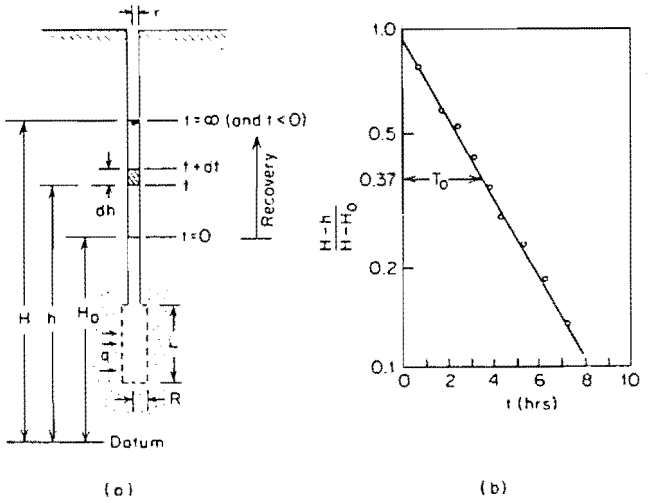

Fig 1 (A.11.3); Hvorslev piezometric test (a) geometry; (b) method of Analysis. (From Freeze and Cherry, 1979).

Hvorslev defined the *basic* time lag, T_0, as

$$T_0 = \frac{\pi r^2}{FK} \qquad (2)$$

When this parameter is substituted in Eq.(1), the solution to the resulting ordinary differential equation, with the initial condition, $h = H_0$ at $t = 0$ is

$$\frac{H - h}{H - H_0} = e^{-t/T_0} \qquad (3)$$

Shape factor in different conditions is described by Cedergren 1967. According to table 1 shape factor for both monitored wells is

$$F = C_s r \quad \text{(well with no screen)}$$

where C_s = shape factor coefficient, r = well radius , C_s is measured by plotting log values of $(H - h)/(H - H_0)$ versus time as shown in Figs 2 and 3.

Observation well or piezometer in aquifer with impervious upper layer	(*f*) Cased hole, uncased or perforated extension into aquifer of finite thickness: (1) $\frac{L_1}{T} \leq 0.20$ (2) $0.2 < \frac{L_2}{T} < 0.85$ (3) $\frac{L_3}{T} = 1.00$ *Note.* R_0 equals effective radius to source at constant head	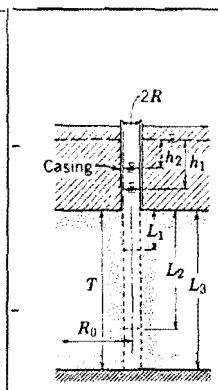	(1) $F = C_s R$ (2) $F = \frac{2\pi L_2}{\ln (L_2/R)}$ (3) $F = \frac{2\pi L_3}{\ln (R_0/R)}$

(From U.S. Navy Bureau of Yards and Docks.)

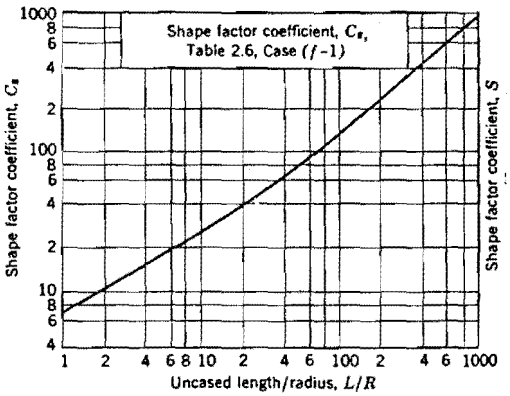

Table 1 (A.11.3); Shape Factor (F) and Shape Coefficient (C_s) (From Cedergren, 1967).

Table A.11.4: Slug Test Data

Well No.	Time (sec)	Water level (m)	$\log \frac{H - h}{H - H_0}$
M36–734	12	1.57	– 0.200
	22.7	2.35	– 3.97
	30	2.78	– 0.553
	38	3.01	– 0.677
	48.1	3.26	– 0.854
M36–1421	2	0.18	– 0.125
	20	0.5	– 0.522
	25	0.545	– 0.638
	33	0.59	– 0.853
	37	0.63	– 0.958

A.11.5: Slug Test Calculations

(A).For well M36–734

$r = 0.05$ m, $C_s = 7$, $T_0 = 23.3$ sec (Fig. 2)

$$F = C_s r$$
$$= 7 \times 0.05$$
$$= 0.35$$

$$K = \frac{\pi r^2}{FT_0}$$
$$= \frac{\pi(0.05)^2}{0.35 \times 23.3}$$
$$= 9.6 \times 10^{-4} \text{ m/s}$$

$$T = KB$$

where K = Hydaulic conductivity, B = Aquifer thickness = 24 m (average),

$$T = 9.6 \times 10^{-4} \times 24$$
$$= 4.3 \times 10^{-3} \text{ m}^2/\text{s}$$

(B). For well 36–1421

$r = 0.0375$ m, $C_s = 7$, $T_0 = 16.35$ (Fig.3)

$$F = C_s r$$
$$= 7 \times 0.0375$$
$$= 0.26$$

$$T = KB$$
$$= 2 \times 10^{-2} \text{ m}^2/\text{s}$$

Fig 2 (A.11.5), Calculating the Time Lag for Slug Test on Well M36/734.

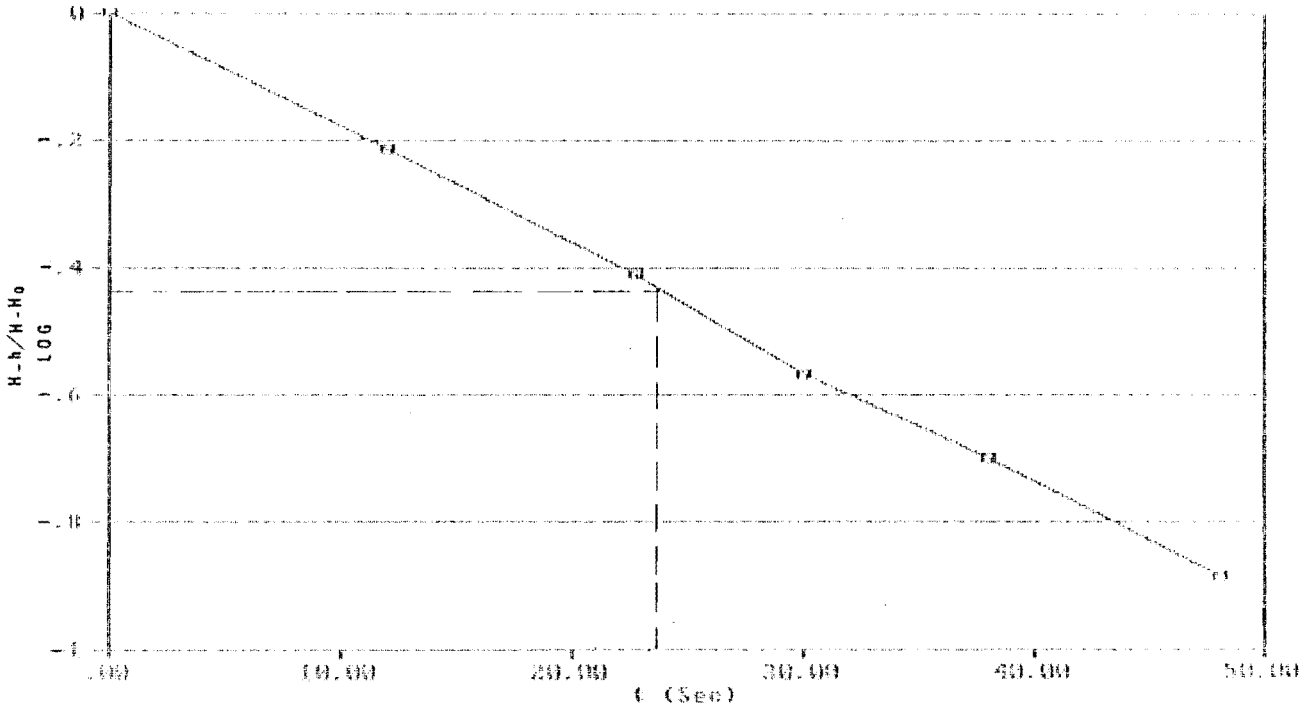

Fig 3 (A.11.5), Calculating the Time Lag for Slug Test on Well M36/1421.

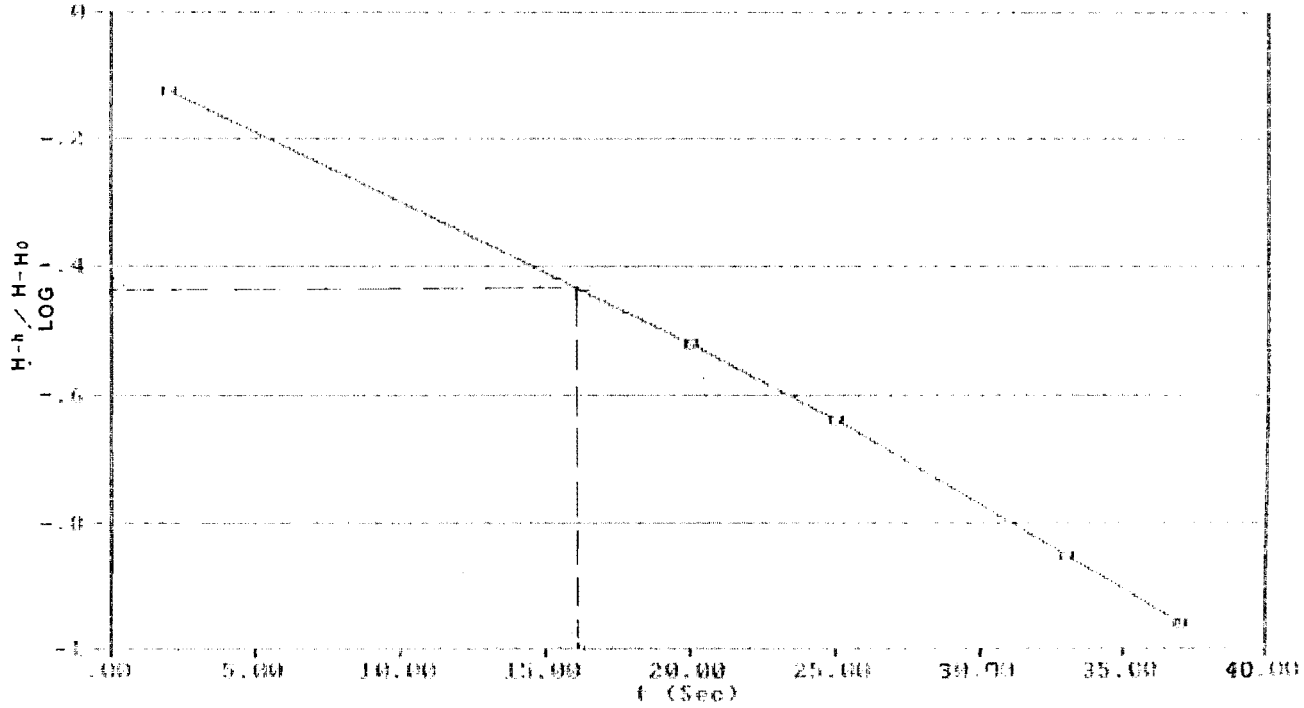

APPENDIX 12

WATER LEVEL MONITORING

Table A.12: Water Level Monitoring

A.12.1

Well No. M36–843
Depth = 9.14 m
Reduced level = 27.0 m
Reference level = + 0.340 m
Grid. Ref. = M36 857 197

Date	Head (m)	Time	Date	Head (m)	Time
			860526	+2.48	1506
860609	+2.47	1140	860617	+2.40	1024
860624	+2.36	0954	860703	+2.07	1300
860708	+1.74	1012	860715	+1.95	1014
860722	+1.95	1003	860731	+2.05	1045
860805	+2.06	0950	860812	+1.77	1021
860819	+2.00	0952	860826	+1.81	1029
860903	+1.96	1040	860909	+2.90	1020
860916	+2.00	0951	861001	+2.16	1410
861007	+1.94	0947	861015	+2.03	–
861021	+2.10	0955	861028	+2.24	0947
861105	+2.16	1040	861112	+2.25	1040
861118	+2.27	1040	861125	+2.13	1216
861201	+2.07	1147	861209	+2.26	1014
861218	+2.36	1353	870107	+2.49	0958
870113	+2.53	1030	870120	+2.85	1049
870127	+2.62	1015	870203	+2.67	1038
870210	+2.68	0949	870217	+2.59	1020
870224	+2.64	1457	870302	+2.58	1059
870310	+2.50	1416	870317	+2.39	1212
870325	+2.44	1036	870331	+2.50	1345
870408	+2.54	1402	870413	+2.58	1421
870421	+2.59	1510	870429	+2.61	1113
870505	+2.52	–	870512	+2.54	1252
870519	+2.46	0934	870526	+2.30	–
870604	+2.40	1040	870609	+2.44	1027
870616	+2.33	1518	870702	+2.24	1045
870707	+2.28	1110	870714	+2.27	1353

A.12.2

Well No. M36–734
Depth = 21.4 m
Reduced level = 10.59 m
Reference level = + 0.100 m
Grid. Ref. = M36 847 175

Date	Head (m)	Time	Date	Head (m)	Time
			860526	+5.27	14.59
860609	+4.35	1132	860617	+3.95	1248
860708	+3.11	1005	860715	+3.22	1019
860722	+3.45	1011	860731	+3.44	1038
860805	+3.50	0959	860812	–	–
861007	+4.48	0594	861015	+4.62	–
861021	p	–	861028	+4.66	0954
861105	+4.80	1030	861112	+4.69	1030
861118	+4.68	1030	861125	–	–
861201	+4.23	1200	861230	+6.75	–
870127	+9.74	1020	870203	+10.35	1444
870210	+8.34	0952	870217	+6.18	1030
870224	+5.17	1503	870302	+5.29	1107
870310	+4.48	1423	870317	+4.17	1322
870325	+4.00	1042	870331	+3.96	1328
870408	+3.96	1439	870413	+3.91	1428
870421	+3.85	1515	870429	+3.88	1120
870505	+3.83		870512	+3.75	1030
870519	+3.72	0938	870526	+3.46	0957
870604	+3.47	1035	870609	+3.54	1020
870616	+3.52	1523	870702	+3.38	1040
870707	+3.36	1105	870714	+3.37	1359

P= Pumping

A.12.3

Well No. M36–1344
Depth = 30 m
Reduced level = 6.78 m
Reference level = + 3.3 m
Grid. Ref. = M36 844 165

Date	Head (m)	Time	Date	Head (m)	Time
860609	+1.78	1147	860617	+1.64	1002
860624	+1.56	0948	860703	+1.37	1235
860708	+1.24	0959	860715	+1.18	1009
860722	+1.23	0958	860731	+1.24	1030
860805	+1.29	0943	860812	+1.21	1015
860819	+1.33	0948	860826	+2.06	1024
860903	+1.90	1026	860909	+1.34	1015
860916	+1.44	0946	861001	+1.64	1400
861007	p	–	861015	+1.85	–
861021	+1.49	0949	861028	+1.65	0945
861105	+1.55	1024	861112	+1.69	1027
861118	+2.03	1040	861125	p	–
861202	+5.15	1142	861209	p	1011
861218	p	1349	860107	p	–
870113	p	–	870120	+12.05	1043
870127	P	1012	870203	+9.00	1449
870210	+6.60	1002	870217	+3.98	1015
870224	+2.74	1453	870302	+3.03	1112
870310	+2.00	1410	870317	+1.77	1340
870325	+1.58	1030	870331	+1.56	1316
870408	+1.62	1444	870413	+1.63	1433
870421	+1.61	1505	870429	+1.67	1105
870505	+1.71	–	870512	+1.51	1332
870519	+1.58	0947	870526	+1.44	–
870604	+1.45	1030	870609	+1.50	1015
870616	+1.50	1518	870702	+1.43	1035
870707	+1.43	1058	870714	+1.44	1403

A.12.4

Well No. M36–1421
Depth = 49.8 m
Reduced level = 4.069 m
Reference level = + 1.22 m
Grid. Ref. = M36 827 146

Date	Head (m)	Time	Date	Head (m)	Time
860610	+0.92	1306	860617	+0.83	0958
860624	+0.82	0944	860703	+0.76	1230
860708	+0.65	0954	860715	+0.54	1004
860722	+0.48	0953	860731	+0.52	1023
860805	+0.56	0938	860812	+0.54	1010
860819	+0.49	0942	860826	+0.44	1019
860903	+0.42	1020	860909	+0.49	1011
860916	+0.61	0941	861001	+0.75	1355
861007	+0.66	0939	861015	p	–
861021	+0.70	0944	861028	+0.82	0939
861105	+0.78	1020	861112	+0.84	1023
861118	+0.80	1010	861125	+1.07	1202
861202	+1.05	1137	861209	+1.18	1008
861218	+2.81	1346	870107	p	–
870113	+3.60	1020	870120	+3.40	1038
870127	+3.54	1015	870203	+3.50	1454
870210	+3.52	1007	870217	+2.44	1010
870224	+1.73	1447	870302	+1.36	1136
870310	+1.00	1405	870317	+0.75	1445
870325	+0.65	1025	870331	+0.66	1310
870408	+0.67	1449	870413	+0.71	1438
870421	+0.87	1510	870429	+0.94	1101
870505	+0.78	–	870512	+0.66	1309
870519	+0.71	1000	870526	+0.65	1004
870604	+0.60	1025	870609	+0.62	1010
870616	+0.64	1530	870702	+0.55	1030
870707	+0.54	1054	870714	+0.53	1408

A.12.5

Well No. M36–1436
Depth = 91 m
Reduced level = 3.212 m
Reference level = + 0.28 m
Grid. Ref. = M36 823 149

Date	Head (m)	Time	Date	Head (m)	Time
860609	–3.30	1121	860617	–3.00	0952
860624	–3.26	0938	860703	–3.30	1230
860708	–3.52	0948	860715	–3.00	0951
860722	–3.05	0939	860731	–3.10	1020
860805	–3.10	0932	860812	–3.00	1001
860819	–3.20	0938	860826	–3.30	1002
860903	–2.56	1010	860909	–3.50	1004
860916	–3.40	0936	861007	–3.5	0937
861015	–3.30	–	861021	–2.10	0955
861028	–3.30	0931	861105	–2.25	1015
861112	–2.30	1020	861118	–2.25	1004
861125	–2.35	1200	861202	–3.25	1233
861209	–3.25	1000	861218	–2.90	1338
870107	–2.75	1008	870113	–3.00	1010
870120	–2.70	1030	870127	–2.70	1003
870203	–	–	870210	–2.30	1018
870217	–2.60	0959	870224	p	–
870302	–3.20	1126	870310	–3.35	1436
870317	–3.35	1503	870325	–3.30	1019
870331	–2.70	1255	870408	–3.30	1436
870413	–3.10	1459	870421	–3.30	1451
870429	–3.30	1049	870505	–2.69	–
870512	–3.40	1336	870519	–3.50	1039
870526	–3.45	1012	870604	–3.50	1020
870609	–3.20	1007	870616	–3.45	1537
870702	–3.03	1027	870707	–2.93	1050
870714	–3.07	1422			

A.12.6

Well No. M36–1437
Depth = 71 m
Reduced level = 3.947 m
Reference level = + 0.700 m
Grid. Ref. = M36 822 152

Date	Head (m)	Time	Date	Head (m)	Time
860609	–2.32	1118	860617	–2.20	0949
860624	–2.35	0935	860703	–2.30	1222
860708	–2.30	0943	860715	–1.75	0947
860722	–1.86	0943	860731	–1.90	1015
860805	–2.28	0928	860812	–1.90	0955
860819	–2.00	0935	860826	–2.30	0958
860903	–2.31	1015	860909	–2.40	1000
860916	–2.06	0930	861001	–2.18	1345
861015	–2.62	–	861021	–2.20	0933
861028	–2.15	0927	861105	–2.19	1005
861112	–2.25	1015	861118	–2.16	1002
861125	–1.78	1150	861202	–2.04	1241
861209	–2.11	0956	861218	–1.75	1330
870107	–1.84	1011	870113	–1.71	1002
870120	–1.61	1002	870127	–1.43	1000
870203	–1.45	1502	870210	–0.78	1030
870217	–1.88	1509	870325	–1.84	1013
870331	–1.70	1248	870408	–1.72	1502
870413	–1.10	1.59	870421	–2.20	1439
870429	–2.13	1041	870505	–2.24	–
870512	–2.13	1340	870519	–2.24	1040
870526	–2.63	1019	870604	–2.25	1015
870609	–2.19	1003	870616	–2.38	1541
870702	–2.28	1025	870707	–2.21	1034
870714	–2.23	1428			

A.12.7

Well No. M36–1422
Depth = 46 m
Reduced level = 3.0 m
Reference level = + 0.15 m
Grid. Ref. = M36 823 149

Date	Head (m)	Time	Date	Head (m)	Time
			860812	–1.03	1110
860819	–1.09	0929	860826	–1.05	1009
860903	–1.15	1005	860909	–1.07	0956
860916	–0.98	0925	861001	–0.94	1336
861007	–0.96	0921	861015	–1.04	–
861021	–1.03	0929	861028	–0.95	0921
861105	–0.87	1005	861112	–0.82	1010
861118	–0.76	1000	861125	–0.30	1145
861202	–0.53	1244	861209	p	0953
861218	–	–	870107	–	–
870113	–	–	870720	–	–
870127	–	–	870203	p	–
870210	p	–	870217	p	–
870224	p	–	870302	–0.26	1145
870310	–0.67	1345	870317	–0.90	1511
870325	–0.99	1009	870331	–0.98	1235
870408	–0.85	1508	870413	–0.94	1510
870421	–0.90	1436	870429	–0.85	1037
870505	–0.87	–	870519	–0.92	1048
870526	–0.96	1023	870604	–1.01	1010
70609	–0.97	1000	870616	–0.98	1546
870702	–1.05	1020	870707	–1.05	1030
870714	–1.05	1432			

A.12.8

Well No. M36–727
Depth = 56.9 m
Reduced level = 2.0 m
Reference level = + 0.45 m
Grid. Ref. = M36 822 147

Date	Head (m)	Time	Date	Head (m)	Time
860609	–1.41	1124	860617	–1.46	0955
860624	–1.56	0941	860703	–1.33	1216
860708	–1.50	0951	860715	–1.74	1002
860722	–1.67	0949	860731	–1.35	1008
860805	–1.80	0935	860812	–1.48	1006
860819	–1540	0940	860826	–1.77	1016
860903	–1.49	1000	860909	–1.39	1007
860916	–1.79	0938	86001	–1.42	1330
861007	–2.27	0935	861015	–1.93	–
861021	–2.20	0941	861028	–1.63	0935
861105	–1.37	1000	861112	–1.42	1000
861118	–1.71	0950	861125	–1.98	1140
861201	–1.73	1231	861209	–2.05	1004
861218	–1.72	1343	870107	–1.32	1006
870113	–1.45	1015	870120	–2.22	1033
870127	–0.76	1006	870203	–0.74	1458
870210	–0.34	1012	870217	–0.47	1007
870224	–1.27	1445	870302	–1.53	1120
870310	–1.20	1401	870317	–1.22	1459
870325	–1.78	1022	870331	–1.20	1304
870408	–1.21	1453	870413	–1.69	1441
870421	–1.28	1457	870429	–1.64	1058
870505	–1.26	–	870512	–1.26	1313
870519	–1.74	1031	870526	–1.32	–
870604	–1.43	1000	870609	–1.38	0955
870616	–1.85	1533	870702	–1.48	–
870707	–1.45	1023	870714	–1.47	1412

A.12.9: Lake Ellesmere Water Level Data (mm) a.m.s.l

Year	1986	1987	Min.	Mean	Max.
Jan	–	920	920	920	920
Feb	1042	930	939	991	1042
Mar	818	890	818	854	890
Apr	975	650	650	812	975
May	1089	882	882	985	1089
Jun	1021	1146	1021	1083	1146
Jly	994	1041	994	1017	1041
Aug	995	842	842	918	995
Sep	740	1025	740	882	1025
Oct	801	–	801	801	801
Nov	669	–	669	669	669
Dec	904	–	904	904	904

APPENDIX 13

SPRING DISCHARGE MONITORING

A.13.1 Methodology

A.13.2 Results

A.13.3 Seasonal Variations

A.13.1 Methodology

1) Discharge monitoring of 27 springs was carried out on a monthly basis. A single reading at the end of each month is considered to be representative of the discharge value for that month. The monitoring was carried out (monthly) between June 1986 and May 1987.

2) The main objective for spring monitoring was to identify the springs with a low discharge variability (larger storage capacity).

3) A calibrated 10 L (for flows less than 35L/min) and 20 L bucket (for flows between 35 and 105L/min) was used for the monitoring.

Table A.13.3

SPRINGS DATA (Discharge)													
Years	1986						1987						
Months	June	July	Aug	Sept	Oct	Nov	Dec	Jan	Feb	March	Apr	May	Va★ (%)
Spring No	Discharge (Lit/Min)												
W.1	.1	14.8	18.8	2	6	3	.1	0	0	.3	.2	.35	5875
W.2.1	4.4	26.3	58.3	8.6	10.8	3	.5	0	0	.35	1	1	2910
W.2.2	2.37	60	105	6.3	15	10	.4	0	0	0	.6	2.1	4700
W.3.1	1.7	20	28	5.14	5.2	19	.5	0	0	1	1.8	2.14	1420
W.3.2	2.04	24	57	3.7	6	37.5	2.4	0	0	.6	.5	1.5	2570
W.3.3	.7	11	16.5	1.1	1.65	9.75	.67	0	0	.1	0	.9	2060
W.3.4	1.1	6	12	1.9	5.4	9	.91	0	0	0	0	.1	1200
W.3.5	.17	2	8	1.5	2.5	2.1	.14	0	0	0	0	.15	1500
W.4.1	.45	9	17	2.6	6	10	.57	.1	.11	.32	.16	1.2	1130
W.4.2	.22	3	5.45	.5	1.7	2.85	.16	0	.05	.15	.12	.15	2868
W.4.3	6.1	40.6	51	13.7	18	26.2	1.5	0	.1	1.03	1.28	3.75	1040
W.4.4	.8	16.5	17	5.49	9.2	12.2	1.2	.115	.05	.32	.29	1.7	1168
W.4.5	2.77	45	45.1	5	8	31.2	1.8	0	0	0	.05	.06	370
W.5.1	2.18	3.2	4.9	1.7	2	2.1	1.15	1.1	.6	1.41	.79	.9	277
W.5.2	2	4.5	8	1	1.3	2.24	.172	0	0	0	.2	.7	1973
W.5.3	6.5	24	21.8	5	6.2	10.5	.71	0	0	0	.15	.72	842
W.5.4	11.3	70	120	10	36	62.2	4.78	0	0	1.68	5.25	6	1500
W.5.5	2.13	90	168	12	24	27	1.84	0	0	.578	.8	2.5	727
W.5.6	1.75	36	50	4.6	7	12	.8	0	0	.54	.9	1.7	2900
W.5.7	2	76	100	8	13.5	17.4	1.04	0	0	.882	1.93	4.71	2980
A.1	5.4	25.5	36	18	25	30	5	0	0	.42	.3	3.6	692
E.1	1.6	4.73	20.2	.65	4.3	7.5	0	0	0	0	.05	.1	5460
E.2.1	.45	1	4	.8	1	3.26	.72	.3	0	0	0	.22	3960
E.2.2	2.3	5	22.6	3	4.6	17.7	3	0	0	0	.44	3.52	753
E.2.3	2.8	13.6	36	10.6	15	31.6	5.1	0	0	.05	.768	1.46	911
E.3.1	.548	1.66	2.34	1.42	2.1	2.6	.91	.6	.62	.75	.62	.9	228
E.3.2	4.1	15	45	3.5	2.5	39.1	1.5	.24	0	0	.3	.7	2250
E.3.3	.25	6	12.9	5.33	9.6	25.5	3	0	0	0	.45	1.14	1231

★ Spring Variability.

Figs A13.3

Springs Discharge
for Kaituna catchment (during 12 months)months

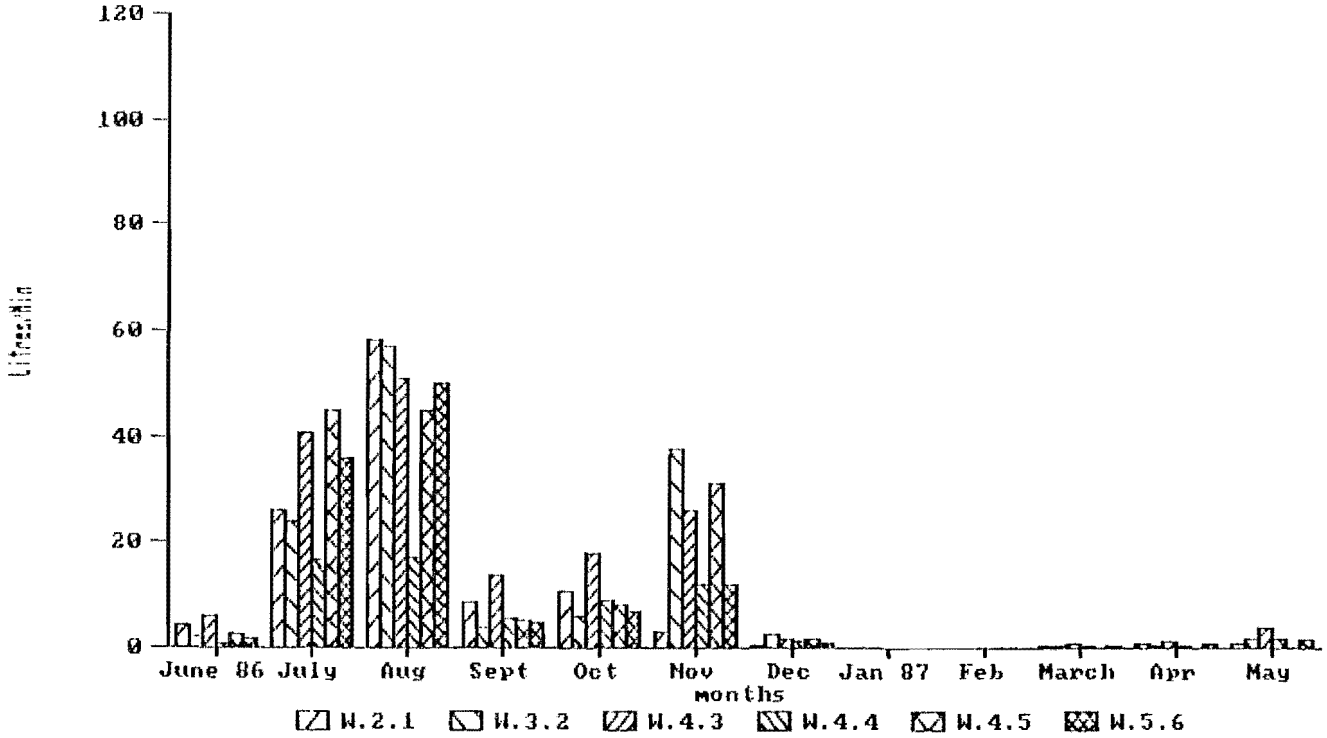

Springs Discharge

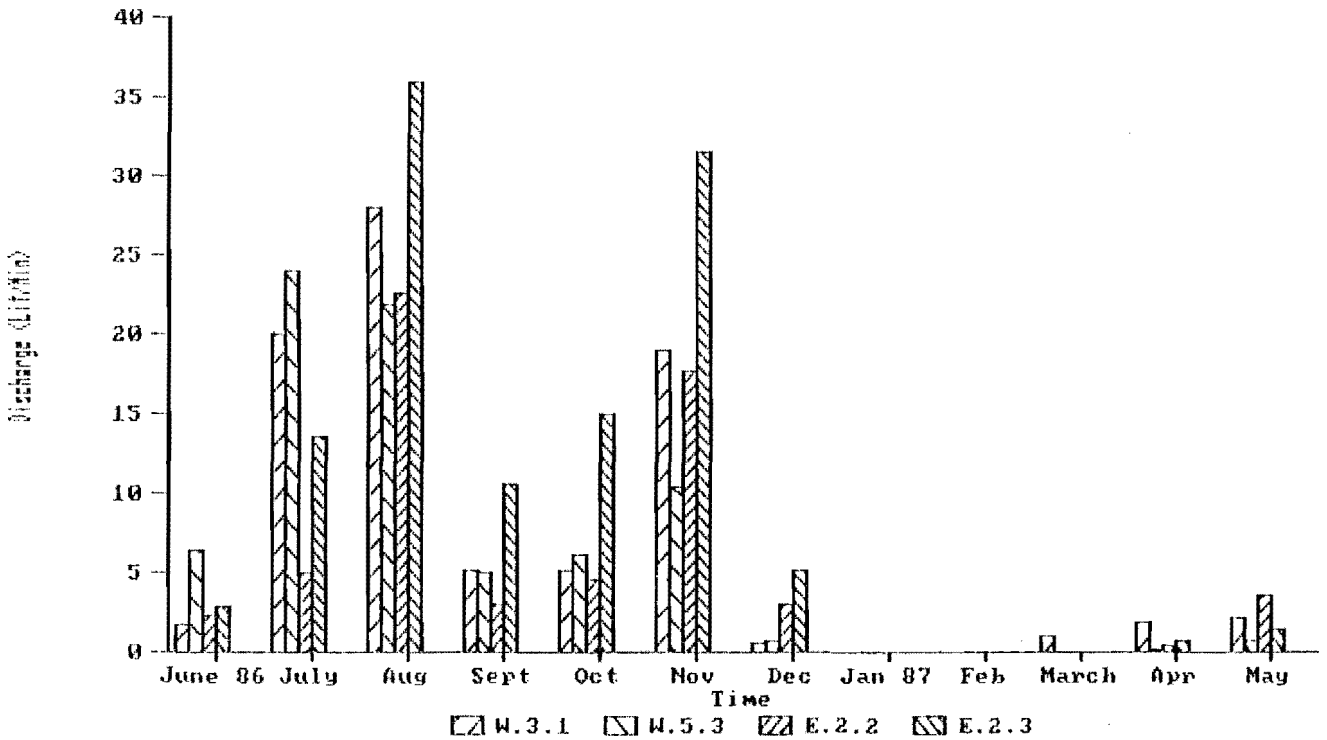

Figs A.13.3
Springs Discharge

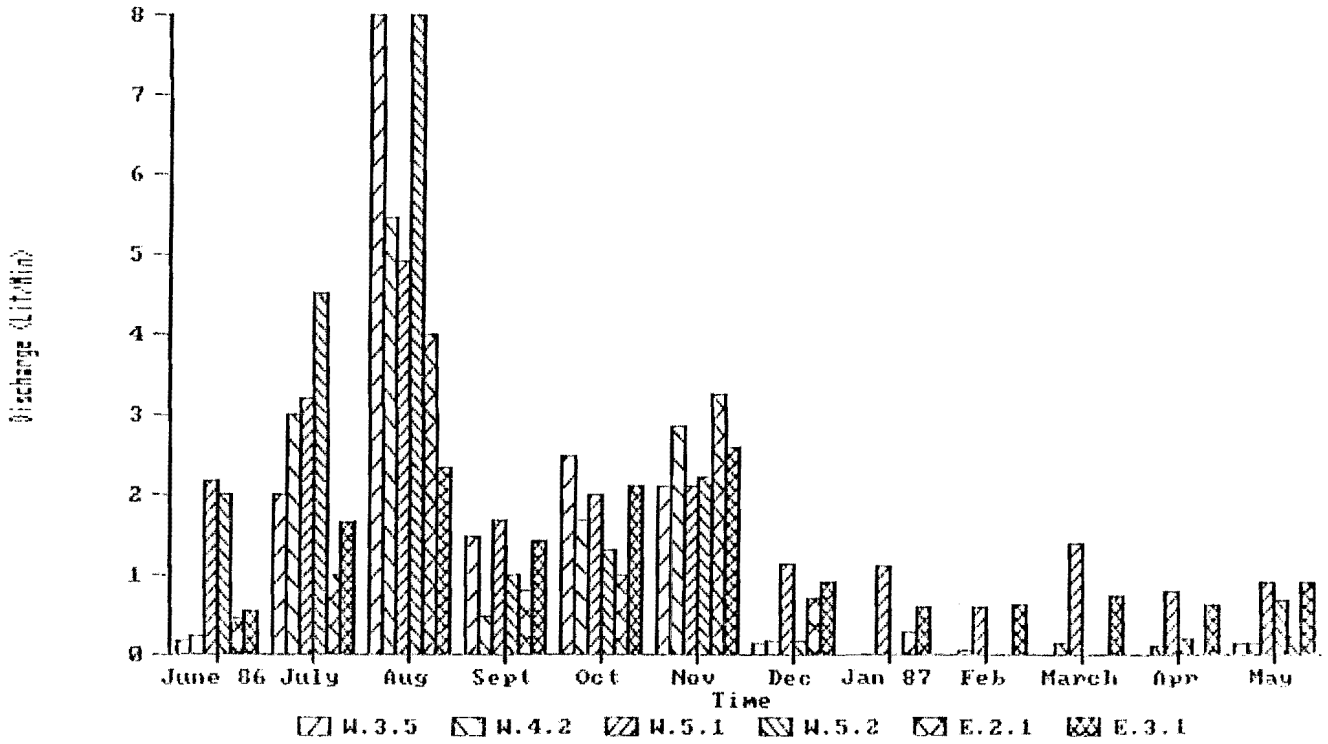

Springs Discharge

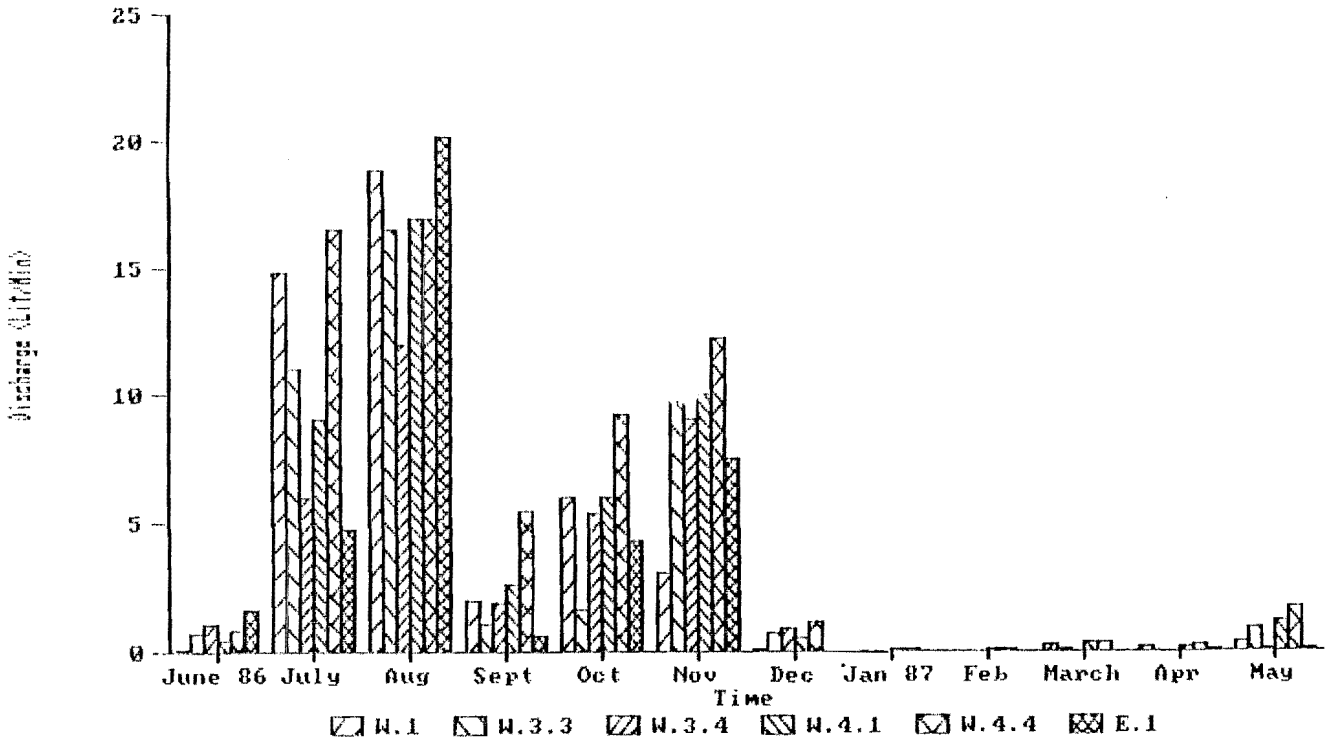

Figs A.13.3

Springs Discharge

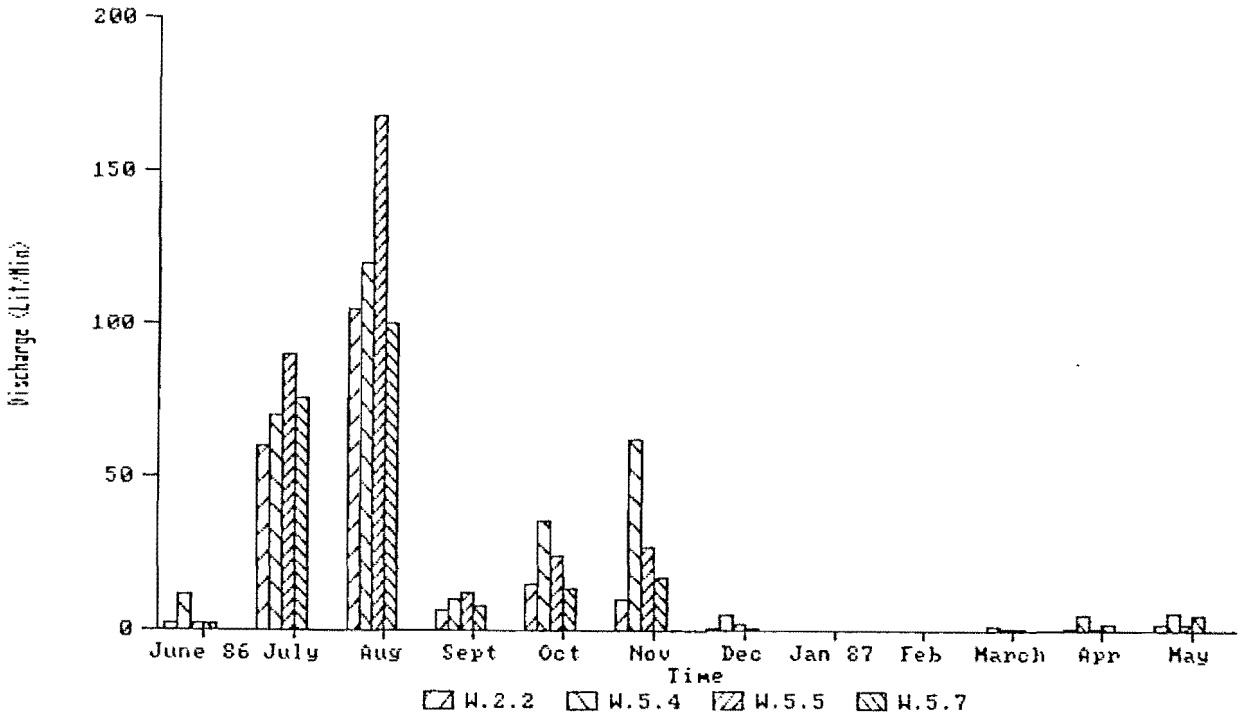

Springs Discharge
for Kaituna catchment (during 12 months)months

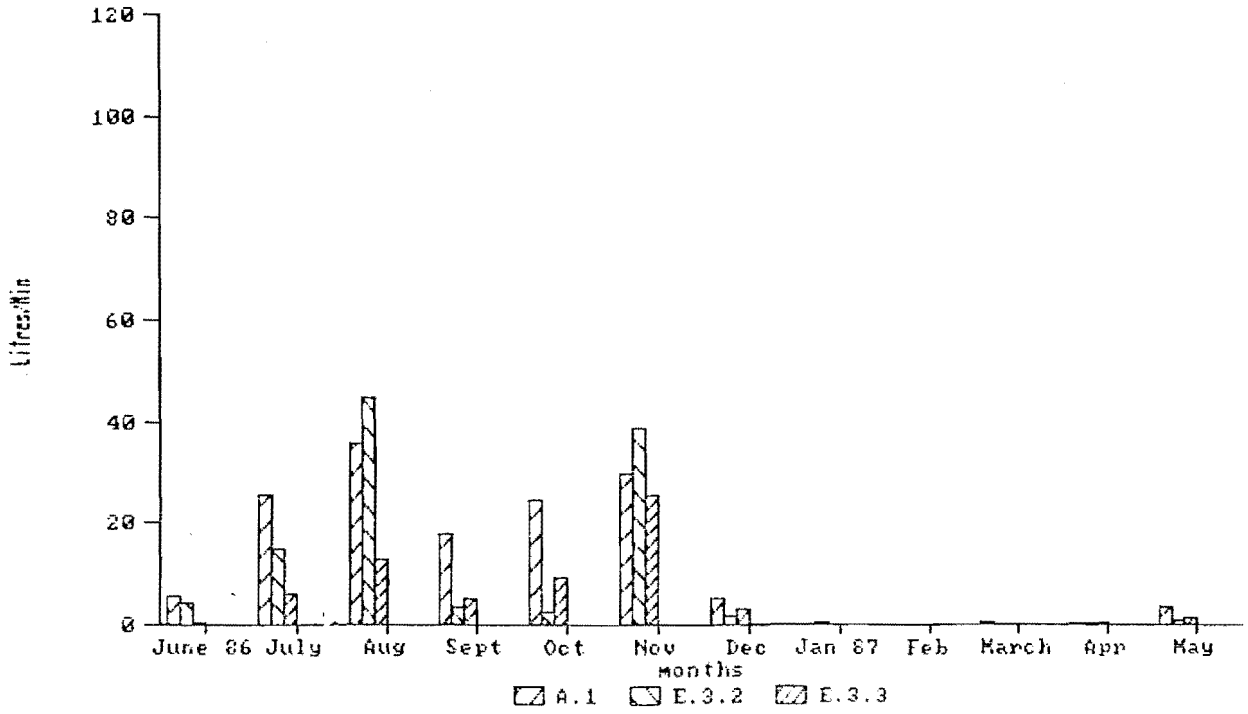

APPENDIX 14

HYDROCHEMICAL AND ENVIRONMENTAL ANALYSIS

A.14.1 Sampling Considerations

A.14.2 New Zealand Drinking Water Standard

A.14.3 World Health Organisation Standard

A.14.4 Guidelines for Interpretation of Water Quality for Trace Elements in Irrigation Water

A.14.5 Conversion factors

A)

Aesthetic Quality

Constituent or characteristic	Unit[a]	Guideline values: Highest Desirable	Guideline values: Excessive	Undesirable effect that may be produced	Document Reference WHO Guidelines Vol. 1
aluminium	g/m³	0.05	0.2	discolouration and deposits; possible corrosion association; special preconditions required for renal dialysis	4.4.3.1
chloride	g/m³	100	250	corrosion, taste threshold between 200 and 300 g/m³	4.4.3.2
chlorobenzenes and chlorophenols	no guideline value set			these compounds can affect taste and odour	4.3.7.5 & 4.3.7.6
colour	true colour units (TCU)[b]	5	30	discolouration and trouble with chlorination	4.4.3.3
copper	g/m³	0.05	1.0	astringent taste, discolouration and corrosion of pipes, and utensils	4.4.3.4
hardness	g/m³ (as $CaCO_3$)	80	200	excessive scale formation, electric element burnout	4.4.3.5
hydrogen sulphide		not detectable by consumer		taste and odour	4.4.3.6
iron	g/m³	0.1	1.0	taste, turbidity, discolouration, deposits, growth of iron bacteria	4.4.3.7
manganese	g/m³	0.05	0.5	taste, turbidity, discolouration, deposits in pipes	4.4.3.8
pH range	-	7.4 to 8.6	7.0 to 8.5	corrosion and scale, unsatisfactory disinfection	4.4.3.10
sodium	g/m³	100	200	taste	4.4.3.11
solids (total dissolved)	g/m³	500	1 000	taste	4.4.3.12
sulphate	g/m³	50	400	corrosion, laxative effect when magnesium present	4.4.3.13
taste and odour	-	-	-	inoffensive to most consumers	4.4.3.14
temperature	-	[c]	[c]	no guideline values set	4.4.3.16
turbidity	nephelometric turbidity units (NTU)	1	5	discolouration; preferably less than 1 NTU for disinfection efficiency	4.4.3.15
zinc	g/m³	5	5	taste, discolouration, deposits	4.4.3.17

[a] g/m³ = mg/l = p.p.m. (parts per million)
[b] True colour is the colour of the water from which the turbidity has been removed. It is measured by the platinum-cobalt standard method [1].
[c] Cool water is generally more palatable. Low water temperature tends to decrease the efficiency of water treatment processes, including disinfection. High water temperature encourages growth of nuisance organisms and intensifies taste, odour, colour and corrosion problems.

B)

Inorganic Constituents of Health Significance

Constituent[a]	Unit[a]	Guideline value	Remarks	Document Reference: N.Z. Standards	Document Reference: WHO Guidelines Vol. 1
arsenic	g/m³	0.05			4.2.2.1
boron	g/m³	0.5	safe level for human intake is 5 g/m³, but some glasshouse plants are damaged above 0.5 g/m³	4.2.2	4.2
cadmium	g/m³	0.005			4.2.2.5
chromium	g/m³	0.05	total chromium		4.2.2.6
cyanide	g/m³	0.1			4.2.2.7
fluoride	g/m³	0.9 to 1.1	deliberately added fluoride	4.2.3	4.2.2.8
lead	g/m³	0.05			4.2.2.10
mercury	g/m³	0.001			4.2.2.11
nitrate	g/m³(N)	10	above the guideline value health of bottle-fed infants is likely to be at risk		4.2.2.13
selenium	g/m³	0.01			4.2.2.14

[a] g/m³ = mg/l = p.p.m. (parts per million).

A.14.2 NZ Drinking Water Standard (NZ Board of Health, 1984), showing guideline values for chemical components of Aesthetic (A) and Inorganic constituents (B).

Substance or property	World Health Org. 1963		Natl. Acad. Sci. Natl. Acad. Eng. 1972
	Maximum acceptable	Maximum allowable	
Alkyl benzyl sulfonate (ABS, LAS, methylene—blue active substances	0.5	1	0.5
Ammonium nitrogen			0.5
Arsenic	—	0.05	0.1
Barium	—	1	1
Cadmium	—	0.01	0.01
Calcium	75	200	—
Chloride	200	600	250
Chromium (hexavalent)	—	0.05	0.05
Color (Pt-Co units)	5	50	75
Copper	1	1.5	1
Cyanide	—	0.2	0.2
Fluoride[a]	—	—	1.4–2.4
Iron (Fe^{2+})	0.3	1	0.3
Lead	—	0.05	0.05
Magnesium	50	150	—
Magnesium and sodium sulfates	500	1000	—
Manganese (Mn^{2+})	0.1	0.5	0.05
Mercury	—	—	0.002
Nitrate nitrogen[b]	—	—	10
Nitrite nitrogen	—	—	1
Organics			
Carbon chloroform extract	0.2	0.5	0.3
Carbon alcohol extract	—	—	1.5
Pesticides			
Aldrin	—	—	0.001
Chlordane	—	—	0.003
DDT	—	—	0.05
Dieldrin	—	—	0.001
Endrin	—	—	0.0005
Heptachlor	—	—	0.0001
Heptachlor epoxide	—	—	0.0001
Lindane	—	—	0.005
Methoxychlor	—	—	1
Toxaphene	—	—	0.005
Organo phosphorus and carbamate insecticides	—	—	0.1
Herbicides			
24-D	—	—	0.02
2,4,5-TP (Silvex)	—	—	0.03
2,4,5-T	—	—	0.002
pH (units)	7–8.5	—	5–9
Phenolic compounds (as phenol)	0.001	0.002	0.000001
Selenium	—	0.01	0.01
Silver	—	—	—
Sulfate	200	400	250

A.14.3 Drinking Water Standard (World Health Organization, 1963, and Natl.Acad.Sci & Natl Acad. Eng, 1972).(from Rahn, 1986).

A

Problems and quality parameters	No problems	Increasing problems	Severe problems
Salinity effects on crop yield:			
Total dissolved-solids concentration (mg/l)	< 480	480-1 920	> 1 920
Deflocculation of clay and reduction in K and infiltration rate:			
Total dissolved-solids concentration (mg/l)	> 320	< 320	< 128
Adjusted sodium adsorption ratio (SAR)	< 6	6-9	> 9
Specific ion toxicity:			
Boron (mg/l)	< 0.5	0.5-2	2-10
Sodium (as adjusted SAR) if water is absorbed by roots only	< 3	3-9	> 9
Sodium (mg/l) if water is also absorbed by leaves	< 69	> 69	
Chloride (mg/l) if water is absorbed by roots only	< 142	142-355	> 355
Chloride (mg/l) if water is also absorbed by leaves	< 106	> 106	
Quality effects:			
Nitrogen in mg/l (excess N may delay harvest time and adversely affect yield or quality of sugar beets, grapes, citrus, avocados, apricots, etc.)	< 5	5-30	> 30
Bicarbonate as HCO_3 in mg/l (when water is applied with sprinklers, bicarbonate may cause white carbonate deposits on fruits and leaves)	< 90	90-520	> 520

B

	Permanent irrigation of all soils	Up to 20 years irrigation of fine textured neutral to alkaline soils (pH 6 to 8.5)
Aluminum	5	20
Arsenic	0.1	2
Beryllium	0.1	0.5
Boron--sensitive crops*	0.75	2
semitolerant crops	1	
tolerant crops	2	
Cadmium	0.01	0.05
Chromium	0.1	1
Cobalt	0.05	5
Copper	0.2	5
Fluoride	1	15
Iron	5	20
Lead	5	10
Lithium--citrus	0.075	0.075
other crops	2.5	2.5
Manganese	0.2	10
Molybdenum	0.01	0.05†
Nickel	0.2	2
Selenium	0.02	0.02
Vanadium	0.1	1
Zinc	2	10

† For acid soils only.

A.14.4 Guideline for Interpretation of Water Quality for Irrigation (A) (from Ayers, 1975) and Recommended Maximum limits in milligrams per litre for trace elements in irrigation water (B) (from Natl. Acad. Sci. & Nat. Acad. Eng. 1972).

(concentrations in mg/l times the conversion factor yields concentration in meq/l)

Chemical Constituent	Conversion Factor
Aluminum (Al^{+3})	0.11119
Ammonium (NH_4^+)	0.05544
Barium (Ba^{+2})	0.01456
Beryllium (Be^{+3})	0.33288
Bicarbonate (HCO_3^-)	0.01639
Bromide (Br^-)	0.01251
Cadmium (Cd^{+2})	0.01779
Calcium (Ca^{+2})	0.04990
Carbonate (CO_3^{-2})	0.03333
Chloride (Cl^-)	0.02821
Cobalt (Co^{+2})	0.03394
Copper (Cu^{+2})	0.03148
Fluoride (F^-)	0.05264
Hydrogen (H^+)	0.99209
Hydroxide (OH^-)	0.05880
Iodide (I^-)	0.00788
Iron (Fe^{+2})	0.03581
Iron (Fe^{+3})	0.05372
Lithium (Li^+)	0.14411
Magnesium (Mg^{+2})	0.08226
Manganese (Mn^{+2})	0.03640
Nitrate (NO_3^-)	0.01613
Nitrite (NO_2^-)	0.02174
Phosphate (PO_4^{-3})	0.03159
Phosphate (HPO_4^{-2})	0.02084
Phosphate ($H_2PO_4^-$)	0.01031
Potassium (K^+)	0.02557
Rubidium (Rb^+)	0.01170
Sodium (Na^+)	0.04350
Strontium (Sr^{+2})	0.02283
Sulfate (SO_4^{-2})	0.02082
Sulfide (S^{-2})	0.06238
Zinc (Zn^{+2})	0.03060

A.14.5 Conversion Factors for Chemical Equivalence (From Hem, 1970).